Universidade Federal do Rio de Janeiro
Escola Politécnica & Escola de Química
Programa de Engenharia Ambiental

Matheus de Andrade Cruz

ADVANCEMENTS TOWARDS FOSSIL ENERGY SUSTAINABILITY: CO_2-RICH NATURAL GAS PROCESSING, MONETIZATION OF FLUE-GAS DESULFURIZATION RESIDUES, AND DECARBONIZATION VIA PHASE-CHANGING ABSORPTION

Rio de Janeiro
2020

UFRJ

Matheus de Andrade Cruz

ADVANCEMENTS TOWARDS FOSSIL ENERGY SUSTAINABILITY: CO_2-RICH NATURAL GAS PROCESSING, MONETIZATION OF FLUE-GAS DESULFURIZATION RESIDUES, AND DECARBONIZATION VIA PHASE-CHANGING ABSORPTION

Doctoral thesis presented to the Environmental Engineering Program, Escola Politécnica & Escola de Química, from Universidade Federal do Rio de Janeiro, as part of the requirements for obtaining a Doctor of Science degree in Environmental Engineering.

Advisors: Ofélia de Queiroz F. Araújo, PhD
José Luiz de Medeiros, DSc.

Rio de Janeiro
2020

CC957a

Cruz, Matheus de Andrade
Advancements towards fossil energy sustainability: CO2-rich natural gas processing, monetization of flue-gas desulfurization residues, and decarbonization via phase-changing absorption / Matheus de Andrade Cruz. -- Rio de Janeiro, 2020.
339 p.

Orientadora: Ofélia de Queiroz Fernandes Araújo.
Coorientador: José Luiz de Medeiros.
Tese (doutorado) - Universidade Federal do Rio de Janeiro, Escola Politécnica, Escola de Química, Programa de Pós-Graduação em Engenharia Ambiental, 2020.

1. Gás natural rico em CO2. 2. Análise exergética. 3. Gases exaustos. 4. Resíduos de FGD. 5. Captura de CO2 por solventes bifásicos. I. de Queiroz Fernandes Araújo, Ofélia, orient. II. de Medeiros, José Luiz, coorient. III. Título.

UFRJ

ADVANCEMENTS TOWARDS FOSSIL ENERGY SUSTAINABILITY: CO_2-RICH NATURAL GAS PROCESSING, MONETIZATION OF FLUE-GAS DESULFURIZATION RESIDUES, AND DECARBONIZATION VIA PHASE-CHANGING ABSORPTION

Matheus de Andrade Cruz

Advisors: Ofélia de Queiroz F. Araújo, PhD
José Luiz de Medeiros, DSc.

Thesis presented to the Program of Environmental Engineering, Escola Politécnica and Escola de Química, of Universidade Federal do Rio de Janeiro, as part of the requirements for the degree of Doctor of Science in Environmental Engineering.

Approved by:

Prof. Ofélia de Queiroz Fernandes Araújo, PhD, UFRJ (Advisor, President)

Prof. José Luiz de Medeiros, DSc, UFRJ (Advisor)

Ana Paula Santana Musse, DSc, Petrobras

Prof. Assed Naked Haddad, DSc, UFRJ

Prof. Bettina Susanne Hoffmann, DSc, UFRJ

Prof. Lidia Yokoyama, DSc, PUC-RJ

Prof. Claudia do Rosário Vaz Morgado, Dsc, UFRJ

Rio de Janeiro
2020

To the memory of my father Marcelo Cruz.
To my mother Cristina, my brother Davi
and my wife Daniele.

.

ACKNOWLEDGMENTS

I would like to express my gratitude to my advisors Prof. Ofélia de Queiroz Fernandes Araújo and Prof. José Luiz de Medeiros, who guided me throughout all the studies developed in this thesis.

I would also like to thank the current and former researchers of the laboratory H2CIN, Alisson Martins, George Brigagão, Igor Wiesberg, Lara Arinelli, and Rui de Castro, which supported me in the execution of experiments and providing computational tools used to developing some topics addressed in this thesis.

I wish to extend my special thanks to the staff of the CE-GN and H2CIN, especially Alex, Wagner, Tiago, Carla and Avanide, for the support in the pilot-plants procurement and construction activities.

Finally, I acknowledge Petrobras and Eneva for their financial support.

RESUMO

CRUZ, M. de A. **Avanços para a sustentabilidade de energias fósseis: processamento de gás natural rico em CO_2, monetização de resíduos de dessulfurização de gases exaustos e descarbonização por absorção com solventes bifásicos**. Tese (Doutorado em Engenharia Ambiental), Programa de Engenharia Ambiental, Escola Politécnica & Escola de Química, Universidade Federal do Rio de Janeiro, 2020. Orientadores: Ofélia de Queiroz Fernandes Araújo e José Luiz de Medeiros.

Visando aumento de eficiência energética e mitigação de impactos ambientais na cadeia de valor de energia fóssil são desenvolvidas/avaliadas novas tecnologias, principalmente de geração/utilização de energia. Assim, essa tese se desdobra em três linhas de pesquisa. Primeiramente, a produção offshore de petróleo e gás tem um histórico de baixa eficiência energética/exergética em relação à produção/utilização de energia no processamento de gás rico em CO_2. Assim, novos conceitos envolvendo compressores centrífugos são avaliados: (i) resfriamento primário a 4ºC com águas profundas, baixando a temperatura da água de resfriamento inter-estágio, com consequente redução do consumo energético de compressores; (ii) substituição de compressores centrífugos superdimensionados com ineficientes reciclos *anti-surge* por compressores menores em paralelo sem reciclo, que reduzem drasticamente a destruição exergética nesses sistemas ao longo de campanhas com carga de gás decrescente. Na segunda vertente do trabalho, é abordada a questão de termoelétricas a carvão que produzem resíduos de dessulfurização de gases exaustos (FGD, do inglês *Flue-Gas Dessulfurization)* fora de especificação para aproveitamento industrial, sendo destinados a aterros. Foi avaliado tratamento para comercialização de resíduos de FGD como aditivo para cimento. Em terceiro lugar, aborda-se a remoção de CO_2 de gases exaustos por soluções aquosas de alcanolaminas, que implica penalidade energética a termoelétricas. São realizados experimentos de captura de CO_2 com solventes bifásicos, desenvolvidos para redução do consumo de energia do processo. No processamento offshore de gás rico em CO_2, é demonstrado que a utilização de captura profunda de água do mar reduz em 2% a 5% o consumo de energia/gás combustível e emissões de CO_2 e em 9,5% o custo dos principais equipamentos de processo. Ademais, compressores com reciclo *anti-surge* mantêm o consumo de energia/gás combustível alto durante toda a campanha de produção, resultando em eficiências exergéticas em torno de 49%/83% entre 25%/100% de carga de gás, enquanto compressores menores em paralelo sem reciclo reduzem a energia/consumo de combustível proporcionalmente à carga de gás, mantendo essa eficiência entre 80% e 88% e eliminando uma turbina a gás. Para usinas a carvão de 360MW, o custo nivelado de energia é reduzido em ~3% com à comercialização de resíduos de FGD. Uma avaliação *gate-to-gate* de impactos ambientais revela que a comercialização do resíduo é ambientalmente menos prejudicial do que dispô-los em aterros. Finalmente, experimentos em uma planta-piloto de pequena escala para captura de CO_2 indicam que soluções aquosas de monoetanolamina/propanol são promissores solventes bifásicos. É apresentado o projeto de uma planta-piloto de maior escala para testes de longa duração com solventes bifásicos.

Palavras-chave: Processamento de gás natural rico em $CO_{2;}$ Análise exergética; Gases exaustos; Absorção por solventes bifásicos; Resíduos de FGD;.

ABSTRACT

CRUZ, M. de A. **Advancements Towards Fossil Energy Sustainability: CO_2-Rich Natural Gas Processing, Monetization of Flue-Gas Desulfurization Residues, and Decarbonization via Phase-Changing Absorption**. Thesis (Doctorate in Environmental Engineering), Programa de Engenharia Ambiental, Escola Politécnica & Escola de Química, Universidade Federal do Rio de Janeiro, 2020. Advisors: Ofélia de Queiroz Fernandes Araújo and José Luiz de Medeiros.

Energy-efficiency and impact mitigation along the fossil-energy value chain drive the development/assessment of new technologies to improve the generation/utilization of fossil-energy. Bearing in mind those targets, this thesis unfolds in three research lines. Firstly, offshore oil/gas production in tropical deep-waters has a track record of low energy/exergy efficiencies regarding gas-fired power production/utilization in CO_2-rich gas processing. Here, new concepts for better utilization of centrifugal compressors are assessed: (i) 4°C deep seawater primary-cooling lowering cooling-water temperature, consequently reducing power consumption of multistage intercooled compression; (ii) substitution of large centrifugal compressors with inefficient anti-surge recycles by multiple-paralleled smaller compressors dramatically reducing exergy destruction in compression systems along offshore campaigns with decreasing gas-load. Secondly, coal-fired power plants produce problematic flue-gas desulfurization (FGD) solid-residues often destined to landfills. Here, monetization was assessed for FGD solids as cement additives. Thirdly, aqueous-amine flue-gas decarbonation entails energy-penalty for power plants. Carbon capture experiments with phase-changing absorption solvents are conducted aiming at energy-penalty reduction. On offshore CO_2-rich gas processing, it is shown that deep-seawater utilization lowers 2%-5% power/fuel-gas consumption and CO_2 emissions, and 9.5% of equipment investment. Moreover, large compressors with anti-surge recycle keep power/fuel-gas consumptions high throughout entire rig campaign entailing exergy efficiencies around 49%/83% at 25%/100% gas-loads, while multiple-paralleled smaller compressors reduce power/fuel-gas consumptions proportionally to gas-load keeping exergy efficiency around 80%-88% throughout campaign, eliminating one gas-turbine. For 360MW coal-fired power plants it is shown that the levelized-cost of energy is reduced ~3% thanks to commercializing FGD residues. Gate-to-gate environment impact assessment unveils upgrading/commercializing as environmentally better than landfilling FGD residues. Finally, experiments on a small decarbonation pilot-plant indicate aqueous-monoethanolamine-propanol solutions as promising CO_2 capture phase-changing solvents. The design of a larger pilot-plant intended to perform long-run trials with phase-changing solvent is presented.

Keywords: CO_2-rich natural gas processing; Exergy analysis; Flue-gas; Phase-changing absorption; FGD residues.

ABBREVIATIONS

AGWA	Acid gas-water-amine
AMP	2-amino-2-methylpropanol
BAT	Best available technologies
BOE	Barrels of oil equivalent
CAPEX	Capital expenditure
CCP	Coal combustion products
CCS	Carbon capture and storage
CCUS	Carbon capture utilization and storage
CW	Cooling-water
DEA	Diethanolamine
DSW	Deep seawater
EKC	Environmental Kuznets curves
EOR	Enhanced oil recovery
EPCI	Engineering, procurement, construction and installation
EROI	Energy return on investment
ERR	Energy return ratios
FBR	Fluidized bed reactor
FCI	Fixed Capital Investment
FGD	Flue-gas desulfurization
FGDR	Flue-gas desulfurization residues
FPSO	Floating production storage and offloading
GDP	Gross domestic product
GHG	Greenhouse gases
GOR	Gas to oil ratio
GT	Gas-turbines
HCDP	Hydrocarbon dew point
LCC	Life cycle cost
LCOE	Levelized cost of electricity
MDEA	Methyldiethanolamine
MEA	Monoethanolamine
NER	Net energy ratio
NG	Natural gas
NGCC	Natural gas combined cycle
O&G	Oil and gas
OPEX	Operational expenditure
P&ID	Process and instrumentation diagram
PCAS	Phase-changing absorption solvents
PCC	Pulverized coal combustion
PM	Particulate matter
SD-FGDR	Semi-dry flue-gas desulfurization residue
SDG	Sustainable development goals
TETA	Triethylenetetramine
TMPDA	Tetramethyl-1,3-propanediamine
TPES	Total primary energy supply
VLCC	Very large crude carriers
WDP	Water dew point
WOR	Water to oil ratio

CONTENT

1. INTRODUCTION

The United Nations established universal access to affordable, reliable and sustainable energy as a goal of the 2030 Agenda for Sustainable Development (United Nations, 2015). Nevertheless, the energy sector has been considered the major responsible for climate changes, accounting for 80% of CO_2 emissions (IEA, 2019a). Furthermore, the extraction, processing and combustion of fossil fuels cause deterioration of air quality, depletion of natural resources among other negative environmental impacts. Since the developed economies are responsible for the major energy demand, they have been leading efforts to replace environmentally non-friendly energy sources (e.g. coal) by natural gas and renewable energy (wind and solar). Additionally, carbon capture utilization and storage (CCUS) technologies are expected innovations in clean-energy grids. However, CCUS deployments and grid transition to renewables are low-paced, comparatively to climate targets – fossil fuels remain responsible for 80% of total primary energy supply (TPES) worldwide, with shares varying across regions.

Frequently, in American countries, the energy demand of the transport sector is predominant and oil share is higher, while, in Asia, heat and power generation is responsible for most of the energy demand, prevailing coal in the energy matrix (IEA, 2020), as depicted in Fig 1.1. This difference in the share of coal-fired energy between developed and developing economies is explained through the Environmental Kuznets Curves (EKC) theory (Stern, Common and Barbier, 1996). In the early '90s, several authors fitted empirical data on environmental degradation versus national income. Most of the plots revealed an inverted U-pattern, as illustrated in Fig. 1.2. According to EKC hypothesis, environmental degradation increases with economic growth only in the least developed economies; at a certain degree of development, an inflection point exists (point A in Fig 1.2) and incomes are reverted in environmental protection. From this stage on, the detrimental effects of economic growth are surpassed by environmental improvements. From point B of Fig. 1.2 onwards, sustainable development is achieved.

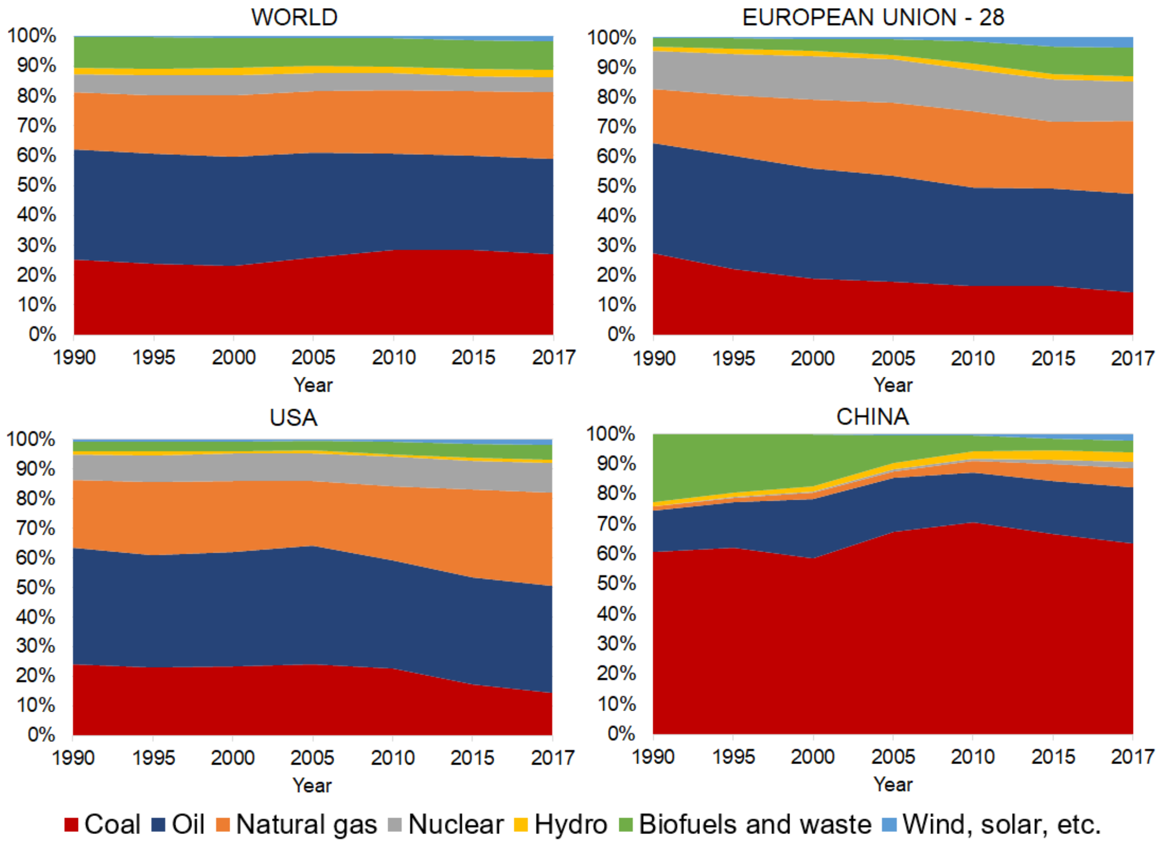

Figure 1.1. Total Primary Energy Supply of the World, European Union, United States of America and China. Graphs are based on data from IEA (2020).

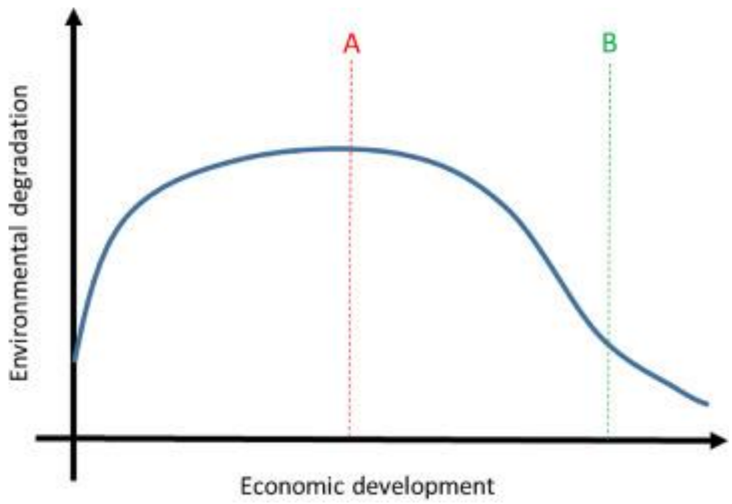

Figure 1.2. The Environmental Kuznet Curve. Line A - inflection point. Line B - sustainable stage of economic development. Source: Vallero and Shulman (2019)

Generally, the level of development of cities and countries is expressed by economic metrics, like gross domestic product (GDP), gross national income (GNI) or purchase power parity (PPP). Environmental degradation is usually expressed as a release rate or concentration of pollutants in natural systems, e.g. particulate matter (PM) concentration or SO_2 flow rate of emissions in the air. However, many other metrics exist to represent the level of environmental degradation and economic development of a region or nation. In fact, sensitivities to localization (country, city) and time (year) do not empirically support the inverted U-patterned of EKCs, and several relevant air pollutants do not follow EKC pattern (Harbaugh, Levinson and Wilson, 2002).

Destek and Sarkodie (2019) investigated the relationship between economic growth, energy consumption, financial development and ecological footprint from 1977 to 2013 in 11 developing economies. The results revealed that, although for certain countries the EKS shape is confirmed, for energy-intensive economies, like China and India, a U-shaped relationship occurred. The authors also found a one-way causality from energy consumption to ecological footprint. Energy is a major driver of economic development but also of environmental degradation. Seeking for economic growth and job creation least developed nations need to increase energy production while avoiding pollution, climate changes and waste generation. EIA (2017) data (Fig. 1.3) corroborates with the findings of Destek and Sarkodie (2019).

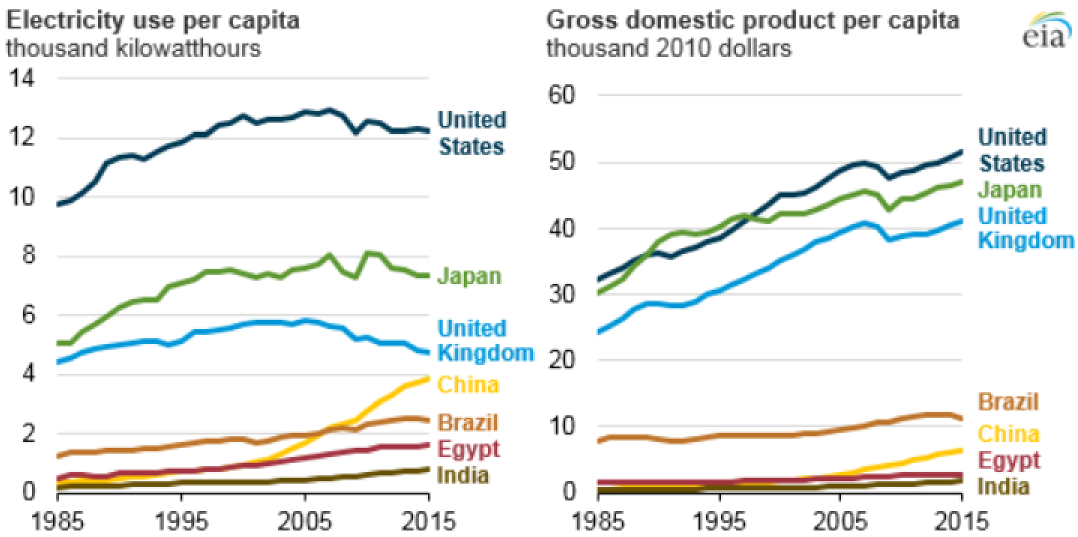

Figure 1.3. Gross Domestic Product and Electricity Use (2011 – 2015) (EIA, 2017)

As an example, in 2008 India had the highest air pollution in the world (Somani, 2013). Not coincidentally, the Indian economy has grown 6.14% per year between 1980 and 2008. India's TPES and energy use per capita increased quickly along these 3 decades pushing the environmental degradation. Fig. 1.3 shows that the developed countries were able to keep GDP growth while reducing the electricity use per-capita over the last 5 years. Differently, developing countries have GDP growth followed by increased electricity use and, consequently, higher environmental degradation.

This scenario shows that fossil fuels will prevail in the TPES in the short to mid-term, demanding technologies to tackle climate change and other negative environmental impacts along the entire fossil-energy value chain, illustrated in Fig. 1.4. Emissions reduction should target reductions of the energy intensity of processes through enhancements of energy efficiency, mitigation of pollutants release and solid wastes management.

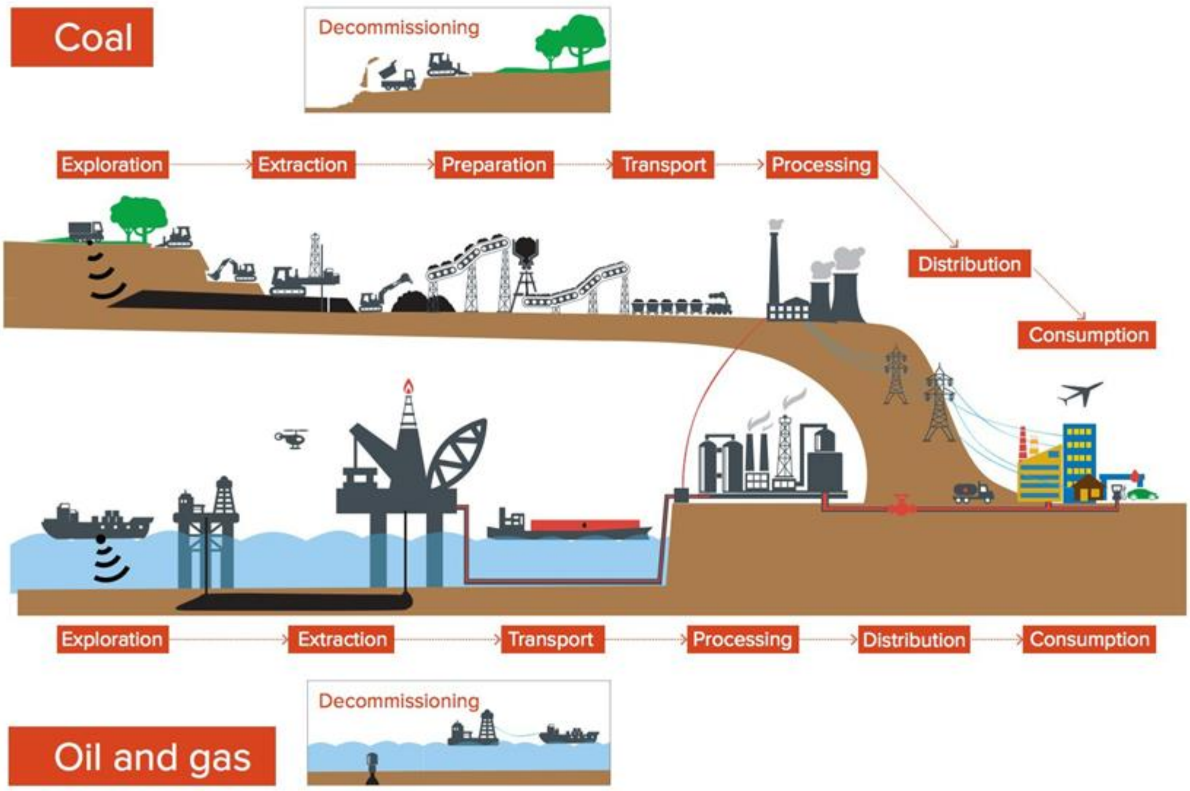

Figure 1.4. Fossil Fuels Value Chain. (InfrastructureUSA, 2015)

In this context, this thesis approaches technological advances in three different fronts within the fossil-energy chain: offshore primary processing of oil and gas; solid waste management of coal-fired power plants and carbon capture from flue-gases, i.e. post-combustion capture. It is worth noting that although post-combustion technologies are mostly employed in power plants it is applicable to other steps of the fossil-energy value chain, e.g. oil production and refining.

1.1. Objectives

Looking for enhancing sustainability of the fossil-energy supply, the objective of this thesis is to assess the technical, economic and/or environmental aspects of three technologies to reduce environmental impacts, respectively three research lines – R1, R2 and R3. This research aims at answering the questions: (i) Are the investigated technologies technically feasible? (ii) Are the technologies advantageous economic and/or environmentally? (iii) Are there bottlenecks or technological challenges to the commercial deployment of the technologies?

1.1.1. Specific Goals

R1 - Offshore Processing of CO_2-Rich Natural Gas

The goal of this research line is to develop and analyze two process modifications in a Floating Production Storage and Offloading (FPSO) unit processing CO_2-rich natural gas: (R1.1) the use of deep seawater (DSW) as primary cooling utility and (R1.2) parallel-compressors scheme to avoid energy expenditure with anti-surge recycles. The main targets of these innovations are the assessment of technical and economic feasibility of the proposed modifications and the resulting reduction of CO_2 emissions. The implementation of an exergy analysis methodology customized to gas processing is a secondary specific objective, inherent to the topic (R1.2).

R1.1 objective is to evaluate the effects of using DSW as an indirect cooling utility in an FPSO. This alternative is compared to the traditional process, which uptakes warmer surface seawater. The comparison addresses energy consumption, economics and CO_2 emissions. More specifically, it seeks to compare:

- Compressor, gas-turbines (GT) and cooling-water (CW) pumping power;
- Heat exchangers duty;
- Equipment weight, equipment cost and revenue from natural gas (NG) production;
- Fuel-gas consumption and CO_2 emissions along the FPSO lifespan;

R1.2 aims to compare the exergy efficiency and power demand of an FPSO operating at peak and partial gas-loads using two process schemes. One with smaller parallel compressors and variable-speed drive versus the traditional design, with anti-surge recycle. Detailed comparisons are:

- Exergy efficiency;
- Energy intensity, in barrels of oil equivalent (BOE) burned per BOE produced;
- Carbon dioxide intensity, in tons of CO_2 emitted per BOE produced;
- Fixed Capital Investment (FCI) and weight of topside equipment resulting from the process modification.

R2 - Desulfurization Residues from Coal-Fired Power Plants

This line aims to investigate the technical, economic and environmental aspects of implementing a thermal treatment of semi-dry Flue-Gas Desulfurization residue (SD-FGDR), a solid by-product contaminated with calcium sulfite ($CaSO_3$). The proposed technology is conceived to avoid landfills occupied by coal ashes mixed with SD-FGDR. This environmental liability is transformed into a resource, used to produce cement. More detailed objectives are:

- Design and construction of a pilot-plant using a fluidized bed reactor (FBR), projected to oxidize $CaSO_3$ to $CaSO_4$ (gypsum). This reactor is used to obtain process parameters needed for scale-up of the technology.
- Economic feasibility analysis of the treatment retrofitted to a coal-fired power plant, including calculation of the final Levelized Cost of Electricity (LCOE).
- Comparison of the environmental performance of the power plant with and without the SD-FGDR treatment.

R3 - CO_2 Capture from Flue-Gases by Phase-Changing Absorption Solvents

The primary objective of this research line is to confirm the potential of energy saving of using phase-changing absorption solvents (PCAS) to capture CO_2 from flue-gases. To fulfill this goal, three major steps are pursued:

- Literature review, selection and preliminary tests of phase-changing absorption solvents (PCAS). At laboratory-scale, basic properties of the selected PCAS are analyzed, e.g. liquid phases behavior, CO_2 loading, density and viscosity.

- Design and construction of a bench-plant for solvent screening, that operates in batch-mode and enables fast absorption and desorption tests, using small volumes of solvent.
- Design of a pilot-plant, that operates in continuous-mode. This pilot-plant has the same layout of an industrial plant and would provide important process parameters, like the energy penalty (GJ/t of CO_2 captured). Future data produced during long run tests can be used to support process simulation and next scale-up design of the technology.

1.2. Justification

Given the potentially catastrophic impacts of climate change, CO_2 emissions have been the focus of environmental and energy-related developments. However, the fossil-energy value chain is responsible for several other negative environmental impacts, to the air, soil and water. It is important to develop and improve the technologies of extraction, processing and conversion of fossil fuels to reduce the environmental footprint of this energy source. The three proposed research lines – R1, R2 and R3 – are justified in the present section.

R1 - Offshore Processing of CO_2-Rich Natural Gas

Given the forecast of 25% increase on energy demand and replacement of coal by NG, the Oil & Gas industry will be in charge of 50% of the global TPES until 2040 (IEA, 2018a). According to the International Association of Oil and Gas Producers (IOGP, 2019), in 2018 the major oil and gas companies produced 1943 MMt of hydrocarbons (HC), with 55.2% of them came from offshore fields. This information justifies the choice and shows the relevance of the approached research lines.

Fossil fuels are believed to contribute to the global energy mix for decades to come, and to be the major energy source in the short to mid-term. Oil and gas (O&G) production from offshore reserves has emitted 115t of greenhouse gases (GHG) per 1000t of HC produced, totalizing 223.4 MMt CO_{2e} in 2018. The IOGP (2019) informs that 71% of the CO_2 emissions (excluded methane) from the O&G industry are related to internal fuel combustion for energy production. Thus, given the environmental concerns and a carbon regulation scenario, it is of utmost importance to improve energy efficiency of O&G operations to reduce CO_2 emissions.

The Brazilian Pre-salt has challenging design conditions, such as the high gas to oil ratio (GOR) and CO_2-rich associated gas. These issues render the primary processing of associated gas more energy-intensive than in conventional fields. There requires CO_2 separation and injection for Enhanced Oil Recovery (EOR) and dispatch of preconditioned gas to onshore processing units, located 150-300km away, demanding high pressures, frequently, near 25000 kPa. These peculiarities strongly impact the cost and energy consumption of the FPSO gas processing plant, and drives research line R1.

R2 - Desulfurization Residues from Coal-Fired Power Plants

In the next decades, coal will have a major participation in the TPES of developing countries, especially in China and India. Consequently, post-combustion technologies to mitigate air pollution are demanded, notedly for sulfur oxides, nitrous oxides and carbon dioxide removal from flue-gas. The first, Flue-gas Desulfurization (FGD), is a fingerprint of coal-fired power plants. Ash yield from coal combustion is between 3% to 49% (Pierce and Dennen, 2009) and some unit operations of power plants also produce solid by-products. Therefore, coal-fired power generation produces a massive amount of the so-called Coal Combustion Products (CCP). In 2017, the total production of CCP was around 1.1 billion metric tons (Harris, Heidrich and Feuerborn, 2019) The majority of CCPs (~64% in 2016) are considered resources and have several large-scale applications. If not utilized, they are piled up in landfills, becoming an environmental liability. Flue-gas desulfurization residues (FGDR) produced by coal-fired power plants can be used as raw materials, e.g. for civil and agricultural applications. However, some pollutants contained in the FGDR might contaminate the local environment, hindering their material reuse. (Phoungthong et al., 2018).

The FGD technology influences the residue composition and potential of utilization. The SD-FGDR is rich in sulfite ($SO_3^{=}$), which limits its use. The ASTM Standard C618 (ASTM, 2015), for example, impose a limit on the $SO_3^{=}$ content to use fly-ash as a cement additive. Therefore, it is not possible to utilize fly-ash as a cement additive when it is mixed to SD-FGDR. Alternative uses of these contaminated ashes are limited. Frequently, large landfills are used to stock the contaminated coal ashes.

Around 40% to 60% of the desulfurization market runs in favor of SD-FGD and the rest uses the wet technology (Blankinship, 2005). As a result, the amount of SD-FGDR produced around the world is very expressive and justifies the research line R2.

R3 - CO_2 Capture from Flue-Gases by Phase-Changing Absorption Solvents

The increase of the CCUS capacity would make the necessity of fossil fuels cut less aggressive when aiming to meet the Paris Agreement global warming goals (Foster and Elzinga, 2015). Without CCUS the fossil energy production must be reduced by 50% until 2040. Considering a scenario where CCUS capacity reaches 7 Gt CO_2/y until 2040 and 11 Gt CO_2/y until 2100, this would be a reduction of 34% on fossil-energy cuts (Copenhagen Economics, 2017). In a more optimistic scenario, the Global CCS Institute (2016) predicts that a capacity of 4 GtCO_2/y would be sufficient to keep global warming below 2ºC. Anyway, CCUS is extremely important to limit global warming. However, the CCUS capacity barely reached 40 MMt/y in 2019 (Global CCS Institute, 2019).

The chemical absorption is currently the more mature technology for large scale post-combustion carbon capture. However, the energy spent to regenerate the solvent – the energy penalty – is considered a major hindrance to the deployment of this technology. The PCAS emerged as an opportunity to reduce this energy penalty and contribute to turning CCUS more economically feasible, increasing its installed capacity. These facts and arguments justify research line R3.

1.3. Outline of the Thesis

This thesis is organized as an assemblage of published articles (Chapters 3, 5 and 6), a submitted article, currently under peer review (Chapter 4), and a conference paper (Chapter 7). A pilot-plant project is included as an additional section of Chapter 7. The research lines R1, R2 and R3 are developed according to the Table 1.1.

Table 1.1. Correlation between scientific production and thesis content.

Research Line	Chapters	References
(R1) Offshore Processing of CO_2-Rich Natural Gas	3	(Cruz, Araújo and de Medeiros, 2018)
	4	Under review. Code *APEN-D-20-00835*
(R2) Desulfurization Residues from Coal-Fired Power Plants	5	(Cruz et al., 2017)
	6	(Cruz et al., 2018)
(R3) CO_2 Capture from Flue-Gases by Phase-Changing Absorption Solvents	7	(Cruz et al., 2019)

Figure 1.5 shows where each research line is supposed to be applied along the fossil energy value chain. R3, identified by blue asterisks in the Figure 1.5, is related to CCUS and could be applied to multiple steps of coal, oil and gas value chains.

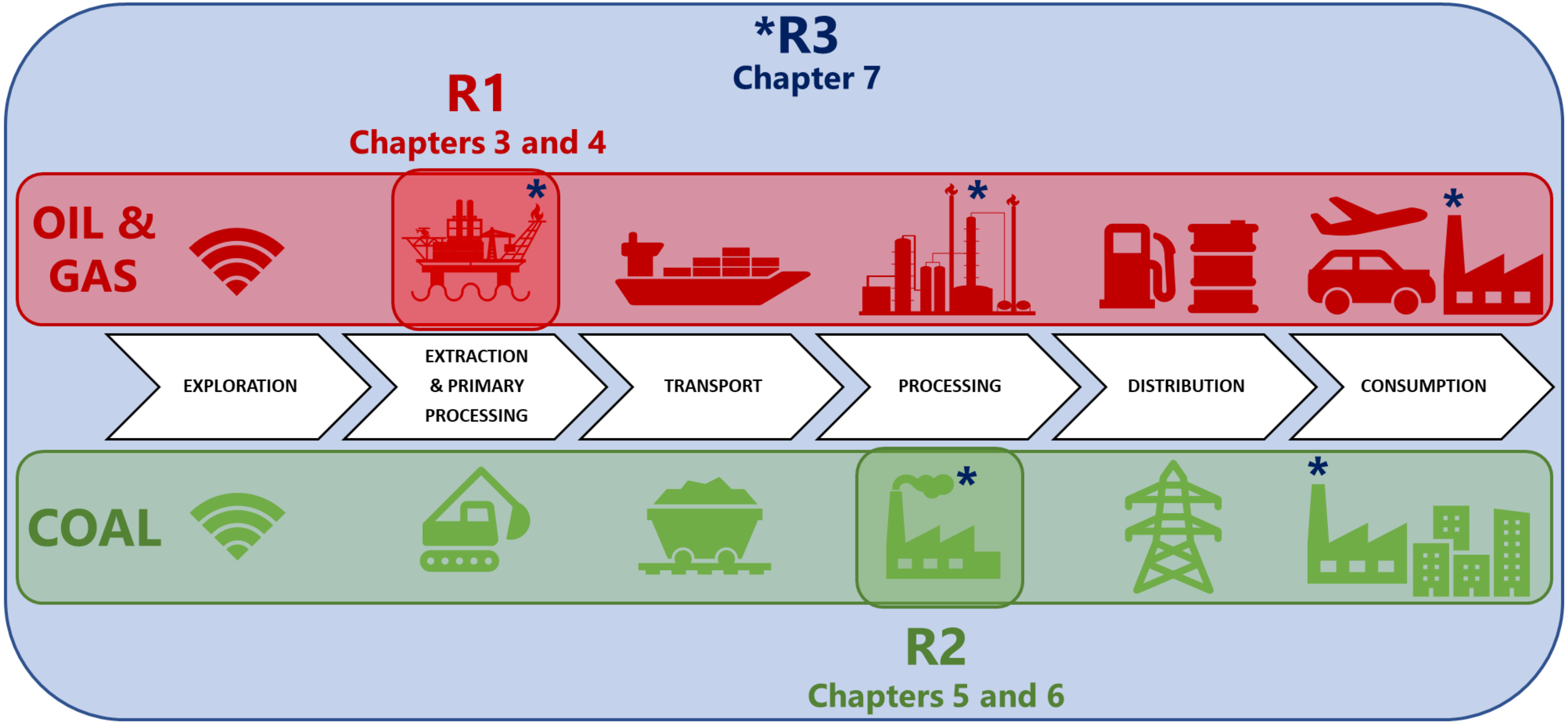

Figure 1.5. Distribution of Research Lines and Chapters of the Thesis Along the Fossil Fuels Value Chain.

Chapter 2 presents a literature review, approaching an overview of each proposed research line. This information supplies a macro perspective, that contextualizes and support the more focused literature review addressed in each chapter. Firstly, referring to R1, general information about the offshore O&G sector, CO_2-rich fields, topside technologies and environmental constraints are presented. Secondly, referring to R2, a compilation of relevant information concerning coal-fired power plants and SD-FGD technologies are presented. Finally, general aspects of traditional post-combustion carbon capture and an extended review about PCAS are presented, complementing research line R3.

In Chapter 3, the article by Cruz, Araújo and De Medeiros (2018) is integrally reproduced, as published. It presents a comparative analysis of using colder DSW uptakes as a primary cooling utility in a FPSO against the traditional surface seawater uptake. The proposed process modification is compared to the base case in terms of power consumption, CO_2 emissions and detailed equipment sizing and cost estimation. Possible extra revenue from natural gas in consequence of fuel gas savings are also estimated.

Chapter 4 contemplates a process design innovation in an offshore CO_2-rich natural gas processing scenario. The use of smaller parallel compressors and variable-speed drive is compared to the traditional layout with anti-surge recycle, at peak and partial gas-loads. A customized exergy analysis methodology is implemented to support the assessment. Processes are compared in terms of exergy efficiency, investment, footprint and emissions.

In Chapter 5, the published article of Cruz et al. (2017) is integrally reproduced. The study addresses a SD-FGDR treatment unit, to promote dry oxidation of calcium sulfite to calcium sulfate. A Brazilian coal-fired power plant facing decision-making process on SD- FGDR destination is regarded as the case study. The main equipment is sized and scaled-up based on the pilot-plant process parameter and patents of similar processes. An economic assessment is performed, including capital, operational and maintenance costs, residue revenue and LCOE. This information is used to determine the impact that the SD-FGDR treatment would imply on the electricity price if it were applied to the analyzed power plant.

In Chapter 6, the article of Cruz et al. (2018) is reproduced. To support decision-making on process configurations to monetize the SD-FGDR, a gate-to-gate assessment of potential environmental impacts is performed. Three scenarios are considered: BASE - the standard power plant, CASE I – the base plant with SD-FGDR treatment, CASE II – bypass of desulfurization system.

Chapter 7 is divided into two subsections. Section 7.1 reproduces the conference paper SDEWES2019.0276 (Cruz et al., 2019), entitled Chemical Absorption of CO_2 from Flue-Gases: Experiments with Phase Changing Solvents in a Bench Scale Plant, presented at the 14th Conference on Sustainable Development of Energy, Water and Environment Systems – Dubrovnik, 2019. This paper presents the state-of-the-art concerning PCAS and selects three of them to be tested in laboratory and in a solvent screening plant. The plant design is briefly presented in the article. One solvent, based on monoethanolamine and 1-propanol, was considered more suitable. Section 7.2 presents the process description, process flow diagram, P&ID, main equipment design and details about the control and automation system of a pilot-plant. The plant is designed to operate in continuous mode, aiming to support the scale-up of the technology to industrial applications.

Chapter 8 encompasses all the research lines presenting and discussing the overall and specific conclusions, findings and highlights of the thesis.

Appendices A to G unveil front pages and a complete bibliography of the publications of the Chapters 3 to 7. When existent, supplementary materials of each chapter are included in the Appendix H.

Appendices F and G unveil front pages and bibliography of further publications and co-authorships.

Appendix I presents design details, process specification, data sheets, draws and pictures of the main equipment of the pilot plant presented in Chapter 7, Section 7.2.

1.4. References of Chapter 1

ASTM, 2015. C618-15, Standard Specification for Coal Fly Ash and Raw or Calcined Natural Pozzolan for Use. Annu. B. ASTM Stand. https://doi.org/10.1520/C0618-15

Blankinship, S., 2005. Looking for a Good Scrubbing: Today's FGD Technology [WWW Document]. Power Eng. URL http://www.power-eng.com/articles/print/volume-109/issue-9/features/looking-for-a-good-scrubbing-todayrsquos-fgd-technology.html (accessed 3.15.17).

Copenhagen Economics, 2017. The future of fossil fuels: How to steer fossil fuels use in a transition to a low-carbon energy system. An analysis of fossil fuels trajectories in low-carbon scenarios.

Cruz, M. de A., Araújo, O.Q.F., de Medeiros, J.L., 2018. Deep seawater intake for primary cooling in tropical offshore processing of natural gas with high carbon dioxide content: Energy, emissions and economic assessments. J. Nat. Gas Sci. Eng. 56, 193–211. https://doi.org/10.1016/j.jngse.2018.06.011

Cruz, M. de A., Araújo, O.Q.F., de Medeiros, J.L., de Castro, R.D.P.V., Ribeiro, G.T., de Oliveira, V.R., 2017. Impact of solid waste treatment from spray dryer absorber on the levelized cost of energy of a coal-fired power plant. J. Clean. Prod. 164. https://doi.org/10.1016/j.jclepro.2017.07.061

Cruz, M. de A., Musse, A.P.S., de Medeiros, J.L., Araújo, O.Q.F., 2019. SDEWES2019.0276 Chemical Absorption of CO2 from Flue Gases: Experiments with Phase Changing Solvents in a Bench Scale Plant, 14th Conference on Sustainable Development of Energy, Water and Environment Systems. Faculty of Mechanical Engineering and Naval Architecture, Zagreb.

Cruz, M.D.A., de Castro, R. de P.V., Araújo, O. de Q.F., de Medeiros, J.L., 2018. Environmental Performance of a Solid Waste Monetization Process Applied to a Coal-Fired Power Plant with Semi-Dry Flue Gas Desulfurization. J. Sustain. Dev. Energy, Water Environ. Syst. 7, 506–520. https://doi.org/http://dx.doi.org/10.13044/j.sdewes.d6.0251

Destek, M.A., Sarkodie, S.A., 2019. Investigation of environmental Kuznets curve for ecological footprint: The role of energy and financial development. Sci. Total Environ. 650, 2483–2489. https://doi.org/https://doi.org/10.1016/j.scitotenv.2018.10.017

Foster, S., Elzinga, D., 2015. The Role of Fossil Fuels in a Sustainable Energy System. UN Chron. LII.

Global CCS Institute, 2019. The Global Status of CCS: 2019, Global CCS Institute. Melbourne, Australia. https://doi.org/10.1007/springerreference_15392

Global CCS Institute, 2016. The Global Status of CCS: 2016. Summary Report. Global CCS Institute, Docklands, AU.

Harbaugh, W.T., Levinson, A., Wilson, D.M., 2002. Reexamining the Empirical Evidence for an Environmental Kuznets Curve. Rev. Econ. Stat. 84, 541–551. https://doi.org/10.1162/003465302320259538

Harris, D., Heidrich, C., Feuerborn, J., 2019. Global aspects on Coal Combustion Products [WWW Document]. Coaltrans Conf. URL https://www.coaltrans.com/insights/article/global-aspects-on-coal-combustion-products (accessed 2.4.20).

IEA, 2020. Data & Statistics - IEA [WWW Document]. Int. Energy Agency. URL https://www.iea.org/data-and-statistics?country=EU28&fuel=Energy supply&indicator=Total primary energy supply (TPES) by source (accessed 1.31.20).

IEA, 2019. CO2 emmisions from fuel combustion. France.

IEA, 2018. 2018 World Energy Outlook: Executive Summary. Oecd/Iea.

InfrastructureUSA, 2015. Fossil Fuel Subsidy Reform: From Rhetoric to Reality [WWW Document]. InfrastructureUSA. URL https://www.infrastructureusa.org/fossil-fuel-subsidy-reform-from-rhetoric-to-reality/ (accessed 3.2.20).

IOGP, 2019. IOGP Environmental performance indicators - 2018 data - Atmospheric emissions Int. Assoc. Oil Gas Prod. URL https://data.iogp.org/Environment/Emissions (accessed 2.4.20).

IPCC, 2014. Climate Change 2014: Synthesis Report. Contribution of Working Groups I, II and III to the Fifth Assessment Report of the Intergovernmental Panel on Climate Change, Intergovernmental Panel on Climate Change. IPCC, Geneva, Switzerland.

Phoungthong, K., He, P.-J., Shao, L.-M., Zhang, H., 2018. Leachate phytotoxicity of flue gas desulfurization residues from coal-fired power plant. Environ. Sci. Pollut. Res. 25, 19808–19817. https://doi.org/https://doi.org/10.1007/s11356-018-2207-8

Pierce, B.S., Dennen, K.O., 2009. The National Coal Resource Assessment Overview. U.S. Geol. Surv. Prof. Pap. 1625, 402.

Somani, A.K., 2013. Environmental Tax Reform and Economic Welfare. Harvard.

Stern, D.I., Common, M.S., Barbier, E.B., 1996. Economic growth and environmental degradation: The environmental Kuznets curve and sustainable development. World Dev. 24, 1151–1160. https://doi.org/10.1016/0305-750X(96)00032-0

United Nations, 2015. Transforming our World: The 2030 Agenda for Sustainable Development. New York. https://sustainabledevelopment.un.org/post2015/transformingourworld.

U.S. EIA, 2017. Link between growth in economic activity and electricity use is changing around the world. U.S. Energy Inf. Adm. URL https://www.eia.gov/todayinenergy/detail.php?id=33812 (accessed 1.31.20).

Vallero, D.A., Shulman, V., 2019. Chapter 1 - Introduction to Waste Management☆, in: Letcher, T.M., Vallero, D.A.B.T.-W. (Second E. (Eds.), . Academic Press, 3–14. https://doi.org/https://doi.org/10.1016/B978-0-12-815060-3.00001-3

Yue, X.L., Gao, Q.X., 2018. Contributions of natural systems and human activity to greenhouse gas emissions. Adv. Clim. Chang. Res. 9, 243–252. https://doi.org/10.1016/j.accre.2018.12.003

2. LITERATURE REVIEW

2.1. R1 – Offshore Primary Processing of CO_2-Rich Natural gas

In 2015, members of the United Nations adopted the Sustainable Development Goals (SDGs) established in the 2030 Agenda for Sustainable Development (United Nations, 2015). The agenda, including SDGs, comprehends a global action plan for social inclusion, environmental sustainability and economic development. The IPIECA, a nonprofit association that promotes the continuous improvement in the O&G sector, published an Atlas (IPIECA, 2017) that lists the positive and negative impacts of this industry within the SDGs. This Atlas also shows initiatives of the sector to contribute to achieving each SDGs. Among several actions, two of them are related to the research line R1 developed in this thesis. Regarding the SDG 7 (affordable and clean energy) the atlas suggests: "*7. By 2030, double the global rate of improvement in energy efficiency; 7.a By 2030, enhance international cooperation to facilitate access to clean energy research and technology, including renewable energy, energy efficiency and advanced and cleaner fossil-fuel technology, and promote investment in energy infrastructure and clean energy technology* (IPIECA, 2017, p. 37).

According to IOGP (2019), 71% of the CO_2 emissions (excluded methane) of the O&G sector are related to internal energy production. In 2011, extraction and transformation of hydrocarbons consumed 6.9% of the energy produced from themselves (IPIECA, 2017) and 3% to 4% of the global TPES (Masnadi et al., 2018). Based on these facts, the IPIECA highlights the importance of improving energy efficiency of O&G production operations, as an alternative to mitigate energy scarcity and GHG emissions worldwide. In this direction, oil companies have worked along the last decades to reduce their flaring, venting and fugitive emissions. Further efforts are needed to reduce energy losses and increase energy efficiency.

2.1.1. Energy and Carbon Intensity of Oil & Gas Production

The oil industry targets to profit from the exploration, production and delivery of energy-carrying substances separated from crude oil – the "energy target" – and supply the net energy produced to society. To discover, extract, process, transport and refine oil into products consumes a large fraction of the energy available in the primary source. Meeting the "energy target”, it is important to measure the energy productivity along the energy supply chain. Amongst many proposed energy return ratios (ERR), energy return on investment (EROI) and net energy ratio (NER) are commonly used to give assessing productivity of energy supply chain. The ERR is sensitive to the primary energy source characteristics. In the O&G industry, relevant characteristics, among others, are GOR, water to oil ratio (WOR), oil density (e.g. °API) and water depth, demanding a bottom-up engineering-based analysis of oilfield operations (Brandt et al., 2015).

Brandt et al. (2015) performed a bottom-up analysis of 40 oil fields around the world. The study employed 3 types of NER: NER_{oil}, NER_{tot} and $NER_{tot,flare}$. The first considers only the energy consumed by oil-related operations; the second includes NG, condensates and internal electricity production operations; and the last includes gas flaring. The production-weighted mean NER_{tot} for all fields is 32.5 MJ/MJ and varied within the range of 10–35 MJ/MJ, excluding fields using thermal EOR. Fig 2.1 shows the regional variation of NERs.

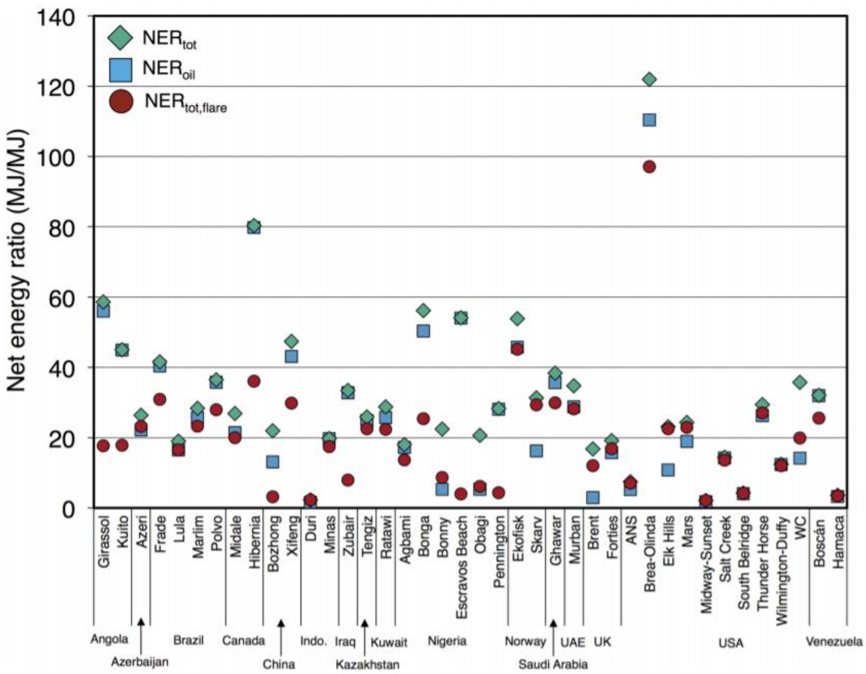

Figure 2.1. Net energy ratio (NER_{tot} and NER_{oil}) of oilfields. Source: Brandt et al. (2015).

From Fig 2.1 it can be noticed that the pre-salt Lula field has a lower NER_{tot} compared to the other Brazilian fields (Marlim, Polvo and Frade). Pre-salt has an exceptionally large GOR and exhibts CO_2-rich associated NG. Additionally, flaring or venting NG or CO_2 is prohibited by local regulations, to mitigate GHG emissions. Consequently, the current pre-salt O&G operation is to separate CO_2 from CO_2-rich NG, compress the CO_2-rich streams and used as

EOR fluid. The pre-treated NG is compressed and transported to onshore processing facilities. The primary conditioning of the CO_2-rich NG reduces the ERRs of the pre-salt oilfields. When flaring is included, many fields present expressively lower NERs. Table 2.1 shows the influence of oilfield characteristics separated by groups. Fields with high WOR and depth presented lower NER_{tot} because of the energy required by lifting; heavy and ultra-heavy oil have even lower NERs, due to the use of thermal recovery; and the thermal recovery sub-group presented the lowest NER_{tot}. (Brandt et al., 2015).

Table 2.1. Total Net Energy Ratio of oilfields. Adapted from Brandt et al. (2015)

	Nº of Fields	Production-Weighted Mean
All fields	40	32.5
High WOR (> 10 bbl water/bbl oil)	6	12.3
Deep (10000ft < depth <15,000ft)	12	29.7
Ultra-deep (depth >15,000ft)	3	22.3
Old (> 40 years old fields)	15	35.9
Heavy oil (15º < API gravity < 22.5º)	10	17.7
Ultra-Heavy oil (API gravity < 15°API)	3	10.6
Thermal EOR	3	2.8

Masnadi et al. (2018) developed and applied a methodology to determine the carbon intensity and well-to-refinery life cycle emissions of 8966 oil fields in 90 countries (98% of oil and condensate production in 2015). The study accounts for GHG emissions of main upstream activities (exploration, drilling and development, production and extraction, surface processing, and transport to the refinery inlet). The summary of this study is illustrated in Fig. 2.2. Given the impossibility of sudden cut on the global oil and gas consumption – unforeseen pandemic crisis of 2020[1], Masnadi et al. (2018) highlighted three main strategies to reduce the carbon intensity of the upstream activities: resource management, resource prioritization, and innovative technologies. The last one is explored through the research line R1 of this thesis, taking the CO_2-rich fields of Pre-salt as a scenario.

[1]In the 2020 pandemic, oil and gas suffered a suden cut.

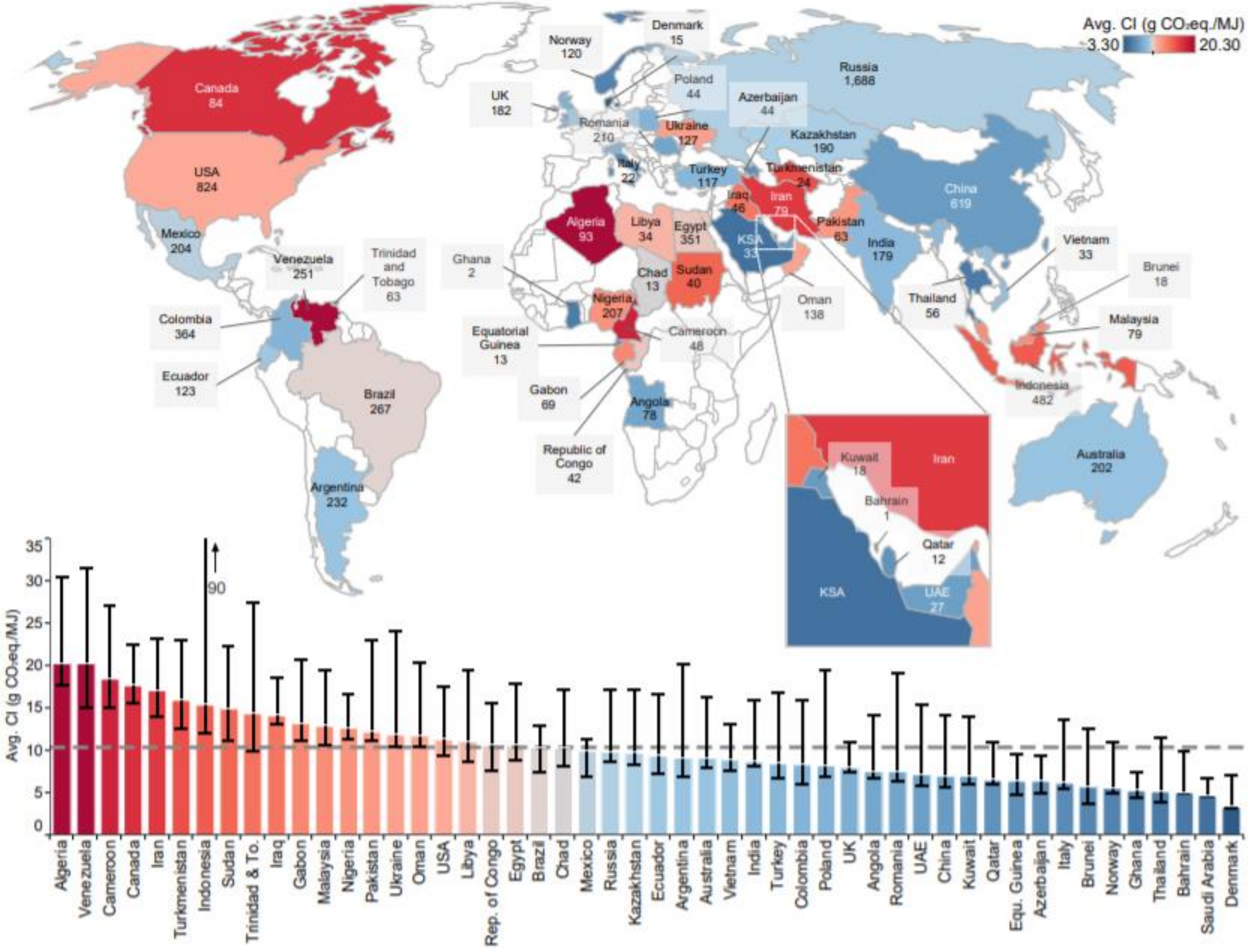

Figure 2.2. Global upstream crude oil carbon intensity (2015). (Masnadi et al., 2018)

2.1.2. CO_2-rich fields implication on FPSO design and energy intensity

The Pre-salt region holds the largest Brazilian oil fields. The fields are located between 150km – 300km far from the coast and the water depth ranges around 1500m – 3000m (ultra-deep waters). The total proven reserves of Petrobras reached 9590 MMboe in 2019. This data did not take into account the giant field of Búzios with reserves estimated in 10000 MMboe). (Petrobras, 2020) In January of 2020, the Pre-salt production reached 2150 MMbbl/d of oil and 84572 MMSm^3/d of NG, totalizing 2682 MMboe/d. This production corresponded to 66.4% of the Brazilian production of oil and gas (ANP, 2020).

Because of the high GOR and CO_2 content found in pre-salt reservoirs, to produce oil a massive flow rate of CO_2-rich gas must be separated and treated, enabling injection of the CO_2-rich stream (EOR) and export of the surplus of pre-treated NG. These constraints impose unusual state-of-the-art production practices like strict control of water dew point (WDP, < 1ppm) and hydrocarbon dew point (HCDP, < 1000ppm); CO_2 separation to achieve a concentration < 3% on NG, and compression to high pressures (25000kPa to 55000kPa). These features demanded new technologies and improvements in the FPSO design and raised the energy demand, carbon intensity and topside equipment weight and cost to unprecedented levels. (Araújo et al., 2017a)

Amongst several advantages, FPSOs are the preferred alternative for remote fields because of its high oil storage capacity and wide deck area to support topside facilities. The largest FPSOs are converted from very large crude carriers (VLCC). These converted FPSOs usually produce up to 180000 bbl/d of oil and processes up to 11 MMSm^3/d of gas with topsides weighing up to 35000t (MODEC, 2019). However, the oil and gas industry demands, especially from pre-salt operators, keep increasing in terms of larger and heavier topsides; greater oil storage and gas processing capacity, accommodations space and extended lifetime (NS Energy, 2019). The increased complexity of primary processing operations also increased the cost of the FPSOs, penalizing offshore production projects. Therefore, the main FPSO suppliers were forced to replace VLCCs for improved and larger hulls.

Concerning market competitivity, Engineering, Procurement, Construction and Installation (EPCI) companies developed new standardized hulls and topside modules. Standardizing resulted on savings in the supply chain and construction phases shortening the delivery time and investment cost of the FPSO (SBM Offshore, 2019), provided financial gains from the earlier start of operations, greater safety and quality.

MODEC (2019) launched the M350 hull, addressing shipbuilding standards:

- Dimensions: 350 m long, 64 m wide, 33 m molded depth;
- Total oil storage capacity of 350000 m³ (2.2 MMbbl);
- 20% larger deck area for topsides, compared to a VLCC, supporting up to 50,000t;
- Increased safety and lifetime of 25 years due to double hull (double sides and double bottom walls);
- Accomodation for 160 workers, and helicopter parking.

MODEC recently signed a sales and purchase agreement to supply the largest FPSO ever delivered to Brazil, Fig. 2.3. The FPSO will be the second application of the M350 hull. This vessel will be deployed at Bacalhau, Block BM-S-8, in the Brazilian pre-salt., with capacity of oil 220,000 bbl oil/d, 2,000,000 bbl of storage capacity and gas processing plant capacity of 15 MMSm³/d, almost threefold higher than the average capacity of an FPSO converted from VLCC (MODEC, 2020).

Figure 2.3. Preliminary Layout of FPSO "Bacalhau" (MODEC, 2020).

Following the same strategy of MODEC, SBM launched the FAST4WARD standardized design (SBM Offshore, 2019), shown in Fig. 2.4, with the following features:

- New-built hull designed for a 30-year lifetime and oil storage capacity of up to 2.3 MMbbl.

- 13% larger deck space compared to a VLCC, with 30% more topside footprint, accommodating up to 50,000t.

Figure 2.4. SBM FAST4WARD FPSO (SBM Offshore, 2019).

Although the new hull designs provide more space and weight to accommodate topside equipment, the extra energy expended to treat extremely high flow rates of CO_2-rich associated gas remains an environmental challenge. For layout simplification and footprint saving, most FPSOs use simple gas turbines to generate power and heat. This generation scheme has low-efficiency and contributes to increasing the carbon intensity of O&G production. Another villain of offshore production sustainability is the use of oversized compressors to match design gas-loads. Most of the time, the gas processing plant operates at partial load and much energy is wasted in anti-surge recycle loops, especially under reduced gas production. A more specific literature review, regarding the investigated technologies to reduce the energy and carbon intensity of the primary processing of CO_2-rich NG is presented in chapters 3 and 4.

2.2. R2 – Desulfurization of Flue-Gases from Coal-Fired Power Plants

2.2.1. Coal-Fired Power Plants

Coal-fired power plants supplied 41% of the electricity demand worldwide in 2016 (WCA, 2017). In the last 20 years, Asia was responsible for 90% of the increase in the global coal-fired capacity. These power plants have an average of 12 years of operation and potentially longer operational lifetime ahead (IEA, 2019b). Coal is responsible for around 25% of the global TPES, but, in some developing nations, coal share is considerably higher, e.g. > 60% in China

(IEA, 2020). Besides GHG (e.g. CO_2 and N_2O), combustion of fossil fuels releases SO_2, NO_X, CO, particulate matter (PM), heavy metals, halide compounds, and dioxins into the atmosphere. SO_2 is formed if sulfur is present in the fuel.

Treated NG is often free of sulfur, coal has a significant content of this element (European Commission, 2006). SO_2 emissions cause detrimental impacts on the environment and to human health. Exposure to high concentrations of SO_2 is linked to respiratory and cardiovascular diseases. SO_2 also leads to acid deposition in the environment and consequent acidification of water bodies and damage to natural vegetation, crops, buildings and monuments (Srivastava and Jozewicz, 2001).

In the face of these impacts, most countries adopted strict limits on SO_2 emissions from power plants. The United States launched initiatives like the Clean Air Act Amendments (CAAA), which includes the Acid Rain SO_2 Reduction Program, focused on reducing SO_2 emissions from thermal power stations (Srivastava and Jozewicz, 2001). To comply with the SO_2 emissions limit, besides using low-sulfur fuel, FGD is necessary. In the European Union, the use of FGD technologies is mandatory for plants with more than 100 MW of capacity. SO_2 emissions limit and recommended FGD technologies are shown in Fig. 2.5 (European Commission, 2006).

Capacity (MW_{th})	SO_2 emission level (mg/Nm^3)						BAT to reach these levels
	Coal and lignite		Peat		Liquid fuels for boilers		
	New plants	Existing plants	New plants	Existing plants	New plants	Existing plants	
50 – 100	200 – 400* 150 – 400* (FBC)	200 – 400* 150 – 400* (FBC)	200 – 300	200 – 300	100 – 350*	100 – 350*	Low sulphur fuel or/and FGD (dsi) or FGD (sds) or FGD (wet) (depending on the plant size). Seawater scrubbing. Combined techniques for the reduction of NO_x and SO_2. Limestone injection (FBC).
100 – 300	100 – 200	100 – 250*	200 – 300 150 – 250 (FBC)	200 – 300 150 -300 (FBC)	100 – 200*	100 – 250*	
>300	20 – 150* 100 – 200 (CFBC/ PFBC)	20 – 200* 100 – 200* (CFBC/ PFBC)	50 – 150 50 – 200 (FBC)	50 – 200	50 – 150*	50 – 200*	

Notes:
FBC: Fluidised bed combustion
CFBC: Circulating fluidised bed combustion
PFBC: Pressurised fluidised bed combustion
FGD(wet): Wet flue-gas desulphurisation
FGD(sds): Flue-gas desulphurisation by using a spray dryer
FGD(dsi): Flue-gas desulphurisation by dry sorbent injection
* Some split views appeared in these values and are reported in Sections 4.5.8 and 6.5.3.3 of the main document.

Figure 2.5. European Union SO_2 emissions limit and recommended technologies (European Commission, 2006).

2.2.2. Flue-gas Desulfurization Systems

Srivastava and Jozewicz (2001) classified the FGD technologies according to the sorbent destination after reacts with SO_2, as shown in Fig 2.6. Once-through systems consider spent sorbent as waste or byproduct. Regenerable processes have an additional step to remove SO_2 from the spent sorbent. Usually, SO_2 is used to produce sulfuric acid or sulfur.

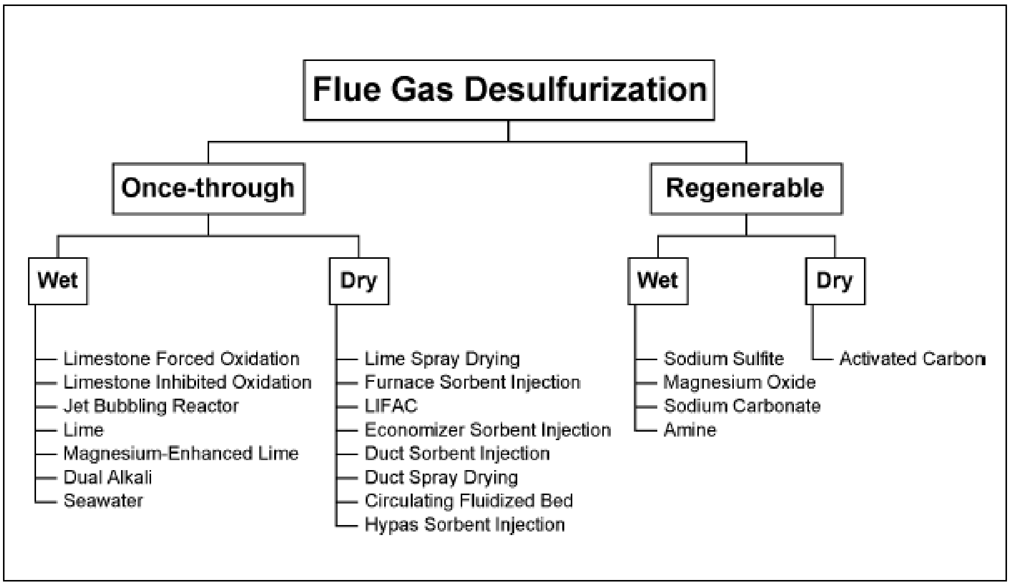

Figure 2.6. Classification of FGD technologies(Srivastava and Jozewicz, 2001).

The Best Available Technologies (BAT) for desulfurization are wet and spray dry scrubbing, with a market share of more than 90%. Wet-FGD has SO_2 removal rate of 92 – 98 % while spray dry scrubber (a SD-FGD technology) has a slightly lower reduction rate of 85 – 92 % (European Commission, 2006). The selection of the FGD technology must consider several factors like power plant capacity, sulfur content of the fuel, capital expenditure (CAPEX), operational expenditure (OPEX), and space availability, sorbent material and water (Ma et al., 2000). In general, SD-FGD is adopted for power plants with less than 300 MW of thermal capacity. Wet-FGD is not considered for plants with less than 100 MW of capacity, due to economic unfeasibility (European Commission, 2006).

The wet-FGD, shown in Fig. 2.7, is the most widely used FGD process, holding more than 80% of the market share. It has a higher performance and lower cost compared to other available technologies. However, its specific water consumption is higher, reaching 250 l/MWh in a subcritical plant. (Carpenter, 2012) Regarding the solid byproducts, the wet-FGD has the advantage to form gypsum ($CaSO_4$), which has several industrial applications.

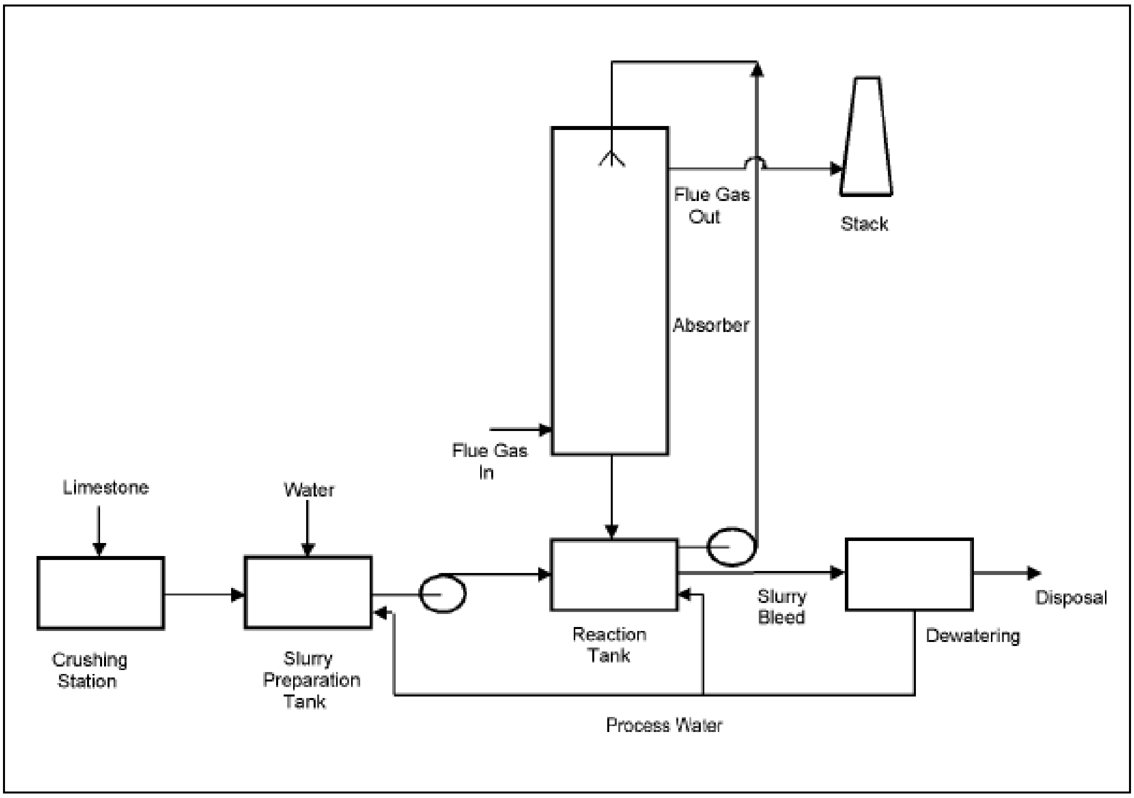

Figure 2.7. Wet FGD Process (Srivastava and Jozewicz, 2001).

Eq. 2.2.1 is the overall reaction of the wet-FGD system, occurring in 4 steps (Eqs. 2.2.1a to 2.2.1e).

$$SO_2 + CaCO_3 + 0.5O_2 + 2H_2O \quad CaSO_4.2H_2O + CO_2 \qquad (2.2.1)$$

SO_2 Absorption:

$$SO_2 + H_2O \leftrightarrow H_2SO_3 \qquad (2.2.1a)$$

$$H_2SO_3 \leftrightarrow H^+ + HSO_3^- \qquad (2.2.1b)$$

Limestone dissolution:

$$CaCO_3 + H_2O \leftrightarrow Ca^{++} + HCO_3^- + OH^- \qquad (2.2.1c)$$

Oxidation:

$$HSO_3^- + O_2 \leftrightarrow H^+ + SO_4^= \qquad (2.2.1d)$$

Precipitation:

$Ca^{++} + SO_4^{=} + 2H_2O \leftrightarrow CaSO_4.2H_2O$ (2.2.1e)

SD-FGD is usually applicable for small to medium-sized power plants (Dehghani and Bridjanian, 2010). This technology, illustrated in Fig. 2.8, trades off efficiency, water use and cost (Sage and Ford, 1996).

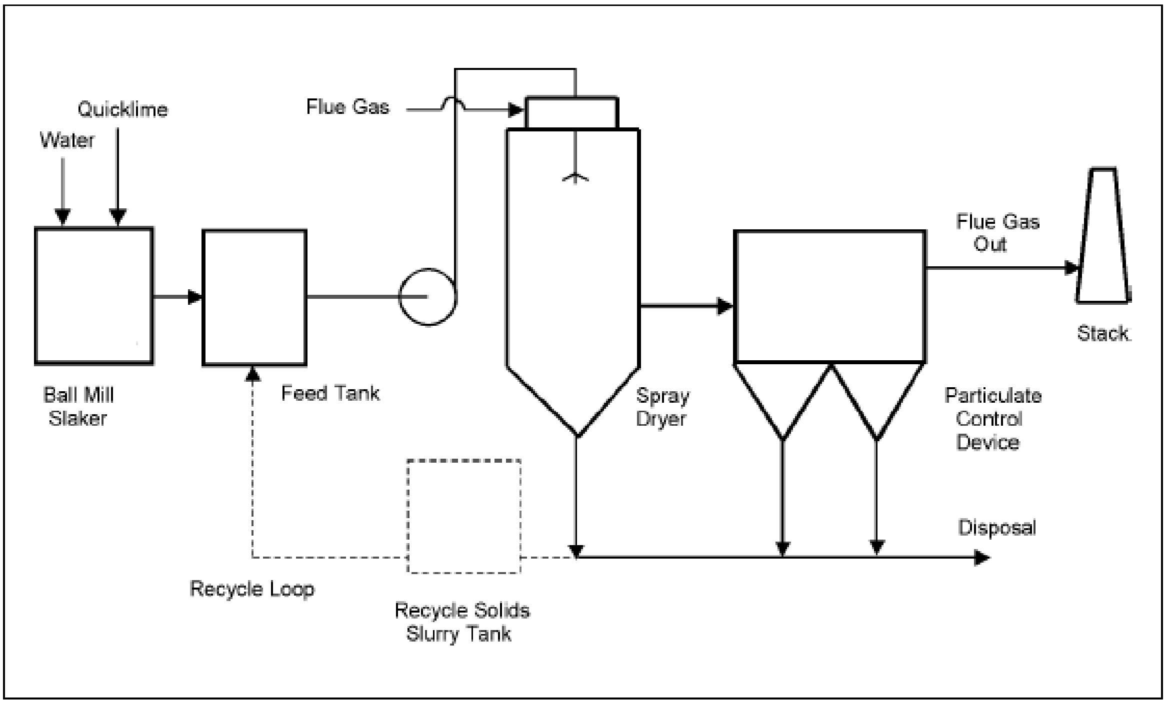

Figure 2.8. Semi-dry FGD Process (Srivastava and Jozewicz, 2001).

The water demand of SD-FGD is 60% lower compared to the humid route. This characteristic makes the semi-dry alternative more attractive in regions under water scarcity, such as the Northeast of Brazil and the Western of the USA. The semi-dry technology installed capacity ranks second worldwide, corresponding to approximately 15% of market share (Carpenter, 2012). However, the application of SD-FGD is limited to low sulfur coal (0% to 3%) (Funch-Jensen and Rubner-Petersen, 2007)

Usually, SD-FGD units have spray dryer vessels where the hot flue-gas contacts a mist of atomized fresh lime slurry (Hill and Zank, 2000). Simultaneous heat and mass transfers remove SO_2 from the flue-gas, according to the Eq. 2.2.2a, and dry the products. The final product is a powder, named desulfurization residue (Dehghani and Bridjanian, 2010).

$SO_2 + Ca(OH)_2 \rightarrow CaSO_3.1/2H_2O + 1/2\ H_2O$ (2.2.2a)

Because the reaction occurs in an atmosphere poor in oxygen and water, instead of forming gypsum, calcium sulfite ($CaSO_3$) predominates. Just a small fraction of calcium sulfite should be oxidized to gypsum, according to the Eq. 2.2.2b.

$$CaSO_3.1/2\ H_2O + 1/2\ O_2 + 3/2\ H_2O \rightarrow CaSO_4.2H_2O \qquad (2.2.2b)$$

Research line R2 develops a technology for utilization of desulfurization residue targeting its use in the cement industry.

2.3. R3 – CO_2 Capture from Flue-Gases by Phase-Changing Solvents

2.3.1. Greenhouse Gases Emissions from Fossil Energy

From 2010 to 2017, the energy sector (electricity, heat generation and transport) accounted for more than two-thirds of total anthropogenic carbon dioxide emissions. The other third was caused by industry and building consumption (IEA, 2019a).

The Global Carbon Budget 2019 (Friedlingstein and Al, 2019) estimates that, from 1850 and 2018, 645 Gt of carbon (GtC) were emitted by human activities. Fossil fuels contributed with almost 66% of these emissions, as depicted in Fig 2.9. In 2018, the GHG emissions from fossil-fueled energy reached 10 GtC/y (Friedlingstein and Al, 2019). The environmental impact of electricity and heat consumption depends on the energy source. Developed countries' share of clean energy from renewable sources (e.g. wind and solar) are increasing lately. However, developing countries, especially China, are still dependent on fossil and low-efficient energy production. The result of such disparity is shown in Fig. 2.10.

CO_2 emissions reached 32.8 billion tons in 2017, increasing after three years of stability. In 2018, the increase accelerated due to global economic growth and a slower pace of penetration of renewables (IEA, 2019a). Atmospheric carbon dioxide concentration reached 411 ppm in December of 2019 (NOAA, 2020), and is currently 40% higher than in the pre-industrial era.

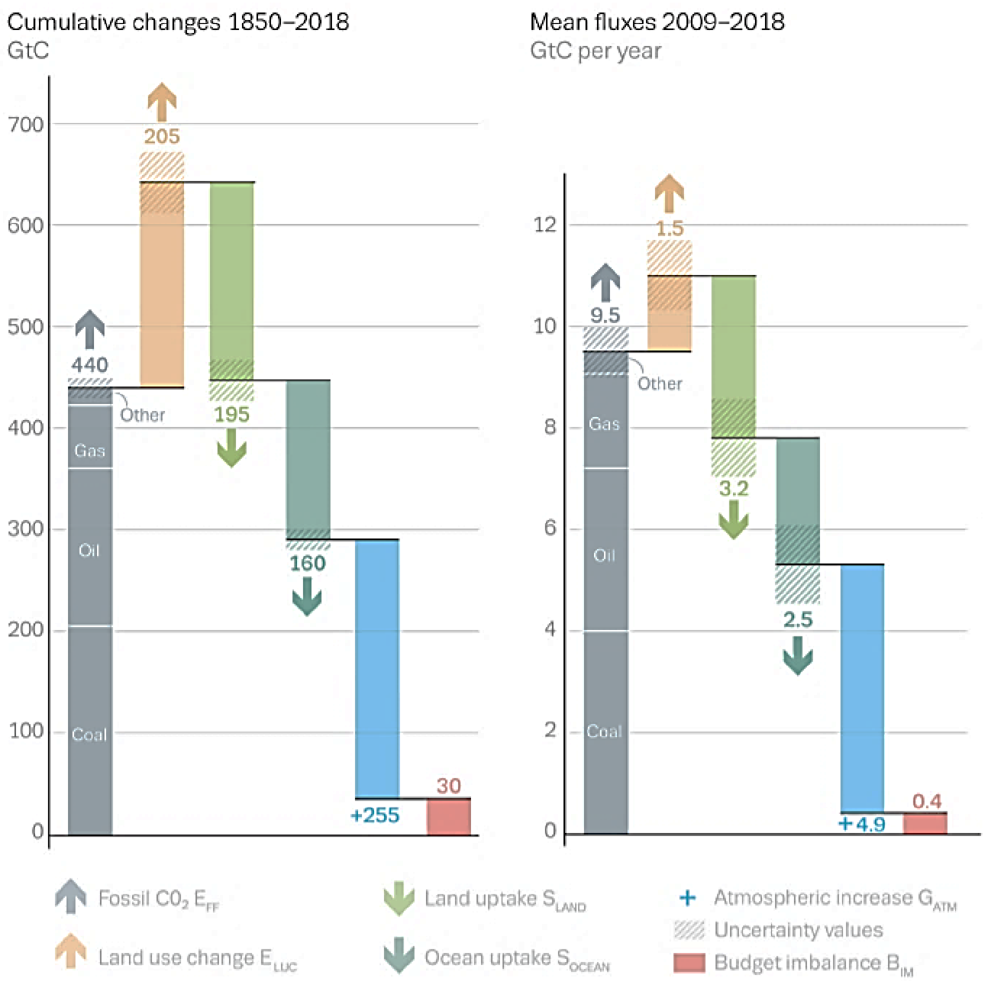

Figure 2.9. Anthropogenic Carbon Flows (Friedlingstein and Al, 2019).

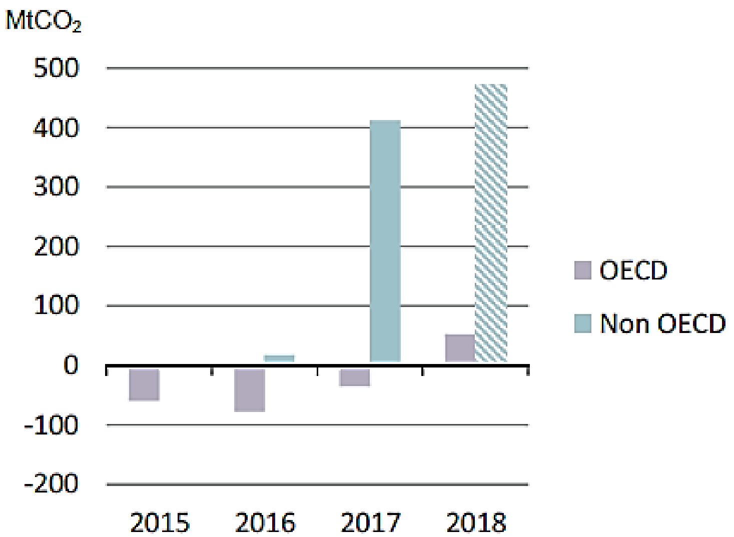

Figure 2.10. Annual Changes in CO_2 Emissions for OECD and Non-OECD countries (IEA, 2019a).

In 2015, the Paris Agreement established targets of maximum temperature increase of 1.5ºC to 2ºC until the end of the century, compared to the pre-industrial era (UNFCCC, 2016). These targets resulted in a "*carbon budget*", which refers to the amount of carbon that could be released until 2100 given the considered temperature target. According to IPCC (2014), the *carbon budget* is around 2900 $GtCO_{2e}$ and 65% of this budget was already consumed by 2011, and the proven fossil fuel reserves exceed the carbon budget by 3 to 6 times. For a 1.5ºC target, 200 $GtCO_{2e}$ could be released to the atmosphere; hence, the current GHG emissions rate should be halved until 2040, despite the global energy demand being expected to increase by 30% to 75% in this period. Clearly, a fast transition from current carbon-intensive energy to a low carbon system (zero or negative emissions) is required (Copenhagen Economics, 2017).

Increased energy efficiency is essential for a quick, feasible and less economically damaging transition (IEA, 2018b). However, most of the current conventional energy production systems are optimized from the process perspective. Opportunities for feasible energy efficiency increase are scarce. Renewable energy sources are claimed to be the ultimate solution to global warming, and its share has been growing worldwide, especially in the European Union. Despite the great environmental advantages, currently, a 100% renewable grid is technically unfeasible. Not to mention the economic issues, the inherent intermittency of wind and solar energies and low energy storage capacity are technical hindrances to renewables' growth. Thus, fossil fuels are expected to remain in the global energy matrix in the mid-term and CCUS is required to achieve negligible or negative emission, as required to meet Paris Agreement goals. (Global CCS Institute, 2019)

2.3.2. Post-Combustion Carbon Capture by Chemical Absorption

The International Energy Agency considers retrofit with CCUS as one of three options to cut GHG emissions from the current 2080 GW of coal-fired installed power capacity. The other options are retrofit with biomass co-firing equipment or prematurely retire coal-based power systems (IEA, 2019b), being these two alternatives more challenging technically and harmful economically. Over the last 20 years, CCUS has evolved from an option to a necessity to mitigate climate change (Global CCS Institute, 2019).

Much of the useful energy (heat and power) production is centralized in thermal power plants, where fossil-fuel combustion produces gases – flue-gases, with contaminants, including CO_2. The flue-gases are treated and emitted to the atmosphere through chimneys. Flue-gases from power plants usually have low pressure (< 150 kPa) and moderate temperature (50ºC – 100ºC). Post-combustion carbon capture technologies aim at mitigating CO_2 emissions from flue-gases before discharging it into the atmosphere. Chemical or physical absorption are the technologies closest to full-scale availability, favoring retrofitting (Araújo and de Medeiros, 2017). However, there are emerging separation technologies, e.g. membrane contactors (de Medeiros et al., 2013; Liu et al., 2020), electrochemical membranes (Tong et al., 2015), or hybrid systems (Frimpong et al., 2019).

Gas-liquid absorption is a preferred choice for post-combustion CO_2 capture because reactive solvents efficiently separate highly diluted CO_2 from flue-gases (Budzianowski, 2016). One of the most recognized and well-established technology for post-combustion carbon capture is chemical absorption with aqueous alkanolamines solutions. Primary, secondary, tertiary and hindered alkanolamines are used in Acid Gas-Water-Amine (AGWA) systems, commonly: monoethanolamine (MEA), diethanolamine (DEA), methyldiethanolamine (MDEA), and 2-amino-2-methylpropanol (AMP), respectively. (de Medeiros, Barbosa and Araújo, 2013)

Modeling of AGWA systems is complex and computationally demanding. The models must deal with nonequilibrium ionic chemical reactions, and heat/mass transfers across vapor-liquid interfaces. Frequently, the necessary physical properties are unavailable and the ions generated by weak dissociations are unknown. High pressures, concentrations, and loadings, make the use of idealities, such as ideal law for gas, inaccurate (de Medeiros, Barbosa and Araújo, 2013) These issues must be circumvented using the methodology of de Medeiros, Barbosa and Araújo (2013), which incorporates molecular species into a chemical equilibrium theory framework using cubic equations of state.

One of the first processes for removing acid gases (CO_2 and H_2S) from NG with MEA was proposed and patented by Bottoms (1930). This process, shown in Fig. 2.10, is also useful to remove CO_2 from flue-gases.

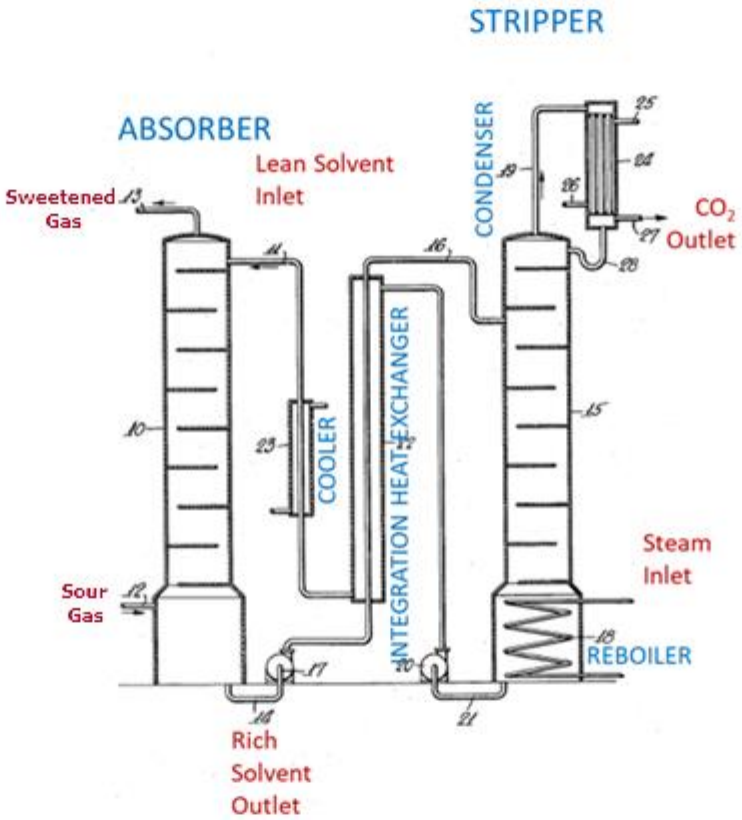

Figure 2.10. Gas-Sweetening Process using Monoethanolamine. Adapted from Bottoms (1930)

The main drawback of the chemical absorption processes using solvents in a closed loop, as in Fig. 2.10, is the energy penalty for solvent regeneration. This penalty is pointed out as the major obstacle to the widespread deployment of full-scale applications of carbon capture by reactive absorption, especially in coal and NG power plants (Boot-Handford et al., 2014). The energy penalty is defined as the energy spent to capture a certain amount of CO_2 from a process stream, usually expressed as GJ/t of CO_2 removed. According to Knudsen et al. (2009), the use of steam from the Rankine cycle to regenerate the solvent at the stripper column consumes between 3.6 and 3.8 GJ/t of CO_2 captured. Carbon Capture and Storage (CCS) can increase approximately 70% the life cycle cost (LCC) of fossil-fueled electricity and cement and, similarly 40% of steel LCC (Zhang et al., 2013). The Bottom's process can no longer be considered the benchmark for CO_2 capture but most of the chemical absorption technologies are based on this concept. Reduced CO_2 loading (kgCO_2/kg of solvent), thermal and oxidative degradation, corrosivity and evaporation losses are often reported as other weaknesses of traditional solvents for CO_2 capture.

In coal-fired power plants, there is a linear relationship between regeneration energy and the overall efficiency of the electricity generation. It is estimated that each GJ/t of CO_2 translates into a 2% decrease in the heat ratio or global efficiency of the plant. Considering thermal plants with efficiency between 40% and 60%, an energy penalty of 5% causes an increase of approximately 10% in fuel consumption. The resulting impact on the electricity price is considerable (Goto, Yogo and Higashii, 2013). More precise quantification of the effect of retrofitting a 500MW Pulverized Coal Combustion plant was performed in the present research using the software IECM v 11 (Rubin, 2018) shows that adding CCS with MEA increased the LCOE by 115% (from 61 $/MWh to 131 $/MWh). The regeneration consumption is 180 MW. Considering a NG combined cycle (NGCC) with the same nominal capacity, the LCOE increased 52% (from 66 $/MWh to 100 $/MWh), with a consumption of 72 MW from the solvent regeneration system. In both cases, most of the CCS energy penalty came from the reboiler consumption of steam, in the solvent regeneration column, as shown in Fig. 2.11.

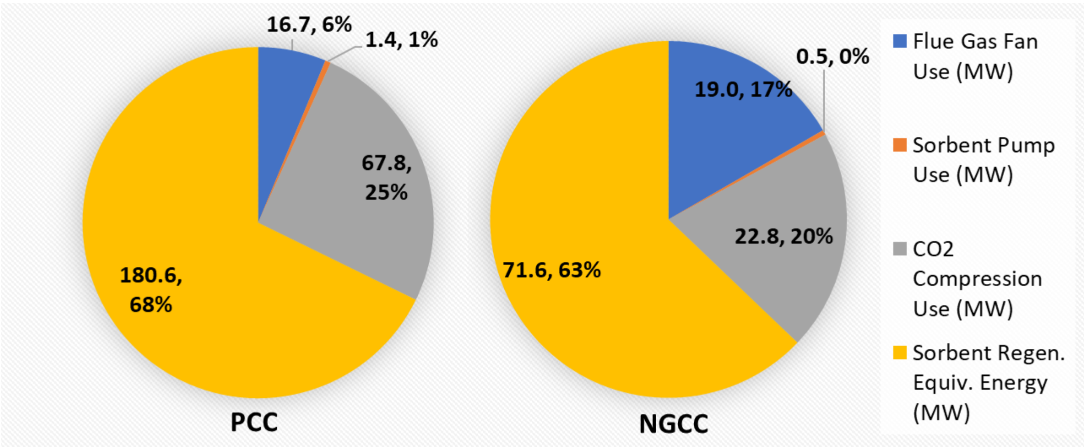

Figure 2.11. CCS energy penalty of Pulverized Coal Combustion and Natural Gas Combined Cycle. Data obtained by the author from simulations using the software IECM v 11 (Rubin, 2018).

These preliminary results motivated the R3 research line, and other developments of solvents and process designs to lower regeneration energy requirements, e.g.: advanced solvents (Goto, Yogo and Higashii, 2013); inter-stage cooling and heating in the absorber and regenerating columns, respectively (Frailie et al., 2013); energy integrations; exhaust gas recycling (Li et al., 2011), among other improvements (Park et al., 2016; Rezazadeh et al., 2017; Sachde; Rochelle, 2014; Zhang; Rochelle, 2014). Industries from the chemical and energy sectors developed solvents and processes that reduced the energy penalty for regeneration by up to 43%, compared to the classic benchmark (MEA 30% - 3.7 GJ/tCO_2), as shown in Table 2.2. Mitsubishi Heavy Industries owns one of the most modern and mature processes, the KM CDR (Kansai Mitsubishi Carbon Dioxide Recovery Process), in pilot and industrial scale in several applications, as shown in Figure 2.12. The Petra Nova joint venture adopted de KM-CDR and is currently the world's largest CCS plant. This plant has capacity to capture 4776 t/d of CO_2, with EOR injection 130 km apart. This capture flow ratio is equivalent to the flue-gas production of a 240 MW power plant (Miyamoto et al., 2017).

Table 2.2. Commercially available chemical absorption CCS technologies.

Process	Company	Solvent	Energy Penalty	Reference
Cansolv	Shell Royal Dutch	DC-103	2.33 GJ/t CO_2	Singh and Stéphenne (2014)
KM CDR	Mitsubishi Heavy	KS-1	2.29 GJ/t CO_2	Kadono et al. (2013)
Process	Industry	KS-2	2.11 GJ/t CO_2	Miyamoto et al. (2017)
Econamine FG+	Fluor Corporation	Amine-Based	3.00* GJ/t CO_2	Mathias, Reddy and O'Connell (2009)

*3.00 GJ/t of steam for reboiler + 2.75 GJ/t for NH_3 refrigeration (gas compression cycle).

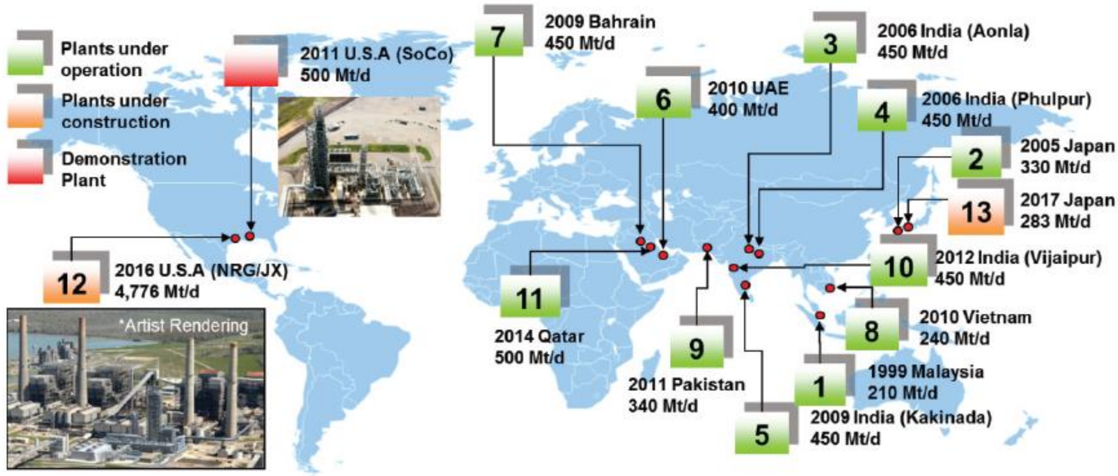

Figure 2.12. KM-CDR applications worldwide (Miyamoto et al., 2017).

Current conventional chemical absorption processes are highly optimized in terms of layout and energy integration. Process design improvement opportunities are scarce. Developments on new solvents, like PCAS, aims at reducing the inherent energy penalty of chemical absorption processes. Such solvents would contribute to the faster deployment of CCUS in industrial scale worldwide, meeting sustainable development goals.

2.3.3. Phase-Changing Absorption Solvents for CO_2 Capture

PCAS are considered advanced solvents for gas-liquid CO_2 absorption. An advanced solvent has a physical or chemical characteristic that enhances the energy performance of a CO_2 capture process. Often, the energy spent with solvent regeneration, using stripping columns, is reduced. Post-combustion processes using advanced solvents could significantly reduce the decarbonization energy penalty, benefiting the energy and other carbon-intensive sectors

(Budzianowski, 2016). Fig 2.13 shows a gas-liquid absorption selection tree, where PCAS (red box, as two immiscible liquid phases) is classified as an advanced solvent. The fundamental property that differentiates a PCAS from other solvent is the formation of immiscible liquid phases triggered by temperature and/or CO_2 loading of the solvent. The energy saving results from the reduced mass of solvent sent to the stripper, considering that only one of the immiscible phases is rich in CO_2. The reboiler duty and possibly the footprint of the stripper column are reduced, resulting in CAPEX and OPEX savings (Coulier et al., 2017; Liebenthal et al., 2013).

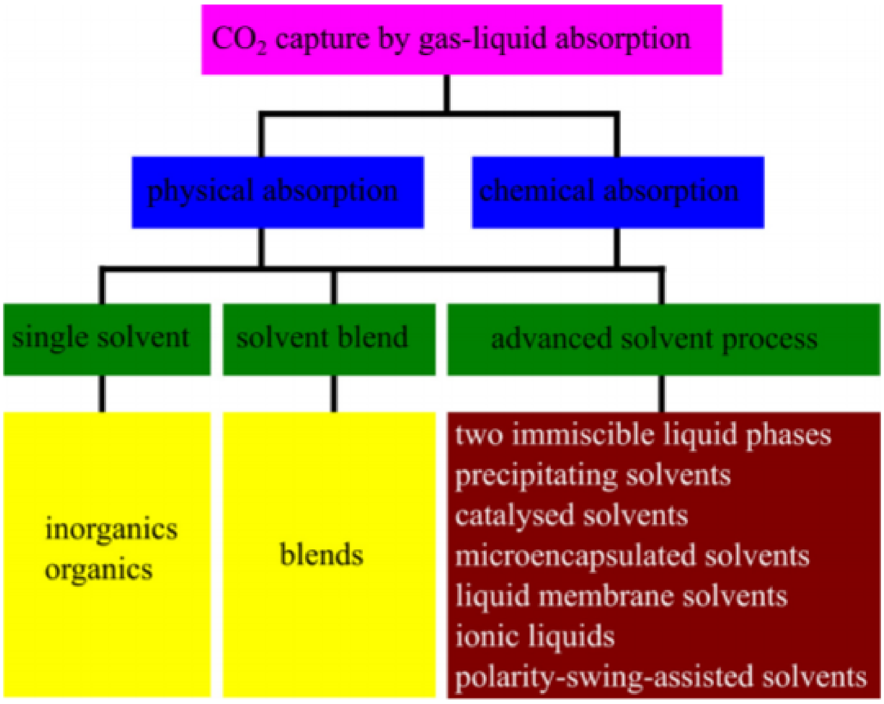

Fig 2.13. Gas-liquid absorption solvents for CO_2 capture. (Budzianowski, 2016).

Three possible scenarios of immiscible liquid phase formation are shown in Fig. 2.14, as a function of temperature. Similar behavior may occur as a function of CO_2 loading instead of temperature. Fig 2.15 illustrates a generic process of phase-split promoted by CO_2 absorption.

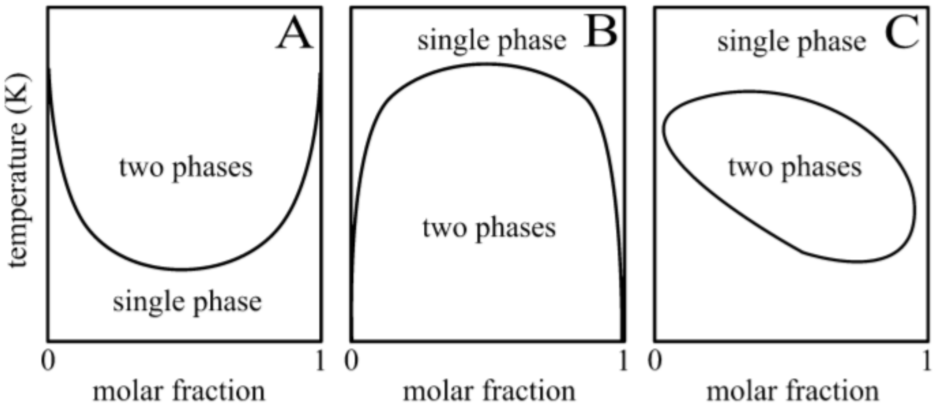

Fig 2.14. Possibilities of immiscible liquid phases formation. (A) lower critical temperature, (B) upper critical temperature, and (C) upper and lower critical temperatures (Budzianowski, 2016).

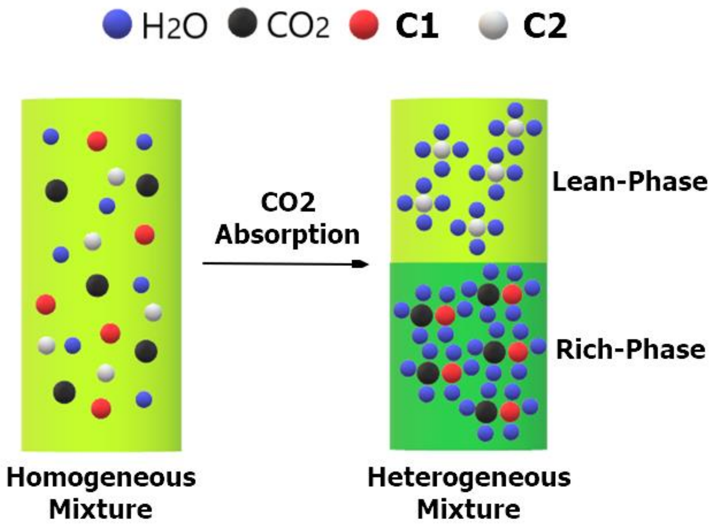

Fig 2.15. Liquid-liquid phase-split promoted by CO_2 capture.

A suitable PCAS should have the following behavior (Budzianowski, 2016):

- Operate homogeneously under scrubbing temperatures.
- Operate as a biphasic mixture (two immiscible liquid phases) under stripping temperatures or after saturation with CO_2.
- Form a CO_2-lean and a CO_2-rich phase, easily separable by gravity.
- Preferably, the volume of the CO_2-rich phase should be smaller than the volume of the lean phase.

Wang et al. (2019) estimated the regeneration energy of several PCAS. The authors considered a 300MW Pulverized Coal Combustion (PCC) power plant using CCS with MEA 30% (w/w) as the baseline. The results are depicted in Fig. 2.16. The PCAS based on triethylenetetramine (TETA) and Tetramethyl-1,3-propanediamine (TMPDA) presented regeneration energy 54% lower than the baseline. MEA/1-propanol ranked second, with a 40% reduction. These results denote the potential benefits of the full-scale application of PCAS on the energy sector. However, the results of Wang et al. (2019) are mostly based on simulation, using Aspen Plus. The lack of information concerning the simulation setup, especially the thermodynamic model calibration, poses a high degree of uncertainty in the accuracy of the energy penalty reported.

A systematic review was performed to determine the state-of-the-art on PCAS. The following group of keywords was chosen as input on Google Scholar: *(("liquid-liquid phase separation" OR "phase transition" OR "de-mixing" OR "phase change solvent" OR "biphasic solvent" OR "thermomorphic") AND ("CO2 capture" OR "CO2 absorption" OR "carbon dioxide capture" OR "carbon dioxide absorption")).* Results were limited to the years 2010 to 2019 and totaled 5.570 articles, and 56 articles were considered more relevant to in depth analysis. Most of the selected articles were published on indexed scientific journals, with high impact factors. An overview of the selected articles reveals that Chinese institutions are responsible for 43% of published papers, followed from France, with 11% of the production, as shown in Fig. 2.17.

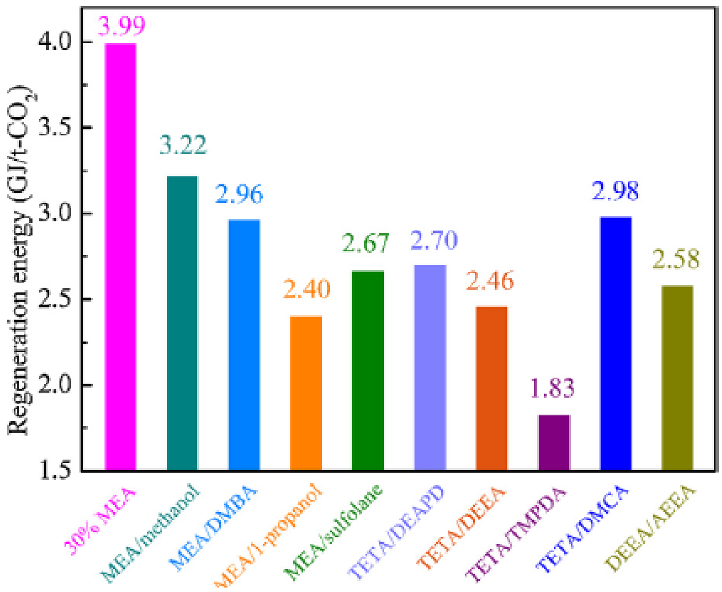

Fig 2.16. Comparison of the regeneration heat of MEA-based and other phase-changing absorption solvents (Wang et al., 2019).

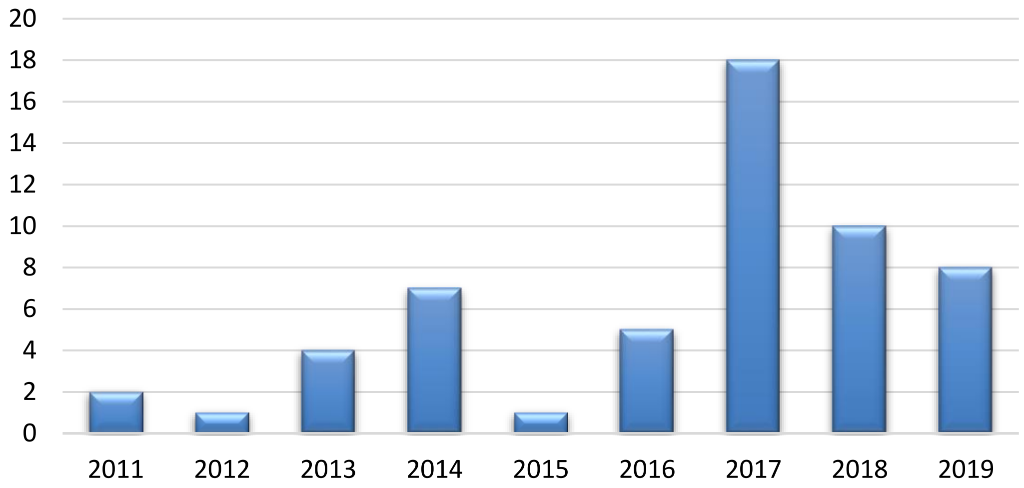

Figure 2.17. Publications on phase-changing absorption solvents from 2010 to 2019.

The review shows a peak of publications on PCAS in 2017 (18 articles) followed by 10 publications in 2018 and 8 until April 2019. Those numbers reflect the relevance and interest on the research line R3 approached in this thesis. Fig. 2.18 presents the most studied topics and chemical components found in the selected articles on PCAS. Most of the selected articles deals with liquid phases behavior and chemical composition of PCAS, and are mostly on laboratory evaluations, rarely targeting pilot plant experiments and process modeling and simulation, denoting the early stage of development on PCAS.

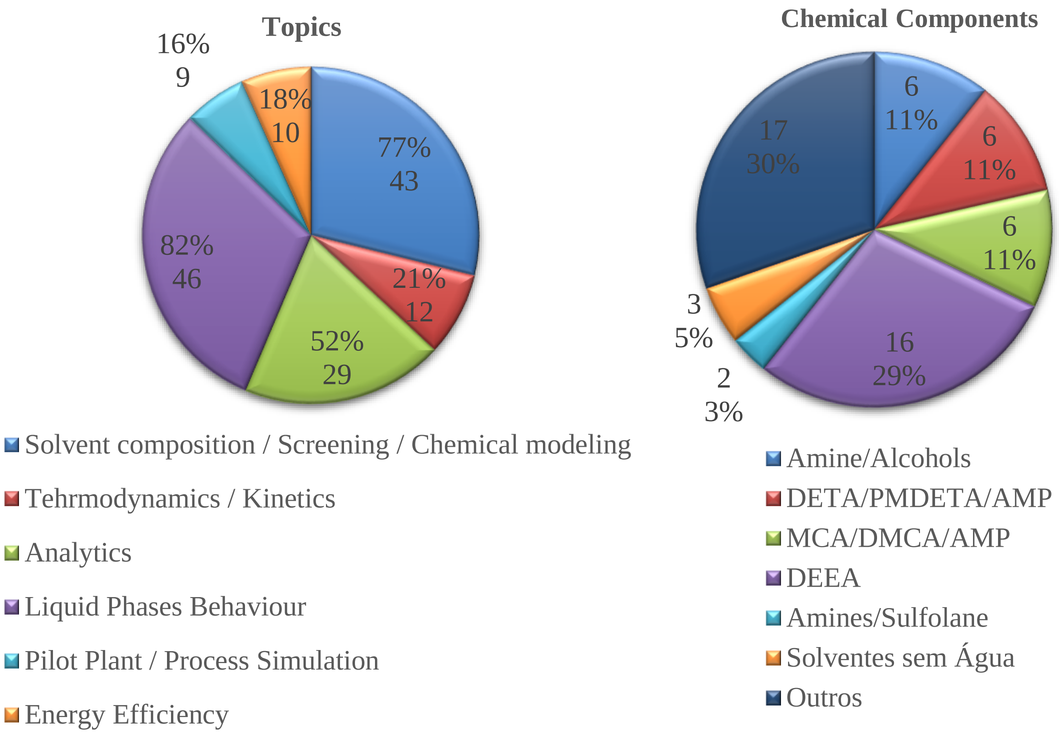

Figure 2.18. Main topics and chemical components related to phase-changing absorption solvents for CO_2 capture.

2.4. References of Chapter 2

ANP, 2020. Boletim da Produção de Petróleo e Gás Natural - Janeiro 2020 [WWW Document]. URL http://www.anp.gov.br/arquivos/publicacoes/boletins-anp/producao/2020-01-boletim.pdf (accessed 3.4.20).

Araújo, O. de Q.F., de Medeiros, J.L., 2017. Carbon capture and storage technologies: present scenario and drivers of innovation. Curr. Opin. Chem. Eng. 17, 22–34. https://doi.org/10.1016/j.coche.2017.05.004

Araújo, O. de Q.F., Reis, A. de C., de Medeiros, J.L., Nascimento, J.F. do, Grava, W.M., Musse, A.P.S., 2017. Comparative analysis of separation technologies for processing carbon dioxide rich natural gas in ultra-deepwater oil fields. J. Clean. Prod. 155, 12–22. https://doi.org/10.1016/j.jclepro.2016.06.073

Boot-Handford, M.E., Abanades, J.C., Anthony, E.J., Blunt, M.J., Brandani, S., Mac Dowell, N., Fernández, J.R., Ferrari, M.-C., Gross, R., Hallett, J.P., Haszeldine, R.S., Heptonstall, P., Lyngfelt, A., Makuch, Z., Mangano, E., Porter, R.T.J., Pourkashanian, M., Rochelle, G.T., Shah, N., Yao, J.G., Fennell, P.S., 2014. Carbon capture and storage update. Energy Environ. Sci. 7, 130–189. https://doi.org/10.1039/C3EE42350F

Bottoms, R.R., 1930. Process for separating acidic gases. US17883901A.

Brandt, A.R., Sun, Y., Bharadwaj, S., Livingston, D., Tan, E., Gordon, D., 2015. Energy Return on Investment (EROI) for Forty Global Oilfields Using a Detailed Engineering-Based Model of Oil Production. PLoS One 10, e0144141.

Budzianowski, W.M., 2016. Explorative analysis of advanced solvent processes for energy efficient carbon dioxide capture by gas–liquid absorption. Int. J. Greenh. Gas Control 49, 108–120. https://doi.org/10.1016/J.IJGGC.2016.02.028

Carpenter, A.M., 2012. Low water FGD technologies. IEA Clean Coal Center.

Copenhagen Economics, 2017. The future of fossil fuels: How to steer fossil fuels use in a transition to a low-carbon energy system. An analysis of fossil fuels trajectories in low-carbon scenarios.

Coulier, Y., Lowe, A.R., Coxam, J.-Y., Ballerat-Busserolles, K., 2017. Thermodynamic Modeling and Experimental Study of CO2 Dissolution in New Absorbents for Post-Combustion CO2 Capture Processes. ACS Sustain. Chem. Eng. acssuschemeng.7b03280. https://doi.org/10.1021/acssuschemeng.7b03280

de Medeiros, J.L., Barbosa, L.C., Araújo, O.D.Q.F., 2013a. Equilibrium approach for CO2 and H2S absorption with aqueous solutions of alkanolamines: Theory and parameter estimation. Ind. Eng. Chem. Res. 52, 9203–9226. https://doi.org/10.1021/ie302558b

de Medeiros, J.L., Nakao, A., Grava, W.M., Nascimento, J.F., Araújo, O. de Q.F., 2013b. Simulation of an offshore natural gas purification process for CO 2 removal with gas-liquid contactors employing aqueous solutions of ethanolamines. Ind. Eng. Chem. Res. 52, 7074–7089. https://doi.org/10.1021/ie302507n

Dehghani, A., Bridjanian, H., 2010. Flue Gas Desulfurization Methods To Conserve the Environment. Pet. Coal.

European Commission, 2006. Integrated Pollution Prevention and Control Reference Document on Best Available Techniques for Large Combustion Plants, Integrated Pollution Prevention and Control.

Frailie, P.T., Madan, T., Sherman, B.J., Rochelle, G.T., 2013. Energy performance of advanced stripper configurations. Energy Procedia 37, 1696–1705. https://doi.org/10.1016/j.egypro.2013.06.045

Friedlingstein, P., Al, E., 2019. Global Carbon Budget 2019. Earth Syst. Sci. Data 11, 1783–1838. https://doi.org/https://doi.org/10.5194/essd-11-1783-2019

Frimpong, R.A., Irvin, B.D., Nikolic, H., Liu, K., Figueroa, J., 2019. Integrated hybrid process for solvent-based CO2 capture using a pre-concentrating membrane: A pilot scale study. Int. J. Greenh. Gas Control 82, 204–209. https://doi.org/10.1016/J.IJGGC.2019.01.016

Funch-Jensen, A., Rubner-Petersen, M., 2007. Semi-dry scrubber technologies: Spray Drying Absorption, in: ESKOM Scrubber Seminar. World Pollution Control Association, Copenhagen, DN, p. 50.

Global CCS Institute, 2019. The Global Status of CCS: 2019, Global CCS Institute. Melbourne, Australia. https://doi.org/10.1007/springerreference_15392

Goto, K., Yogo, K., Higashii, T., 2013. A review of efficiency penalty in a coal-fired power plant with post-combustion CO2 capture. Appl. Energy 111, 710–720. https://doi.org/10.1016/J.APENERGY.2013.05.020

Hill, F.F., Zank, J., 2000. Flue gas desulphurization by spray dry absorption. Chem. Eng. Process. Process Intensif. https://doi.org/10.1016/S0255-2701(99)00077-X

IEA, 2020. Data & Statistics - IEA [WWW Document]. Int. Energy Agency. URL https://www.iea.org/data-and-statistics?country=EU28&fuel=Energy supply&indicator=Total primary energy supply (TPES) by source (accessed 1.31.20).

IEA, 2019a. CO2 emmisions from fuel combustion [WWW Document]. URL https://webstore.iea.org/download/direct/2505?fileName=CO2_Emissions_from_Fuel_Combustion_2019_Overview.pdf

IEA, 2019b. World Energy Outlook - Executive Summary [WWW Document]. Int. Energy Agency. URL www.iea.org

IEA, 2018. Perspectives for the Energy Transition: The Role of Energy Efficicency [WWW Document]. URL http://www.iea.org/publications/freepublications/publication/Perspectives for the Energy Transition - The Role of Energy Efficiency.pdf (accessed 7.2.18).

IOGP, 2019. IOGP Environmental performance indicators - 2018 data - Atmospheric emissions [WWW Document]. Int. Assoc. Oil Gas Prod. URL https://data.iogp.org/Environment/Emissions (accessed 2.4.20).

IPCC, 2014. Climate Change 2014: Synthesis Report. Contribution of Working Groups I, II and III to the Fifth Assessment Report of the Intergovernmental Panel on Climate Change, Intergovernmental Panel on Climate Change. IPCC, Geneva, Switzerland.

IPIECA, 2017. Mapping the Oil and Gas Industry To the Sustainable Development Goals: an Atlas [WWW Document]. URL http://www.ipieca.org/media/3093/mapping_og_to_sdg_atlas_lr_2017.pdf

Kadono, K., Suzuki, A., Iijima, M., Ohishi, T., Tanaka, H., Hirata, T., Kondo, M., 2013. New Energy Efficient Processes and Newly Developed Absorbents for Flue Gas CO2 Capture. Energy Procedia 37, 1785–1792. https://doi.org/10.1016/J.EGYPRO.2013.06.055

Knudsen, J.N., Jensen, J.N., Vilhelmsen, P.J., Biede, O., 2009. Experience with CO2 capture from coal flue gas in pilot-scale: Testing of different amine solvents. Energy Procedia 1, 783–790. https://doi.org/10.1016/j.egypro.2009.01.104

Li, H., Haugen, G., Ditaranto, M., Berstad, D., Jordal, K., 2011. Impacts of exhaust gas recirculation (EGR) on the natural gas combined cycle integrated with chemical absorption CO2 capture technology. Energy Procedia 4, 1411–1418. https://doi.org/10.1016/j.egypro.2011.02.006

Liebenthal, U., Di D. Pinto, D., Monteiro, J.G.M.S., Svendsen, H.F., Kather, A., 2013. Overall process analysis and optimisation for CO2 Capture from coal fired power plants based on phase change solvents forming two liquid phases. Energy Procedia 37, 1844–1854. https://doi.org/10.1016/j.egypro.2013.06.064

Liu, B., Tang, C., Li, X., Wang, B., Zhou, R., 2020. High-performance SAPO-34 membranes for CO2 separations from simulated flue gas. Microporous Mesoporous Mater. 292, 109712. https://doi.org/10.1016/J.MICROMESO.2019.109712

Ma, X., Kaneko, T., Tashimo, T., Yoshida, T., Kato, K., 2000. Use of limestone for SO2removal from flue gas in the semidry FGD process with a powder-particle spouted bed. Chem. Eng. Sci. https://doi.org/10.1016/S0009-2509(00)00090-7

Masnadi, M.S., El-Houjeiri, H.M., Schunack, D., Li, Y., Englander, J.G., Badahdah, A., Monfort, J.-C., Anderson, J.E., Wallington, T.J., Bergerson, J.A., Gordon, D., Koomey, J., Przesmitzki, S., Azevedo, I.L., Bi, X.T., Duffy, J.E., Heath, G.A., Keoleian, G.A., McGlade, C., Meehan, D.N., Yeh, S., You, F., Wang, M., Brandt, A.R., 2018. Global carbon intensity of crude oil production. Science (80-.). 361, 851–853. https://doi.org/10.1126/science.aar6859

Mathias, P.M., Reddy, S., O’Connell, J.P., 2009. Quantitative evaluation of the aqueous-ammonia process for CO2 capture using fundamental data and thermodynamic analysis. Energy Procedia 1, 1227–1234. https://doi.org/10.1016/J.EGYPRO.2009.01.161

Miyamoto, O., Maas, C., Tsujiuchi, T., Inui, M., Hirata, T., Tanaka, H., Yonekawa, T., Kamijo, T., 2017. KM CDR ProcessTM Project Update and the New Novel Solvent Development. Energy Procedia 114, 5616–5623. https://doi.org/10.1016/J.EGYPRO.2017.03.1700

MODEC, 2020. MODEC Awarded Contract by Equinor to Supply FPSO for offshore field in Brazil [WWW Document]. Modec Inc. URL https://www.modec.com/news/2020/20200130_pr_bacalhau_en.html (accessed 3.4.20).

MODEC, 2019. M350 NEW BUILT FPSO HULL [WWW Document]. URL https://www.gastechevent.com/media/41272/m350_e_brochure.pdf (accessed 3.6.20).

NOAA, 2020. ESRL Global Monitoring Division - Global Greenhouse Gas Reference Network [WWW Document]. US Dep. Commer. Earth Syst. Res. Lab. URL https://www.esrl.noaa.gov/gmd/ccgg/trends/ (accessed 2.2.20).

NS Energy, 2019. MODEC unveils two next-generation new built FPSO hulls [WWW Document]. NS Energy Bus. URL https://www.nsenergybusiness.com/news/modec-built-fpso-hulls/ (accessed 3.6.20).

Park, T., Bae, J., Lee, C.J., Lee, J.M., 2016. A Sequential Method for Determining Optimal Stripper Pressure and Terminal Pressure in CO2Capture and Liquefaction Process Using MEA. IFAC-PapersOnLine 49, 657–662. https://doi.org/10.1016/j.ifacol.2016.07.250

Petrobras, 2020. Fechamos o ano de 2019 com ótimo desempenho operacional [WWW Document]. Blog Fatos e Dados. URL https://petrobras.com.br/fatos-e-dados/fechamos-o-ano-de-2019-com-otimo-desempenho-operacional.htm (accessed 3.4.20).

Rezazadeh, F., Gale, W.F., Rochelle, G.T., Sachde, D., 2017. Effectiveness of absorber intercooling for CO2 absorption from natural gas fired flue gases using monoethanolamine solvent. Int. J. Greenh. Gas Control 58, 246–255. https://doi.org/10.1016/j.ijggc.2017.01.016

Rezazadeh, F., Gale, W.F., Sachde, D., Rochelle, G.T., 2014. Absorber intercooling configurations using aqueous piperazine for capture from sources with 4 to 27% CO2. Energy Procedia 63, 1637–1656. https://doi.org/10.1016/j.egypro.2014.11.174

Rubin, E.S., 2018. Integrated Environmental Control Model [WWW Document]. Carnegie Mellon. URL https://www.cmu.edu/epp/iecm/index.html (accessed 7.26.18).

Sage, P.W., Ford, N.W.J., 1996. Review of sorbent injection processes for low-cost sulphur dioxide control. Proc. Inst. Mech. Eng. Part A J. Power Energy. https://doi.org/10.1243/PIME_PROC_1996_210_031_02

SBM Offshore, 2019. SBM Offshore-Fast4Ward ® [WWW Document]. URL https://www.sbmoffshore.com/wp-content/uploads/2019/09/SEPT-2019-FAST4WARD-BROCHURE.pdf (accessed 3.4.20).

Singh, A., Stéphenne, K., 2014. Shell Cansolv CO2 capture technology: Achievement from First Commercial Plant. Energy Procedia 63, 1678–1685. https://doi.org/10.1016/J.EGYPRO.2014.11.177

Srivastava, R.K., Jozewicz, W., 2001. Flue gas desulfurization: The state of the art. J. Air Waste Manag. Assoc. https://doi.org/10.1080/10473289.2001.10464387

Tong, J., Zhang, L., Han, M., Huang, K., 2015. Electrochemical separation of CO2 from a simulated flue gas with high-temperature ceramic-carbonate membrane: New observations. J. Memb. Sci. https://doi.org/10.1016/j.memsci.2014.12.017

UNFCCC, 2016. Report of the Conference of the Parties, Addendum Part two: Action taken by the Conference at its twenty-first session [WWW Document]. URL http://unfccc.int/resource/docs/2015/cop21/eng/10a01.pdf (accessed 7.14.16).

United Nations, 2015. Transforming our World: The 2030 Agenda for Sustainable Development [WWW Document]. URL https://sustainabledevelopment.un.org/content/documents/21252030 Agenda for Sustainable Development web.pdf (accessed 3.5.20).

Wang, R., Liu, S., Wang, L., Li, Q., Zhang, S., Chen, B., Jiang, L., Zhang, Y., 2019. Superior energy-saving splitter in monoethanolamine-based biphasic solvents for CO2 capture from coal-fired flue gas. Appl. Energy 242, 302–310. https://doi.org/10.1016/J.APENERGY.2019.03.138

WCA, 2017. Coal & Electricity [WWW Document]. World Coal Assoc. URL https://www.worldcoal.org/coal/uses-coal/coal-electricity (accessed 3.14.17).

Zhang, J., Qiao, Y., Wang, W., Misch, R., Hussain, K., Agar, D.W., 2013. Development of an energy-efficient CO2 capture process using thermomorphic biphasic solvents. Energy Procedia 37, 1254–1261. https://doi.org/10.1016/j.egypro.2013.05.224

Zhang, Y., Rochelle, G.T., 2014. Absorber Performance with High CO2. Energy Procedia 63, 1329–1338. https://doi.org/10.1016/j.egypro.2014.11.142

3. DEEP SEAWATER INTAKE FOR PRIMARY COOLING IN TROPICAL OFFSHORE PROCESSING OF NATURAL GAS WITH HIGH CARBON DIOXIDE CONTENT: ENERGY, EMISSIONS AND ECONOMIC ASSESSMENTS

This chapter is published a full-length original article in the Journal of Natural Gas Science and Engineering

CRUZ, M. DE A.; ARAÚJO, O. DE Q. F.; DE MEDEIROS, J. L. Deep seawater intake for primary cooling in tropical offshore processing of natural gas with high carbon dioxide content: Energy, emissions and economic assessments. **Journal of Natural Gas Science and Engineering**, v. 56, n. June, p. 193–211, 2018.

Abstract

In deepwaters offshore oil-gas rigs, centrifugal compressor trains are major power consumers, requiring intercoolers conventionally designed assuming surface seawater for primary cooling, limiting compressor inlet gas temperatures to 40°C at tropical sites. On the other hand, at tropical deepwaters the available deep seawater at 4ºC can be exploited to reduce compression power – nearly proportional to inlet gas absolute temperature – entailing energy, economic and environmental benefits. This work considers a new primary cooling for deepwaters offshore platforms based on deep seawater (DSW) intake at 4ºC from depths around 900 m, reducing the outlet temperature of intercoolers to 12ºC. DSW intake alternative is assessed in terms of power consumption, CO_2 emissions and economy employing detailed equipment sizing and cost estimation. Depending on gas flow rate, it is shown that DSW intake lowers compressors power up to 9.2%, besides several indirect benefits: elimination of one CO_2 compressor; 30% less heat transfer areas; 4.5% less fuel gas consumption; 4% less gas turbines power; 9.5% (15 MMUS$) less investment; 14.4% (226 t) less topside weight, while making refrigeration unnecessary for dew point adjustment. DSW intake also entails 5% more efficient energy usage and 9327 tCO_2/y less emissions, boosting economic performance under carbon taxation.

Keywords: Deep seawater intake; Deepwater oil production; Offshore natural gas processing; FPSO; Gas compression; Energy usage efficiency.

Supplementary Materials for this chapter are found in the Appendix H, Section A.

Abbreviations

CAPEX	Capital Expenditures
CW	Cooling-Water
DSW	Deep Seawater
EIA	Environmental Impacts Assessment
EOR	Enhanced Oil Recovery
FLNG	Floating Liquefied Natural Gas Plant
FPSO	Floating Production, Storage and Offloading
GHG	Greenhouse Gas
GOR	Gas-to-Oil Ratio
GT	Gas Turbine
HCDP	Hydrocarbon Dew-Point
HCDPA	Hydrocarbon Dew-Point Adjustment
HDPE	High Density Polyethylene
HHV	Higher Heating Value
LHV	Lower Heating Value
MP	Membrane Permeation
NG	Natural Gas
NPSH	Net Positive Suction Head
OPEX	Operational Expenditures
OTEC	Offshore Thermal Energy Conversion
PFD	Process Flow Diagram
PR-EOS	Peng-Robinson Equation of State
RH	Relative Humidity
SW	Seawater
TSA	Temperature Swing Adsorption
US$	US Dollar
VLCC	Very Large Crude Carrier
WDPA	Water Dew Point Adjustment
WHRU	Waste Heat Recovery Unit
WOR	Water-to-Oil Ratio.

Nomenclature

A_0	Effective outside heat transfer surface (m^2)
bbl/d	Barrels per day
CO_{2Eq}	Carbon dioxide equivalent
F	*LMTD* correction factor
MW	Molecular Mass
$MMSm^3/d$	Millions of Standard m^3 (293 K, 101.33 kPa) per day
n	Polytropic exponent
N	Number of compression stages
P	Absolute pressure (kPa, bar)
q	Mass flow rate (kg/h)
Q	Heat duty (kW)
R	Ideal gas constant (8.314 kJ/kmol.K)
r_p	Compression ratio
T	Absolute temperature (K)
U	Overall heat transfer coefficient ($kW/m^2.K$)

W Brake horsepower (kW)
Z Compressibility factor

Greek Symbols

η_p Polytropic efficiency
ΔP Head loss (kPa)
ΔT_M Corrected mean temperature difference (K)

3.1. Introduction

Since 2000, offshore fields respond for ≈30% of the world production of oil and natural gas (Rui et al., 2017). Due to still modest competitiveness of renewable energy sources, fossil sources will continue to play significant role in global energy matrix in the short to mid-term, especially natural gas (NG). However, oil price decline and new climate change mitigation policies – e.g. carbon taxation – have been a challenge to this industry. CO_2 emission taxation is already a reality in many countries, with Sweden imposing the highest tax of 140 US$/t (IEA, 2016). According to the International Association of Oil and Gas Producers (IOGP, 2016) main oil and gas companies emitted 280 Mt CO_{2Eq} of greenhouse gases (GHG) in 2015, of which 68% is related to fuel combustion for in-place energy production. Thus, energy usage efficiency and CO_2 emissions are becoming not solely an environmental, but also, an economic issue for oil and gas producers. As energy usage efficiency and CO_2 emissions are inversely interrelated concepts, using processing strategies with higher energy usage efficiency implies lowering CO_2 emissions, alleviating the environmental burden of oil and gas industries. In other words, there is no option to the carbon fossil industry but questing for better energy usage efficiency.

3.1.1. Offshore Oil and Gas Processing: Improving Efficiency of Energy Usage

New developments on offshore oil and gas primary processing represent opportunities to, cumulatively, improve efficiency of energy usage, reduce GHG emissions, lower topsides footprint and, consequently, reduce costs. All these effects contribute to increase the economic and environmental feasibility of offshore oil and gas production. The literature presents several recent works on energy assessment and optimization of primary processing on offshore oil and gas rigs, comprising measures to improve energy usage efficiency (Nguyen et al., 2016a), better power generation schemes with organic cycles (Pierobon et al., 2013), air-bottoming cycles (Pierobon and Haglind, 2014), steam-bottoming cycles (Nguyen et al., 2014a), heat-exchanger network optimization for minimum energy consumption (Pierobon et al., 2013; Pierobon and Haglind, 2014; Nguyen et al., 2014a) and offshore power production via combined cycles (Rivera-Alvarez et al., 2015). To improve energy usage efficiency of the process as a whole, including carbon capture units such as post-combustion amine plants, Nguyen et al. (2014b; 2016b) constructed multi-objective frameworks for optimizing CO_2 mitigation alternatives and platform lifecycle, using as working scenario an ending-life oil and gas offshore platform in the Norwegian North Sea.

As easily verified in these works, offshore oil and gas production follows a standard practice of centralizing multiple production wells in a single offshore processing unit, with topside equipment designed to separate and process oil, gas and water (Asibor et al., 2013). At ultra-deep waters distant from coast, Floating Production Storage and Offloading (FPSO) units configure the preferred choice of platform type (Gallo et al., 2017; Araújo et al., 2017; Ataújo and de Medeiros, 2017). Several works (Rivera-Alvarez et al., 2015; Gallo et al., 2017; Araújo et al., 2017; Voldsund et al., 2013; Nguyen et al., 2013; Teixeira et al., 2016) performed steady-state energy and exergy analysis of gas and oil processing on FPSOs and other offshore rigs, unveiling the common fact that compressors and gas turbines (GT) are major power sinks and power sources where exergy is mostly destroyed (Voldsund et al., 2014). This is particularly true for centrifugal compressors operating at partial load, when Joule-Thomson depressurizing recycles are used to sustain gas flow rate at sufficient levels to prevent surge (GPSA, 2004), despite the great rate of exergy destruction entailed by such anti-surge strategies.

3.1.2. Deep Seawater Intake at Tropical Latitudes

Based on this last fact, the present work assesses the potential increase of energy usage efficiency of offshore gas processing by employing deep seawater (DSW) intake for primary cooling of a FPSO operating on deepwaters at tropical sites. As compressor machinery is dominant in gas processing FPSOs Eq (3.1), which is commonly used (GPSA, 2004) to calculate brake horsepower of centrifugal compressors, can demonstrate the interrelationship between temperature of primary cooling and FPSO energy usage efficiency, where r_p, n, η_P, W, q, Z, R, T_1, MW respectively represent compression ratio, polytropic exponent, polytropic efficiency, brake horsepower (kW), gas flow rate (kg/h), average compressibility factor, ideal gas constant (8.314 kJ/kmol.K), gas inlet absolute temperature (K) and gas molar mass (kg/kmol). Eq (3.1) shows that the power of centrifugal compressors is nearly proportional to the gas inlet absolute temperature, which is indirectly linked to the primary cooling temperature.

$$W = \frac{q.Z.R.T_1\left\{r_P^{\frac{n-1}{n}} - 1\right\}}{3600.\eta_P.MW.(n-1)/n} \tag{3.1}$$

On a FPSO the primary cooling source is seawater (SW), as displayed in Fig. 3.1, where it is seen that SW operates in open loop. It is aspired by SW pumps, passes through plate heat exchangers and returns to the ocean. In the plate exchangers, SW absorbs heat from the closed-loop cooling water (CW) coming warm from process heat exchangers. The cooled CW is then returned to the process plant by CW pumps. The main CW demanding units are intercoolers and aftercoolers of gas compression trains, whose heat duties have the same magnitude of the powers of the respective precedent compression stages. Therefore, inlet SW temperature indirectly imposes a lower bound on the temperature of gas leaving intercoolers and aftercoolers, affecting total compression power and energy usage efficiency of FPSOs.

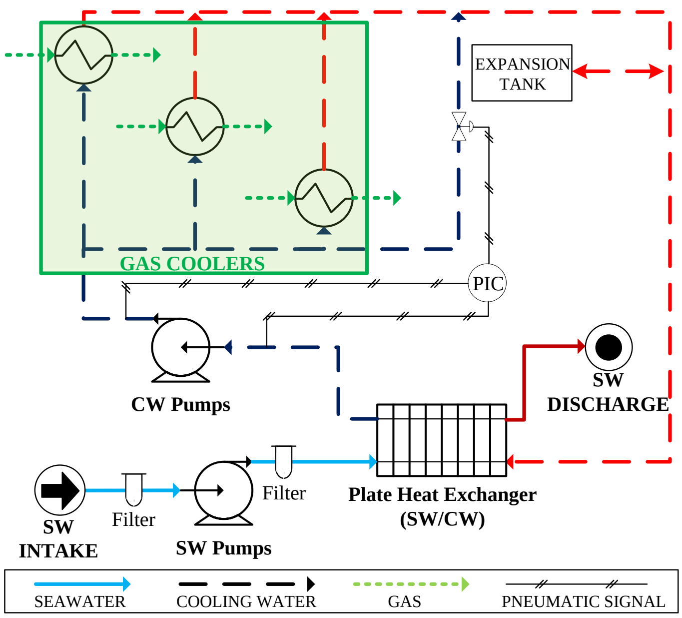

Figure 3.1. FPSO CW circuit cooled by SW intake

Shallow-water offshore platforms were also studied assuming SW intake at 8°C for primary cooling (Nguyen et al., 2016b; Pierobon et al., 2013; Pierobon and Haglind, 2014; Nguyen et al., 2014a; Voldsund et al., 2014). The underlying reason is that such units are situated at high latitudes (e.g. Norwegian North Sea). On the other hand, at tropical or sub-tropical deepwaters – e.g. Gulf of Mexico, South Atlantic Brazilian Pre-Salt and South-East Asia – the surface SW is much hotter, attaining 25ºC to 32ºC in the summer. This entails lowest CW temperature near to 35ºC, implying that hot compression gases can be cooled down to 40ºC (313 K) only.

On the other hand, at tropical deepwaters, SW temperature falls continuously becoming almost constant beyond 800 m of depth and attaining a seabed temperature around 4ºC as shown in Fig. 3.2 for tropical latitudes of the South Atlantic on Pre-Salt basin. Thus, DSW intake below 900 m of depth is less cost-effective, implying that the layer between 800 m and 900 m of depth is established as the best temperature-cost compromise for positioning DSW intake (Rogez, 2012). This demonstrates that DSW intake is more relevant for FPSOs located at tropical seas, where differences of up to 28ºC can be observed between surface SW and DSW. On the other hand, on high latitude seas the maximum temperature difference from surface SW to DSW is less than ≈8ºC, entailing that DSW intake is less interesting in such cases.

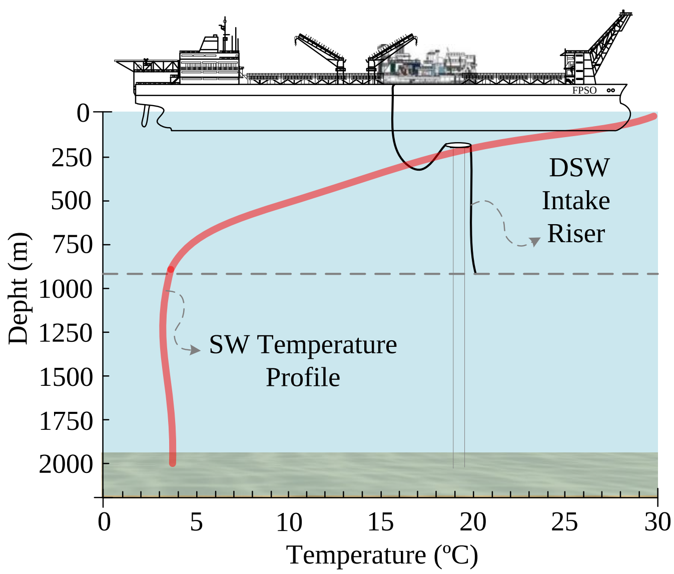

Figure 3.2. DSW intake and thermal profile of deepwaters at tropical latitudes in the South Atlantic

DSW intake at 4ºC allows to cool down CW to 7ºC and, consequently, compressor outlet gas to 12ºC (285K), excepting in cases where there is risk of gas hydrate formation and/or of attaining lower bound of equipment working temperature. Eq. (3.1) shows that a decrease of 28K (e.g. from 313 K to 285 K) of gas inlet temperature reduces compression power approximately by 9%, which can be achieved by adopting DSW intake to cool the CW circuit. Additionally, DSW intake leads to other indirect benefits: (i) elimination of refrigeration for Hydrocarbon Dew Point Adjustment (HCDPA); (ii) reduction of area and weight of heat exchangers; (iii) decrease of gas turbines power; (iv) decrease of fuel gas consumption; (v) elimination of one stage in CO_2 compression train (i.e., only three stages instead of the usual four); and (vi) reduction of the dehydration load of Temperature Swing Adsorption (TSA) units for Water Dew Point Adjustment (WDPA).

3.1.3. Present Work

The literature shows a growing interest in optimization of energy usage efficiency of offshore platforms. In this context, DSW intake is a factor to be considered for better energy usage efficiency of offshore rigs as it can effectively reduce compressor power on tropical deep-waters. Despite this, there are only a handful of literature works that studied DSW intake for obtaining resources and improving energy usage efficiency of plants, where only a fraction of them considered offshore gas processing applications. Rogez (2012) analyzed high capacity (≈30,000 m^3/h) 800 m depth DSW intake at 5ºC to floating liquefied NG (FLNG) platforms and offshore thermal energy conversion (OTEC) systems, demonstrating its theoretical feasibility, but without field validation. Wei et al. (1980) discussed DSW for mariculture and nuclear power plant cooling. Blomster and Stanimirov (2004) considered the manufacture of ≈600m polyethylene pipes for DSW applications. Petkovic et al. (1993) analyzed flexible or rigid ducts for suctioning 500 m depth DSW at 7ºC. These studies were motivated by expected gains achieved with DSW intake in terms of energy, weight and costs, but did not attempt quantitative assessment of the technology.

The present work contributes to filling this gap. It is presented a quantitative assessment of the effects of using DSW intake in terms of power consumption, economic responses (capital investment and revenues) and CO_2 emissions of a typical oil and gas processing FPSO operating on the Brazilian Pre-Salt. The choice of this scenario is relevant for implementation of DSW alternative, due to the stringent design conditions of oil and gas FPSO's in this area, such as unusual high gas to oil ratio (GOR) and high %CO_2 in raw NG. These conditions demand proper CO_2 separation, CO_2-rich fluid dispatch to enhanced oil recovery (EOR) and NG exportation to onshore plants (Araújo and de Medeiros, 2017). Compression of CO_2-rich fluid to EOR and exportation gas, both at high pressures, has strong impact on capital investment and power consumption of the FPSO. In this context, the potential of innovation of

DSW intake was evaluated comparing conventional surface SW intake with DSW intake, in terms of the following items of performance: (i) power of compressors, GTs, CW pumps and SW/DSW pumps; (ii) gas processing plant layout; (iii) equipment weight, capital expenditures (CAPEX) and NG exportation revenues; (iv) power demand, fuel gas consumption and CO_2 emissions along project life; (v) energy usage efficiency of FPSO gas processing plant; and (vi) sensitivity analysis in carbon taxation scenarios.

3.2. Methods

Table 3.1 presents the two considered scenarios of SW/DSW intake for assessment of impacts on FPSO gas processing plant.

Table 3.1. Scenarios for comparison of SW intake schemes

	BASE-CASE	DSW-CASE
SW Intake Temperature	32ºC	4ºC
Cold CW Temperature	35ºC	7ºC
CW ΔT	20ºC	20ºC
Hot CW Temperature	55ºC	27ºC
SW Outlet Temperature	<40ºC	<12ºC
Cooled Gas Temperature	40ºC	12ºC

CW ΔT: CW change of temperature

The procedure depicted in Fig. 3.3 was applied to the FPSO gas processing plant under traditional surface SW intake as Base-Case and the alternative DSW-Case using DSW intake. The design gas processing capacity is considered 5 MMSm³/d. Both cases were evaluated under five gas processing loadings – 100%, 75%, 50% and 25% of full design capacity – resulting in ten simulation cases.

Anti-surge recycle loops were adjusted to maintain the design gas flow rate through compressors (≈5 MMSm³/d). Specific simulation tools were employed considering the diversity of FPSO unit operations for oil, gas and utilities. The oil and gas processing plants – including CW/SW circuits and GTs – were simulated with HYSYS 8.8 (Aspentech) using Peng-Robinson Equation of State (PR-EOS) for thermodynamic modeling. GT simulations were validated with Thermoflex (Thermoflow Inc.), employing 25 simulations of the selected GT at same capacity and ambient conditions of temperature, pressure and air humidity. Equipment sizing and cost estimation were executed with HYSYS 8.8, Aspen Exchanger Design and Rate 8.8 and Aspen Capital Cost Estimator 8.8 (Aspentech).

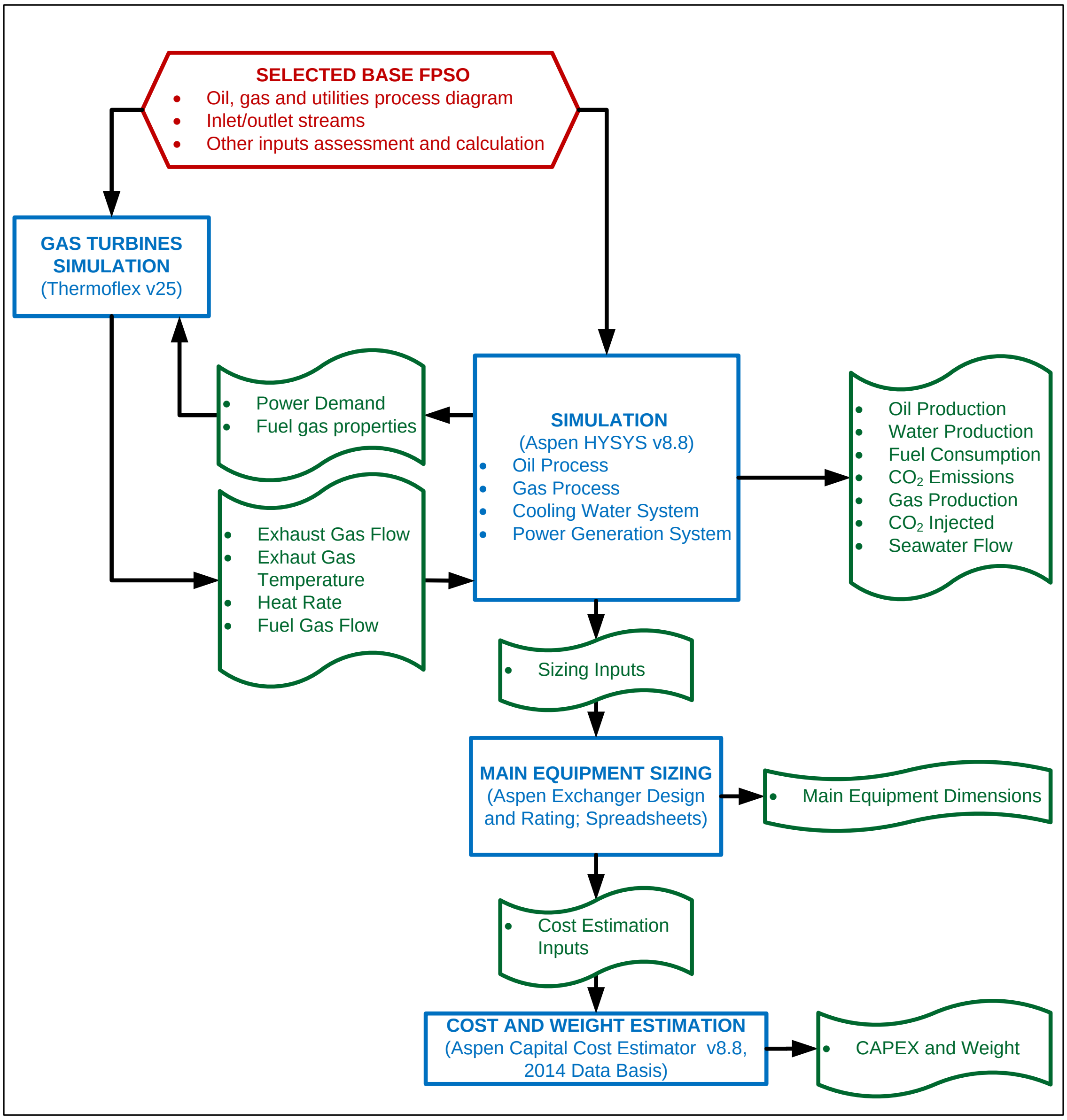

Figure 3.3. Procedure flowchart for this study

3.2.1. Base-Case Definition

The operation conditions of FPSO *Cidade de Paraty* were chosen to define the Base-Case in this study. It operates at Brazilian Pre-Salt since 2013 with processing capacity of 5 MMSm³/d of gas and 100,000 bbl/d of oil. Information concerning this FPSO was extracted from the Environmental Impacts Assessment (EIA) of the Activity of Production and Flow of Oil and Gas from Santos Basin Pre-Salt Pole – Stage 1 (Petrobras, 2013), from now on simply referred as EIA. Real operational and inlet data from EIA are available in the Internal Appendix IA, of chapter 3 (Tables IA.1, IA.2 and IA.3, Figs. IA.1 and. IA.2).

FPSOs operating on Pre-Salt fields are not allowed to flare associated gas. Therefore, gas processing plants contemplates CO_2 removal from NG, destination of the CO_2-rich fluid to EOR, and exportation of treated NG through pipelines to onshore plants. This imposes high compression power demand, configuring an application niche for DSW alternative. Fig. IA.1 depicts the block diagram of the *Cidade de Paraty* topside processing plant, including CW system. The gas production profile along project life is supplied by EIA (Petrobras, 2013) in Fig. IA.2, where the gas profile of %CO_2 is an estimated curve built with the only two values, initial and final, provided by EIA, respectively, 8%mol and 55%mol. In the real situation, the continuous increase of CO_2 content of associated gas affects equally both DSW-Case and Base-Case: flow rate of re-injection compression trains (C-700 and C-600) increases, while the flow rate of NG exportation compressors (C-500) decreases. Due to such continually changing conditions and lack of all necessary data, the rigorous evaluation of this effect was not attempted in this work. Instead, the design %CO_2 of raw NG was herein assumed constant at 15% mol, the time-average %CO_2 of the raw gas profile in Fig. IA.2. This way the complexity of the problem and the number of explored cases could be kept at workable levels. The average gas plant feed is shown in Table IA.1.

3.2.2. Oil Processing Plant

The oil processing plant was simulated to obtain the flow rate, composition, temperature and pressure of the raw gas that feeds the gas processing plant. HYSYS extension GOR Adjustment was used for crude feed modeling. Flow rates, compositions, pressure and temperature of oil, gas and water streams in Table IA.1 were used as inputs. Three-phase crude arrives from thirteen risers after 2223 m of sub-sea elevation change from the reservoir at 41368 kPa and 40ºC. Gas streams were separated from the crude feed at three pressures: 1850 kPa, 667.7 kPa and 250 kPa. GOR and water-to-oil ratio (WOR) targets were set to 268.2 Sm^3/m^3 and 0.02537 m^3/m^3, respectively, to achieve the predicted flows of oil, gas and water considering the year (Fig. IA.2) of maximum gas production of 4.750184 $MMSm^3/d$ with 111462 bbl/d of oil and 2906 bbl/d of water. Oil plant process flow diagram (PFD) for simulation and GOR Adjustment settings are in Fig. A1.1 (Supplement A1 of Supplementary Materials at Appendix H).

3.2.3. Gas Processing Plant Simulation: Base-Case

Fig. 3.4 is a simplified PFD of the gas processing plant for the Base-Case. The simulation PFD is shown in Fig. A1.3 (Supplement A1 of Supplementary Materials at Appendix H) Gas streams 103, 206 and 201, coming from the high, medium and low-pressure oil-gas separators, feed the gas plant. Table 3.2 summarizes data of compressor sets.

Table 3.2. Centrifugal compressors summary: Base-Case

PFD AREA	100	200	500	600	700	900
Compressor Service	Main	Gas Recovery	Gas Export	CO_2	Injection	C_3 Cycle
Number of Stages	1	2	2	4	1	1
Inlet Pressure (kPa)	1800	250	4500	400	25000	476.6
Discharge Pressure (kPa)	5200	1800	25000	25000	55000	1738
Gas cooler 1 ΔP (kPa)	50	25	50	25	50	-
Gas cooler 2 ΔP (kPa)	-	50	50	25	-	-
Gas cooler 3 ΔP (kPa)	-	-	-	50	-	-
Gas cooler 4 ΔP (kPa)	-	-	-	50	-	-
Pressure Ratio/Stage	2.9167	2.7708	2.3649	2.8385	2.2020	3.6466
1st stage actual flow (m^3/h)	12027	1317	2894	12939	313	1885
2nd stage actual flow (m^3/h)	-	1848	1110	4728	-	-
3rd stage actual flow (m^3/h)	-	-	-	1583	-	-
4th stage actual flow (m^3/h)	-	-	-	467	-	-
1st stage polytropic efficiency	82%	74%	77%	83%	57%	75%
2nd stage polytropic efficiency	-	75%	73%	79%	-	-
3rd stage polytropic efficiency	-	-	-	74%	-	-
4th stage polytropic efficiency	-	-	-	70%	-	-

Eq. (3.2) is used to calculate the compression ratio r_P of a compression stage belonging to a N-staged compressor train, inlet pressure P_0 and final discharge pressure P_N , where ΔP_i represents the head loss in the i^{th} intercooler. The polytropic efficiency is determined via GPSA (2004), which presents efficiency of centrifugal compressors for several flow rate ranges. These data allowed building the correlation of Fig. A1.4 (Supplement A1 of Supplementary Materials at Appendix H) to predict polytropic efficiency from gas flow rate.

$$P_0 * r_P^N - \sum_{i=1}^{N} \Delta P_i * r_P^{N-i} - P_N = 0 \qquad (3.2)$$

Five simulations were executed. The first is a simulation for equipment sizing at design conditions adopting maximum compressor operational flow rates from EIA (Fig. IA.1). The four additional simulations assume 100%, 75%, 50% and 25% of the total gas plant capacity. The 100% capacity corresponds to 4.75 $MMSm^3/d$ of gas flow rate referring to the year of maximum gas production in Fig. IA.2. Flow rates of anti-surge recycles were adjusted to keep design flow rates of all compression stages.

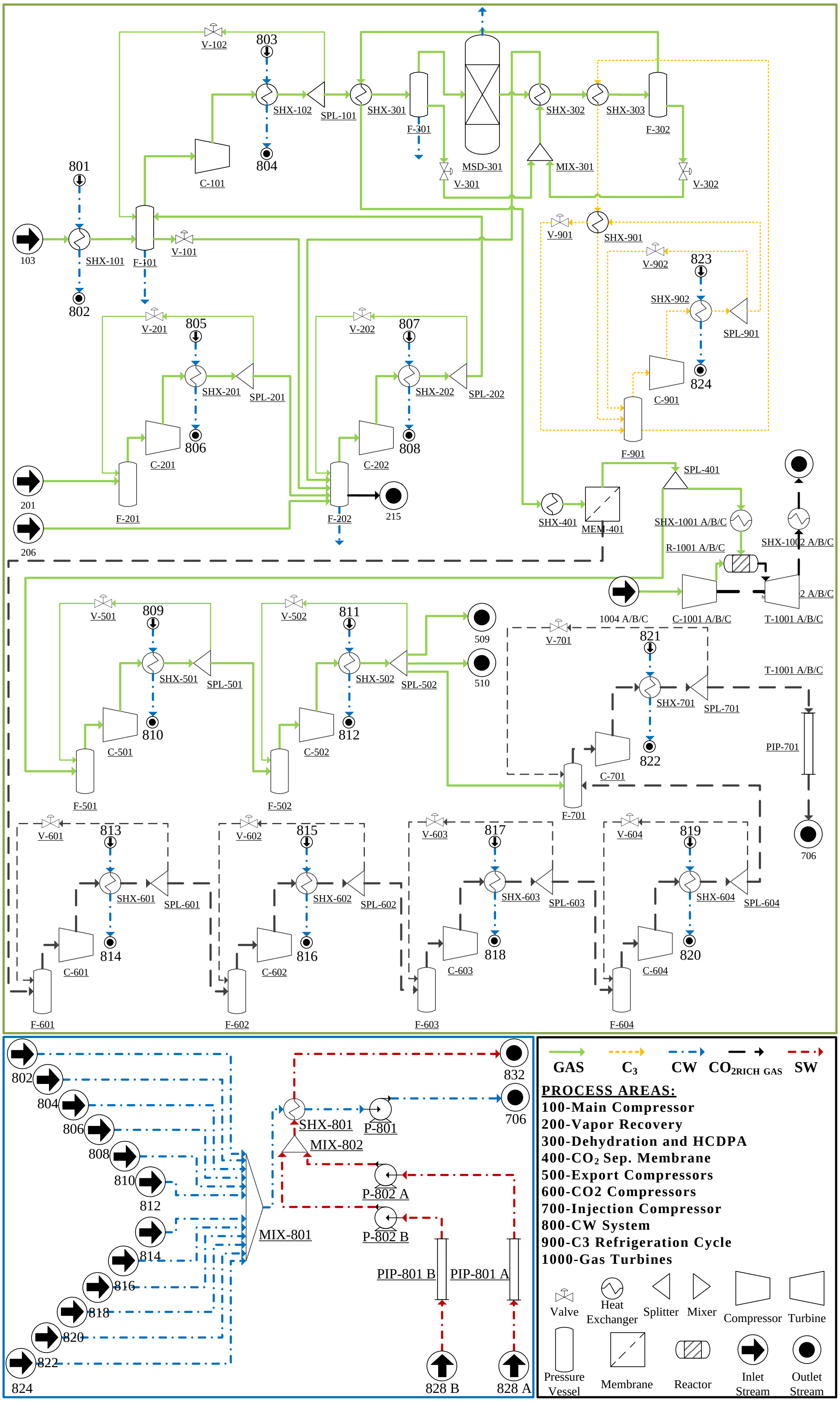

Figure 3.4. PFD of gas processing plant: Base-Case

Heat exchangers specifications, including CW and gas temperatures, are shown in Table A1.3, (Supplement A1, Suppl. Mat.). A propane refrigeration cycle cooled by CW was used for hydrocarbon dew-point adjustment (HCDPA). For a HCDP of 10ºC, the propane evaporator temperature was 0ºC with 476.6 kPa of dew pressure, while the condenser temperature was 50ºC with bubble pressure of 1738 kPa. CO_2 separation was executed by a membrane permeation (MP) unit, which was the same in both Base-Case and DSW-Case, eliminating the need to calculate its contribution to costs and equipment weight in the comparative analysis. Despite MP units can be installed as customized user operations in HYSYS PFDs for designing MP area (Arinelli et al., 2017), here MP CAPEX has no importance, so that the MP unit was simulated via a simple stream calculator using as specifications the feed stream and the desired %CO_2 in retentate (5%mol) and in permeate (56.6%mol) as in EIA (Petrobras, 2013). Assuming permeation of only CO_2 and CH_4, compositions and flow rates of permeate and retentate were determined by mass balances, while the respective temperatures followed via energy balance.

The CW circuit was designed considering gas processing at 100% capacity, giving the highest CW consumption, with most anti-surge loops disabled, except in the compressor train of CO_2 rich fluid to EOR. In this case the flow rate of EOR compressors was lower than their specific design value, corresponding to all processed gas being injected to EOR due to inexistent subsea pipelines.

3.2.4. Gas Processing Plant Simulation: DSW-Case

The approach of the Base-Case was adapted according to the particularities of DSW-Case simplified PFD in Fig. 3.5, which corresponds to the simulation PFD in Fig. A1.5 (Supplement A1 of Supplementary Materials at Appendix H). Due to the lower CW temperature the process was modified: (i) Propane refrigeration cycle (Area 900) was unnecessary as a mere cooler attains the HCDPA target using CW at 7ºC; (ii) gas at 12ºC from intercoolers allowed to use only three CO_2 compression stages (Area 600), without overpassing compressor threshold temperature of ~180ºC; (iii) at partial load (75%, 50%, 25% of maximum gas capacity), the anti-surge control is activated to keep compressor design flow rates.

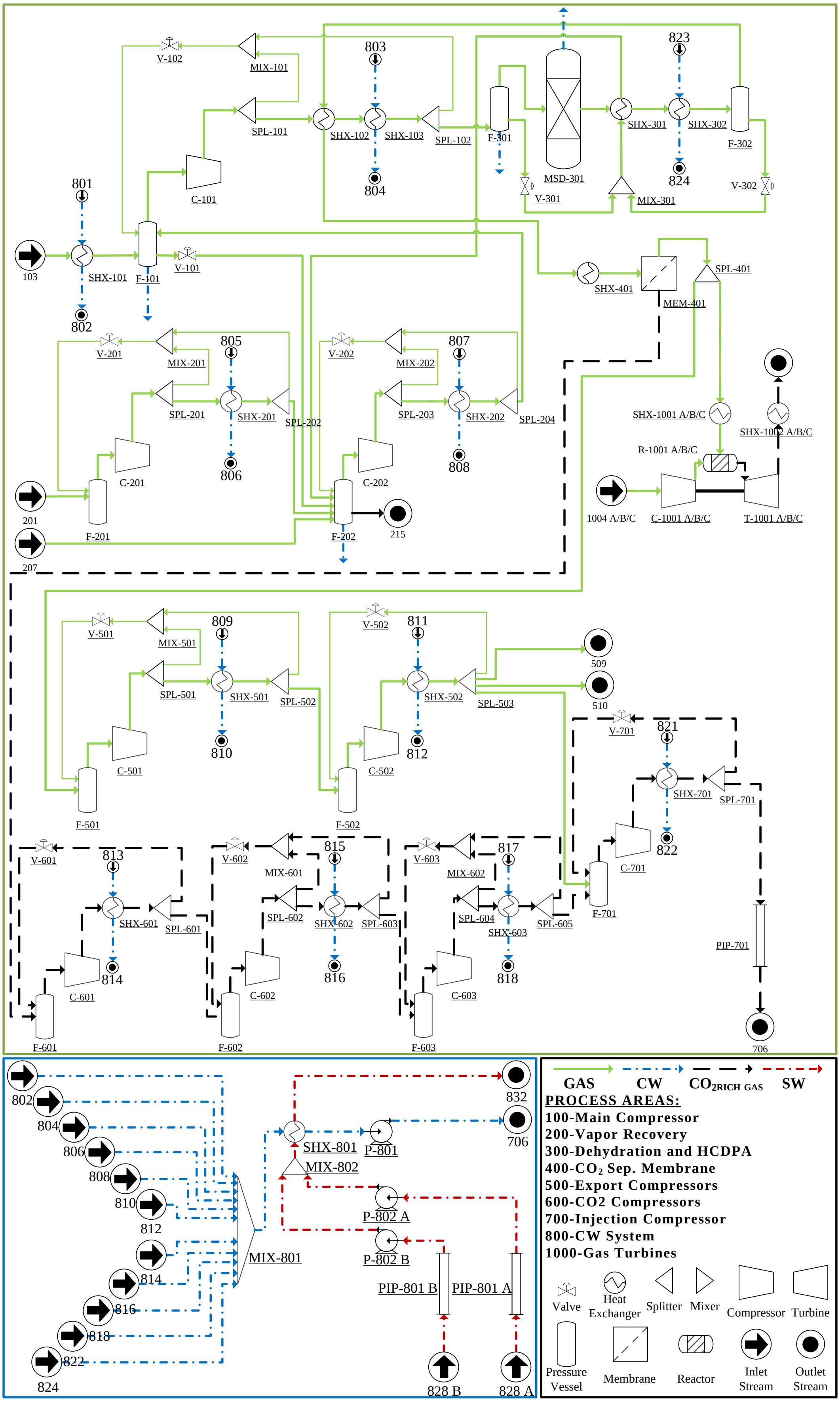

Figure 3.5. PFD of gas processing plant: DSW-Case

However, Joule-Thomson effects in anti-surge valves resulted in very low temperatures in some suction lines. That could lead to hydrate formation and freezing for non-dehydrated gas (e.g. compressors C-101, C-201 and C-202 in Fig. 3.5), besides issues of low carbon steel resistance. Hydrate and freezing conditions were detected via HYSYS Hydrate-Analysis tool, so that whenever hydrate conditions were detected, hot-bypasses (i.e. recycling hot gas from compressor outlet before intercooling) set the temperature after anti-surge valves to at least 3ºC above hydrate temperature. Temperatures below 0ºC were detected in compressors C-501, C-602 and C-603, and hot-bypasses were used to set suction temperature to 5ºC, also avoiding expensive stainless-steel compressors. Anti-surge recycles and hot by-passes were adjusted to reach design flow rates and minimum temperatures of compression stages. Table 3.3 shows compressors parameters of the DSW-Case with supplementary information in Tables A1.4 to A1.7 (Supplement A1, Suppl. Mat.). Heat exchangers specifications – including CW and gas temperatures – are in Table A1.8 (Supplement A1, Suppl. Mat.)

Table 3.3. Centrifugal compressors summary: DSW-Case

	Process Area				
	100	200	500	600	700
Compressor Service	Main	Gas Recovery	Gas Export	CO_2	Injection
Number of Stages	1	2	2	3	1
Inlet P (kPa)	1800	250	4500	400	25000
Discharge P (kPa)	5200	1800	25000	25000	55000
Gas cooler 1 ΔP (kPa)	50	25	50	25	50
Gas cooler 2 ΔP (kPa)	-	50	50	25	-
Gas cooler 3 ΔP (kPa)	-	-	-	50	-
Pressure Ratio/Stage	2.9167	2.7708	2.3649	3.9974	2.2020
1st stage actual flow (Sm³/h)	10437	1317	2894	12888	313
2nd stage actual flow (Sm³/h)	-	1431	835	2943	-
3rd stage actual flow (Sm³/h)	-	-	-	581	-
1st stage polytropic efficiency	82%	74%	77%	83%	57%
2nd stage polytropic efficiency	-	74%	72%	77%	-
3rd stage polytropic efficiency	-	-	-	71%	-

3.2.5. Gas Turbines (GT) Simulation

The Base-Case uses four aero-derivate GT model GE LM 2500, a spare included. Each GT has a dedicated waste heat recovery unit or WHRU (Teixeira et al., 2016; Nguyen et al., 2016b) fed with the respective exhaust gas. GT is simulated integrating an adiabatic air compressor, a combustion reactor and an adiabatic expander, as shown in Area 1000 of Figs. 3.4 and 3.5. GT simulation model in HYSYS was calibrated against GT simulation with Thermoflex 25 by adjusting compressor and expander adiabatic efficiencies to match power and air/fuel ratio to match exhaust temperature. At operation conditions of the Base-Case and the DSW-Case GT simulations were validated against Thermoflex results. Due to lower power demand of DSW-

Case, a smaller GE LM2500 GT model was prescribed, with 26.7 MW gross power (ISO conditions) – instead of the 28.2 MW GT model of Base-Case – burning fuel gas of nearly same composition of Base-Case in Table A.2. Table 3.4 summarizes GT information at three conditions.

Table 3.4. Selected gas turbine (GT) data

CONDITION	BASE-CASE			DSW-CASE		
	Iso	Design	Operation	Iso	Design	Operation
Fuel	Methane	Fuel Gas	Fuel Gas	Methane	Fuel Gas	Fuel Gas
Altitude (m)	0	0	0	0	0	0
P (kPa)	101.33	101.33	101.33	101.33	101.33	101.33
T (°C)	15	23	30	15	23	30
Relative Humidity	60%	87%	77%	60%	87%	77%
Filter ΔP (kPa)	0.0	1.0	1.0	0.0	1.0	1.0
Exhaust Duct ΔP (kPa)	0.0	0.5	0.5	0.0	0.5	0.5
Net power (MW)[1]	28.176	23.536	25.78	26.718	22.172	24.337
Compressor Efficiency[2]	83.9%	83.9%	84.2%	86.0%	85.2%	85.7%
Expander Efficiency[2]	88.0%	88.0%	88.0%	87.5%	87.5%	87.5%
Fuel Gas Flow (kg/s)[1]	1.53	1.537	1.648	1.459	1.46	1.571
Inlet Air Flow (kg/s)[1]	85.85	76.27	80.85	82.25	75.55	77.06
Fuel LHV (kJ/Sm^3)[3]	32824	40737	40737	32824	40750	40750
Heat Rate (kJ/kWh)[1]	9622	10213	9998	9676	10299	10096
GT Efficiency (Yield)[1]	37.4%	35.2%	36.0%	37.2%	35.0%	35.7%
Combustion T (°C)[2]	1192	1201	1196	1170	1183	1179
Exhaust T (°C)[1]	513	523.7	519.5	512.4	525.1	521.9
Exhaust Flow (kg/s)[1]	86.66	77.0	81.6	83.07	73.26	77.83
Fuel Consumption (MMSm^3/d)[1]	0.198	0.142	0.152	0.1890	0.1345	0.1447
CO_2 Emissions (t/d)[1]	366	354	380	349	337	362

1 - From GE LM2500 GT simulation with Thermoflex
2 - From GT simulation with HYSYS
3 - Table IA.2

The adiabatic efficiency of GT air axial compressor varies from 78% to 87%, while the adiabatic efficiency of GT expander depends on temperature in the combustion chamber, varying from 84% at 1200ºC to 92% at 1288ºC (Boyce, 2002). Air temperature and relative humidity (RH) affect GT power output and were considered the same in HYSYS and Thermoflex runs, respectively as 23ºC and 87% according to EIA – as design premise, the maximum air temperature and minimum RH were 30ºC and 77%. This effect is represented in Fig. A1.6 (Supplement A1 of Supplementary Materials at Appendix H) as a power surface of GE LM2500 versus RH and ambient temperature.

3.2.6. SW Intake and CW Circuit

For the Base-Case (Fig. 3.4) the total CW flow rate through the SW/CW plate exchanger SHX-801 was obtained adding all CW exchanger outlets (streams 802 to 824), while SW was fed from two headers (PIP-801 A/B). The CW system was designed to operate at 100% of gas processing capacity of 5.0 MMSm³/d at 735.5 kPa of discharge pressure of pumps P-801 and P-802A/B. SW flow rate was calculated by a controller (SVC-801) setting HX-801 outlet temperature to 40ºC, the SW disposal limit temperature according to local legislation (CONAMA, 2011). The NPSH is a critical issue in designing SW intake pipes as insufficient suction head leads to cavitation. Table 3.5 details the design of SW intake pipes for the Base-Case. The DSW-Case was designed with same parameters excepting the final DSW temperature of 11ºC (Table 3.1) and the intake pipe length of 900 m giving 1550 m of total equivalent pipe length instead the 380 m of the Base-Case.

Table 3.5. SW intake pipe sizing: Base-Case

Total Equivalent Pipe Length (m)[1]	380
Net Elevation to Sea Level (m)[2]	-2.0
Absolute Pipe Roughness (mm)[3]	0.0015
Max Allowed ΔP (kPa)[4]	60
Suction Filter ΔP (kPa)	30
Max Flow Velocity (m/s)	2.0
External Heat Transfer	Isothermal
Max SW Flow Rate per Pipe (m³/h)[5]	2000

1 - SW intake at 30m depth and 350m of equivalent length;
2 - Fig. A1.7 (Supplement A1 of Supplementary Materials at Appendix H); 3 - HDPE pipes;
4 – Rogez (2012); 5 - Limited by pump maximum flow

3.2.7. Equipment Sizing

Equipment sizing was performed to allow cost and weight estimations. Reducing CW temperature strongly affects compressors, HCDPA, NG dehydration TSA units, GTs, pumps, NG intercoolers and aftercoolers. Heat exchangers demand special attention as they had to be resized due to DSW intake effects on flow rate and temperature of inlet and outlet process streams. Heat exchangers were designed (TEMA, 2007) with Eq. (3.3), where A_0 is the effective heat transfer surface (m²), Q is the heat duty (kW), U is the overall heat transfer coefficient (kW/m².K) and ΔT_M is the corrected mean temperature difference (K) calculated via Eq. (3.4) for constant U, where $LMTD$ is the log mean temperature difference (K), F is the correction factor dependent of exchanger TEMA type and tube passes, and *GTTD* and *LTTD* are greater and lower terminal temperature differences (K).

$$A_0 = Q/(U * \Delta T_M) \tag{3.3}$$

$$\Delta T_M = LMTD * F = \left(\frac{GTTD - LTTD}{ln(GTTD / LTTD)} \right) * F \tag{3.4}$$

All variables in Eq. (3.3) are affected by changes of flow rate and inlet/outlet temperatures. Furthermore, construction materials, pressure rating and other parameters could also vary, impacting exchanger costs. Therefore, detailed heat exchanger sizing was necessary for evaluation of DSW intake impacts. Rigorous Aspen Exchanger Design and Rating v8.8 was used to size shell-and-tube exchangers and CW-SW plate exchangers, with all necessary information in Tables S2-1, S2-2, S2-3 and A2.4 (Supplement A2, Suppl. Mat.). In DSW-Case, the low temperature of compressed gas allows 6.4% reduction of water content in the NG feed to the molecular sieve TSA dehydration unit, entailing bed size reductions and/or extending TSA cycle, both advantageous aspects that were disregarded in the present analysis.

3.2.8. Equipment Costs and Weights

CAPEX and weight of equipment were estimated via Aspen Capital Cost Estimator 8.8 (ASPENTECH, 2014 data basis). Detailed information for such estimates is available in Tables A3.1 to A3.12 (Supplement A3, Suppl. Mat.).

3.2.9. Power and Fuel Gas Consumptions

The FPSO total power demand was based on plant simulation results and on complementary FPSO power consumption data from Martins et al. (2014) in Table A1.10 (Supplement A1, Suppl. Mat.). Results allowed calculation of fuel gas consumption at 100%, 75%, 50% and 25% of gas processing capacity, which were fitted against percentage of gas processing load in Fig. 3.6. These correlations were used to predict FPSO annual consumptions of power and fuel gas as shown in Fig. 3.7, assuming 8760 hours per year and process load between 18% and 100% of gas processing capacity according to raw gas feeds forecasted along 23 years of FPSO operation in Fig. IA.2. Tables IA.1 and IA.2 display the average compositions of raw NG and fuel gas, respectively.

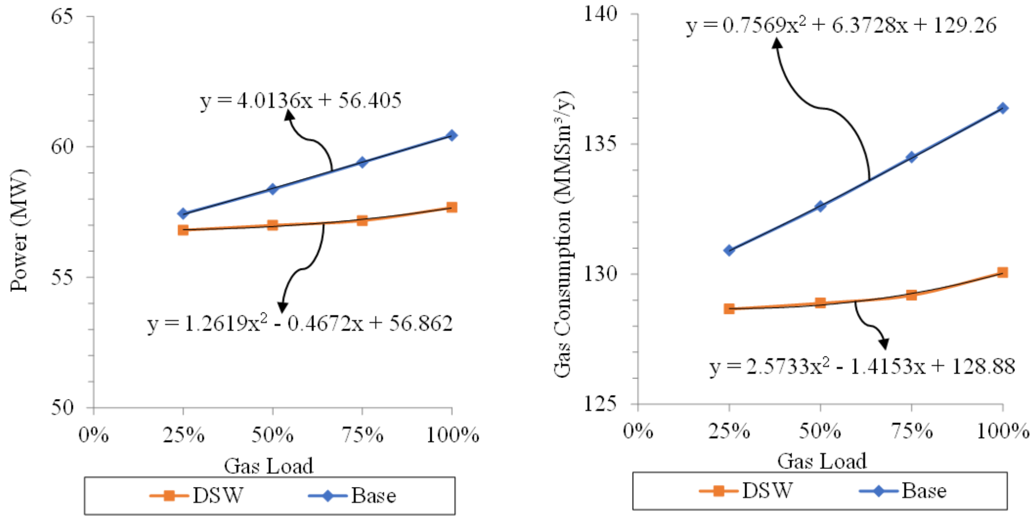

Figure 3.6. Power demand (y) and fuel gas consumption (z) *vs* gas processing load (x) for Base-Case and DSW-Case

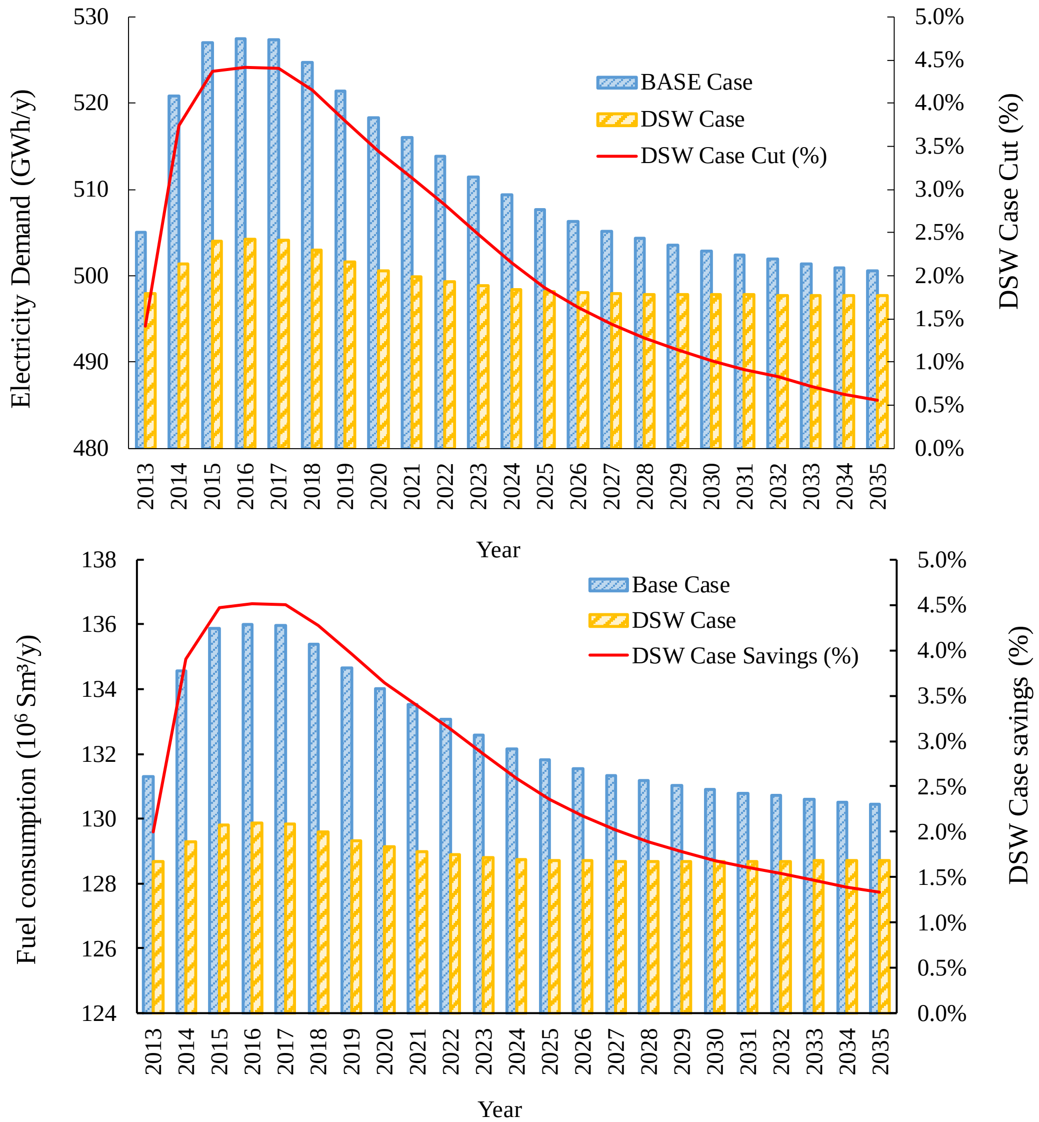

Figure 3.7. Predicted FPSO consumptions of electricity and fuel gas

3.3. Results and Discussion

Simulations, equipment sizing and economic analysis generated a massive amount of data that is organized and used to calculate secondary information and final results. A selection of the most significant results is presented in this section. Complementary results are available in Supplement A4, Suppl. Materials.

3.3.1. Process Simulation Results

3.3.1.1. Compressors

DSW intake at 4ºC decreased total compression design power by 9.0% (3.217 MW), as shown in Table A4.1 (Supplement A4 of Supplementary Materials at Appendix H). However, larger variations of power were found for some compressors (Fig. 3.8), as compressor power does not depend solely on inlet gas temperature. Compressor C-901 was excluded due to elimination of the refrigeration cycle for HCDPA (i.e. 100% power reduction). Furthermore, substitution of surface SW intake (Base-Case) by DSW intake reduced one stage of the CO_2 rich gas compression train (C-600) (i.e. 100% power reduction of C-604). Compression ratio per stage moved from 2.8 to 4.0, increasing stage power from 18% up to 38%, compared to the same stages of the Base-Case. As a rule, the higher the number of intercooled compression stages, the lower the power of the compression train as a whole (as it approaches the isothermal compression limit) and the higher the investment – as the cost of N stages grows with $\approx N*(Power/N)^{0.6}$. Prescribing three stages in C-600 instead of four in DSW-Case entails an increase in the power of each stage for two reasons: (i) higher stage compression ratio, and (ii) higher temperature increase per stage. But, as a whole, the design power of C-600 was reduced by 4% or 0.35 MW. This was possible because the lower number of stages was compensated by the lower temperature of gas inlets in virtue of DSW primary cooling.

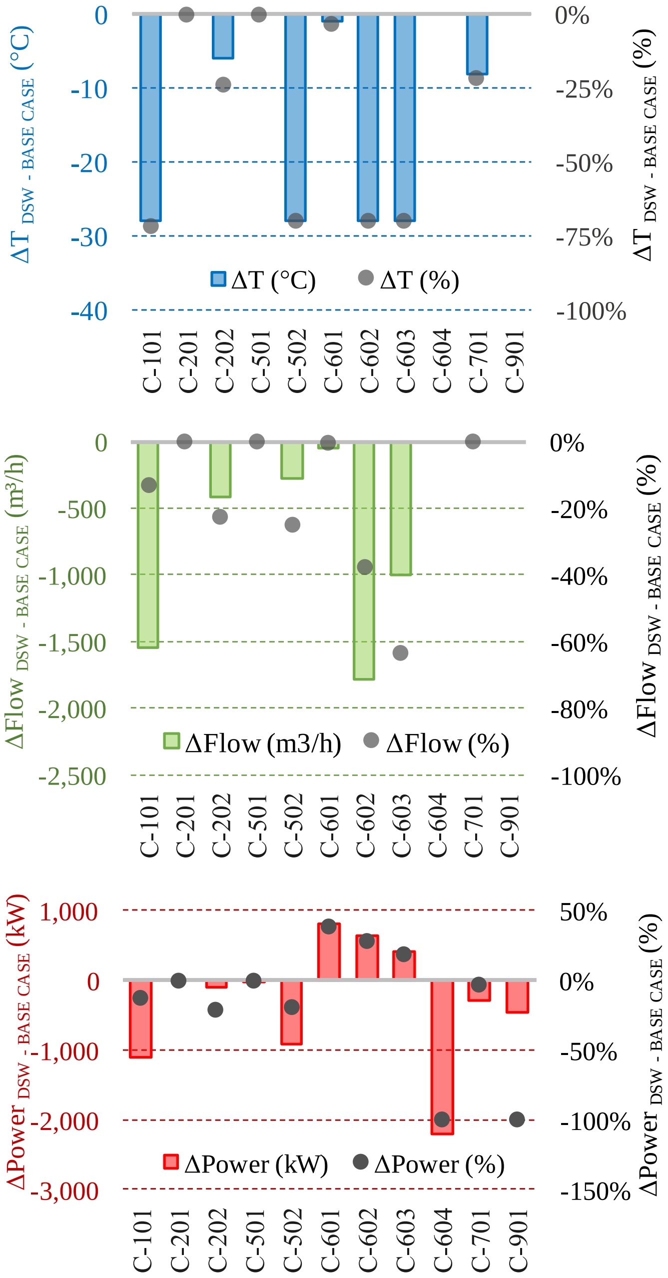

Figure 3.8. Variation of compressor performances from Base-Case to DSW-Case
***C-604 and C-901 power reductions of 100% mean they are absent in DSW-Case**

Compressors C-202 and C-502 benefited from reduced inlet flow rate and temperature achieving ≈20% of power reduction at full gas load. Comparison of compressor powers at partial loads is shown in Figs. S4-1 and A4.2 (Supplement A4 of Supplementary Materials at Appendix H). Fig. 3.9 demonstrates that the total power savings achieved in DSW-Case decreases as raw NG feed flow rate decreases, since anti-surge flow rates increase. Also, gas cooling from Joule-Thomson effect in anti-surge recycling valves limits the benefits of colder CW.

Additionally, compressors exhibited different power behavior due to process constraints in DSW-Case: gas hydrate and ice formations and minimum operating temperature of compressor materials. Thus, DSW-Case requires hot-bypasses in some compressors, to avoid such low temperature issues. From 25% to 100% of gas processing capacity, DSW intake entails 3% to 9.2% of compressor power savings.

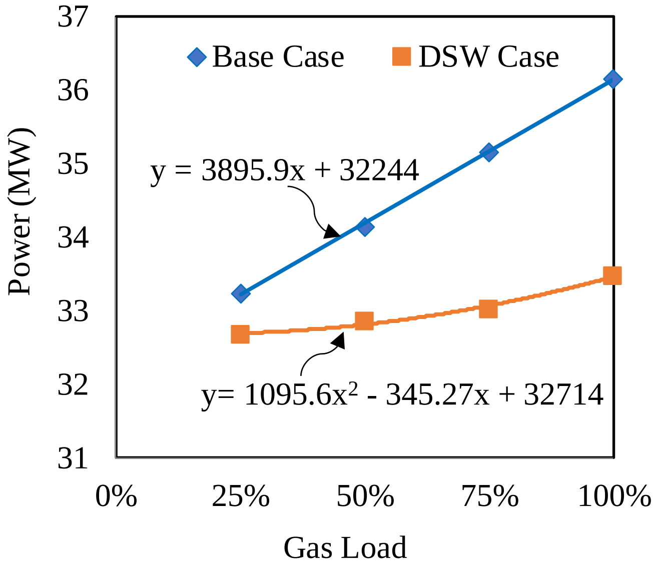

Figure 3.9. Total compressors power (y, MW) *vs* gas processing load (x, %).

As %CO_2 in associated gas increases along project lifetime, it is expected that flow rates of injection gas (C-700) and CO_2 rich gas (C-600) compression trains increase, accompanied by a decrease of the flow rate of NG exportation compressor C-500. On one hand, due to elimination of one compressor stage, the benefit of DSW intake on total design power of C-600 is modest (4% or 0.35 MW) relatively to Base-Case. On the other hand, NG compressors (C-500) running with extra gas cooling from DSW reached ≈1.0 MW lower design power. Thus, if %CO_2 increases in the raw NG feed, the advantage of DSW intake decreases. Nevertheless, if the original four stages of C-600 are maintained, the increase of %CO_2 in associated gas would favor DSW intake.

3.3.1.2. Heat Exchangers

Fig. 3.10 shows the differences in terms of duty, *LMTD* and area of heat exchangers, with exchanger IDs provided in Table A.3. Detailed exchanger results are shown in Table A4.2 (Supplement A4, Suppl. Mat.). A reduction of 6% in total heat exchangers duty was achieved in the DSW-Case, but the total heat exchange area reduction was almost negligible (1.6%). But considering shell-and-tube exchangers apart from SW plate exchangers, the respective area reduction reaches 29%. This entails an expressive decrease in weight and costs, because shell-and-tube exchangers for high-pressure gas have higher specific cost (\$/m²) and weight (kg/m²) relatively to low-pressure SW plate exchangers.

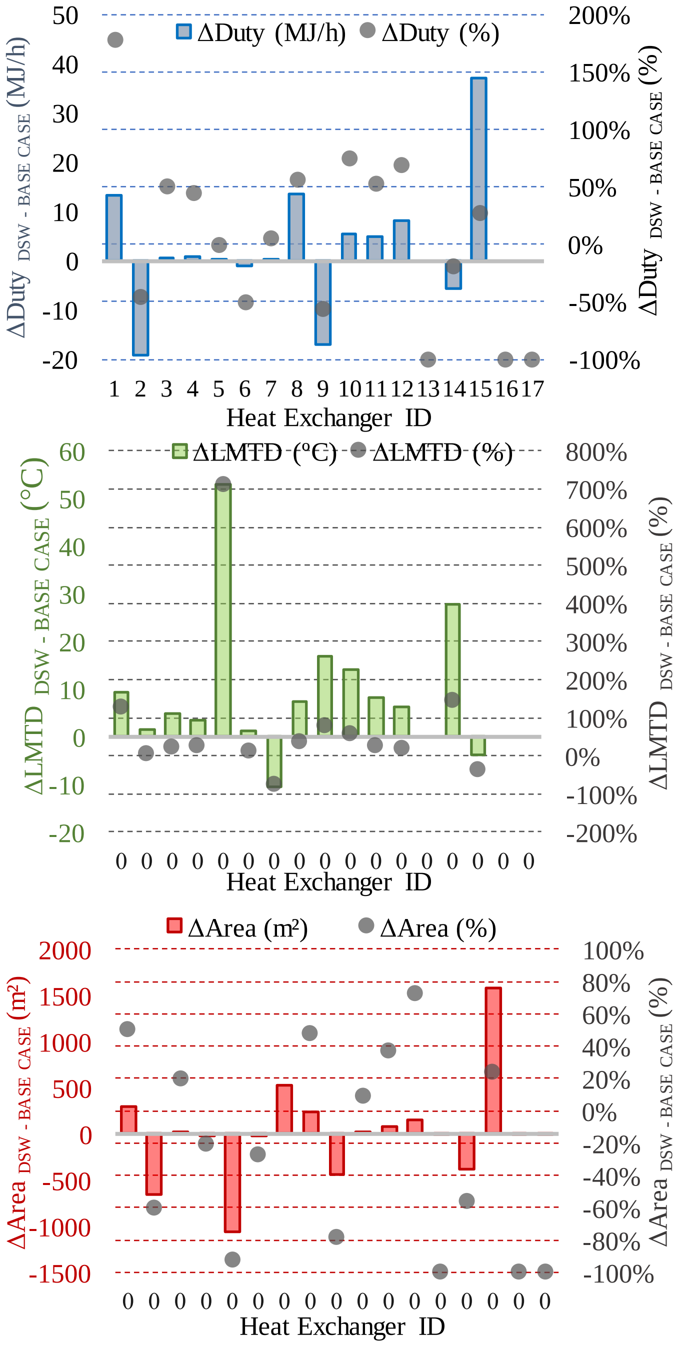

Figure 3.10. Variations of heat exchanger performances from Base-Case to DSW-Case
***Exchangers 13, 16 and 17 with 100% of area and duty reductions were absent in DSW-Case**

3.3.1.3. Gas Turbines (GTs)

Total power demands were calculated as 61.6 MW and 58.8 MW for Base-Case and DSW-Case, respectively. Considering three operating GTs, the average power per GT was 20.5 MW for Base-Case and 19.6 MW for DSW-Case. Fig. 3.11 shows the calculated power demand of compressors, CW pumps and other FPSO consumers of power. The spare power corresponds to the idle share of total generation capacity, considering the three selected GT power generation at design condition (30ºC and 94% RH), i.e. 3 x 23.5 MW for Base-Case and 3 x 22.2 MW for DSW-Case.

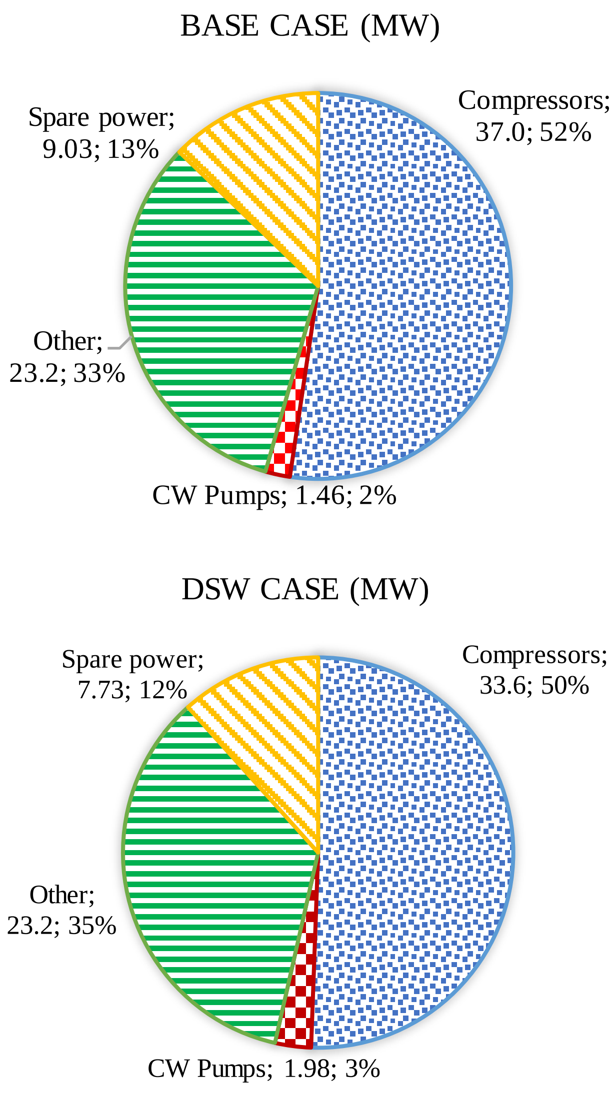

Figure 3.11. FPSO power consumers (MW) by equipment category

GTs simulation with HYSYS reproduced the same performance of the respective simulations with Thermoflex 25 for Base-Case and DSW-Case. An example of validation for full gas load at design conditions (air at 23ºC and 87% RH) is shown in Table A4-3 (Supplement A4 of Supplementary Materials at Appendix H) and GT performance comparisons at partial load are depicted in Figs. A4.2 and A4.3 (Supplement A4 of Supplementary Materials at Appendix H). Fig. 3.12 summarizes the most relevant results. It is shown that GTs of DSW-Case operate with loads from 1% to 5% greater than for the Base-Case, but the effect on efficiency is negligible at 100% gas load and reaches less than 1% for 25% gas load. CO_2 emissions are directly proportional to fuel gas consumption, presenting reductions between 1.5% and 4.5% depending on % gas load.

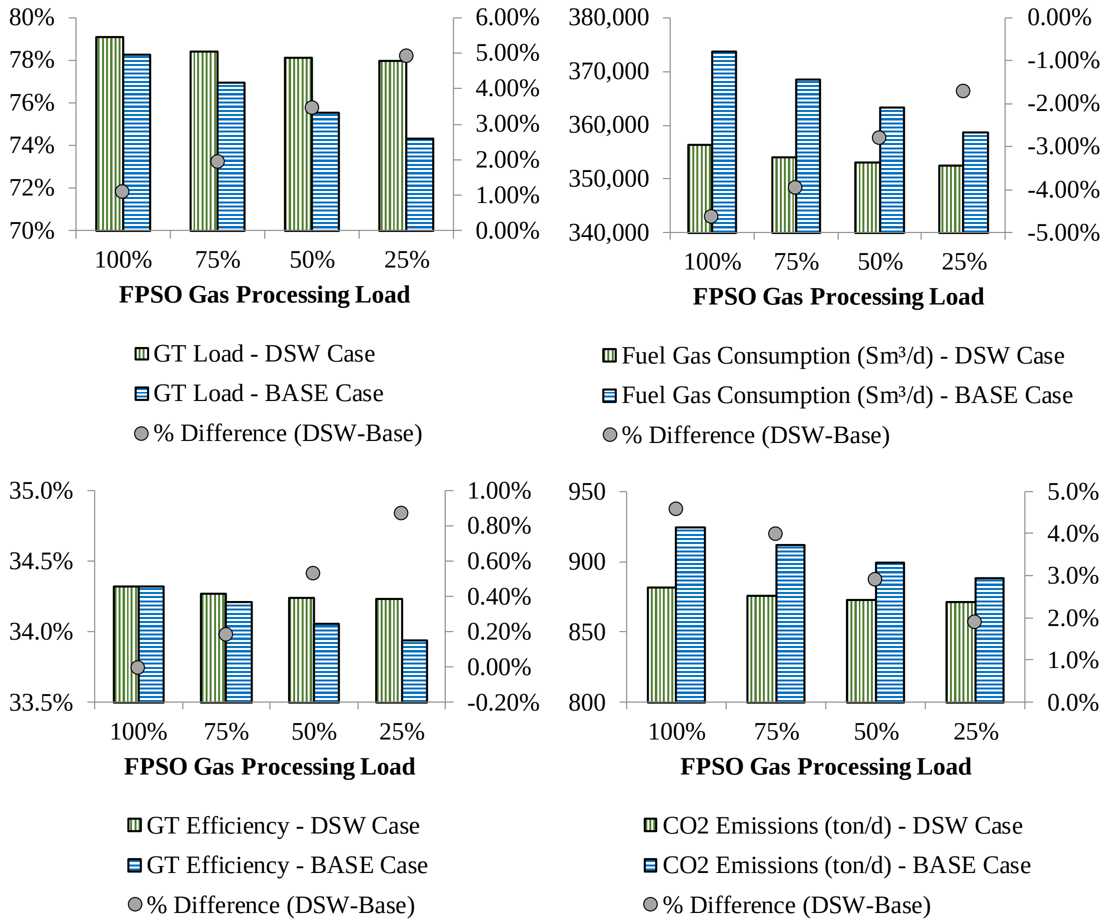

Figure 3.12. Gas turbine (GTs) relative performances of DSW-Case and Base-Case *vs* % gas plant load

3.3.1.4. Pumps

The design SW flow rate of the DSW-Case was 31% greater than Base-Case. Nevertheless, this result is almost irrelevant because, as shown in Fig. 3.11, pumps are responsible for less than

3% of total FPSO power consumption. A summary of pumps results is in Table A4.4 (Supplement A4, Suppl. Mat.).

3.3.2. Energy Usage Efficiency and CO_2 Emissions

The energy usage efficiency of the gas plant is compared in terms of MWh/Sm³ of treated NG exported. From 25% up to 100% of gas load, the DSW-Case achieved an increase from 2.7% up to 5.0% in energy usage efficiency as shown in Fig. 3.13.

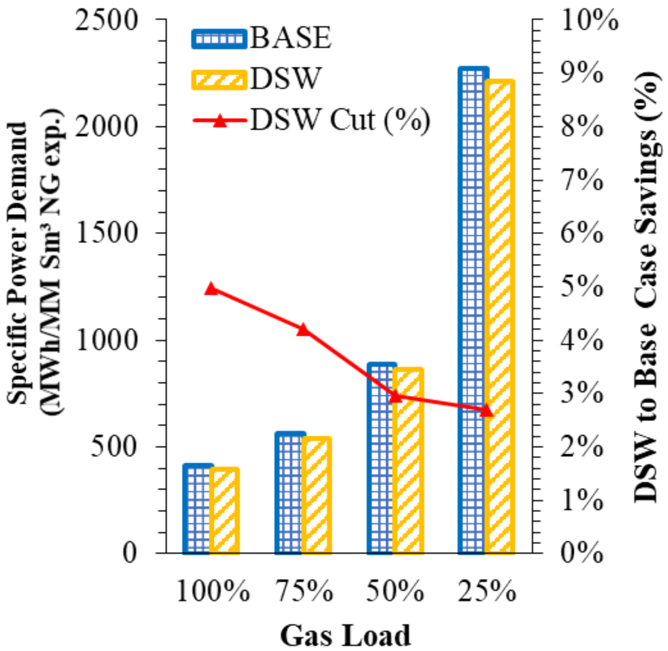

Figure 3.13. FPSO Specific Power Demand (MWh/MM Sm³ NG exported) and its % savings in DSW-Case relative to Base-Case *vs* gas plant % load

Fig. 3.14 shows the comparison of CO_2 emissions for DSW-Case and Base-Case along the FPSO lifetime. DSW-Case emits 1.5% to 4.2% less CO_2 than Base-Case, depending on the year of operation. An average emission reduction of 9327 tCO_2/y was achieved. The total reduction for 23 years of operation is 214,500 tCO_2, or 3% of Base-Case emissions. Besides making FPSO operation more environmentally sound, DSW intake can be more profitable in case of carbon taxation as shown in the sensitivity analysis of Fig. 3.15, where the range of carbon taxes is based on World Energy Outlook 2016 (IEA, 2016). The annual extra savings due to lower carbon emissions of DSW-Case were negligible for 1 US$/$tCO_2$ taxation but could become relevant for higher carbon taxes. Considering in Fig. 3.15 the maximum carbon taxation (130 US$/t) and gas production, the savings could reach 2.1 MMUS$/y.

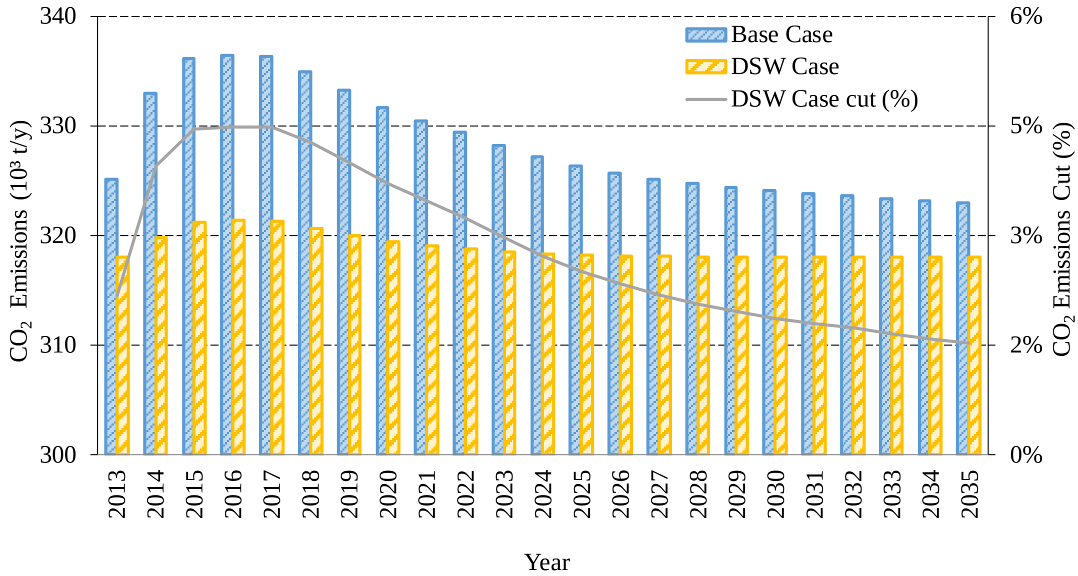

Figure 3.14. FPSO CO_2 emissions along project lifecycle

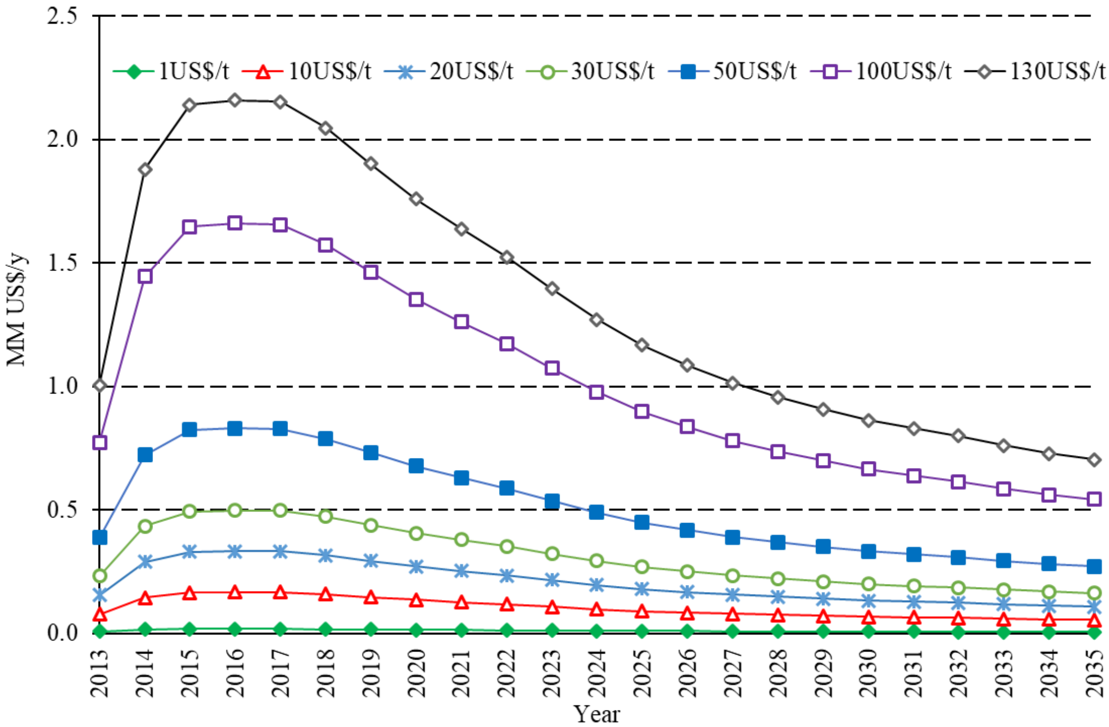

Figure 3.15. Sensitivity of avoided carbon taxation costs (MMUS$/y) with carbon tax along FPSO lifecycle with DSW-Case

3.3.3. Equipment Weight and Capital Costs

Equipment weight and CAPEX were estimated with ASPEN Capital Cost Estimator 8.8. A summary of results is presented in Table 3.6. Detailed results of equipment weight and CAPEX are available for Base-Case and DSW-Case in Tables A4.5 to A4.10, (Supplement A4, Suppl.

Mat.). CAPEX savings in the DSW-Case does not include the potential reduction of FPSO hull cost due to reducing topside weight. Additionally, an extra income of 6.2 MMUS$ (net present value) is achieved by the DSW-Case, considering extra NG revenues due to lower fuel gas consumption. Total savings correspond to 1.33% of FPSO total fixed investment estimated as 1.6 Billion US$, while the estimated CAPEX reduction by DSW intake is ~15 MMUS$. It is worth noting that DSW intake may become less attractive according to the magnitude of its lifecycle cost – CAPEX plus all maintenance costs of DSW intake piping and connections. Hence, the obtained savings in virtue of DSW intake of ~21 MMUS$ considering CAPEX and OPEX of the gas plant, may be overshadowed by the lifecycle cost of the intake piping itself, in which case the DSW intake solution would be rendered economically unfeasible.

A rough estimative of (non-installed) piping cost for DSW intake at 900 m of depth is ~1.0 MMUS$ for two parallel 26” x 1200 m risers (710 mm nominal diameter) made of high density polyethylene (HDPE 100), with nominal pressure class 1600 kPa (PN 16) and standard diameter ratio 11 (SDR 11), which is rated at ~US$ 440/m. However, the real lifecycle cost depends on the installed structure to keep the risers in the right position (buoys, anchors, cables) and its maintenance expenses. Moreover, the challenge to implement the new technology goes beyond economic calculations. Intake design, pipelines lifetime, installation and maintenance are determinant aspects to prove the technical economic feasibility of DSW intake technology.

Table 3.6. Summary of equipment weight and CAPEX results

Equipment	Total Weight (t)		Δ (t)	Δ (%)	CAPEX (MM US$)		Δ (MMUS$)	Δ (%)
	BASE CASE	DSW CASE			BASE CASE	DSW CASE		
Compressors	349	306	43	-14	80.2	77.2	-2.93	-3,7
Exchangers	529	357	150	-42	39.2	34.4	-4.81	-12
GTs	902	858	44	-5.1	36.9	29.2	-7.69	-21
CW Pumps	18	21	-3.4	16	1.97	2.39	0.42	22
TOTAL	1798	1572	-226	-14	158	143	-15	-9.5

3.3.4. Extra NG Revenues

As seen in the DSW-Case, DSW intake can lower fuel gas consumption and increase NG exportation from 0.2% to 2.0% on FPSO lifecycle according to % gas load. However, the actual additional NG revenues are lower than the resulting reduction of fuel gas burned, because part of the additional treated gas is reinjected due to unavailability of sub-sea pipelines whose implementation normally follows a different scheduling. Nevertheless, DSW intake could allow extra revenues according to the availability of pipeline capacity to export such extra gas. This potential extra NG exportation effect is shown in Fig. 3.16. Fig. 3.17 depicts a sensitivity analysis of the potential extra annual revenues from NG exportation for NG price ranging from 4 US$/MMBTU to 14 US$/MMBTU.

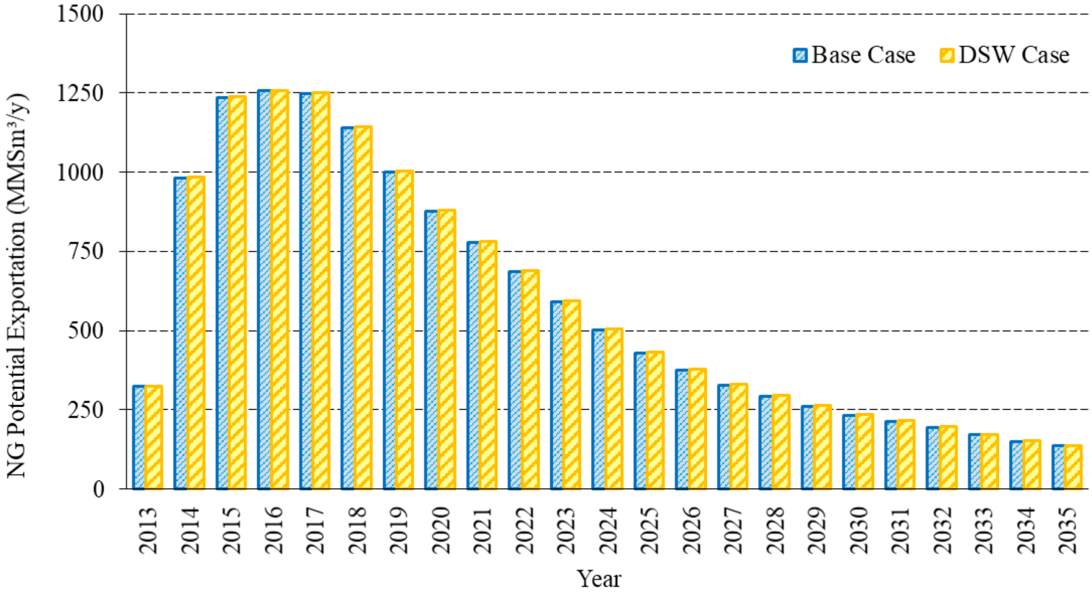

Figure 3.16. NG potential exportation of Base-Case and DSW-Case along FPSO lifecycle

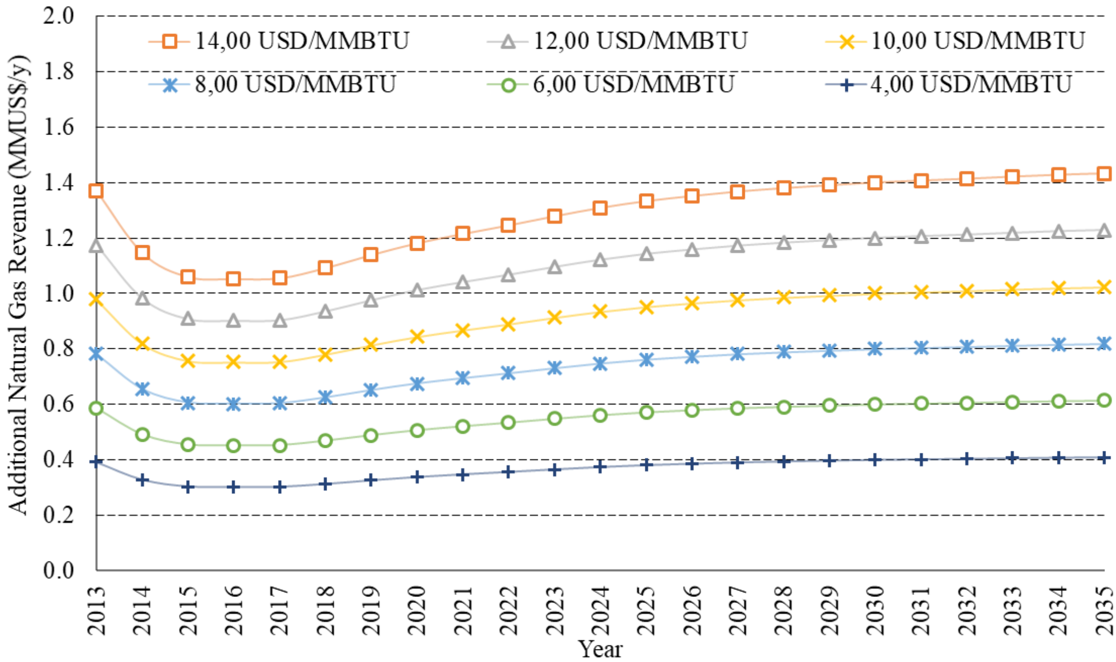

Figure 3.17. Sensitivity of extra NG annual revenues (MMUS$/y) with NG price along FPSO lifecycle

3.4. Conclusions

This work investigated the gains of power consumption, economic responses and CO_2 emissions as conventional surface SW intake is replaced by deep seawater (DSW) intake at 900 m of depth for use as primary cooling of FPSOs processing CO_2 rich NG at tropical deepwaters. The investigation consisted in comparing a Base-Case gas plant with conventional surface SW intake against the proposed alternative DSW-Case gas plant with DSW intake. The Base-Case corresponds to a selected FPSO (*Cidade de Paraty*) operating in Brazil Pre-Salt basin and processing a nominal flow rate of 5 MMSm^3/d of raw NG with average CO_2 content of 15%mol. The resulting variations of gas processing layout, electricity generation capacity, energy usage efficiency and CO_2 emissions were assessed using rigorous thermodynamic simulation and specific engineering software for detailed process design and cost analysis. Results showed reduction of CO_2 emissions and increase in energy usage efficiency from 2.7% to 5.0%, depending on % gas processing load, where the highest value corresponds to full gas processing load.

Equipment sizing and costs were estimated for Base-Case and DSW-Case and compared. DSW intake promotes modest CAPEX and topside weight savings if compared to total FPSO cost and weight, but results are expressive considering only the gas processing and electricity generation modules. Furthermore, DSW intake also leads to other indirect advantages like less fuel gas consumption, less CO_2 emission, less FPSO power demand, elimination of the refrigeration cycle for hydrocarbon dew-point adjustment (HCDPA) and 6% reduction of water content in the gas feed to dehydration TSA units for water dew-point adjustment (WDPA), which could result in extended TSA cycle and/or smaller molecular sieve bed, lowering TSA weight and CAPEX. Modifications on gas processing capacity, HCDPA and WDPA systems, NG CO_2 content, exportation/injection ratio and other processing characteristics would lead to different DSW intake impacts on FPSO energy usage efficiency, CAPEX, operational costs and equipment weight.

Although the study has reached its main goals, there were some limitations of scope due to the huge size of the problem and the already massive calculations to report. Firstly, the effect of the continuous increase of CO_2 content in the associated gas along project lifetime was disregarded; i.e. the analysis only considered the average lifetime value of 15%mol CO_2 in the raw NG. Secondly, for the same reason, it was not possible to investigate DSW intake effects over the usual range of FPSO gas processing capacities and CO_2 content in the feed gas, e.g., 2.0 – 12.0 MMSm³/d and 5%mol - 80%mol, respectively. Thirdly, the impact of DSW intake on gas dehydration units using expensive TSA cycles was detected as advantageous, but was not adequately measured. In the same way, it was not assessed the potential impact of DSW intake on certain specific gas processing alternatives such as HCDPA via Joule-Thomson expansion or supersonic separator instead of propane refrigeration; CO_2 separation via chemical absorption or supersonic separator or cryogenic distillation instead of MP, or even hybrid capture processes (e.g., chemical absorption coupled to MP) instead of pure MP.

Additionally, the DSW flow along the intake piping was considered isothermal at 4°C, which is not realistic as some heavy insulation would be necessary on the 900 m risers, impacting DSW intake costs. Nevertheless, it is straightforward to estimate the profile of temperature along the intake risers in order to obtain DSW temperature at the inlet of the plate heat exchanger (DSW/CW). Another aspect has to do with the lack of specificity of the cost estimation method for offshore plants and ultra-high pressures (> 20000 kPa), probably resulting in underestimated equipment fixed investment (CAPEX). In connection to this point, lifecycle cost evaluation of the installed piping for DSW intake must also be performed in order to determine the ultimate feasibility of DSW intake technology.

By last, the feasibility of DSW intake should be also investigated within a continuous or mixed-integer non-linear optimization framework so that certain features that were assumed pre-defined and constant in this study could vary in order to seek optimum values, configurations and dimensioning. For instance, the present analysis showed that certain FPSO units become problematic if cooled with cold CW at 7ºC, being preferable to use traditional CW with conventional thermal range 35ºC-55ºC. Therefore a possible optimization formulation would consider two independent CW circuits – 35ºC-55ºC CW and 7ºC-27ºC CW, the latter requiring more expensive lines with insulation, etc – whose service heat loads, allocation points, exchanger/pump dimensioning and circulation flow rates are continuous or mixed-integer decision variables to be sought. Opportunely, two independent seawater intakes could also be considered as primary cooling – conventional SW and DSW – whose flow rates and intake dimensioning (e.g. riser diameters and pumps) are also passive of mixed-integer optimization. In this case, it is conceivable to let free the exiting temperature of DSW in the plate exchanger to reach the maximum environmental limit of 40ºC for disposal (counterpointing the narrow DSW thermal range stipulated in Table 3.1), this way reducing DSW flow rate and the cost of deep-intake piping, insulations, pumps and footprint for the same total heat load. Relaxing the exiting temperature of DSW seems a reasonable point to be questioned by optimizations as it has some thermodynamic support in the context of exergy analysis. In the present study DSW is returned to the sea at 11ºC only (Table A1.8, Supplement A1, Suppl. Mat.) with a huge flow rate of 1.64 m^3/s (Table A4.4, Supplement A4, Suppl. Mat.). This represents a valuable flow of exergy (relative to reference SW environment at 32ºC) being wasted in the present DSW implementation. This flow of wasted exergy could be reduced by returning a lower flow rate of hotter DSW to the sea at the expenses of using larger heat exchangers in the process.

3.5. References of Chapter 3

Araújo O de QF, Reis A de C, de Medeiros JL, Nascimento JF, Grava WM, Musse APS. Comparative analysis of separation technologies for processing carbon dioxide rich natural gas in ultra-deepwater oil fields. J. Clean. Prod. 2017; 155:12–22, doi:10.1016/j.jclepro.2016.06.073.

Araújo O de QF and de Medeiros JL. Carbon capture and storage technologies: present scenario and drivers of innovation. Current Opinion in Chemical Engineering 2017, 17, 22–34, doi 10.1016/j.coche.2017.05.004

Arinelli LO, Trotta TAF, Teixeira AM, de Medeiros JL, Araújo O de QF. Offshore Processing of CO2 Rich Natural Gas with Supersonic Separator versus Conventional Routes. J. of Nat. Gas Sci. and Eng. 2017, 46, 199-221, doi 10.1016/j.jngse.2017.07.010

Asibor E, Marongiu-Porcu M, Economides MJ. Oil production optimization without natural gas constraints: The harvesting of upstream natural gas. J. Nat. Gas Sci. Eng. 2013; 15:59–68, doi:10.1016/j.jngse.2013.09.004.

Blomster TJ, Stanimirov M. Continuously extruded long length polyethylene pipes for seawater intakes and marine outfalls. Desalination 2004; 166:275–286, doi:10.1016/j.desal.2004.06.082.

Boyce MP. GasTurbine Engineering Handbook. 2nd Ed. Houston, Gulf Professional Publishing, 2002.

CONAMA. Resolução CONAMA 430/2011. DOU 2011:9.

Gallo WLR, Gallego AG, Acevedo VL, Dias R, Ortiz HY, Valente BA. Exergy analysis of the compression systems and its prime movers for a FPSO unit. J. Nat. Gas Sci. Eng. 2017; 44:287–298, doi:10.1016/j.jngse.2017.04.023.

GPSA. Engineering Data Book. 20th Ed., Gas Processors Suppliers Association, 2004.

IEA. World Energy Outlook 2016. 2016.

IOGP. Environmental Performance Indicators - 2015 data. London: 2016.

Martins PM, Delfino B, Fachini R. Projeto de Sistemas Oceânicos II. FPSO Campo de Libra. UFRJ 2014. http://www.deno.oceanica.ufrj.br/deno/prod_academic/relatorios/2014/RafaelFachini+BrunoDelfino/relat2/relat2_completo.htm (accessed January 1, 2017).

Nguyen T-V, Pierobon L, Elmegaard B, Haglind F, Breuhaus P, Voldsund M. Exergetic assessment of energy systems on North Sea oil and gas platforms. Energy 2013; 62:23–36, doi:10.1016/j.energy.2013.03.011.

Nguyen T-V, Tock L, Breuhaus P, Maréchal F, Elmegaard B. Oil and gas platforms with steam bottoming cycles: System integration and thermoenvironomic evaluation. Appl. Energy 2014; 131:222–237, doi:10.1016/j.apenergy.2014.06.034.

Nguyen T-V, Fülöp TG, Breuhaus P, Elmegaard B. Life performance of oil and gas platforms: Site integration and thermodynamic evaluation. Energy 2014; 73, doi:10.1016/j.energy.2014.06.021.

Nguyen T-V, Voldsund M, Breuhaus P, Elmegaard B. Energy efficiency measures for offshore oil and gas platforms. Energy 2016; 117:325–40, doi:10.1016/j.energy.2016.03.061.

Nguyen T-V, Tock L, Breuhaus P, Maréchal F, Elmegaard B. CO2-mitigation options for the offshore oil and gas sector. Appl. Energy 2016; 161:673–694, doi:10.1016/j.apenergy.2015.09.088.

Petkovic MAL, Sattamini SR, Moraes CAC, Cavalcanti GN. Sistema de captação de água a grandes profundidades para plataformas semi-submersíveis de produção. PI9102045A, 1993.

Petrobras. Polo Pre-Sal - Bacia de Santos - Etapa 1. IBAMA 2013. http://licenciamento.ibama.gov.br/Petroleo/Producao/Producao - Polo Pre-Sal - Bacia de Santos - Etapa 1 - Petrobras/ (accessed July 4, 2017).

Pierobon L, Nguyen T Van, Larsen U, Haglind F, Elmegaard B. Multi-objective optimization of organic Rankine cycles for waste heat recovery: Application in an offshore platform. Energy 2013; 58, doi:10.1016/j.energy.2013.05.039.

Pierobon L, Haglind F. Design and optimization of air bottoming cycles for waste heat recovery in off-shore platforms. Appl. Energy 2014; 118, doi:10.1016/j.apenergy.2013.12.026.

Rivera-Alvarez A, Coleman MJ, Ordonez JC. Ship weight reduction and efficiency enhancement through combined power cycles. Energy 2015; 93, doi:10.1016/j.energy.2015.08.079.

Rogez F. Deep large seawater intakes: a common solution for Floating LNG in oil & gas industry and OTEC in marine renewable energy. 4th Int. Conf. Ocean Energy, 2012, 1–6.

Rui Z, Li C, Peng F, Ling K, Chen G, Zhou X. Development of industry performance metrics for offshore oil and gas project. J. Nat. Gas Sci. Eng. 2017; 39:44–53, doi:10.1016/j.jngse.2017.01.022.

Teixeira AM, Arinelli LO, de Medeiros JL, Araújo OQF. Exergy Analysis of monoethylene glycol recovery processes for hydrate inhibition in offshore natural gas fields. J. of Nat. Gas Sci. and Eng. 2016, 35, 798-813, doi 10.1016/j.jngse.2016.09.017

TEMA. Standards of the Tubular Exchanger Manufacturers Association. 9th ed. Tarrytown, NY: Tubular Exchanger Manufacturers Association, INC.; 2007.

Voldsund M, Ertesvag IS, He W, Kjelstrup S. Exergy analysis of the oil and gas processing on a north sea oil platform a real production day. Energy 2013; 55:716–727, doi:10.1016/j.energy.2013.02.038.

Voldsund M, Nguyen T-V, Elmegaard B, Ertesvåg IS, Røsjorde A, Jøssang K, et al. Exergy destruction and losses on four North Sea offshore platforms: A comparative study of the oil and gas processing plants. Energy 2014; 74:45–58, doi:10.1016/j.energy.2014.02.080.

Wei C, Huang B-J, Kong M-S. Engineering Analysis of Pumping Cold Deep Nutrient-Rich Seawater for Mariculture and Nuclear Power Plant Cooling. Ocean. Eng. 1980; 7:501–520.

3.6. Appendix 3A: *Cidade de Paraty* Plant, Gas Production, Inlet Streams, Fuel Gas and Exchanger IDs

Table 3A.1. Gas plant inlet streams for simulation from EIA

	OIL	GAS	WATER
Temperature (°C)	40	40	40
Pressure (kPa)	41368	41368	41368
Composition (mol fraction)			
CO_2	0.0000	0.1513	0.0000
H_2S	0.0000	0.0000	0.0000
N_2	0.0000	0.0051	0.0000
Methane	0.0000	0.6396	0.0000
Ethane	0.0000	0.0924	0.0000
Propane	0.0050	0.0591	0.0000
i-Butane	0.0019	0.0099	0.0000
n-Butane	0.0081	0.0207	0.0000
i-Pentane	0.0065	0.0052	0.0000
n-Pentane	0.0122	0.0075	0.0000
C_6*	0.0295	0.0063	0.0000
C_7*	0.0559	0.0009	0.0000
C_8*	0.0777	0.0016	0.0000
C_9*	0.0658	0.0005	0.0000
C_10*	0.0604	0.0000	0.0000
C_11*	0.0405	0.0000	0.0000
C_12*	0.0537	0.0000	0.0000
C_13*	0.0488	0.0000	0.0000
C_14*	0.0436	0.0000	0.0000
C_15*	0.0308	0.0000	0.0000
C_16*	0.0339	0.0000	0.0000
C_17*	0.0224	0.0000	0.0000
C_18*	0.0236	0.0000	0.0000
C_19*	0.0224	0.0000	0.0000
C20+*	0.3573	0.0000	0.0000
H2O	0.0000	0.0000	1.0000
MM C20+		500	
Density C20+		0.9496	

Table 3A.2. Fuel Gas Properties (Base-Case from EIA)

	Base Case	DSW Case
Pressure (kPa)	3500	3500
Temperature (°C)	22.5	22.5
LHV (kJ/kg)	43487	43486
HHV (kJ/kg)	47848	47847
Molar Mass (kg/kgmol)	22.91	22.92
COMPOSITION (Mol Fraction)		
N_2	0.00672	0.00673
CO_2	0.05000	0.05000
Methane	0.69910	0.70100
Ethane	0.14380	0.14000
Propane	0.06802	0.06966
n-Butane	0.01684	0.01687
n-Pentane	0.00567	0.00583
Hexane	0.00093	0.00099
Isobutane	0.00892	0.00892

Table 3A.3. Heat Exchangers IDs in Fig. 3.10

Base-Case		DSW-Case	
ID in Fig. 3.10	TAG	ID in Fig. 3.10	TAG
1	SHX-101	1	SHX-101
2	SHX-102	2	SHX-103
3	SHX-201	3	SHX-201
4	SHX-202	4	SHX-202
5	SHX-301	5	SHX-102
6	SHX-302	6	SHX-301
7	SHX-303	7	SHX-302
8	SHX-501	8	SHX-501
9	SHX-502	9	SHX-502
10	SHX-601	10	SHX-601
11	SHX-602	11	SHX-602
12	SHX-603	12	SHX-603
13	SHX-604	14	SHX-701
14	SHX-701	15	SHX-801
15	SHX-801		
16	SHX-901		
17	SHX-902		

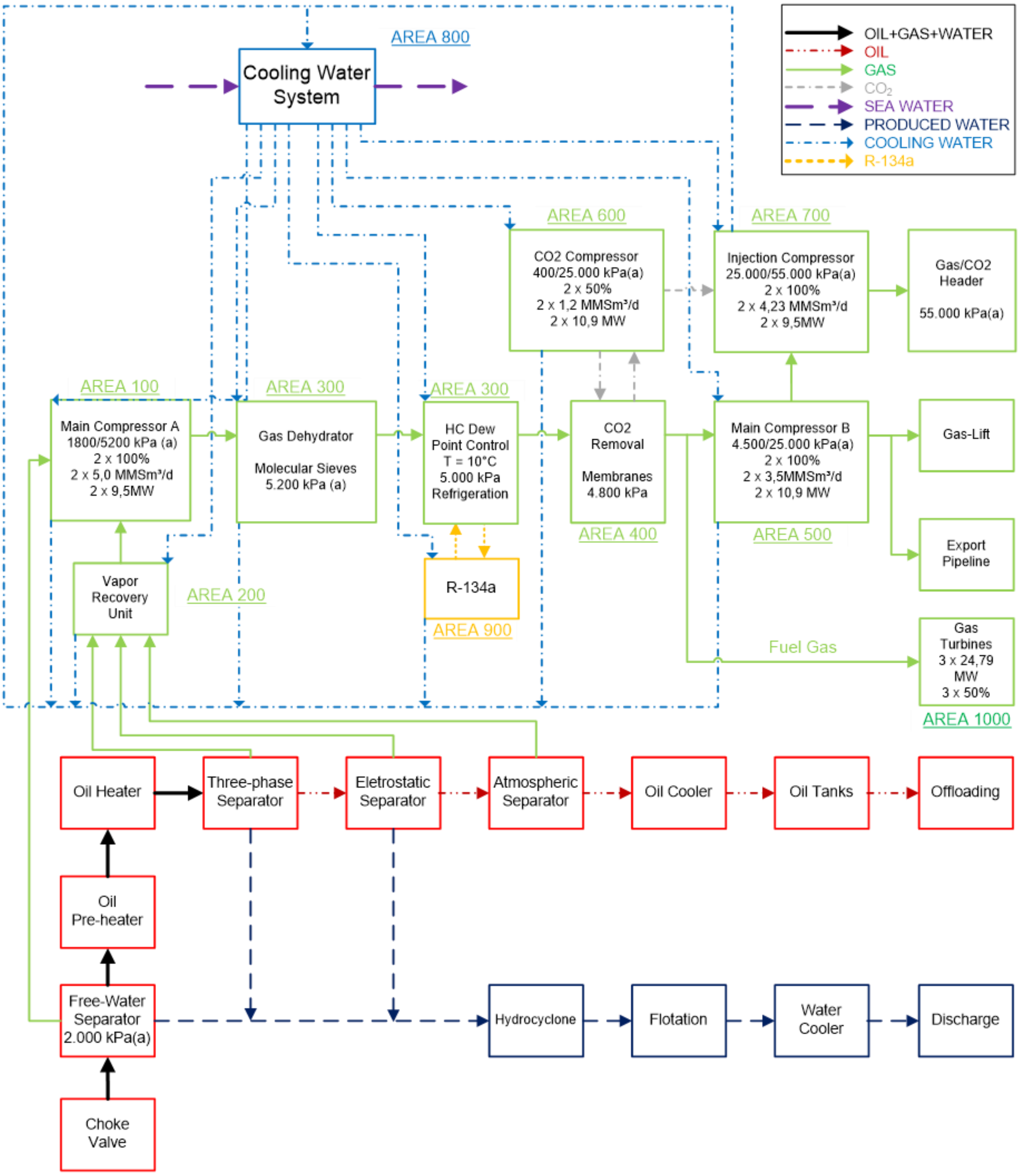

Figure 3A.1. Block diagram of topside plant of FPSO *Cidade de Paraty*

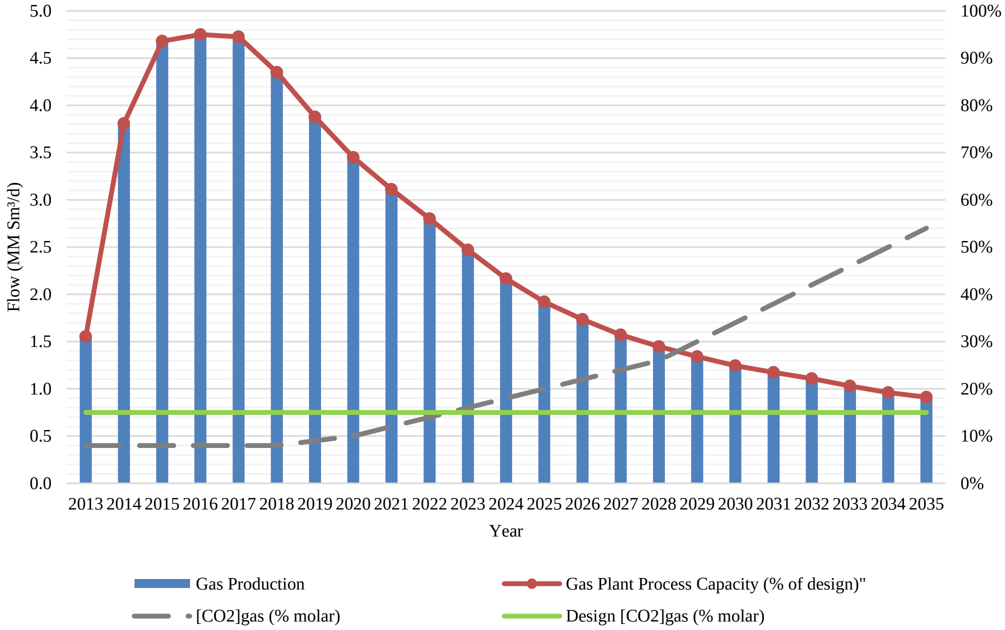

Figure 3A.2. Forecasted gas production
(%CO_2 curve estimated with only initial 8%mol and final 55%mol from EIA)

4. EXERGY, ENERGY AND EMISSIONS ANALYSIS OF COMPRESSORS SCHEMES IN OFFSHORE RIGS: CO_2-RICH NATURAL GAS PROCESSING

This chapter was submitted as a full-length original article to the Journal of Natural Gas Science and Engineering, in February, 22th of 2020. Manuscript Code: JNGSE-D-20-00340

Abstract

Deepwater oil and associated gas productions resort to floating rigs operating at continuously decreasing gas-loads during the last three quarters of the field campaign. As centrifugal compressors are sized at maximum loads, anti-surge recycles are used making operation inefficient in terms of power consumption and emissions per oil barrel produced. Smaller paralleled compressors and variable-speed drivers are investigated at peak and partial gas-loads and compared to traditional anti-surge recycle designs in terms of exergy efficiency, investment, footprint and emissions. Oversized compressors with anti-surge recycles result in almost constant power consumption along process lifespan, regardless the gas-load, increasing fuel and CO_2 intensities as gas-load decreases and attaining exergy efficiencies of 49% and 83% at 25% and 100% gas-loads, respectively. On the other hand, with variable-speed drivers and smaller paralleled compressors, power consumption becomes proportional to gas-load with exergy efficiencies always between 80% and 88%, and attaining 11% and 39% less power consumptions at 100% and 25% gas-loads. Moreover, CO_2 intensity and investment are, respectively 34% and 3% less than in traditional layouts with oversized compressors. These savings resulted from eliminating a gas turbine thanks to lower power demand when no anti-surge recycles are used.

Keywords: Offshore gas processing; CO_2-rich natural gas; Centrifugal compressors; Anti-surge recycle; Exergy analysis; CO_2 emissions.

Supplementary Materials for this chapter are found in the Appendix H, Section B.

Abbreviations

BOE Equivalent Oil Barrel; bbl/d Barrels per Day; CW Cooling-Water; EOR Enhanced Oil Recovery; FPSO Floating Production, Storage & Offloading; GT Gas-Turbine; HCDPA Hydrocarbon Dew-Point Adjustment; MMSm^3/d Million Standard m^3 per Day; MP Membrane-Permeation; MPSC Multiple-Paralleled Smaller Compressors; MMUSD Million US Dollars; NG Natural Gas; PHW Pressurized-Hot-Water; PR-EOS Peng-Robinson Equation-of-State; RER Reference Environmental Reservoir; RPM Revolutions per Minute; SW Seawater; SSLC Single-Shaft Larger Compressors; WDPA Water Dew-Point Adjustment; VRU Vapor-Recovery Unit; VSD Variable-Speed Driver.

Nomenclature

$\dot{B}$	*Exergy flow rate (kW)*
CO_{2eq}	*CO_2 equivalent*
F_j	***jth*** *feed flow rate (kmol/s)*
FCI	*Fixed Capital Investment (MMUSD)*
$\bar{H}$	*Molar enthalpy (kJ/kmol)*
K_j	***jth*** *product flow rate (kmol/s)*
LMTD	*Log-Mean temperature difference (^oC)*
nc, nfs, nps	*Numbers of components/feeds/products*
nwi, nwe	*Numbers of imported/exported powers*
P, Q	*Pressure (bar,kPa), Heat duty (kW)*
R	*Ideal gas constant ($R=8.314*10^{-5}bar.m^3/mol.K$)*
$\bar{S}$	*Molar entropy (kJ/kmol.K)*
T, $\bar{V}$	*Temperature (K), Molar volume (m^3/kmol)*
$\dot{W}$	*Shaft-Power (MW)*
Y, Z	*Molar fraction, Compressibility factor*

Greek Symbols

μ_k	*Chemical potential of k^{th} species*
η, η_P	*Exergy and polytropic efficiencies*
$\dot{\Omega}_S$	*Entropy creation rate (kW/K)*

Superscripts

exported, imported	*Exported, Imported*
W	*Mechnical power*

Subscripts

Burn, Emitted	*Combustion, Emitted*
in, in.total	*Inlet, Total Inlet*
inj	*Full-Injection*
out, out,total	*Outlet, Total Outlet*
Produced, Exp	*Produced, Exported*

4.1. Introduction

According to the International Energy Agency (IEA, 2018), the global energy demand will increase by ~25% until 2040, making oil and natural gas (NG) responsible for ~50% of the global energy consumption in the same period. Additionally, NG partially replaces coal in power generation until 2030, becoming the second source in the global energy matrix (Copenhagen Economics, 2017). In 2018 oil and NG were responsible for 5.2 gigatonnes of CO_2 equivalent (CO_{2eq}) liberated into the atmosphere, where ~2/3 of such emissions resulted from in-place power/heat productions (IOGP, 2016). Meanwhile, the Paris Agreement forced the oil-and-gas industry to limit operational emissions, resulting that major oil companies worldwide are now considering climate-change policies on planning and investment decisions; i.e., environmental and economic objectives must be balanced because regulatory policies, such as carbon-taxation and efficiency standards, can affect supply/demand and prices of fossil fuels (Chevron, 2018).

Given the growing oil-gas demands, deepwater oil-gas fields attracted investments worldwide in which Floating Production, Storage and Offloading (FPSO) vessels are the preferred production concept for large-scale projects at remote offshore locations without pipeline systems, primarily due to lower installation-decommissioning costs, flexibility and large storage capacity (Araújo et al., 2017). Currently, 186 FPSOs operate worldwide, with 24 FPSO awards expected by 2020, 8 of them in Pre-Salt Basin, Brazil (Rystad Energy, 2019).

A typical FPSO operates with low-efficiency power-producing, power-consuming and heat-producing systems. On one hand, gas-turbines (GT) are the main power-producing systems and operate without heat-recovery steam-generators; i.e., only waste-heat recovery units transfer some heat from flue-gas to pressurized-hot-water (PHW) and combined-cycles are vetoed due to footprint/weight/safety restrictions. On the other hand, major power-consuming systems are single-shaft large centrifugal compressors (SSLC) designed for high gas-loads, which waste power in anti-surge gas recycles at low gas-loads as shown in Cruz et al. (2018) who investigated benefits of deep-seawater to cool cooling-water (CW) for SSLC trains that respond for 52% of the power demand of a Pre-Salt FPSO processing CO_2-rich NG and dispatching CO_2 to Enhanced Oil Recovery (EOR).

New oil-and-gas sector regulations have demanded technology improvements to mitigate environmental impacts of offshore units. Rational and optimized energy utilization leads to less power/emission intensive FPSOs. Pierobon et al. (2014) investigated waste-heat recovery in offshore rigs. Allahyarzadeh-Bidgoli et al. (2018) performed energy optimization of Pre-Salt FPSOs. Barrera, Bazzo and Kami (2015), Reis and Gallo (2018) and Veloso et al. (2018) studied optimization of FPSO power production with organic Rankine-Cycles, while Roussanaly et al. (2018) techno-economically analyzed offshore power generation with carbon capture and storage.

4.1.1. Exergy Analysis of Offshore Rigs

Nguyen et al. (2013) performed exergy analyses of North Sea oil-gas rigs, while Voldsund et al. (2014) investigated the respective exergy destructions. Nguyen et al. (2014) exergetically analyzed upstream oil plants on mature fields and Gallo et al. (2017) performed energy/exergy analyses of Pre-Salt FPSOs, concluding that SSLCs stand as major power sinks whose anti-surge recycles increasingly devour exergy as gas-load decreases.

The exergy concept for open systems combines the 1st and 2nd Laws of Thermodynamics. The exergy flow rate of a stream is the maximum obtainable power when reaching equilibrium with a reference environment reservoir (RER) (Teixeira et al., 2016). Exergy analysis assesses exergy flows, discriminating wasted exergy to the environment and exergy destruction due to irreversibilities. Both can be minimized, though the latter invoke different approaches for reduction. Exergy destruction is a reflex of systemic irreversibilities requiring interventions for better exergy efficiency (Soundararajan et al., 2014). However, system re-design is problematic. FPSO design is constrained by equipment technology (e.g., efficiencies), field characteristics and export conditions (oil/gas temperature, pressure and specifications). Additionally, economic and operational risks must be considered in new designs. There are works on exergy-based design optimization and on minimizing energy degradation, normally disregarding economy implications. Panton et al. (2014) compared conventional and electrified oil-gas platforms via exergy analysis, while da Silva and de Oliveira (2018) determined exergy cost of oil-gas offshore production and Silva et al. (2019) exergetically analyzed gas-turbines on offshore rigs.

As seen above, many works have applied exergy analysis to offshore rigs and FPSOs, but none has used exergy assessments to compare SSLC with new compressor schemes.

4.1.2. The Present Work

Due to rough working conditions and long distance to coast, deep-water offshore oil production with associated gas has a past of extreme exergy inefficiency. About 25 years ago it was a common practice of some oil companies to simply burn all produced gas – exceeding power/heating/gas-lift utilizations – through bizarrely giant flares requiring huge radiation shields for crew protection. With the advent of climate-change such absurd practices were banned, and a growing interest in better FPSO exergy efficiency appeared in the literature. But even nowadays oil is still the supreme goal in deep-water enterprises and gas is, not rarely, considered worthless in the sense that power-consuming systems are designed for less efficient operation privileging low investment; e.g., SSLC schemes with inefficient anti-surge recycles at low gas-load. Gallo et al. (2017) suggested replacing SSLC by multiple-paralleled smaller compressors (MPSC), which are gradually turned-off as gas production falls, but they did not develop MPSC. Replacing SSLC by MPSC to rule out anti-surge recycles can increase FPSO exergy efficiency at the expense of rising fixed capital investment (FCI); hence a trade-off appears between FCI and exergy efficiency, requiring further examination. This study fills this gap comparing SSLC and MPSC in offshore oil-gas rigs on following grounds: (i) exergy efficiency; (ii) power demand, fuel consumption and CO_2 emissions per equivalent oil barrel (BOE) produced; and (iii) FCI/footprint. Calculations adopted rigorous thermodynamic simulation of processes, exergy analysis with two RER definitions and 2nd Law consistency checks.

4.2. Methods

For deep-water oil-gas FPSOs handling CO_2-rich NG, MPSC is proved to have benefits over SSLC. To do this, SSLC and MPSC comparisons on exergy conservation, power consumption and capital/footprint grounds were conducted at three FPSO gas-loads (~100%, ~50%, ~25%) representing phases of typical Pre-Salt FPSO campaigns. Two RER approaches (RER-1, RER-2) were considered for exergy analysis, entailing 6 process simulations and 12 exergy analyses performed. FCI/footprint analyses contemplate only 100% gas-load, upon which MPSC and SSLC gas-plants were sized; i.e., the design condition. Fig. 4.1 is a flowchart of steps in this study: (i) red-hexagon consolidates literature information and data from environmental impact assessments of the real FPSO (Cruz et al., 2018) selected for this study; (ii) blue-boxes represent computational tasks for process simulation, exergy analysis, equipment sizing and FCI/footprint estimation; and (iii) green-flags represent task inputs and/or task results.

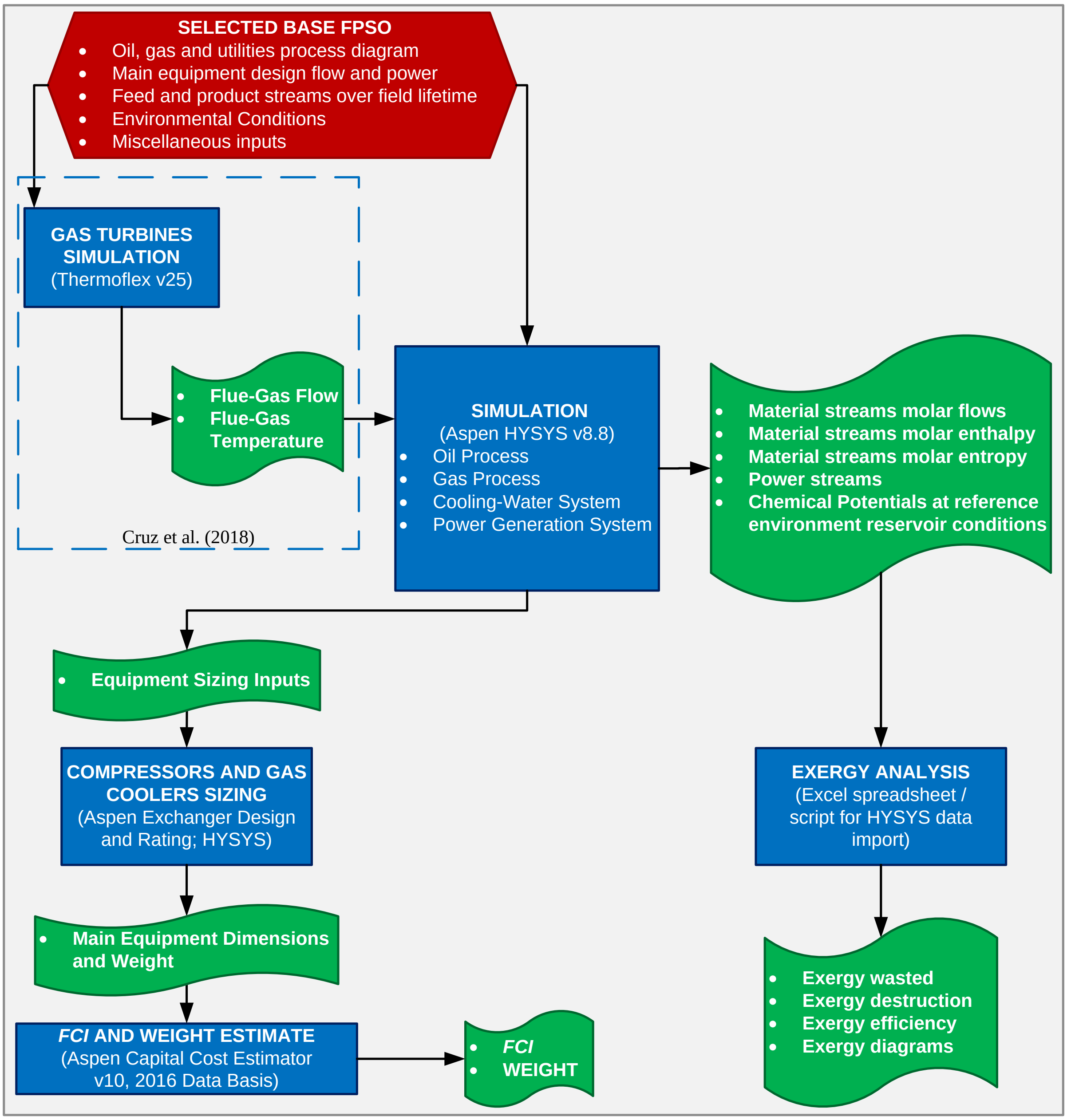

Figure 4.1. Study Flowchart.

4.2.1. Process Simulation

The chosen FPSO (Cruz et al., 2018) operates on Pre-Salt (Santos) Basin with gas and oil respective capacities of 5 MMSm³/d and 100,000 bbl/d. On Pre-Salt fields, CO_2 separation, EOR injection and NG exportation require high pressures, entailing highly power-intensive gas processing due to massive use of SSLC centrifugal compressors. FPSO and oil-gas field data come from Santos Basin Environmental Impacts Assessment (Petrobras, 2013) as the profiles (Fig. 4.2) of oil/gas/CO_2 productions and %mol CO_2 of raw NG along field lifetime, where the large circles represent three phases of field campaign: maximum (year 4), medium (year 10) and minimum (year 18) gas-loads at which the FPSO respectively operates at ~100%/~50%/~25% of design gas capacity. Steady-state FPSO configurations, SSLC-Case and MPSC-Case, were simulated at ~100%/~50%/~25% gas-loads. Fig. 4.3 depicts SSLC-Case flowsheet with 319 material-streams, 40 power-streams and 197 units. The legends auto-explain Fig. 4.3, where red-box and green-box respectively envelope oil-plant and gas-plant; blue-box encloses CW system; grey-box envelopes power generation gas-turbines; and black-box represents FPSO topside with streams 1-10 as feeds/products. All envelopes were simulated, except the production-water plant (Fig. 4.3, bottom) because it is not affected by gas-plants nor generate feeds to them. The oil-plant is absent in exergy/economic analyses since it is not affected by SSLC/MPSC gas-plants.

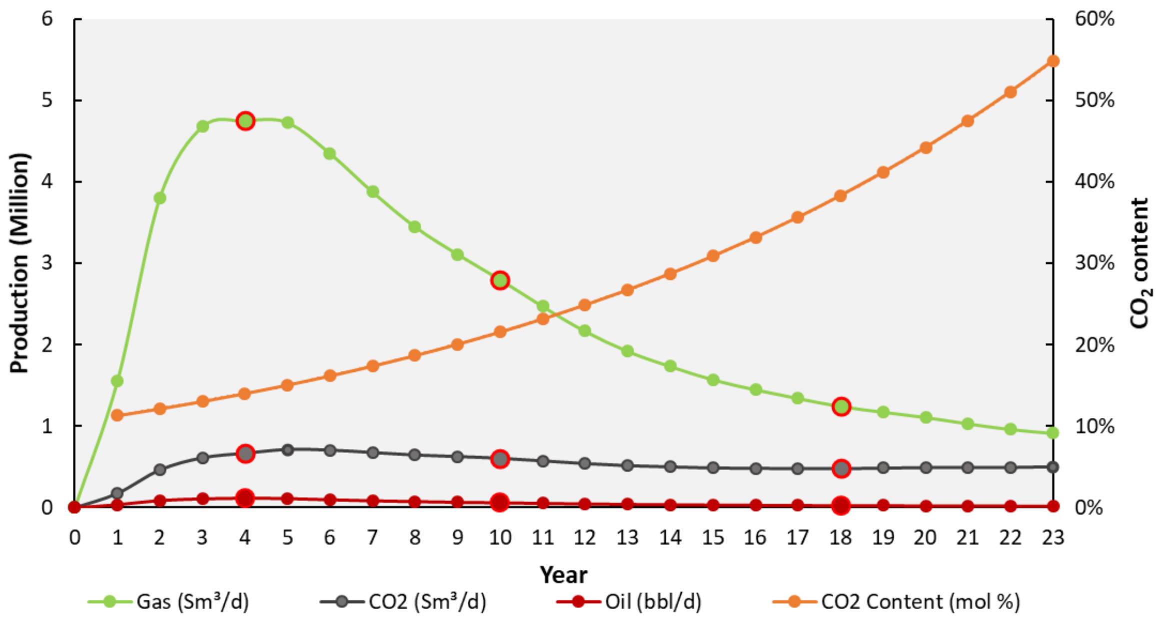

Figure 4.2. Oil/gas/CO_2 productions along field lifetime. (Petrobras, 2013).

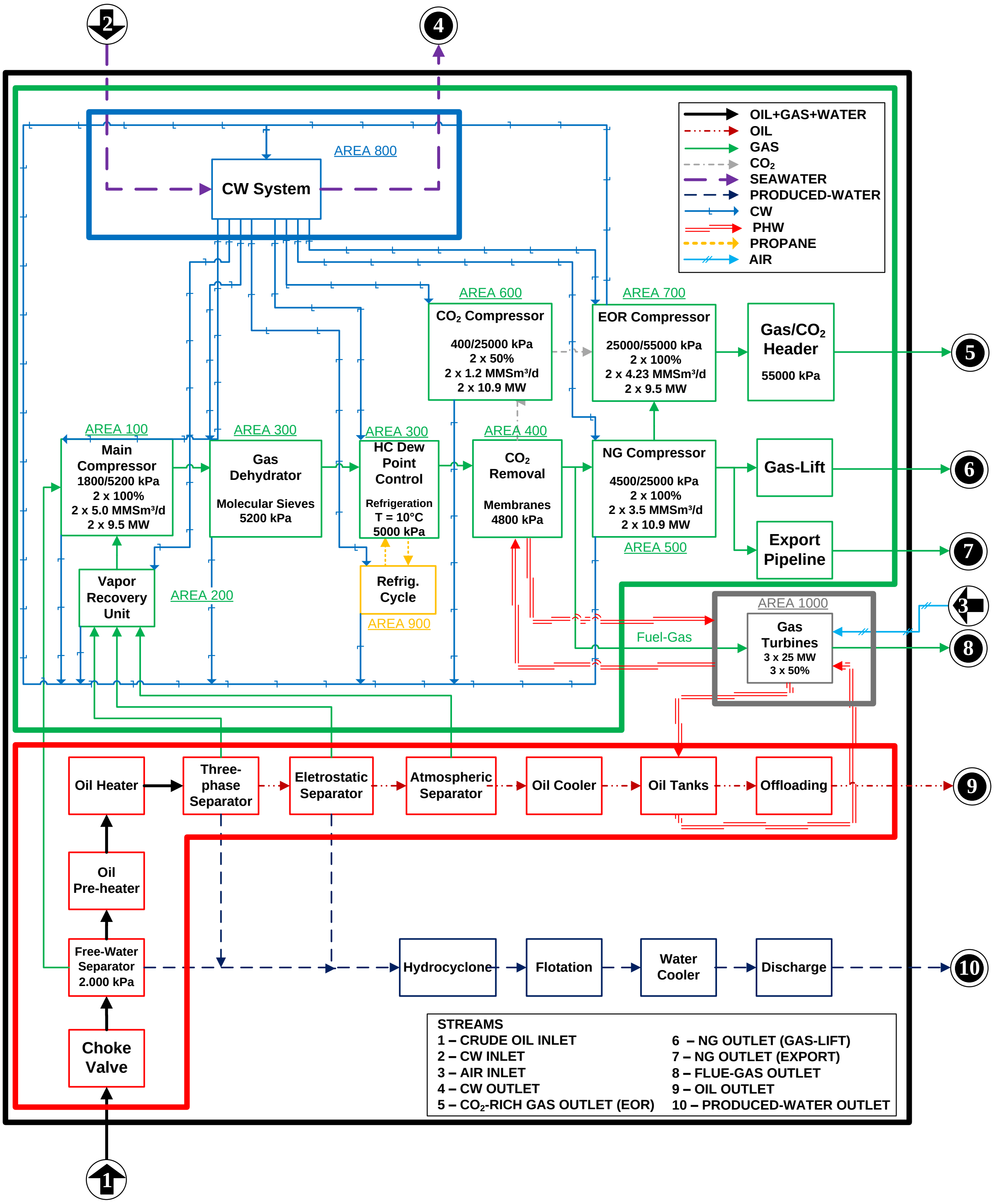

Figure 4.3. SSLC-Case: oil-plant (red), gas-plant (green) and water-plant (bottom-right).

4.2.1.1. Oil-Plant

Fig. 4.4 depicts the oil-plant flowsheet with oil and produced-water inputs in Table 4.1 at ~100%/~50%/~25% gas-loads. Oil-plant feeds the gas-plant with raw gas streams that vary according to gas-load (Table 4.2) and is the same for SSLC-Case and MPSC-Case.

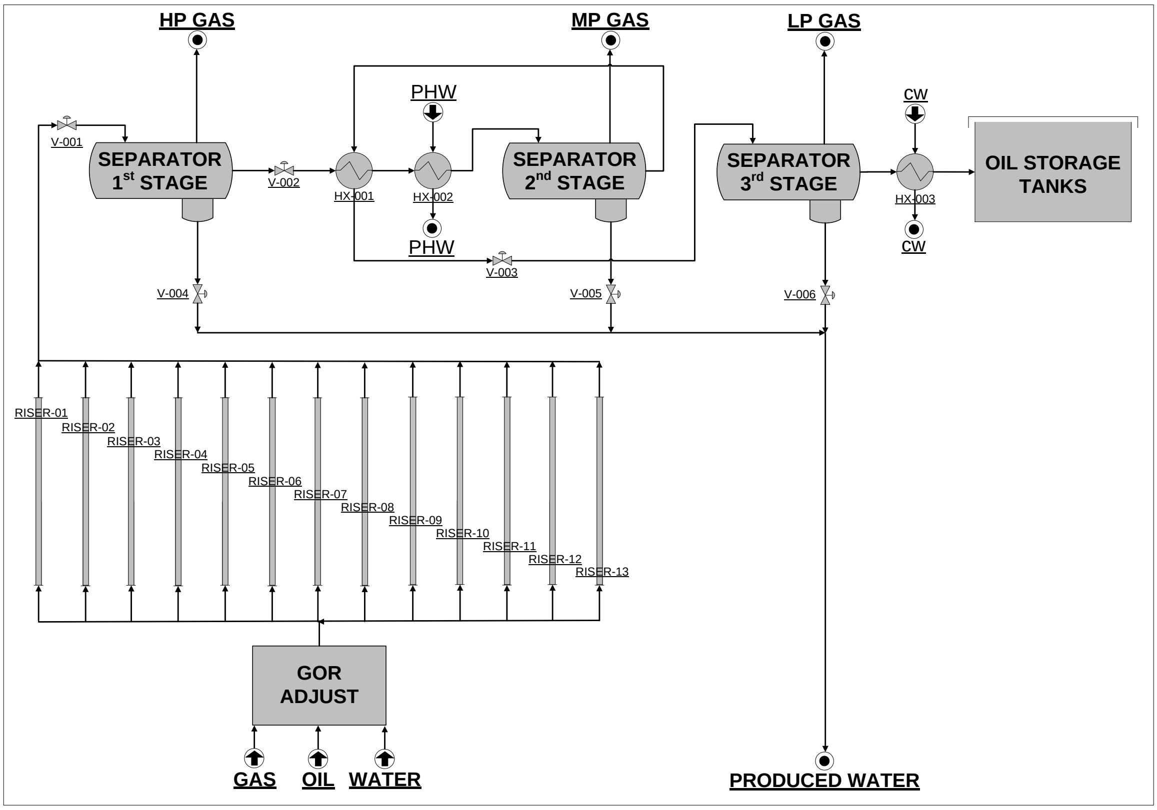

Figure 4.4. Oil-Plant (HP=high-pressure, MP=medium-pressure, LP=low-pressure)

Table 4.1. Oil-Plant: simulation inputs.

FPSO Gas-Load	*100%*	*50%*	*25%*
Operational Year	*4*	*10*	*18*
Oil (bbl/d)	*111467*	*56771*	*24037*
Production-Water (bbl/d)	*2907*	*41748*	*79153*
Raw NG (Sm^3/d)	*4750184*	*2801137*	*1244432*
CO_2 (Sm^3/d)	*664971*	*603644*	*476677*
Gas-Oil Separators	*3*	*3*	*3*
Gas-Oil Ratio (Sm^3/m^3)	*257*	*294*	*303*
Water-Oil Ratio (m^3/m^3)	*0.025*	*0.691*	*3.09*
Reservoir Temperature (°C)	*40*	*40*	*40*
Reservoir Pressure (kPa)	*41368*	*41368*	*41368*

Table 4.2. Oil-Plant: raw NG streams.

FPSO Gas-Load	*100%*			*50%*			*25%*		
Gas-Oil Separator	*1st*	*2nd*	*3rd*	*1st*	*2nd*	*3rd*	*1st*	*2nd*	*3rd*
Gas Stream	*101*	*208*	*201*	*270*	*320*	*370*	*420*	*470*	*520*
MMSm³/d	*4.44*	*0.25*	*0.06*	*2.65*	*0.12*	*0.03*	*1.19*	*0.05*	*0.01*
T(ºC)	*20*	*60*	*44*	*29*	*60*	*48*	*36*	*60*	*44*
P(kPa)	*1850*	*655*	*250*	*1850*	*655*	*250*	*1850*	*655*	*250*
Mol Fractions									
CO_2	*0.1410*	*0.1774*	*0.2471*	*0.2126*	*0.2451*	*0.3417*	*0.3610*	*0.4114*	*0.5111*
H_2	*0.0000*	*0.0000*	*0.0000*	*0.0000*	*0.0000*	*0.0000*	*0.0000*	*0.0000*	*0.0000*
N_2	*0.0057*	*0.0003*	*0.0011*	*0.0051*	*0.0003*	*0.0010*	*0.0041*	*0.0003*	*0.0007*
Methane	*0.0000*	*0.0000*	*0.0000*	*0.0000*	*0.0000*	*0.0000*	*0.0000*	*0.0000*	*0.0000*
Ethane	*0.6993*	*0.1839*	*0.1705*	*0.6309*	*0.1585*	*0.1519*	*0.5053*	*0.1379*	*0.1133*
Propane	*0.0898*	*0.1849*	*0.1426*	*0.0834*	*0.1576*	*0.1198*	*0.0678*	*0.1230*	*0.0850*
i-Butane	*0.0444*	*0.2408*	*0.2056*	*0.0442*	*0.2152*	*0.1722*	*0.0374*	*0.1571*	*0.1212*
n-Butane	*0.0050*	*0.0411*	*0.0436*	*0.0055*	*0.0395*	*0.0380*	*0.0049*	*0.0285*	*0.0274*
i-Pentane	*0.0092*	*0.0830*	*0.0879*	*0.0103*	*0.0819*	*0.0780*	*0.0096*	*0.0596*	*0.0572*
n-Pentane	*0.0014*	*0.0155*	*0.0209*	*0.0018*	*0.0165*	*0.0195*	*0.0018*	*0.0125*	*0.0153*
n-Hexane	*0.0017*	*0.0200*	*0.0275*	*0.0022*	*0.0216*	*0.0259*	*0.0023*	*0.0166*	*0.0208*
n-Heptane	*0.0008*	*0.0103*	*0.0185*	*0.0011*	*0.0119*	*0.0180*	*0.0013*	*0.0097*	*0.0157*
n-Octane	*0.0003*	*0.0041*	*0.0093*	*0.0004*	*0.0048*	*0.0091*	*0.0006*	*0.0042*	*0.0087*
n-Nonane	*0.0001*	*0.0020*	*0.0059*	*0.0002*	*0.0025*	*0.0058*	*0.0003*	*0.0021*	*0.0055*
n-Decane	*0.0000*	*0.0006*	*0.0021*	*0.0001*	*0.0007*	*0.0021*	*0.0001*	*0.0006*	*0.0020*
n-C11	*0.0000*	*0.0002*	*0.0008*	*0.0000*	*0.0002*	*0.0008*	*0.0000*	*0.0002*	*0.0008*
n-C12	*0.0000*	*0.0000*	*0.0002*	*0.0000*	*0.0001*	*0.0002*	*0.0000*	*0.0000*	*0.0002*
H_2O	*0.0000*	*0.0000*	*0.0002*	*0.0000*	*0.0000*	*0.0002*	*0.0000*	*0.0000*	*0.0002*
Ar	*0.0014*	*0.0357*	*0.0161*	*0.0022*	*0.0435*	*0.0157*	*0.0033*	*0.0362*	*0.0148*

4.2.1.2. Gas-Plant, Cooling-Water System and Power Generation

Gas-plant, GT power generation and CW system of SSLC-Case and MPSC-Case were simulated in HYSYS using Peng-Robinson Equation-of-State (PR-EOS) with Free-Water for thermodynamic modeling of oil/gas/CO2/water process streams and HYSYS-Steam-Table for CW, PHW and seawater (SW) streams. Air temperature (23ºC), relative humidity (87%) and SW temperature (23ºC near sea surface) represent average values at FPSO location (Petrobras, 2013), which are necessary for GT simulations (validated in Cruz et al., 2018) and CW calculations. Fig. 4.5 depicts SSLC-Case flowsheet comprising gas-plant, CW system and GT area, where VRU, MP, WDPA, HCDPA, C3, C3+, C6+ respectively stand for Vapor-Recovery Unit, Membrane-Permeation, Water Dew-Point Adjustment, Hydrocarbon Dew-Point Adjustment, propane, propane-and-heavier-alkanes, and hexane-and-heavier-alkanes. HCDPA is set at 3ºC to guarantee C6+ below 0.1%mol, avoiding MP condensation issues. MP CO2 separation was simulated using HYSYS MP Extension (Arinelli et al., 2019).

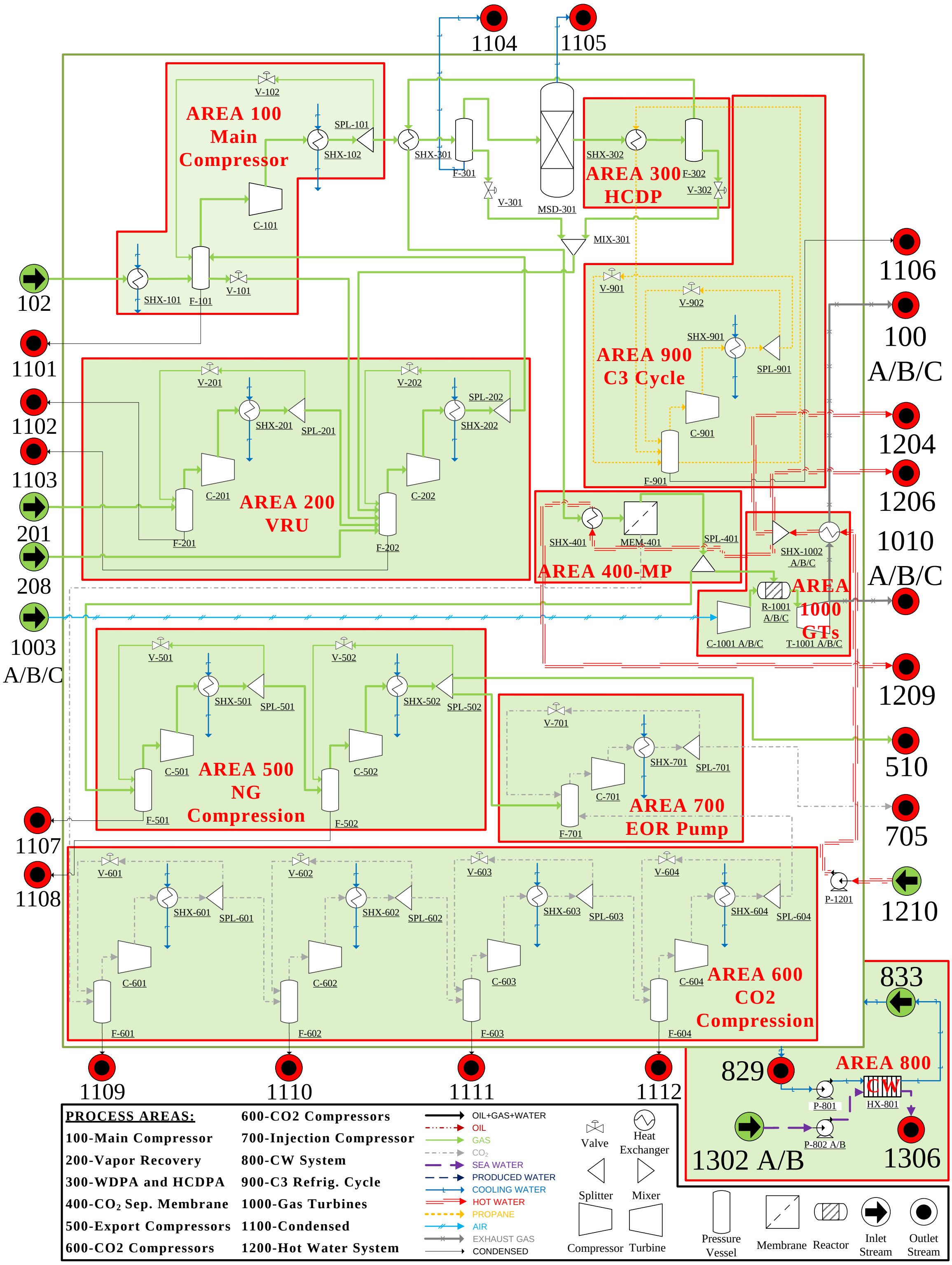

Figure 4.5. SSLC-Case: gas-plant, CW system and GT area.

4.2.1.3. MPSC-Case Simulation

MPSC-Case is modeled as the SSLC-Case (Figs. 4.3-4.5) just replacing some SSLC compressors with anti-surge recycles by sets of MPSCs deprived of anti-surge control. This eliminates exergy destruction by anti-surge recycles in MPSC-Case. The number of equal MPSCs replacing a given large SSLC in MPSC-Case is defined using the minimum achievable flow rate via variable-speed drivers (VSD) which decrease RPM of SSLC to avoid surge at low inlet flow rates. VSD can also move the operating point to the optimal efficiency region via RPM manipulation, regardless inlet flow variations (Albusaidi and Pilidis, 2015). Since VSD flows are limited to 50%–60% of design flows, 55% of design inlet flow is assumed as VSD lower limit. Therefore, if a SSLC experiences less than 55% flow rate at ~25% FPSO gas-load, it is replaced in MPSC-Case by a set of MPSCs each one designed somewhat above such minimum SSLC flow and totaling little above the integral SSLC flow at 100% FPSO gas-load. Thus, at 100% FPSO gas-load all MPSCs are active and are turned off, one-at-a-time, as FPSO gas-load falls. Since the polytropic efficiency of centrifugal compressors varies with flow rate, MPSC efficiencies were estimated via a correlation of Cruz et al. (2018).

However, the minimum VSD flow is limited to 50%–60% of the compressor design flow. In this work, 55% of the design inlet volumetric flow is adopted as limit. Below this limit, the inlet flow is divided and smaller paralleled compressors are considered. When the gas-load becomes lesser than 55% of design capacity one of the smaller compressors is turned off and the operation proceeds with the other one. Table 4.3 shows the compressors scheme for SSLC-Case and MPSC-Case. The polytropic efficiency of centrifugal compressors varies with inlet flow rate. This effect is considered in this study, as observed in Table 4.3. The polytropic efficiency is estimated using a correlation of Cruz et al. (2018).

4.2.2. Exergy Analysis of Processes

Exergy analysis follows Teixeira et al. (2016), with main steps described in the following.

4.2.2.1. Process division into subsystems

Fig. 4.5 shows such division for SSLC-Case, which is the same for MPSC-Case. Envelopes for exergy analyses of subsystems expose feed/product material-streams, CW/PHW/SW streams and power-streams.

4.2.2.2. Energy and mass balances

Energy-Mass balances are solved through process simulation (Sec. 4.2.1) obtaining process parameters, material-streams properties and power-streams for determination of inlet/outlet exergy flows.

4.2.2.3. RER Configuration

RER is an infinite ground-level equilibrium system constituted of process species at temperature T_0, pressure P_0 and i^{th} chemical potential μ_i^0 ($i=1..nc$). Exergy flow rates (kW) of material-streams are relative to the chosen RER; i.e., exergy flows depend on the associated material-streams and also on RER definition, while for power-streams the exergy flows are the respective power values. Adequate RER definition is crucial for a useful exergy analysis (Dinçer and Rosen, 2013); i.e., inappropriate RER choices would entail enormous values of inlet/outlet exergy flows of material-streams, making exergy destruction rates – which do not depend on RER choice – relatively insignificant. In such cases, exergy efficiencies would have artificially high values close to 100%, making the assessment useless.

Two RER definitions are adopted: RER-1 and RER-2. Both initially consist of standard dry air ($N_2=78.08\%mol$, $O_2=20.95\%mol$, $Ar=0.93\%mol$ and $CO_2=0.04\%mol$) at $T_0=298.15\ K$, $P_0=1.013\ bar$, which was put in equilibrium with an infinite body of liquid water becoming water-saturated at $T_0=298.15\ K$, $P_0=1.013\ bar$. The existence of liquid water in RER is convenient to lower exergy flows of numerous CW/PHW/SW streams. At this point, the calculation of μ_i^0 for $i\in\{N_2,O_2,Ar,CO_2,H_2O\}$ is immediate as an atmospheric ideal gas mixture. The differences between RER-1 and RER-2 emerge from the different μ_i^0 states chosen for the hydrocarbons of raw NG. RER-1 is adequate for combustion or chemically reactive processes (e.g., GTs), while RER-2 is appropriate for non-reactive processes (e.g., compressors, valves, exchangers and physical separation operations). In RER-1, the μ_i^0 of hydrocarbons is obtained from μ_i^0 $i\in\{N_2,O_2,Ar,CO_2,H_2O\}$ via chemically equilibrated gas-phase combustion reactions (e.g., $\mu_{CH_4}^0=\mu_{CO_2}^0+2\mu_{H_2O}^0-2\mu_{O_2}^0$, $\mu_{C_2H_6}^0=2\mu_{CO_2}^0+3\mu_{H_2O}^0-3.5\mu_{O_2}^0$, etc), entailing very low μ_i^0 for hydrocarbons and giving high exergy flows for NG streams. On the other hand, in RER-

2 hydrocarbons are not chemically equilibrated with air species; i.e., they are physically added to the water-saturated air at low contents compatible with typical atmospheres surrounding oil-gas facilities (e.g., *44.1 ppm-mol* for CH_4, etc) based on microseepage studies (Chang et al., 2014). The gas phase composition of RER-2 is updated due to the small hydrocarbon contents, but the ideal gas behavior is still valid. RER-2 is critical for exergy analysis of non-reactive processes that do not change the number of molecules; i.e., in RER-2 the μ_i^0 of hydrocarbons are not too low. This reduces the "chemical part" of exergy flows of feed/product streams of physical operations, enhancing the visibility of their exergy destructions and producing meaningful exergy efficiencies. Regardless of RER-1 or RER-2 choices, the rate of exergy destruction is always the same for a given steady-state operation, but the exergy efficiency is calculated with inlet exergy flows and, as such, is very dependent of RER choice.

μ_i^0 for $i \in \{N_2, O_2, Ar, CO_2, H_2O\}$ are calculated respecting HYSYS enthalpy/entropy reference-states for the chosen thermodynamic packages. PR-EOS for process gas/oil/water streams and HYSYS-Steam-Table for CW/PHW/SW streams have the same water reference-states; i.e., have datum compatibility. Since HYSYS does not export chemical potentials, μ_i^0 for $i \in \{N_2, O_2, Ar, CO_2, H_2O\}$ is calculated with ideal gas formula in the left term of Eq. (1), where P^* is a sufficiently low pressure for pure *i* ideal gas at T_0. For light gases $\{N_2, O_2, Ar, CO_2\}$ $P^*=P_0$ is chosen, while for water $P^*=0.01\ bar$ is adequate. $\mu_i^{Pure}(T_0, P^*)$ is obtained for a pure *i* stream at (T_0, P^*) via the right term in Eq. (4.1) with PR-EOS. For trace hydrocarbon *i* in RER-2, Eq. (1) is used with pure *i* at $P^*=0.01\ bar$. Table 4.3 presents molar fractions (y_i^0) and μ_i^0 for NG species in RER-1 and RER-2.

$$\mu_i^0 = \mu_i^{Pure}(T_0, P^*) + RT_0.\,ln\left(\frac{P_0 y_i^0}{P^*}\right), \mu_i^{Pure}(T_0, P^*) = \bar{H}_i^{Pure}(T_0, P^*) - T_0.\,\bar{S}_i^{Pure}(T_0, P^*) \quad (4.1)$$

Table 4.3. RER-1 and RER-2: gas molar fractions (y_i^0) and chemical potentials (μ_i^0) for NG operations.

	RER-1		***RER-2***	
T(K)	*T_0=298.15*		*T_0=298.15*	
P(bar)	*P_0=1.0133*		*P_0=1.0133*	
Species	y_i^0	μ_i^0 ***(kJ/mol)***	y_i^0	μ_i^0 ***(kJ/mol)***
N_2	*0.7593*	*-47.4*	*0.7593*	*-47.4*
O_2	*0.2037*	*-52.5*	*0.2037*	*-52.5*
H_2O	*0.0276*	*-301.3*	*0.0276*	*-301.3*
Argon	*0.0090*	*-47.1*	*0.0090*	*-47.1*
CO_2	*0.0004*	*-464.2*	*0.0004*	*-464.2*
CH_4	*N/A*	*-961.7*	*4.41E-05*	*-154*
C_2H_6	*N/A*	*-1648*	*4.12E-11*	*-201*
C_3H_8	*N/A*	*-2335*	*2.31E-11*	*-212*
i-C_4H_{10}	*N/A*	*-3022*	*4.48E-12*	*-247*
C_4H_{10}	*N/A*	*-3022*	*1.17E-11*	*-228*
i-C_5H_{12}	*N/A*	*-3709*	*6.33E-12*	*-237*
C_5H_{12}	*N/A*	*-3709*	*6.58E-12*	*-242*
C_6H_{14}	*N/A*	*-4395*	*3.29E-12*	*-268*
C_7H_{16}	*N/A*	*-5082*	*1.65E-12*	*-303*
C_8H_{18}	*N/A*	*-5769*	*8.23E-13*	*-313*
C_9H_{20}	*N/A*	*-6455*	*4.11E-13*	*-379*
$C_{10}H_{22}$	*N/A*	*-7142*	*2.06E-13*	*-416*
$C_{11}H_{24}$	*N/A*	*-7829*	*1.03E-13*	*-452*
$C_{12}H_{26}$	*N/A*	*-8516*	*5.14E-14*	*-487*

4.2.2.4. Exergy Flow of Inlet/Outlet Energy/Material Streams

Eqs. (4.2a)-(4.2b) calculate inlet/outlet exergy flows of a system regarding the chosen RER (Teixeira et al., 2016), where $\dot{B}_{in}, \dot{B}_{out}$ are inlet/outlet exergy flow rates (kW) of material-streams, while $\dot{B}_{in}^W, \dot{B}_{out}^W$ respectively comprehend sums of positive power-streams $\dot{W}_j^{imported}, \dot{W}_j^{exported}$ on the right-hand side of Eqs. (4.2a)-(4.2b) that are imported/exported by the system (e.g., electricity to compressors/pumps drivers). All terms of Eqs. (4.2a)-(4.2b) were extracted from HYSYS simulations and exported to spreadsheets via an automatized procedure to avoid mistakes.

$$\dot{B}_{in.total} = \dot{B}_{in} + \dot{B}_{in}^W = \sum_{j=1}^{nfs} F_j \left(\bar{H}_{Fj} + P_0\bar{V}_{Fj} - T_0\bar{S}_{Fj} - \sum_{k=1}^{nc} \mu_k^0 y_{k,Fj} \right) + \sum_{j=1}^{nwi} \left| \dot{W}_j^{imported} \right| \qquad (4.2a)$$

$$\dot{B}_{out.total} = \dot{B}_{out} + \dot{B}^{W}_{out} = \sum_{j=1}^{nps} K_j \left(\bar{H}_{Kj} + P_0 \bar{V}_{Kj} - T_0 \bar{S}_{Kj} - \sum_{k=1}^{nc} \mu^0_k y_{k,Kj} \right) + \sum_{j=1}^{nwe} \left| \dot{W}^{exported}_j \right| \quad (4.2b)$$

4.2.2.5. Exergy Balances and Exergy Destructions

Eq. (4.3) calculates the exergy destruction rate (kW) of a system ($\Delta\dot{B}$) by subtracting Eqs (4.2a) and (4.2b). It can be proved that $\Delta\dot{B}$ is also $\dot{W}^{LOST}$, the rate of lost work given in Eq. (4.4) via the rate of entropy creation in the Universe ($\dot{\Omega}_S$) due to the system steady-state operation (Teixeira et al., 2016).

$$\Delta\dot{B} = (\dot{B}_{out} + \dot{B}^{W}_{out}) - (\dot{B}_{in} + \dot{B}^{W}_{in}) \quad (4.3)$$

$$\dot{W}^{LOST} = T_0 . \dot{\Omega}_S \quad (4.4)$$

A total of six exergy balances – for SSLC-Case and MPSC-Case with three gas-loads each – were conducted for RER-1 and RER-2. Material-streams and power-streams are classified as inlet or outlet and are attributed to a system or subsystem. Fig. 4.5 depicts the subsystems for SSLC-Case and MPSC-Case, including the respective overall gas-plants. RER-1 is suitable only for exergy analysis of GT area, while all other subsystems and gas-plants use RER-2.

4.2.2.6. Exergy Efficiencies

Exergy efficiencies of oil/gas processing with RER-1 leads to useless high values due to high chemical exergy of hydrocarbons; i.e., RER-1 exergy efficiencies via Eq. (4.5a) tend to be numerically high and similar for corresponding systems/subsystems of SSLC-Case and MPSC-Case at analogous gas-loads. Moreover, they also present low sensitivity to process changes and are inefficient for exploring potential FPSO improvements and trade-offs.

On the other hand, RER-2 exergy analysis of non-reactive systems allows using simple exergy efficiency formulas, Eq (4.5a), to compare SSLC-Case and MPSC-Case, excluding the respective GT areas which are appropriate for RER-1 efficiencies. To validate the present methods, exergy efficiencies of GTs with RER-1 were calculated via Eq. (4.5b) and compared with counterparts of Gallo et al. (2017) in Appendix 4.A.

$$\eta = \frac{\dot{B}_{out,total}}{\dot{B}_{in,total}} \tag{4.5a}$$

$$\eta_{GT} = \frac{\dot{B}_{out,electricity}}{\dot{B}_{in,fuel-gas}} \tag{4.5b}$$

4.2.3. Energy Metrics

SSLC-Case and MPSC-Case are also compared via energy metrics such as Fuel Intensity ($BOE_{Burn}/10^3.BOE_{Produced}$), CO_2 Intensity ($tCO_{2Emitted}/10^3.BOE_{Produced}$) and FPSO Power Consumption – considering ≈23MW of background power consumption (Cruz et al., 2018).

4.2.4. Economic and Footprint Assessments

Equipment *FCI* and weight were estimated for SSLC-Case and MPSC-Case via Aspen Capital-Cost Estimator (2016-database). The inputs for turbo-generators are power (kVA) and GT-driver type. MPSC-Case heat exchangers were sized to smaller duties in Table 4.4 from corresponding exchangers of SSLC-Case downsized proportionally to the ratios of heat duty (*Q*) per log-mean temperature difference (*LMTD*) at 100% gas-load (data in Table B1.2, Supplementary Materials) Table 4.5 presents compressors data extracted from simulation at 100% gas-load for *FCI* and weight estimation. *FCI* of heat exchangers of SSLC-Case were estimated with data in Table B2.1.1 (Supplementary Materials).

Table 4.4. Heat exchanger areas: SSLC-Case and MPSC-Case.

TAG	***Area SSLC (m^2)****	***Δ(Q/LMTD)***	***Area MPSC (m^2)***	***Paralleled Exchangers MPSC***	***Total Design-Area MPSC (m^2)***	***Spares***	***Identical Exchangers SSLC***	***Identical Exchangers MPSC***
HX-102	*1093.0*	*52.8%*	*516.2*	*2*	*1032.5*	*1*	*2*	*3*
HX-202	*41.0*	*65.0%*	*14.3*	*3*	*43.0*	*1*	*2*	*4*
HX-204	*108.5*	*71.5%*	*30.9*	*3*	*92.7*	*1*	*2*	*4*
HX-501	*505.5*	*67.7%*	*163.4*	*3*	*490.2*	*1*	*2*	*4*
HX-502	*563.6*	*67.7%*	*182.3*	*3*	*546.8*	*1*	*2*	*4*
HX-601	*254.4*	*19.5%*	*204.7*	*1*	*204.7*	*1*	*2*	*2*
HX-602	*198.7*	*18.9%*	*161.2*	*1*	*161.2*	*1*	*2*	*2*
HX-603	*203.3*	*18.6%*	*165.6*	*1*	*165.6*	*1*	*2*	*2*
HX-604	*239.4*	*18.8%*	*194.4*	*1*	*194.4*	*1*	*2*	*2*
HX-701_exp	*683.2*	*76.7%*	*159.0*	*1*	*867.9*	*1*	*2*	*2*
HX-702_inj		*48.1%*	*354.4*	*2*		*1*	*2*	*3*
HX-901	*8.6*	*46.6%*	*4.6*	*2*	*9.2*	*1*	*2*	*3*

**Cruz et al. (2018)*

Table 4.5. Compressors: data for *FCI* and weight estimation.

SSLC-Case																
TAG	***Casing Material***	***Flow^{Inlet} (m³/h)***	***P^{Inlet} (kPag)***	***T^{Inlet} (°C)***	***$P^{Discharge}$ (kPag)***	***MW (kg/kmol)***	***Cp/Cv***	***Z^{Inlet}***	***Z^{Outlet}***	***Tubes Material***	***Driver***	***Driver Power (kW)***	***Reduced Gear Driver***	***Paralleled Machines***	***Identical Items***
C-101	*CS*[#]	*10477*	*1699*	*20.3*	*5149*	*24.33*	*1.335*	*0.921*	*0.921*	*SS316L*	*Motor*	*8223*	*No*	*1*	*2*
C-201	*CS*	*1100*	*124*	*38.55*	*556*	*39.12*	*1.163*	*0.964*	*0.964*	*SS316L*	*Motor*	*139*	*No*	*1*	*2*
C-202	*CS*	*1878*	*531*	*20.45*	*1749*	*38.22*	*1.211*	*0.901*	*0.901*	*SS316L*	*Motor*	*605*	*No*	*1*	*2*
C-501	*CS*	*2808*	*4399*	*32.3*	*10541*	*22.27*	*1.467*	*0.868*	*0.868*	*CS*	*Motor*	*4577*	*No*	*1*	*2*
C-502	*CS*	*1029*	*10491*	*38.39*	*24949*	*22.27*	*1.872*	*0.88*	*0.88*	*SS316L*	*Motor*	*4635*	*No*	*1*	*2*
C-601	*CS*	*10635*	*299*	*31.63*	*1034*	*30.62*	*1.302*	*0.986*	*0.986*	*CS*	*Motor*	*2123*	*No*	*1*	*2*
C-602	*CS*	*3867*	*1009*	*37.31*	*3051*	*30.62*	*1.329*	*0.967*	*0.967*	*CS*	*Motor*	*2241*	*No*	*1*	*2*
C-603	*CS*	*1288*	*3026*	*32.38*	*8775*	*30.62*	*1.443*	*0.923*	*0.923*	*SS316L*	*Motor*	*2238*	*No*	*1*	*2*
C-604	*CS*	*377*	*8725*	*29.71*	*24949*	*30.62*	*2.050*	*0.886*	*0.886*	*SS316L*	*Motor*	*2032*	*No*	*1*	*2*
C-701	*CS*	*584*	*24899*	*31.08*	*34470**	*24.16*	*1.88*	*1.137*	*1.137*	*SS316L*	*Motor*	*7767*	*No*	*1*	*2*
C-901	*CS*	*1929*	*279*	*0.17*	*1619*	*44.10*	*1.179*	*0.791*	*0.791*	*CS*	*Motor*	*494*	*No*	*1*	*2*
MPSC-Case															
TAG	***Casing Material***	***Flow^{Inlet} (m³/h)***	***P^{Inlet} (kPag)***	***T^{Inlet} (°C)***	***$P^{Discharge}$ (kPag)***	***MW (kg/kmol)***	***Cp/Cv***	***Z^{Inlet}***	***Z^{Outlet}***	***Tubes Material***	***Driver***	***Driver Power (kW)***	***Reduced Gear Driver***	***Paralleled Machines***	***Identical Items***
C-101 A/B	*CS*	*5240*	*1699*	*20.4*	*5149*	*24.34*	*1.335*	*0.921*	*0.921*	*SS316L*	*Motor*	*4059*	*Yes*	*2*	*3*
C-201 A/B/C	*CS*	*402*	*124*	*40*	*556*	*39.07*	*1.162*	*0.965*	*0.965*	*SS316L*	*Motor*	*43*	*Yes*	*3*	*4*
C-202 A/B/C	*CS*	*619*	*531*	*20.68*	*1749*	*38.25*	*1.211*	*0.901*	*0.901*	*SS316L*	*Motor*	*180*	*Yes*	*3*	*4*
C-501 A/B/C	*CS*	*952*	*4399*	*33.78*	*10541*	*22.27*	*1.461*	*0.870*	*0.870*	*CS*	*Motor*	*1619*	*Yes*	*3*	*4*
C-502 A/B/C	*CS*	*349*	*10491*	*40*	*24949*	*22.27*	*1.851*	*0.879*	*0.879*	*SS316L*	*Motor*	*1584*	*Yes*	*3*	*4*
C-601	*CS*	*10635*	*299*	*30.78*	*1034*	*30.62*	*1.276*	*0.986*	*0.986*	*CS*	*Motor*	*1707*	*Yes*	*1*	*2*
C-602	*CS*	*3867*	*1009*	*40*	*3051*	*30.62*	*1.327*	*0.968*	*0.968*	*CS*	*Motor*	*1824*	*Yes*	*1*	*2*
C-603	*CS*	*1287*	*3026*	*40*	*8775*	*30.62*	*1.426*	*0.931*	*0.931*	*SS316L*	*Motor*	*1864*	*Yes*	*1*	*2*
C-604	*CS*	*377*	*8725*	*40*	*24949*	*30.62*	*1.887*	*0.908*	*0.908*	*SS316L*	*Motor*	*1762*	*Yes*	*1*	*2*
C-701 A	*CS*	*121*	*24899*	*40*	*34470**	*30.62*	*2.192*	*1.048*	*1.048*	*SS316L*	*Motor*	*1552*	*Yes*	*1*	*2*
C-701 B/C	*CS*	*296*	*24899*	*40*	*34470**	*24.13*	*1.879*	*1.136*	*1.136*	*SS316L*	*Motor*	*3685*	*Yes*	*2*	*3*
C-901 A/B	*CS*	*970*	*279*	*-6*	*1619*	*44.10*	*1.186*	*0.777*	*0.777*	*CS*	*Motor*	*229*	*Yes*	*2*	*3*

[#]*Carbon-Steel.* **Aspen Capital-Cost Estimator limit ($P^{Discharge,C\text{-}701}$=54949 kPag).*

4.3. Results and Discussion

4.3.1. Energy and Environmental Analyses

Six simulation cases – SSLC-Case and MPSC-Case at ≈100%/≈50%/≈25% gas-loads – comprehend a large amount of data, hence only relevant information is presented. Table 4.6 shows compressor flow rates of SSLC-Case and the counterparts of MPSC-Case.

Table 4.6. Compressor schemes: SSLC-Case and MPSC-Case.

	SSLC-Case					***MPSC-Case***					
	Inlet Flow (m³/h) at FPSO %Gas-Load			η_p	***VSD Min. Flow (m³/h)***	***Parallel Comps.***	***Design Flow (m³/h)***	***VSD Min. Flow (m³/h)***	***Total Flow (m³/h)***	***Min. Flow (m³/h)***	η_p
TAG	***100%***	***50%***	***25%***								
C-101	*10477*	*6418*	*2943*	*82%*	*5239*	*2*	*5239*	*2881*	*10477*	*2881*	*79%*
C-201	*1100*	*610*	*219*	*74%*	*550*	*3*	*367*	*202*	*1100*	*202*	*69%*
C-202	*1878*	*974*	*415*	*75%*	*939*	*3*	*626*	*344*	*1878*	*344*	*71%*
C-501	*2802*	*1286*	*243*	*77%*	*1401*	*3*	*934*	*514*	*2802*	*514*	*72%*
C-502	*1027*	*473*	*91*	*73%*	*514*	*3*	*342*	*188*	*1027*	*188*	*69%*
C-601	*10635*	*9198*	*6289*	*83%*	*5318*	*1*	*10635*	*5850*	*10635*	*5850*	*82%*
C-602	*3867*	*3368*	*2343*	*79%*	*1933*	*1*	*3867*	*2127*	*3867*	*2127*	*78%*
C-603	*1288*	*1114*	*767*	*74%*	*644*	*1*	*1288*	*708*	*1288*	*708*	*73%*
C-603*	*1288*		*1001*		*644*						
C-604	*377*	*316*	*204*	*70%*	*189*	*1*	*377*	*207*	*377*	*207*	*69%*
C-604*	*377*		*324*		*189*						
C-701	*121*	*100*	*64*	*68%*	*61*	*1*	*121*	*67*	*576*	*67*	*65%*
C-701*	*576*		*108*		*288*	*2*	*227*	*125*			*67%*
C-901	*1929*	*1331*	*601*	*75%*	*964*	*2*	*964*	*530*	*1929*	*530*	*72%*

**Full-injection mode.*

Only the CO_2 compressors (C-600) were not divided into MPSCs because as the gas-load reduces, the %CO_2 of raw gas increases, giving CO_2 flow rates always above 55% of design capacity for such SSLCs (Table 4.6, *VSD Min. Flow*); i.e., VSD alone can prevent surge. In all other cases, two or more compressors in parallel were necessary to achieve minimum flow with VSD. As compressor efficiencies slightly reduce as flow rate decreases, the advantage of dismissing anti-surge recycles is shadowed a little. Fig. 4.6 shows compressor gas-loads versus FPSO gas-load for SSLC-Case and MPSC-Case. In SSLC-Case compressors generally operate above 80% of design capacities for 100% FPSO gas-load, while at 25% gas-load all compressors operate below 60% of design capacities, being C-700 – EOR compressor – the only exception since it must inject all processed gas if gas exportation is not possible (i.e., full-injection mode). Consequently, C-700 operates at 15%-20% of its design capacity when NG is being exported; i.e., in SSLC-Case all compressors operate at high recycle ratios, especially the C-700.

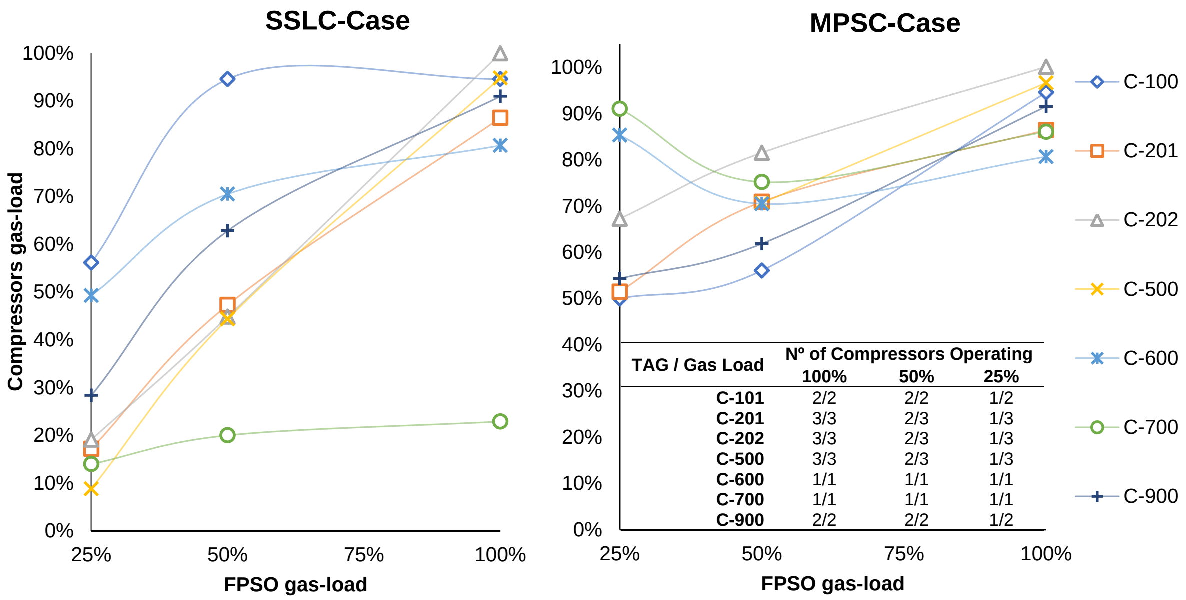

Figure 4.6. Compressors gas-loads versus FPSO gas-load.

As FPSO gas-load decreases in MPSC-Case, compressors operate above 55% of design capacities along the entire FPSO lifetime. It is only necessary to shut down part of the paralleled compressors (as in the table inside Fig. 4.6) and using VSD to make anti-surge recycles unnecessary. Fig. 4.7 demonstrates MPSC power savings, showing power consumption of SSLC-Case almost constant along FPSO lifespan due to anti-surge recycles that keep compressor design flow at partial gas-loads. Fig. 4.8 shows total power consumption of SSLC-Case modestly decreasing as gas-load reduces, while MPSC-Case shows power savings of 11% and 39% respectively at 100% and 25% gas-loads due to absence of anti-surge recycles.

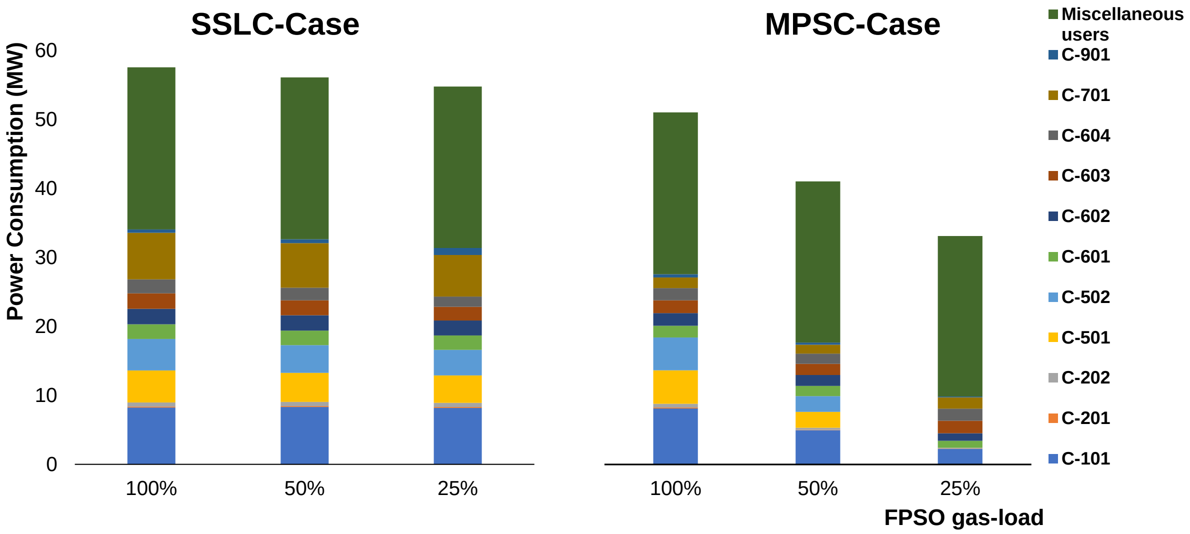

Figure 4.7. Power consumptions versus FPSO gas-load: compressors and miscellaneous units.

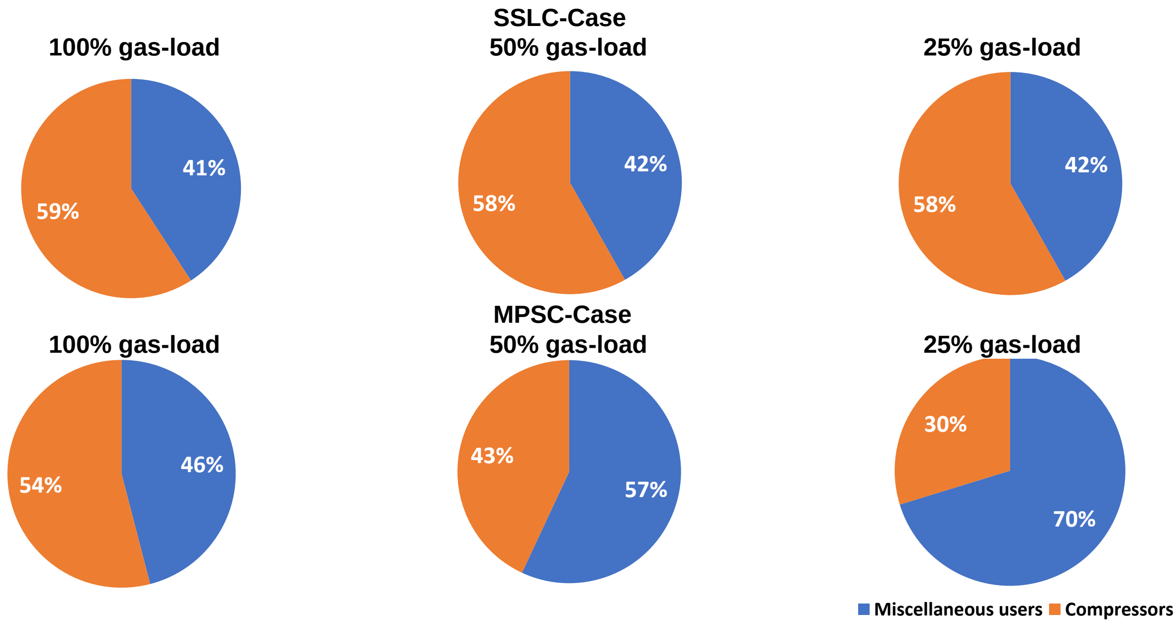

Figure 4.8. Compressor share of total power consumption versus FPSO gas-load.

In MPSC-Case at 25% gas-load, the power consumption of compressors is not anymore the greatest share, while in SSLC-Case compressors continue to be the greatest power sink due to anti-surge gas recycles, as depicted in Fig. 4.8. The SSLC-Case gas-plant consumes a considerable fraction of its carbon input, especially at low gas-loads. Given the current climate-change scenario, it is important to increase the usable energy ratio of oil-gas production. Consequently, the carbon intensity of FPSO products should be reduced to meet sustainability commitments. There are many energy return ratios reported in the literature; e.g., energy return on investment (EROI) and net energy ratio (NER). In this work, net energy ratio and carbon intensity of oil-gas are respectively reported in terms of fuel-gas consumption and tCO_2 emitted both per BOE produced. These ratios are reported in Fig 4.9 to unveil the different energy productivities of SSLC-Case and MPSC-Case gas-plants at 25%/50%/100% gas-loads.

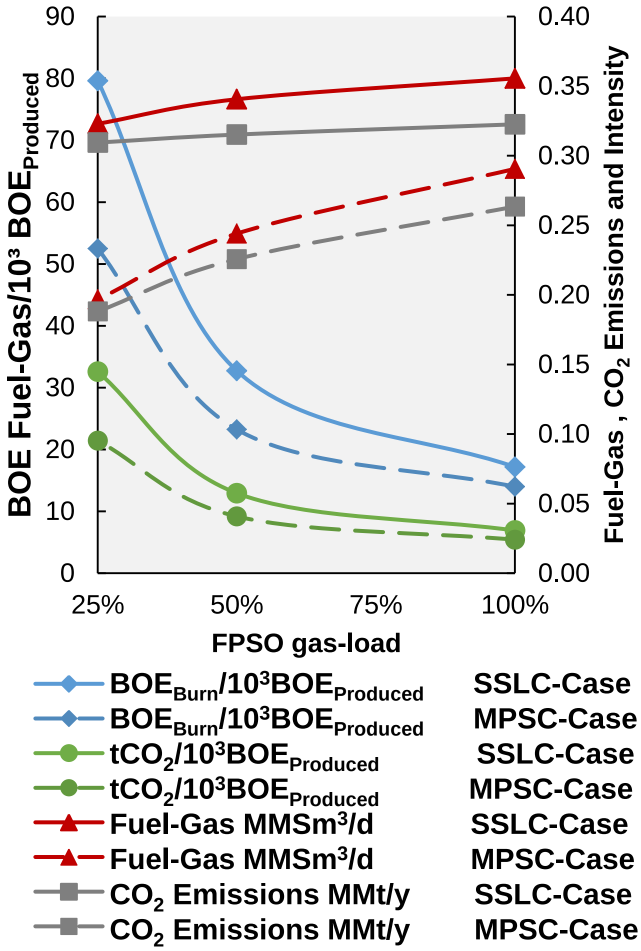

Figure 4.9. SSLC-Case and MPSC-Case: Fuel-Gas and CO_2 intensities versus FPSO gas-load.

The power consumption of compressors has a significant impact on FPSO fuel-gas consumption and CO_2 emissions. Therefore, SSLC-Case energy and environmental performance are drastically affected by its anti-surge recycles, as demonstrated in Fig. 4.9, which also shows that MPSC-Case is more environmentally friendly in terms of net energy ratio and CO_2 intensity, especially at low gas-loads. At 25% gas-load the fuel-gas and CO_2 intensities of MPSC-Case are 34% lower than the counterparts of SSLC-Case. More results are available in Supplementary Materials, Sec. B2.1 (SSLC-Case) and Sec. B2.2 (MPSC-Case).

4.3.2. Exergy Analysis

To shed more light on the thermodynamic advantages of MPSC-Case over SSLC-Case, 12 exergy analyses were performed for MPSC-Case and SSLC-Case, with RER-1 and RER-2, at three FPSO gas-loads. Exergy flows and exergy balances for each gas-load of MPSC-Case and SSLC-Case, are available in Supplementary Materials B, Section B3.

Fig 4.10 reports overall flow rates of exergy destruction and wasted for SSLC-Case and MPSC-Case considering RER-1. RER-1 is satisfactory only for exergy analysis of GTs, because it makes other exergy flows quite invariant compared to changes observed in GTs exergy flows; that is, RER-1 makes the exergy efficiency of physical units falsely high (~99%) in all gas-loads and cases. This results from the enormous values of inlet/outlet chemical part of the exergy flows that are invariant in physical units, making changes of physical exergy insignificant. Fig 4.10 shows that at 100% gas-load the rate of exergy destruction and wasted is similar for SSLC-Case and MPSC-Case, where GTs are major exergy destructors and exergy wasters comparatively to other systems, because GTs operate with highest spontaneity and irreversibility on FPSO topside thanks to highly irreversible combustion chemical reactions. Considering flue-gas contributing to the outlet exergy flow, the exergy efficiency of GTs via Eq. (4.5a) is ≈61% for both SSLC-Case and MPSC-Case at any FPSO gas-loads. On the other hand, operating at 25% gas-load, there is a reduction of 46.7% on the flows of destroyed plus wasted (flue-gas+ SW discharge) exergy of the overall MPSC-Case vis-à-vis SSLC-Case, confirming the thermodynamic superiority of MPSC-Case over SSLC-Case.

Fig 4.11 depicts SSLC-Case and MPSC-Case exergy Sankey diagrams for GTs with RER-1 at all gas-loads, showing that inlet and outlet GT exergy flows are almost the same in SSLC-Case (Fig. 4.11, left), including the exergy destruction rate, no matter the FPSO gas-load. The SSLC anti-surge recycles keep constant compressor inlet gas flows, consequently FPSO power and fuel-gas consumptions are almost constant as gas-load decreases (Fig. 4.8). Therefore, GTs operate at almost constant throughput along FPSO lifetime. Counterpointing this, in MPSC-Case (Fig. 4.11, right) as FPSO gas-load decreases, inlet fuel-gas exergy flow decreases, as well as the flows of destroyed exergy, wasted exergy (flue-gas and SW discharge) and electricity, all consequences of inexistent anti-surge recycles.

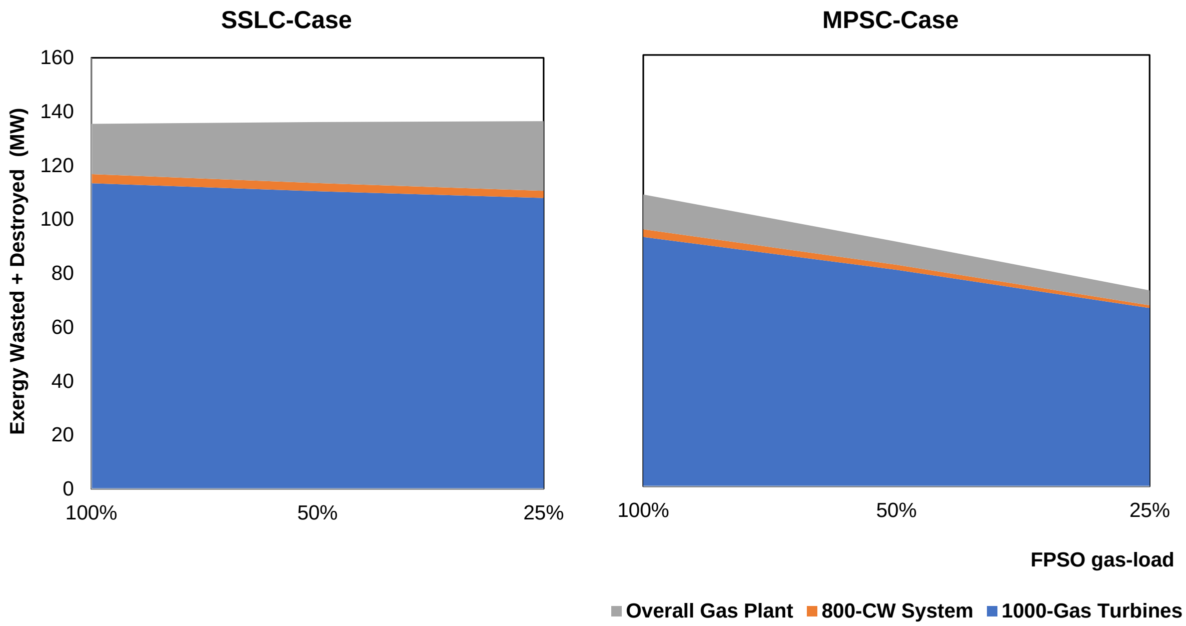

Figure 4.10. Destroyed and wasted exergy versus FPSO gas-load with RER-1.

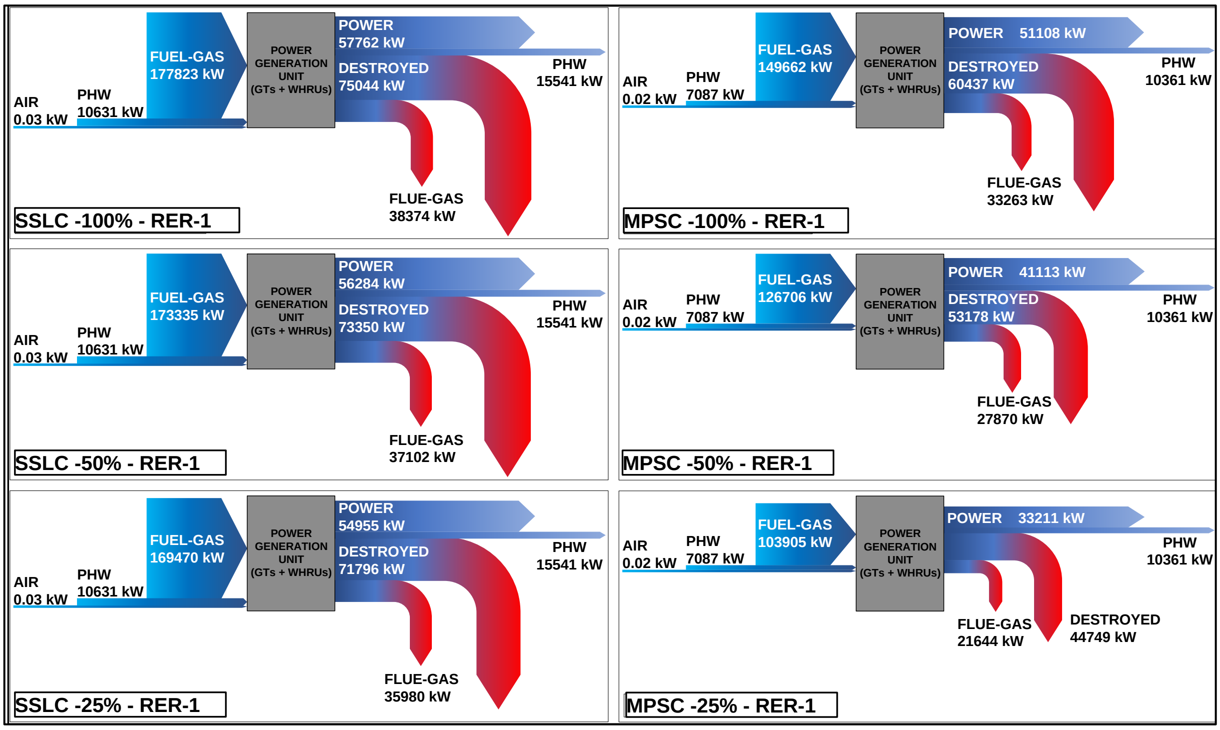

Figure 4.11. Exergy Sankey diagrams for GT power generators with RER-1: SSLC-Case (left) and MPSC-Case (right) at various FPSO gas-loads.

Fig 4.12 depicts flow rates of exergy destruction with RER-2 for subsystems of SSLC-Case and MPSC-Case, including overall exergy efficiencies via Eq. (4.5a) for the respective gas-plants (green-box, Fig. 4.3). The exergy destruction rates are differences between inlet and outlet exergy flow rates across the boundaries of subsystems in Fig. 4.5. Fig. 4.12 shows that RER-2 exergy analysis is much more sensitive to irreversibilities in physical subsystems (compressors, exchangers, separators) in comparison with RER-1 exergy analysis, unveiling that total exergy destruction rates of MPSC-Case gas-plant are 32.5%, 62.2% and 78.6% lower than the SSLC-Case gas-plant counterparts at 100%/50%/25% FPSO gas-loads, respectively. It is also interesting to observe that while exergy destruction rate increase with gas-load in MPSC-Case the opposite is seen in SSLC-Case, proving that the increased activity of anti-surge recycles at decreasing FPSO gas-loads increase exergy destruction rates even at low FPSO gas-loads.

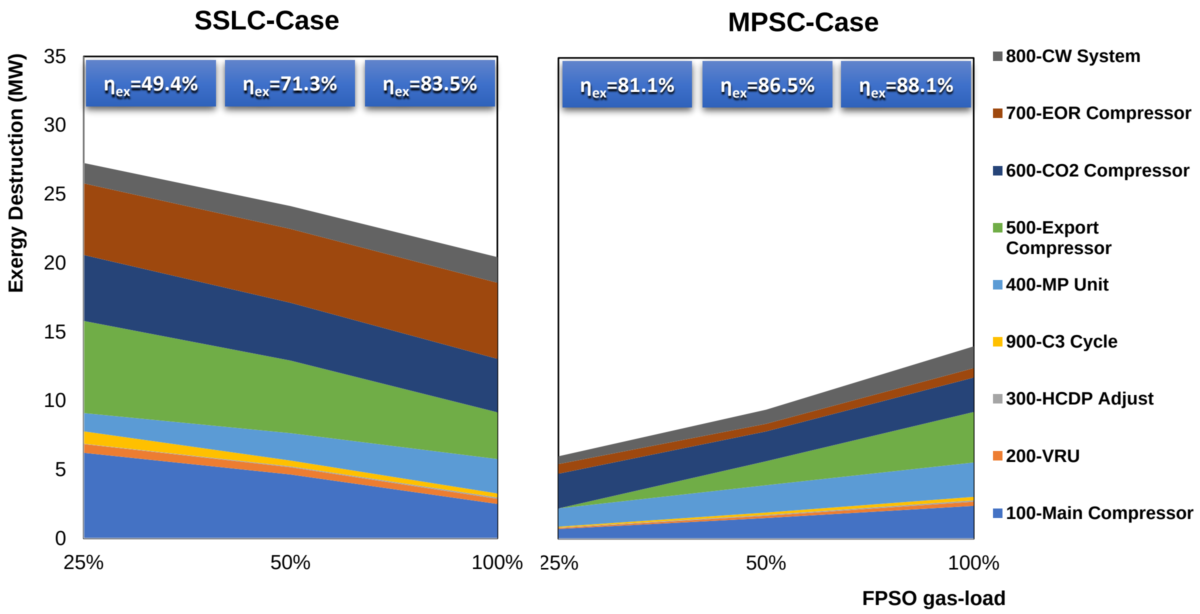

Figure 4.12. Exergy destruction rate versus FPSO gas-load with RER-2: SSLC-Case, MPSC-Case.

Fig. 4.13 depicts exergy Sankey diagrams with RER-2 for SSLC-Case and MPSC-Case at 25%/50%/100% FPSO gas-loads, showing increasing exergy destruction rate of SSLC-Case as FPSO gas-load decreases. At 25% FPSO gas-load, 37% of the inlet exergy flow is destroyed in SSLC-Case gas-plant (green-box, Fig. 4.3). As a result, the decreases of outlet NG exergy (53% at 50% gas-load and 91% at 25% gas-load) are more pronounced than the respective decreases in the feed gas (respectively, 43% and 76%). In MPSC-Case, on the other hand, the decreases of outlet NG exergy flow rate are proportional to the gas feed reductions. The exception is for FPSO gas-load below 25%, because the entire gas is necessary as fuel-gas for power production. Operating at such extremely low gas-load would demand several small paralleled compressors (in MPSC-Case) or full gas recycles (in SSLC-Case), becoming both SSLC-Case and MPSC-Case very inefficient in terms of *FCI* and/or energy use, respectively. Adding such low NG load to the CO_2-rich EOR stream seems to be a more reasonable solution, which was adopted in MPSC-Case at 25% FPSO gas-load in Fig. 4.13.

Figure 4.13. Exergy Sankey diagrams versus FPSO gas-load with RER-2: SSLC-Case, MPSC-Case.

Figs 4.14 and 4.15 show percent exergy destructions of gas-plant, GTs, CW system and subsystems, respectively considering RER-1 and RER-2. Percent exergy destructions in Fig. 4.14 are obtained with absolute destructions (Fig. 4.10) and inlet exergy flow rates of envelopes in Fig. 4.3. Percent exergy destructions are similar for GT and CW envelopes of SSLC-Case and MPSC-Case, but, the high percent exergy destruction of CW system is illusionary and consequence of the very low inlet exergy flow rates of CW streams in RER-1 which create high relative values. Thanks to the anti-surge recycles of SSLC-Case, the percent exergy destruction of gas-plant envelope increases as gas-load reduces. Without such anti-surge recycles in MPSC-Case gas-plant, such increase is almost unnoticeable.

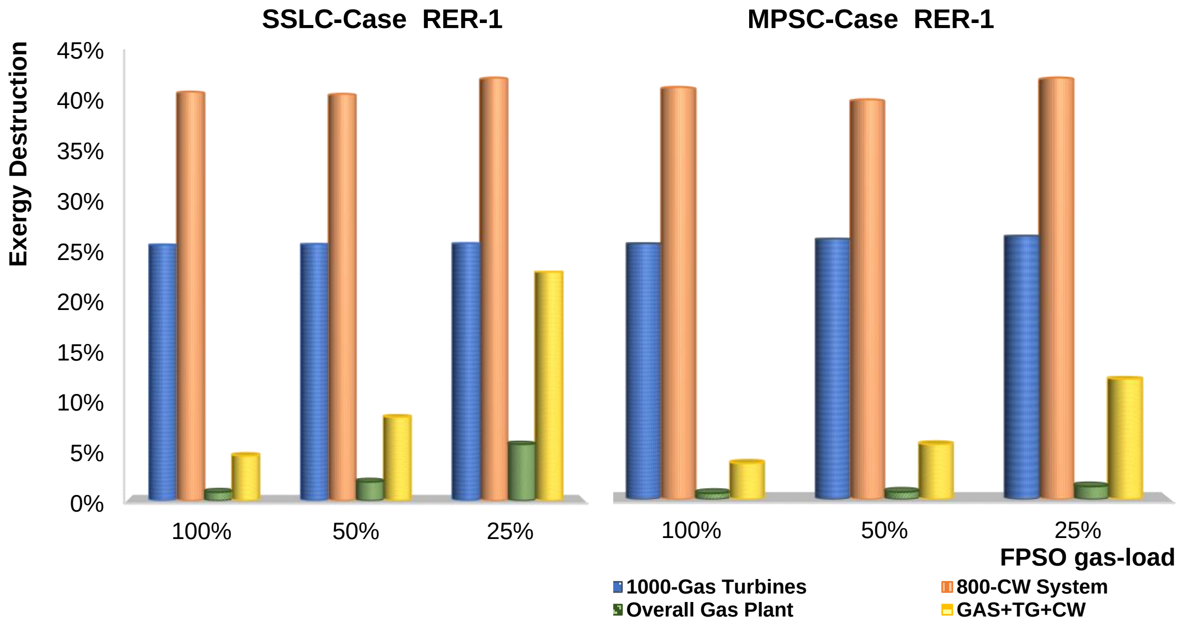

Figure 4.14. Exergy destructions (%) versus gas-load with RER-1: SSLC-Case, MPSC-Case.

Fig. 4.15 provides segmented portraits of percent exergy destructions of SSLC-Case and MPSC-Case gas-plants using RER-2. Percent exergy destructions are calculated with absolute destructions (Fig. 4.12) and respective inlet exergy flow rates of subsystems. Gas-plant percent exergy destructions in Fig. 4.15 are much higher than Fig. 4.14 counterparts. The underlying reason has to do with the considered RER: Despite RER invariance of absolute exergy destructions, RER-1 embodies chemical exergy in inlet exergy flows, dramatically inflating them and appreciably reducing percent destructions, while RER-2 put inlet exergy flows into appropriate scales entailing better discrimination of gas-plant irreversibilities. Fig. 4.15 also evinces gas-export compressors (C-500) as the SSLC-Case subsystem with highest percent exergy destruction at 25% gas-load, but at 100% gas-load – i.e., design flow – percent destruction goes down thanks to no utilization of anti-surge recycle. EOR compressor (C-700) and CO_2 compressors (C-600) behave differently, keeping high percent exergy destruction even at 100% gas-load, since they always operate with high anti-surge recycle ratios due to large sizing suited for full-injection operation mode. In MPSC-Case most compressors operate with low percent exergy destruction comparatively to SSLC-Case.

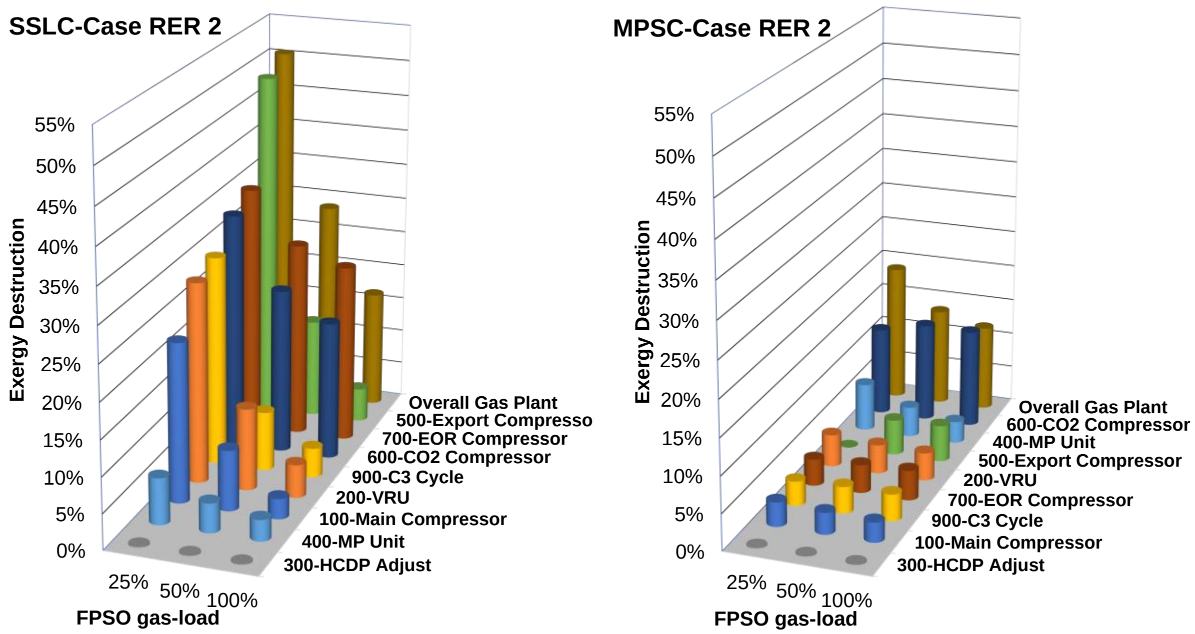

Figure 4.15. Exergy destructions (%) with RER-2: SSLC-Case, MPSC-Case.

4.3.2.1. Exergy Analysis: Consistency Check

Following Teixeira et al. (2016), the consistency of exergy analysis can be checked by calculating the lost power (work) $\dot{W}^{LOST}$ using two thermodynamically independent routes: via the rate of exergy destruction $\Delta\dot{B}$ in Eq. (4.3) and via the 2nd Law $\dot{W}^{LOST}$ formula in Eq. (4.4). Since all calculations of exergy flows rely on steady-state simulation of heavy flowsheets, with hundreds of streams and dozens numerically iterated recycles, followed by a numerically-intensive treatment with thermodynamic properties extracted from the flowsheet already incorporating some round-off errors, it is natural that $\Delta\dot{B}$ and $\dot{W}^{LOST}$ present some unavoidable discrepancy. In the present study, very low discrepancies smaller than 0.1% were encountered for the majority of the 12 exergy analyses. The exception corresponds to SSLC-Case at 100% gas-load with RER-1, which reached 1% of discrepancy between $\Delta\dot{B}$ and $\dot{W}^{LOST}$. Results of consistency checks are in Tables B3.2.1 to B3.2.4, Supplementary Materials B, Section B3.2.

4.3.3. Investment and Footprint Assessments

MPSC-Case frankly outperformed SSLC-Case on energy-efficiency and exergy-efficiency grounds. But it is also important to compare *FCI* and costs of SSLC-Case and MPSC-Case to establish, or not, the economic feasibility of MPSC-Case and of MPSC design in FPSOs. Fig. 4.16 summarizes *FCI* comparison of SSLC-Case and MPSC-Case. Considering only compressors and intercollers/aftercoolers, MPSC-Case has a 27% greater *FCI*, or 15.3MMUSD. However, since one less GT is necessary in MPSC-Case, there is also a *FCI* reduction of 19.7MMUSD, resulting a final MPSC-Case *FCI* (compressors, intercollers/aftercoolers and GTs) 4.4MMUSD lower than the SSLC-Case counterpart. Therefore, in addition to being more energy/exergy efficient, MPSC-Case design also entailed 3% of *FCI* savings. However, the risk of using only two GTs in MPSC-Case is evident: at 100% gas-load GTs would operate at ≈99% of design capacity; i.e., with zero clearance for extra demand. Operation with 3 GTs – now at 67% of design load at 100% gas-load – is safer.

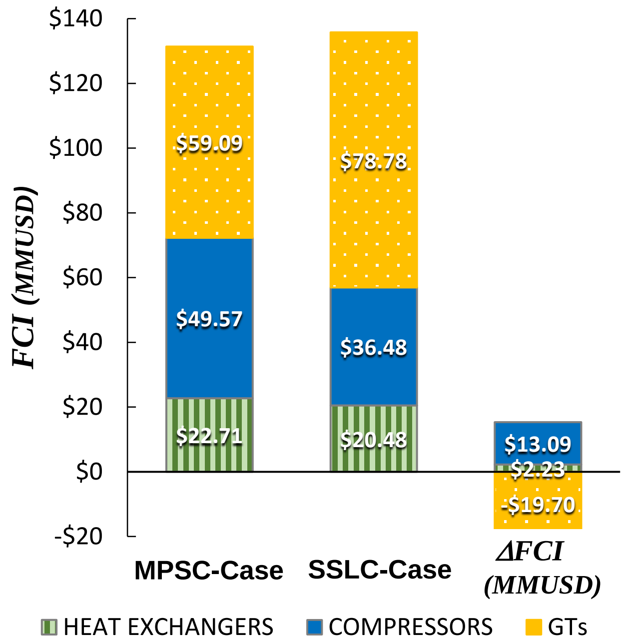

Figure 4.16. *FCI* comparison: MPSC-Case versus SSLC-Case.

4.3.4. Weight Comparison

Fig. 4.17 compares equipment weights showing MPSC-Case with ≈115 t more weight than SSLC-Case. Despite the criticality of equipment weight and footprint on FPSO topside, the weight difference of only ≈*4%* against MPSC-Case is acceptable vis-à-vis its sound exergy, energy and environmental benefits.

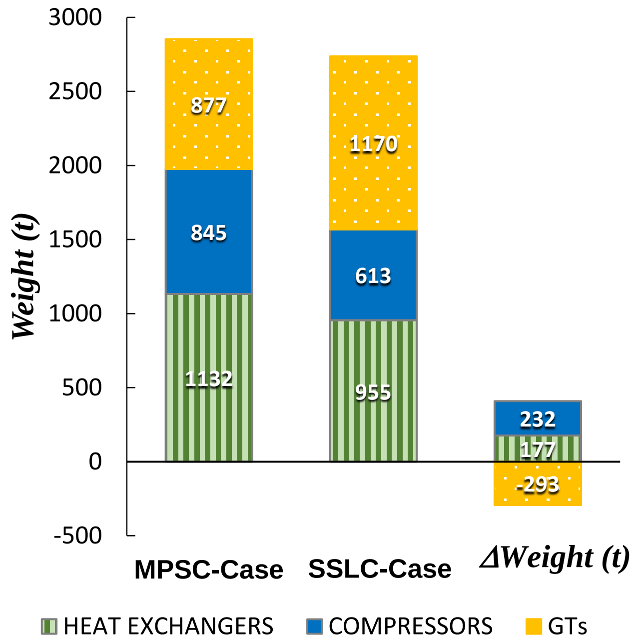

Figure 4.17. Equipment weight comparison: MPSC-Case versus SSLC-Case.

4.4. Conclusions

Process simulations, exergy analyses and *FCI*/footprint estimation of FPSO gas-plants adopting different compressor schemes – SSLC-Case (single-shaft larger compressors with anti-surge recycles) and MPSC-Case (multiple-paralleled smaller compressors without anti-surge recycles) – were performed unveiling an outstanding superiority of MPSC-Case over SSLC-Case on exergy-efficiency, energy-efficiency and environment grounds, contrasted by a small superiority of SSLC-Case in terms of *FCI*/footprint.

SSLC-Case and MPSC-Case were compared in terms of exergy-efficiency, *FCI*/footprint and CO_2 emissions. Simulations revealed that oversized compressors with anti-surge recycles (SSLC-Case) lead to almost constant power consumption along the field lifespan, regardless the gas-load processed. Consequently, fuel-gas and CO_2 intensities increase in SSLC-Case as gas-load decreases. It was shown that the efficiency of compressors can be kept high using VSD and smaller paralleled compressors. Moreover, the proposed MPSC-Case eliminates anti-surge recycles, turning the power demand proportional to gas-load, improving FPSO fuel-gas and CO_2 intensities.

Exergy analyses were conducted using two Reference Environmental Reservoirs, RER-1 and RER-2. RER-1 inflates exergy flows with the high chemical exergy of hydrocarbons, producing too high exergy efficiencies of physical operations (e.g., compressors, exchangers and separators); i.e., the modest irreversibilities of physical operations and of the entire gas-plant are masked giving exergy efficiencies for SSLC-Case and MPSC-Case always close to ~99%, regardless the gas-load. However, RER-1 is useful for chemically reactive operations with high spontaneity such as gas-turbines and combustors. For such operations, RER-1 produces reliable exergy efficiencies because there is huge rate of exergy destruction in gas-fired systems corresponding to high fractions of the inlet exergy flow. Counterpointing this, RER-2 deflates exergy flows by excluding the high chemical exergy of hydrocarbons, entailing that the exergy assessments of physical operations and of typical gas-plants (i.e., gas-turbines excluded) are now meaningful. Exergy analyses corroborate the simulation achievements, unveiling that MPSC-Case entails a much lower FPSO exergy destruction rate according to both RER-1 and RER-2. For FPSO gas-load ranging from 25% to 100%, the RER-2 exergy efficiency of SSLC-Case lies between 49% and 83%, whereas the counterpart of MPSC-Case is always from 81% to 88%.

Investment and footprint assessments indicate that MPSC-Case, besides being more exergy-efficient, energy-efficient and environmentally adequate, also entails 3% of *FCI* savings, despite increasing only 4% the equipment weight. The lower power demand of MPSC-Case allowed one less GT in the FPSO, compensating the *FCI*/footprint increases of compressors and exchangers.

In summary, MPSC-Case has much superior exergy/energy and environmental performances relatively to SSLC-Case. Surprisingly, the superiority of MPSC-Case extends to economic grounds, thanks to the elimination of a GT power generator. In a carbon taxation scenario, MPSC-Case would be even more profitable.

4.5. References of Chapter 4

Albusaidi, W., Pilidis, P., 2015. An iterative method to derive the equivalent centrifugal compressor performance at various operating conditions: Part I: Modelling of suction parameters impact. Energies 8, 8497–8515. https://doi.org/10.3390/en8088497

Allahyarzadeh-Bidgoli, A., Salviano, L.O., Dezan, D.J., de Oliveira Junior, S., Yanagihara, J.I., 2018. Energy optimization of an FPSO operating in the Brazilian Pre-salt region.

Energy 164, 390–399. https://doi.org/10.1016/J.ENERGY.2018.08.203

Araújo, O.Q.F., Reis, A.C., de Medeiros, J.L., Nascimento, J.F., Grava, W.M., Musse, A.P.S., 2017. Comparative analysis of separation technologies for processing carbon dioxide rich natural gas in ultra-deepwater oil fields. J. Clean. Prod. 155, 12–22. https://doi.org/10.1016/j.jclepro.2016.06.073

Arinelli, L.O., de Medeiros, J.L., Teixeira, A.M., Araújo, O.Q.F., 2019. Modeling of Supersonic Separators and Membrane Permeation Units for Processing of CO2-Rich Natural Gas with HYSYS Implementation, in: Offshore Processing of CO2-Rich Natural Gas with Supersonic Separator: Multiphase Sound Speed, CO2 Freeze-Out and HYSYS Implementation. Springer International Publishing, Cham, pp. 163–213. https://doi.org/10.1007/978-3-030-04006-2_6

Barrera, J.E., Bazzo, E., Kami, E., 2015. Exergy analysis and energy improvement of a Brazilian floating oil platform using Organic Rankine Cycles. Energy 88, 67–79. https://doi.org/10.1016/J.ENERGY.2015.03.091

Chang, K., Baril, R., Hull, M., Pepe, N.T.M., Nwachuku, I.B., Doezema, L.A., 2014. Microseepage of C2-C5 alkanes over the Baldwin Hills in Los Angeles. Atmos. Environ. 87, 170–174. https://doi.org/10.1016/j.atmosenv.2014.01.047

Chevron, 2018. Climate Change Resilience: A Framework for Decision Making. https://www.chevron.com/ -/media/shared-media/documents/climate-change-resilience.pdf (Accessed 21-October-2019).

Copenhagen Economics, 2017. The future of fossil fuels: How to steer fossil fuels use in a transition to a low-carbon energy system. An analysis of fossil fuels trajectories in low-carbon scenarios. http://www.energy-transitions.org/sites/default/files/ETC - Copenhagen Economics - The future of fossil fuels - Summary Paper.pdf (Accessed 2-July-2018).

Cruz, M.A., Araújo, O.Q.F., de Medeiros, J.L., 2018. Deep seawater intake for primary cooling in tropical offshore processing of natural gas with high carbon dioxide content: Energy, emissions and economic assessments. J. Nat. Gas Sci. Eng. 56, 193–211. https://doi.org/10.1016/j.jngse.2018.06.011

da Silva, J.A.M., de Oliveira Junior, S., 2018. Unit exergy cost and CO2 emissions of offshore petroleum production. Energy 147, 757–766. https://doi.org/10.1016/j.energy.2018.01.100

Dinçer, I., Rosen, M. EXERGY : Energy, Environment and Sustainable Development. Elsevier Science. https://doi.org/https://doi.org/10.1016/C2010-0-68369-6

Gallo, W.L.R., Gallego, A.G., Acevedo, V.L., Dias, R., Ortiz, H.Y., Valente, B.A., 2017. Exergy analysis of the compression systems and its prime movers for a FPSO unit. J. Nat. Gas Sci. Eng. 44, 287–298. https://doi.org/10.1016/j.jngse.2017.04.023

Veloso, T.G.C., Sotomonte, C.A.R., Coronado, C.J.R., Nascimento, M.A.R., 2018. Multi-objective optimization and exergetic analysis of a low-grade waste heat recovery ORC application on a Brazilian FPSO. Energy Convers. Manag. 174, 537–551.

https://doi.org/10.1016/j.enconman.2018.08.042

IEA, 2018. 2018 World Energy Outlook: Executive Summary. Oecd/Iea. https://webstore.iea.org/ download/summary/190?fileName=English-WEO-2018-ES.pdf (Accessed 21-October-2019).

IOGP, 2016. Environmental Performance Indicators - 2015 data, IOGP. London. www.iogp.org (Accessed 21-October-2019).

Silva, F.C.N., Flórez-Orrego, D., de Oliveira Junior, S., 2019. Exergy assessment and energy integration of advanced gas turbine cycles on an offshore petroleum production platform. Energy Convers. Manag. 197, 111846. https://doi.org/10.1016/j.enconman.2019.111846

Nguyen, T., Pierobon, L., Elmegaard, B., Haglind, F., Breuhaus, P., Voldsund, M., 2013. Exergetic assessment of energy systems on North Sea oil and gas platforms. Energy 62, 23–36. https://doi.org/10.1016/j.energy.2013.03.011

Nguyen, T.V., Jacyno, T., Breuhaus, P., Voldsund, M., Elmegaard, B., 2014. Thermodynamic analysis of an upstream petroleum plant operated on a mature field. Energy. https://doi.org/ 10.1016/j.energy.2014.02.040

Panton, L.K., Eide, B., Solutions, A., Førde, T., 2014. Exergy analysis of conventional and electrified oil and gas platforms. Norwegian University of Science and Technology. https://ntnuopen.ntnu.no/ntnu-xmlui/bitstream/handle/11250/235802/757579_FULLTEXT01.pdf?sequence=2&isAllowed=y (Accessed 23-October-2019).

Petrobras, 2013. Polo Pre-Sal - Bacia de Santos - Etapa 1. IBAMA. http://licenciamento.ibama.gov.br/ Petroleo/Producao/Producao - Polo Pre-Sal - Bacia de Santos - Etapa 1 - Petrobras/ (Accessed 4-July-2017).

Pierobon, L., Benato, A., Scolari, E., Haglind, F., Stoppato, A., 2014. Waste heat recovery technologies for offshore platforms. Appl. Energy 136. https://doi.org/10.1016/j.apenergy.2014.08.109

Reis, M.M.L., Gallo, W.L.R., 2018. Study of waste heat recovery potential and optimization of the power production by an organic Rankine cycle in an FPSO unit. Energy Convers. Manag. 157, 409–422. https://doi.org/10.1016/J.ENCONMAN.2017.12.015

Roussanaly, S., Aasen, A., Anantharaman, R., Danielsen, B., Jakobsen, J., Heme-De-Lacotte, L., Neji, G., Sødal, A., Wahl, P.E., Vrana, T.K., Dreux, R., 2019. Offshore power generation with carbon capture and storage to decarbonise mainland electricity and offshore oil and gas installations: A techno-economic analysis. Appl. Energy 233–234, 478–494. https://doi.org/10.1016/j.apenergy.2018.10.020

Rystad Energy, 2019. FPSO market is booming with Brazil fueling demand. https://www.rystadenergy.com/newsevents/news/press-releases/FPSO-market-is-booming-with-Brazil-fueling-demand/ (Accessed 21-October-2019).

Soundararajan, K., Ho, H.K., Su, B., 2014. Sankey diagram framework for energy and exergy flows. Appl. Energy 136, 1035–1042. https://doi.org/10.1016/j.apenergy.2014.08.070

Teixeira, A.M., Arinelli, L.O., de Medeiros, J.L., Araújo, O.Q.F., 2016. Exergy Analysis of Monoethylene glycol recovery processes for hydrate inhibition in offshore natural gas fields. J. Nat. Gas Sci. Eng. 35, 798–813. https://doi.org/10.1016/J.JNGSE.2016.09.017

Voldsund, M., Nguyen, T.V., Elmegaard, B., Ertesvåg, I.S., Røsjorde, A., Jøssang, K., Kjelstrup, S., 2014. Exergy destruction and losses on four North Sea offshore platforms: A comparative study of the oil and gas processing plants. Energy 74, 45–58. https://doi.org/10.1016/j.energy.2014.02.080

Appendix 4A: Comparison of Exergy Efficiencies of Gas-Turbines

Exergy flows of FPSO gas-plants were calculated with a novel methodology (Teixeira et al., 2016) mostly using RER-2. On the other hand, GTs exergy efficiency of SSLC-Case and MPSC-Case were determined with exergy flows according to RER-1 via Eq. (4.5a). However, the exergy efficiency of GTs according to Gallo et al. (2017) in Eq. (4.5b) offers an opportunity to compare and validate the present approach. This comparison is available in Table 4A.1 which shows that, despite the completely different methodologies for exergy flows, the present exergy efficiency of GTs using RER-1 and Eq. (4.5b) gave values very close to the value of Gallo et al. (2017).

Table 4A.1. Exergy Efficiency Comparison for GTs (Eq. (4.5b) with RER-1).

	This work		***Gallo et al. (2017)***
	100% Gas-Load SSLC-Case	*100% Gas-Load MPSC-Case*	*100% Gas-Load*
FPSO Gas-Load [MMSm^3/d]	*4.75*	*4.75*	*6.00*
Active GTs	*3*	*3*	*3*
Net Power [kW]	*57762*	*51108*	*69134*
η_{GT}	*32.5%*	*34.1%*	*33.8%*

5. IMPACT OF SOLID WASTE TREATMENT FROM SPRAY DRYER ABSORBER ON THE LEVELIZED COST OF ENERGY OF A COAL-FIRED POWER PLANT

This chapter is published a full-length original article in the Journal of Cleaner Production.

CRUZ, M. DE A. et al. Impact of solid waste treatment from spray dryer absorber on the levelized cost of energy of a coal-fired power plant. **Journal of Cleaner Production**, v. 164, 2017.

Abstract

Coal-fired power plants with semi-dry flue-gas desulfurization (semi-dry FGD) system produce daily tones of ashes contaminated with calcium sulfite. To turn this solid waste useful, e.g. to the cement industry, and avoid landfill disposal, the present study suggests a semi-dry FGD solid waste treatment unit, that promotes the dry oxidation of the calcium sulfite to calcium sulfate. Sizing of main equipment using pilot-plant data and patents allows economic evaluation of capital expenditure, operational and maintenance costs, and sale of the treated residue, allowing estimation of levelized cost of energy to assess the impact of the technology on the electricity price of a power plant using the proposed solid waste treatment unit. As base case, a Brazilian coal-fired power plant facing decision making process on semi-dry FGD waste destination is selected. Results demonstrate that the semi-dry FGD, without the solid treatment unit, has total levelized cost of energy increased in 0.56% (from 94.44 to 94.97 \$/MWh) resulting from solids waste disposal. If the treated semi-dry FGD waste was transferred (at zero revenue) as additive to a cement industry, the levelized cost of energy of the power plant would remain approximately unchanged. This is because the increase of 0.51\$/MWh resulting from the investment and operation and maintenance cost of the treatment unit is compensated by the decrease of 0.53\$/MWh, in virtue of the avoided waste disposal costs. However, if the commercialization as raw material of the treated semi-dry FGD waste is considered, a reduction of 2.83 \$/MWh (~3%) on the levelized cost of energy (to 92.14 \$/MWh) would occur. In both cases, the proposed treatment unit shows small impact on the total power plant levelized cost of energy, besides solving the solid management problems of landfill saturation, land use and costs related to landfill maintenance. Thus, it is adequate to implement the semi-dry FGD waste treatment unit on the power plant in question. The conclusion can be extended to plants with similar design and economic parameters.

Keywords: Coal-Fired Power Plant; Flue-Gas Desulfurization; Spray Dryer Absorbers; Solid Waste Treatment; Calcium Sulphite Oxidation; Levelized Cost of Energy.

Supplementary Materials for this chapter are found in Appendix H, Section C.

Nomenclature

Abbreviations

CAPEX	Capital Expenditure
FBR	Fluidized Bed Reactor
FGD	Flue-Gas Desulfurization
IECM	Integrated Environmental Control Model software
OPEX	Operational Expenditure
PCC	Pulverized Coal Combustion
PFD	Process Flow Diagram
SDA	Spray Dryer Absorber

Roman letters

AE	Annual energy output (MWh/yr)
D	Diameter (m)
f	Annuity factor (%)
HHV	Higher Heating Value (kJ/kg)
L	Length (m)
LCOE	Levelized cost of energy ($/MWh)
MM	Molecular mass (kmol/kg)
n	Polytrophic exponent
P	Pressure (kPa)
Pw	Power (kW)
R_i	Reaction number *i*, where *i* is a counter
q	Flow rate (kg/h)
R	Gas constant (J/mol.K)
r_p	Pressure ratio
t	Lifetime of the plant (yr)
T	Temperature (K)
TAC	Total annualized capital costs ($/yr)
Z	Average compressibility factor
z	Discount Rate (%)

Greek Letters

ΔH_r	Enthalpy of reaction (kcal/mol)
η_p	Polytrophic efficiency

5.1. Introduction

Brazilian electricity matrix is dominated by hydropower generation. However, because of the recent water scarcity crisis in Brazil, hydroelectricity has been supplemented with electrical power generated by thermal power plants, resulting in 18% increase during 2013-2014 and presently represents 28.2% of the total Brazilian electricity source. In this same period, electricity produced by coal power plants has increased 24.2%, with mineral coal representing 9.6% of the thermopower source in Brazil (EPE, 2015a). The Brazilian energy demand will increase in an average of 3.6% yearly until 2019, thus it is expected that the use of coal-fired power plants continues to increase in short to medium term (EPE, 2015b). Furthermore, an average power plant technical lifetime of about 40 years for coal compared to 34 years for gas and 34 years for oil-fired power plants is estimated (Farfan and Breyer, 2017), indicating that the next decade will sustain supply of fossil energy accompanied by growing environmental legislation and policies. Consequently, technologies for reducing post-combustion emissions will assume a protagonist role, notedly for carbon dioxide and sulfur oxides, the latter – flue-gas desulfurization (FGD) being a fingerprint of coal-fired power plants.

The commercial application of FGD is a challenge in terms of removal efficiency, price and availability of sorbent (Ma et al., 2000). Wet limestone FGD system is the most widely used process for flue-gas desulfurization because of its high performance and reduced operating cost (Cordoba, 2015). Less capital-intensive alternatives to wet FGD are sought, but are characterized by modest SO_2 removal despite reduced capital costs (Sage and Ford, 1996). semi-dry flue-gas desulfurization (semi-dry FGD) is an intermediate between dry and wet flue-gas scrubbing, with slightly lower costs than wet FGD, but presents residue disposal problems (Sage and Ford, 1996).

Nevertheless, about 12% of USA power plants were using semi-dry FGD systems in 2007. (EPRI, 2009) According to Alston Power, the market was running about 40% - 60% in favour of semi-dry FGD. The semi-dry technology has typically been employed on small to moderate size plants. Because of size limitations on the absorber tower, the maximum power served by a spray dryer is about 250 – 350 MW. Power plants with semi-dry FGD usually burns low-sulfur coal, in virtue of a limit of 95% on SO_2 removal efficiency. The semi-dry technology is interesting in regions where the water supply is limited (e.g., northeast of Brazil and western of the United States), because it consumes 30-40 less water than Wet-FGD. In terms of capital expenditure (CAPEX), the cost of a semi-dry FGD is about 60% lower than the wet technology.(Blankinship, 2005) Environmental impact analyses of FGD alternatives are available (Wu et al., 2017), they mostly treat energy consumption - resource consumption and pollutant emissions, despite solid residues being recognized as the most critical for FGD technologies (Feng et al., 2014).

The semi-dry FGD solid waste is basically composed of calcium sulfite ($CaSO_3$), varying amounts of unreacted fly ashes and lime. Most units do not present fly ash pre-collectors, often resulting in semi-dry FGD waste with high ash percentage (EPRI, 2009). Fly ashes from combustion of mineral coal show very low agglomerating property, but, in the presence of water, react with calcium hydroxide ($Ca(OH)_2$), at ambient temperature, to form aggregating (pozzolanic) compounds (Thomas, 2007; ABNT, 2015). In USA only 22% is used in commercial applications, with mining applications representing 83% of its use. Other uses include oil/gas field services, cementitious products, cement replacement in concrete (pozzolanic material), engineering applications, agriculture, soil stabilization and as wet FGD sorbent (ACAA, 2014).

Most coal-fired power plants that use semi-dry FGD systems currently dispose its solid residue on landfills. The solids transportation and landfill maintenance is expensive, unhealthy to local workers (EPRI, 1998) and unsustainable in long term, because the landfill becomes saturated, as could be noticed in Fig.5.1. The power plant complex of Pecém, shown in Fig. 5.1, has three 360 MW coal-fired power plants units, with semi-dry FGD for SO_2 control. The start-up occurred in 2012 and after 4 years of operation 2 ash landfills becomes saturated and a third one is being built. In Brazil and USA, among other countries, the use of semi-dry FGD systems is expected to grow, or at least be maintained, creating the need for increased alternatives for utilization for the semi-dry FGD waste.

Fig. 5.1. Ash landfills of a Brazilian coal-fired power plant in December of 2016.
Source: Google Earth (satellite images) and personal archive (landfill picture).

Among possible uses, FGD gypsum is recognized as a substitute for natural gypsum in the cement industry (Galos et al., 2002). In fact, as stated by Mikulčić et al. (2016), the challenge for the cement industry is to use alternative raw materials especially wastes originated from other industries, highlighting, among others, fly ashes and gypsum from coal power plants.

To explore this synergy, i.e., the use of the semi-dry FGD waste as pozzolanic material, solids treatment to comply with standards are required. Besides other parameters, standards (e.g., ABNT, 2015; ASTM, 2015) define threshold limit for $CaSO_3$ content in the semi-dry FGD waste. For instance, in Brazil, when $CaSO_3$ exceeds 5% (mass) it is considered inadequate to be sold as pozzolanic or cementitious material. The Brazilian ABNT standard (ABNT, 2015) is similar to the American ASTM Standard C618 (ASTM, 2015).

In this context of expanding energy demand, continued share of coal among energy supply sources, intensification of legislation to enforce SO_2 emissions and the social, economic and environmental impacts of landfill as destination to semi-dry FGD waste, this study evaluates the effect on the levelized cost of electricity (LCOE) posed by using a treatment unit. Specifically, the work approaches a new technology which employs fluidized bed reactor

(FBR) to convert the $CaSO_3$ present in the semi-dry FGD waste by high temperature dry oxidation, resulting in residue compliance with the class C pozzolanic material standard. Additionally, a comparison is presented of the LCOE with FGD solids management and the LCOE of the original project, i.e., landfill destination.

The LCOE is recognized worldwide as one of the most adequate methodology to compare and evaluate the economic competitiveness of different electricity generation technologies. (Tolmasquim, 2016) The LCOE gives the cost of the energy that is generated over the lifetime of a given power plant per unit of energy produced. In a simple manner, it is calculated by dividing the total annualized cost of the power plant by the total annual energy generated in the same period (Santoyo-Castelazo and Azapagic, 2014; Short et al., 1995). The total annualized cost is based on a levelized average lifetime cost approach, using the discounted cash flow (DCF) methodology. Several general, local and technology specific assumptions must be considered for various technical and economic parameters. Costs are calculated at the plant level (busbar), and do not include transmission and distribution costs, nor considers other systemic costs or externalities beyond CO_2 emissions (IEA and NEA, 2015). A detailed procedure describing how to calculate the LCOE is supplied by NREL (Short et al., 1995) and IEA (2016). To standardize and simplify LCOE calculation, several computational tools are available. For coal-fired power plant, the IECM (Berkenpas and Grol, 2009) by Rochedo et al. (2016).

Although the semi-dry FGD waste treatment solves the solid waste problem, it demands CAPEX for building the solid waste treatment unit (FBR and auxiliary equipment), Operation and maintenance (O&M) fixed and variable costs, and consumes energy (the air used to oxidize $CaSO_3$ must be slightly compressed (by a blower) and sometimes heated above 500 ºC). Although this costs increases the LCOE, it allows revenues (pozzolanic/cementitious material and reduction of landfill related costs), which could render it profitable.

Hence, the main objective of this study is determining the impact of the semi-dry FGD waste treatment unit on the LCOE of a coal-fired power plant. The work is organized in four sections. In Section 2, process premises and methods of calculating LCOE are presented. Results and discussion follows in Section 3 and main conclusions are given in Section 4. Supplementary material is available on line with results from Aspen Process Economic Analyzer (Aspentech Inc) and details for FBR sizing.

5.2. Process Premises and Methods

The block diagram of Fig. 5.2 presents the calculation procedure used in this study.

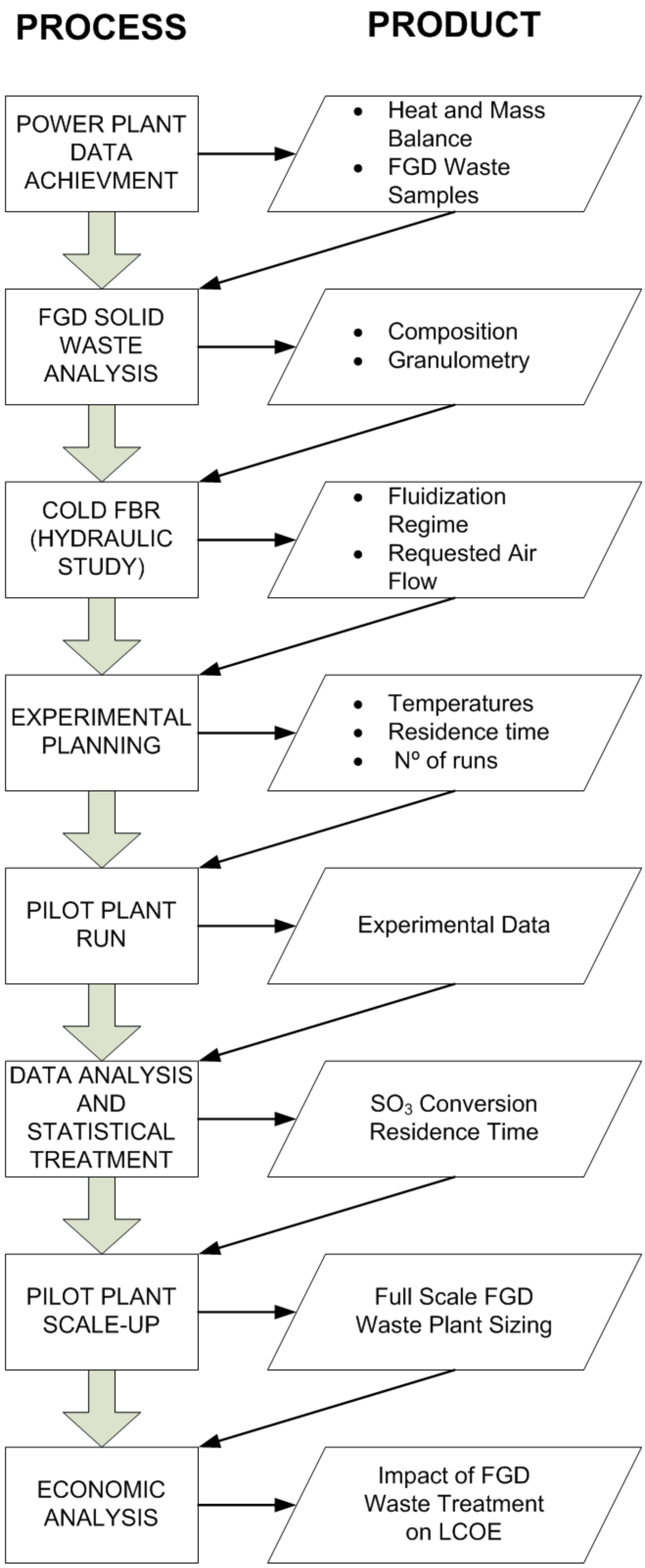

Fig. 5.2 block diagram of calculation procedure

The work is based on a 360 MW coal-fired power plant. This is a conventional pulverized coal combustion (PCC) plant, located in the Brazilian northeast. Coal from Colombia is supplied to the power plant. It is transported by ship and sent from the port terminal to the coal stock by a mechanical belt.

The proposed semi-dry FGD waste treatment unit is based on a pilot-plant, designed and constructed by the authors. It is composed of a fluidized bed reactor (FBR), where occurs oxidation of $CaSO_3$, an air compressor, a heater, a cyclone, an economizer and an air filter. The cyclone collect particles above 10 μm back to the FBR. The economizer recovers part of the heat of the exhaust air from the FBR. The air filter avoids emission of small particles, below 10 μm, to the atmosphere. The pilot-plant FBR has a diameter of 200 mm and 1100 mm of height. Depending on temperature and residence time, conversions of $CaSO_3$ in $CaSO_4$ up to 90% is reached. Fig. 5.3 presents a diagram of the pilot-plant.

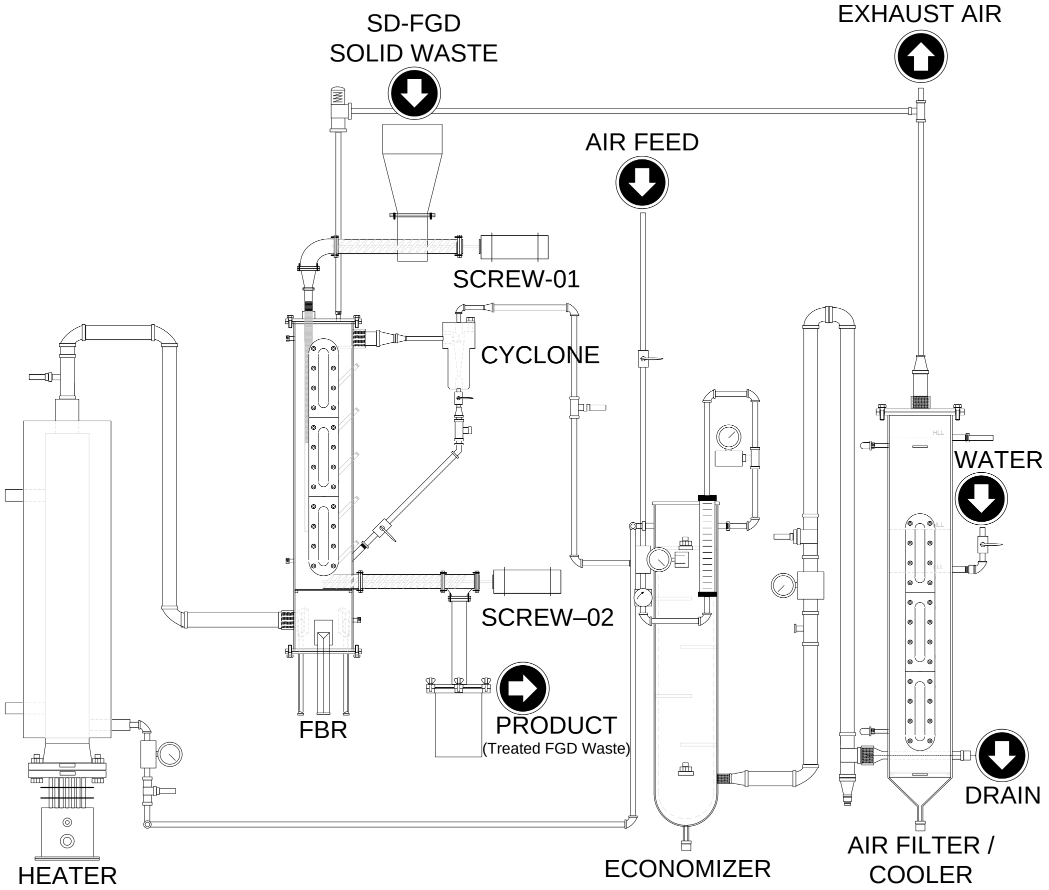

Fig. 5.3. Diagram of the semi-dry FGD waste treatment pilot-plant

A simplified process flow diagram of the power plant and the semi-dry FGD waste treatment unit was developed and is presented in Fig. 5.4.

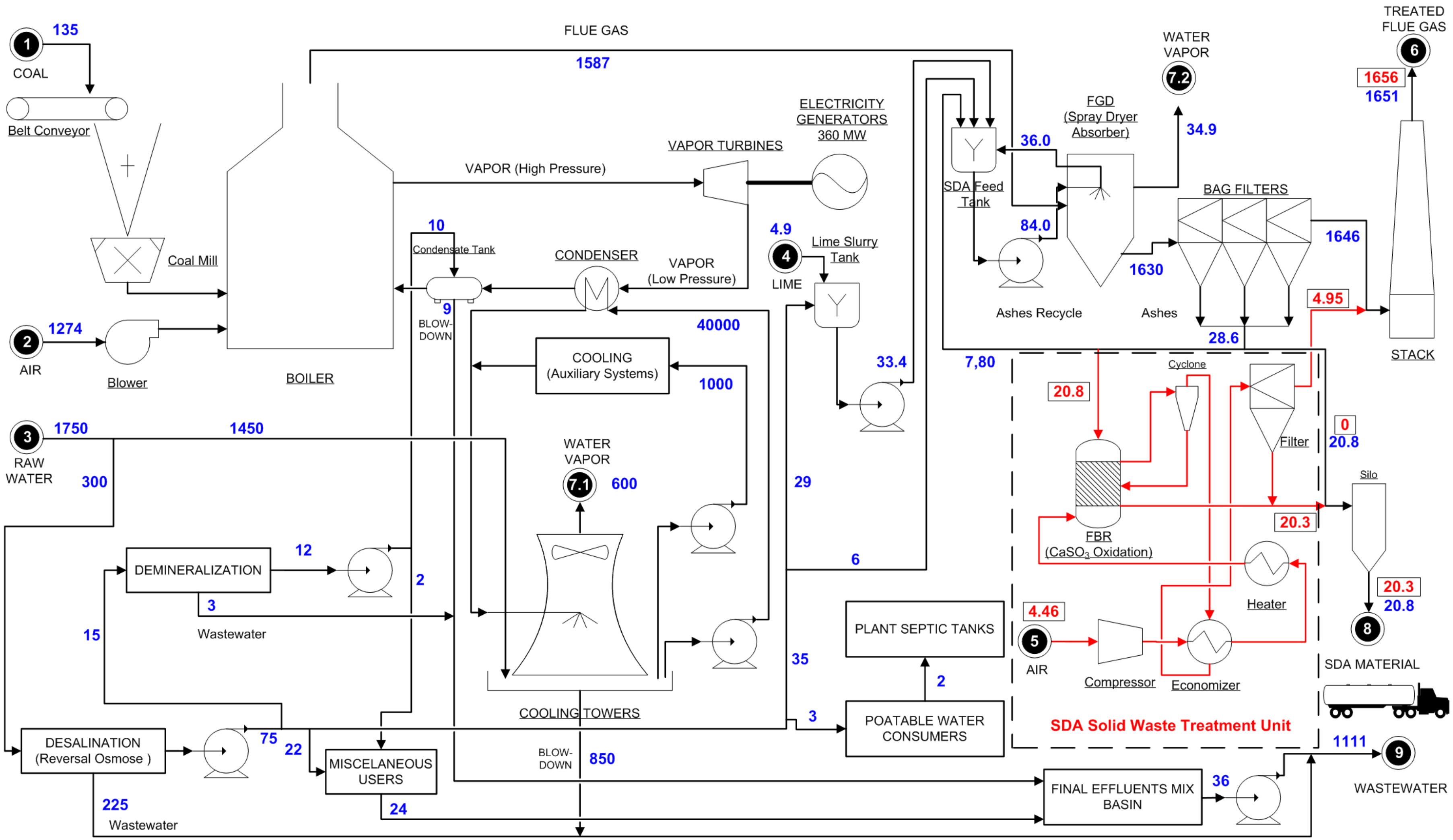

Fig. 5.4. Process flow diagram of the coal-fired power plant and the semi-dry FGD waste treatment unit (indicated with a dashed box). Numbers along stream arrows indicate original mass balance, while numbers within boxes correspond to mass balance of modified power plant (with solid waste treatment).

5.2.1. Power Plant

The global mass balance of the power plant follows the original layout (without treatment of the semi-dry FGD waste) of the reference power plant. The main process streams are represented in the simplified process flow diagram presented on Fig. 5.4, where mass flows are expressed in tons per hour. Original power plant streams mass flow (t/h) represented by numbers along stream arrows, and the semi-dry FGD waste treatment unit with numbers inside boxes.

To perform the heat balance and validate the mass balance of the reference PCC plant, the software IECM v 9.2.1 (Berkenpas; Grol, 2009) is adopted. Main set parameters are based on the power plant's data book and environmental impacts assessment (EIA) study (DEEPL, 2008). Fig. 5.5 presents the plant representation on IECM interface.

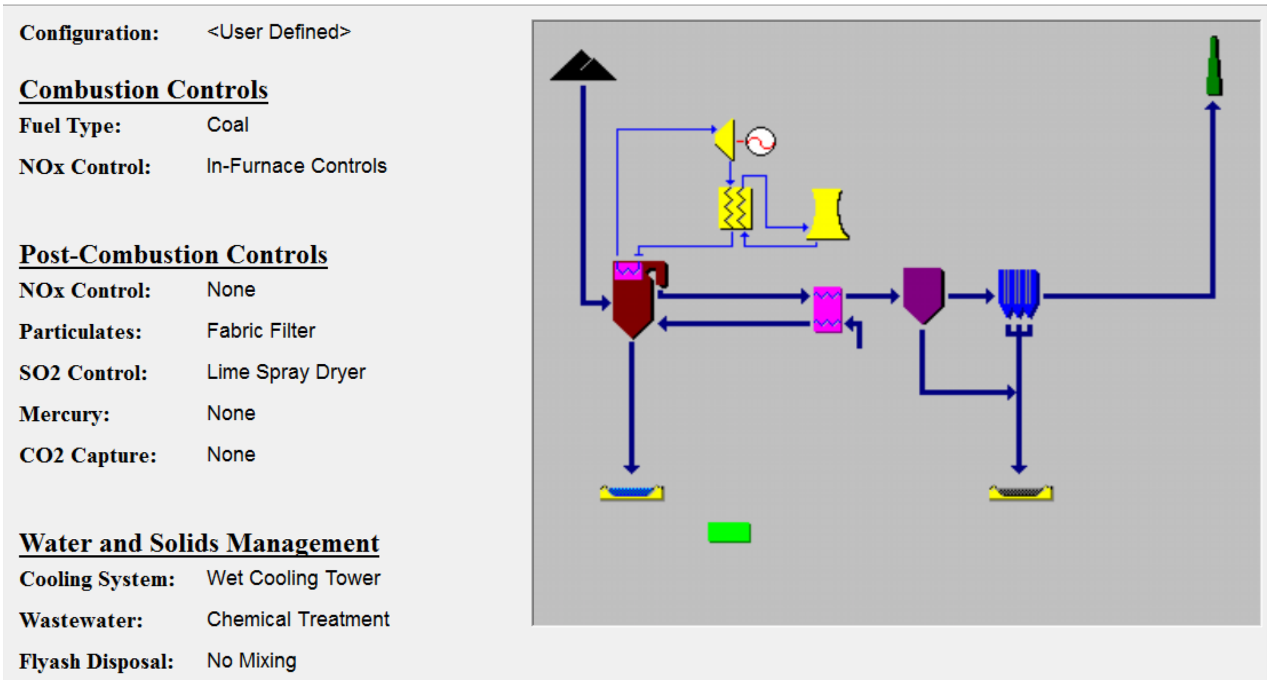

Fig. 5.5. PCC Base Plant Design. Source: IECM v 9.2.1 Interface.

5.2.2. Semi-dry FGD waste Treatment Unit

Basically, all information to design auxiliary equipment of the semi-dry FGD waste treatment unit depends on the determination of the inlet and outlet FBR air flow (Section C1 of Supplementary Materials C). The FBR heat and mass balances follow information presented by Jons et al. (1987) and in data acquired from the pilot-plant experiments (not reported). FBR inlet and outlet air streams (standard and actual volumetric flows) of the full-scale plant are determined using the process simulator PRO-II v9.3 (Schneider Electric SimSci), as presented in Fig. 5.6. Compressor power and heaters duty are also determined with the simulator. The economizer is designed using the Aspen Exchanger Design and Rating v8.8 (Aspentech Inc).

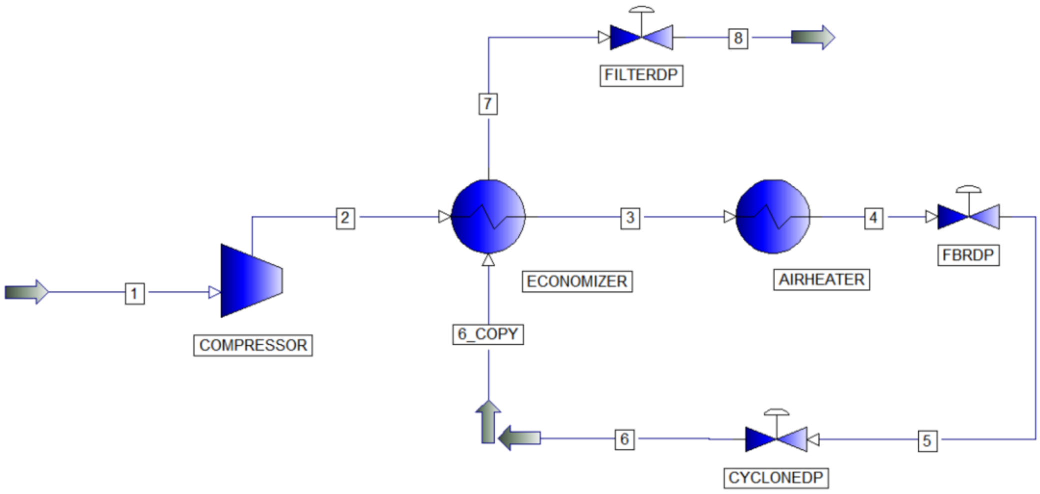

Fig. 5.6. Simulation diagram of the pilot fluidization plant (PRO-II). Valves with DP after equipment names represents the pressure drop of the referred equipment.

5.2.3. Levelized Cost of Energy

The LCOE of the coal-fired power plant is calculated using the software IECM v 9.2.1 (Berkenpas; Grol, 2009), while the LCOE for the semi-dry FGD waste treatment unit is based on main equipment economic analysis, performed in Aspen Process Economic Analyzer v8.8 (APEA, Aspentech Inc) (results are presented in Section C2 of the Supplementary Materials C. APEA can estimate CAPEX and O&M of a given industrial process, based on main equipment specification. Tables C2.1 and C2.2, from Supplementary Materials C, present the equipment specifications and main economic parameters assumed in APEA for CAPEX, O&M and LCOE evaluation of the semi-dry FGD waste treatment unit.

5.2.4. Semi-dry FGD waste Treatment Unit Heat and Mass Balance

The set of reactions expected to occur inside the FBR is presented in Table 5.1 (Jons et al., 1987).

Table 5.1. FBR set of reactions.

Reaction	ΔH_r (kcal/mol)	Temperature Range (ºC)
R_1 - $CaSO_3.½ H_2O \rightarrow CaSO_3 + ½ H_2O$	6.87	370-390
R_2 - $CaSO_4.2 H_2O \rightarrow CaSO_4 + 2 H_2O$	26.07	130-150
R_3 - $Ca(OH)_2 \rightarrow CaO + H_2O$	25.7	> 470
R_4 - $CaSO_3 + ½ O_2 \rightarrow CaSO_4$	-65.8	> 550

The semi-dry FGD waste composition and mass flow, shown in Table 5.2, is obtained from the heat and mass balance of the reference power plant. This is the worst expected case, as it considers coal with 1.5% of sulphur, on a weight basis. When the coal sulphur content is lower, SO_2 content in the fly-ash decreases.

Table 5.2. Composition of the semi-dry FGD waste – worst case, coal with 1.5% of sulfur.

Mass Flow (t/h)		20.78
Composition (mass %)		
	$CaSO_3.½H_2O$	38.40%
	$CaSO_4.2H_2O$	0.00%
	$Ca(OH)_2$	8.30%
	$CaSO_3$	0.00%
	$CaSO_4$	0.00%
	CaO	0.00%
	H_2O	2.00%
	Fly-ashes (inert)	51.30%

Based on Angevine et al. (1985), considering a temperature of 550 ºC and 5% of O_2 in excess, it is possible to achieve a SO_3 mass composition of 3.2% on the treated residue, complying with ASTM Standard C618(ASTM, 2015) for class C or F fly ash, that establishes a limit of 5% (mass) of SO_3 for this type of cement additive. A conversion of 91.3% is considered for reaction R_4 and 100% for reactions R_1, R_2 and R_3 (Table 5.1). These results are considered in performing the heat and mass balance of the semi-dry FGD waste treatment unit. The semi-dry FGD waste heat capacity used to estimate the energy consumption due to the heating of the residue from 80 ºC to 550 ºC is considered 730 J/kg.K, the same value of a class C fly ash (Bentz et al., 2011). The inlet and outlet air flow and composition is calculated in function of the FBR demand (reactions R_1 to R_4 of Table 5.1).

The detailed calculation is presented in Table C1.2, Section C1 of Supplementary Materials C. The air is pre-heated to 350 ºC by the economizer. The heater is designed to complete the service, rising the air temperature to the set-point (550 ºC). It is worth noting that the energy supplied by the oxidation of $CaSO_3$ and integration with steam purges of the power plant could bring the air heating energy input to zero. Thus, the air heater could be used only for the start-up of the system.

5.2.5. Equipment Scale-up and Sizing

5.2.5.1. Fluidized Bed Reactor

As the FBR is not available in industrial scale, determination of the fluidization air flow needs to be estimated. In the pilot scale, where FBR deals with a 10% w/w $CaSO_3.½H_2O$ feed, the ratio of fluidization air flow to stoichiometric air flow is 3.75. Since in this study the $CaSO_3$ mass fraction is 38.4%, the stoichiometry air flow with 5% of oxygen (O_2) excess is considered sufficient to promote bed fluidization. The length/diameter (L/D) ratio of the full scale FBR is considered the same of the pilot scale equipment (L/D=5), as well as the maximum level of solids inside the reactor (30% of L). The maximum residence time of the semi-dry FGD waste is considered 500 seconds, based in Jons et al. (1987).

5.2.5.2. Air Compressor

A fan, air blower or compressor is necessary to make the air stream passes through the economizer, air heater, FBR, cyclones and air filter, reaching the end of the process with a pressure slightly higher than atmospheric, with estimated pressure drop of 1.5 bar. As the air inlet is nearly at atmospheric pressure, the necessary absolute outlet pressure of the compressor is 250 kPa, and the pressure ratio is 2.47. This range of pressure ratio turns the use of fans and common blowers inappropriate, being a compressor more adequate for the service.

The power of centrifugal compressor is calculated using Eq. 5.1 (GPSA, 2004).

$$\boldsymbol{Pw} = \frac{\boldsymbol{q}\,.\boldsymbol{Z}.\boldsymbol{R}.\boldsymbol{T}.\left[(\boldsymbol{r_P})^{\frac{(\boldsymbol{n-1})}{\boldsymbol{n}}} - \boldsymbol{1}\right]}{\boldsymbol{3.600}\,.\boldsymbol{\eta_P}.\boldsymbol{MM}.\frac{\boldsymbol{n-1}}{\boldsymbol{n}}} \tag{5.1}$$

where $\boldsymbol{Pw}$ is the brake horsepower (kW), q is the gas flow rate (kg/h), $\boldsymbol{Z}$ is the average compressibility factor, R is the gas constant (8.314 kJ/kmol.K), $\boldsymbol{T}$ is the gas inlet temperature (K), $\boldsymbol{MM}$ is the molecular mass (kmol/kg), $\boldsymbol{r_P}$ is the pressure ratio, $\boldsymbol{n}$ is the polytrophic exponent and $\boldsymbol{\eta_P}$ is the polytrophic efficiency. The pressure ratio is calculated dividing the outlet pressure, P_2 (kPa), by the inlet pressure P_1 (kPa). P_2 is considered 250 kPa (gauge). P_1 is the atmospheric pressure (0 kPa gauge). η_p is considered 80%, q of inlet air stream (stream 1 of Fig. 5.5), 4460 kg/h, is calculated in function of the FBR demand (see Table C1.2 of Section C1 of Supplementary Materials C).

5.2.5.3. Air Heater

Although it is expected that the energy supplied by the oxidation of $CaSO_3$ and integration with steam purges from the closed loop steam cycle could heat the air inside the reactor to the required level (550 ºC), as by the reaction R_4 (see Table 5.1), the air heater is necessary to start-up the system and to heat the air when the SO_3 content in the semi-dry FGD waste is lower than expected, in function of the use of a coal with less sulphur. In this case, the oxidation reaction could not be sufficient to supply the necessary energy input and the air heater must have capacity to reach the reaction R_4 temperature set-point. PRO-II is used to calculate the heater duty, to heat the air from the compressor discharge temperature (~130 ºC) to 550 ºC. It was assumed that during the start-up no heat is recovered by the economizer. A maximum pressure drop of 30 kPa is considered in the process side of the heater.

5.2.5.4. Economizer

The economizer recovers part of the heat of the exhaust air from the FBR to pre-heat the air coming from the compressor to 350 ºC. Inlet and outlet streams temperatures and pressures are obtained from the simulation. A vertical BEU TEMA type shell-and-tube heat exchanger is considered. The design of the equipment is developed on Aspen Heat Exchanger Design and

Rating software (Aspentech Inc). A maximum pressure drop of 30 kPa is considered on shell and tubes sides.

5.2.5.5. Cyclone and Air Filter

A preliminary sizing of both equipment is not required, as the economic analysis tool (APEA) demands only the air flow to estimate costs, obtained from process simulation.

5.2.6. Semi-dry FGD Waste Treatment Unit Levelized Cost of Energy

Traditionally, the LCOE can be calculated by Eq. 5.2 (Santoyo-Castelazo and Azapagic, 2014).

$$\boldsymbol{LCOE = TAC/AE} \tag{5.2}$$

where, $LCOE$ is the levelized or unit cost of energy ($/MWh), TAC is the total annualised cost of generating electricity ($/yr) and AE is the annual energy generation (MWh/yr). TAC is the sum of annualized capital costs ($/yr), fixed costs ($/yr), variable costs ($/yr) and fuel costs ($/yr). However, sale of treated semi-dry FGD waste could be deducted from the annual variable cost parcel of *TAC*. The annualised capital costs are calculated multiplying the total capital cost by an annuity factor (*f*), that is calculated according to Eq. 5.3 (Santoyo-Castelazo and Azapagic, 2014).

$$\boldsymbol{f = z(1+z)\, e^{t}/[(1+z)e^{t} - 1)]} \tag{5.3}$$

where, z is the discount rate (%) and t is the lifetime of the plant (yr). The discount rate measures the time value of the money, it is used to calculate the present value of a cash flow and, often, to account the inherent risk of an investment.

The proper selection of the discount rate is very important to any economic analysis and depends on several factors, as rate of return, risk premium, planning horizon, interest rates and taxes. Therefore, discount rates vary from place to place, industry to industry and company to company (Short et al., 1995). In the present study, a nominal discount rate of 8% is assumed, based on Tomalsquim (2016). A lifetime of 30 years is considered for the power plant to calculate the LCOE of the semi-dry FGD waste treatment unit. Furthermore, this study considers that the treated residue can be used as cement kiln raw material, assumed as 47 $/t (an approximate value in Brazil).

Tables C2.1 and C2.2, Section C2 of Supplementary Materials C, present the equipment specifications and main economic parameters assumed on APEA to perform CAPEX, O&M and LCOE evaluation of the semi-dry FGD waste treatment unit.

5.2.7. Levelized Cost of Energy of the Coal-Fired Power Plant

Tables 5.3 and 5.4 summarize the main parameters input for IECM tool, adapted to reproduce the reference power plant heat and mass balances and performance.

Table 5.3. IECM input parameters.

Set Parameters	**Value**	**Reference**
Capacity Factor (%)	85	(Tolmasquim, 2016)
Ambient Air Dry Bulb Temperature (°C)	27	ENEVA
Ambient Air Pressure (MPa)	0.1013	Plant at sea level
Relative Humidity (%)	80.84	ENEVA
Discount Rate (%)	8.0	(Tolmasquim, 2016)
Plant or Project Book Life (yr)	30	
Federal Tax Rate (%)	15	Minimum IECM value
State Tax Rate (%)	2	(DEEPL, 2008)
Property Tax rate (%)	0	Government incentive program
Internal Cost of Electricity (COE)	Total Plant COE	
O&M Escalation Rate (%/yr)	3.5	APEA
Coal Cost ($/ton)	90	(Tolmasquim, 2016)
Gross Electrical Output (MW)	373.8	ENEVA
Steam cycle type	Sub-Critical	(DEEPL, 2008)
Boiler Efficiency (%)	90	(DEEPL, 2008)
Gas Temperature Exiting Economizer (°C)	307	ENEVA
Gas Temperature Exiting Air Preheater (°C)	118	ENEVA
Miscellaneous (%MW)	5	Set to reach reference heat rate (10097 kJ/kWh)
Construction time (yr)	4	(Tolmasquim, 2016)
Royalties Fees (%)	0	Imported Coal, royalty free.
Number of Operating Jobs	80	(DEEPL, 2008)
Maximum SO_2 removal (%)	95	(DEEPL, 2008)
Reagent Stoichiometry (molCa/molS in)	1.27	Set to reach the reference CaO consumption (4.9 t/h)
Ca content of lime (%)	90	(DEEPL, 2008)
SDA Power Requirement (% gross MW)	0.38	Set to reach the reference value (1.4 MW)
Cooling Water Inlet Temperature (°C)	39	ENEVA
Tower overdesign factor (% total load)	20	Set to reach the reference cooling water flow (~ 40000 t/h)
Tower Power Requirement (% gross MW)	0.719	Set to reach reference (2.688 MW)

Table 5.4. IECM Customized Fuel and Ash Properties.

Fuel		Ash	
Higher Heating Value (kJ/kg)	25289	Composition (wt%)	
Composition (wt%)		SiO_2	59.00
Carbon	60.66	Al_2O_3	22.00
Hydrogen	4.40	Fe_2O_3	8.00
Oxygen	9.38	CaO	2.50
Chlorine	0.03	MgO	1.50
Sulfur	1.50	Na_2O	0.70
Nitrogen	1.23	K_2O	1.80
Ash	10.80	TiO_2	1.10
Moisture	12.00	P_2O_5	0.30
Total	100.00	SO_3	2.50
Default Cost ($/t)	90.00	MnO_2	0.00
		Other	0.60
		Total	100.00

Source: (DEEPL, 2008)

5.3. Results and Discussion

5.3.1. Semi-dry FGD waste Treatment Unit Heat and Mass Balance

Based on information from Tables 5.1, 5.2 and fly ash heat capacity (730 J/kg.K), the heat balance of the FBR is performed.

The inlet air and semi-dry FGD waste heating demands are 248 kW and 1980 kW, respectively. Reaction R_1 demands 494 kW, reaction R_2 does not occur with the considered semi-dry FGD waste composition, reaction R_3 demands 697 kW and reaction R_4 (exothermic) liberates 4260 kW. The final heat balance gives -841 kW. Hence, considering all stated premises, the reaction could be auto sufficient in terms of energy. Additional energy is necessary only to start up the FBR (diesel) and to supply the compressor (electricity).

The semi-dry FGD waste production is estimated in 20.3 t/h. The treated residue has final composition of $CaSO_3$ of 3.66%, complying with the ASTM standard (< 5.0%). The FBR air demand is estimated in 4,460.0 kg/h and the calculated outlet air flow as 4,491.0 kg/h (6.9 Sm^3/h). Detailed information on the calculation of mass flow and composition of the treated semi-dry FGD waste is presented in Supplement C (Table C2.1) as well as the inlet and outlet air mass flows, which promote the oxidation of the $CaSO_3$ inside the FBR. (Table C2.2).

5.3.2. Semi-dry FGD Waste Treatment Unit Economic Analysis

Considering the main equipment specification of Table C2.1 (Section C2 of Supplementary Materials C), CAPEX and OPEX of the semi-dry FGD waste treatment unit are estimated. The main equipment cost and weight are individually presented in Table C2.3, Section C2 of Supplementary Materials C. The final economic analysis (CAPEX and OPEX) is shown in Table 5.5.

Table 5.5. Semi-dry FGD waste Treatment Unit CAPEX and OPEX Analysis Summary.

Item	**Value**
Total Project Capital Cost ($)	6,804,026.36
Total Products Sales ($/yr)	7,108,999.10
Total Operating Labor and Maintenance Cost ($/yr)	573,261.31
Total Utilities Cost ($/yr)	112,257.85
Total Operating Cost ($/yr)	1,049,948.80
Operating Labor Cost ($/yr)	558,825.00
Maintenance Cost ($/yr)	14,436.31
Operating Charges ($/yr)	25
Plant Overhead ($/yr)	286,630.66
Subtotal Operating Cost ($/yr)	972,174.82
General and Administration Cost ($/yr)	77,773.99

From Table 5.5, it can be noticed that, in 1 year of operation, the semi-dry FGD waste revenue could pay all the capital investment on its treatment unit. Details on the treated semi-dry FGD waste sales are presented in Table 5.6.

Table 5.6. SDA Solids Commercialization.

Products Sales per Hour ($/h)	954.1
Product Name	Ash + SDA Residue
Product Rate (t/h)	20.3
Product Unit Cost ($/t)*	47
Product Rate per Period (t/yr)	151,255.30
Product Sales ($/yr)	7,108,999.10

*Considering sale as cement kiln raw material in Brazil.

With data provided by APEA, it is possible to calculate LCOE of the semi-dry FGD waste treatment unit, as shown in Table 5.7. It is worth noting that the impact of the treatment unit on the power plant LCOE depends on the revenue price of the treated residue.

Table 5.7. SDA Solids Treatment LCOE.

Discount Rate	8%
f	8.88%
Annualized Capital Cost ($/yr)	604,384.20
O&M Fixed Cost ($/yr)	573,261.31
O&M Variable Cost ($/yr)	-6,996,741.25
Fuel Cost ($/yr)	0.00
TAC ($/yr)	-5,819,095.74
TAC w/o product sales ($/yr)	1,289,903.36
Capacity Factor	85%
AE (MWh/yr)	2,535,000
LCOE without product sales ($/MWh)	0.51
LCOE with product sales ($/MWh)	-2.30

5.3.3. IECM Results for the Coal Fired Power Plant

Considering the input parameters of Tables 5.3 and 5.4, IECM produces a comprehensive set of results. For the intended analysis, a realistic coal and calcium oxide (CaO) consumption is fundamental, to produce the informed flow of semi-dry FGD waste (20.8 t/h). The mass balance results are presented in Figs. 5.7 and 5.8. Other important parameter is the net plant heat rate, that reflects the final net efficiency of the plant.

Results demonstrate that the SO_2 control (semi-dry FGD), without the solid treatment unit, has total LCOE of 19.56 $/MWh, where 0.53 $/MWh (2.7%) corresponds to the semi-dry FGD waste disposal. Thus, the total plant LCOE is increased in 0.56% (from 94.44 to 94.97 $/MWh) resulting from disposal of the semi-dry FGD waste.

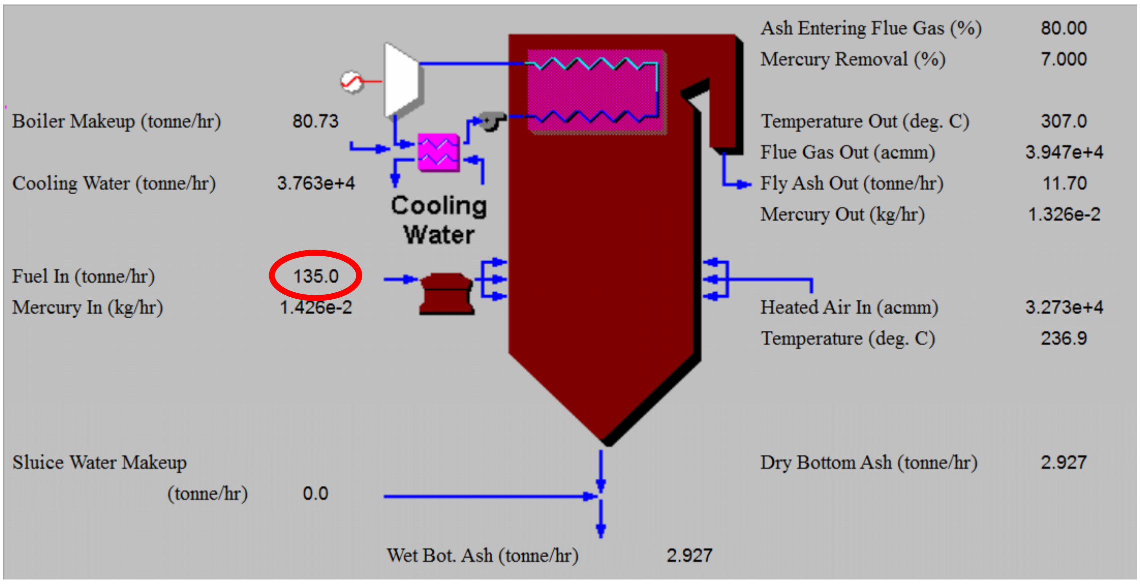

Fig. 5.7. Boiler Diagram. Source: IECM v 9.2.1 Interface.

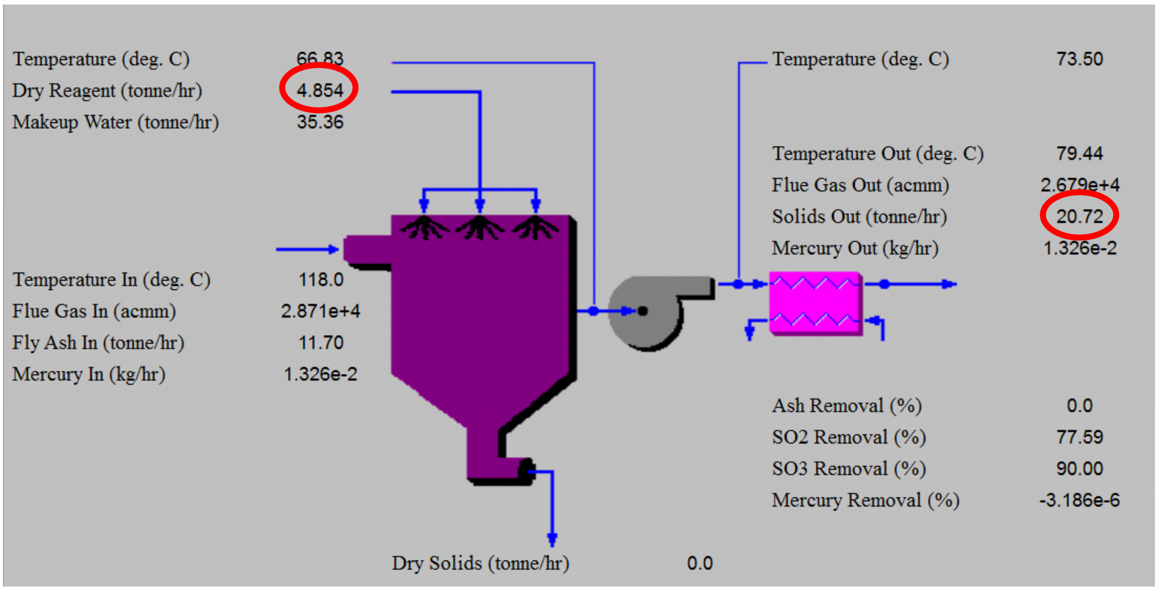

Fig. 5.8. Semi-dry FGD Diagram. Source: IECM v 9.2.1 Interface.

To validate the consistence and accuracy of the IECM results, key performance parameters are compared with values reported in the literature and reference power plant information, presented in Table 5.8, which shows that all key performance parameters are in strong agreement with the literature and reference power plant data. This accuracy is relevant to reach a realistic LCOE result. IECM calculates LCOE, or revenue required from electricity price, based on the total O&M and annualized capital costs, presented in Table 5.9.

Table 5.8. Overall PCC Plant Performance Validation.

Performance Parameter	**Result**	**Reference Value***	**Deviation (%)**
Coal Consumption (ton/h)	135	135	0.00%
Primary Fuel Input (MW)	948.06	942.35	0.61%
Gross Electrical Output (MW)	373.8	373.8	0.00%
Plant Electricity Requirements			
Base Plant Use (MW)	28.6		
In-Furnace NOx Use (MW)	0		
Fabric Filter Use (MW)	1.152		
Spray Dryer Use (MW)	1.140	1.14	0.00%
Cooling Tower Use (MW)	2.688	2.688	0.00%
Wastewater Plant Use (MW)	0.016		
Net Electrical Output (MW)	340.2	336	1.25%
Annual Power Generation (kWh/yr)	2.535×10^9		
Gross Plant Heat Rate, HHV (kJ/kWh)	9133		
Net Plant Heat Rate, HHV (kJ/kWh)	10030	10097	-0.66%
Net Plant Efficiency, HHV (%)	35.82	35.8	0.06%
CaO Consumption (t/h)	4.85	4.9	-0.94%
Ash Production	20.72	20.8	-0.38%

*Reference values from the power plant data (ENEVA) and Environmental Impacts Assessment Study (DEEPL, 2008).

Table 5.9. PCC Plant Total Cost.

Technology	***Fixed O&M (M$/yr)***	***Variable O&M (M$/yr)***	***Total O&M (M$/yr)***	***Annualized Capital (M$/yr)***	***Levelized Annual Cost (M$/yr)***
Combustion NOx Control	0.1181	0	0.1181	0.4622	0.5803
TSP Control	1.552	3.21	4.762	2.584	7.347
SO_2 Control	7.452	6.862	14.31	5.248	19.56
Subtotal	9.122	10.07	19.19	8.295	27.49
Cooling Tower	2.032	5.061	7.092	3.909	11
Wastewater Control	0.776	0.3172	1.093	0.96	2.053
Base Plant	63.63	87.65	151.3	48.86	200.1
Land	0	0	0	5.02E-02	5.02E-02
Total	**75.56**	**103.1**	**178.7**	**62.08**	**240.7**

Based on Table 5.9, information, IECM calculates total capital required, capital required per net kW, annual revenue required and, the objective of this study, LCOE ($/MWh), as shown in Table 5.10.

Table 5.10. PCC plant cost summary.

Technology	***Capital Required (M$)***	***Capital Required ($/kW-net)***	***Revenue Required (M$/yr)***	***Revenue Required ($/MWh)***
Combustion NOx Control	5.344	15.71	0.5803	0.2289
Post-Combustion NOx Control	0	0	0	0
Mercury Control	0	0	0	0
TSP Control	29.88	87.82	7.347	2.898
SO_2 Control	60.67	178.3	19.56	7.717
Combined SOx/NOx Control	0	0	0	0
CO_2 Control	0	0	0	0
Subtotal	95.89	281.9	27.49	10.84
Cooling Tower	45.19	132.8	11	4.34
Wastewater Control	11.1	32.62	2.053	0.8099
Base Plant	564.9	1660	200.1	78.95
Land	0.5798	1.704	5.02E-02	1.98E-02
Emission Taxes	0	0	0	0
Total	**717.7**	**2109**	**240.7**	**94.97**

The final LCOE is 94.97 $/MWh. This value strongly depends on the considered discount rate. For a discount rate of 7%, closer to the one assumed in this study (8%), the International Energy Agency (IEA and NEA, 2015) presents a range of 75 – 110 $/MWh for the LCOE of coal-fired power plant. Thus, it can be considered that the LCOE calculated using IECM is in good agreement with the international values, allowing to determine the impact of the semi-dry FGD waste treatment unit on LCOE, as presented in Table 5.11.

Table 5.11. Final LCOE Comparison for Base PCC and PCC + SDA Solid Treatment Plants

Case	***PCC***	***PCC + Solids Treatment***
Air Compressor Power (MW)	-	0.135
Net Electrical Power Output (MW)	340.200	340.065
Plant Efficiency	35.88%	35.87%
Reference Plant LCOE ($/MWh)	94.97	94.97
FGD waste disposal cost ($/MWh)	0.53	0.00
LCOE with FGD waste sales ($/MWh)		92.14
LCOE reduction with FGD waste sales		3.0%
LCOE without FGD waste sales ($/MWh)		94.95
LCOE reduction without FGD waste sales ($/MWh)		0.02%

As shown in Table 5.11, there is no need of a heater for operating the semi-dry FGD waste treatment unit, because the exothermic oxidation of $CaSO_3$ (R_4) can supply all the energy required to heat air and solids flow and promote the endothermic reactions ($R_{1,}$ $R_{2,}$ and R_3). The only energy requirement is from the air compressor power demand (0.135 MW), merely 0.04% of the PCC plant net power output (340 MW). Thus, the only factors that considerably impact LCOE are CAPEX and O&M costs of the semi-dry FGD waste treatment unit, and the revenue from treated residue price.

If the treated semi-dry FGD waste was transferred (at zero cost and null revenue) as additive to a cement industry, LCOE of the power plant would remain approximately the same, because the increase of 0.51$/MW resulting from CAPEX and O&M costs of the treatment unit is compensated by the decrease of 0.53$/MWh, in virtue of the avoided semi-dry FGD waste disposal costs. However, if commercialization as raw material of the treated semi-dry FGD waste (for cement kiln) is considered, there is a reduction of 3% (2.83 $/MWh) on the power plant LCOE (to 92.14 $/MWh).

It is worth noting that that regional economic scenarios may change the impact of semi-dry FGD waste treatment on LCOE. For instance, Liu et al. (2016) surveyed 7 coal fired-power plants in China to collect detailed field data to examine the costs and benefits of flue-gas desulfurization. They state that a PCC plant in China which installs and properly operate FGD equipment can receive 15 Yuan/MWh (~2.89 $/MWh) premium tariff on top of their on-grid tariffs. However, their study shows that this incentive is insufficient to cover FGD costs of most of the sample plants surveyed. Liu et al. (2016) propose that, to cope with the penalty on LCOE, in China's scenario of dispatch regulation, allocating generation hour based on the pollutant emission would provide strong incentive for sulfur dioxide mitigation.

Lastly, coal fired generation with CCS has estimated LCOE of 139.5 $/MWh (EIA, 2017), a penalty of 44.5 $/MWh, considering the reference power plant (without solid waste treatment) of the present work (~95 $/MWh). Comparatively, semi-dry-FGD has positive impact in LCOE, and the proposed semi-dry FGD waste treatment would turn a penalty of 0.53$/MWh (because of semi-dry FGD waste disposal cost) in an extra revenue (as LCOE is reduced in 2.83 $/MWh).

Aiming to show the impact of variations on treated semi-dry FGD waste revenue price, a sensitivity analysis of LCOE, based on variation of final product price between 0 and 100 $/ton is presented in Fig. 5.9. Remembering that, the base price adopted in the present study was 47 $/ton (points with black board on Fig. 5.9). The detailed calculation is presented on supplementary material Tables C3.1 e C3.2, Section C3 of Supplementary Materials C.

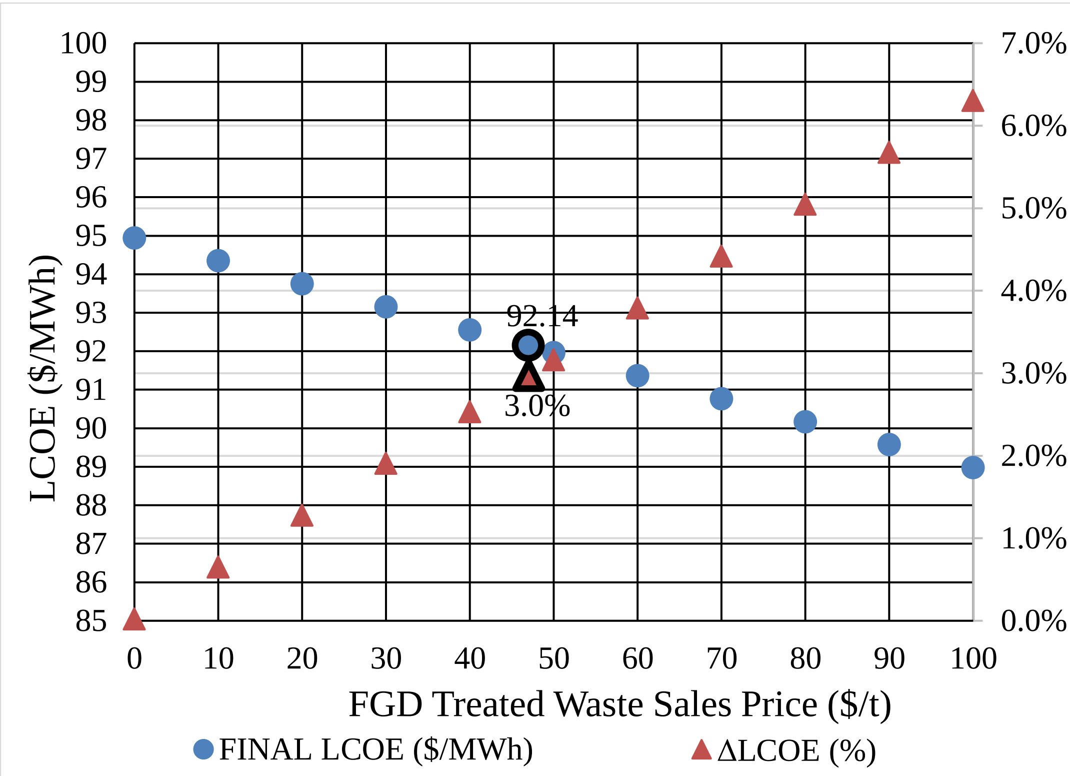

Fig. 5.9. Sensitivity Analysis of LCOE versus Treated Semi-dry FGD Residue Revenue Price

The sensitivity analysis shown a linear variation on the LCOE according to the treated semi-dry FGD residue revenue price. Even if the residue were donated for free there is no impact on LCOE, because of the saving with landfill disposal (0.53 \$/MWh). If the revenue price increases about 100% behind the base value, the impact on LCOE would be more 3.3% of decrease, achieving a final value of 89 \$/MWh, or 6.3% of decrease (based on the reference plant, that is 95 \$/MWh).

5.4. Conclusions

This study analyzes the impact on LCOE from installing a semi-dry FGD waste treatment unit in a real PCC power plant (the reference power plant) that is currently facing decision making process on semi-dry FGD waste destination. The calculated LCOE, 94.97 \$/MWh, is consistent with world values for this type of power plant. The analysis shows that the extra energy demanded by the novel semi-dry FGD waste treatment unit is nearly negligible due to the exothermicity of the $CaSO_3$ oxidation reaction and the proposed economizer for heating air and solids inlet streams. The power necessary to air compressor operation is only 0.04% of the PCC plant net power output (340 MW). Thus, the only factors that impact LCOE are cost (CAPEX and O&M) of the semi-dry FGD waste treatment unit and the residue revenue price.

Furthermore, this study demonstrates that, if the residue revenue is not considered, the achieved reduction in LCOE is only 0.02% (0.02 \$/MWh). If the residue is commercialized as a raw material for cement kiln, the LCOE could be reduced in ~3% (2.83 \$/MWh) to 92.14 \$/MWh. Therefore, with or without treated semi-dry FGD waste revenue, the proposed treatment unit has a negative, but small, impact on the total power plant LCOE, besides solving the problem of landfill saturation, land use and costs related to landfill maintenance. Thus, it is adequate to implement the semi-dry FGD waste treatment unit on PCC power plants with similar design and financial parameters compared to the reference coal-fired power plant studied in this work.

5.5. References of Chapter 5

ACAA. American Coal Ash Association. Beneficial Use of Coal Combustion Products. An American Recycling Success Story, 2014 Available at: https://www.acaa-usa.org/Portals/9/Files/PDFs/Production-and-Use-Brochure.pdf. Last access date: 4/7/2016.

Angevine, P.A., Bengtsson, S., Koudijs, G.P. Method for oxidation of flue gas desulfurization absorbent and the product produced thereby. US Patent No. 4544542, 195. ABNT. Associação Brasileira de Normas Técnicas. NBR 12653 - Materiais pozolânicos, 2015. Available at: http://www.abntcatalogo.com.br/, Last access date: 4/7/2016.

ASTM. C618-15, Standard Specification for Coal Fly Ash and Raw or Calcined Natural Pozzolan for Use. Annu. B. ASTM Stand, 2015. http://dx.doi.org/10.1520/C0618-15.

Bentz, D.., Peltz, M., Duran-Herrera, A., Valdez, P., Juarez, C. Thermal properties of high-volume fly ash mortars and concretes. J. Build. Phys. 34, 263–275, 2011. http://dx.doi.org/10.1177/1744259110376613.

Berkenpas, M.B. (Carnegie M.U., Grol, E.P.E. (National E.T.L., 2009. Integrated Environmental Control Model User Manual. U.S. Department of Energy, Pittsburgh, PA. Cordoba, P. Status of Flue Gas Desulphurisation (FGD) systems from coal-fired power plants: Overview of the physic-chemical control processes of wet limestone FGDs. Fuel, 144, 274-286, 2015. http://dx.doi.org/10.1016/j.fuel.2014.12.065.

Blankinship, S. Looking for a Good Scrubbing: Today’s FGD Technology. Power Eng. 109, 9; 19-24, 2005. Available at: http://www.power-eng.com/articles/print/volume-109/issue-9/features/looking-for-a-good-scrubbing-todayrsquos-fgd-technology.html Last access date: 03/15/2017.

DEEPL. Diferencial Energia Empreendimentos e Participação Ltda. Estudo de Impacto Ambiental (EIA). Empreendimento da Usina Termoelétrica Porto do Itaqui (UTE Porto do Itaqui), 2008.

EIA. U.S. Energy Information Agency. Levelized Cost and Levelized Avoided Cost of New Generation Resources in the Annual Energy Outlook 2016, August 2016. Available at: http://www.eia.gov/outlooks/aeo/pdf/electricity_generation.pdf. Last access date: 01/23/2017.

EPE. Empresa de Pesquisa Energética. Balanço Energético Nacional 2015, 2015a. Available at: https://ben.epe.gov.br/downloads/Relatorio_Final_BEN_2015.pdf Last access date: 4/7/2016.

EPE. Empresa Brasileira de Planejamento Energético. Previsões de carga para o Planejamento Anual da Operação Energética 2015 – 2019 1a Revisão Quadrimestral, 2015b. Rio de Janeiro.

EPRI. Electric Power Research Institute. Coal Ash: Its origin, disposal, use and potential health issues. Report from EPRI's Environment Division. Environmental Focus. Palo Alto, CA, 1998. Available at: http://ecosmartconcrete.com/docs/trepri98.pdf. Last access date: 01/23/2017.

EPRI. Electric Power Research Institute. Characterization of Spray Dryer Absorber Products for Use in Cement and Concrete Applications 1017580. Palo Alto, CA, 2009.

Farfen, J., Breyer, C. Structural changes of global power generation capacity towards sustainability and the risk of stranded investments supported by a sustainability indicator. Journal of Cleaner Production, 141, 370–384, 2017. http://dx.doi.org/10.1016/j.jclepro.2016.09.068.

Feng, C., Gao, X., Tang, Y., Zhang, T. Comparative life cycle environmental assessment of flue gas desulphurization technologies in China. Journal of Cleaner Production, 68, 81-92, 2014. http://dx.doi.org/10.1016/j.jclepro.2013.10.023.

Galos, K. A., Smakowski, T.S., Szlugaj, J. Flue-gas desulphurisation products from Polish coal-fired power-plants. Applied Energy, 75(3-4), 257–265, 2003. http://dx.doi.org/10.1016/S0306-2619(03)00039-4.

GPSA. Gas Processors Suppliers Association. Engineering Data Book, 20th ed., 2004. Gas Processors Association, Tulsa, Oklahoma.

IEA, NEA. Projected Costs of Generating Electricity. Organisation for Economic Co-operation and Development/International Energy Agency, and Organisation for Economic Co-operation and Development/Nuclear Energy Agency, Paris, 2015 Edition. Available at: https://www.iea.org/Textbase/npsum/ElecCost2015SUM.pdf. Last access date: 1/23/2017.

Jons, E.S., Liborius, E., Veltman, P.L., Vernenkar, K.N., 1987. Method for treating by-products from flue gas. US Patent 4666694.

Liu, X., Lin, B., Zhang, Y. Sulfur dioxide emission reduction of power plants in China: current policies and implications. Journal of Cleaner Production, 113, 133–143, 2016. http://dx.doi.org/10.1016/j.jclepro.2015.12.046.

Ma, X., Kaneko, T., Tashimo, T., Yoshida, T., Kato, K. Use of limestone for SO_2 removal from flue gas in the semidry FGD process with a powder-particle spouted bed. Chemical Engineering Science, 55(20), 4643-4652, 2000. http://dx.doi.org/10.1016/S0009-2509(00)00090-7.

Mikulčić, H., Klemeš, J. J., Vujanović, M., Urbaniec, K., Duić, N. Reducing greenhouse gasses emissions by fostering the deployment of alternative raw materials and energy sources in the cleaner cement manufacturing process. Journal of Cleaner Production, 136, Part B, 119–132, 2016. http://dx.doi.org/10.1016/j.jclepro.2016.04.145.

Rochedo, P.R.R., Costa, I.V.L., Império, M., Hoffmann, B.S., Merschmann, P.R. de C., Oliveira, C.C.N., Szklo, A., Schaeffer, R., 2016. Carbon capture potential and costs in Brazil. J. Clean. Prod. 131, 280–295. http://dx.doi.org/10.1016/j.jclepro.2016.05.033.

Sage, P. W., Ford, N. W. J. Review of Sorbent Injection Processes for Low-Cost Sulphur Dioxide Control. Proceedings of the Institution of Mechanical Engineers, Part A: Journal of Power and Energy, 210 (3), 183-190, 1996. Available at: http://journals.sagepub.com/doi/pdf/10.1243/PIME_PROC_1996_210_031_02. Last access date: 01/23/2017.

Santoyo-Castelazo, E., Azapagic, A., 2014. Sustainability assessment of energy systems: integrating environmental, economic and social aspects. J. Clean. Prod. 80, 119–138. http://dx.doi.org/10.1016/j.jclepro.2014.05.061

Short, W., Packey, D.J., Holt, T., 1995. A Manual for the Economic Evaluation of Energy Efficiency and Renewable Energy Technologies. National Renewable Energy Laboratory (NREL), Colorado.

Thomas, M. Optimizing the Use of Fly Ash in Concrete. Portland Cement Association. Illinois, USA, 2007. Available at: http://www.cement.org/docs/default-source/fc_concrete_technology/is548-optimizing-the-use-of-fly-ash-concrete.pdf. Last access date: 01/23/2017.

Tolmasquim, M.T., 2016. Energia Termelétrica: Gás Natural, Biomassa, Carvão, Nuclear, 1st ed. Empresa de Pesquisa Energética (EPE), Rio de Janeiro.

Wu, X., Wu, K., Zhang, Y., Hong, Q., Zheng, C., Gao, X., Cen, K., 2017. Comparative life cycle assessment and economic analysis of typical flue-gas cleaning processes of coal-fired power plants in China. J. Clean. Prod. 142, 3236–3242. doi:10.1016/j.jclepro.2016.10.146

6. ENVIRONMENTAL PERFORMANCE OF A SOLID WASTE MONETIZATION PROCESS APPLIED TO A COAL-FIRED POWER PLANT WITH SEMI-DRY FLUE-GAS DESULFURIZATION

This chapter is published a full-length original article in the Journal of Journal of Sustainable Development of Energy, Water and Environment Systems

Abstract

Mixing of semi-dry flue-gas desulfurization solids and fly-ash from coal-fired power plants results in a solid waste contaminated by calcium sulfite. Therefore, it becomes useless for industry and is often landfilled. To support decision-making on process configurations to monetize this solid residue a gate-to-gate life cycle assessment was performed, considering three scenarios: BASE case – standard 360 MW power plant, CASE I – base plant adopting dry thermal oxidation treatment of spray dryer solids, CASE II – bypass of desulfurization system. Cases I and II allow commercialization of the solid residue as class C fly-ash. Evaluated alternatives were compared based on quantitative potential environmental impacts, using United States Environmental Protection Agency waste reduction algorithm. Based on the results, the BASE case was more aggressive to the environment, due to solid waste production. CASE II increased photochemical oxidation and acidification potentials. CASE I was the more environmentally friendly but demands additional capital and operational expenditure.

Keywords: Calcium sulfite dry oxidation, Coal fired power plant, Life cycle assessment, Semi-dry flue-gas desulfurization, Solid waste treatment, Spray dryer absorbers

Nomenclature

$M_{j,\mathrm{out}}$	output mass flows of j streams	[-]
MW	molecular weight	[kg mol/kg]
n	polytropic exponent	[-]
Pw	power	[kW]
P_i	Pressure at i, where i is a counter	[kPa]
q	gas flow rate	[kg/h]
R	universal gas constant (8.314 J/molK)	[-]
r_p	pressure ratio	[-]
T	temperature	[K]
x_{kj}	k component composition on j output stream	[-]
Z	compressibility factor	[-]

Greek letters

α	impacts categories
η_P	polytropic efficiency
Ψ_{ki}	normalized score of i category and k component

Abbreviations

AP	Acidification Potential
ATP	Aquatic Toxicity Potential
CCP	Coal Combustion Products
EPRI	Electric Power Research Institute
FBR	Fluidized Bed Reactor
FGD	Flue-Gas Desulfurization
GDP	Gross Domestic Product
GHG	Greenhouse Gas
GWP	Global Warming Potential
HTPE	Human Toxicity Potential by Exposure
HTPI	Human Toxicity Potential by Ingestion
LCA	Life Cycle Assessment
ODP	Ozone Depletion Potential
PCC	Pulverized Coal Combustion
PCOP	Photochemical Oxidation Potential
PEI	Potential of Environmental Impacts
PFD	Process Flow Diagram
SDA	Spray Dryer Absorber
SD-FGD	Semi-dry Flue-Gas Desulfurization
SD-FGD-R	Semi-dry Flue-Gas Desulfurization Solid Residue
TTP	Terrestrial Toxicity Potential
WAR	Waste Reduction Algorithm

6.1. Introduction

Coal-fired power plants are responsible to fuel 41% of global electricity demand [1]. In some countries, this share is much higher. In China for instance, the world's largest coal producer and consumer, the use of coal for power generation is not expected to decrease in the short to medium term [2]. Despite the on-going transition to a low carbon economy driving a move to renewable sources of energy, the supply of base-load remains dependent on fossil fuel to face their intermittent supply. In this scenario, coal is the most plentiful, and one of the cheapest, among fossil alternatives. As an example, the water scarcity crisis that occurred in Brazil, during 2013-2015, limited the hydropower generation. It is known that the majority of Brazilian electricity is supplied by hydro sources [3], this source is responsible to supply 65% of the total electricity demand [4]. As result, electricity from coal-fired power plants has increased 24.2%, presently, mineral coal represents 9.6% of the thermoelectric power source in Brazil [5].

In the face of the huge amount of solid waste produced by coal-fired power plants, many initiatives were raised in the last decades, aiming to improve waste management of such processes. Common associated solid wastes are: fly and bottom ash, flue-gas desulfurization sludges, boiler blowdown and coal pile runoff, chemicals and other materials related to power plants operation. Within all named solid wastes, fly-ash, bottom ash, slag and scrubber sludge are the ones produced in higher volume [6].

Coal combines organic and mineral components in varying proportions, with ash yields ranging from 3 to 49%. Consequently, coal power generation produces significant amounts of solid wastes, Coal Combustion Products (CCP), consisting of fly-ash, bottom ash, boiler slag, and material from Flue-Gas-Desulfurization (FGD, process applied to flue-gas stream to chemically trap sulfur) [7]. The term coal ash has been used to refer to all the different ash types [8]. CCP is composed basically of non-combustible minerals and a small fraction of unreacted carbon [1]. Depending on burner and pollution control technologies (e.g., FGD), the solid wastes composition varies significantly. Wet CCP is disposed in large surface impoundments while dry CCP is disposed in landfills. To reduce landfill occupation, there is a need for utilization of CCP into valuable materials.

Semi-Dry FGD (SD-FGD) is a technology that uses Spray Dryer Absorption (SDA) to control Sulfur dioxide (SO_2) emissions by flue-gases, by chemical reaction with lime. According to Electric Power Research Institute [9], in 2007, about 12% of USA power plants were using SD-FGD systems, whose water use is 30 to 40% lower than the Wet-FGD technology, being attractive in regions where water supply is limited. However, while Wet-FGD CCP has commercial value for gypsum production, SD-FGD solid is almost useless, having landfills as usual destination. In general, CCP produced by SD-FGD systems is composed of Calcium sulfite ($CaSO_3$), fly-ash and unreacted lime. Most power plants with SD-FGD do not have fly-ash pre-collectors resulting in solid waste with high ash content (> 50%).

CCP plays an important role in the cement industry. Besides reducing the need for landfill space, the use of fly-ash as substitute for traditional cement brings environmental benefits: Greenhouse Gas (GHG) emissions and primary raw material reduction. In fact, CCP has been used for decades, as a substitute for mined or manufactured materials, lowering construction costs [10]. Fly-ash is not required to pass through the clinker kiln, an energy-intensive step of Portland cement production. Furthermore, concrete from fly-ash is durable, strong and corrosion resistant [11]. There are patented processes for dry oxidation of $CaSO_3$ from SD-

FGD waste into Calcium sulfate ($CaSO_4$). In general they claim technologies to transform CCP into cementitious material or suitable for other applications. Patent 4,478,810, authored by Bloss *et al.* [12], claims a method of treating final products from FGD. Patent 4,544,542, authored by Angevine *et al.* [13], claims a method for oxidation of FGD absorbent and the product produced thereby. Patent 4,666,694, authored by Jons *et al.* [14], claims a method for treating by-products from flue-gas.

Alternative methods aiming to improve CCP properties and applications have also been highlighted in the literature. Li *et al.* [15] reported improving the pozzolanic degree of fly-ash using chemical activators solutions of Sodium hydroxide (NaOH), Sodium sulfate (Na_2SO_4) and Sodium chloride (NaCl) injected into the fluidized fly-ash through a side spray device, in a Fluidized Bed Reactor (FBR). Ren-ping *et al.* [16] studied the oxidation characteristics of ashes containing $CaSO_3$. SDA material has been used commercially to manufacture cement in Germany after treatment in a fluidized bed process [17]. In fact, post-treatment is necessary since the use of SD-FGD solid residue as cementitious (pozzolanic) material must comply with the ASTM C618 standard or similar country-specific standards [18]. According to ASTM C618, when the $CaSO_3$ content of fly-ash exceeds 5% by mass, it is considered inadequate for commercialization as cement additive or replacement material for concrete.

Despite the economic advantage of using SD-FGD waste as cement, the commercial application of this residue remains a challenge. In USA only 22% of SD-FGD residue is used, with mining applications representing 83% of this use. In general, coal fired power plants with SD-FGD dispose its solid waste on landfills, with massive land use. In USA, the production of SD-FGD waste was about 3.5×10^6 tonnes in 2009 and is expected to double by 2019 [9].

Clearly, increased utilization of SD-FGD solid residue is needed [19]. The SD-FGD waste landfill is a potential source of contaminants. Besides landfill soil and nearby vegetation ash contamination, leaching of CCP landfills could carry toxic substances, like mercury [2], hexavalent chromium [20] and other contaminants [21], posing potential impact to groundwater.

Additionally, landfill construction and maintenance present economic penalty to electricity generation. Furthermore, the air inside and around the landfill is unhealthy to local workers, because of the high concentration of particulate matter.

Animal tests revealed that SD-FGD waste is not a skin sensitizer but, is irritating to eyes. If ingested, it is an irritant to the digestive tract, causing gastro-intestinal disturbances, erosion or hemorrhage. A moderately acute oral and injection toxicity was indicated in animals. Sulfites are recognized as a food allergen. Breathing difficulty, sneezing, throat swelling and hives could be observed after minutes of ingestion. The inhalation of sulfite aerosol caused mild lung changes in rats and effects on respiratory tract of dogs [22].

Attempts to add use and commercial value to fly-ash appear in the literature since decades. Mulder [23] investigated mechanical properties of coal fly-ash for road base construction material application. Camilleri *et al.* [24] studied the viability of use of fly-ash from coal-fired power plant as a cement replacement in concrete mixes. Today this topic is still being explored by many researchers. Use as Geopolymer is proposed by Chindaprasirt and Rattanasak [25] and Xu *et al.* [26]. Doudart de la Grée *et al.* [27] investigated the use of fly-ashes as building materials. Ding *et al.* [28] proposed the recovery of alumina from fly-ash.

A Brazilian coal-fired power plant complex, located in the Northeast region, is considering an alternative destination for its SDA solid waste. This complex has 3 identical 360 MW Pulverized Coal Combustion (PCC) power plants, equipped with SD-FGD for reduction of SO_2 emissions. After 4 years of operation, 2 landfills, with total area of ~79,500 m^2 of area, became almost full with CCP and a third one is being built for operation guarantee (see Figure 6.1).

Aiming to solve the environmental challenge related to CCP landfilling, a SD-FGD waste treatment pilot-plant was designed and constructed at the Federal University of Rio de Janeiro [29]. It is based on the above-mentioned patents information with a modified layout and innovative equipment design. The main equipment is a FBR, to oxidize $CaSO_3$, reducing the sulfite (SO_3^{-2}) content of the FGD waste, allowing the treated residue to be used as pozzolanic material. The FBR of mini-pilot plant has diameter of 200 mm and 1,100 mm of height. The pilot-plant has a heater, a cyclone (to collect and return particles above 10 μm back to the FBR), an economizer (to partially recover the heat of the hot outlet air stream leaving the cyclone) and an air filter (to avoid emission to the atmosphere of small particles, not captured by the cyclone). de Castro *et al.* [29] reported SO_3^{-2} content reduction to below 5%w/w under dry oxidation on FBR at temperatures above 500 °C.

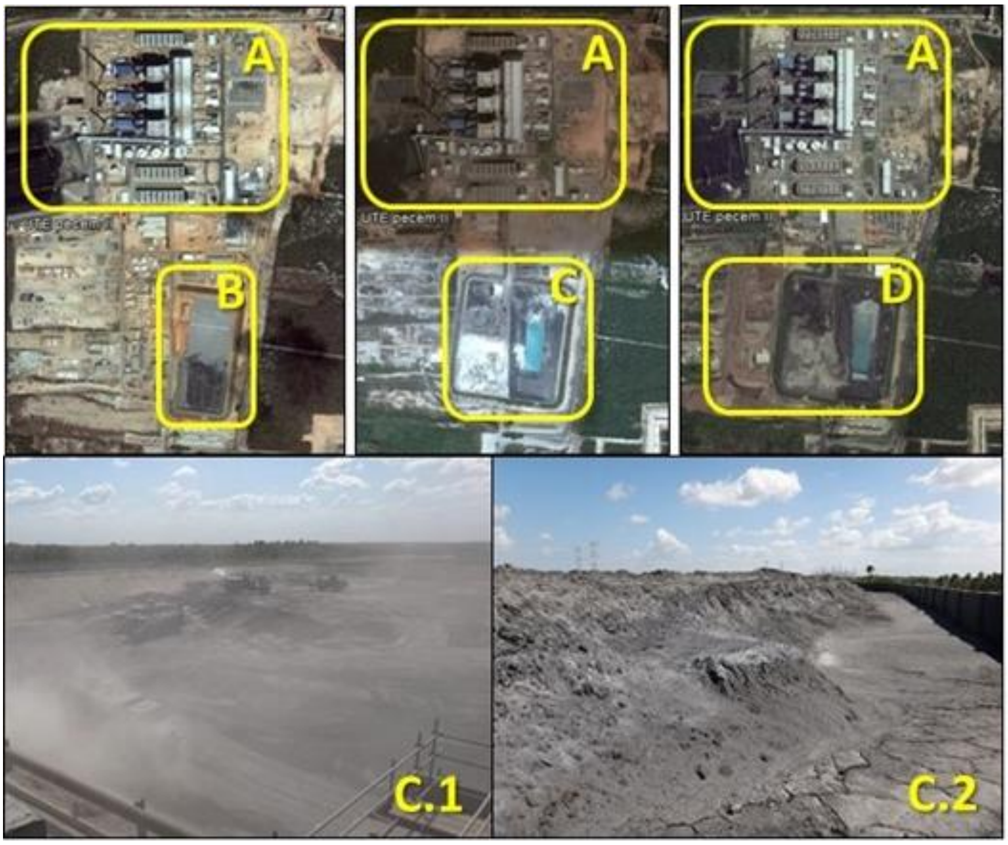

Figure 6.1. Time evolution of ash landfills at a Brazilian coal fired power plant [source: Google Earth (satellite images) and site pictures (landfills 1 and 2): 3 × 360 MW power plants (a); year of 2012 – power plant operations start-up – Landfill I (b); year of 2015 – Landfill I is full, Landfill II in use (c); Landfill II in 2015 (c.1); Landfill I in 2015 (c.2) and year of 2017 – Landfill II is almost full, and Landfill III is under construction (d)]

Based on experimental results of de Castro *et al.* [29] and patent information [13], this work assesses the potential environmental impacts avoided if a full-scale SD-FGD waste treatment unit were put in operation. For a full-scale plant, an air compressor is required to supply air at the FBR pressure. Pressure losses through the economizer, air heater, FBR, cyclone and filter are estimated in 150 kPa, and the compressor pressure ratio is 2.47.

Environmental impacts of waste management are assessed using Waste Reduction Algorithm (WAR) [30] for three alternative destinations of CCP: BASE case, CASE I and CASE II. BASE case is the coal-fired power plant (Figure 6.1) operating with the FGD process and the resulting CCP destined to landfills, considered as waste on WAR. CASE I adapts the power plant to operate with the proposed full-scale FGD waste treatment unit, converting the SDA residue into a class C pozzolanic material. Although CASE I manages CCP without increasing SO_2 emissions, it demands capital investments (CAPEX) for building the solid waste treatment unit. Although the air used to oxidize $CaSO_3$ must be heated above 400-600

°C, the oxidation reaction is exothermic and, depending on the residue composition, could be autothermic. However, extra energy is necessary (e.g., for plant start-up or compensation of heat losses). Integration with hot gases, vapor purge or combustion air from the power plant process would avoid fuel consumption. CASE II consists of turning-off the SD-FGD, making possible to commercialize the residue directly as Class C pozzolanic material, because ashes are not contaminated by desulfurization products.

It is worth noting that CASE I is an environmentally friendly approach for CCP management, while CASE II prioritizes economic performance at the expense of environmental impacts. That alternative is legally possible only if the SO_2 concentration in exhausted gas complies with local environmental regulation (in Brazil, 400 mg/Nm³, according to CONAMA 03/1990 [31][2]). Adjusting the FGD operation and using low sulfur coal, SO_2 emissions will probably be very close to the regulation limit. In the event of surpassing emission limit, increased atmospheric pollution would result, comparatively to CASE I and BASE case.

The main objective of the study is to evaluate, based on a gate-to-gate Life Cycle Assessment (LCA) methodology, the environmental performance of the three CCP management alternatives, considering a set of environmental impact metrics (i.e., not restricted to solely evaluating SO_2 emissions). The results aim to quantify how much CASE I is less polluting than CASE II and BASE case, proving the relevance of SDA waste treatment unit for coal-fired power plants operating with SD-FGD system.

The present results and the proposed methodology contribute to the decision-making process of CCP managing of coal-fired power plants using SD-FGD. No similar work was found in the scientific literature, proving the originality of this study.

6.2. Materials and Methods

The assessment of environmental impacts of a process or product systems is useful as a decision-making tool and can be achieved using LCA [4]. ISO 14040 [32] establish four basic steps to perform a LCA:

- Goal and scope definition;
- Inventory analysis;
- Impact assessment;
- Interpretation of results.

[2] See Erratum, item 1.

6.2.1. Goal and scope

The main goal is support decision-making on process configurations to monetize mixed coal combustion products from a 360 MW pulverized coal power plant with semi-dry FGD. A gate-to-gate life cycle assessment is performed, considering three scenarios: BASE – standard power plant [33], CASE I – base plant adopting dry thermal oxidation treatment of spray dryer solids, CASE II – bypass of desulfurization system. Cases I and II allow commercialization of the solid residue as class C fly-ash.

6.2.2. Heat and mass balances, and streams inventory

A global mass balance of each process was performed, classifying the streams as: inlet, waste outlet and product outlet. These streams are based on the Process Flow Diagram (PFD) of the Brazilian Coal-Fired power plant pictured in Figure 6.2, used as case study of the proposed methodology. The missing information was calculated from mass balance.

The power plant is supplied with Colombian Coal, with composition assumed as similar to Colombian field IGM 1238 [34]. The considered set of reactions expected to occur inside the FBR and the SDA solid residue composition and mass flow is presented by Cruz *et al.* [33]. The last was obtained from the heat and mass balances of the power plant used as case study and considers coal with 1.5%w/w of sulfur.

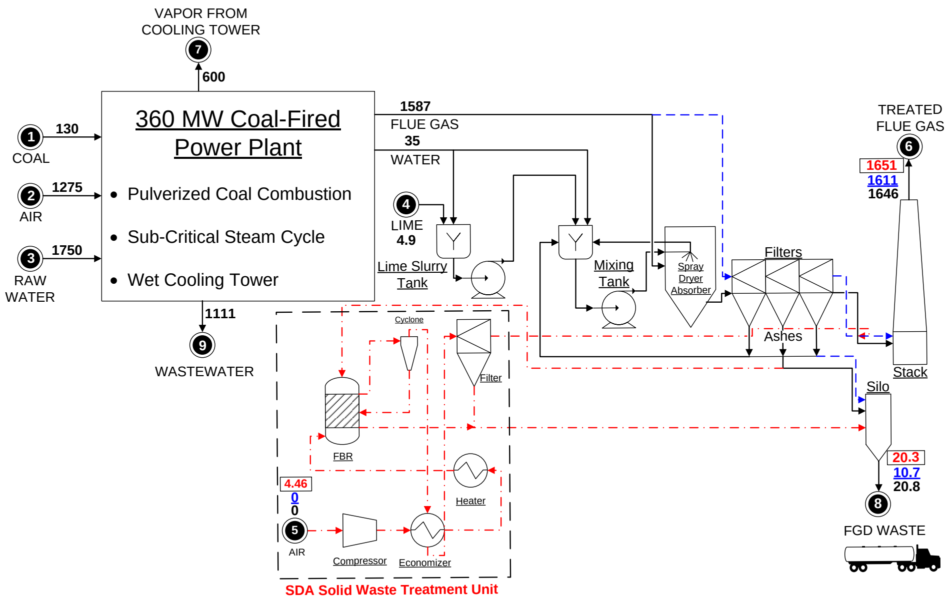

Figure 6.2. Flow diagram of the coal-fired power plant with SD-FGD waste treatment unit (dashed box), numbers in black indicate mass flow of original power plant [t/h], while red numbers within boxes correspond to CASE I and underlined blue numbers correspond to CASE II

Based on Angevine *et al.* [13], considering a temperature of 550 °C and 5% of excess O_2, it is possible to achieve a SO_3 mass composition of 3.2% on the treated SDA waste, complying with ASTM Standard C-618 [18] Sulfur trioxide (SO_3) limit for class C or F fly-ash. Based on experiments of de Castro *et al.* [29], a conversion of 91.3% was considered for SO_3 oxidation reaction. These results were considered for mass and energy balances of SDA treatment unit of CASE I. The specific heat of SDA residue, used to estimate energy consumption for heating the SDA residue from 80 °C to 550 °C was considered 730 J/kgK, the same value of a class C fly-ash [35].

As the FBR does not exist in industrial scale, the fluidization air flow was estimated. In a pilot scale FBR dealing with a 10%w/w $CaSO_3 \times ½H_2O$ feed, the flow ratio of fluidization air to stoichiometric air was taken as 3.75. Considering the calcium sulfite mass fraction as 38.4%, the stoichiometry air flow with 5% of O_2 excess was considered enough to promote bed fluidization. The air compressor power was calculated by eq. (6.1) [36]:

$$Pw = \frac{q \times Z \times R \times T \left[(r_{\mathrm{P}})^{\frac{(n-1)}{n}} - 1 \right]}{3{,}600 \times \eta_{\mathrm{P}} \times MW \ \frac{n-1}{n}} \tag{6.1}$$

where *Pw* is the brake horsepower [kW], *q* is the gas flow rate [kg/h], *Z* is the average compressibility factor, *R* is the gas constant (8.314 kJ/kmolK), *T* is the gas inlet temperature [K], *MW* is the molecular mass [kg mol/kg], r_P is the pressure ratio, *n* is the polytropic exponent and η_P is the polytropic efficiency. The pressure ratio is calculated dividing the outlet pressure, P_2 [kPa], by the inlet pressure P_1 (kPa). P_2 is considered 250 kPa (gauge). P_1 is the atmospheric pressure (0 kPa gauge). η_P is considered 80%, *q* of inlet air stream (stream 1 of Figure 6.3), calculated as a function of the FBR demand.

The air is pre-heated to 250 °C by the economizer. The heater service is to heat the air to the reactor temperature (550 °C). However, the energy supplied by the oxidation of $CaSO_3$ and integration with high temperature steam purges from the closed loop steam cycle could bring the air heating energy input to zero (the air heater can be used only for the start-up of the system). The SDA power consumption was obtained from the Environmental Impacts Assessment Study of the power plant used as case study [37].

6.2.3. Waste Reduction Algorithm Methodology

Evaluated alternatives are compared based on quantitative Potential Environmental Impacts (PEI), using United States Environmental Protection Agency (USEPA) Waste Reduction Algorithm [38]. To compare the environmental friendliness of chemical processes, WAR algorithm uses the concept of PEI balance. It is based on the idea that the PEI of a certain amount of material and energy can be defined as the effect that they would have on the environment if they were emitted [30]. As PEI is a conceptual quantity, it cannot be directly measured, but can be calculated from measurable parameters, using functional relations [38]. The balance considers the flow of PEI (mass + energy) across the process boundary [PEI/h]. From the balance, PEI indexes are calculated, providing the degree of environmental friendliness of the process.

WAR algorithm describes the Potential of Environmental Impacts Rate [PEI/h] for each category using the eq. (6.2) [38]:

$$\hat{\mathrm{I}}_{\mathrm{out}} = \sum_{i}^{\mathrm{category}} (\alpha_i) \sum_{j}^{\mathrm{stream}} \left(M_{j,\mathrm{out}}\right) \sum_{k}^{\mathrm{component}} \left(x_{kj}\psi_{ki}\right) \tag{6.2}$$

where $\hat{\mathrm{I}}_{\mathrm{out}}$ is the output PEI rate, α_i is the user defined weight factor for the i^{th} impact category, $M_{j,\mathrm{out}}$ is the output mass flow of the j^{th} stream, x_{kj} is the composition of the k^{th} component in the j^{th} output stream, Ψ_{ki} is the normalized score of i^{th} impact category for the k^{th} component (score_{ki} /<score_{ki}>). <score_{ki}> is the average score of all components in a same category. According to Young and Cabezas [30], WAR classifies PEI in impact categories, with the global PEI resulting from their weighted sum (with user defined weights). Table 6.1 shows the impact categories and weights adopted for the current evaluation. The objective of the study is comparing scenarios. Therefore, the weight and absolute value of each category individually does not matter in the proposed analysis.

We are interested in the difference between cases. Using different weights for some categories might be considered an attempt to manipulating the conclusions. Thus, it was decided to keep all weights equal to 1, for all the 3 cases.

The inventory streams of cases BASE, I and II were used as input of WAR algorithm, through the software WAR GUI Version 1.0.17 (2008), namely chemical composition and flow rates of mass streams entering and leaving the process. Energy input were ignored (considered zero) since all the alternative cases present similar energy use.

Table 6.1. WAR environmental impacts categories and adopted weights

Impact	Description	Weight
HTPI	Human Toxicity Potential by Ingestion	1
HTPE	Human Toxicity Potential by Exposure	1
ATP	Aquatic Toxicity Potential	1
TTP	Terrestrial Toxicity Potential	1
GWP	Global Warming Potential	1
ODP	Ozone Depletion Potential	1
PCOP	Photochemical Oxidation Potential	1
AP	Acidification Potential	1

6.3. Results and Discussion

The methodology stated on the last section was successfully applied and the main results are presented below.

6.3.1. Fluidized Bed Reactor heat and mass balance

According to Cruz *et al.* [33], the mass flow of SDA solid residue is 20.8 tons/h, fly ash specific heat is 730 J/kgK. The initial $CaSO_3 \times ½H_2O$ content on SDA residue is 38.4%w/w, with 2% of water (humidity), 8.3% of Calcium hydroxide [$Ca(OH)_2$] and 51.3% of inert minerals (fly-ash). Therefore, it is possible to calculate the heat balance around the FBR, product mass flow and composition as well as the air mass flows (in and out) to promote CCP oxidation inside the FBR, as shown in Tables 6.2-6.4.

Table 6.2. FBR heat balance

Item	Energy [kW]
Air heating	372
Solids heating	1,980
Reaction 1 ($CaSO_3 \times ½H_2O \rightarrow CaSO_3 + H_2O$)	494
Reaction 2 ($CaSO_4 \times ½H_2O \rightarrow CaSO_4 + H_2O$)	0.0
Reaction 3 [$Ca(OH)_2 \rightarrow CaO + H_2O$]	697
Reaction 4 ($CaSO_3 + ½O_2 \rightarrow CaSO_4$)	−4,260
Balance	−717

Table 6.3. FBR product stream

Component	*MW* [g/mol]	Flow [mol/h]	Flow [kg/h]	Composition [% weight]
$CaSO_3 \times ½H_2O$	129	-	-	0.00
$CaSO_4 \times 2H_2O$	172	-	-	0.00
$Ca(OH)_2$	74	-	-	0.00
$CaSO_3$	120	6,186	742	3.7
$CaSO_4$	136	55,671	7,571	37.3
CaO	56	23,307	1,305	6.5
H_2O	18	-	-	0.00
Inert	-	-	10,660	52.5
	Total		20,279	100.0

Table 6.4. FBR air inlet and outlet streams

FBR air inlet stream				
Component	*MW* [g/mol]	Flow [mol/h]	Flow [kg/h]	% Molar [mole %]
O_2	32	32,475	1,039	21.0
N_2	28	122,167	3,421	79.0
Air	29	154,642	4,460	100.0
FBR air outlet stream				
Component	*MW* [g/mol]	Flow [mol/h]	Flow [kg/h]	% Molar [mole %]
O_2	32	4,639	148	2.3
N_2	28	122,167	3,421	59.8
H_2O	18	77,325	1,392	37.9
Air	24	204,131	4,961	100.0

The FBR heat balance shows that, considering all stated premises, the reaction could be self-sufficient in terms of energy, and energy input is necessary only to start up the FBR and to supply the compressor. As shown in Table 6.5, the extra energy is 1,275 kW. This is only 0.35% of the plant turbine power output (360 MW) and was not considered in the WAR algorithm analysis.

Table 6.5. Overall power plant heat balance for CASE I and CASE II

Case	Unit	I	II
Coal consumption	[tons/h]	135	135
Boiler duty	[kW]	987,368	987,368
Turbine output	[kW]	360,000	360,000
Compressor power	[kW]	135	0.00
SDA consumption	[kW]	1,140	0.00
Net electrical power output	[kW]	358,725	360,000
SDA + Ash treatment energy penalty	[kW]	1,275	0.00
SDA + Ash treatment energy penalty	[%]	0.35	0.00
Plant efficiency (LHV)	[%]	36.33	36.46

6.3.2. Waste Reduction Algorithm Results

Based on streams inventory, the PEI generation rate of each case (BASE, I and II) were calculated using the software WAR. Tables 6.6-6.8 show the streams inventory of each case.

The results for each environmental impact category and the total PEI rate are summarized in Figure 6.3.

Table 6.6. BASE case streams inventory

Stream	1	2	3	4	5	6	7	8	9
Type	Inlet	Inlet	Inlet	Inlet	Inlet	Waste outlet	Waste outlet	Waste outlet	Waste outlet
Name	Coal	Air inlet 1	Raw water	Lime	Air inlet 2	Flue-gas	Water vapor	FGD waste	Wastewater
Flow [tons/h]	129	1,275	1,750	4.9	-	1,646	600	20.4	857
Coal	1.000	-	-	-	-	-	-	-	-
N_2	-	0.8113	-	-	0.8113	0.6845	-	-	-
O_2	-	0.1887	-	-	0.1887	0.0508	-	-	-
H_2O	-	-	1.0000	-	-	0.0761	1.0000	0.0200	1.000
SO_2	-	-	-	-	-	0.0002	-	-	-
CO_2	-	-	-	-	-	0.1884	-	-	-
SiO_2	-	-	-	-	-	-	-	0.1319	-
Al_2O_3	-	-	-	-	-	-	-	0.1391	-
CaO	-	-	-	0.9500	-	-	-	0.1368	-
MgO	-	-	-	0.0500	-	-	-	0.0144	-
Fe_2O_3	-	-	-	-	-	-	-	0.0649	-
TiO_2	-	-	-	-	-	-	-	0.0094	-
P_2O_5	-	-	-	-	-	-	-	0.0030	-
$CaSO_3$	-	-	-	-	-	-	-	0.3840	-
SO_4^*	-	-	-	-	-	-	-	0.0964	-

Table 6.7. CASE I streams inventory

Stream	1	2	3	4	5	6	7	8	9
Type	Inlet	Inlet	Inlet	Inlet	Inlet	Waste outlet	Waste outlet	Product	Waste outlet
Name	Coal	Air inlet 1	Raw water	Lime	Air inlet 2	Flue-gas	Water vapor	Fly-ash	Wastewater
Flow [tons/h]	129	1,275	1,750	4.9	4.9	1,651	600	20.4	857
Coal	1.000	-	-	-	-	-	-	-	-
N_2	-	0.8113	-	-	0.8113	0.6845	-	-	-
O_2	-	0.1887	-	-	0.1887	0.0508	-	-	-
H_2O	-	-	1.0000	-	-	0.0761	1.0000	-	1.000
SO_2	-	-	-	-	-	0.0002	-	-	-
CO_2	-	-	-	-	-	0.1884	-	-	-
SiO_2	-	-	-	-	-	-	-	0.1352	-
Al_2O_3	-	-	-	-	-	-	-	0.1426	-
CaO	-	-	-	0.9500	-	-	-	0.1195	-
MgO	-	-	-	0.0500	-	-	-	0.0148	-
Fe_2O_3	-	-	-	-	-	-	-	0.0665	-
TiO_2	-	-	-	-	-	-	-	0.0097	-
P_2O_5	-	-	-	-	-	-	-	0.0031	-
$CaSO_3$	-	-	-	-	-	-	-	0.0365	-
SO_4^*	-	-	-	-	-	-	-	0.4722	-

*See Erratum, item 2.

Table 6.8. CASE II streams inventory

Stream	1	2	3	4	5	6	7	8	9
Type	Inlet	Inlet	Inlet	Inlet	Inlet	Waste outlet	Waste outlet	Product	Waste outlet
Name	Coal	Air inlet 1	Raw water	Lime	Air inlet 2	Flue-gas	Water vapor	Fly-ash	Wastewater
Flow [tons/h]	129	1,275	1,715	0	0	1,611	600	10.7	921
Coal	1.0000	-	-	-	-	-	-	-	-
N_2	-	0.8113	-	-	0.8113	0.6942	-	-	-
O_2	-	0.1887	-	-	0.1887	0.0487	-	-	-
H_2O	-	-	1.0000	-	-	0.0582	1.0000	-	1.000
SO_2	-	-	-	-	-	0.0028	-	-	-
CO_2	-	-	-	-	-	0.1961	-	-	-
SiO_2	-	-	-	-	-	-	-	0.2572	-
Al_2O_3	-	-	-	-	-	-	-	0.2712	-
CaO	-	-	-	0.9500	-	-	-	0.1048	-
MgO	-	-	-	0.0500	-	-	-	0.0281	-
Fe_2O_3	-	-	-	-	-	-	-	0.1264	-
TiO_2	-	-	-	-	-	-	-	0.0184	-
P_2O_5	-	-	-	-	-	-	-	0.0059	-
$CaSO_3$	-	-	-	-	-	-	-	-	-
SO_4[*]	-	-	-	-	-	-	-	0.1880	-

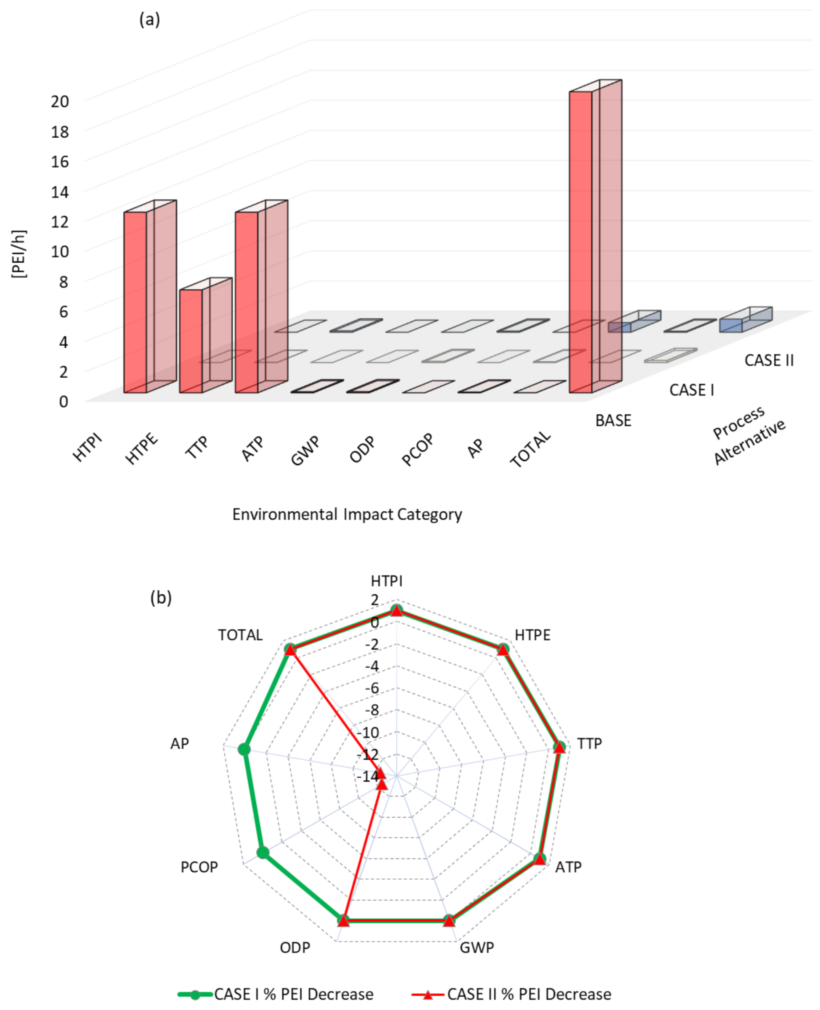

Figure 6.3. Environmental impact assessment: PEI/h for each impact categories (a) and decrease of PEI generation rates for CASE I and CASE II with respect to BASE case (b)

[*]See Erratum, item 2.

Table 6.6 refers to BASE case streams inventory. On BASE case it can be noticed that the stream 8 is considered as waste, because the 20.4 tons/h of SD-FGD solid is landfilled. Table 6.7 represents CASE I, this is the only one when the stream 5 (air) is not zero. This air is used on the FBR reactor, to oxidize the $CaSO_3$ to $CaSO_4$. On Tables 6.7 and 6.8 the stream 8 is considered a product, and not a waste. In this way, environmental impacts of those streams are not considered by the software on PEI generation rates. On Table 6.8 (CASE II), it is noticed that the solids production (stream 8) is lower. It happens because FGD is out of operation. There is no lime consumption (stream 4 flow is zero), the only solid waste source is coal combustion. CASE II presents a 2% decrease on water consumption (stream 3). The reason is that FGD uses 35 tons/h of water, that evaporates on the SDA. It is shown by the difference on waste flue-gas mass flow (stream 6) of CASE II, compared to CASE I and BASE case. Stream 6 of CASE I presents a higher flow because the air used by the FBR is mixed with the flue-gas from boiler. CASE II presents a lower flow because, as the flue-gases do not pass through SDA, no water vapor is mixed with this stream.

Figure 6.3a shows clearly that BASE case scores are higher in categories related to human health and terrestrial toxicity (HTPI, HTPE and TTP), proving that FGD waste is indeed an environmental problem. As the PEI rate of these categories were an order of magnitude higher related to the other ones, results are presented in Figure 6.4, for PEI generation rates [PEI/h] in categories ATP, GWP, ODP, PCOP, AP, and decrease in PEI generation of CASES I and II with respect to BASE case.

The absence of SO_2 recovery system resulted in a photochemical oxidation and acidification potential PEI generation rate 1,245% higher for CASE II. That happens because these categories are directly affected by SO_2 emissions. The total PEI generation reduction of CASE I was approximately 500% related to CASE II, showing definite inferiority of CASE II with respect to CASE I. It is worth noting that CASES I and II have very lower Total PEI generation rates since both CCP (solid wastes from FGD) comply with specifications for commercial use, hence being considered products and, as such, are not computed as waste (reducing PEI generation) by WAR. Clearly, the more environmentally friendly alternative to FGD solid waste problem is CASE I.

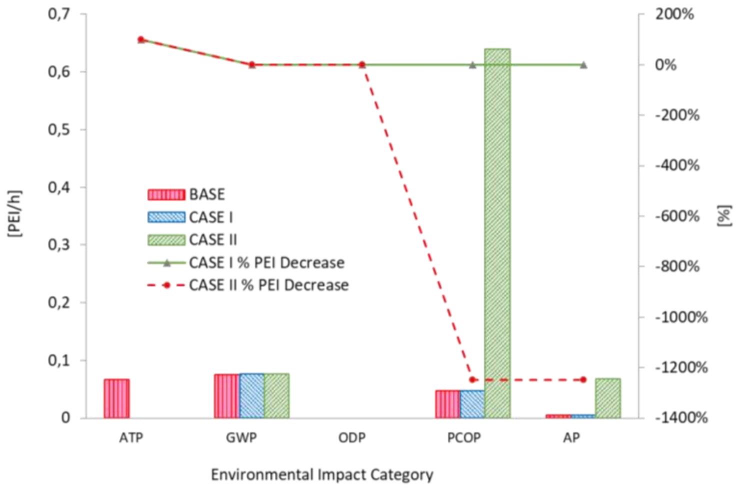

Figure 6.4. PEI generation rates [PEI/h] for categories ATP, GWP, ODP, PCOP, AP and decrease in PEI generation of Cases I and II with respect to BASE case

6.4. Conclusions

Heat and mass balances were performed for three modes of operation of the Semi-Dry FGD section of a Coal Fired power plant in the northeast of Brazil. WAR results demonstrated that BASE case is much more aggressive to the environment, due to the large amount of useless FGD waste produced. The treatment of FGD waste (CASE I) or the bypass of the SDA system (CASE II) were compared separately, as alternatives to transform the solid waste into a class C fly-ash. Because of the SDA system bypassing, SO_2 emission was responsible for increasing PCOP and AP by 1,245%. CASE I was demonstrated to be the more environmentally friendly alternative, although resulting in capital expenditure to install an FBR and auxiliary equipment, to oxidize $CaSO_3$ and solve the problem of landfill use. The SDA and FBR operation also entail an increment of operational expenditures, like energy (1,275 kW or 0.35% of the total turbine power output), water (35 t/h) and lime consumption (4.9 tons/h).

Both Cases I and II allow the commercialization of the solids coming from the SDA as class C fly-ash. Thus, considering only the economic point of view, CASE II is better, but this study proves that the environmental impacts related to SO_2 emissions increases dramatically, and could be prohibitive in countries where the environmental legislation is more restrictive, like in Western Europe and USA. CASE I is more sustainable, because it solves SO_2 emissions, while reducing environmental impacts in other impact categories, contrarily to

CASE II, which favors economics, increasing air pollution to mitigate landfill related environmental impacts. In the long term, depending on the ash and cement market, CASE I could become profitable, resulting from commercialization of treated CCP. Future work must include new data from the recently improved pilot plant and ash analytical methodology, aiming to generate a more accurate streams inventory. Results from this work could be validated, using other LCA software and data basis, like SimaPro and Ecoinvent. Use of low-grade heat from power plant could favor the economic and environmental performance of the full-scale SD-FGD treatment system. This effect must be investigated, and results included in future LCA studies.

6.5. References of Chapter 6

1. World Coal Association, Coal & Electricity, 2017, https://www.worldcoal.org/coal/uses-coal/coal-electricity, [Accessed: 14-March-2017]

2. Wang, Y., Duan, Y., Yang, L., Huang, Z., Meng, S. and Zhao, C., Mercury Speciation and Emission from the Coal-fired Power Plant Filled with Flue Gas Desulfurization Equipment, *Can. J. Chem. Eng.*, Vol. 88, No. 5, pp 867-873, 2010, https://doi.org/10.1002/cjce.20331

3. de Almeida Prado, F. A., da Silva, A. L. R., Avila, E. M. and Matsuyama, G., Clean Energy Certification in Brazil: A Proposal, *J. Sustain. Dev. Energy, Water Environ. Syst.*, Vol. 3, No. 1, pp 95-105, 2015, https://doi.org/10.13044/j.sdewes.2015.03.0007

4. Geller, M. T. B. and Meneses, A. A. M., Life Cycle Assessment of a Small Hydropower Plant in the Brazilian Amazon, *J. Sustain. Dev. Energy, Water Environ. Syst.*, Vol. 4, No. 4, pp 379-391, 2016, https://doi.org/10.13044/j.sdewes.2016.04.0029

5. Empresa de Pesquisa Energética (EPE), National Energetic Balance 2015 (in Portuguese), 2015, https://ben.epe.gov.br/downloads/S%25c3%25adntese do Relat%25c3%25b3rio Final_2015_Web.pdf, [Accessed: 07-April-2016]

6. Row, R. W., Developments in the Management of Wastes from Coal-fired Power Plants, *Waste Manag.*, Vol. 14, No. 3, pp 299-308, 1994, https://doi.org/10.1016/0956-053X(94)90076-0

7. Pierce, B. S. and Dennen, K. O., The National Coal Resource Assessment Overview, *U.S. Geol. Surv. Prof. Pap.*, Vol. 1625, No. F, p 402, 2009.

8. Heidrich, C., Feuerborn, H.-J. and Weir, A., Coal Combustion Products: A Global Perspective, *Proceedings of the World of Coal Ash Conference*, Lexington, Kentucky, USA, 2013.

9. Electric Power Research Institute (EPRI), Characterization of Spray Dryer Absorber Products for Use in Cement and Concrete Applications 1017580, Palo Alto, California,

USA, 2009.

10. American Coal Ash Association (ACAA), Key Findings 2015, Coal Combustion Products Utilization, U.S. Historical Perspective and Forecast, 2015.

11. World Coal Association (WCA), Coal Combustion Products, 2018, https://www.worldcoal.org/coal/uses-coal/coal-combustion-products, [Accessed: 14-March-2017]

12. Bloss, W. and Mohn, U., Method of Treating Final Products from Flue Gas Desulfurization, Patent Number 4,478,810, 1984.

13. Angevine, P. A., Bengtsson, S. and Koudijs, G. P., Method for Oxidation of Flue Gas Desulfurization Absorbent and the Product Produced Thereby, Patent Number 4,544,542, 1985.

14. Jons, E. S., Liborius, E., Veltman, P. L. and Vernenkar, K. N., Method for Treating By-Products from Flue Gas, Patent Number 4,666,694, 1987.

15. Li, C., Zhu, H., Wu, M., Wu, K. and Jiang, Z., Pozzolanic Reaction of Fly Ash Modified by Fluidized Bed Reactor-vapor Deposition, *Cem. Concr. Res.*, Vol. 92, pp 98-109, 2017, https://doi.org/10.1016/j.cemconres.2016.11.016

16. Liu, R., Guo, B., Ren, A. and Bian, J., The Chemical and Oxidation Characteristics of Semi-dry Flue Gas Desulfurization Ash from a Steel Factory, *Waste Manag. Res.*, Vol. 28, No. 10, pp 865-871, 2010, https://doi.org/10.1177/0734242X09339952

17. Electric Power Research Institute (EPRI), A Review of Literature Related to the Use of Spray Dryer Absorber Material Production, Characterization, Utilization Applications, Barriers, and Recommendations, 1014915, Technical Report, Palo Alto, California and Grand Forks, North Dakota, USA, 2007.

18. ASTM, C618-15, Standard Specification for Coal Fly Ash and Raw or Calcined Natural Pozzolan for Use, *Annual Book of ASTM Standards*, p 5, ASTM International, West Conshohocken, Pennsylvania, USA, 2015.

19. American Coal Ash Association (ACAA), Beneficial Use of Coal Combustion Products, An American Recycling Success Story, 2014, https://www.acaa-usa.org/Portals/9/Files/PDFs/Production-and-Use-Brochure.pdf, [Accessed: 07-April-2016]

20. Huggins, F. E., Rezaee, M., Honaker, R. Q. and Hower, J. C., On the Removal of Hexavalent Chromium from a Class F Fly Ash, *Waste Manag.*, Vol. 51, pp 105-110, 2016, https://doi.org/10.1016/j.wasman.2016.02.038

21. Hjelmar, O., Leachate from Land Disposal of Coal Fly Ash, *Waste Manag. Res.*, Vol. 8, No. 6, pp 429-449, 1990, https://doi.org/10.1016/0734-242X(90)90019-J

22. European Chemicals Agency (ECHA), Product of Semi-Dry Absorption method of Flue Gas Desulphurization – Registration Dossier, https://echa.europa.eu/registration-dossier/-/registered-dossier/15224/7/2/2#, [Accessed: 30-March-2017]

23. Mulder, E., A Mixture of Fly Ashes as Road Base Construction Material, *Waste Manag.*, Vol. 16, No. 1, pp 15-20, 1996, https://doi.org/10.1016/S0956-053X(96)00026-8

24. Camilleri, J., Sammut, M. and Montesin, F. E., Utilization of Pulverized Fuel Ash in Malta, *Waste Manag.*, Vol. 26, No. 8, pp 853-860, 2006, https://doi.org/10.1016/j.wasman.2005.11.022

25. Chindaprasirt, P. and Rattanasak, U., Utilization of Blended Fluidized Bed Combustion (FBC) Ash and Pulverized Coal Combustion (PCC) Fly Ash in Geopolymer, *Waste Manag.*, Vol. 30, No. 4, pp 667-672, 2010, https://doi.org/10.1016/j.wasman.2009.09.040

26. Xu, H., Li, Q., Shen, L., Zhang, M. and Zhai, J., Low-reactive Circulating Fluidized Bed Combustion (CFBC) Fly Ashes as Source Material for Geopolymer Synthesis, *Waste Manag.*, Vol. 30, No. 1, pp 57-62, 2010, https://doi.org/10.1016/j.wasman.2009.09.014

27. Doudart de la Grée, G. C. H., Florea, M. V. A., Keulen, A. and Brouwers, H. J. H., Contaminated Biomass Fly Ashes – Characterization and Treatment Optimization for Reuse as Building Materials, *Waste Manag.*, Vol. 49, pp 96-109, 2016, https://doi.org/10.1016/j.wasman.2015.12.023

28. Ding, J., Ma, S., Shen, S., Xie, Z., Zheng, S. and Zhang, Y., Research and Industrialization Progress of Recovering Alumina From Fly Ash: A Concise Review, *Waste Manag.*, Vol. 60, pp 375-387, 2017, https://doi.org/10.1016/j.wasman.2016.06.009

29. de Castro, R. de P. V., de Medeiros, J. L., Araújo, O. de Q. F., Cruz, M. de A., Ribeiro, G. T. and de Oliveira, V. R., Fluidized Bed Treatment of Residues of Semi-dry Flue Gas Desulfurization Units of Coal-fired Power Plants for Conversion of Sulfites to Sulfates, *Energy Convers. Manag.*, Vol. 143, pp 173-187, 2017, https://doi.org/10.1016/j.enconman.2017.03.078

30. Young, D. M. and Cabezas, H., Designing Sustainable Processes with Simulation: The Waste Reduction (WAR) Algorithm, *Comput. Chem. Eng.*, Vol. 23, No. 10, pp 1477-1491, 1999, https://doi.org/10.1016/S0098-1354(99)00306-3

31. National Environment Council (CONAMA), CONAMA Resolution No. 003 from June 28th 1990 (in Portuguese), 1990.

32. The International Standards Organisation, Environmental Management — Life Cycle Assessment — Principles and Framework, ISO 14040, 2006.

33. Cruz, M. de A., Araújo, O. de Q. F., de Medeiros, J. L., de Castro, R. de P. V., Ribeiro, G. T. and de Oliveira, V. R., Impact of Solid Waste Treatment from Spray Dryer Absorber on the Levelized Cost of Energy of a Coal-fired Power Plant, *J. Clean. Prod.*, Vol. 164, pp 1623-1634, 2017, https://doi.org/10.1016/j.jclepro.2017.07.061

34. Tewalt, S. J., Finkelman, R. B., Torres, I. E. and Simoni, F., Colombia, World Coal Quality Inventory: South America, 2006, http://pubs.usgs.gov/of/2006/1241/Chapter 5-Colombia.pdf, [Accessed: 28-May-2015]

35. Bentz, D., Peltz, M., Duran-Herrera, A., Valdez, P. and Juarez, C., Thermal Properties of

High-volume Fly Ash Mortars and Concretes, *J. Build. Phys.*, Vol. 34, No. 3, pp 263-275, 2011, https://doi.org/10.1177/1744259110376613

36. GPSA, *Engineering Data Book* (20th ed.), Gas Processors Suppliers Association, Tulsa, Oklahoma, USA, 2004.

37. Diferencial Energia Empreendimentos e Participação Ltda (DEEPL), Environmetal Impact Assessment, Port of Itaqui Power Plant Enterprise (in Portuguese), p 1395, Rio de Janeiro, Brasil, 2008.

38. Cabezas, H., Bare, J. C. and Mallick, S. K., Pollution Prevention with Chemical Process Simulators: The Generalized Waste Reduction (WAR) Algorithm — Full Version, *Comput. Chem. Eng.*, Vol. 23, No. 4-5, pp 623-634, 1999, https://doi.org/10.1016/S0098-1354(98)00298-1

7. CO_2 CAPTURE FROM FLUE-GASES BY PHASE-CHANGING ABSORPTION SOLVENTS

This first part of this chapter is based on the conference paper SDEWES2019.0276, presented at the 14th Sustainable Development on Environment Water and Energy Systems Conference – Dubrovnik – 2019. Additional content is included on the second part, to update and complement this topic.

7.1. Chemical Absorption of CO2 from Flue-Gases: Experiments with Phase-Changing Solvents in a Bench-Scale Plant

Cruz, M. de A. et al. (2019) **SDEWES2019.0276 Chemical Absorption of CO2 from Flue-Gases: Experiments with Phase Changing Solvents in a Bench Scale Plant**, 14th Conference on Sustainable Development of Energy, Water and Environment Systems. Edited by A. Mudrovčić and M. Ban. Zagreb: Faculty of Mechanical Engineering and Naval Architecture. Available at: https://www.dubrovnik2019.sdewes.org/.

Abstract

The energy penalty of solvent regeneration is a barrier for the deployment of chemical absorption post-combustion carbon capture. Phase-changing absorption solvents have been proposed to overcome this issue. CO_2 absorption triggers phase separation with only the CO_2-rich phase requiring regeneration, potentially reducing energy demand. A systematic review supports the choice of a set of solvents for experimental investigation, based on economic, process and energy-related criteria. Until now the selected absorbents were only investigated in laboratory scale. They need to move from lab to industrial scale to contribute to the global warming mitigation. Three selected biphasic solvents are selected and tested, to confirm the results reported by its developers. Solvent A, based on monoethanolamine/1-propanol, was considered the more suitable one. This blend presented 26% of reduction on the lower (CO_2-rich) liquid phase, compared to the initial volume of fresh solvent. monoethanolamine is the more traditional chemical absorbent for CO_2 capture applications and both components can be considered standard chemicals (low-cost), which is a remarkable advantage. The viscosity of the CO_2-rich phase of solvent A is 10 mPa.s at 25ºC, which is considered low compared to other candidates. Solvent B, based on diethylene-triamine and N,N,N’,N”,N”-pentamethyldiethylenetriamine, was disregarded for further evaluations. It presented only 10% of volume reduction on CO_2 rich phase and prohibitively high viscosity (360 mPa.s at 40ºC). Furthermore, chemical components of this solvent are considered specialty (high cost).

Solvent C, based on N-methylcyclohexylamine and N,N-dimethylcyclohexylamine, was also disregarded for further tests. Although the costs of its chemical components are in the same range of monoethanolamine and the CO_2-rich liquid phase presents an acceptable viscosity (58 mPa.s at 25ºC), this blend had an issue. It presented solids precipitation on the CO_2 rich phase, what is a potential source of operational problems on industrial application. Solvent A was the only one tested on a bench scale screening plant, designed for absorption and desorption of chemical absorption solvents. This blend presented a CO_2 loading of 2.8 mol/kg on the lower phase, 76% higher than MEA 30%. It is an opportunity to reduce the energy penalty of carbon capture of CO_2 by chemical absorption. The solvent A was selected to further evaluation on a continuous mode pilot-plant (under construction).

Keywords: Post-combustion carbon capture, phase change solvents, biphasic solvents, chemical absorption pilot plant, combustion exhaust gases.

Nomenclature

AMP	2-amino-2-methyl-1-propanol
CCS	Carbon Capture and Storage
DEEA	Diethylaminoethanol
DETA	Diethylene-triamine
DMCA	N,N-dimethylcyclohexylamine
LLPS	Liquid-liquid phase separation
LPST	Liquid phase separation temperature
MAPA	N-Methyl-1,3-Propanediamine
MCA	N-methylcyclohexylamine
MEA	Monoethanolamine
PCAS	Phase-changing absorption solvents
PCASP	Phase-change absorption screening plant
PMDETA	N,N,N’,N”,N”-pentamethyldiethylenetriamine
TBS	Termomorphic biphasic solvent

7.1.1. Introduction

Paris Agreement established a compromise to keep the global warming below 2ºC to the end of this century. It imposes at least 70% emissions reductions through 2050, compared to 2010 levels. (IPCC, 2014b) Carbon Capture and Storage (CCS) is expected to account for 14% (140Gt) of this target, considering the power and industrial sectors. (Global CCS Institute, 2017) Nevertheless, the pace of CCS development is not enough to achieve this goal. (IEA, 2016) Cost is a remarked hindrance to CCS deployment on industries where CO_2 separation step is not inherent to the process. CCS could bring up to 70% addition on lifecycle cost of production for power generation, 68% for cement production and 41% for steel manufacturing. (Global CCS Institute, 2017)

Major CCS costs come from the energy penalty of capture and compression processes. Usually, CO_2 capture corresponds to 65% - 80% of this penalty on power plants. (Goto; Yogo; Higashii, 2013) Chemical absorption with alkanolamines is a mature post-combustion capture process for exhaust gases with low CO_2 partial pressure (4 – 30 kPa). Gas scrubbing with an aqueous solution of monoethanolamine (MEA) is the benchmark technology. (Rochelle, 2009; Rubin; Chen; Rao, 2007) The first process was proposed by Bottoms (1930) and imposes an energy consumption of 3.7 GJ/ton of CO_2 captured. (Knudsen et al., 2009) Major energy demand comes from desorption of CO_2 from the solvent. Usually, heat is supplied by low-pressure steam, from boilers or steam cycles. As a result, the net energy efficiency of those processes is impaired. For each GJ/ton CO_2 reduced, 2% net efficiency improvement is achieved on coal-fired power plants. (Goto; Yogo; Higashii, 2013). Additionally, low CO_2 absorption capacity per mol of solvent (loading), thermal and oxidative degradation and corrosivity are frequently reported as weaknesses of MEA. (Zhang et al., 2013)

Process improvements and optimization on conventional amine scrubbing have been exhaustively studied. The energy penalty of Bottom's process cannot be considered a reference nowadays. (Boot-Handford et al., 2014) Frailie et al. (2013) evaluated inter-stage cooling and heating on absorber and stripper columns, respectively. Li et al. (2011) investigated heating integration and exhaust gas recycle. Park et al. (2016) performed an optimization study concerning stripper pressure. Rochelle and collaborators deeply investigated absorber performance (Zhang; Rochelle, 2014) and intercooling (Rezazadeh et al., 2014, 2017). Commercial processes applying state-of-the-art technology combines process optimization and advanced solvents. KM-CDR process reached an energy penalty of 2.11 GJ/ton of CO_2 captured, about 43% lower than early MEA scrubbing processes. (Miyamoto et al., 2017) Nevertheless, the energy penalty of carbon capture by chemical absorption still being a barrier for its deployment. However, there are few opportunities for energy saving and lifecycle cost reduction of CCS by amine scrubbing.

7.1.1.1. Phase-changing absorption solvents

Phase-changing absorption solvents (PCAS) emerged as a real opportunity to cut the energy penalty of carbon capture. Most PCAS are called thermomorphic, which means that they present a lower critical CO_2 loading that is a function of temperature. After saturated in CO_2 and above a certain temperature, liquid-liquid phase separation (LLPS) occurs. (Budzianowski, 2016) Preferably, one phase must be rich and other lean on CO_2 (Raynal et al., 2014) and liquid phase separation temperature (LPST) must be higher than absorption temperature. Thereby, the CO_2 lean phase is recycled to the absorber and only the rich phase is sent to desorption. It entails reduced circulation rate and reboiler heat duty. (Coulier et al., 2017; Liebenthal et al., 2013) Some PCAS presents lower desorption temperature, enabling the use of low-grade heat. Higher desorption pressure is another possibility, reducing CO_2 compression penalty.

Early PCAS was already demonstrated in pilot scale. DMX process (Raynal et al., 2014) reported a specific reboiler heat consumption of 2.5 GJ/t of CO_2, 19% reduction on energy penalty and 20% lower cost of CO_2 avoided, compared to MEA runs. BiCAP process (Lu, 2017) reported 34% of energy penalty reduction and 50% reduction on the cost of CO_2 avoided. Both DMX and BiCAP used undisclosed proprietary blends of PCAS. DEEA (Diethylaminoethanol) and MAPA (N-Methyl-1,3-Propanediamine) aqueous solutions was tested in Gløshaugen (NTNU/SINTEF) pilot plant. The average reboiler duty was 2.3 GJ/t of CO_2 (Pinto et al., 2014), 30% lower than the benchmark (MEA).

Recently, new PCAS (Barzagli; Mani; Peruzzini, 2017; Wang et al., 2017; Zhang et al., 2013, 2017a, 2017b; Zhou et al., 2017) emerged, aiming to overtake weaknesses of early ones, notedly: proprietary blends, low net CO_2 loading, LPST below absorption temperature, high cost of employed unconventional amines and high viscosity of loaded solution. This work selected three PCAS in the early stage of development from literature. Table 7.1 lists retail prices of all components of selected PCAS, for comparison.

Table 7.1. Retail price of PCAS chemicals (Sigma-Aldrich, 2018)

Component	Structural Formula	Price (US$/liter)	Component	Structural Formula	Price (US$/liter)
MEA	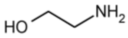	51.00	DMCA	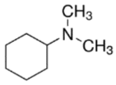	74.60
DEEA	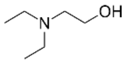	54.50	AMP	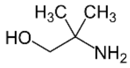	56.50
MAPA	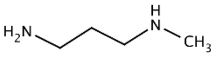	297.50	DETA	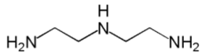	63.40
1-propanol	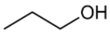	79.50	PMDETA	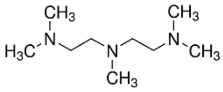	270.00
MCA	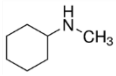	383.65			

The first blend is MEA/1-propanol/H_2O, claimed by Zhang et al. (2017a, 2017b) as a promising PCAS, because it is based on MEA, the most common CO_2 absorbent and 1-propanol, an ordinary alcohol. 1-propanol presents affordable prices, in the same order of magnitude of MEA (see Table 7.1). The author performed tests in a simple lab absorption apparatus. Basically, pure CO_2 was bubbled in an Erlenmeyer flask, filled with the absorption solvent. Preliminary results confirmed LPST at around 30ºC. The volume of rich phase could be reduced up to 67% of the initial volume of solvent with loading up to 2.6 molCO_2/kg of solvent, 30% higher than MEA 30% (w/w). The author suggested that more tests, in pilot scale, are required to demonstrate the suitability and potential for energy penalty reduction of this PCAS.

The second was developed by Zhou et al. (2017), being composed of diethylene-triamine (DETA) and N,N,N',N'',N''-pentamethyldiethylenetriamine (PMDETA). That blend is not cost attractive as the first one, especially because PMDETA price (see Table 7.1). But bulk orders are available for both components, with much more affordable prices. The advantage is that, usually, none of them needs special permits of army or police to be purchased in large quantities. Another advantage is the improved loading (0.613 mol CO_2/mol amine), 21% higher than MEA and 26% higher than DEEA/MAPA. LPST is 50ºC, within the temperature range of flue-gases from power plants. The volume of rich phase is 57% of total solvent volume. The author reported 2.3 GJ/t of CO_2 (reduction of 38% compared to MEA). Once again, tests were performed in small glass apparatus on the lab. Pilot scale experiments are required, to prove the advantage of using this PCA in full-scale CCS applications.

Lastly, Zhang et al. (2013) studied a so-called TBS (termomorphic biphasic solvent), that mixes N-methylcyclohexylamine (MCA) as an absorption activator, N,N-dimethylcyclohexylamine (DMCA), as regeneration promoter and amine 2-amino-2-methyl-1-propanol (AMP), as a solubilizer to increase LPST. This PCAS do not use expensive amines, as shown in Table 7.1, and performs well in terms of CO_2 loading (3.5 molCO_2/kg – 75% higher than MEA). LPST is between 30ºC - 40 ºC. Desorption occurs at 80 ºC, enabling the use of low-grade heat. Experiments were performed in bench scale plant but used glass columns of only 0.04 mm inner diameter at atmospheric pressure. The author reported 2.0 GJ/t of CO_2 (reduction of 46% compared to MEA). However, this result could be unrealistic, because of wall effects and other consequences of such small-scale plant.

PCAS with high viscosity could be a challenge for pumping systems. Zhang et al. (2013) reported viscosities of 16 mPa.s for loaded TBS-3, what is higher than MEA (3.3 mPa.s) but lower than DETA/PMDETA (250 mPa.s (Zhou et al., 2017)) and MEA/1-propanol (60 mPa.s (Zhang et al., 2017b)). The effect of viscosity on the full-scale system must be considered on choosing the more suitable PCAS.

7.1.1.2. Solvent Testing Plant (Batch)

Technical, economic and environmental performance of large-scale post-combustion processes with selected PCAS are necessary to prove the advantage of such solvents over early ones. Move from lab to pilot scale plants is the first step to achieve this goal. In this work, a bench scale screening plant is constructed to the preliminary evaluation of selected PCAS. Based on lab preliminary tests and techno-economic criteria, suitable PCAS are tested on the screening plant. Based on the results of this work and previous pilot plant studies, a continuous mode pilot plant will be designed. Data from experiments in both, bench and pilot-scale plants, will support mathematical modeling and computational simulation of full-scale CCS using PCAS.

The absorption capacity of solvents is affected by testing methods, solvent composition, temperature (of gas and solvent), pressure, and gas composition. (Huertas et al., 2015) To reproduce the results of previous studies, the bench scale plant is designed to run experiments at the same conditions used by authors. In future tests, a more realistic standard condition must be set, to enable comparison between different PCAS. Therefore, the bench plant must be able to work with a wide range of CO_2, O_2 and N_2 flows (gas composition), temperatures and pressures. It is also important to keep the solvent temperature constant along with the experiment, using a process thermostat.

Although showing promising results, most previous studies were performed at lab conditions (ambient temperature and pressure, small glass apparatus and bubbling pure CO_2 into a few milliliters of solvent). However, higher temperature (40 - 70ºC) low CO_2 partial pressures (5 – 30 kPa) and oxygen (1% - 15%) are found in flue-gases from power stations, gas-turbines, furnaces, refinery, cement and steel plants (Ulrich, 2010). As a result, the loading reported at lab conditions, by previous studies, could be overestimated compared to real conditions. Consequently, the overall energy penalty of the process is underestimated.

Oxygen irreversibly reacts with amines along the time, reducing it CO_2 absorption capacity. (Huertas et al., 2015) Considering aqueous solutions concentrations between 12% and 42% (w/w) the process is controlled by kinetics and O_2 mass transfer. However, MEA loss due to oxidative degradation is in the range of 0.29 – 0.73 kg per ton of CO_2 captured in large scale processes. (Thong et al., 2012) Therefore, this effect is expected to be negligible for batch experiments with virgin PCAS, but relevant for the continuous mode pilot plant.

Low CO_2 partial pressures and higher temperature reduces the capture efficiency of the absorption process. Lower efficiency means increased saturation time for batch experiments and higher absorbent flux (reboiler duty) and column size for continuous process. Once again, CO_2 partial pressure is not so relevant parameter for batch experiments, but very important to a continuous process.

The main objective of this work is evaluating selected PCAS, in terms of CO_2 absorption capacity and rate, volume ratio and viscosity of upper and lower liquid phases. Besides process and energetic matters, economic, environmental and safety inherent characteristics of PCAS components will be taken into account on solvent choice. Results support continuous pilot-plant design and operation. The more suitable PCAS is selected to a trial test and further studied on a batch pilot plant and, in the future, tested at a continuous mode pilot-plant (under construction).

7.1.2. Methodology

7.1.2.1. Preliminary experiments

Preliminary absorption experiments (Figure 7.1) are performed with the three selected PCAS, at the lab, to observe the phase-change behavior and properties (density and viscosity) of liquid phases. Tests were executed at ambient temperature (around 25 ºC), based on previous studies, according to Table 7.2. These preliminary tests consisted of bubbling a pure CO_2 gas stream into a recipient containing 50 ml of solvent, as shown in Figure 7.2. The gas flow is kept constant until there is no more difference between the absorption liquid and the ambient temperatures. It means that the solvent is already saturated because the absorption reaction is exothermic. The required chemical components to formulate the PCAS are gathered in Table 7.1. MEA was purchased from Oxiteno S.A, 1-propanol (99.5%) from Isofar, MCA, DMCA, DETA, PMDETA, and AMP were obtained from Merck (Sigma-Aldrich, Inc).

Figure 7.1. Absorption Preliminary Tests Apparatus

Table 7.2. Selected phase-change absorption solvents - composition

PCAS	Components	Total Amine Mole Concentration	Components Mole Concentration					Reference
A	MEA/1-propanol	5.00	5.00	:	5.35			(Zhang et al., 2017a)
B	DETA/PMDETA	5.00	4.00	:	1.00			(Zhou et al., 2017)
C	MCA/DMCA/AMP	5.50	1.00	:	3.00	:	1.50	(Zhang et al., 2013)

Feed gas flow and composition used on absorption experiments are shown in Table 7.3.

Table 7.3. Absorption tests – feed gas parameters

T	P	Gas Vol. Flow (NLPM)		CO_2 Partial Pressure
(ºC)	(kPa)	Air	CO_2	(kPa)
25	101.3	-	0.50	101

Preliminary absorption experiments are performed to enable comparison between results obtained by this work and reference ones. It employs a standard gas composition, without O_2, SO_x, and NO_x. Such contaminants could react with amines and modify some results.

7.1.2.2. Phase-Change Absorption Screening Plant (PCASP)

The PCASP is shown in Figures 7.2 and 7.3. It is a bench unit, mainly comprised of two bubble columns (V-02 and V-03, with 0.1 m diameter and 0.675 m of height), where absorption and desorption PCAS tests take place. A supervisory control and data acquisition (SCADA) system (Elipse E3) is used to control and record temperatures, pressures, flow rates, and gas CO_2 concentrations at strategic points of the system. Gas cylinders (from Linde Gases LTDA.) supplies CO_2 (99.8% at 5800 kPa) and Nitrogen (N_2) (99.8% at 20000 kPa). Dry compressed air can be used to adjust Oxygen (O_2) composition of the feed gas. The flows of all inlet gases are measured by thermal mass flow controllers (Brooks SLA 5800 series). Standard flow is double checked by local rotameters. Maximum standard flows of CO_2, air, and N_2 are 3 normal liters per minute (NLPM), 10 NLPM and 15 NLPM, respectively. The CO_2 pressure regulator and the downstream pipe has an electrical trace, enabling gas heating and avoiding frozen. Streams of CO_2, air, and N_2 are mixed and follows to vessel V-01. If a humid and warm gas is desired (to simulate a flue-gas from a real power plant), V-01 must be partially filled with water and its immersed electrical resistance turned on. The feed gas temperature can be set in the range of 30ºC – 50ºC. Experiments can be realized between 101.3 and 500 kPa, resulting in feed gas CO_2 partial pressures in the range of 5 – 500 kPa.

Figure 7.2. Absorption & Desorption Screening Plant

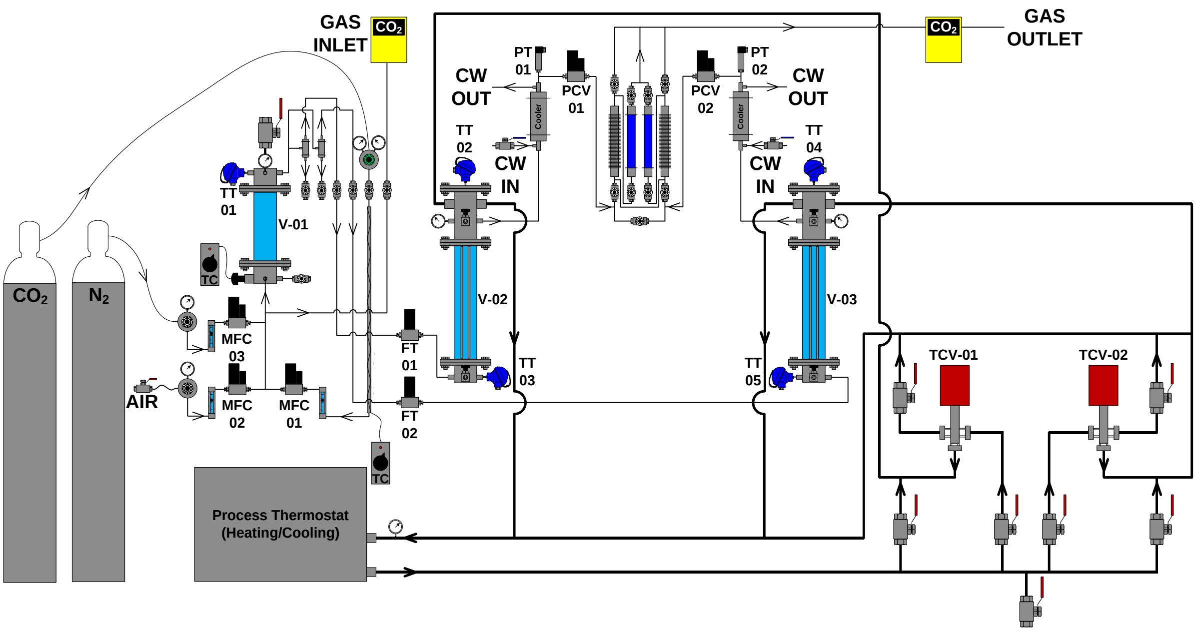

Figure 7.3. Absorption & Desorption Screening Plant Flowsheet

Two different solvents can be tested simultaneously. Each vessel (V-02 and V-03) can receive up to 4 liters of solvent, considering the maximum level as half of the vessel height). Filled with 5 kg of 5 mm glass beads, the inventory of solvent is reduced to 1.5 liters of solvent. These vessels have internal coils. Inside these coils a thermal fluid (Kryo 65) flows, coming from a process thermostat (Lauda Integral XT-150). This equipment enables to keep the temperature constant during absorption (cooling mode) and desorption (heating mode). TCV-01 and TCV-02 are 3-way temperature control valves (Badger Meter RCV type 1118 with electronic actuator model EVA-1). They adjust the thermal fluid flow in each coil, enabling individually set the temperature inside V-01 and V-02. Each vessel has a water condenser and a silica gel filter after gas outlet, to reduce solvent loss and avoid liquids and humidity into CO_2 sensors.

7.1.2.3. Absorption Experiment Using the PCASP

Procedure and Setup:

Solvent temperature set-point: 30°C during absorption; 40 ºC after solvent saturation

- Absorption vessel pressure (V-02): 101.3 kPa
- Gas composition: 16.7% CO_2 + 83.3% dry air (9 min); 66.7% CO_2 + 33.3% dry air (10 min); 100% CO_2 (28 min)
- CO_2 flow: 2.0 l/min
- Airflow: 10.0 l/min (9 min); 1.0 l/min (10 min). Air was used to increase the feed gas flow, promoting heat and composition homogenization inside absorption vessel (V-02)
- Solvent: 1.5 liters of solvent A (5M MEA/6M 1-propanol)

The CO_2 absorption rate was calculated by the difference between the inlet and outlet gas concentration as proposed by Wang et al. (2013), according to Equation (7.1):

$$r_{CO_2} = \frac{273.15 \times P\ Q_g\ (C_{in} - C_{out})}{101.3 \times 22.4\ T} \tag{7.1}$$

Where r_{CO_2} is the CO_2 instantaneous absorption rate (mol/min), P is the absorption pressure (kPa), Q_g is the CO_2 standard flow rate (l/min), C_{in} and C_{out} are the CO_2 concentrations on inlet and outlet gas streams (% vol.) and T is the absorption temperature (K).

The CO_2 concentration of the feed and lean gas can be continuously monitored by in-line infrared sensors (Witt model PA 7.0). CO_2 loading in liquid phases is analyzed by the Chittick method. (Zhang et al., 2018) The viscosity of liquid phases is measured using a viscometer (Brookfield DV1). Density is determined by Mettler Toledo DM40 density meter.

7.1.3. Results and Discussion

7.1.3.1. Preliminary tests

The three tested PCAS candidates (A, B and C) formed two phases after being loaded with CO_2. This is the first criterion that must be regarded before considering a test on the PCASP.

Although it was confirmed the formation of two phases after CO_2 absorption by solvents A, B, and C, there was a 26% reduction in the volume of the lower (supposedly CO_2 rich) phase of solvent A, 10% in the lower phase of the solvent B and 20% of solvent C. The modest volume reduction of solvent B would lead to negligible reduction in the energy penalty of regeneration. The viscosity of each phase of the solvents was also analyzed, as shown in Figure 7.5. High viscosity could be a challenge for pumping systems and must be considered when aiming a full-scale application.

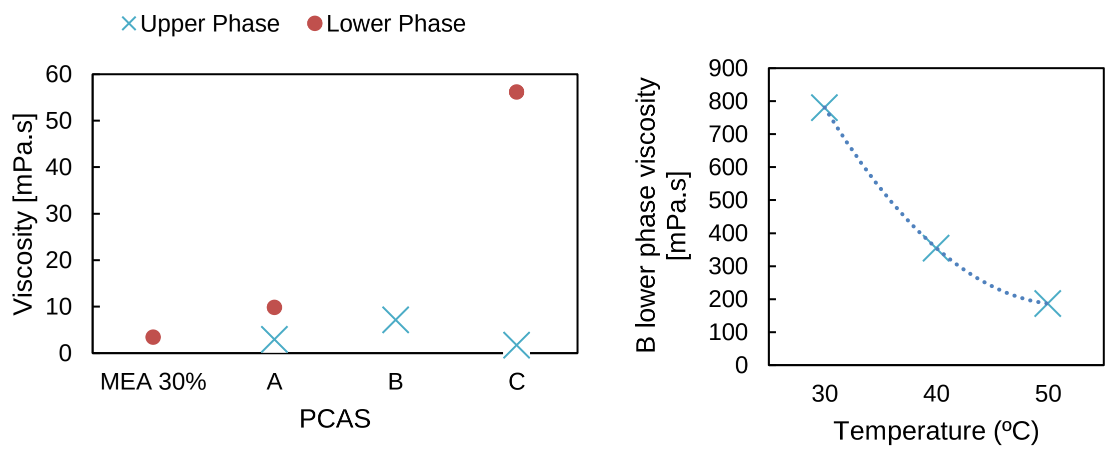

Figure 7.5. Viscosity of liquid phases after CO_2 absorption at 25°C – (A) 5M MEA/4M 1-propanol; (B) 4M DETA/1 M PMDETA; (C) 1M MCA/3M DMCA/1.5M AMP. Viscosity versus temperature of solvent B.

Solvent B presented high viscosity for the lower phase, exceeding the maximum value supported by the viscometer (1200 mPa.s) at 25 °C. Heating was required to enable a measure of lower phase viscosity, as shown in Figure 7.6. The viscosity only reaches the values reported by Zhou et al. (2017) (250 mPa.s) above 50ºC. This viscosity is prohibitive because brings operation and maintenance issues on industrial application. This characteristic together with the low reduction of volume of the CO2 rich phase resulted in the elimination of solvent B from further experiments on PCASP.

The viscosity of the lower phase of solvents A and C was around 183% and 1500% greater than the reference (30% MEA), respectively. The slightly higher viscosity of A could imply marginal impacts on the overall energy penalty of the process, but this effect could be more representative for solvent C. Besides presented a moderate viscosity, crystals precipitation was noted in solvent C after standing at ambient temperature. The precipitate can bring operational problems – e.g. clogging of liquid dispersers and process pipes. For this reason, the use of solvent C may not be convenient on plants designed for liquid-liquid PCAS. Another negative point of C was difficult on visualizing the liquid-liquid interface, due to the color similarity of the two phases. For these reasons, solvent C was not tested on the PCASUS.

7.1.3.2. Absorption Experiments on the PCASP

The solvent started to become saturated in CO_2 after 40 minutes of absorption. This event was visually observed by the increased turbidity of the solvent inventory, by the gas temperature drop (Figure 7.6) and by the increase in CO_2 concentration at the gas outlet (Figure 7.7). The solvent was considered fully saturated after 46 minutes (Figure 7.7) when the liquid became totally turbid and the CO_2 concentration at the outlet reached 100%. At this stage, the set-point of the temperature control valve (TV-01) was modified to 40 °C. After 70 minutes, when the liquid temperature reached 34 °C, the phase split began, and the gas feed was interrupted to stop the stirring and enable the total liquid-liquid separation. The turbid interface gradually narrowed until becoming a line dividing the two liquid phases (Figure 7.6). At the end of the experiment, samples of the upper and lower phases were collected. The CO_2 loading, density, and viscosity of each phase were analyzed, and results are shown in Table 7.4. The instant CO_2 absorption rate was calculated according to Equation 7.1 and is shown in Figure 7.7.

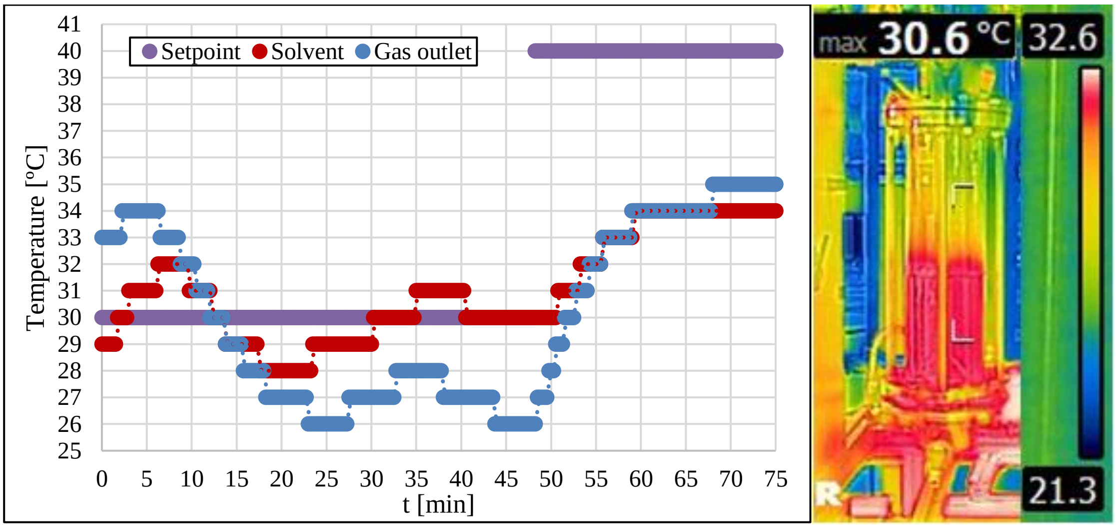

Figure 7.6. Average solvent A (5M MEA/6M 1-propanol) temperature along with the test at PCASP (left side). Thermal image of the vessel during the experiment (right side).

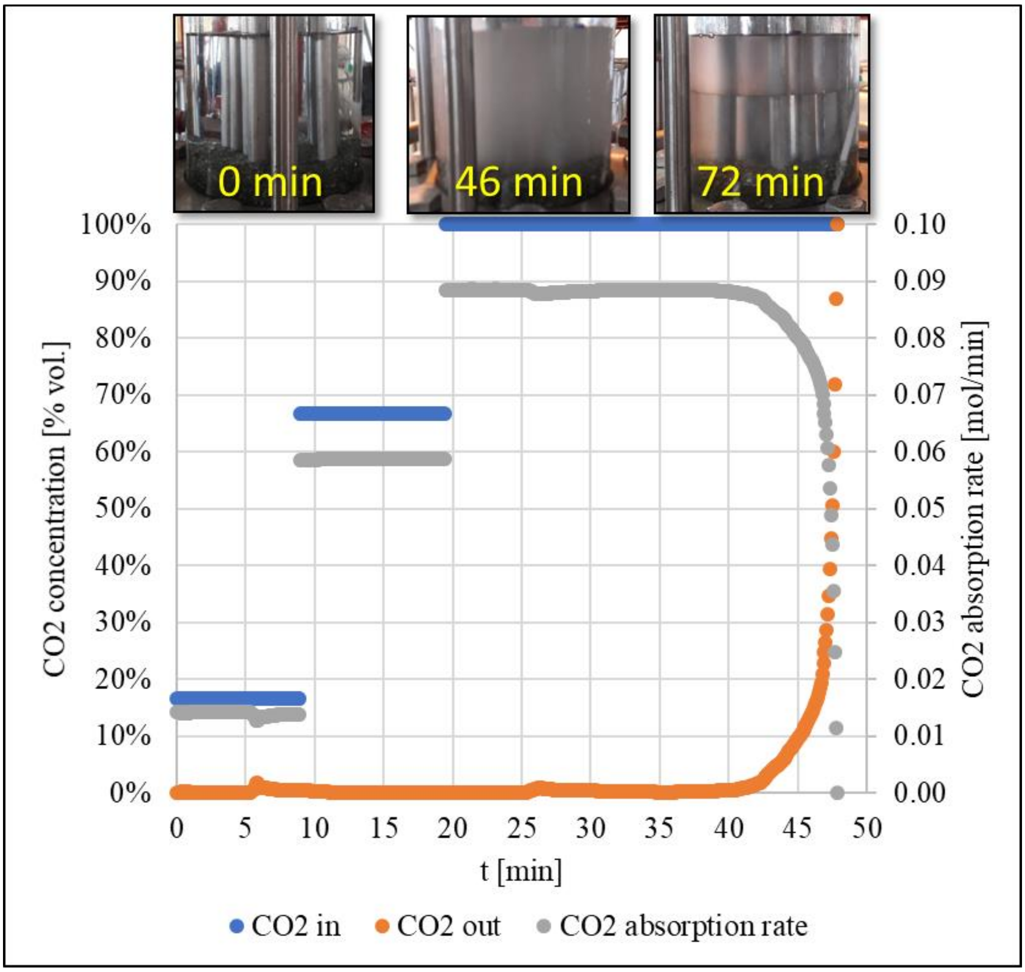

Figure 7.7. Gas CO_2 concentration and absorption rate of solvent A (5M MEA/6M 1-propanol) along with the test at PCASP

Table 7.4. Main results of the test of solvent A (5M MEA/6M 1-propanol) on the PCASP compared with results of ZHANG et al. (2017a).

Property	**Lower Phase**			**Upper Phase**		
	This work	Ref.*	Diff.	This work	Ref.*	Diff.
Density (g/cm³)	1.11	1.06	5.1%	0.86	0.79	8.9%
Viscosity (cP)	10	12	-16.7%	3	N/A	N/A
CO_2 loading (mol/kg)	2.80	3.00	-6.5%	0.47	0.49	-4.6%
Volume (ml)	1050	-	-	450	-	-

*****(Zhang et al., 2017a)

The CO_2 loading, densities, and viscosities are in agreement with the results reported by Zhang et al. (2017a). According to the present study, the loading of solvent A is 76% higher than MEA 30%. Measure the energy penalty reduction of the carbon capture process depends on further desorption experiments, that enables to determine the cyclic capacity of the solvent. Nevertheless, it is possible to infer that solvent A would bring energy savings and reduced stripper footprint when applied to a carbon capture process. The energy penalty benefit comes from the increased loading of CO_2 per mol of solvent that is sent to the stripper. If the CO_2 loading of the lower phase were the same as MEA 30% solutions, the reduction on the initial volume of solvent would have no consequence on the regeneration energy. The reduction of the lower phase (30%) compared to the initial volume of solvent was almost the same volume of 1-propanol added to the MEA 30% solution. According to Wang et al., (2019), the only advantage off add 1-propanol to the solvent is that it works as a physical solvent, increasing the diffusivity of the CO_2 and consequently its solubility and absorption rate. After reach a critical loading, carbamates encircled by water expels 1-propanol molecules, forming another liquid phase. This effect is named salting-out.

7.1.3.3. Potential Energy Savings from the use of PCAS (solvent A)

The presence of 1-propanol (even in low concentration) on the lower phase is an advantage. Alcohols have a low dielectric constant, promoting solvent regeneration. (Zhang et al., 2017a).

Simulating a capture process using the same PCAS considered in this study (MEA 30%/1-propanol 40% w/w) Wang et al. (2019) reported an energy penalty of 2.87 GJ/t, setting a pressure of 200 kPa at the stripper, which resulted in a temperature of 127 ºC on the reboiler. The energy saving estimated by Wang et al. (2019) is 28% lower than the baseline (MEA 30% - 3.99 GJ/tCO_2). Disregarding simulation constrains and accuracy, the major source of energy penalty is the volume reduction coming from the split of the rich liquid phase considered by Wang et al. (2019) and also reported in the present study. The author reported a 43.6% volume fraction of the upper phase against the total income solution while in the experiments performed in the present study this fraction is 30%. This factor influence MEA concentration, CO_2 loading on rich phase and the flow rate of the solvent sent to the stripper, which directly influences the reboiler duty and temperature and stripper CO_2 recovery.

The feed gas of a NGCC flue-gas has a CO_2 partial pressure ranging around 5 to 10 kPa. Wang considered a partial pressure of 16 kPa (compatible with PCC flue-gas), which makes the chemical absorption process less intensive on energy. Using a NGCC flue-gas entails a higher solvent per CO_2 flow ratio (capture ratio) increasing the energy penalty.

7.1.4. Conclusion

This study investigated the state-of-the-art on PCAS. Three blends of solvents were selected and submitted to preliminary tests. One of them was elected to be tested on a batch screening plant, named PCASP, designed to evaluate biphasic solvents properties and phase change behavior during absorption and desorption of CO_2 coming from the synthetic exhaust gas. The test confirmed that using PCAS based on MEA and 1-propanol is an opportunity to reduce the energy penalty of carbon capture of CO_2 by chemical absorption.

The next step is testing the best PCAS under different compositions and absorption conditions, simulating a more realistic flue-gas (higher temperature, pressure, presence of contaminants and lower CO_2 partial pressure). Desorption experiments also must be executed to confirm the cyclic capacity and comparison with results reported by other authors. Results will serve as a reference to the design of a pilot plant that will expose the solvent to a continuous process and long runs, in order to evaluate more precisely the energy penalty, degradation of the solvent and other process parameters. This information is necessary to validate the simulation and scale-up of a full-scale application of a PCAS.

7.2. Pilot Plants Developed for Testing CO_2 Capture with Phase-Changing Absorption Solvents

A pilot plant was designed to perform long-run experiments with PCAS, to up scaling the first plant, PCASP, presented in section 7.1 – the Phase-Changing Absorption Pilot Plant (PCAPP). This section describes the two plants.

7.2.1. Phase-Changing Absorption Solvents Screening Unit - PCASP

The PCASP was presented in section 7.1 and is detailed in this section. The construction of the plant lasted six months and was finished in January 2018. Fig.7.8 shows the unit.

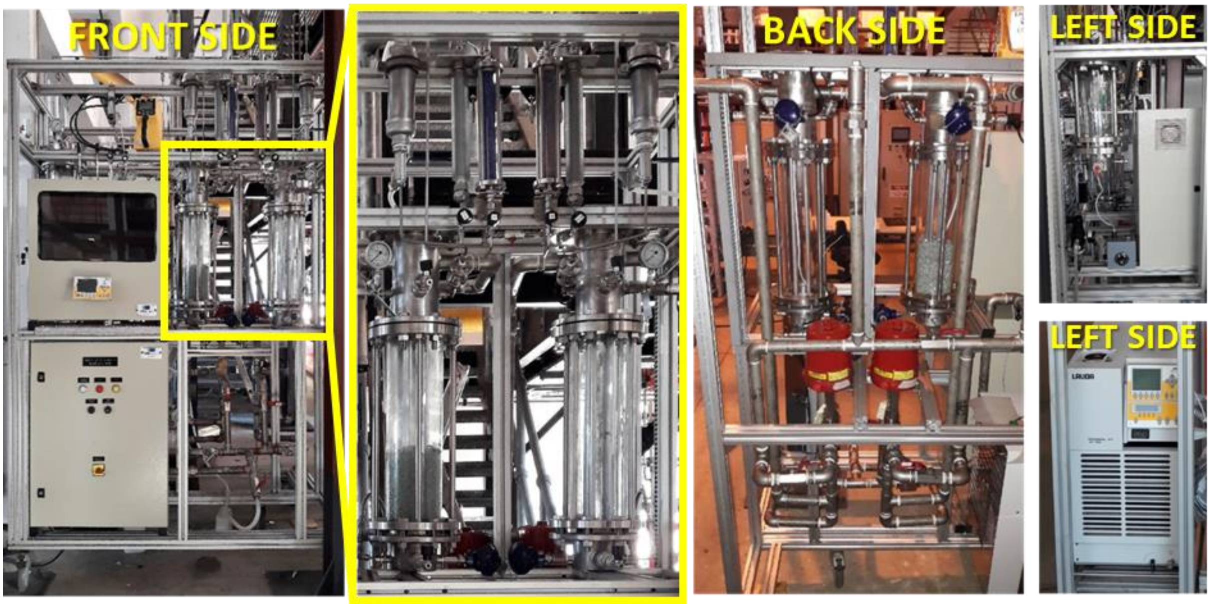

Figure 7.8. PCASP Overview

On the front side of the plant, the control and automation panels and the two main vessels are visualized. On the opposite side, are installed the temperature control valves and thermal fluid piping. On the left side, the process thermostat and the gas heating and water saturation vessel are placed. The commissioning and startup of the plant were performed in May 2018 and experiments were performed along 2018 and 2019. A 5M MEA solution was used to perform an absorption test with a CO_2-rich feed gas. The plant provided a capture efficiency >90%. The skid has three glass absorption vessels. Each vessel has a temperature sensor (PT-100) and a mechanic pressure gauge. The inlet and outlet gas flows are connected to the CO_2 analyzers. Temperature, gas flows and CO_2 concentration trends were registered at the SCADA of the PCASP, as shown in Fig. 7.9.

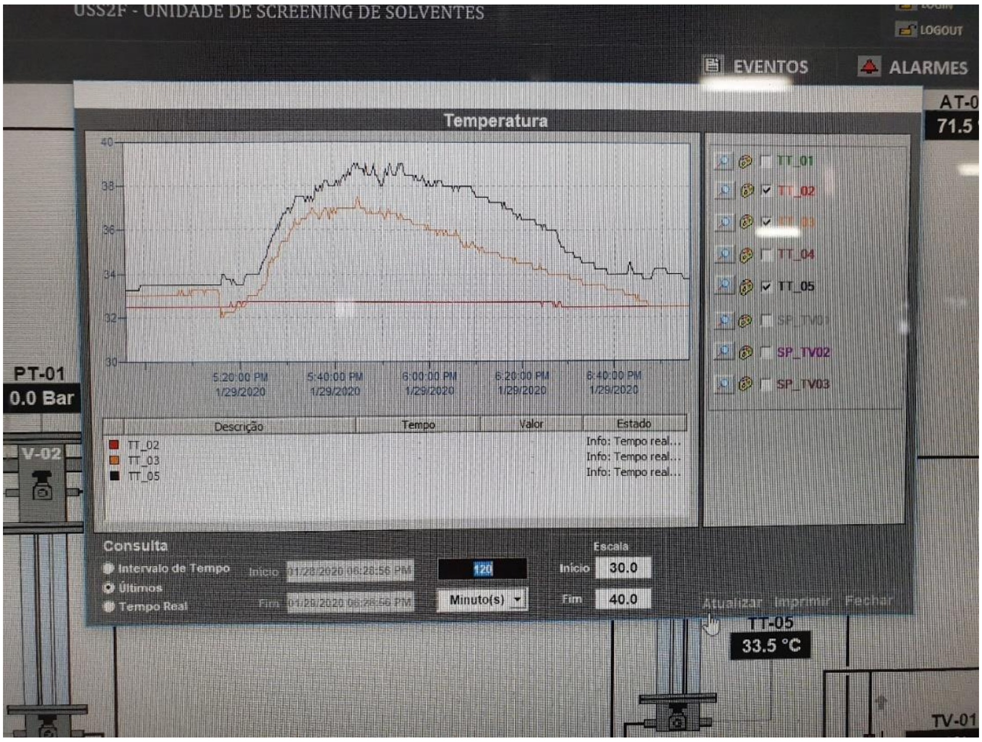

Figure 7.9. Temperature trends in typical PCAS experiment.

7.2.2. Phase-Changing Absorption Pilot-Plant - PCAPP

This section presents the process description and basic engineering design data related to the PCAPP, a pilot-plant intended to testing PCAS in continuous mode. The PCAPP will be located in the *Natural Gas Center of Excellence* (*CE-GN*). The CE-GN has the process utilities described in Table 7.5.

Table 7.5 CE-GN Available Utilities

UTILITY	PROCESS PARAMETERS
Chilled Cooling-Water	5°C
Tower Cooling-Water	28ºC
Compressed air	800 kPag
N_2 gas	400 kPag (generator)/10000 kPag (cylinder)
CO_2 gas	5700 kPag (cylinder)
Mixed Gas (30%CO_2/70%N_2)	15000 kPag (tank)
Electricity	380V triphasic 60Hz (AC) 220V monophasic 60Hz (AC)
Heating (thermal fluid)	Up to 150ºC (11,2 kW)

The PCAPP is designed to capture CO_2 from low-pressure flue-gases with PCAS. The main difference with relation to conventional chemical absorption units is the liquid-liquid separation vessel placed downstream the absorber bottom liquid outlet. The PCAPP process flow diagram is depicted in Figure 7.10. The P&ID of the plant is available in Fig. 7.11.

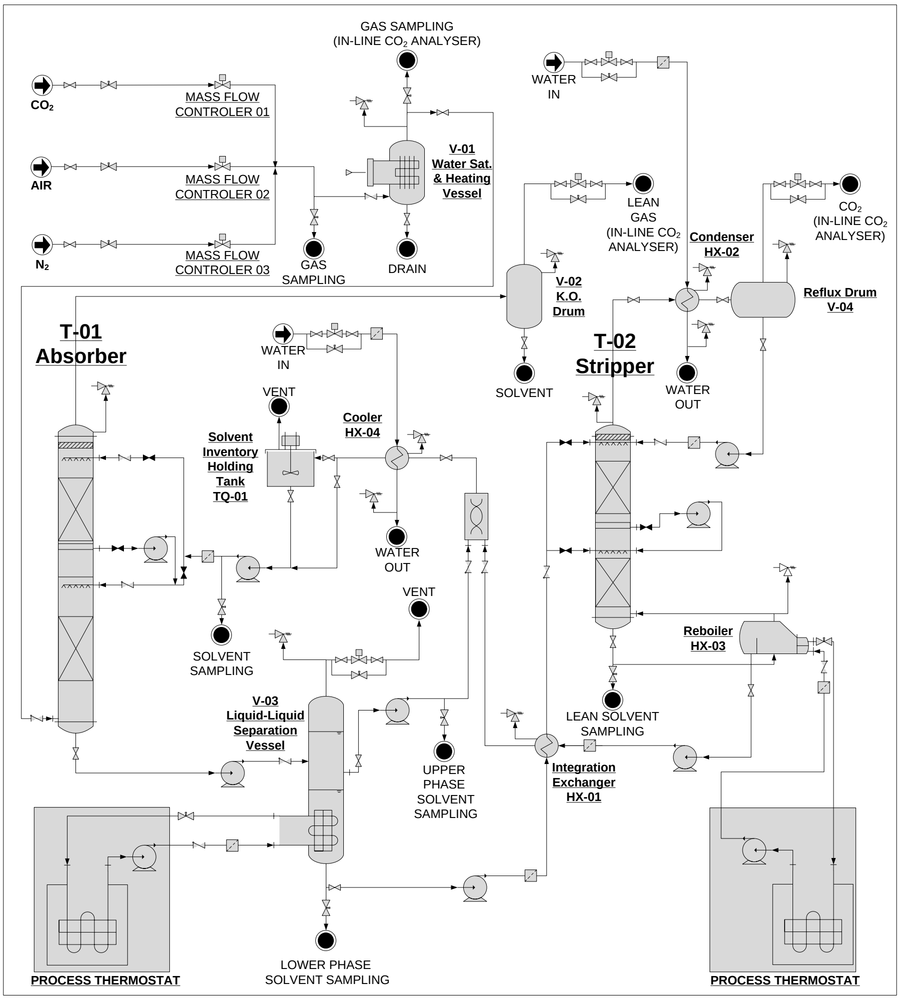

Figure 7.10. PCAPP Flowsheet

The plant is designed to absorb a maximum flow rate of 5kg/h of CO_2. Table 7.6 shows the range of CO_2 concentration and partial pressure considered – the higher the CO_2 partial pressure the more favored is the absorption. The NGCC flue-gases are well known to present low CO_2 partial pressures (4 – 8 kPa) making the chemical absorption less efficient. The considered partial pressures are expected on flue-gases from NGCC power plants and some refinery units.

Table 7.6. Design CO_2 partial pressures and dry flue-gas mass flows

CO_2 Composition		SFG Mass Flow	SFG Inlet Pressure	CO_2 Partial Pressure
% mass	% mol	kg/h	kPag.	kPag
5,0	~3,5	94,7	100 – 200	3.5 - 7.0
10,0	~7,0	50,0	50 – 200	3.5 - 14
15,0	~10	33,4	50 – 200	5.0 - 20
20,0	~14	25,0	50 – 200	7.0 - 28

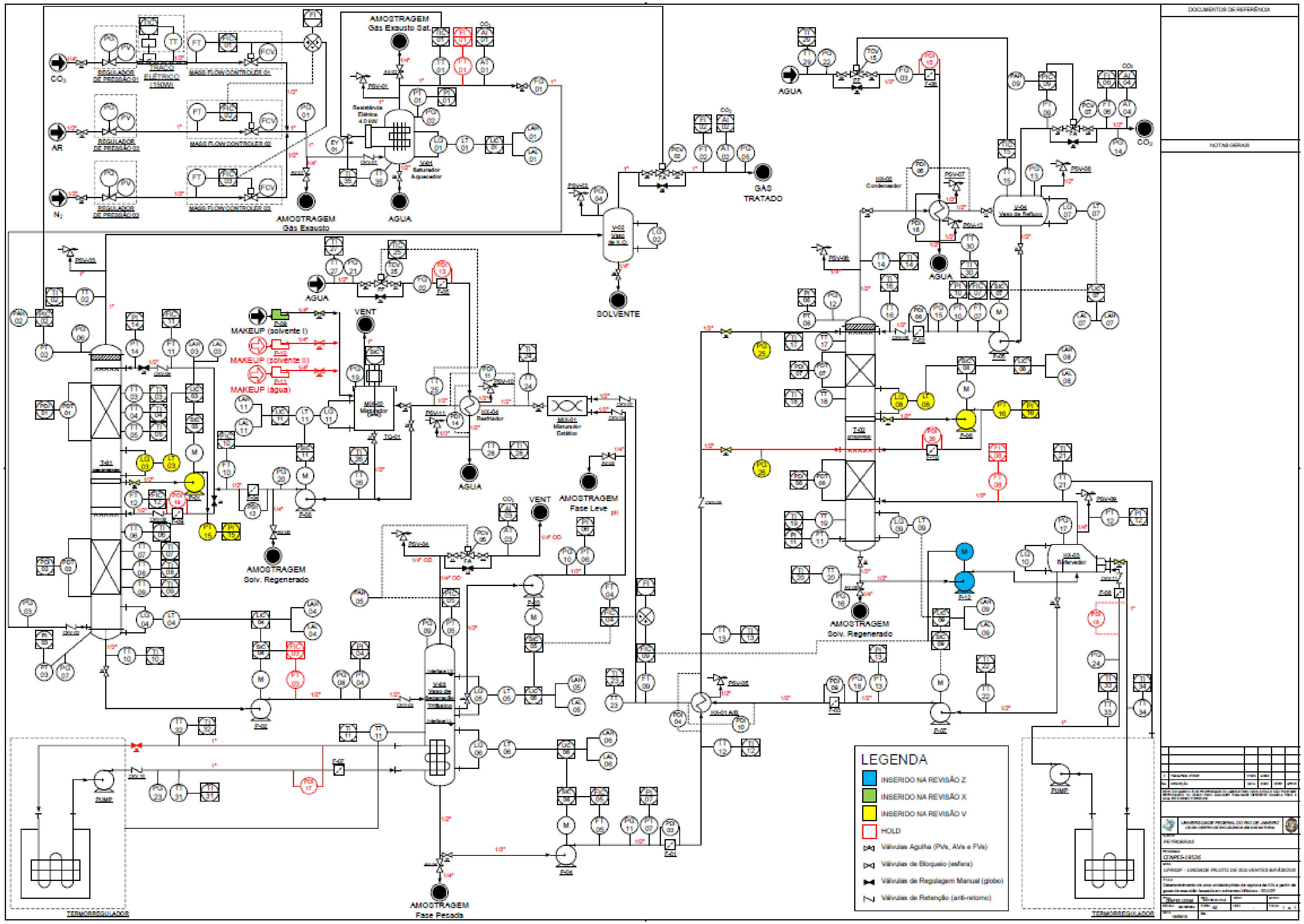

Figure 7.11. PCAPP P&ID

- **Synthetic Flue-Gas Production**

The synthetic flue-gas (SFG) is produced by mixing N_2, Air and CO_2. The SFG composition is manipulated using mass-flow controllers (MFCs 1 to 3, Fig 7.11). Before reaching the MFC, the pressure of each gas stream is broken by a pressure regulator. For safety reasons, the inlet gas pressures must be set to a maximum of 500 kPa. The dry SGF is sent to the heating and saturation vessel (V-01), where it could be bubbled in hot water if a more realistic flue-gas composition is desired. The SFG from V-01 proceed to the absorption column (T-01).

- **CO_2 Absorption**

The CO_2-rich SFG (SFG_{rich}) is fed at the bottom of the (T-01), where it passes through two sections of a 2.2m height packed beds, countercurrent to the lean solvent ($SOLV_{lean}$). CO_2 is selectively removed from the SFG_{rich} by chemical absorption, and the lean gas leaves the T-01 (SFG_{lean}). $SOLV_{lean}$ is fed at the top of each packed bed. A knock-out drum (V-02) is placed downstream of the T-01 top gas outlet. This vessel is designed to hold eventual entrained liquid. The minimum CO_2 capture efficiency of the T-01 must be 90% (weight basis). The T-01 is designed to operate between 50 and 200 kPag. This parameter is controlled by a pressure control valve (PCV-01), which acts adjusting the outlet flow of SFG_{lean}. The pump P-02 sends the CO_2-rich solvent to the liquid-liquid separation vessel (V-03).

- **Liquid Phases Split**

Most of the investigated solvents present spontaneous phase-split under absorption temperature after loaded in CO_2. However, some of them (TBS) need to be heated to 50ºC - 80ºC (depending on the PCAS) to start the liquid phase separation. Hence, the V-03 was provided with an internal heater. The heat is delivered by thermal fluid circulation guided by a process thermostat. Inside the V-03, total liquid-liquid phase split occurs, forming a CO_2-rich liquid phase ($SOLV_{richp}$) and a CO_2-lean liquid phase ($SOLV_{leanp}$). The $SOLV_{leanp}$ is sent back to the tank of solvent (TQ-01) by pump P-03. $SOLV_{richp}$ is pumped by P-04 to the top of the regeneration column (T-02). Before reaching the T-02, $SOLV_{richp}$ is pre-heated at the integration heat exchanger HX-01. Manipulation of V-03 pressure is possible and optionally releases CO_2. In this case, V-03 would work as a batch solvent regenerator.

- **Solvent Regeneration**

Pre-heated $SOLV_{richp}$ follows a downward path through the packed beds of T-02, in countercurrent with vapor coming from the reboiler (HX-03), when CO_2 is stripped from $SOLV_{richp}$. The CO_2-rich hot gas ($HOTGAS_{rich}$) leaves T-02 from the top and is couled to nearly 40ºC at the condenser (HX-02). From HX-02, the cooled stream is sent to the reflux drum (V-04) where the condensed liquid is separated from the saturated CO_2-rich gas ($SATGAS_{rich}$). The $SATGAS_{rich}$ passes through the CO_2 analyzer AI-04 and leaves the system. The condensate returns to the top of T-02, through pump P-05. HX-02 uses chilled water (5 ºC) as a cold utility.

The stripper temperature and pressure have a remarkable effect on energy consumption and solvent flow rate. The pressure of the T-02 is controlled between 150 - 400 kPa by PCV-02. The reboiler uses thermal fluid as a heat source to promote the partial vaporization of the solvent. For MEA-based solvents, the maximum reboiler pressure is ≅300 kPa. Higher pressures imply temperatures above 130ºC and consequent MEA degradation and heat-stable salts formation. The lean solvent ($SOLV_{lean}$) is pumped from the bottom of T-02 to the reboiler by P-12. This pump is necessary because of the low height of the liquid column between the T-02 bottom outlet nozzle and the reboiler inlet nozzle. This liquid column could not be enough to surpass the reboiler internal pressure flooding the tower.The hot lean solvent ($HOTSOLV_{lean}$) from the bottom of the reboiler is sent to the TQ-01 by pump P-07. Before reaching the tank, $HOTSOLV_{lean}$ is partially cooled at the HX-01 and is mixed with the $SOLV_{leanp}$, forming the lean solvent stream ($SOLV_{lean}$). $SOLV_{lean}$ is cooled to 40ºC at the HX-04 and finally returns to TQ-01. HX-04 uses chilled water as a cold utility. The regenerated solvent is recirculated to T-01 top by pump P-08.

The detailed procedure of designing the pilot plant is available in Appendix I.

7.3. References of Chapter 7

Aspentech. Aspen HYSYS. Disponível em: <https://www.aspentech.com/en/products/engineering/aspen-hysys>. Acesso em: 3 mar. 2020.

Barzagli, F., Mani, F., Peruzzini, M., 2017. Novel water-free biphasic absorbents for efficient CO2capture. Int. J. Greenh. Gas Control. https://doi.org/10.1016/j.ijggc.2017.03.010

Boot-Handford, M.E., Abanades, J.C., Anthony, E.J., Blunt, M.J., Brandani, S., Mac Dowell, N., Fernández, J.R., Ferrari, M.-C., Gross, R., Hallett, J.P., Haszeldine, R.S., Heptonstall, P., Lyngfelt, A., Makuch, Z., Mangano, E., Porter, R.T.J., Pourkashanian, M., Rochelle, G.T., Shah, N., Yao, J.G., Fennell, P.S., 2014. Carbon capture and storage update. Energy Environ. Sci. 7, 130–189. https://doi.org/10.1039/C3EE42350F

Bottoms, R.R., 1930. Process for separating acidic gases. US17883901A.

Budzianowski, W.M., 2016. Explorative analysis of advanced solvent processes for energy efficient carbon dioxide capture by gas–liquid absorption. Int. J. Greenh. Gas Control 49, 108–120. https://doi.org/10.1016/J.IJGGC.2016.02.028

Coulier, Y., Lowe, A.R., Coxam, J.-Y., Ballerat-Busserolles, K., 2017. Thermodynamic Modeling and Experimental Study of CO2 Dissolution in New Absorbents for Post-Combustion CO2 Capture Processes. ACS Sustain. Chem. Eng. acssuschemeng.7b03280. https://doi.org/10.1021/acssuschemeng.7b03280

Frailie, P.T., Madan, T., Sherman, B.J., Rochelle, G.T., 2013. Energy performance of advanced stripper configurations. Energy Procedia 37, 1696–1705. https://doi.org/10.1016/j.egypro.2013.06.045

Global CCS Institute, 2017. The Global Status of CCS: 2017. Melbourne, Australia.

Goto, K., Yogo, K., Higashii, T., 2013. A review of efficiency penalty in a coal-fired power plant with post-combustion CO2 capture. Appl. Energy 111, 710–720. https://doi.org/10.1016/J.APENERGY.2013.05.020

Huertas, J.I., Gomez, M.D., Giraldo, N., Garzón, J., 2015. CO2 Absorbing Capacity of MEA. J. Chem. 2015, 1–7. https://doi.org/10.1155/2015/965015

IEA, 2016. 20 Years of Carbon Capture and Storage - Accelerating Future Deployment. Paris, France.

IPCC, 2014. Climate Change 2014: Synthesis Report. Contribution of Working Groups I, II and III to the Fifth Assessment Report of the Intergovernmental Panel on Climate Change. Geneva, Switzerland.

Knudsen, J.N., Jensen, J.N., Vilhelmsen, P.J., Biede, O., 2009. Experience with CO2 capture from coal flue gas in pilot-scale: Testing of different amine solvents. Energy Procedia 1, 783–790. https://doi.org/10.1016/j.egypro.2009.01.104

Koch-Glitsch. KG-TOWER® Software. Disponível em: <https://koch-glitsch.com/kg-tower-software>. Acesso em: 2 mar. 2020.

Li, H., Haugen, G., Ditaranto, M., Berstad, D., Jordal, K., 2011. Impacts of exhaust gas recirculation (EGR) on the natural gas combined cycle integrated with chemical absorption CO2 capture technology. Energy Procedia 4, 1411–1418. https://doi.org/10.1016/j.egypro.2011.02.006

Liebenthal, U., Di D. Pinto, D., Monteiro, J.G.M.S., Svendsen, H.F., Kather, A., 2013. Overall process analysis and optimisation for CO2 Capture from coal fired power plants based on phase change solvents forming two liquid phases. Energy Procedia 37, 1844–1854. https://doi.org/10.1016/j.egypro.2013.06.064

Lu, Y., 2017. Development of a Novel Biphasic CO 2 Absorption Process with Multiple Stages of Liquid–Liquid Phase Separation for Post-Combustion Carbon Capture. DOE/NETL, Pittsburgh, PA.

Micropump. Pumps - Micropump. Disponível em: <http://www.micropump.com/product_list.aspx?ProductFamilyID=5>. Acesso em: 3 mar. 2020.

Miyamoto, O., Maas, C., Tsujiuchi, T., Inui, M., Hirata, T., Tanaka, H., Yonekawa, T., Kamijo, T., 2017. KM CDR ProcessTM Project Update and the New Novel Solvent Development. Energy Procedia 114, 5616–5623. https://doi.org/10.1016/J.EGYPRO.2017.03.1700

Park, T., Bae, J., Lee, C.J., Lee, J.M., 2016. A Sequential Method for Determining Optimal Stripper Pressure and Terminal Pressure in CO2Capture and Liquefaction Process Using MEA. IFAC-PapersOnLine 49, 657–662. https://doi.org/10.1016/j.ifacol.2016.07.250

Pinto, D.D.D., Knuutila, H., Fytianos, G., Haugen, G., Mejdell, T., Svendsen, H.F., 2014. CO2 post combustion capture with a phase change solvent. Pilot plant campaign. Int. J. Greenh. Gas Control 31, 153–164. https://doi.org/10.1016/j.ijggc.2014.10.007

Raynal, L., Briot, P., Dreillard, M., Broutin, P., Mangiaracina, A., Drioli, B.S., Politi, M., La Marca, C., Mertens, J., Thielens, M.L., Laborie, G., Normand, L., 2014. Evaluation of the DMX process for industrial pilot demonstration - methodology and results. Energy Procedia 63, 6298–6309. https://doi.org/10.1016/j.egypro.2014.11.662

Rezazadeh, F., Gale, W.F., Rochelle, G.T., Sachde, D., 2017. Effectiveness of absorber intercooling for CO2 absorption from natural gas fired flue gases using monoethanolamine solvent. Int. J. Greenh. Gas Control 58, 246–255. https://doi.org/10.1016/j.ijggc.2017.01.016

Rezazadeh, F., Gale, W.F., Sachde, D., Rochelle, G.T., 2014. Absorber intercooling configurations using aqueous piperazine for capture from sources with 4 to 27% CO2. Energy Procedia 63, 1637–1656. https://doi.org/10.1016/j.egypro.2014.11.174

Rochelle, G.T., 2009. Amine Scrubbing for CO2 Capture. Science (80-.). 325, 1652 LP – 1654.

Rubin, E.S., Chen, C., Rao, A.B., 2007. Cost and performance of fossil fuel power plants with CO2capture and storage. Energy Policy 35, 4444–4454. https://doi.org/10.1016/j.enpol.2007.03.009

Sigma-Aldrich, 2018. Order Preview.

Thong, D., Dave, N., Feron, P., Azzi, M., 2012. Process Modelling for Amine-based PostCombustion Capture Plant.

Ulrich, J., 2010. Flue Gas Analysis in Industry: Practical Guide for Emission and Process

Measurements, 2nd ed. TESTO. https://doi.org/0981.2773/hd/R/08.2004

Wang, L., An, S., Li, Q., Yu, S., Wu, S., 2017. Phase change behavior and kinetics of CO2absorption into DMBA/DEEA solution in a wetted-wall column. Chem. Eng. J. https://doi.org/10.1016/j.cej.2016.12.033

Wang, R., Liu, S., Wang, L., Li, Q., Zhang, S., Chen, B., Jiang, L., Zhang, Y., 2019. Superior energy-saving splitter in monoethanolamine-based biphasic solvents for CO2 capture from coal-fired flue gas. Appl. Energy 242, 302–310. https://doi.org/10.1016/J.APENERGY.2019.03.138

Wang, Z., Fang, M., Pan, Y., Yan, S., Luo, Z., 2013. Amine-based absorbents selection for CO2 membrane vacuum regeneration technology by combined absorption–desorption analysis. Chem. Eng. Sci. 93, 238–249. https://doi.org/10.1016/J.CES.2013.01.057

Zhang, J., Qiao, Y., Wang, W., Misch, R., Hussain, K., Agar, D.W., 2013. Development of an energy-efficient CO2 capture process using thermomorphic biphasic solvents. Energy Procedia 37, 1254–1261. https://doi.org/10.1016/j.egypro.2013.05.224

Zhang, S., Shen, Y., Shao, P., Chen, J., Wang, L., 2018. Kinetics, Thermodynamics, and Mechanism of a Novel Biphasic Solvent for CO 2 Capture from Flue Gas. Environ. Sci. Technol. 52, 3660–3668. https://doi.org/10.1021/acs.est.7b05936

Zhang, W., Jin, X., Tu, W., Ma, Q., Mao, M., Cui, C., 2017a. A Novel CO2 Phase Change Absorbent: MEA/1-propanol/H2O. Energy & Fuels acs.energyfuels.7b00090. https://doi.org/10.1021/acs.energyfuels.7b00090

Zhang, W., Jin, X., Tu, W., Ma, Q., Mao, M., Cui, C., 2017b. Development of MEA-based CO2 phase change absorbent. Appl. Energy 195, 316–323. https://doi.org/10.1016/j.apenergy.2017.03.050

Zhang, Y., Rochelle, G.T., 2014. Absorber Performance with High CO 2. Energy Procedia 63, 1329–1338. https://doi.org/10.1016/j.egypro.2014.11.142

Zhou, X., Liu, F., Lv, B., Zhou, Z., Jing, G., 2017. Evaluation of the novel biphasic solvents for CO2capture: Performance and mechanism. Int. J. Greenh. Gas Control. https://doi.org/10.1016/j.ijggc.2017.03.013

8. CONCLUSIONS AND SUGGESTIONS

The causal nexus of economic growth, energy consumption and ecological footprint is reviewed in this thesis. A challenging scenario of increasing energy demand constrained by global warming is presented. The persistence and high share of fossil sources in the global TPES for the next decades are also evidenced. Aiming to mitigate some environmental impacts of carbon-based power, this thesis identifies technological gaps within the fossil energy value chain. Four technologies, related to three research lines (R1, R2 and R3), are proposed and evaluated through technical, economic and/or environmental assessments.

In general, the technologies and alternative process designs developed in this thesis proved to be beneficial in at least one of the three considered dimensions (technical, economic or environmental). The technologies have the potential to be applied in full-scale and achieve commercial maturity. However, to reach this stage more R&D effort to scale-up and troubleshooting technical issues is necessary. The utilization of the proposed technologies would raise the competitiveness and support decision-making on some chains of the fossil energy production process. It makes clear that energy efficiency is a key point in future developments. However, the economic impacts of new technologies are the main barrier to its development, especially in developing and poor countries. Meet the triple bottom line of sustainability on the fossil-energy sector is a challenging task. The introduction of a carbon tax would be the way towards a sustainable future. The taxation would favor environmental-friendly technologies, like the ones proposed in this thesis.

More specific findings, contributions and answers to the questions that motivated the development of the present thesis are addressed below, separated by research line.

8.1. R1 - Offshore Processing of CO_2-Rich Natural Gas

R1.1. Deep Seawater Intake for Primary Cooling in Tropical Offshore Processing of Natural Gas with High Carbon Dioxide Content: Energy, Emissions and Economic Assessments

The use of DSW intake at 900 m of depth instead of conventional seawater intake as the primary cooling utility of a FPSO is investigated. The resulting variations of gas processing layout, electricity generation capacity, energy usage efficiency and CO_2 emissions were assessed.

The overall energy usage efficiency increase with DSW intake is in the range of 2.7% to 5.0%, depending on the gas processing flow. The highest value corresponds to full capacity. The CO_2 emissions had decreased in the same proportion, thanks to the reduced fuel gas consumption for power generation. The use of DSW promotes modest cost and weight savings when the entire FPSO is considered, but the results are more expressive considering only the gas processing plant and power generation units. Furthermore, DSW intake also leads to other indirect advantages like the elimination of the refrigeration cycle for HCDPA and 6% reduction of water content in the gas feed to dehydration TSA units for WDPA. The last could result in further cost and energy savings, not assessed in this investigation. The study reached its main goals, but some simplification was considered to limit the scope of the investigation. It was necessary because of the complexity and size of the FPSO flowsheet and the massive calculation workforce demanded to perform the necessary assessments. Some limitations of the cost estimation software, like equipment pressure and size, could lead to underestimated cost and weight.

As a recommendation for future work, a lifecycle cost evaluation of the DSW intake pipelines must be performed to determine the ultimate feasibility of the investigated technology. Additionally, the feasibility of DSW intake should be investigated within a continuous or mixed-integer non-linear optimization framework so that certain features that were assumed pre-defined and constant in this study could vary to seek optimum performance. For instance, the present analysis showed that certain FPSO units become problematic if cooled with cold CW at 7ºC. Therefore, a possible optimization formulation would consider two independent CW circuits, working at two temperature ranges – 35ºC-55ºC and 7ºC-27ºC – whose service heat loads, allocation points, exchanger/pump sizing and circulation flow rates are continuous or mixed-integer decision variables to be sought. In this case, it is conceivable to let the outlet temperature of DSW in the plate exchanger free, up to the regulated outlet limit of 40ºC. The DSW flow rate and the cost of intake piping, insulations and pumps would be minimized. Relaxing the exiting temperature of DSW seems a reasonable point to be questioned by optimizations as it has some thermodynamic support in the context of exergy analysis. The flow of wasted exergy could be reduced by returning a lower flow rate of hotter DSW to the sea at the expense of using larger plate heat exchangers in the process.

R1.2. Exergy, Energy and Emissions Analysis of Compressors Schemes in Offshore Rigs: CO_2-Rich Natural Gas Processing

An alternative process layout applied to the offshore processing of CO_2-Rich NG is developed and evaluated. MPSC (multiple paralleled smaller compressors) are proposed instead of conventional SSLC (single-shaft larger compressors with anti-surge recycles). SSLC-Case and MPSC-Case were compared in terms of exergy efficiency, FCI, footprint, CO_2 and energy intensities. This integrated holistic approach is unusual in conventional studies. Simulations revealed that oversized compressors with anti-surge recycle lead to almost constant power consumption along the field lifespan, even with a falling gas flow being processed. Consequently, fuel-gas and CO_2 intensities increase as gas-load decreases. It is shown that the efficiency of compressors is kept higher using VSD and smaller paralleled compressors. Moreover, eliminating anti-surge recycles the FPSO power demand becomes proportional to gas-load, reducing fuel-gas and CO_2 intensities.

Regarding the exergy analysis, two Reference Environmental Reservoirs are considered, RER-1 and RER-2. RER-1 inflates exergy flows with the high chemical exergy of hydrocarbons, producing too high exergy efficiencies for physical operations, e.g. compressors, exchangers and separators. Therefore, the exergy efficiencies for SSLC-Case and MPSC-Case are always ~99%, no matter the gas-load. RER-1 is considered useful for chemically reactive operations with high spontaneity, such as gas turbines and combustors in general. For such operations, RER-1 produces reliable exergy efficiencies. RER-2 deflates exergy flows by excluding the high chemical exergy of hydrocarbons, making the exergy assessments of physical operations and the overall gas plant meaningful. Exergy analyses corroborate the simulation achievements, unveiling that MPSC-Case entails a much lower FPSO exergy destruction rate. For FPSO gas-load ranging from 25% to 100%, the RER-2 exergy efficiency of SSLC-Case lies between 49% and 83%, whereas the MPSC-Case is always from 81% to 88%.

Besides being more exergy and energy-efficient, MPSC-Case leads to 3% of *FCI* savings, despite increasing only 4% the overall equipment weight. The lower power demand of MPSC-Case allowed removal of one GT in the FPSO, compensating the *FCI* and footprint increases of compressors and exchangers. In a carbon taxation scenario, MPSC-Case would be even more profitable.

Aiming to prove the technical feasibility potential of innovation of using MPSC, future work would address dynamic simulation of the compression systems. It would validate the proposed process design under several operation modes. The developed methodology of exergy analysis would also be applied to further evaluation of DSW intake. Additionally, the DSW intake and MPSC designs would be mixed and evaluated simultaneously.

8.2. R2 - Desulfurization Residues from Coal-Fired Power Plants

The environmental burden of SD-FGDR landfills is introduced. A treatment of SD-FGDR through dry-oxidation is proposed to make this residue useful. In Chapter 5 the impact of the treatment in the LCOE of a real PCC power plant facing decision-making process on SD-FGDR destination is assessed. A LCOE of 94.97 $/MWh is calculated for a conventional PCC, in agreement with reported values of similar power plants. The energy demanded by the novel SD-FGDR treatment unit is negligible due to the exothermal nature of the $CaSO_3$ oxidation reaction and the pre-heater of inlet air and solids. The air compressor power is only 0.04% of the net power plant output (340 MW). The LCOE is impacted by the investment, operation and maintenance costs of the SD-FGDR treatment unit and the residue revenue price. Disregarding the commercialization of residue the LCOE increases only 0.02%. If the residue is sold as a raw material for cement kiln, the LCOE decreases by ~3%, to 92.14 $/MWh. Therefore, the SD-FGDR revenue has a small beneficial impact on the LCOE, besides solving the landfill environmental issues and maintenance cost. In conclusion, this study demonstrates that it is technically and economically feasible to implement the dry-oxidation SD-FGDR treatment on the investigated PCC power plants and others with similar design.

In Chapter 6, an assessment of the environmental impacts of three different SD-FGDR management scenarios is performed for the same PCC power plant considered in Chapter 5. Heat and mass balances were calculated for each alternative. It is shown that the Base Case has a higher rate of potential environmental impacts due to the massive production of SD-FGDR. The Base Case is compared to the PCC operating with the treatment of the residue (CASE I) or the bypass of the SDA system (CASE II). CASE I and CASE II enable selling the SD-FGDR mixed with coal ashes as class C fly-ash. The SDA bypassing lead to higher SO_2 emissions and an increase of 1245% in the photochemical oxidation and acidification potentials. It is concluded that using de SD-FGDR treatment is a more environmental-friendly alternative.

Considering only the economic point of view, bypass the FGD is better, but this study proves that the environmental impacts related to SO_2 emissions increase dramatically and could be prohibitive in countries where environmental legislation is restrictive, like in Western Europe and the USA. CASE I is more sustainable because it solves SO_2 emissions while reducing other environmental impact categories. In the long term, depending on the ash and cement market, CASE I could become profitable, because of the revenue of fly-ash.

Future work must include updated data from pilot-plant runs and improvements on the ash composition analytical methodology. These data would enable a more accurate streams inventory. This inventory could serve as input for extended LCA. The use of low-grade heat coming from the power plant could favor the economic and environmental performance of a full-scale SD-FGDR treatment system. This effect must be investigated, and results included in future studies.

8.3. R3 - CO_2 Capture from Flue-Gases by Phase-Changing Absorption Solvents

The state-of-the-art in PCAS is investigated. Solvents were selected and preliminary tests performed to confirm phase-changing behavior, CO_2 loading and other relevant process parameters. One solvent was selected for further evaluation in a batch screening plant, named PCASP. The plant is designed to perform absorption and desorption tests using a synthetic exhaust gas. The test confirmed that the PCAS based on MEA and 1-propanol has the potential to reduce the energy penalty of CO_2 carbon capture by chemical absorption using conventional and affordable chemical components.

The next step is testing the best PCAS under different compositions and absorption conditions, simulating a more realistic flue-gas (higher temperature, pressure, presence of contaminants and lower CO_2 partial pressure). Desorption experiments also must be executed to confirm the cyclic capacity and support comparison with results reported by other authors.

A pilot plant is designed to operate in continuous mode. It will enable submit solvents to long run experiments. The pilot experiments will support a more precise estimation of the potential energy penalty, solvent loss and degradation rate, and other useful process parameters. Pilot data is necessary to validate process simulations and to scale-up the PCAS technology.

APPENDIX A. PUBLISHED PAPER OF CHAPTER 3 - JNGSE

CRUZ, M. DE A.; ARAÚJO, O. DE Q. F.; DE MEDEIROS, J. L. Deep seawater intake for primary cooling in tropical offshore processing of natural gas with high carbon dioxide content: Energy, emissions and economic assessments. **Journal of Natural Gas Science and Engineering**, v. 56, n. June, p. 193–211, 2018.

Journal of Natural Gas Science and Engineering 56 (2018) 193–211

Contents lists available at ScienceDirect

Journal of Natural Gas Science and Engineering

journal homepage: www.elsevier.com/locate/jngse

Deep seawater intake for primary cooling in tropical offshore processing of natural gas with high carbon dioxide content: Energy, emissions and economic assessments

Matheus de Andrade Cruz, Ofélia de Queiroz Fernandes Araújo, José Luiz de Medeiros*

Escola de Química, Federal University of Rio de Janeiro. Av. Athos da Silveira Ramos, 149. CT, E, Ilha do Fundão, Rio de Janeiro, RJ 21.941-972 Brazil

ARTICLE INFO

Keywords:
Deep seawater intake
Deepwater oil production
Offshore natural gas processing
FPSO
Gas compression
Energy usage efficiency

ABSTRACT

In deepwaters offshore oil-gas rigs, centrifugal compressor trains are major power consumers, requiring inter-coolers conventionally designed assuming surface seawater for primary cooling, limiting compressor inlet gas temperatures to 40 °C at tropical sites. On the other hand, at tropical deepwaters the available deep seawater at 4 °C can be exploited to reduce compression power – nearly proportional to inlet gas absolute temperature – entailing energy, economic and environmental benefits. This work considers a new primary cooling for deep-waters offshore platforms based on deep seawater (DSW) intake at 4 °C from depths around 900 m, reducing the outlet temperature of intercoolers to 12 °C. DSW intake alternative is assessed in terms of power consumption, CO_2 emissions and economy employing detailed equipment sizing and cost estimation. Depending on gas flow rate, it is shown that DSW intake lowers compressors power up to 9.2%, besides several indirect benefits: elimination of one CO_2 compressor; 30% less heat transfer areas; 4.5% less fuel gas consumption; 4% less gas turbines power; 9.5% (15 MMUS$) less investment; 14.4% (226 t) less topside weight, while making refrigeration unnecessary for dew point adjustment. DSW intake also entails 5% more efficient energy usage and 9327 tCO_2/y less emissions, boosting economic performance under carbon taxation.

1. Introduction

Since 2000, offshore fields respond for ≈30% of the world production of oil and natural gas (Rui et al., 2017). Due to still modest competitiveness of renewable energy sources, fossil sources will continue to play significant role in global energy matrix in the short to mid-term, especially natural gas (NG). However, oil price decline and new climate change mitigation policies – e.g. carbon taxation – have been a challenge to this industry. CO_2 emission taxation is already a reality in many countries, with Sweden imposing the highest tax of 140 US$/t (IEA, 2016). According to the International Association of Oil and Gas Producers (IOGP, 2016) main oil and gas companies emitted 280 Mt CO_{2Eq} of greenhouse gases (GHG) in 2015, of which 68% is related to fuel combustion for in-place energy production. Thus, energy usage efficiency and CO_2 emissions are becoming not solely an environmental, but also, an economic issue for oil and gas producers. As energy usage efficiency and CO_2 emissions are inversely interrelated concepts, using processing strategies with higher energy usage efficiency implies lowering CO_2 emissions, alleviating the environmental burden of oil and gas industries. In other words, there is no option to the carbon fossil industry but questing for better energy usage efficiency.

1.1. Offshore oil and gas processing: improving efficiency of energy usage

New developments on offshore oil and gas primary processing represent opportunities to, cumulatively, improve efficiency of energy usage, reduce GHG emissions, lower topsides footprint and, consequently, reduce costs. All these effects contribute to increase the economic and environmental feasibility of offshore oil and gas production. The literature presents several recent works on energy assessment and optimization of primary processing on offshore oil and gas rigs, comprising measures to improve energy usage efficiency (Nguyen et al., 2016a), better power generation schemes with organic cycles (Pierobon et al., 2013), air-bottoming cycles (Pierobon and Haglind, 2014), steam-bottoming cycles (Nguyen et al., 2014a), heat-exchanger network optimization for minimum energy consumption (Pierobon et al., 2013; Pierobon and Haglind, 2014; Nguyen et al., 2014a) and offshore power production via combined cycles (Rivera-Alvarez et al., 2015). To improve energy usage efficiency of the process as a whole, including carbon capture units such as post-combustion amine plants, Nguyen

* Corresponding author.
E-mail address: jlm@eq.ufrj.br (J.L. de Medeiros).

https://doi.org/10.1016/j.jngse.2018.06.011
Received 16 February 2018; Received in revised form 28 May 2018; Accepted 5 June 2018
1875-5100/

APPENDIX B. PAPER SUBMITED OF CHAPTER 4 – JNGSE

Title: Exergy, Energy and Emissions Analysis of Compressors Schemes in Offshore Rigs: CO2-Rich Natural Gas Processing

Authors: Matheus de Andrade Cruz, Ofélia de Q.F. Araújo*, José Luiz de Medeiros**

**Escola de Química, Federal University of Rio de Janeiro. Av. Athos da Silveira Ramos, 149. CT, Bl. E, Ilha do Fundão, Rio de Janeiro, RJ, Brazil. CEP: 21.941-972*

Manuscript Code: JNGSE-D-20-00340

Elsevier Editorial System(tm) for Journal of Natural Gas Science & Engineering
Manuscript Draft

Manuscript Number:

Title: Exergy Analysis of Compressor Schemes: Offshore Processing of Natural Gas with High Carbon Dioxide Content

Article Type: Full Length Article

Keywords: Offshore gas processing;
CO2-rich natural gas;
Centrifugal compressors;
Anti-surge recycle;
Exergy analysis;
CO2 emissions

Corresponding Author: Professor José Luiz Luiz de Medeiros, DSc

Corresponding Author's Institution: Federal University of Rio de Janeiro

First Author: Matheus A Cruz, MSc

Order of Authors: Matheus A Cruz, MSc; Ofélia Q Araújo, PhD; José Luiz Luiz de Medeiros, DSc

Abstract: Deepwater oil and associated gas productions resort to floating rigs operating at continuously decreasing gas-loads during the last three quarters of the field campaign. As centrifugal compressors are sized at maximum loads, anti-surge recycles are used making operation inefficient in terms of power consumption and emissions per oil barrel produced. Smaller paralleled compressors and variable-speed drivers are investigated at peak and partial gas-loads and compared to traditional anti-surge recycle designs in terms of exergy efficiency, investment, footprint and emissions. Oversized compressors with anti-surge recycles result in almost constant power consumption along process lifespan, regardless the gas-load, increasing fuel and CO2 intensities as gas-load decreases and attaining exergy efficiencies of 49% and 83% at 25% and 100% gas-loads, respectively. On the other hand, with variable-speed drivers and smaller paralleled compressors, power consumption becomes proportional to gas-load with exergy efficiencies always between 80% and 88%, and attaining 11% and 39% less power consumptions at 100% and 25% gas-loads. Moreover, CO2 intensity and investment are, respectively 34% and 3% less than in traditional layouts with oversized compressors. These savings resulted from eliminating a gas turbine thanks to lower power demand when no anti-surge recycles are used.

Research Data Related to this Submission

There are no linked research data sets for this submission. The following reason is given:
Data will be made available on request

APPENDIX C. PUBLISHED PAPER OF CHAPTER 5 – JCLEPRO

CRUZ, M. DE A. et al. Impact of solid waste treatment from spray dryer absorber on the levelized cost of energy of a coal-fired power plant. **Journal of Cleaner Production**, v. 164, 2017a.

Journal of Cleaner Production 164 (2017) 1623–1634

Contents lists available at ScienceDirect

Journal of Cleaner Production

journal homepage: www.elsevier.com/locate/jclepro

Impact of solid waste treatment from spray dryer absorber on the levelized cost of energy of a coal-fired power plant

Matheus de Andrade Cruz [a, *], Ofélia de Queiroz Fernandes Araújo [a], José Luiz de Medeiros [a], Rui de Paula Vieira de Castro [a], Gabriel Travagini Ribeiro [b], Vanessa Reich de Oliveira [c]

[a] Federal University of Rio de Janeiro, Rio de Janeiro, Brazil
[b] Energia Pecém – EDP, São Gonçalo do Amarante, Ceará, Brazil
[c] ENEVA S.A., Rio de Janeiro, Brazil

ARTICLE INFO

Article history:
Received 26 January 2017
Received in revised form
16 May 2017
Accepted 8 July 2017
Available online 12 July 2017

Handling Editor: Yutao Wang

Keywords:
Coal-fired power plant
Flue gas desulfurization
Spray dryer absorbers
Solid waste treatment
Calcium sulphite oxidation
Levelized cost of energy

ABSTRACT

Coal-fired power plants with semi-dry flue gas desulfurization (semi-dry FGD) system produce daily tones of ashes contaminated with calcium sulphite. To turn this solid waste useful (e.g. to the cement industry) and avoid landfill disposal, the present study suggests a semi-dry FGD solid waste treatment unit, that promotes the dry oxidation of calcium sulfite to calcium sulfate. Sizing of main equipment using pilot-plant and patents data allows economic evaluation of capital expenditure, operational and maintenance costs, and sale of the treated residue, which permits estimation of levelized cost of energy to assess the impact of the technology on the electricity price of a power plant using the proposed solid waste treatment unit. As base case, a Brazilian coal-fired power plant facing decision making process on semi-dry FGD waste destination is selected. Results demonstrate that the semi-dry FGD, without the solid treatment unit, has total levelized cost of energy increased in 0.56% (from 94.44 to 94.97 \$/MWh) resulting from solids waste disposal. If the treated semi-dry FGD waste was transferred (at zero revenue) as additive to a cement industry, the levelized cost of energy of the power plant would remain approximately unchanged. This is because the increase of 0.51\$/MWh resulting from the investment and operation and maintenance cost of the treatment unit is compensated by the decrease of 0.53\$/MWh, in virtue of the avoided waste disposal costs. However, if the commercialization as raw material of the treated semi-dry FGD waste is considered, a reduction of 2.83 \$/MWh (~3%) on the levelized cost of energy (to 92.14 \$/MWh) would occur. In both cases, the proposed treatment unit shows small impact on the total power plant levelized cost of energy, besides solving the solid management problems of landfill saturation, land use and costs related to landfill maintenance. Thus, it is adequate to implement the semi-dry FGD waste treatment unit on the power plant in question. The conclusion can be extended to plants with similar design and economic parameters.

1. Introduction

The Brazilian electricity matrix is dominated by hydropower generation. However, because of the recent water scarcity crisis in Brazil, hydroelectricity has been supplemented with electrical power generated by thermal power plants, resulting in 18% increase during 2013–2014 and presently represents 28.2% of the total Brazilian electricity sources. In this same period, electricity produced by coal power plants has increased 24.2%, with mineral coal representing 9.6% of the thermopower sources in Brazil (EPE, 2015a). The Brazilian energy demand will increase in an average of 3.6% yearly until 2019, thus it is expected that the use of coal-fired power plants will continue to increase in short to medium term (EPE, 2015b). Furthermore, an average power plant technical lifetime of about 40 years for coal compared to 34 years for gas and 34 years for oil-fired power plants is estimated (Farfen and Breyer, 2017), indicating that the next decade will sustain supply of fossil energy accompanied by growing environmental legislation and

* Corresponding author.
E-mail addresses: mcruz@poli.ufrj.br (M.A. Cruz), ofelia@eq.ufrj.br (O.Q.F. Araújo), jlm@eq.ufrj.br (J.L. de Medeiros), rui@eq.ufrj.br (R.P.V. de Castro), gabriel.travagini@edpenergiapecem.com.br (G.T. Ribeiro), vanessa.oliveira@eneva.com.br (V.R. de Oliveira).

http://dx.doi.org/10.1016/j.jclepro.2017.07.061
0959-6526/© 2017 Elsevier Ltd. All rights reserved.

APPENDIX D – PUBLISHED PAPER OF CHAPTER 6 - JSDEWES

CRUZ, M. D. A. et al. Environmental Performance of a Solid Waste Monetization Process Applied to a Coal-Fired Power Plant with Semi-Dry Flue Gas Desulfurization. **Journal of Sustainable Development of Energy, Water and Environment Systems**, v. 7, n. 3, p. 506–520, 2018.

Journal of Sustainable Development of Energy, Water and Environment Systems

http://www.sdewes.org/jsdewes

Year 2019, Volume 7, Issue 3, pp 506-520

Environmental Performance of a Solid Waste Monetization Process Applied to a Coal-Fired Power Plant with Semi-Dry Flue Gas Desulfurization

Matheus de Andrade Cruz[*1], *Rui de Paula Vieira de Castro*[2], *Ofélia de Queiroz Fernandes Araújo*[3], *José Luiz de Medeiros*[4]

[1]School of Chemistry, Federal University of Rio de Janeiro, Athos da Silveira Ramos Ave. 149, Block E, Ilha do Fundão, Rio de Janeiro, Brazil
e-mail: mcruz@poli.ufrj.br

[2]School of Chemistry, Federal University of Rio de Janeiro, Athos da Silveira Ramos Ave. 149, Block E, Ilha do Fundão, Rio de Janeiro, Brazil
e-mail: rui@eq.ufrj.br

[3]School of Chemistry, Federal University of Rio de Janeiro, Athos da Silveira Ramos Ave. 149, Block E, Ilha do Fundão, Rio de Janeiro, Brazil
e-mail: ofelia@eq.ufrj.br

[4]School of Chemistry, Federal University of Rio de Janeiro, Athos da Silveira Ramos Ave. 149, Block E, Ilha do Fundão, Rio de Janeiro, Brazil
e-mail: jlm@eq.ufrj.br

Cite as: de Andrade Cruz, M., de Castro, R. de P. V, Araújo, O. de Q. F., de Medeiros, J. L., Environmental Performance of a Solid Waste Monetization Process Applied to a Coal-Fired Power Plant with Semi-Dry Flue Gas Desulfurization, J. sustain. dev. energy water environ. syst., 7(3), pp 506-520, 2019,
DOI: https://doi.org/10.13044/j.sdewes.d6.0251

ABSTRACT

Mixing of semi-dry flue gas desulfurization solids and fly-ash from coal-fired power plants results in a solid waste contaminated by calcium sulfite. Therefore, it becomes useless for industry and is often landfilled. To support decision-making on process configurations to monetize this solid residue a gate-to-gate life cycle assessment was performed, considering three scenarios: BASE case – standard 360 MW power plant, CASE I – base plant adopting dry thermal oxidation treatment of spray dryer solids, CASE II – bypass of desulfurization system. Cases I and II allow commercialization of the solid residue as class C fly-ash. Evaluated alternatives were compared based on quantitative potential environmental impacts, using United States Environmental Protection Agency waste reduction algorithm. Based on the results, the BASE case was more aggressive to the environment, due to solid waste production. CASE II increased photochemical oxidation and acidification potentials. CASE I was the more environmentally friendly but demands additional capital and operational expenditure.

KEYWORDS

Calcium sulfite dry oxidation, Coal fired power plant, Life cycle assessment, Semi-dry flue gas desulfurization, Solid waste treatment, Spray dryer absorbers.

* Corresponding author

APPENDIX E – CONFERENCE PAPER – SDEWES 2019

Cruz, M. de A. et al. (2019) **SDEWES2019.0276 Chemical Absorption of CO2 from Flue Gases: Experiments with Phase Changing Solvents in a Bench Scale Plant**, 14th Conference on Sustainable Development of Energy, Water and Environment Systems. Edited by A. Mudrovčić and M. Ban. Zagreb: Faculty of Mechanical Engineering and Naval Architecture. Available at: https://www.dubrovnik2019.sdewes.org/.

SDEWES2019.0276

Post-Combustion Carbon Capture: Investigation of Chemical Absorption with Phase-Changing Solvents in a Bench-Scale Plant Operating in Batch Mode

M.D.A. Cruz*[1], A.P. Musse[1], J. Luiz De Medeiros[2], O. Araujo[1]

[1]Federal University of Rio de Janeiro, Brazil; [2]Federal University of Rio de Janeiro, Escola de Química, Brazil (*mcruz@poli.ufrj.br)

Abstract

The energy penalty of solvent regeneration is a barrier for the deployment of chemical absorption post-combustion carbon capture. Phase-changing absorption solvents have been proposed to overcome this issue. CO_2 absorption triggers phase separation with only the CO_2-rich phase requiring regeneration, potentially reducing energy demand. A systematic review supports the choice of a set of solvents for experimental investigation, based on economic, process and energy-related criteria. Until now the selected absorbents were only investigated in laboratory scale. They need to move from lab to industrial scale to contribute to the global warming mitigation. Three selected biphasic solvents are selected and tested, to confirm the results reported by its developers. Solvent A, based on monoethanolamine/1-propanol, was considered the more suitable one. This blend presented 26% of reduction on the lower (CO_2-rich) liquid phase, compared to the initial volume of fresh solvent. monoethanolamine is the more traditional chemical absorbent for CO_2 capture applications and both components can be considered standard chemicals (low-cost), which is a remarkable advantage. The viscosity of the CO_2-rich phase of solvent A is 10 mPa.s at 25ºC, which is considered low compared to other candidates. Solvent B, based on diethylene-triamine and N,N,N',N",N"-pentamethyldiethylenetriamine, was disregarded for further evaluations. It presented only 10% of volume reduction on CO_2 rich phase and prohibitively high viscosity (360 mPa.s at 40ºC). Furthermore, chemical components of this solvent are considered specialty (high cost). Solvent C, based on N-methylcyclohexylamine and N,N-dimethylcyclohexylamine, was also disregarded for further tests. Although the costs of its chemical components are in the same range of monoethanolamine and the CO_2-rich liquid phase presents an acceptable viscosity (58 mPa.s at 25ºC), this blend had an issue. It presented solids precipitation on the CO_2 rich phase, what is a potential source of operational problems on industrial application. Solvent A was the only one tested on a bench scale screening plant, designed for absorption and desorption of chemical absorption solvents. This blend presented a CO_2 loading of 2.8 mol/kg on the lower phase, 76% higher than MEA 30%. It is an opportunity to reduce the energy penalty of carbon capture of CO_2 by chemical absorption. The solvent A was selected to further evaluation on a continuous mode pilot-plant (under construction). Based on thermodynamic process simulation, the use of the solvent A in replacement of MEA 30% could result in a decrease of 7.9% on the regeneration energy penalty.

APPENDIX F – PUBLISHED PAPER - ECM

DE CASTRO, R. DE P. V. et al. Fluidized bed treatment of residues of semi-dry flue gas desulfurization units of coal-fired power plants for conversion of sulfites to sulfates. **Energy Conversion and Management**, v. 143, 2017.

Energy Conversion and Management 143 (2017) 173–187

Contents lists available at ScienceDirect

Energy Conversion and Management

journal homepage: www.elsevier.com/locate/enconman

Fluidized bed treatment of residues of semi-dry flue gas desulfurization units of coal-fired power plants for conversion of sulfites to sulfates

Rui de Paula V. de Castro [a], José Luiz de Medeiros [a], Ofélia de Queiroz Fernandes Araújo [a,*], Matheus de Andrade Cruz [b], Gabriel Travagini Ribeiro [c], Vanessa Reich de Oliveira [c]

[a] Escola de Química, Federal University of Rio de Janeiro, Rio de Janeiro, Brazil
[b] PEA, Escola Politécnica, Federal University of Rio de Janeiro, Rio de Janeiro, Brazil
[c] ENEVA S.A., Rio de Janeiro, Brazil

ARTICLE INFO

Article history:
Received 16 December 2016
Received in revised form 25 March 2017
Accepted 27 March 2017
Available online 7 April 2017

Keywords:
Calcium sulfite
Coal power plant
Fluidized bed reactor
Response surface methodology
Semi-dry FGD residues

ABSTRACT

Coal-fired power plants with semi-dry flue gas desulfurization produce several metric tons per day of residues with 10–18%w/w of hemi-hydrated calcium sulfite. The rest of the 90–80%w/w of such residues contains silica, aluminium-silicates and calcium/magnesium carbonates, sulfates and hydroxides. This material could be added to cement, but sulfites degrade the cement quality and lead to costs of landfill disposal. To test upgrading desulfurization residues to turn it into an acceptable cement feedstock, a pilot plant was built to oxidize residues with hot air converting sulfites to sulfates. This pilot comprehends a fluidized bed reactor, an air heater, a cyclone and a heat recovery exchanger. Its operation showed that residues react favorably under fluidization. The effect of independent variables, residence time and temperature, was investigated and sulfite conversions up to 89.4% were observed. With statistical treatment of pilot experimental data, response surface of conversion of sulfites to sulfates was developed, allowing to estimate the effect of independent coordinates on conversion and the optimal oxidation conditions. Experimental data and model predictions showed agreement leading to low estimated variance.

1. Introduction

Coal-fired power plants play a vital role in electricity generation worldwide. According to World Coal Association, coal-fired power plants currently are responsible by 41% of global electricity production and the global coal demand is projected to increase 15% until 2040, mainly due to the growing energy demand of Asian economies such as China and India [1]. New plant efficiencies, tight emissions controls and cleaner technologies are expected to comply with this increasing demand of coal energy via-à-vis the increasing climate concerns.

The primary flue gas (FG) of a typical 360 MW coal-fired power plant comprehends impressive flow rates of problematic gases, e.g. ≈452 t/h of carbon dioxide (CO_2) and ≈4.2 t/h of sulfur dioxide (SO_2). In order to abate the atmospheric emissions of SO_2 the flue gas (FG) is treated in the operation known as Flue Gas Desulphurization (FGD), which is located just prior the liberation of FG into the atmosphere.

1.1. FGD systems of coal-fired power plants

There are a few FGD technologies for coal-fired power plants. An important aspect in connection with FGD systems in such plants is the presence of very fine fly-ash, which can be deposited with the solid FGD residues. FGD systems of coal-fired plants are generally classified as Dry or Semi-Dry FGD and Wet FGD.

In Wet FGD the FG at the dew point is contacted in large vessels with a fine-grain aqueous slurry of grinded limestone containing calcium carbonate ($CaCO_3$) and magnesium carbonate ($MgCO_3$) with air injected in the bottom. In the Wet FGD SO_2 is the only component of FG which reacts with the slurry of limestone via Eqs. (1a)–(1d) producing basically a slurry of hydrated calcium sulfate or gypsum ($CaSO_4{\cdot}2H_2O$), magnesium sulfate ($MgSO_4{\cdot}6H_2O$), calcium sulfite ($CaSO_3{\cdot}0.5H_2O$), magnesium sulfite ($MgSO_3{\cdot}6H_2O$) and CO_2 gas. As the weight ratio sulfates:sulfites is ≈5 (w/w), an important economic factor of Wet FGD is the exportation of gypsum as a masonry feedstock. For the 360 MW coal power plant, the flow rate of 4.2 t/h of SO_2 in the FG will entail a production of ≈9 t/h of gypsum + sulfites or ≈28 t/h of solids (gypsum + sulfites + fly-ashes + limestone) with a consumption of ≈7 t/h of limestone and ≈39 t/h of water.

* Corresponding author.
E-mail address: ofelia@eq.ufrj.br (O.d.Q F. Araújo).

http://dx.doi.org/10.1016/j.enconman.2017.03.078
0196-8904/

APPENDIX G – PUBLISHED PAPER – Petróleo & Gás

CRUZ, M. DE A. et al. Estudo de mercados de GNL, GLP, propano e butano liquefeitos, visando aproveitamento comercial do gás natural do pré-sal. **Revista Petróleo & Gás**, v. 369, p. 16–22, 2017b.

Artigo Técnico

Estudo dos mercados de GNL, GLP, propano e butano liquefeitos, visando aproveitamento comercial do gás natural do Pré-sal

Matheus de Andrade Cruz
PRH-41 (PEA), UFRJ

Dárley Carrijo de Melo
Cenpes, Petrobras

José Luiz de Medeiros; Ofélia de Q. F. Araújo
Escola de Química, Universidade Federal do Rio de Janeiro

Resumo

Investimentos de grande soma têm sido feitos no polo Pré-sal da Bacia de Santos, visando o desenvolvimento dos seus campos e aumento da produção de óleo. Com isso, há expectativa de que a produção de gás natural (GN) dobre até 2030. Esse GN pode ser reinjetado, com o objetivo de aumentar a recuperação de óleo dos campos, ou escoado para terra, por gasodutos. Essa última alternativa depende da expansão da malha de gasodutos, ou seja, mais investimento, mas abriria oportunidades para redução do déficit nacional do mercado de GNL e exploração dos mercados mundiais de C_3, C_4 e GLP, contribuindo para o desenvolvendo da economia brasileira. O principal objetivo do estudo é fornecer subsídios para definir-se a melhor estratégia de utilização do GN produzido no Pré-sal. São estudadas as cadeias produtivas desses produtos e apresentadas unidades de processamento e seus custos típicos. A seguir é apresentado o mercado nacional e internacional de GNL, GLP, C_3 e C_4. O comércio exterior brasileiro foi estudado através das ferramentas Radar Comercial e Alice Web. Evidenciaram-se a complexidade e o dinamismo do mercado de GNL, C_3, C_4 e GLP. A análise dos dados de comércio exterior indica que o mercado de GNL é muito maior (em volume e valores, a nível nacional e internacional) que o de GLP, C_3 e C_4 e que os maiores consumidores desses produtos pertencem à região Ásia-Pacífico, com destaque para o Japão, Coréia e China. O Radar Comercial indica que a prioridade deve ser dada a projetos de de C_3 e C_4. Projetos de GLP não seriam tão oportunos para o Brasil. Com isso, investir em URLs e UFLs pode ser mais interessante do que em UPGNs..Além disso, haveria maior disponibilização de gás natural no Brasil, reduzindo o déficit da balança comercial de GNL, hoje importado para complementar o suprimento de gás natural ao mercado nacional.

1. Introdução

A partir do gás natural (GN) bruto são obtidos diversos produtos, tais como: o Gás Natural Especificado, Gás Natural liquefeito (GNL), Gás Liquefeito de Petróleo (GLP), Propano Liquefeito (C_3), Butano Liquefeito (C_4) e Gasolina Natural (C_{5+}). Como será mostrado, o Brasil sempre foi importador destes produtos.

A figura 1 mostra que a oferta doméstica de GN, a partir dos campos da Petrobras e de seus parceiros, deve mais que dobrar até 2030, refletindo os investimentos que têm sido feitos para aumentar a produção e o escoamento do GN produzido no polo Pré-sal. Tal previsão assume a premissa de escoamento do GN, dos campos *offshore* para terra. Inicialmente são previstas três rotas, com capacidade total de 40,8 MM Sm³/d, como ilustrado pela figura 2. Porém, há campos do Pré-sal com previsão de gerar até 100 MM Sm³/d de GN no pico da produção, o que demonstra a necessidade de mais gasodutos de exportação.

Figura 1. Oferta de GN da Petrobras 2013-2030.
Fonte: Petrobras

APPENDIX H – SUPPLEMENTARY MATERIALS

SUPPLEMENTARY MATERIALS A

CRUZ, M. DE A.; ARAÚJO, O. DE Q. F.; DE MEDEIROS, J. L. Deep seawater intake for primary cooling in tropical offshore processing of natural gas with high carbon dioxide content: Energy, emissions and economic assessments. **Journal of Natural Gas Science and Engineering**, v. 56, n. June, p. 193–211, 2018.

Supplement A1. Simulation Methodology

Supplement A2. Equipment Sizing

Supplement A3. Cost and Weight Estimation

Supplement A4. Simulation, Sizing and CAPEX Results

References of Supplementary Materials A

Supplement A1 – Simulation Methodology

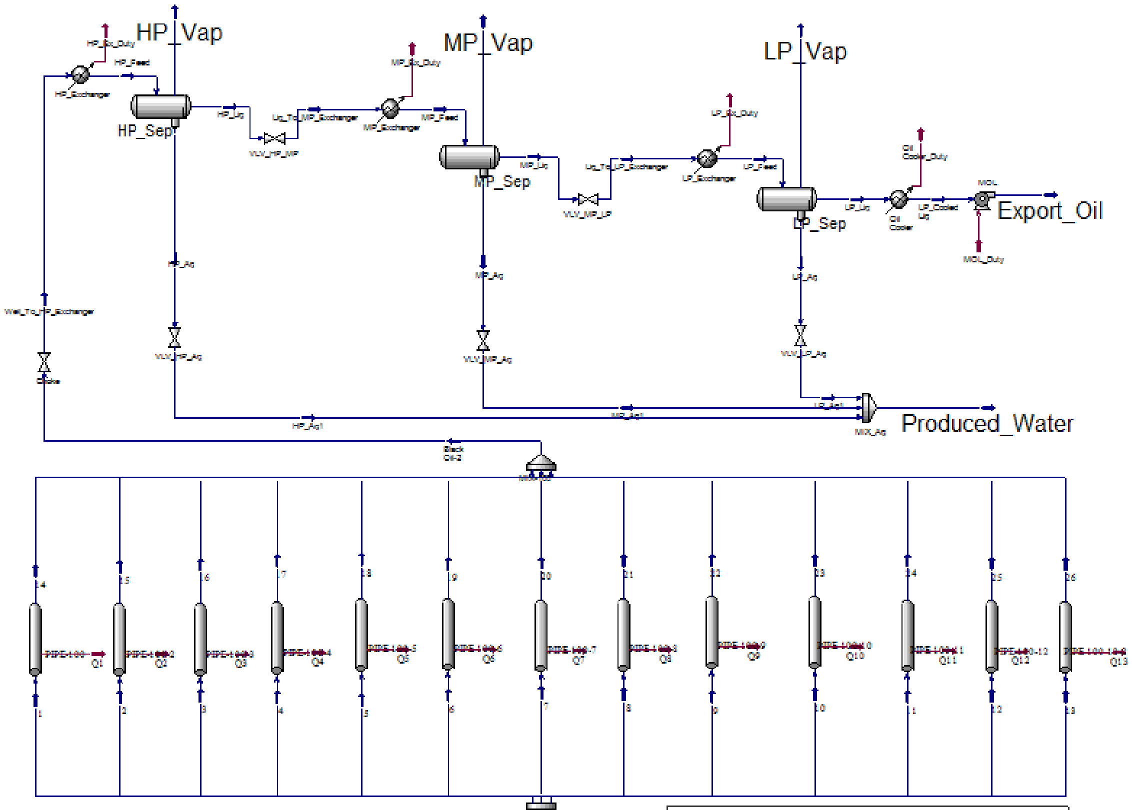

SPRDSHT-1		
B1: 1st Stage Std Gas Flow	4566682	Nm3/d(gas)
B2: 2nd Stage Std Gas Flow	116041	Nm3/d(gas)
B3: 3rd Stage Std Gas Flow	67461,1	Nm3/d(gas)
B4: Total Gas Flow	4750184	Nm3/d(gas)
B5: Std Liq Vol Flow Spec	111462	barrel/day
B6: Std Ideal Liq Vol Flow	2906	barrel/day
B8:Flow/Riser (actual m³/d)	2260	

Figure A1.1. Oil Plant Simulation Flowsheet

BASE CASE

```
SEQ          DESCRIPTION
----  ----------------------------------------
        BEGIN CONTROL LOOP FOR 'SVC-101'      <--+
  1   HX 'SHX-101'                               |
  2   CONTROLLER 'SVC-101'                       |
        END CONTROL LOOP FOR 'SVC-101'        -->+
        BEGIN RECYCLE LOOP 'LOOP1'            <-----+
  3   FLASH 'F-101'                                 |
  4   VALVE 'V-101'                                 |
  5   COMPRESSOR 'C-101'                            |
        BEGIN CONTROL LOOP FOR 'SVC-102'      <--+  |
  6   HX 'SHX-102'                               |  |
  7   CONTROLLER 'SVC-102'                       |  |
        END CONTROL LOOP FOR 'SVC-102'        -->+  |
  8   SPLITTER 'SPL-101'                            |
  9   VALVE 'V-102'                                 |
 10   FLASH 'F-301'                                 |
 11   VALVE 'V-301'                                 |
 12   STRM CALC 'MSD-301'                           |
 13   HX 'SHX-301'                                  |
 14   HX 'SHX-302'                                  |
        BEGIN CONTROL LOOP FOR 'SVC-901'      <--+  |
 15   HX 'SHX-303'                               |  |
 16   CONTROLLER 'SVC-901'                       |  |
        END CONTROL LOOP FOR 'SVC-901'        -->+  |
 17   HX 'SHX-901'                                  |
 18   FLASH 'F-901'                                 |
 19   COMPRESSOR 'C-901'                            |
 20   SPLITTER 'SPL-901'                            |
 21   VALVE 'V-902'                                 |
        BEGIN CONTROL LOOP FOR 'SVC-902'      <--+  |
 22   HX 'SHX-902'                               |  |
 23   VALVE 'V-901'                              |  |
 24   CONTROLLER 'SVC-902'                       |  |
        END CONTROL LOOP FOR 'SVC-902'        -->+  |
 25   FLASH 'F-302'                                 |
 26   VALVE 'V-302'                                 |
 27   MIXER 'MIX-301'                               |
 28   FLASH 'F-201'                                 |
 29   COMPRESSOR 'C-201'                            |
        BEGIN CONTROL LOOP FOR 'SVC-201'      <--+  |
 30   HX 'SHX-201'                               |  |
 31   CONTROLLER 'SVC-201'                       |  |
        END CONTROL LOOP FOR 'SVC-201'        -->+  |
 32   SPLITTER 'SPL-201'                            |
 33   VALVE 'V-201'                                 |
 34   COMPRESSOR 'C-202'                            |
        BEGIN CONTROL LOOP FOR 'SVC-202'      <--+  |
 35   HX 'SHX-202'                               |  |
 36   CONTROLLER 'SVC-202'                       |  |
        END CONTROL LOOP FOR 'SVC-202'        -->+  |
 37   SPLITTER 'SPL-202'                            |
 38   VALVE 'V-202'                                 |
 39   FLASH 'F-202'                                 |
        END RECYCLE LOOP 'LOOP1'              ----->+
        BEGIN MVC LOOP FOR 'MVC-401'          <--+
 40   HX 'SHX-401'                               |
 41   STRM CALC 'MEM-401'                        |
 42   FLASH 'F-002'                              |
 43   MVC 'MVC-401'                              |
        END MVC LOOP FOR 'MVC-401'            -->+
        BEGIN MVC LOOP FOR 'MVC-1001A'        <-----+
 44   SPLITTER 'SPL-401'                            |
 45   FLASH 'F-003'                                 |
 46   VALVE 'V-1001'                                |
 47   SPLITTER 'SPL-1001'                           |
 48   VALVE 'V-1002A'                               |
 49   COMPRESSOR 'C-1001A'                          |
 50   CONV REAC 'R-1001A'                           |
        BEGIN RECYCLE LOOP 'LOOP2'            <--+  |
 51   EXPANDER 'T-1001A'                         |  |
 52   SPLITTER 'SPL-1002A'                       |  |
 53   HX 'SHX-1001A'                             |  |
        END RECYCLE LOOP 'LOOP2'              -->+  |
 54   MVC 'MVC-1001A'                               |
        END MVC LOOP FOR 'MVC-1001A'          ----->+
        BEGIN RECYCLE LOOP 'LOOP3'            <-----+
 55   FLASH 'F-501'                                 |
 56   COMPRESSOR 'C-501'                            |
        BEGIN CONTROL LOOP FOR 'SVC-501'      <--+  |
 57   HX 'SHX-501'                               |  |
 58   CONTROLLER 'SVC-501'                       |  |
        END CONTROL LOOP FOR 'SVC-501'        -->+  |
 59   SPLITTER 'SPL-501'                            |
 60   VALVE 'V-501'                                 |
        END RECYCLE LOOP 'LOOP3'              ----->+
```

DSW CASE

```
SEQ          DESCRIPTION
----  ----------------------------------------
        BEGIN CONTROL LOOP FOR 'SVC-101'      <--+
  1   HX 'SHX-101'                               |
  2   CONTROLLER 'SVC-101'                       |
        END CONTROL LOOP FOR 'SVC-101'        -->+
        BEGIN RECYCLE LOOP 'LOOP2'            <--------+
  3   FLASH 'F-101'                                    |
  4   VALVE 'V-101'                                    |
  5   COMPRESSOR 'C-101'                               |
  6   SPLITTER 'SPL-101'                               |
  7   HX 'SHX-102'                                     |
        BEGIN CONTROL LOOP FOR 'SVC-102'      <--+     |
  8   HX 'SHX-103'                               |     |
  9   CONTROLLER 'SVC-102'                       |     |
        END CONTROL LOOP FOR 'SVC-102'        -->+     |
 10   SPLITTER 'SPL-102'                               |
 11   MIXER 'MIX-101'                                  |
 12   VALVE 'V-102'                                    |
 13   FLASH 'F-301'                                    |
 14   VALVE 'V-301'                                    |
 15   STRM CALC 'MSD-301'                              |
 16   HX 'SHX-301'                                     |
        BEGIN CONTROL LOOP FOR 'SVC-301'      <--+     |
 17   HX 'SHX-302'                               |     |
 18   CONTROLLER 'SVC-301'                       |     |
        END CONTROL LOOP FOR 'SVC-301'        -->+     |
 19   FLASH 'F-302'                                    |
 20   VALVE 'V-302'                                    |
 21   MIXER 'MIX-301'                                  |
        BEGIN RECYCLE LOOP 'LOOP1'            <-----+  |
 22   FLASH 'F-201'                                 |  |
 23   COMPRESSOR 'C-201'                            |  |
 24   SPLITTER 'SPL-201'                            |  |
        BEGIN CONTROL LOOP FOR 'SVC-201'      <--+  |  |
 25   HX 'SHX-201'                               |  |  |
 26   CONTROLLER 'SVC-201'                       |  |  |
        END CONTROL LOOP FOR 'SVC-201'        -->+  |  |
 27   SPLITTER 'SPL-202'                            |  |
 28   MIXER 'MIX-201'                               |  |
 29   VALVE 'V-201'                                 |  |
        END RECYCLE LOOP 'LOOP1'              ----->+  |
 30   COMPRESSOR 'C-202'                               |
 31   SPLITTER 'SPL-203'                               |
        BEGIN CONTROL LOOP FOR 'SVC-202'      <--+     |
 32   HX 'SHX-202'                               |     |
 33   CONTROLLER 'SVC-202'                       |     |
        END CONTROL LOOP FOR 'SVC-202'        -->+     |
 34   SPLITTER 'SPL-204'                               |
 35   MIXER 'MIX-202'                                  |
 36   VALVE 'V-202'                                    |
 37   FLASH 'F-202'                                    |
        BEGIN MVC LOOP FOR 'MVC-401'          <--+     |
 38   HX 'SHX-401'                               |     |
 39   STRM CALC 'MEM-401'                        |     |
 40   MVC 'MVC-401'                              |     |
        END MVC LOOP FOR 'MVC-401'            -->+     |
        BEGIN MVC LOOP FOR 'MVC-1001A'        <-----+  |
        ENTER RECYCLE LOOP 'LOOP2'                  |  |
 41   SPLITTER 'SPL-401'                            |  |
 42   VALVE 'V-1001'                                |  |
 43   SPLITTER 'SPL-1001'                           |  |
 44   VALVE 'V-1002A'                               |  |
 45   COMPRESSOR 'C-1001A'                          |  |
 46   CONV REAC 'R-1001A'                           |  |
        END RECYCLE LOOP 'LOOP2'              -------->+
        BEGIN RECYCLE LOOP 'LOOP3'            <--+  |
 47   EXPANDER 'T-1001A'                         |  |
 48   SPLITTER 'SPL-1002A'                       |  |
 49   HX 'SHX-1001A'                             |  |
        END RECYCLE LOOP 'LOOP3'              -->+  |
 50   MVC 'MVC-1001A'                               |
        END MVC LOOP FOR 'MVC-1001A'          ----->+
        BEGIN RECYCLE LOOP 'LOOP4'            <--+
 51   FLASH 'F-501'                              |
 52   COMPRESSOR 'C-501'                         |
 53   SPLITTER 'SPL-501'                         |
        BEGIN MVC LOOP FOR 'MVC-501'          <-----+
        ENTER RECYCLE LOOP 'LOOP4'               |  |
 54   HX 'SHX-501'                               |  |
 55   SPLITTER 'SPL-502'                         |  |
 56   MIXER 'MIX-501'                            |  |
 57   VALVE 'V-501'                              |  |
        END RECYCLE LOOP 'LOOP4'              -->+  |
 58   MVC 'MVC-501'                                 |
        END MVC LOOP FOR 'MVC-501'            ----->+
        BEGIN RECYCLE LOOP 'LOOP5'            <-----+
 59   FLASH 'F-502'                                 |
 60   COMPRESSOR 'C-502'                            |
        BEGIN CONTROL LOOP FOR 'SVC-502'      <--+  |
 61   HX 'SHX-502'                               |  |
 62   CONTROLLER 'SVC-502'                       |  |
        END CONTROL LOOP FOR 'SVC-502'        -->+  |
 63   SPLITTER 'SPL-503'                            |
 64   VALVE 'V-502'                                 |
        END RECYCLE LOOP 'LOOP5'              ----->+
```

```
    BEGIN RECYCLE LOOP 'LOOP4'                        <-----+
61  FLASH 'F-502'                                           |
62  COMPRESSOR 'C-502'                                      |
    BEGIN CONTROL LOOP FOR 'SVC-502'                  <--+  |
63  HX 'SHX-502'                                         |  |
64  CONTROLLER 'SVC-502'                                 |  |
    END CONTROL LOOP FOR 'SVC-502'                    -->+  |
65  SPLITTER 'SPL-502'                                      |
66  VALVE 'V-502'                                           |
    END RECYCLE LOOP 'LOOP4'                          ----->+
67  SPLITTER 'SPL-503'
    BEGIN RECYCLE LOOP 'LOOP5'                        <-----+
68  FLASH 'F-601'                                           |
69  COMPRESSOR 'C-601'                                      |
    BEGIN CONTROL LOOP FOR 'SVC-601'                  <--+  |
70  HX 'SHX-601'                                         |  |
71  CONTROLLER 'SVC-601'                                 |  |
    END CONTROL LOOP FOR 'SVC-601'                    -->+  |
72  SPLITTER 'SPL-601'                                      |
73  VALVE 'V-601'                                           |
    END RECYCLE LOOP 'LOOP5'                          ----->+
    BEGIN RECYCLE LOOP 'LOOP6'                        <-----+
74  FLASH 'F-602'                                           |
75  COMPRESSOR 'C-602'                                      |
    BEGIN CONTROL LOOP FOR 'SVC-602'                  <--+  |
76  HX 'SHX-602'                                         |  |
77  CONTROLLER 'SVC-602'                                 |  |
    END CONTROL LOOP FOR 'SVC-602'                    -->+  |
78  SPLITTER 'SPL-602'                                      |
79  VALVE 'V-602'                                           |
    END RECYCLE LOOP 'LOOP6'                          ----->+
    BEGIN RECYCLE LOOP 'LOOP7'                        <-----+
80  FLASH 'F-603'                                           |
81  COMPRESSOR 'C-603'                                      |
    BEGIN CONTROL LOOP FOR 'SVC-603'                  <--+  |
82  HX 'SHX-603'                                         |  |
83  CONTROLLER 'SVC-603'                                 |  |
    END CONTROL LOOP FOR 'SVC-603'                    -->+  |
84  SPLITTER 'SPL-603'                                      |
85  VALVE 'V-603'                                           |
    END RECYCLE LOOP 'LOOP7'                          ----->+
    BEGIN RECYCLE LOOP 'LOOP8'                        <-----+
86  FLASH 'F-604'                                           |
87  COMPRESSOR 'C-604'                                      |
    BEGIN CONTROL LOOP FOR 'SVC-604'                  <--+  |
88  HX 'SHX-604'                                         |  |
89  CONTROLLER 'SVC-604'                                 |  |
    END CONTROL LOOP FOR 'SVC-604'                    -->+  |
90  SPLITTER 'SPL-604'                                      |
91  VALVE 'V-604'                                           |
92  MIXER 'MIX-701'                                         |
    END RECYCLE LOOP 'LOOP8'                          ----->+
    BEGIN RECYCLE LOOP 'LOOP9'                        <-----+
93  FLASH 'F-701'                                           |
94  COMPRESSOR 'C-701'                                      |
    BEGIN CONTROL LOOP FOR 'SVC-701'                  <--+  |
95  HX 'SHX-701'                                         |  |
96  CONTROLLER 'SVC-701'                                 |  |
    END CONTROL LOOP FOR 'SVC-701'                    -->+  |
97  SPLITTER 'SPL-701'                                      |
98  VALVE 'V-701'                                           |
    END RECYCLE LOOP 'LOOP9'                          ----->+
99  PIPE 'PIP-701'
100 MIXER 'MIX-801'
    BEGIN CONTROL LOOP FOR 'SVC-801'                  <-----+
101 PIPE 'PIP-801A'                                         |
102 PUMP 'P-802A'                                           |
103 PIPE 'PIP-801B'                                         |
104 PUMP 'P-802B'                                           |
105 MIXER 'MIX-802'                                         |
106 HX 'SHX-801'                                            |
    BEGIN CONTROL LOOP FOR 'SVC-802'                  <--+  |
107 PUMP 'P-801'                                         |  |
108 CONTROLLER 'SVC-802'                                 |  |
    END CONTROL LOOP FOR 'SVC-802'                    -->+  |
109 CONTROLLER 'SVC-801'                                    |
    END CONTROL LOOP FOR 'SVC-801'                    ----->+
```

```
65  SPLITTER 'SPL-504'
    BEGIN RECYCLE LOOP 'LOOP6'                        <-----+
66  FLASH 'F-601'                                           |
67  COMPRESSOR 'C-601'                                      |
    BEGIN CONTROL LOOP FOR 'SVC-601'                  <--+  |
68  HX 'SHX-601'                                         |  |
69  CONTROLLER 'SVC-601'                                 |  |
    END CONTROL LOOP FOR 'SVC-601'                    -->+  |
70  SPLITTER 'SPL-601'                                      |
71  VALVE 'V-601'                                           |
    END RECYCLE LOOP 'LOOP6'                          ----->+
    BEGIN RECYCLE LOOP 'LOOP7'                        <--+
72  FLASH 'F-602'                                        |
73  COMPRESSOR 'C-602'                                   |
    BEGIN MVC LOOP FOR 'MVC-602'                      <-----+
    ENTER RECYCLE LOOP 'LOOP7'                           |  |
74  SPLITTER 'SPL-602'                                   |  |
75  HX 'SHX-602'                                         |  |
76  SPLITTER 'SPL-603'                                   |  |
77  MIXER 'MIX-601'                                      |  |
78  VALVE 'V-602'                                        |  |
    END RECYCLE LOOP 'LOOP7'                          -->+  |
79  MVC 'MVC-602'                                           |
    END MVC LOOP FOR 'MVC-602'                        ----->+
    BEGIN RECYCLE LOOP 'LOOP8'                        <--+
80  FLASH 'F-603'                                        |
81  COMPRESSOR 'C-603'                                   |
    BEGIN MVC LOOP FOR 'MVC-603'                      <-----+
    ENTER RECYCLE LOOP 'LOOP8'                           |  |
82  SPLITTER 'SPL-604'                                   |  |
83  HX 'SHX-603'                                         |  |
84  SPLITTER 'SPL-605'                                   |  |
85  MIXER 'MIX-602'                                      |  |
86  VALVE 'V-603'                                        |  |
    END RECYCLE LOOP 'LOOP8'                          -->+  |
87  MVC 'MVC-603'                                           |
    END MVC LOOP FOR 'MVC-603'                        ----->+
88  MIXER 'MIX-701'
    BEGIN RECYCLE LOOP 'LOOP9'                        <-----+
89  FLASH 'F-701'                                           |
90  COMPRESSOR 'C-701'                                      |
    BEGIN CONTROL LOOP FOR 'SVC-701'                  <--+  |
91  HX 'SHX-701'                                         |  |
92  CONTROLLER 'SVC-701'                                 |  |
    END CONTROL LOOP FOR 'SVC-701'                    -->+  |
93  SPLITTER 'SPL-701'                                      |
94  VALVE 'V-701'                                           |
    END RECYCLE LOOP 'LOOP9'                          ----->+
95  PIPE 'PIP-701'
96  MIXER 'MIX-801'
    BEGIN CONTROL LOOP FOR 'SVC-801'                  <-----+
97  PIPE 'PIP-801A'                                         |
98  PUMP 'P-802A'                                           |
99  PIPE 'PIP-801B'                                         |
100 PUMP 'P-802B'                                           |
101 MIXER 'MIX-802'                                         |
102 HX 'SHX-801'                                            |
    BEGIN CONTROL LOOP FOR 'SVC-802'                  <--+  |
103 PUMP 'P-801'                                         |  |
104 CONTROLLER 'SVC-802'                                 |  |
    END CONTROL LOOP FOR 'SVC-802'                    -->+  |
105 CONTROLLER 'SVC-801'                                    |
    END CONTROL LOOP FOR 'SVC-801'                    ----->+
```

Figure A1.2. Simulation Calculation Sequence

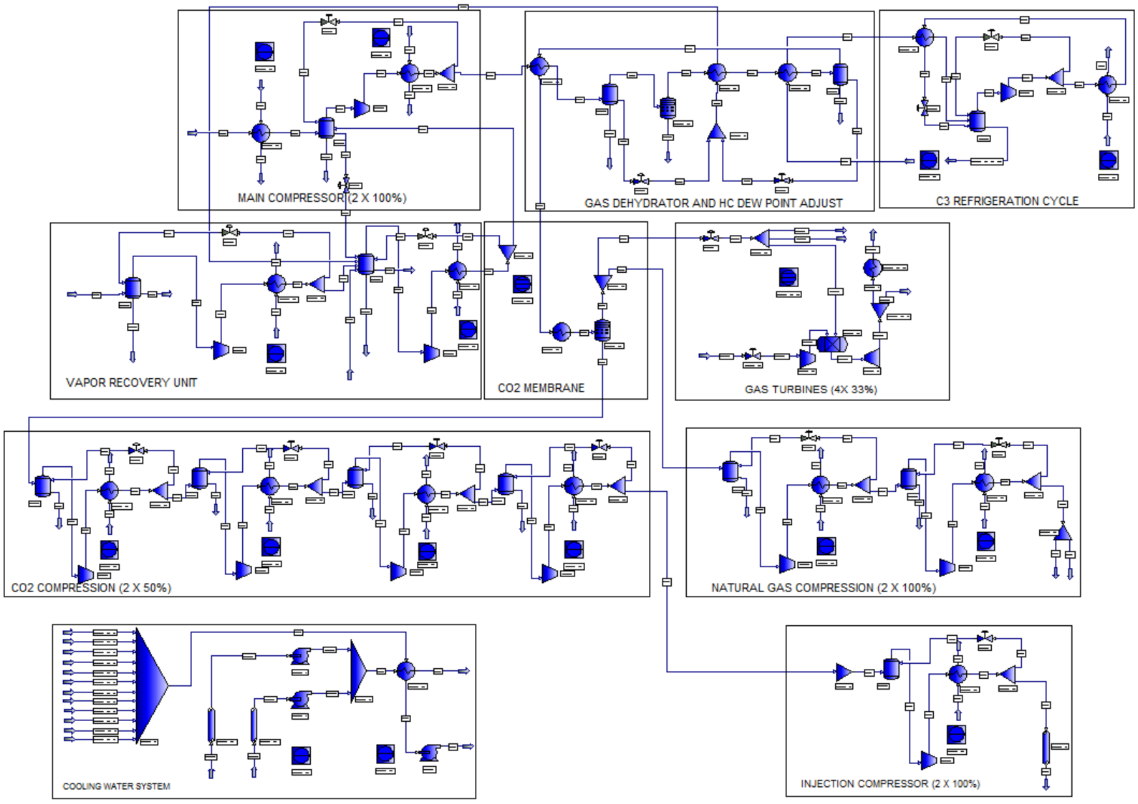

Figure A1.3. Simulation Flowsheet: Base-Case

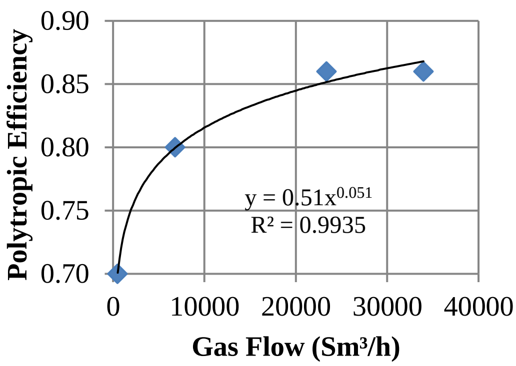

Figure A1.4 – Polytropic efficiency versus gas flow rate (Fitted with data fromn Fig. 13-23 of GPSA [2])

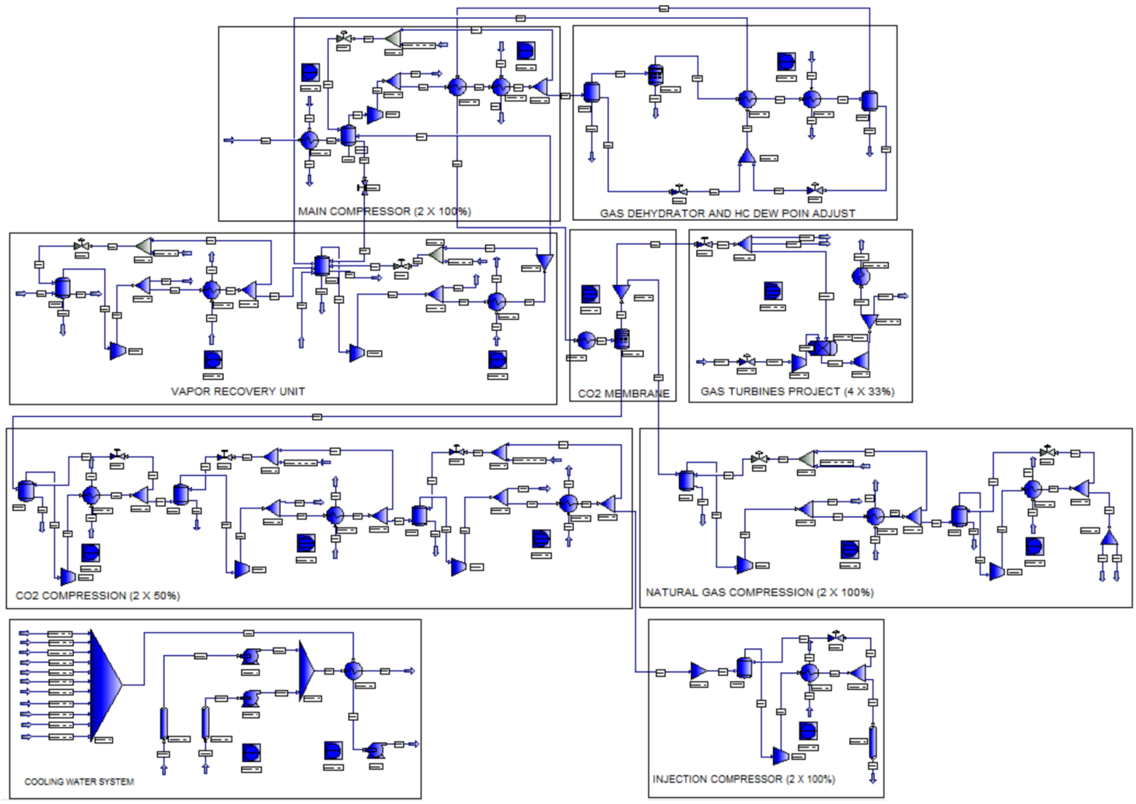

Figure A1.5. Simulation Flowsheet: DSW-Case

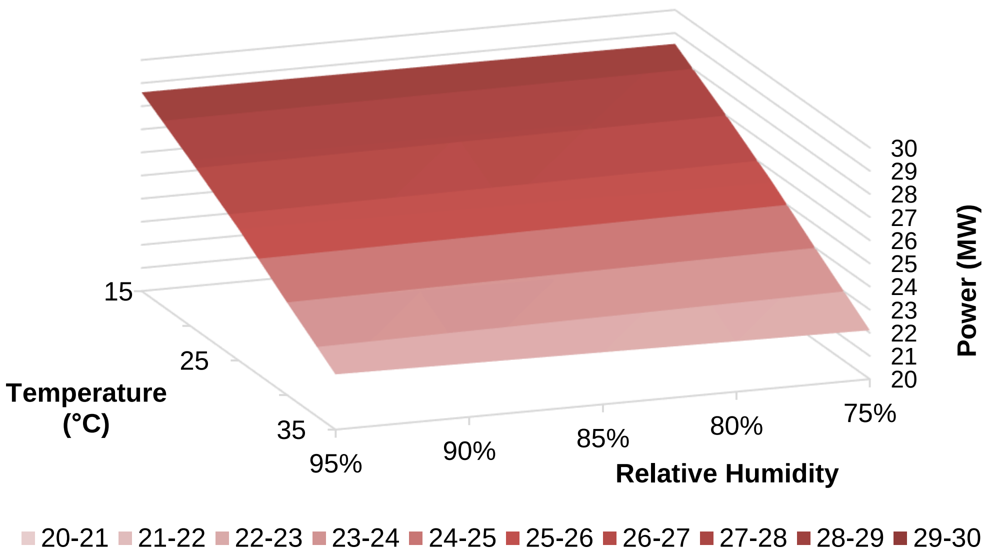

Figure A1.6. GE LM2500 GT Power vs Air Temperature and Relative Humidity

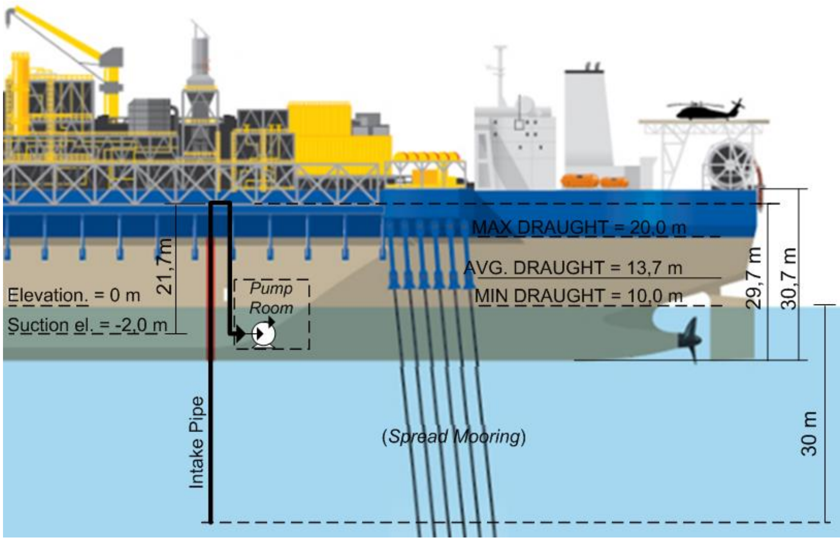

Figure A1.7. Base-Case Seawater Intake System (based on EIA [1])

Table A1.1. Simulation of Plant Inlet Streams (EIA (Petrobras, 2013))

	OIL	GAS	WATER
Temperature (°C)	40	40	40
Pressure (kPa)	41368	41368	41368
Composition (mol fraction)			
CO_2	0.0000	0.1513	0.0000
H_2S	0.0000	0.0000	0.0000
N_2	0.0000	0.0051	0.0000
Methane	0.0000	0.6396	0.0000
Ethane	0.0000	0.0924	0.0000
Propane	0.0050	0.0591	0.0000
i-Butane	0.0019	0.0099	0.0000
n-Butane	0.0081	0.0207	0.0000
i-Pentane	0.0065	0.0052	0.0000
n-Pentane	0.0122	0.0075	0.0000
C_6*	0.0295	0.0063	0.0000
C_7*	0.0559	0.0009	0.0000
C_8*	0.0777	0.0016	0.0000
C_9*	0.0658	0.0005	0.0000
C_10*	0.0604	0.0000	0.0000
C_11*	0.0405	0.0000	0.0000
C_12*	0.0537	0.0000	0.0000
C_13*	0.0488	0.0000	0.0000
C_14*	0.0436	0.0000	0.0000
C_15*	0.0308	0.0000	0.0000
C_16*	0.0339	0.0000	0.0000
C_17*	0.0224	0.0000	0.0000
C_18*	0.0236	0.0000	0.0000
C_19*	0.0224	0.0000	0.0000
C20+*	0.3573	0.0000	0.0000
H2O	0.0000	0.0000	1.0000
MM C20+		500	
Density C20+		0.9496	

Table A1.2. Compressors Flows and Anti-Surge Recycle – Base-Case

Compressor	Design Flow (MMSm³/d)	Base-Case 100% Operation 5.0 MM Sm³/d		Base-Case 75% Operation 3.75 MM Sm³/d		Base-Case 50% Operation 2.5 MM Sm³/d		Base-Case 25% Operation 1.25 MM Sm³/d	
		Flow	Recycle	Flow	Recycle	Flow	Recycle	Flow	Recycle
C-101	5.082	5.082	0.0%	5.082	25.2%	5.081	50.3%	5.085	75.3%
C-201	0.071	0.071	0.0%	0.071	26.0%	0.071	52.0%	0.071	76.0%
C-202	0.302	0.302	0.0%	0.301	26.0%	0.301	52.0%	0.301	77.0%
C-501	3.500	3.506	0.0%	3.506	27.5%	3.508	50.1%	3.504	82.8%
C-502	3.500	3.506	0.0%	3.506	27.5%	3.508	50.1%	3.504	82.8%
C-601	1.200	1.200	16.6%	1.200	37.5%	1.200	58.3%	1.200	79.1%
C-602	1.200	1.200	16.6%	1.200	37.5%	1.200	58.3%	1.200	79.1%
C-603	1.200	1.200	16.6%	1.200	37.5%	1.200	58.3%	1.200	79.1%
C-604	1.200	1.200	16.6%	1.200	37.5%	1.200	58.3%	1.200	79.1%
C-701	4.230	4.231	76.4%	4.230	82.3%	4.230	88.2%	4.230	94.1%
C-901	0.254	0.254	0.0%	0.254	18.5%	0.254	37.8%	0.254	57.0%

Table A1.3. Heat Exchangers Specification – Base-Case

ID in Fig. 10	TAG	Utility Fluid	T_{in} (°C)	T_{out} (°C)	ΔP (kPa)	Specification	Value (°C)	ΔP gas (kPa)
1	SHX-101	CW	35	45	100	Hot Fluid T	40	50
2	SHX-102	CW	35	55	50	Hot Fluid T	40	50
3	SHX-201	CW	35	50	50	Hot Fluid T	40	25
4	SHX-202	CW	35	55	50	Hot Fluid T	40	50
5	SHX-301	-				Hot Fluid T	5	50
6	SHX-302	-				Hot T_{in} – Cold T_{out}	3	50
7	SHX-303	Propane	0	0	13.8	Hot Fluid T	10	50
8	SHX-501	CW	35	55	100	Hot Fluid T	40	50
9	SHX-502	CW	35	55	100	Hot Fluid T	40	50
10	SHX-601	CW	35	55	50	Hot Fluid T	40	25
11	SHX-602	CW	35	55	50	Hot Fluid T	40	25
12	SHX-603	CW	35	55	100	Hot Fluid T	40	50
13	SHX-604	CW	35	55	50	Hot Fluid T	40	50
14	SHX-701	CW	35	55	50	Hot Fluid T	40	50
15	SHX-801	SW	32	40	60	Hot Fluid T	35	60
16	SHX-901	-				ºC Above Dew Point	10	0
17	SHX-902	CW	35	55	50	Hot Fluid Vapor Fraction	0	0

Table A1.4. Anti-Surge Control Loop, Hot Bypass Flow and Minimum Allowable Temperature – DSW-Case (100% gas capacity)

Compressor	Design Mass Flow (MMSm³/d)	Simulated Flow (MM Sm³/d)	% Anti-Surge Recycle	Hot Bypass (Sm³/d)	Hydrate T (°C)	Min. T (°C)
C-101	4.956	4.956	0.0%	0	8.7/0	5
C-201	0.071	0.071	0.0%	0	-7.8/0	5
C-202	0.238	0.238	0.0%	0	3.6/0	5
C-501	3.500	3.520	0.0%	0	-	5
C-502	3.500	3.520	0.0%	0	-	5
C-601	1.200	1.201	16.5%	0	-	5
C-602	1.200	1.201	16.5%	4228	-	5
C-603	1.200	1.201	16.5%	51291	-	5
C-701	4.200	4.230	76.3%	0	-	5

Table A1.5. Surge Control Loop, Hot Bypass Flow and Minimum Allowable Temperature – DSW-Case (75% gas capacity)

Compressor	Design Mass Flow (MMSm³/d)	Simulated Flow (MM Sm³/d)	% Anti-Surge Recycle	Hot Bypass (Sm³/d)	Hydrate T (°C)	Min. T (°C)
C-101	4.956	4.956	25.0%	300000	8.7/0	5
C-201	0.071	0.071	27.0%	1500	-7.8/0	5
C-202	0.238	0.239	26.0%	12500	3.6/0	5
C-501	3.500	3.503	27.1%	180000	N/P	5
C-502	3.500	3.503	27.1%	0	N/P	5
C-601	1.200	1.200	37.5%	0	N/P	5
C-602	1.200	1.200	37.5%	75222	N/P	5
C-603	1.200	1.200	37.5%	191159	N/P	5
C-701	4.200	4.230	82.3%	0	N/P	5

Table A1.6. Anti-Surge Control Loop, Hot Bypass Flow and Minimum Allowable Temperature – DSW-Case (50% gas capacity)

Compressor	Design Mass Flow (MMSm³/d)	Simulated Flow (MM Sm³/d)	% Anti-Surge Recycle	Hot Bypass (Sm³/d)	Hydrate T (°C)	Min. T (°C)
C-101	4.956	4.956	50.0%	525000	8.7/0	5
C-201	0.071	0.070	52.5%	3750	-7.8/0	5
C-202	0.238	0.239	51.0%	39000	3.5/0	5
C-501	3.500	3.502	54.5%	820000	N/P	5
C-502	3.500	3.502	54.5%	0	N/P	5
C-601	1.200	1.201	58.4%	0	N/P	5
C-602	1.200	1.201	58.4%	146977	N/P	5
C-603	1.200	1.201	58.4%	332054	N/P	5
C-701	4.200	4.230	88.2%	0	N/P	5

Table A1.7. Anti-Surge Control Loop, Hot Bypass Flow and Minimum Allowable Temperature – DSW-Case (25% gas capacity)

Compressor	Design Mass Flow ($MMSm^3/d$)	Simulated Flow ($MM\ Sm^3/d$)	% Anti-Surge Recycle	Hot Bypass (Sm^3/d)	Hydrate T (°C)	Min. T (°C)
C-101	4.956	4.956	75.0%	750000	8.7/0	5
C-201	0.071	0.071	77.0%	6750	-7.8/0	5
C-202	0.238	0.239	76.1%	58000	3.5/0	5
C-501	3.500	3.503	82.3%	1440000	N/P	5
C-502	3.500	3.503	82.3%	0	N/P	5
C-601	1.200	1.200	79.2%	0	N/P	5
C-602	1.200	1.200	79.2%	217204	N/P	5
C-603	1.200	1.200	79.2%	470246	N/P	5
C-701	4.200	4.230	94.1%	0	N/P	5

Table A1.8. Heat Exchangers Specification – DSW-Case

ID Fig. 10	TAG	Utility Fluid	T_{in} (°C)	T_{out} (°C)	ΔP (kPa)	Specification	Value (°C)	ΔP gas (kPa)
1	SHX-101	CW	7	17	100	Hot Fluid T	12	50
2	SHX-103	CW	7	27	50	Hot Fluid T	20	50
3	SHX-201	CW	7	27	50	Hot Fluid T	12	25
4	SHX-202	CW	7	27	50	Hot Fluid T	12	50
5	SHX-102	-	-	-	50	Cold Fluid T	35	50
6	SHX-301	-			50	Hot T_{in} – Cold T_{out}	3	50
7	SHX-302	CW	7	13	50	Hot Fluid T	10	50
8	SHX-501	CW	7	27	100	Hot Fluid T	12	50
9	SHX-502	CW	7	27	100	Hot Fluid T	40	50
10	SHX-601	CW	7	27	50	Hot Fluid T	12	25
11	SHX-602	CW	7	27	50	Hot Fluid T	12	25
12	SHX-603	CW	7	27	100	Hot Fluid T	12	50
14	SHX-701	CW	7	27	50	Hot Fluid T	40	50
15	SHX-801	SW	4	11	60	Hot Fluid T	7	60

Table A1.9. Fuel Gas Properties

CASE	BASE	DSW
Pressure (kPa)	3500	3500
Temperature (°C)	22.5	22.5
LHV (kJ/kg)	43487	43486
HHV (kJ/kg)	47848	47847
Molar Mass (kg/kgmol)	22.91	22.92
COMPOSITION (MOLAR FRACTION)		
N_2	0.00672	0.00673
CO_2	0.05000	0.05000
Methane	0.69910	0.70100
Ethane	0.14380	0.14000
Propane	0.06802	0.06966
n-Butane	0.01684	0.01687
n-Pentane	0.00567	0.00583
Hexane	0.00093	0.00099
Isobutane	0.00892	0.00892

Table A1.10. FPSO Typical Electricity Consumers

ENGINE ROOM AND VESSEL	POWER (kW)
Compressors	1000
Oil Treatment Panel	300
Engine Command Panel	2190
Cranes	290
Offloading Hose Reel	150
Hot Water Pumps	90
Inert Gas Generator	125
Deaerator Pump	132
Naval Lighting	150
Hypochlorite Generator	330
Main Generation/ Auxiliary Equipment	112
Ballast System	110
Emergency Cooling Pump	95
Emergency Hot Water	90
Inert Gas Generator Cooling Pump	110
ACCOMODATIONS -100 people	
Miscellaneous Equipment	157
Gym	0.59
Laundry	7.14
Hospital	2.89
Kitchen	36.34
Others	39.14
Electric Devices	96.50
PROCESS (Oil, Gas, Water)	
Flare System	2300
CO_2 removal	1500
Gas Dehydration, Fuel Gas and HCDP	560
Injection Manifolds	155
Oil Processing and Treatment	5000
Sulfates Removal and Water Injection System	300
Chemical Storage	3500
Utilities	515
Laydown Area	65
Automation	1200
Pipe Rack	1450
Flare Tower	655
Laboratory	350
Cooling Water Pumps	2000
TOTAL	**23.16 MW**

(adapted from Martins et. al (2014) (Martins; Delfino; Fachini, 2014)**)**

Supplement A2 – Equipment Sizing

Table A2.1. Heat Exchangers Sizing – Base-Case

	RHX-101	RHX-102	RHX-201	RHX-202
Heat Duty	SHX-101	SHX-102	SHX-201	SHX-202
Hot Fluid Side	Tubes	Tubes	Tubes	Tubes
Cold Fluid Side	Shell	Shell	Shell	Shell
$\Delta P_{max\ shell}$/Shell (kPa)	50	50	25	50
$\Delta P_{max\ tubes}$/Shell (kPa)	25	50	50	50
Number of Shells in Serie	2	1	1	1
Number of Shells in Parallel	1	1	1	1
Number of Tube Passes /Shell	1	4	2	2
TEMA Type	AEL	NFU	NFU	NFU
Shell Diameter (mm)	900	1800	350	500
Shell Material	A 516	A 516	A 516	A 516
Tubes Material	Inconel	Inconel	Inconel	Inconel
Tubes Abs. Roughness (mm)	0.04572	0.04572	0.04572	0.04572
Tubes Outer Diameter (mm)	25.4	19.05	19.05	19.05
Tubes BWG	18	18	18	18
Tubes Length (m)	5.7	6.096	6.096	6.096
Pitch (mm)	31.7	25.4	25.4	25.4
Tubes Pattern	Triangular 30°	Triangular 30°	Triangular 30°	Triangular 30°
Baffles Type	Single	Double	Single	Single
Baffles Cut (%)	25	30	25	25
Baffles Spacing (mm)	250	350	150	170
Fouling Resistance (m^2.K/kW)	0.17611	0.17611	0.17611	0.17611

Table A2.1. Heat Exchangers Sizing – Base-Case (Continued)

	RHX-301	RHX-302	RHX-303	RHX-501
Heat Duty	SHX-301	SHX-302	SHX-303	SHX-501
Hot Fluid Side	Shell	Tubes	Tubes	Tubes
Cold Fluid Side	Tubes	Shell	Shell	Shell
$\Delta P_{max\ shell}$/Shell (kPa)	25	50	50	50
$\Delta P_{max\ tubes}$/Shell (kPa)	25	50	0	50
Number of Shells in Series	2	1	1	2
Number of Shells in Parallel	1	1	1	1
Number of Tube Passes /Shell	2	2	2	2
TEMA Type	BHM	NFU	NFU	DFU
Shell Diameter (mm)	1150	750	800	800
Shell Material	A 516	SS316	A 516	A 516
Tubes Material	Inconel	316LS	316LS	316LS
Tubes Abs. Roughness (mm)	0.04572	0.04572	0.04572	0.04572
Tubes Outer Diameter (mm)	19.05	25.4	25.4	19.05
Tubes BWG	18	18	18	18
Tubes Length (m)	11.6	4.5	6.6	10.6
Pitch (mm)	25.4	31.7	31.7	25.4
Tubes Pattern	Triangular 30°	Triangular 30°	Triangular 30°	Triangular 30°
Baffles Type	Single	Single	Single	Double
Baffles Cut (%)	25	25	25	33
Baffles Spacing (mm)	350	120	150	600
Fouling Resistance (m^2.K/kW)	0.17611	0.17611	0.17611	0.17611

Table A2.1. Heat Exchangers Sizing – Base-Case (Continued)

	RHX-502	RHX-601	RHX-602	RHX-603
Heat Duty	SHX-502	SHX-601	SHX-602	SHX-603
Hot Fluid Side	Tubes	Tubes	Tubes	Tubes
Cold Fluid Side	Shell	Shell	Shell	Shell
$\Delta P_{max\ shell}$/Shell (kPa)	50	50	50	50
$\Delta P_{max\ tubes}$/Shell (kPa)	50	50	50	50
Number of Shells in Serie	2	1	2	-
Number of Shells in Parallel	1	2	1	-
Number of Tube Passes /Shell	2	2	2	-
TEMA Type	DFU	NFU	NFU	DFU
Shell Diameter (mm)	800	900	700	550
Shell Material	A 516	A 516	A 516	A 516
Tubes Material	316LS	A179	A179	316LS
Tubes Abs. Roughness (mm)	0.04572	0.04572	0.04572	0.04572
Tubes Outer Diameter (mm)	19.05	19.05	19.05	19.05
Tubes BWG	16	18	18	18
Tubes Length (m)	11.8	8.4	11	9.4
Pitch (mm)	25.4	25.4	25.4	25.4
Tubes Pattern	Triangular 30°	Triangular 30°	Triangular 30°	Triangular 30°
Baffles Type	Double	Single	Double	-
Baffles Cut (%)	33	30	30	-
Baffles Spacing (mm)	750	300	500	-
Fouling Resistance (m².K/kW)	0.17611	0.17611	0.17611	0.17611

Table A2.1. Heat Exchangers Sizing – Base-Case (Continued)

	RHX-604	RHX-701	RHX-901	RHX-902
Heat Duty	SHX-604	SHX-701	SHX-901	SHX-902
Hot Fluid Side	Tubes	Shell	Shell	Tubes
Cold Fluid Side	Shell	Tubes	Tubes	Shell
$\Delta P_{max\ shell}$/Shell (kPa)	50	50	0	50
$\Delta P_{max\ tubes}$/Shell (kPa)	50	50	0	50
Number of Shells in Serie	-	-	1	1
Number of Shells in Parallel	-	-	1	1
Number of Tube Passes /Shell	-	-	1	6
TEMA Type	DFU	DFU	BEM	AJL
Shell Diameter (mm)	-	-	325	850
Shell Material	A516	A516	A 516	A 516
Tubes Material	316LS	316LS	A179	A179
Tubes Abs. Roughness (mm)	0.04572	0.04572	0.04572	0.04572
Tubes Outer Diameter (mm)	19.05	19.05	25.4	19.05
Tubes BWG	-	-	18	18
Tubes Length (m)	-	-	1.5	5.2
Pitch (mm)	-	-	31.7	25.4
Tubes Pattern	-	-	Triangular 30°	Triangular 30°
Baffles Type	-	-	-	Single
Baffles Cut (%)	-	-	-	25
Baffles Spacing (mm)	-	-	-	80
Fouling Resistance (m².K/kW)	0.17611	0.17611	0.17611	0.17611

Table A2.2. Plate Heat Exchangers HX-801 Sizing – Base-Case

	Cold Side	Hot Side
Fluid	SW	CW
Mass Flow (kg/s)	calculated	162.9 x 4
Inlet Temperature (°C)	32	53.6
Outlet Temperature (°C)	40	35
Outlet Pressure (kPa abs.)	800	500
ΔP max (kPa)	60	60
Fouling Resistance (m².K/W)	0.3	0.2

Table A2.3. Heat Exchangers Sizing – DSW-Case

	RHX-101	RHX-102	RHX-103	RHX-201	RHX-202
Heat Duty	SHX-101	SHX-102	SHX-103	SHX-201	SHX-202
Hot Fluid Side	Tubes	Shell	Tubes	Tubes	Tubes
Cold Fluid Side	Shell	Tubes	Shell	Shell	Shell
$\Delta P_{max\ shell}$/Shell (kPa)	50	50	50	50	50
$\Delta P_{max\ tubes}$/Shell (kPa)	25	50	50	25	25
Number of Shells in Serie	2	1	1	1	2
Number of Shells in Parallel	1	2	1	1	1
Number of Tube Passes /Shell	2	1	2	2	2
TEMA Type	AEL	BHM	NFU	NFU	NFU
Shell Diameter (mm)	1280	450	1000	350	400
Shell Material	A 516	A 516	A 516	A 516	A 516
Tubes Material	Inconel	Inconel	Inconel	Inconel	Inconel
Tubes Abs. Roughness (mm)	0.04572	0.04572	0.04572	0.04572	0.04572
Tubes Outer Diameter (mm)	25.4	19.05	19.05	19.05	19.05
Tubes BWG	18	18	18	18	18
Tubes Length (m)	4.3	3.1	11.6	12	8.4
Pitch (mm)	31.7	25.4	25.4	25.4	25.4
Tubes Pattern	Triangular 30°	Triangular 30°	Triangular 30°	Triangular 30°	Triangular 30°
Baffles Type	Single	Single	Double	Single	Single
Baffles Cut (%)	25	25	30	25	25
Baffles Spacing (mm)	400	250	500	200	250
Fouling Resistance (m².K/kW)	0.17611	0.17611	0.17611	0.17611	0.17611

Table A2.3. Heat Exchangers Sizing – DSW-Case (continued)

	RHX-301	RHX-302	RHX-501	RHX-502
Heat Duty	SHX-301	SHX-302	SHX-501	SHX-502
Hot Fluid Side	Shell	Tubes	Tubes	Tubes
Cold Fluid Side	Tubes	Shell	Shell	Shell
$\Delta P_{max\ shell}$/Shell (kPa)	50	50	50	50
$\Delta P_{max\ tubes}$/Shell (kPa)	50	50	50	50
Number of Shells in Serie	1	2	2	1
Number of Shells in Parallel	1	1	1	1
Number of Tube Passes /Shell	6	2	2	2
TEMA Type	BHM	NFU	DFU	DFU
Shell Diameter (mm)	500	1000	1050	620
Shell Material	A 516	A 516	A 516	A 516
Tubes Material	SS 316	SS 316	SS 316	SS 316
Tubes Abs. Roughness (mm)	0.04572	0.04572	0.04572	0.04572
Tubes Outer Diameter (mm)	25.4	25.4	19.05	19.05
Tubes BWG	18	18	18	16
Tubes Length (m)	4.7	10.4	9	9
Pitch (mm)	31.7	31.7	25.4	25.4
Tubes Pattern	Triangular 30°	Triangular 30°	Triangular 30°	Triangular 30°
Baffles Type	Single	Double	Double	Double
Baffles Cut (%)	25	30	33	33
Baffles Spacing (mm)	500	280	850	400
Fouling Resistance (m^2.K/kW)	0.17611	0.17611	0.17611	0.17611

Table A2.3. Heat Exchangers Sizing – DSW-Case (continued)

	RHX-601	RHX-602	RHX-603	RHX-701
Heat Duty	SHX-601	SHX-602	SHX-603	SHX-701
Hot Fluid Side	Tubes	Tubes	Tubes	Tubes
Cold Fluid Side	Shell	Shell	Shell	Shell
$\Delta P_{max\ shell}$/Shell (kPa)	50	50	50	50
$\Delta P_{max\ tubes}$/Shell (kPa)	50	50	50	50
Number of Shells in Serie	1	1	-	-
Number of Shells in Parallel	1	1	-	-
Number of Tube Passes /Shell	2	2	-	-
TEMA Type	NFU	NFU	DFU	DFU
Shell Diameter (mm)	900	780	-	-
Shell Material	A 516	A 516	A516	A516
Tubes Material	A179	A179	SS316	SS316
Tubes Abs. Roughness (mm)	0.04572	0.04572	0.04572	0.04572
Tubes Outer Diameter (mm)	19.05	19.05	19.05	19.05
Tubes BWG	18	18	-	-
Tubes Length (m)	9.2	12	-	-
Pitch (mm)	25.4	25.4	-	-
Tubes Pattern	Triangular 30°	Triangular 30°	-	-
Baffles Type	Single	Single	-	-
Baffles Cut (%)	25	30	-	-
Baffles Spacing (mm)	500	650	-	-
Fouling Resistance (m^2.K/kW)	0.17611	0.17611	0.17611	0.17611

Table A2.4. Plate Heat Exchangers HX-801 Sizing – DSW-Case

	Cold Side	Hot Side
Fluid	SW	CW
Mass Flow (kg/s)	818.5 x 2	133.1 x 5
Inlet Temperature (°C)	4	23.8
Outlet Temperature (°C)	11	7
Outlet Pressure (kPa abs.)	800	500
ΔP max (kPa)	60	60
Fouling Resistance (m².K/W)	0.3	0.2

Supplement A3 – Cost and Weight Estimation

Table A3.1. Inputs for Compressors CAPEX Estimation – Base-Case

	C-101	C-201	C-202	C-501	C-502	C-601
Compressor Material	CS	CS	CS	CS	CS	CS
Inlet Flow (m³/h)	11975.6	1238.5	1838.7	2894.0	1110.4	12939.3
Inlet Pressure (kPag)	1699	149	566	4399	10491	299
Inlet Temperature (°C)	39.48	55	25.01	28.86	40	30
Discharge Pressure (kPag)	5149	591	1749	10541	24949	1034
Gas Mol. Mass	25.35	39.83	34.50	22.56	22.56	31.87
Cp/Cv	1.3049	1.1579	1.2179	1.4858	1.8807	1.308
Z_{inlet}	0.9462	0.9837	0.9517	0.8555	0.7451	0.9879
Z_{outlet}	0.9484	0.9744	0.9317	0.8923	0.9366	0.9887
Tubes Material	SS316L	SS316L	SS316L	CS	SS316L	CS
Driver	Motor	Motor	Motor	Motor	Motor	Motor

Table A3.1. Inputs for Compressors CAPEX Estimation – Base-Case (continued)

	C-602	C-603	C-604	C-701	C-901
Compressor Material	CS	CS	CS	CS	CS
Inlet Flow (m³/h)	605	609	613	702	904
Inlet Pressure (kPag)	606	610	614	703	905
Inlet Temperature (°C)	4727.7	1583.2	466.5	312.8	1884.9
Discharge Pressure (kPag)	1009	3025	8724	24899	375
Gas Mol. Mass	40	40	40	37.42	0
Cp/Cv	3050	8774	24949	54949	1637
Z_{inlet}	31.87	31.87	31.87	25.22	44.10
Z_{outlet}	1.3316	1.436	1.9648	n/a	1.1992
Tubes Material	0.97	0.9147	0.7607	n/a	0.898
Driver	0.976	0.949	0.9419	n/a	0.7835
Compressor Material	CS	SS316L	SS316L	SS316L	CS
Inlet Flow (m³/h)	Motor	Motor	Motor	Motor	Motor

Table A3.2. Inputs for Heat Exchangers CAPEX Estimation – Base-Case

	SHX-101	SHX-102	SHX-201	SHX-202	SHX-301
Heat Exchange Area (m^2)[1]	587.50	1093.00	41.00	108.50	1153.00
Number of Shells[2]	2	1	1	1	2
TEMA Type[3]	AEL	NFU	NFU	NFU	BHM
Tubes Material [2]	Inconel	Inconel	Inconel	Inconel	Inconel
Tubes Operation P (kPag) [1]	1749	5149	591	1749	4799
Tubes Design P (kPag) [4]	2094	5494	761	2094	5144
Tubes Operation T (°C) [1]	55	126	116	92	35
Tubes Design T (°C) [5]	125	156	146	125	125
Tubes Ext. Diameter (mm) [2]	25.4	25.4	19.1	19.1	25.4
Shell Material[2]	A 516	A 516	A 516	A 516	A 516
Shell Operation P (kPag) [1]	438	438	438	438	5099
Shell Design P (kPag) [4]	608	608	608	608	5444
Shell Operation T (°C) [1]	45	55	50	55	40
Shell Design T (°C) [5]	125	125	125	125	125
Tubes Length (m) [2]	5.70	9.00	10.00	12.20	11.60
Tubes BWG [2]	18	18	18	18	18
Pitch (mm) [2]	31.7	25.4	25.4	25.4	25.4
Tubes Pattern [2]	Triangular 30°	Triangular 30°	Triangular 30°	Triangular 30°	Triangular 30°
Shell Diameter (mm) [1]	900	1800	350	500	1150
Channel Material	A 516	A 516	A 516	A 516	A 516
Head Material	A 516	A 516	A 516	A 516	A 516
Clad Material	Inconel	Inconel	Inconel	Inconel	Inconel
Clad Side	Head	Head	Head	Head	Head
Number of Tube Passes/Shell[2]	1	4	2	2	2
Number of /Shell[2]	1	2	2	2	4

Table A3.2. Inputs for Heat Exchangers CAPEX Estimation – Base-Case (continued)

	SHX-302	SHX-303	SHX-501	SHX-502	SHX-601
Heat Exchange Area (m^2)[1]	1153	76,8	128,2	505,5	563,6
Number of Shells[2]	2	1	1	2	2
TEMA Type[3]	BHM	NFU	NFU	DFU	DFU
Tubes Material [2]	Inconel	316LS	316LS	316LS	316LS
Tubes Operation P (kPag) [1]	4799	4899	4849	10541	24949
Tubes Design P (kPag) [4]	5144	5244	5194	11068	26196
Tubes Operation T (°C) [1]	35	21,6	18	102	110
Tubes Design T (°C) [5]	125	22	22	132	140
Tubes Ext. Diameter (mm) [2]	19.05	25.4	25.4	19.05	19.05
Shell Material[2]	A 516	SS316	A 516	A 516	A 516
Shell Operation P (kPag) [1]	5099	616	375	438	438
Shell Design P (kPag) [4]	5444	786	545	608	608
Shell Operation T (°C) [1]	40	-11	-1	55	55
Shell Design T (°C) [5]	125	-41	-31	125	125
Tubes Length (m) [2]	11.6	4.5	6.6	10.6	11.8
Tubes BWG [2]	18	18	18	18	16
Pitch (mm) [2]	25.4	31.7	31.7	25.4	25.4
Tubes Pattern[2]	Triangular 30°	Triangular 30°	Triangular 30°	Triangular 30°	Triangular 30°
Shell Diameter (mm) [1]	1150	750	800	800	800
Channel Material	A 516	316L	A 516	316L	316L
Head Material	A 516	316L	A 516	316L	316L
Clad Material	Inconel	-	-	-	-
Clad Side	Head	-	-	-	-
Number of Tube Passes/Shell[2]	2	2	2	2	2
Number of Passes /Shell[2]	4	2	2	2	2

Table A3.2. Inputs for Heat Exchangers CAPEX Estimation – Base-Case (continued)

	SHX-602	SHX-603	SHX-901	SHX-902
Heat Exchange Area (m^2)[1]	198.7	203.3	8.64	266.1
Number of Shells[2]	1	2	1	1
TEMA Type[3]	NFU	DFU	BEM	AJL
Tubes Material [2]	A179	316LS	A179	A179
Tubes Operation P (kPag) [1]	3050	8774	375	438
Tubes Design P (kPag) [4]	3395	9213	545	608
Tubes Operation T (°C) [1]	142	150	10	45
Tubes Design T (°C) [5]	172	180	22	125
Tubes Ext. Diameter (mm) [2]	19.05	19.05	19.05	19.05
Shell Material[2]	A 516	A 516	A 516	A 516
Shell Operation P (kPag) [1]	438	438	1637	1637
Shell Design P (kPag) [4]	608	608	1807	1807
Shell Operation T (°C) [1]	55	55	50	66
Shell DesignT (°C) [5]	125	125	125	125
Tubes Length (m) [2]	11	9.4	1.5	5.2
Tubes BWG [2]	18	18	18	18
Pitch (mm) [2]	25.4	25.4	31.7	25.4
Tubes Pattern[2]	Triangular 30°	Triangular 30°	Triangular 30°	Triangular 30°
Shell Diameter (mm) [1]	700	550	325	850
Channel Material	A 516	316L	A 516	A 516
Head Material	A 516	316L	A 516	A 516
Clad Material	-	-	-	-
Clad Side	-	-	-	-
N° Tube Passes/Shell[2]	2	2	1	6
N° of Passes /Shell[2]	2	2	1	1

Notes:
[1] From simulation
[2] From Table B-1
[3] From Table B-1
[4] Calculated by Aspen Capital cost Estimator
[5] Calculated by Aspen Capital cost Estimator

Table A3.3. Inputs for Heat Exchangers SHX-604 and SHX-701 CAPEX Estimation – Base-Case

	SHX-604	SHX-701
U (W/m².K)	591	629
UA (W/K)	141477	429733
Heat Exchange Area (m²)	239.4	683.2
Number of Shells	2	2
TEMA Type	DFU	DFU
Tubes Material	316LS	316LS
Tubes Operation P (kPag)	24949	54949
Tubes Design P (kPag)	26196	57696
Tubes Operation T (°C)	147	103
Tubes Design T (°C)	177	133
Tubes Ext. Diameter (mm)	19.05	19.05
Shell Material	A516	A516
Shell Operation P (kPag)	438	438
Shell Design P (kPag)	608	608
Shell Operation T (°C)	55	55
Shell DesignT (°C)	125	125
Tubes Length (m)	0	0
Tubes BWG	-	-
Pitch (mm)	-	-
Tubes Pattern	-	-
Shell Diameter (mm)	-	-
Channel Material	316L	316L
Head Material	316L	316L
Clad Material	-	-
Clad Side	-	-
N° Tube Passes/Shell	2	2
N° of Passes /Shell	2	2

Table A3.4. Inputs for Plate Heat Exchanger SHX-801 CAPEX Estimation – Base-Case

	SHX-801
Number of Heat Exchangers	3 + 1 spare
Heat Exchange Area (m²)[1]	2415.5
Number of Plates[1]	669
Operation P (kPag)	792.85
Design P (kPag)	963
Operation T (°C)	53.6
Design T (°C)	125
Material	titanium

[1] Heat exchange area and number of plates from Aspen Exchanger Design and Rating.

Table A3.5. Inputs for CW System Pumps CAPEX Estimation – Base-Case

	P1	P2
Model	DCP API 610	DCP API 610
Pumps in Operation	1x100%	2x50%
Spares	1	1
Material	Carbon Steel	Steel/Copper
Flow (L/s)[1]	647.7	564.4
Head (m)[1]	36.6	75.4

[1] From Simulation

Table A3.6. Inputs for Gas Turbines CAPEX Estimation – Base-Case

Gas Turbines in Operation[1]	3
Spares[1]	1
Design Power (kW) [1]	28491
Power Factor	0.9
Power (kVA) [2]	31657

[1] From EIA(Petrobras, 2013); [2] Power (kVA) = Power (kW) / Power Factor

Table A3.7 – Inputs for Compressors CAPEX Estimation – DSW-Case

	C-101	C-201	C-202	C-501	C-502	C-601	C-602	C-603	C-701
Compressor Material	CS	CS	CS	CS	CS	CS	CS	CS	CS
Inlet Flow (m^3/h)	10428	1239	1426	2894	835	12888	2943	581	313
Inlet Pressure (kPag)	1699	149	566	4399	10491	299	1473	6165	24899
Inlet Temperature (°C)	10.7	55.0	19.3	28.9	12.0	28.9	12.0	12.0	28.7
Discharge Pressure (kPag)	5149	591	1749	10541	24949	1498	6190	24949	54949
Gas Mol. Mass	24.78	39.83	33.41	22.56	22.56	31.84	31.84	31.84	25.21
Cp/Cv	1.353	1.158	1.230	1.486	2.474	1.309	1.392	2.036	n/a
Z_{inlet}	0.928	0.984	0.953	0.855	0.616	0.988	0.940	0.739	n/a
Z_{outlet}	0.929	0.974	0.937	0.892	0.873	0.990	0.960	0.947	n/a
Tubes Material	SS316L	SS316L	SS316L	CS	SS316L	CS	CS	SS316L	SS316L
Driver	Motor	Motor	Motor	Motor	Motor	Motor	Motor	Motor	Motor

Table A3.8. Inputs for Heat Exchangers CAPEX Estimation – DSW-Case

	SHX-101	SHX-102	SHX-103	SHX-201
Heat Exchange Area (m^2)[1]	883.20	89.30	439.00	49.20
Number of Shells[2]	2	2	1	1
TEMA Type[3]	AEL	BHM	NFU	NFU
Tubes Material [2]	Inconel	Inconel	Inconel	Inconel
Tubes Operation P (kPag) [1]	1749	4799	5099	591
Tubes Design P (kPag) [4]	2094	5144	5444	761
Tubes Operation T (°C) [1]	55	35	70	116
Tubes Design T (°C) [5]	125	125	125	146
Tubes Ext. Diameter (mm) [2]	25.4	19.1	19.1	19.1
Shell Material[2]	A 516	A 516	A 516	A 516
Shell Operation P (kPag) [1]	438	5149	438	438
Shell Design P (kPag) [4]	608	5494	608	608
Shell Operation T (°C) [1]	7	96	27	27
Shell DesignT (°C) [5]	22	126	125	125
Tubes Length (m) [2]	4.30	3.10	11.60	12.00
Tubes BWG [2]	18	18	18	18
Pitch (mm) [2]	31.7	25.4	25.4	25.4
Tubes Pattern[2]	Triangular 30°	Triangular 30°	Triangular 30°	Triangular 30°
Shell Diameter (mm) [1]	1280	450	1000	350
Channel Material	A 516	A 516	A 516	A 516
Head Material	A 516	A 516	A 516	A 516
Clad Material	Inconel	-	Inconel	Inconel
Clad Side	Head	-	Head	Head
N° Tube Passes/Shell[2]	1	1	2	2
N° of Passes /Shell[2]	1	2	2	2

Table A3.8. Inputs for Heat Exchangers CAPEX Estimation – DSW-Case (continued)

	SHX-202	SHX-301	SHX-302	SHX-501
Heat Exchange Area (m^2)[1]	91.60	91.6	62.6	660
Number of Shells[2]	2.00	2	1	2
TEMA Type[3]	NFU	NFU	BHM	NFU
Tubes Material [2]	Inconel	Inconel	SS 316	SS 316
Tubes Operation P (kPag) [1]	1749	1749	616	4849
Tubes Design P (kPag) [4]	2094	2094	786	5194
Tubes Operation T (°C) [1]	89	89	-19	18
Tubes Design T (°C) [5]	125	125	-49	22
Tubes Ext. Diameter (mm) [2]	19.1	19.05	25.4	25.4
Shell Material[2]	A 516	A 516	A 516	A 516
Shell Operation P (kPag) [1]	438	438	4899	438
Shell Design P (kPag) [4]	608	608	5244	608
Shell Operation T (°C) [1]	27	27	20	7
Shell DesignT (°C) [5]	125	125	22	22
Tubes Length (m) [2]	8.40	8.4	4.7	10.4
Tubes BWG [2]	18	18	18	18
Pitch (mm) [2]	25.4	25.4	31.7	31.7
Tubes Pattern[2]	Triangular 30°	Triangular 30°	Triangular 30°	Triangular 30°
Shell Diameter (mm) [1]	400	400	500	1000
Channel Material	A 516	A 516	A 516	A 516
Head Material	A 516	A 516	A 516	A 516
Clad Material	Inconel	Inconel	-	-
Clad Side	Head	Head	-	-
Number of Tube Passes/Shell[2]	2,00	2	6	2
Number of Passes /Shell[2]	2,00	2	4	2

Table A3.8. Inputs for Heat Exchangers CAPEX Estimation – DSW-Case (continued)

	SHX-502	SHX-601	SHX-602
Heat Exchange Area (m^2)[1]	748.7	125.8	272
Number of Shells[2]	2	1	1
TEMA Type[3]	DFU	DFU	NFU
Tubes Material [2]	SS 316	SS 316	A179
Tubes Operation P (kPag) [1]	10541	24949	6190
Tubes Design P (kPag) [4]	11068	26196	6535
Tubes Operation T (°C) [1]	102	70	149
Tubes Design T (°C) [5]	132	125	179
Tubes Ext. Diameter (mm) [2]	19.05	19.05	19.05
Shell Material[2]	A 516	A 516	A 516
Shell Operation P (kPag) [1]	438	438	438
Shell Design P (kPag) [4]	608	608	608
Shell Operation T (°C) [1]	27	27	27
Shell Design T (°C) [5]	125	125	125
Tubes Length (m) [2]	9	9	12
Tubes BWG [2]	18	16	18
Pitch (mm) [2]	25.4	25.4	25.4
Tubes Pattern[2]	Triangular 30°	Triangular 30°	Triangular 30°
Shell Diameter (mm) [1]	1050	620	780
Channel Material	316L	316L	A 516
Head Material	316L	316L	A 516
Clad Material	-	-	-
Clad Side	-	-	-
Number of Tube Passes/Shell[2]	2	2	2
Number of Passes /Shell[2]	2	2	2

[1] From simulation
[2] From Table B-3
[3] From Table B-3
[4] Calculated by Aspen Capital cost Estimator
[5] Calculated by Aspen Capital cost Estimator

Table A3.9. Inputs for Heat Exchangers SHX-603, SHX-701 CAPEX Estimation – DSW-Case

	SHX-603	SHX-701
U (W/m².K)	433	463
UA (W/K)	152561	140588
Heat Exchange Area (m²)	352.3	303.6
Number of Shells	1	1
TEMA Type	DFU	DFU
Tubes Material	SS316	SS316
Tubes Operation P (kPag)	24949	54949
Tubes Design P (kPag)	26196	57696
Tubes Operation T (°C)	150	90
Tubes Design T (°C)	180	125
Tubes Ext. Diameter (mm)	19.05	19.05
Shell Material	A516	A516
Shell Operation P (kPag)	438	438
Shell Design P (kPag)	608	608
Shell Operation T (°C)	27	27
Shell Design T (°C)	125	125
Tubes Length (m)	0	0
Tubes BWG	-	-
Pitch (mm)	-	-
Tubes Pattern	-	-
Shell Diameter (mm)	-	-
Channel Material	316L	316L
Head Material	316L	316L
Clad Material	-	-
Clad Side	-	-
Number Tube Passes/Shell	2	2
Number of Passes /Shell	2	2

Table A3.10. Inputs for Plate Heat Exchanger SHX-801 CAPEX Estimation – DSW-Case

	SHX-801
Numberof Heat Exchangers	4 + 1 spare
Heat Exchange Area (m²)[1]	1908.2
Number of Plates[1]	687
Operation P (kPag)	792.85
Design P (kPag)	963
Operation T (°C)	23.8
Design T (°C)	125
Material	titanium

[1] Heat exchange area and number of plates from Aspen Exchanger Design and Rating.

Table A3.11. Inputs for CW System Pumps CAPEX Estimation – DSW-Case

	P1	P2
Model	DCP API 610	DCP API 610
Pumps in Operation	1x100%	2x50%
Spares	1	1
Material	Carbon Steel	Steel/Copper
Flow (L/s)[1]	664.7	818.5
Head (m)[1]	36.6	75.1

[1] From Simulation

Table A3.12. Inputs for Gas Turbines CAPEX Estimation – DSW-Case

GTs in Operation[1]	3
Spares[1]	1
Design Power (kW) [1]	27017
Power Factor	0.9
Power (kVA) [2]	30019

[1] From EIA (Petrobras, 2013)
[2] Power (kVA) = Power (kW) / Power Factor

Supplement A4 – Simulation, Sizing and CAPEX Results

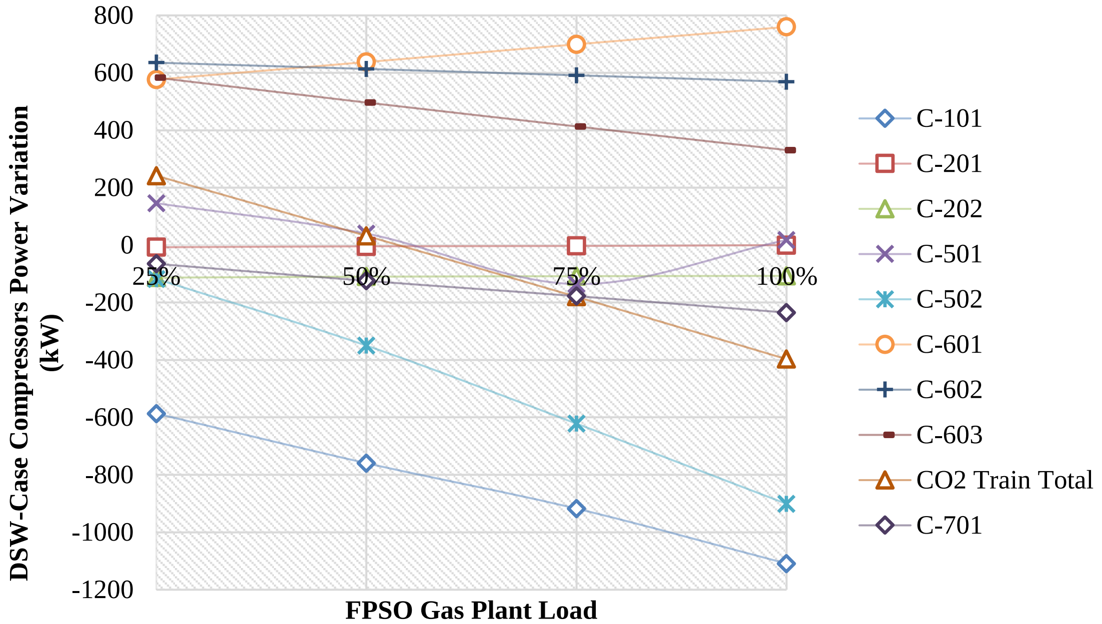

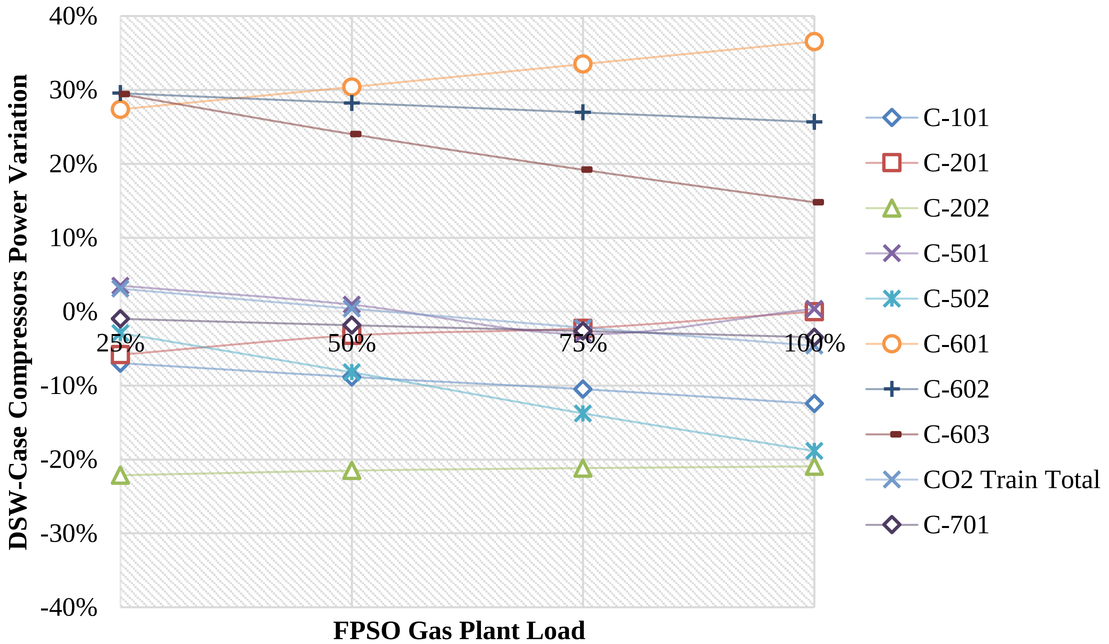

Figure A4.1. DSW-CASE compressors power reduction at partial load

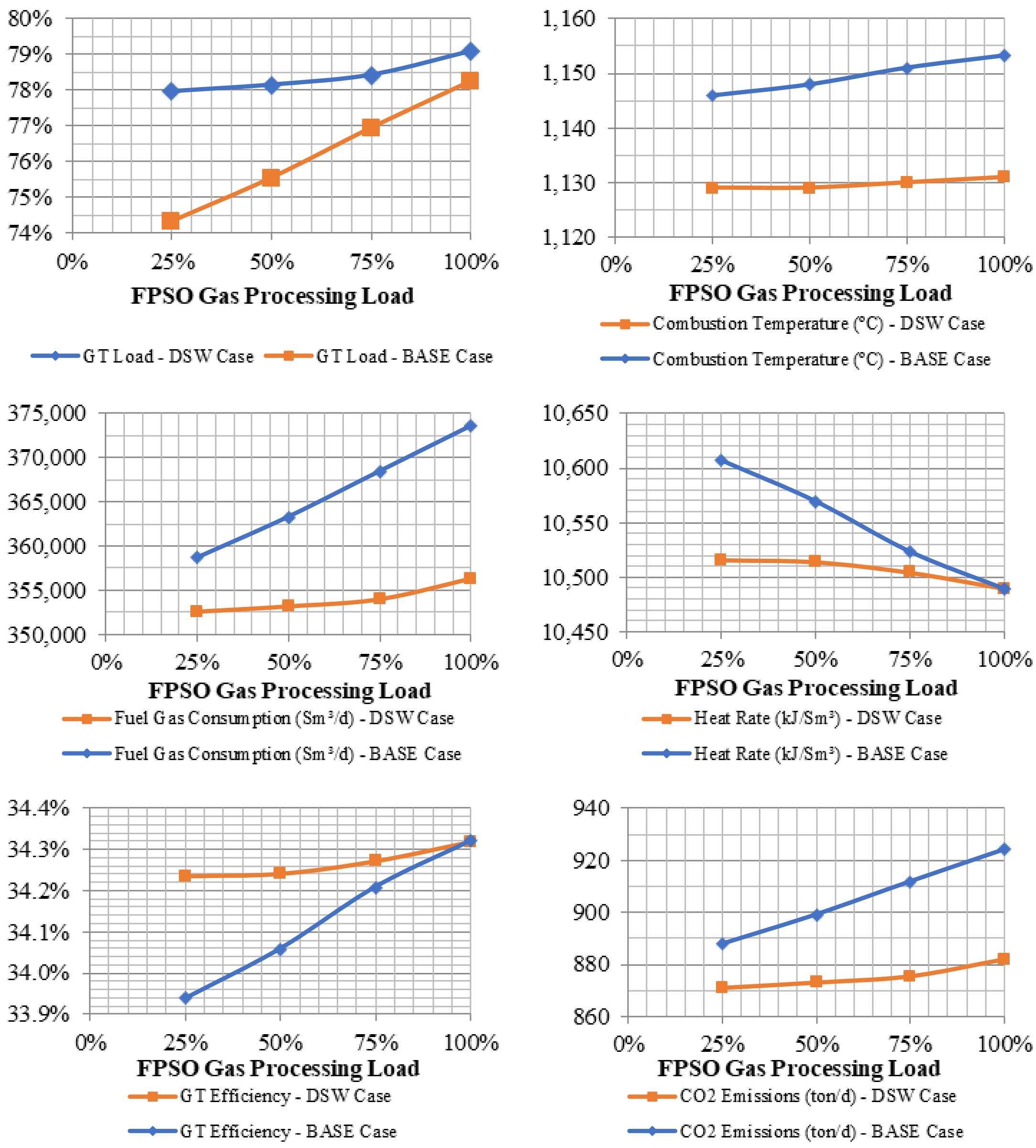

Figure A4.2. Gas turbines (GTs) performance comparison at partial load

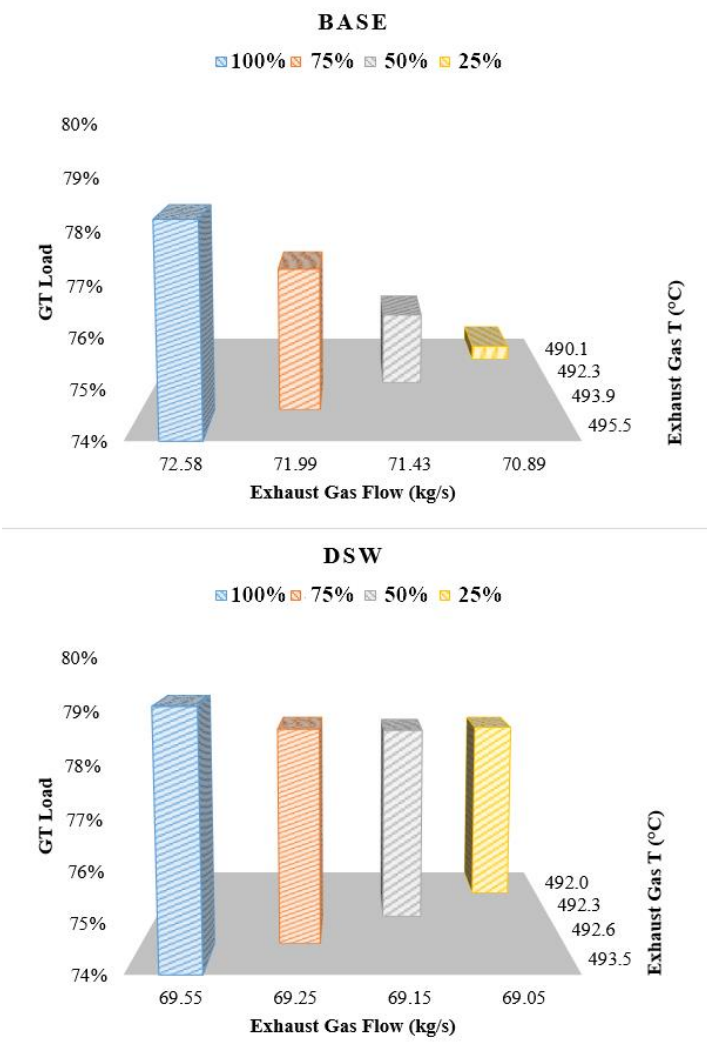

Figure A4.3. Gas turbines (GTs) load versus exhaust gas flow rate and temperature

Table A4.1. Compressors Results

CASE	BASE			DSW			
TAG	Inlet Flow (m^3/h)	Inlet T (ºC)	Power (kW)	Inlet Flow (m^3/h)	Inlet T (ºC)	Power (kW)	Power Cut
C-101	11,976	39	8,901	10,428	11	7,792	12.5%
C-201	1,239	55	137	1,239	55	137	0.0%
C-202	1,839	25	511	1,426	19	404	20.9%
C-501	2,894	29	4,596	2,894	29	4,595	0.0%
C-502	1,110	40	4,768	835	12	3,856	19.1%
C-601	12,939	30	2,080	12,888	29	2,879	-38.4%
C-602	4,728	40	2,234	2,943	12	2,866	-28.3%
C-603	1,583	40	2,301	581	12	2,718	-18.1%
C-604	466	40	2,196	-	-	-	-
C-701	313	37	7,672	313	29	7,385	3.7%
C-901	1,885	0	455	-	-	-	-
TOTAL			35,850			32,633	9.0%

Table A4.2. Heat Exchangers Results and Comparison

CASE		Q (MJ/h)			LMTD			A_0 (m^2)		
BASE	DSW	BASE	DSW	ΔQ	BASE	DSW	ΔLMTD	BASE	DSW	ΔA_0
SHX-101	SHX-101	7.43	20.7	179%	7.30	16.6	127%	588	883	50%
SHX-102	SHX-103	42.3	23.1	-45%	23.5	25.0	6%	1,093	439	-60%
SHX-201	SHX-201	1.02	1.53	51%	20.2	25.0	24%	41.0	49.2	20%
SHX-202	SHX-202	1.98	2.87	45%	12.7	16.2	27%	109	86.1	-21%
SHX-301	SHX-102	11.4	11.4	0%	7.50	60.5	712%	1,153	89.3	-92%
SHX-302	SHX-301	1.84	0.92	-50%	10.0	11.3	13%	85.7	62.6	-27%
SHX-303	SHX-302	4.57	4.87	6%	14.5	3.90	-73%	128	660	415%
SHX-501	SHX-501	24.1	37.7	57%	18.8	26.1	39%	506	749	48%
SHX-502	SHX-502	30.1	13.2	-56%	20.9	37.8	81%	564	126	-78%
SHX-601	SHX-601	7.08	12.4	75%	24.5	38.6	57%	254	277	9%
SHX-602	SHX-602	9.17	14.0	53%	28.8	36.9	28%	199	272	37%
SHX-603	SHX-603	12.0	20.2	69%	30.6	36.8	20%	203	352	73%
SHX-604	-	15.2	-	-	29.8	-	-	239	-	-
SHX-701	SHX-701	29.3	23.6	-19%	19.0	46.7	146%	683	304	-56%
SHX-801	SHX-801	131	168	28%	10.4	6.50	-37%	6,649	8,232	24%
SHX-901	-	0.20	-	-	43.5	-	-	8.60	-	-
SHX-902	-	6.22	-	-	10.0	-	-	288	-	-
	TOTAL	335	355	6%				12,791	12,581	1.6%

Table A4.3. GTs Simulation Validation against Thermoflex Results

Gas Turbines Parameters	Base-Case			DSW-Case		
(air at 23ºC and 87% RH)	HYSYS	Thermoflex	Error	HYSYS	Thermoflex	Error
Compressor Efficiency	84.2%	N/A	-	85.7%	-	-
Turbine Efficiency	88.0%	N/A	-	87.5%	-	-
Net Power (kW) (generator eff. = 97%)	25754	25780	-0.10%	24300	24337	-0.15%
Gas Inlet Flow (kg/s)	1.650	1.648	0.09%	1.571	1.571	0.03%
Air Inlet Flow(kg/s)	80.85	80.85	0.00%	77.06	77.06	0.00%
Fuel LHV (kJ/Sm^3) (from simulation)	40737	40737	0.00%	40751	40750	0.00%
Heat Rate (kJ/kWh)[1]	10017	9998	0.19%	10114	10096	0.18%
Efficiency[2]	35.9%	36.0%	0.19%	35.6%	35.7%	0.18%
Exhaust Gas Temperature (°C)	519.5	519.5	0.00%	521.9	521.9	0.00%
Fire Temperature (°C)	1196	N/A	-	1179	-	-
Exhaust Gas Flow (kg/s)	81.67	81.61	0.07%	77.85	77.83	0.02%

[1] Heat Rate = (Fuel Flow*Fuel LHV*3600) / Net Power
[2] Efficiency = 3600 / Heat Rate

Table A4.4. CW, SW and DSW Pumps: Summary of Design Results

Pump	CW P-801 (1x 100%)		Δ (%)
	BASE-CASE	DSW-CASE	
Flow (L/s)	647.7	664.7	2.6
Head (m)	36.6	36.4	-0.5
Power (kW)	307.5	315.6	2.6
Pump	SW/DSW P-802 A/B (2 x 50%)		Δ (%)
	BASE-CASE	DSW-CASE	
Flow (L/s)	564.4	818.5	31.0%
Head (m)	75.4	75.1	-0.4%
Power (kW)	553.5	802.7	31.0%
NPSH (kPa)	45	32	-28.0%

Table A4.5. Compressors: Summary of Weight Results

Compressor	Weight (t)			
	BASE-CASE	DSW-CASE	Δ	Δ (%)
C-101	74	62.6	-11.4	-15%
C-201	9.4	9.4	0.0	0%
C-202	14.4	13.2	-1.2	-8%
C-501	47.8	47.8	0.0	0%
C-502	43.4	38.6	-4.8	-11%
C-601	34.6	45.2	10.6	31%
C-602	29.2	35.0	5.8	20%
C-603	33	33.0	0.0	0%
C-604	28.6	-	-28.6	-
C-701	20.8	20.8	0.0	0%
C-901	13.8	-	-13.8	-
TOTAL	349	305.6	-43.4	-12%

Table A4.6. Heat Exchangers: Summary of Weight Results

Case		Weight (t)			
BASE	DSW	BASE-CASE	DSW-CASE	Δ	Δ (%)
SHX-101	SHX-101	34.8	60.4	25.6	74%
SHX-102	SHX-103	57.2	8.8	-48.4	-64%
SHX-201	SHX-201	2.4	20.4	18.0	33%
SHX-202	SHX-202	6.0	3.2	-2.8	-7%
SHX-301	SHX-102	120	5.6	-114.4	-93%
SHX-302	SHX-301	5.8	6.6	0.8	14%
SHX-303	SHX-302	8.2	34.0	25.8	315%
SHX-501	SHX-501	30.8	47.6	16.8	55%
SHX-502	SHX-502	48.8	13.2	-35.6	-73%
SHX-601	SHX-601	11.0	12.0	1.0	9%
SHX-602	SHX-602	9.4	13.2	3.8	40%
SHX-603	SHX-603	14.0	33.0	19.0	136%
SHX-604	-	23.6	-	-23.6	-
SHX-701	SHX-701	57.6	26.8	-30.8	-53%
SHX-801	SHX-801	86.0	102.6	16.6	14%
SHX-901	-	1.04	-	-1.0	-
SHX-902	-	12.8	-	-12.8	-
	TOTAL	529,4	387.4	-142.0	-27%

Table A4.7. CW System: Summary of Weight Results

Pumps	Weight (t)		Δ	Δ (%)
	BASE-CASE	DSW-CASE		
P-801	7.60	7.80	0.20	2.6%
P-802 A/B	10.40	13.60	3.20	30.8%
TOTAL	18.00	21.40	3.40	18.9%

Table A4.8. Compressors CAPEX Comparison

Compressor	CAPEX US$[1]		Δ (%)
	BASE-CASE	DSW-CASE	
C-101	6,741,600	5,650,400	-16.2%
C-201	1,839,700	1,839,700	0.0%
C-202	2,267,600	2,187,900	-3.5%
C-501	4,539,800	4,539,800	0.0%
C-502	4,970,100	4,608,200	-7.3%
C-601	3,458,700	4,728,600	36.7%
C-602	2,804,500	3,674,100	31.0%
C-603	3,625,000	3,964,700	9.4%
C-604	3,677,200	-	-
C-701	3,155,200	3,155,500	0.0%
C-901	2,077,400	-	-
TOTAL	39,156,800	34,348,900	-12.3%

[1] For two pieces of equipment (one spare)

Table A4.9. Heat Exchangers CAPEX Comparison

Heat Exchanger		CAPEX US$[1]		Δ (%)
		BASE-CASE	DSW-CASE	
SHX-101	SHX-101	2,568,200	3,526,400	37.3%
SHX-102	SHX-103	4,503,900	2,259,000	-49.8%
SHX-201	SHX-201	404,500	428,700	6.0%
SHX-202	SHX-202	832,400	859,800	3.3%
SHX-301	SHX-102	4,945,300	946,400	-80.9%
SHX-302	SHX-301	504,800	380,100	-24.7%
SHX-303	SHX-302	570,900	1,468,500	157.2%
SHX-501	SHX-501	2,138,300	3,047,000	42.5%
SHX-502	SHX-502	4,199,700	1,796,000	-57.2%
SHX-601	SHX-601	307,700	327,400	6.4%
SHX-602	SHX-602	255,700	384,000	50.2%
SHX-603	SHX-603	1,247,800	2,860,700	129.3%
SHX-604	-	2,799,100	-	-
SHX-701	SHX-701	4,549,500	2,694,100	-40.8%
SHX-801	SHX-801	6,594,500	8,213,300	24.5%
SHX-901	-	123,800	-	-
SHX-902	-	336,000	-	-
	TOTAL	36,882,100	29,191,400	-20.9%

[1] For two pieces of equipment (one spare)

Table A4.10. CW Pumps CAPEX Comparison

Pumps	CAPEX US$[1]		Δ (%)
	BASE-CASE	DSW-CASE	
P-801	740,700	759,500	2.5%
P-802	1,228,500	1,633,900	24.8%
TOTAL	$1,969,200	$2,393,400	17.7%

[1] For two pieces of equipment (one spare)

References of Supplement A

Boyce MP. GasTurbine Engineering Handbook. 2nd Ed. Houston: Gulf Professional Publishing; 2002.

TEMA. Standards of the Tubular Exchanger Manufacturers Association. 9th ed. Tarrytown, NY: Tubular Exchanger Manufacturers Association, INC.; 2007.

SUPPLEMENTARY MATERIALS B

Title: Exergy, Energy and Emissions Analysis of Compressors Schemes in Offshore Rigs: CO2-Rich Natural Gas Processing

Authors: Matheus de Andrade Cruz, Ofélia de Q.F. Araújo*, José Luiz de Medeiros**

**Escola de Química, Federal University of Rio de Janeiro. Av. Athos da Silveira Ramos, 149. CT, Bl. E, Ilha do Fundão, Rio de Janeiro, RJ, Brazil. CEP: 21.941-972*

Manuscript Code: JNGSE-D-20-00340

Supplement B1 – Heat Exchangers

Table B1.1. Heat Exchangers Design and Materials

	SHX-101	SHX-202	SHX-204	SHX-501	SHX-502	SHX-601	SHX-602	SHX-603	SHX-604	SHX-701	SHX-901
Heat Exchange Area (m^2)[1]	1093	41.0	108.5	505,5	563,6	254.4	198.7	203.3	239.4	683.2	266.1
Number of Shells[1]	1	1	1	2	2	1	1	2	2	2	1
TEMA Type[1]	NFU	NFU	NFU	DFU	NFU	NFU	NFU	DFU	DFU	DFU	AJL
Tubes Material [1]	Inconel	Inconel	Inconel	316LS	316LS	A179	A179	316LS	316LS	316LS	A179
Tubes Design P (kPag) [1]	5494	761	2094	11068	20500[2]	1204.05	3395	9213	20500[3]	20500[4]	608
Tubes Ext. Diameter (mm) [1]	25.4	19.05	19.05	19.05	19.05	19.05	19.05	19.05	19.05	19.05	19.05
Shell Material[1]	A 516	A 516	A 516	A 516	A 516	A 516	A 516	A 516	A516	A516	A 516
Shell Design P (kPag) [1]	608	608	608	608	608	608.0	608	608	608	608	1789
Tubes Pattern [1]	Triangular 30°	Triangular 30°	Triangular 30°	Triangular 30°	Triangular 30°	Triangular 30°	Triangular 30°	Triangular 30°	Triangular 30°	Triangular 30°	Triangular 30°
Shell Diameter (mm) [1]	1800	350	500	800	800	900	700	550	-	-	850
Channel Material	316L	316L	316L	316L	316L	A 516	A 516	316L	316L	316L	A 516
Number of Tube Passes/Shell[1]	4	2	2	2	2	2	2	2	2	2	6
Number of Passes /Shell[1]	2	2	2	2	2	2	2	2	2	2	1

Notes:

[1] From Cruz et al. (2018)

[2] Pressure limited to 20500 kPa by ACCEv10. The real design pressure of the HX-502 is 26196 kPag

[3] Pressure limited to 20500 kPa by ACCEv10. The real design pressure of the HX-604 is 26196 kPag

[4] Pressure limited to 20500 kPa by ACCEv10. The real design pressure of the HX-701 is 57696 kPag

Table B1.2. Heat Exchangers Area Estimation for Multiple Smaller Compressors in Parallel Case

SSLC	HX-102	HX-202	HX-204	HX-501	HX-502	HX-601	HX-602	HX-603	HX-604	HX-701		HX-901
Q (MJ/h)	30569	645	2405	25301	28914	7358	8997	10937	12892	25797		5679
UA (MJ/h.°C)	1846	35	165	1273	1414	295	320	383	489	1530		314
LMTD (°C)	16.6	18.4	14.6	19.9	20.4	25.0	28.1	28.5	26.3	16.9		18.1
Min. Approach (°C)	5	5	5	5	5	5	5	5	5	5		10
MSCP	**HX-102**	**HX-202**	**HX-204**	**HX-501**	**HX-502**	**HX-601**	**HX-602**	**HX-603**	**HX-604**	**HX-701 exp**	**HX-702 inj**	**HX-901**
Q (MJ/h)	15089	202	720	8748	9918	5862	7496	9594	11921	7103	14853	2788
UA (MJ/h.°C)	872	12	47	411	457	237	260	312	397	356	794	168
LMTD (°C)	17.3	16.5	15.4	21.3	21.7	24.7	28.9	30.7	30.0	19.9	18.7	16.6
Min. Approach (°C)	5	5	5	5	5	5	5	5	5	5	5	10
DIFFERENCE (SSLC-MSCP)												
$Q_{reduction}$ (MJ/h)	15480	443	1685	16554	18996	1496	1500	1343	970	18694	10944	2891
$Q_{reduction}$ (%)	50.6%	68.6%	70.1%	65.4%	65.7%	20.3%	16.7%	12.3%	7.5%	72.5%	42.4%	50.9%
LMTD (°C)	-0.75	1.90	-0.75	-1.38	-1.24	0.25	-0.76	-2.20	-3.66	-3.08	-1.85	1.45
LMTD (%)	-4.5%	10.3%	-5.2%	-7.0%	-6.1%	1.0%	-2.7%	-7.7%	-13.9%	-18.3%	-11.0%	8.0%
Q/LMTD (MJ/h.°C)	974	23	118	861	957	58	60	71	92	1174	736	146
Q/LMTD (%)	52.8%	65.0%	71.5%	67.7%	67.7%	19.5%	18.9%	18.6%	18.8%	76.7%	48.1%	46.6%
AREA												
Design Area of SSLC (m²)*	1093	41	108.5	505.5	563.6	254.4	198.7	203.3	239.4	683.2		8.64
Design Area of MSCP (m²)	516.2	14.3	30.9	163.4	182.3	204.7	161.2	165.6	194.4	159.0	354.4	4.8
Exchangers in Parallel MSCP	2	3	3	3	3	1	1	1	1	1	2	2
Total Required Area MSCP (m²)	1032	43	93	490	547	205	161	166	194	868		9
Spares (SSLC AND MSCP)	1	1	1	1	1	1	1	1	1	1	1	1
Nº of identical exchangers SSLC	2	2	2	2	2	2	2	2	2	2	2	2
Nº of identical exchangers MSCP	3	4	4	4	4	2	2	2	2	2	3	3

*from Cruz et al. (2018)

Supplement B2 – Process Simulation

B2.1. SSLC-Case

Table B2.1.1. Compressors and Pumps Simulation Power - SSLC

COMPRESSORS AND PUMPS	
C-101 Std Gas Flow (Sm³/d)	5000318
C-201 Std Gas Flow (Sm³/d)	70793
C-202 Std Gas Flow (Sm³/d)	341542
C-501 Std Gas Flow (Sm³/d)	3499879
C-502 Std Gas Flow (Sm³/d)	3499879
C-601 Std Gas Flow (Sm³/d)	1200505
C-602 Std Gas Flow (Sm³/d)	1200505
C-603 Std Gas Flow (Sm³/d)	1200505
C-604 Std Gas Flow (Sm³/d)	1200505
C-701 Std Gas Flow (Sm³/d)	4229609
C-901 Std Gas Flow (Sm³/d)	226185
C-101 Power (kW)	8223
C-201 Power (kW)	139
C-202 Power (kW)	605
C-501 Power (kW)	4635
C-502 Power (kW)	4577
C-601 Power (kW)	2123
C-602 Power (kW)	2241
C-603 Power (kW)	2238
C-604 Power (kW)	2032
C-701 Power (kW)	6744
C-901 Power (kW)	494
C-200 Total power (kW)	744
C-500 Total power (kW)	9212
C-600 Total power (kW)	8634
Compressors Total power (kW)	34050
Pumps power (kW)	481
Other users power (kW)	23164
Total drivers power (kW)	34531
Total power demand (kW)	57695
Power per GT (kW)	19232

Table B2.1.2. Gas Turbines Simulation: SSLC-Case

1000 - GAS TURBINES	
NG Mass Flow/GT (kg/s)	1.29
NG Mass Flow/GT (kg/h)	4652
NG Std Gas Flow (Sm^3/d)	118533
NG Vapour Fraction	1
NG Higher Heating Value (kJ/kg)	43500
NG Lower Heating Value (kJ/kg)	47945
NG Pressure (kPa)	3500
NG Temperature (ºC)	27.5
NG Molecular Weight	22.27
AIR Mass Flow (kg/s)	65.57
AIR Mass Flow (kg/h)	236055
AIR Std Gas Flow (Sm^3/d)	4667006
AIR INLET Pressure (kPa)	101.3
AIR INLET Temperature (ºC)	23.0
C-1001 Power (kW)	34319
T-1001 Power (kW)	54150
NET Power (kW)	19831
Net Electricity (kW -97% gen. eff.)	19237
Heat Rate (BTU/kWh)	11246
LHV Efficiency (%)	32.01
Exhaust Gas Mass Flow (kg/s)	66.19
Exhaust Gas Mass Flow (kg/h)	238299
Exhaust Gas Temperature (ºC)	518.5
Fire Temperature (ºC)	1177.5
Exhaust CO2 Comp (mole %)	3.3%
Exhaust CO2 Emissions (kg/h)	12275
Total NG Consumption (kg/h - 3 TGs)	13955
Total NG Consumption (Sm^3/h - 3 TGs)	355598
Total CO2 Emissions (kg/h - 3 TGs)	36825
GT used capacity (%)	74.62%
Power demand/GT (kW)	19232
Check Power (generated - demand) (kW)	4.8
Error ((generated - demand)/demand) (kW)	0.025%
Loss due to Gen. Efficiency (3%) (kW)	594.9

Table B2.1.3. Propane Refrigeration Cycle Simulation: SSLC-Case

900 - C3 REFRIGERATION CYCLE	
Liquid T sat (ºC)	-7
Liquid P sat (kPa)	380
Vapor T sat (ºC)	50
Vapor P sat (kPa)	1720
Stream 901 T (ºC)	-6.0
Stream 905 T (ºC)	45
Superheating (ºC)	1.0
Subcooling (ºC)	5
HX-303 ΔH (kJ/kg)	244.2
C-901 ΔH (kJ/kg)	101.1
Pot / ton refrig.	1.45
COP	2.42
Stream 901 Mass Flow (kg/h)	15977
Stream 902 std gas flow (Sm³/d)	226185
Stream 902 mass flow (kg/h)	17576
NG Inlet T (ºC)	10
NG Outlet T (ºC)	3
HX-303 Duty (kJ/h)	3902082
HX-303 BTU/h	3698393
T.R.	308
Condenser CW flow (kg/h)	131744
CW inlet T (ºC)	35
CW outlet T (ºC)	45
Condenser Duty (kJ/h)	5679369
Outlet Gas C6+ content (ppmv)	483

Table B2.1.4. Cooling-Water System Simulation: SSLC-Case

800 - COOLING WATER SYSTEM	
HX-003 Mass Flow (kg/h)	228442
HX-102 Mass Flow (kg/h)	354331
HX-201 Mass Flow (kg/h)	1843
HX-202 Mass Flow (kg/h)	7474
HX-203 Mass Flow (kg/h)	19748
HX-204 Mass Flow (kg/h)	27880
HX-501 Mass Flow (kg/h)	293281
HX-502 Mass Flow (kg/h)	335161
HX-601 Mass Flow (kg/h)	85288
HX-602 Mass Flow (kg/h)	104282
HX-603 Mass Flow (kg/h)	126772
HX-604 Mass Flow (kg/h)	149429
HX-701 Mass Flow (kg/h)	299029
HX-901 Mass Flow (kg/h)	131744
TOTAL CW INLET (kg/h)	2164705
CW OUTLET STREAM T (ºC)	35.0
SW OUTLET STREAM T (ºC)	40.0
CW INLET STREAM T (ºC)	52.7
SW INLET STREAM T (ºC)	23.0

B2.2. MPSC-Case

Table B2.2.1. Compressors and Pumps Simulation Power: MPSC-Case

COMPRESSORS AND PUMPS		
	Flow (Sm^3/d)	Power (kW)
C-101 A	2364552	4059
C-101 B	2364552	4059
C-201 A	20109	43
C-201 B	20109	43
C-201 C	20109	43
C-202 A	97030	180
C-202 B	97030	180
C-202 C	97030	180
C-501 A	1124749	1619
C-501 B	1124749	1619
C-501 C	1124749	1619
C-502 A	1124749	1584
C-502 B	1124749	1584
C-502 C	1124749	1584
C-601	968160	1707
C-602	968160	1824
C-603	968160	1864
C-604	968160	1762
C-701 A	968160	1552
C-901 A	103459	229
C-901 B	103459	229
C-100 Total	4729104	8118
C-200 Total	291090	669
C-500 Total	3374248	9607
C-600 Total	968160	7158
C-900 Total	206919	459
Compressors Total power (kW)	27562	
Pumps power (kW)	382	
Other users power (kW)	23164	
Total drivers power (kW)	27944	
Total power demand (kW)	51108	
Power per GT (kW)	25554	

Table B2.2.2. Gas Turbines Simulation: MPSC-Case

1000 - GAS TURBINES	
NG Mass Flow/GT (kg/s)	1.63
NG Mass Flow/GT (kg/h)	5873
NG Std Gas Flow (Sm³/d)	149637
NG Vapour Fraction	1
NG Higher Heating Value (kJ/kg)	43500
NG Lower Heating Value (kJ/kg)	47945
NG Pressure (kPa)	3500
NG Temperature (ºC)	27.5
NG Molecular Weight	22.27
AIR Mass Flow (kg/s)	80.10
AIR Mass Flow (kg/h)	288371
AIR Std Gas Flow (Sm³/d)	5701330
AIR INLET Pressure (kPa)	101.3
AIR INLET Temperature (ºC)	23.0
C-1001 Power (kW)	41338
T-1001 Power (kW)	67682
NET Power (kW)	26344
Net Electricity (kW -97% gen. eff.)	25554
Heat Rate (BTU/kWh)	10688
LHV Efficiency (%)	33.68
Exhaust Gas Mass Flow (kg/s)	80.92
Exhaust Gas Mass Flow (kg/h)	291300
Exhaust Gas Temperature (ºC)	519.5
Fire Temperature (ºC)	1191.8
Exhaust CO2 Comp (mole %)	3.4%
Exhaust CO2 Emissions (kg/h)	15491
Total NG Consumption (kg/h - 3 TGs)	11745
Total NG Consumption (Sm³/h - 3 TGs)	299274
Total CO2 Emissions (kg/h - 3 TGs)	30982
GT used capacity (%)	99.1%
Power demand/GT (kW)	25554
Check Power (generated - demand) (kW)	0.3
Error ((generated - demand)/demand) (kW)	0.001%
Loss due to Gen. Efficiency (3%) (kW)	790.3

Table B2.2.3. Propane Refrigeration Cycle Simulation: MPSC-Case

900 - C3 REFRIGERATION CYCLE	
Liquid T sat (ºC)	-7
Liquid P sat (kPa)	380
Vapor T sat (ºC)	50
Vapor P sat (kPa)	1720
Stream 901 T (ºC)	-6.1
Stream 905 T (ºC)	45
Superheating (ºC)	0.9
Subcooling (ºC)	5
HX-303 ΔH (kJ/kg)	244.1
C-901 ΔH (kJ/kg)	102.7
Pot / ton refrig.	1.47
COP	2.38
Stream 901 Mass Flow (kg/h)	16079
Stream 902 std gas flow (Sm^3/d)	206919
Stream 902 mass flow (kg/h)	16079
NG Inlet T (ºC)	10
NG Outlet T (ºC)	3
HX-303 Duty (kJ/h)	3925034
HX-303 BTU/h	3720148
T.R.	310
Condenser CW flow (kg/h)	64681
CW inlet T (ºC)	35
CW outlet T (ºC)	45
Condenser Duty (kJ/h)	2788247
Outlet Gas C6+ content (ppmv)	482

Table B2.2.4. Cooling-Water System Simulation: MPSC-Case

800 - COOLING WATER SYSTEM	
HX-003 Mass Flow (kg/h)	228442
HX-102 A/B Mass Flow (kg/h)	354331
HX-201 Mass Flow (kg/h)	1843
HX-202 Mass A/B/C Flow (kg/h)	7474
HX-203 Mass Flow (kg/h)	19748
HX-204 A/B/C Mass Flow (kg/h)	27880
HX-501 A/B/C Mass Flow (kg/h)	293281
HX-502 A/B/C Mass Flow (kg/h)	335161
HX-601 Mass Flow (kg/h)	85288
HX-602 Mass Flow (kg/h)	104282
HX-603 Mass Flow (kg/h)	126772
HX-604 Mass Flow (kg/h)	149429
HX-701 A Mass Flow (kg/h)	299029
HX-901 A/B Mass Flow (kg/h)	131744
TOTAL CW INLET (kg/h)	2164705
CW OUTLET STREAM T (ºC)	35.0
SW OUTLET STREAM T (ºC)	40.0
CW INLET STREAM T (ºC)	52.7
SW INLET STREAM T (ºC)	23.0

Supplement B3 – Exergy Analysis

B3.1. Determination of exergy flows of streams

- *RER-1*

Table B3.1.1 Streams exergy flow- Single-shaft compressors – 100% FPSO gas -load – RER-1

Stream	*Stream Type S/P*	*Direction In/Out*	*System*	*H (kJ/kgmol)*	*S (kJ/kgmol.K)*	*Flow (kgmol/s)*	$\sum N_k.\mu_k^0$ *(kW)*	$H\text{-}T_0S + P_0V - \sum N_k.\mu_k^0$ *(kW)*	S_K *(kW)*	*Check Ex >0*
102	S	IN	Overall Gas Plant	-123689	163.76	2.173	-2281951.7	1907850.8	-105369	OK
201	S	IN	Overall Gas Plant	-156362	183.40	0.030	-51158.7	44918.0	-1609	OK
208	S	IN	Overall Gas Plant	-176963	176.71	0.098	-173097.0	150557.8	-5144	OK
803	S	IN	Overall Gas Plant	-284622	56.26	5.463	-1646213.1	151.2	-91031	OK
805	S	IN	Overall Gas Plant	-284622	56.26	0.028	-8563.0	0.8	-474	OK
807	S	IN	Overall Gas Plant	-284622	56.26	0.115	-34726.0	3.2	-1920	OK
809	S	IN	Overall Gas Plant	-284622	56.26	0.304	-91748.2	8.4	-5073	OK
811	S	IN	Overall Gas Plant	-284622	56.26	0.430	-129531.9	11.9	-7163	OK
813	S	IN	Overall Gas Plant	-284622	56.26	4.522	-1362576.3	125.2	-75347	OK
815	S	IN	Overall Gas Plant	-284622	56.26	5.168	-1557150.0	143.0	-86106	OK
817	S	IN	Overall Gas Plant	-284622	56.26	1.315	-396246.1	36.4	-21911	OK
819	S	IN	Overall Gas Plant	-284622	56.26	1.608	-484492.7	44.5	-26791	OK
821	S	IN	Overall Gas Plant	-284622	56.26	1.955	-588977.4	54.1	-32569	OK
823	S	IN	Overall Gas Plant	-284622	56.26	2.304	-694244.5	63.8	-38390	OK
825	S	IN	Overall Gas Plant	-284622	56.26	4.611	-1389279.6	127.6	-76823	OK
827	S	IN	Overall Gas Plant	-284622	56.26	2.031	-612079.3	56.2	-33846	OK
804	S	OUT	Overall Gas Plant	-283068	61.15	5.463	-1646213.1	724.9	98948	OK
806	S	OUT	Overall Gas Plant	-284235	57.51	0.028	-8563.0	1.2	484	OK
808	S	OUT	Overall Gas Plant	-283067	61.15	0.115	-34726.0	15.4	2087	OK

810	S	OUT	Overall Gas Plant	-283846	58.74	0.304	-91748.2	20.9	5297	OK
812	S	OUT	Overall Gas Plant	-283068	61.15	0.430	-129531.9	57.0	7786	OK
814	S	OUT	Overall Gas Plant	-283068	61.15	4.522	-1362576.3	600.0	81900	OK
816	S	OUT	Overall Gas Plant	-283068	61.15	5.168	-1557150.0	685.7	93595	OK
818	S	OUT	Overall Gas Plant	-283068	61.15	1.315	-396246.1	174.5	23817	OK
820	S	OUT	Overall Gas Plant	-283068	61.15	1.608	-484492.7	213.4	29121	OK
822	S	OUT	Overall Gas Plant	-283068	61.15	1.955	-588977.4	259.4	35401	OK
824	S	OUT	Overall Gas Plant	-283068	61.15	2.304	-694244.5	305.7	41729	OK
826	S	OUT	Overall Gas Plant	-283068	61.15	4.611	-1389279.6	611.8	83505	OK
828	S	OUT	Overall Gas Plant	-283846	58.74	2.031	-612079.3	139.7	35340	OK
510	S	OUT	Overall Gas Plant	-99659	134.20	1.624	-1891287.2	1664873.1	64552	OK
402	S	OUT	Overall Gas Plant	-96058	156.34	0.174	-202695.8	177915.9	8059	OK
705	S	OUT	Overall Gas Plant	-245894	118.13	0.474	-332775.6	199653.4	16581	OK
1101	S	OUT	Overall Gas Plant	-285888	52.58	0.000	-67.6	0.0	3	OK
1102	S	OUT	Overall Gas Plant	-284367	57.17	0.000	-50.2	0.0	3	OK
1103	S	OUT	Overall Gas Plant	-180135	87.06	0.025	-78540.9	73445.3	638	OK
1104	S	OUT	Overall Gas Plant	-286955	49.90	0.003	-783.2	0.6	38	OK
1105	S	OUT	Overall Gas Plant	-286501	49.58	0.001	-234.8	0.1	11	OK
1106	S	OUT	Overall Gas Plant	-122967	80.40	0.000	0.0	0.0	0	OK
1107	S	OUT	Overall Gas Plant	-127699	118.00	0.000	0.0	0.0	0	OK
1108	S	OUT	Overall Gas Plant	-97645	145.67	0.000	0.0	0.0	0	OK
1109	S	OUT	Overall Gas Plant	-239637	172.98	0.000	0.0	0.0	0	OK
1110	S	OUT	Overall Gas Plant	-239613	164.78	0.000	0.0	0.0	0	OK
1111	S	OUT	Overall Gas Plant	-240373	154.22	0.000	0.0	0.0	0	OK
1112	S	OUT	Overall Gas Plant	-242403	140.59	0.000	0.0	0.0	0	OK
C-101_P	P	IN	Overall Gas Plant					8222.8	0	OK
C-201_P	P	IN	Overall Gas Plant					139.0	0	OK
C-202_P	P	IN	Overall Gas Plant					604.8	0	OK
C-501_P	P	IN	Overall Gas Plant					4635.3	0	OK
C-502_P	P	IN	Overall Gas Plant					4576.7	0	OK
C-601_P	P	IN	Overall Gas Plant					2122.9	0	OK

C-602_P	P	IN	Overall Gas Plant					2241.1	0	OK
C-603_P	P	IN	Overall Gas Plant					2237.8	0	OK
C-604_P	P	IN	Overall Gas Plant					2031.7	0	OK
C-701_P	P	IN	Overall Gas Plant					6744.0	0	OK
C-901_P	P	IN	Overall Gas Plant					493.8	0	OK
1208	S	IN	Overall Gas Plant	-277139	77.42	0.767	-231168.6	955.8	-17590	OK
1209	S	OUT	Overall Gas Plant	-277945	75.40	0.767	-231168.6	796.7	17131	OK
102	S	IN	GAS+TG+CW	-123689	163.76	2.173	-2281951.7	1907850.8	-105369	OK
201	S	IN	GAS+TG+CW	-156362	183.40	0.030	-51158.7	44918.0	-1609	OK
208	S	IN	GAS+TG+CW	-176963	176.71	0.098	-173097.0	150557.8	-5144	OK
510	S	OUT	GAS+TG+CW	-99659	134.20	1.624	-1891287.2	1664873.1	64552	OK
705	S	OUT	GAS+TG+CW	-245894	118.13	0.474	-332775.6	199653.4	16581	OK
1101	S	OUT	GAS+TG+CW	-285888	52.58	0.000	-67.6	0.0	3	OK
1102	S	OUT	GAS+TG+CW	-284367	57.17	0.000	-50.2	0.0	3	OK
1103	S	OUT	GAS+TG+CW	-180135	87.06	0.025	-78540.9	73445.3	638	OK
1104	S	OUT	GAS+TG+CW	-286955	49.90	0.003	-783.2	0.6	38	OK
1105	S	OUT	GAS+TG+CW	-286501	49.58	0.001	-234.8	0.1	11	OK
1106	S	OUT	GAS+TG+CW	-122967	80.40	0.000	0.0	0.0	0	OK
1107	S	OUT	GAS+TG+CW	-127699	118.00	0.000	0.0	0.0	0	OK
1108	S	OUT	GAS+TG+CW	-97645	145.67	0.000	0.0	0.0	0	OK
1109	S	OUT	GAS+TG+CW	-239637	172.98	0.000	0.0	0.0	0	OK
1110	S	OUT	GAS+TG+CW	-239613	164.78	0.000	0.0	0.0	0	OK
1111	S	OUT	GAS+TG+CW	-240373	154.22	0.000	0.0	0.0	0	OK
1112	S	OUT	GAS+TG+CW	-242403	140.59	0.000	0.0	0.0	0	OK
1003-A	S	IN	GAS+TG+CW	-6020	164.49	2.285	-125039.0	0.0	-111286	OK
1003-A	S	IN	GAS+TG+CW	-6020	164.49	2.285	-125039.0	0.0	-111286	OK
1003-A	S	IN	GAS+TG+CW	-6020	164.49	2.285	-125039.0	0.0	-111286	OK
1009-A	S	OUT	GAS+TG+CW	-19509	192.30	2.329	-190682.2	12623.1	132626	OK
1009-A	S	OUT	GAS+TG+CW	-19509	192.30	2.329	-190682.2	12623.1	132626	OK
1009-A	S	OUT	GAS+TG+CW	-19509	192.30	2.329	-190682.2	12623.1	132626	OK
1010-A	S	OUT	GAS+TG+CW	-16646	196.12	0.024	-1926.1	168.2	1366	OK

1010-A	S	OUT	GAS+TG+CW	-16646	196.12	0.024	-1926.1	168.2	1366	OK
1010-A	S	OUT	GAS+TG+CW	-16646	196.12	0.024	-1926.1	168.2	1366	OK
1201-A	S	IN	GAS+TG+CW	-278742	73.33	4.158	-1252981.4	3543.6	-90311	OK
1201-A	S	IN	GAS+TG+CW	-278742	73.33	4.158	-1252981.4	3543.6	-90311	OK
1201-A	S	IN	GAS+TG+CW	-278742	73.33	4.158	-1252981.4	3543.6	-90311	OK
1204	S	OUT	GAS+TG+CW	-277139	77.42	6.193	-1866058.4	7715.2	141991	OK
1206	S	OUT	GAS+TG+CW	-277139	77.42	5.515	-1661717.3	6870.4	126442	OK
1209	S	OUT	GAS+TG+CW	-277945	75.40	0.767	-231168.6	796.7	17131	OK
1303-A	S	IN	GAS+TG+CW	-285558	53.18	17.466	-5262603.5	81.4	-275068	OK
1303-B	S	IN	GAS+TG+CW	-285558	53.18	17.466	-5262603.5	81.4	-275068	OK
1306	S	OUT	GAS+TG+CW	-284236	57.51	34.931	-10525207.1	1525.4	594950	OK
835	S	OUT	GAS+TG+CW	-284620	56.27	3.522	-1061333.6	98.1	58695	OK
802	S	IN	GAS+TG+CW	-284234	57.51	3.522	-1061333.6	157.6	-59995	OK
Other users	P	OUT	GAS+TG+CW					23164.0	0	OK
Gen Loss	P	OUT	GAS+TG+CW					594.9	0	OK
Gen Loss	P	OUT	GAS+TG+CW					594.9	0	OK
Gen Loss	P	OUT	GAS+TG+CW					594.9	0	OK
1003-A	S	IN	1000-GT	-6020	164.49	2.285	-125039.0	0.0	-111286	OK
1003-A	S	IN	1000-GT	-6020	164.49	2.285	-125039.0	0.0	-111286	OK
1003-A	S	IN	1000-GT	-6020	164.49	2.285	-125039.0	0.0	-111286	OK
1002-A	S	IN	1000-GT	-96058	158.13	0.058	-67565.3	59274.5	-2717	OK
1002-A	S	IN	1000-GT	-96058	158.13	0.058	-67565.3	59274.5	-2717	OK
1002-A	S	IN	1000-GT	-96058	158.13	0.058	-67565.3	59274.5	-2717	OK
1009-A	S	OUT	1000-GT	-19509	192.30	2.329	-190682.2	12623.1	132626	OK
1009-A	S	OUT	1000-GT	-19509	192.30	2.329	-190682.2	12623.1	132626	OK
1009-A	S	OUT	1000-GT	-19509	192.30	2.329	-190682.2	12623.1	132626	OK
1010-A	S	OUT	1000-GT	-16646	196.12	0.024	-1926.1	168.2	1366	OK
1010-A	S	OUT	1000-GT	-16646	196.12	0.024	-1926.1	168.2	1366	OK
1010-A	S	OUT	1000-GT	-16646	196.12	0.024	-1926.1	168.2	1366	OK
C1001A	P	IN	1000-GT					34318.9	0	OK

C1001A	P	IN	1000-GT					34318.9	0	OK
C1001A	P	IN	1000-GT					34318.9	0	OK
T1001A	P	OUT	1000-GT					54150.4	0	OK
T1001A	P	OUT	1000-GT					54150.4	0	OK
T1001A	P	OUT	1000-GT					54150.4	0	OK
1201-A	S	IN	1000-GT	-278742	73.33	4.158	-1252981.4	3543.6	-90311	OK
1201-A	S	IN	1000-GT	-278742	73.33	4.158	-1252981.4	3543.6	-90311	OK
1201-A	S	IN	1000-GT	-278742	73.33	4.158	-1252981.4	3543.6	-90311	OK
1202-A	S	OUT	1000-GT	-277139	77.42	4.158	-1252981.4	5180.5	95341	OK
1202-A	S	OUT	1000-GT	-277139	77.42	4.158	-1252981.4	5180.5	95341	OK
1202-A	S	OUT	1000-GT	-277139	77.42	4.158	-1252981.4	5180.5	95341	OK
1303-A	S	IN	800-CW System	-285558	53.18	17.466	-5262603.5	81.4	-275068	OK
1303-B	S	IN	800-CW System	-285558	53.18	17.466	-5262603.5	81.4	-275068	OK
830	S	IN	800-CW System	-283242	60.61	33.378	-10057161.8	4037.5	-599089	OK
1306	S	OUT	800-CW System	-284236	57.51	34.931	-10525207.1	1525.4	594950	OK
832	S	OUT	800-CW System	-284615	56.26	33.378	-10057161.8	1145.6	556141	OK
P-802A	P	IN	800-CW System					74.3	0	OK
P-802B	P	IN	800-CW System					74.3	0	OK
P-801	P	IN	800-CW System					185.7	0	OK

Table B3.1.2. Streams exergy flow- Single-shaft compressors – 50% FPSO gas load – RER-1

Stream	*Stream Type S/P*	*Direction In/Out*	*System*	*H (kJ/kgmol)*	*S (kJ/kgmol.K)*	*Flow (kgmol/s)*	$\sum N_k.\mu_k^0$ *(kW)*	$H-T_0S+P_0V-\sum Nk.\mu_k^0$ *(kW)*	S_K *(kW)*	*Check Ex >0*
102	S	IN	Overall Gas Plant	-146519	164.81	1.298	-1321446.9	1067969.5	-63338	OK
201	S	IN	Overall Gas Plant	-178368	183.66	0.016	-26695.9	22925.0	-881	OK
208	S	IN	Overall Gas Plant	-204760	176.13	0.046	-74560.7	62658.7	-2416	OK
803	S	IN	Overall Gas Plant	-284622	56.26	5.843	-1760425.3	161.7	-97347	OK
805	S	IN	Overall Gas Plant	-284622	56.26	0.040	-12180.4	1.1	-674	OK
807	S	IN	Overall Gas Plant	-284622	56.26	0.103	-31057.8	2.9	-1717	OK
809	S	IN	Overall Gas Plant	-284622	56.26	0.132	-39764.9	3.7	-2199	OK
811	S	IN	Overall Gas Plant	-284622	56.26	0.340	-102381.6	9.4	-5661	OK
813	S	IN	Overall Gas Plant	-284622	56.26	3.392	-1022120.6	93.9	-56520	OK
815	S	IN	Overall Gas Plant	-284622	56.26	3.648	-1099152.0	101.0	-60780	OK
817	S	IN	Overall Gas Plant	-284622	56.26	1.290	-388600.7	35.7	-21489	OK
819	S	IN	Overall Gas Plant	-284622	56.26	1.586	-477876.2	43.9	-26425	OK
821	S	IN	Overall Gas Plant	-284622	56.26	1.899	-572142.2	52.6	-31638	OK
823	S	IN	Overall Gas Plant	-284622	56.26	2.167	-652824.6	60.0	-36099	OK
825	S	IN	Overall Gas Plant	-284622	56.26	4.376	-1318543.4	121.1	-72912	OK
827	S	IN	Overall Gas Plant	-284622	56.26	1.703	-513218.8	47.1	-28380	OK
804	S	OUT	Overall Gas Plant	-283068	61.15	5.843	-1760425.3	775.2	105813	OK
806	S	OUT	Overall Gas Plant	-284235	57.51	0.040	-12180.4	1.8	689	OK
808	S	OUT	Overall Gas Plant	-283067	61.15	0.103	-31057.8	13.8	1867	OK
810	S	OUT	Overall Gas Plant	-283846	58.74	0.132	-39764.9	9.1	2296	OK
812	S	OUT	Overall Gas Plant	-283068	61.15	0.340	-102381.6	45.1	6154	OK
814	S	OUT	Overall Gas Plant	-283068	61.15	3.392	-1022120.6	450.1	61436	OK
816	S	OUT	Overall Gas Plant	-283068	61.15	3.648	-1099152.0	484.0	66066	OK
818	S	OUT	Overall Gas Plant	-283068	61.15	1.290	-388600.7	171.1	23357	OK
820	S	OUT	Overall Gas Plant	-283068	61.15	1.586	-477876.2	210.4	28724	OK
822	S	OUT	Overall Gas Plant	-283068	61.15	1.899	-572142.2	252.0	34390	OK

824	S	OUT	Overall Gas Plant	-283068	61.15	2.167	-652824.6	287.5	39239	OK
826	S	OUT	Overall Gas Plant	-283068	61.15	4.376	-1318543.4	580.6	79253	OK
828	S	OUT	Overall Gas Plant	-283846	58.74	1.703	-513218.8	117.1	29632	OK
510	S	OUT	Overall Gas Plant	-100232	134.01	0.760	-899225.2	792870.0	30167	OK
402	S	OUT	Overall Gas Plant	-96657	155.92	0.167	-197235.7	173422.3	7698	OK
705	S	OUT	Overall Gas Plant	-273140	115.63	0.414	-273791.9	146509.9	14180	OK
1101	S	OUT	Overall Gas Plant	-285676	53.53	0.001	-175.4	0.0	9	OK
1102	S	OUT	Overall Gas Plant	-284732	56.03	0.000	-99.7	0.0	5	OK
1103	S	OUT	Overall Gas Plant	-180790	86.07	0.016	-51431.5	48151.2	405	OK
1104	S	OUT	Overall Gas Plant	-287076	50.34	0.002	-599.4	0.5	30	OK
1105	S	OUT	Overall Gas Plant	-286416	49.88	0.001	-158.6	0.1	8	OK
1106	S	OUT	Overall Gas Plant	-118741	94.93	0.000	0.0	0.0	0	OK
1107	S	OUT	Overall Gas Plant	-132940	108.54	0.000	0.0	0.0	0	OK
1108	S	OUT	Overall Gas Plant	-99269	141.93	0.000	0.0	0.0	0	OK
1109	S	OUT	Overall Gas Plant	-266265	171.66	0.000	0.0	0.0	0	OK
1110	S	OUT	Overall Gas Plant	-266266	163.39	0.000	0.0	0.0	0	OK
1111	S	OUT	Overall Gas Plant	-267244	152.16	0.000	0.0	0.0	0	OK
1112	S	OUT	Overall Gas Plant	-269677	137.26	0.000	0.0	0.0	0	OK
C-101_P	P	IN	Overall Gas Plant					8313.4	0	OK
C-201_P	P	IN	Overall Gas Plant					136.5	0	OK
C-202_P	P	IN	Overall Gas Plant					603.1	0	OK
C-501_P	P	IN	Overall Gas Plant					4196.2	0	OK
C-502_P	P	IN	Overall Gas Plant					4027.6	0	OK
C-601_P	P	IN	Overall Gas Plant					2109.2	0	OK
C-602_P	P	IN	Overall Gas Plant					2219.4	0	OK
C-603_P	P	IN	Overall Gas Plant					2159.1	0	OK
C-604_P	P	IN	Overall Gas Plant					1846.1	0	OK
C-701_P	P	IN	Overall Gas Plant					6438.8	0	OK
C-901_P	P	IN	Overall Gas Plant					574.5	0	OK
1208	S	IN	Overall Gas Plant	-277139	77.42	0.457	-137799.6	569.7	-10485	OK
1209	S	OUT	Overall Gas Plant	-277945	75.40	0.457	-137799.6	474.9	10212	OK

102	S	IN	GAS+TG+CW	-146519	164.81	1.298	-1321446.9	1067969.5	-63338	OK
201	S	IN	GAS+TG+CW	-178368	183.66	0.016	-26695.9	22925.0	-881	OK
208	S	IN	GAS+TG+CW	-204760	176.13	0.046	-74560.7	62658.7	-2416	OK
510	S	OUT	GAS+TG+CW	-100232	134.01	0.760	-899225.2	792870.0	30167	OK
705	S	OUT	GAS+TG+CW	-273140	115.63	0.414	-273791.9	146509.9	14180	OK
1101	S	OUT	GAS+TG+CW	-285676	53.53	0.001	-175.4	0.0	9	OK
1102	S	OUT	GAS+TG+CW	-284732	56.03	0.000	-99.7	0.0	5	OK
1103	S	OUT	GAS+TG+CW	-180790	86.07	0.016	-51431.5	48151.2	405	OK
1104	S	OUT	GAS+TG+CW	-287076	50.34	0.002	-599.4	0.5	30	OK
1105	S	OUT	GAS+TG+CW	-286416	49.88	0.001	-158.6	0.1	8	OK
1106	S	OUT	GAS+TG+CW	-118741	94.93	0.000	0.0	0.0	0	OK
1107	S	OUT	GAS+TG+CW	-132940	108.54	0.000	0.0	0.0	0	OK
1108	S	OUT	GAS+TG+CW	-99269	141.93	0.000	0.0	0.0	0	OK
1109	S	OUT	GAS+TG+CW	-266265	171.66	0.000	0.0	0.0	0	OK
1110	S	OUT	GAS+TG+CW	-266266	163.39	0.000	0.0	0.0	0	OK
1111	S	OUT	GAS+TG+CW	-267244	152.16	0.000	0.0	0.0	0	OK
1112	S	OUT	GAS+TG+CW	-269677	137.26	0.000	0.0	0.0	0	OK
1003-A	S	IN	GAS+TG+CW	-6020	164.49	2.223	-121685.1	0.0	-108301	OK
1003-A	S	IN	GAS+TG+CW	-6020	164.49	2.223	-121685.1	0.0	-108301	OK
1003-A	S	IN	GAS+TG+CW	-6020	164.49	2.223	-121685.1	0.0	-108301	OK
1009-A	S	OUT	GAS+TG+CW	-19578	192.21	2.266	-185559.9	12203.3	128991	OK
1009-A	S	OUT	GAS+TG+CW	-19578	192.21	2.266	-185559.9	12203.3	128991	OK
1009-A	S	OUT	GAS+TG+CW	-19578	192.21	2.266	-185559.9	12203.3	128991	OK
1010-A	S	OUT	GAS+TG+CW	-16636	196.14	0.023	-1874.3	163.9	1330	OK
1010-A	S	OUT	GAS+TG+CW	-16636	196.14	0.023	-1874.3	163.9	1330	OK
1010-A	S	OUT	GAS+TG+CW	-16636	196.14	0.023	-1874.3	163.9	1330	OK
1201-A	S	IN	GAS+TG+CW	-278742	73.33	4.158	-1252981.4	3543.6	-90311	OK
1201-A	S	IN	GAS+TG+CW	-278742	73.33	4.158	-1252981.4	3543.6	-90311	OK
1201-A	S	IN	GAS+TG+CW	-278742	73.33	4.158	-1252981.4	3543.6	-90311	OK
1204	S	OUT	GAS+TG+CW	-277139	77.42	2.623	-790324.3	3267.6	60137	OK
1206	S	OUT	GAS+TG+CW	-277139	77.42	9.395	-2830820.5	11704.0	215401	OK

1209	S	OUT	GAS+TG+CW	-277945	75.40	0.457	-137799.6	474.9	10212	OK
1303-A	S	IN	GAS+TG+CW	-285558	53.18	15.652	-4716189.7	73.5	-246509	OK
1303-B	S	IN	GAS+TG+CW	-285558	53.18	15.652	-4716189.7	73.5	-246509	OK
1306	S	OUT	GAS+TG+CW	-284236	57.51	31.304	-9432379.3	1367.2	533179	OK
835	S	OUT	GAS+TG+CW	-284620	56.27	3.650	-1099717.2	102.0	60817	OK
802	S	IN	GAS+TG+CW	-284234	57.51	3.650	-1099717.2	163.3	-62164	OK
Other users	P	OUT	GAS+TG+CW					23164.0	0	OK
Gen Loss	P	OUT	GAS+TG+CW					579.7	0	OK
Gen Loss	P	OUT	GAS+TG+CW					579.7	0	OK
Gen Loss	P	OUT	GAS+TG+CW					579.7	0	OK
1003-A	S	IN	1000-GT	-6020	164.49	2.223	-121685.1	0.0	-108301	OK
1003-A	S	IN	1000-GT	-6020	164.49	2.223	-121685.1	0.0	-108301	OK
1003-A	S	IN	1000-GT	-6020	164.49	2.223	-121685.1	0.0	-108301	OK
1002-A	S	IN	1000-GT	-96657	157.69	0.056	-65745.2	57778.2	-2595	OK
1002-A	S	IN	1000-GT	-96657	157.69	0.056	-65745.2	57778.2	-2595	OK
1002-A	S	IN	1000-GT	-96657	157.69	0.056	-65745.2	57778.2	-2595	OK
1009-A	S	OUT	1000-GT	-19578	192.21	2.266	-185559.9	12203.3	128991	OK
1009-A	S	OUT	1000-GT	-19578	192.21	2.266	-185559.9	12203.3	128991	OK
1009-A	S	OUT	1000-GT	-19578	192.21	2.266	-185559.9	12203.3	128991	OK
1010-A	S	OUT	1000-GT	-16636	196.14	0.023	-1874.3	163.9	1330	OK
1010-A	S	OUT	1000-GT	-16636	196.14	0.023	-1874.3	163.9	1330	OK
1010-A	S	OUT	1000-GT	-16636	196.14	0.023	-1874.3	163.9	1330	OK
C1001A	P	IN	1000-GT					33398.4	0	OK
C1001A	P	IN	1000-GT					33398.4	0	OK
C1001A	P	IN	1000-GT					33398.4	0	OK
T1001A	P	OUT	1000-GT					52722.4	0	OK
T1001A	P	OUT	1000-GT					52722.4	0	OK
T1001A	P	OUT	1000-GT					52722.4	0	OK
1201-A	S	IN	1000-GT	-278742	73.33	4.158	-1252981.4	3543.6	-90311	OK

1201-A	S	IN	1000-GT	-278742	73.33	4.158	-1252981.4	3543.6	-90311	OK
1201-A	S	IN	1000-GT	-278742	73.33	4.158	-1252981.4	3543.6	-90311	OK
1202-A	S	OUT	1000-GT	-277139	77.42	4.158	-1252981.4	5180.5	95341	OK
1202-A	S	OUT	1000-GT	-277139	77.42	4.158	-1252981.4	5180.5	95341	OK
1202-A	S	OUT	1000-GT	-277139	77.42	4.158	-1252981.4	5180.5	95341	OK
1303-A	S	IN	800-CW System	-285558	53.18	15.652	-4716189.7	73.5	-246509	OK
1303-B	S	IN	800-CW System	-285558	53.18	15.652	-4716189.7	73.5	-246509	OK
830	S	IN	800-CW System	-283253	60.57	30.168	-9090005.8	3621.1	-541158	OK
1306	S	OUT	800-CW System	-284236	57.51	31.304	-9432379.3	1367.2	533179	OK
832	S	OUT	800-CW System	-284615	56.26	30.168	-9090005.8	1035.4	502658	OK
P-802A	P	IN	800-CW System					66.0	0	OK
P-802B	P	IN	800-CW System					66.0	0	OK
P-801	P	IN	800-CW System					163.7	0	OK

Table B3.1.3. Streams exergy flow- Single-shaft compressors – 25% FPSO gas load – RER-1

Stream	*Stream Type S/P*	*Direction In/Out*	*System*	*H (kJ/kgmol)*	*S (kJ/kgmol.K)*	*Flow (kgmol/s)*	*$\sum N_k.\mu_k^0$ (kW)*	*$H-T_0S+P_0V-\sum N_k.\mu_k^0$ (kW)*	*S_K (kW)*	*Check Ex >0*
102	S	IN	Overall Gas Plant	-193477	164.61	0.581	-536568.9	395934.5	-28303	OK
201	S	IN	Overall Gas Plant	-225649	181.98	0.006	-7996.2	6352.3	-317	OK
208	S	IN	Overall Gas Plant	-254181	174.38	0.019	-25648.8	19752.7	-996	OK
803	S	IN	Overall Gas Plant	-284622	56.26	5.658	-1704929.6	156.6	-94278	OK
805	S	IN	Overall Gas Plant	-284622	56.26	0.006	-1714.2	0.2	-95	OK
807	S	IN	Overall Gas Plant	-284622	56.26	0.094	-28201.7	2.6	-1559	OK
809	S	IN	Overall Gas Plant	-284622	56.26	0.046	-13809.6	1.3	-764	OK
811	S	IN	Overall Gas Plant	-284622	56.26	0.338	-101853.6	9.4	-5632	OK
813	S	IN	Overall Gas Plant	-284622	56.26	2.702	-814069.2	74.8	-45016	OK
815	S	IN	Overall Gas Plant	-284622	56.26	2.584	-778458.4	71.5	-43047	OK
817	S	IN	Overall Gas Plant	-284622	56.26	1.261	-380016.5	34.9	-21014	OK
819	S	IN	Overall Gas Plant	-284622	56.26	1.523	-458840.6	42.1	-25373	OK
821	S	IN	Overall Gas Plant	-284622	56.26	1.702	-512874.3	47.1	-28360	OK
823	S	IN	Overall Gas Plant	-284622	56.26	1.749	-526925.7	48.4	-29137	OK
825	S	IN	Overall Gas Plant	-284622	56.26	4.031	-1214669.5	111.6	-67168	OK
827	S	IN	Overall Gas Plant	-284622	56.26	1.730	-521244.5	47.9	-28823	OK
804	S	OUT	Overall Gas Plant	-283068	61.15	5.658	-1704929.6	750.8	102478	OK
806	S	OUT	Overall Gas Plant	-284235	57.51	0.006	-1714.2	0.2	97	OK
808	S	OUT	Overall Gas Plant	-283067	61.15	0.094	-28201.7	12.5	1695	OK
810	S	OUT	Overall Gas Plant	-283846	58.74	0.046	-13809.6	3.2	797	OK
812	S	OUT	Overall Gas Plant	-283068	61.15	0.338	-101853.6	44.9	6122	OK
814	S	OUT	Overall Gas Plant	-283068	61.15	2.702	-814069.2	358.5	48931	OK
816	S	OUT	Overall Gas Plant	-283068	61.15	2.584	-778458.4	342.8	46791	OK
818	S	OUT	Overall Gas Plant	-283068	61.15	1.261	-380016.5	167.3	22842	OK
820	S	OUT	Overall Gas Plant	-283068	61.15	1.523	-458840.6	202.1	27579	OK
822	S	OUT	Overall Gas Plant	-283068	61.15	1.702	-512874.3	225.9	30827	OK

824	S	OUT	Overall Gas Plant	-283068	61.15	1.749	-526925.7	232.0	31672	OK
826	S	OUT	Overall Gas Plant	-283068	61.15	4.031	-1214669.5	534.9	73010	OK
828	S	OUT	Overall Gas Plant	-283846	58.74	1.730	-521244.5	119.0	30096	OK
510	S	OUT	Overall Gas Plant	-100257	134.26	0.145	-170754.8	150458.6	5763	OK
402	S	OUT	Overall Gas Plant	-97821	154.85	0.158	-192265.0	169550.5	7250	OK
705	S	OUT	Overall Gas Plant	-309848	111.68	0.289	-175364.1	76147.5	9570	OK
1101	S	OUT	Overall Gas Plant	-286104	52.78	0.001	-326.1	0.1	17	OK
1102	S	OUT	Overall Gas Plant	-284945	55.42	0.000	-28.3	0.0	2	OK
1103	S	OUT	Overall Gas Plant	-192339	87.03	0.005	-18581.5	17396.6	140	OK
1104	S	OUT	Overall Gas Plant	-287549	50.63	0.001	-207.0	0.2	10	OK
1105	S	OUT	Overall Gas Plant	-286423	49.85	0.000	-80.9	0.0	4	OK
1106	S	OUT	Overall Gas Plant	-83662	201.20	0.000	0.0	0.0	0	OK
1107	S	OUT	Overall Gas Plant	-130193	106.31	0.006	-12628.2	11685.2	184	OK
1108	S	OUT	Overall Gas Plant	-100086	139.52	0.000	0.0	0.0	0	OK
1109	S	OUT	Overall Gas Plant	-302035	169.53	0.000	0.0	0.0	0	OK
1110	S	OUT	Overall Gas Plant	-302152	160.91	0.000	0.0	0.0	0	OK
1111	S	OUT	Overall Gas Plant	-303646	147.99	0.000	0.0	0.0	0	OK
1112	S	OUT	Overall Gas Plant	-306947	130.49	0.000	0.0	0.0	0	OK
C-101_P	P	IN	Overall Gas Plant					8161.0	0	OK
C-201_P	P	IN	Overall Gas Plant					138.2	0	OK
C-202_P	P	IN	Overall Gas Plant					612.2	0	OK
C-501_P	P	IN	Overall Gas Plant					3970.1	0	OK
C-502_P	P	IN	Overall Gas Plant					3702.3	0	OK
C-601_P	P	IN	Overall Gas Plant					2091.4	0	OK
C-602_P	P	IN	Overall Gas Plant					2174.0	0	OK
C-603_P	P	IN	Overall Gas Plant					1979.2	0	OK
C-604_P	P	IN	Overall Gas Plant					1484.6	0	OK
C-701_P	P	IN	Overall Gas Plant					6032.8	0	OK
C-901_P	P	IN	Overall Gas Plant					1005.6	0	OK
1208	S	IN	Overall Gas Plant	-277139	77.42	0.208	-62806.1	259.7	-4779	OK
1209	S	OUT	Overall Gas Plant	-277945	75.40	0.208	-62806.1	216.5	4654	OK

102	S	IN	GAS+TG+CW	-193477	164.61	0.581	-536568.9	395934.5	-28303	OK
201	S	IN	GAS+TG+CW	-225649	181.98	0.006	-7996.2	6352.3	-317	OK
208	S	IN	GAS+TG+CW	-254181	174.38	0.019	-25648.8	19752.7	-996	OK
510	S	OUT	GAS+TG+CW	-100257	134.26	0.145	-170754.8	150458.6	5763	OK
705	S	OUT	GAS+TG+CW	-309848	111.68	0.289	-175364.1	76147.5	9570	OK
1101	S	OUT	GAS+TG+CW	-286104	52.78	0.001	-326.1	0.1	17	OK
1102	S	OUT	GAS+TG+CW	-284945	55.42	0.000	-28.3	0.0	2	OK
1103	S	OUT	GAS+TG+CW	-192339	87.03	0.005	-18581.5	17396.6	140	OK
1104	S	OUT	GAS+TG+CW	-287549	50.63	0.001	-207.0	0.2	10	OK
1105	S	OUT	GAS+TG+CW	-286423	49.85	0.000	-80.9	0.0	4	OK
1106	S	OUT	GAS+TG+CW	-83662	201.20	0.000	0.0	0.0	0	OK
1107	S	OUT	GAS+TG+CW	-130193	106.31	0.006	-12628.2	11685.2	184	OK
1108	S	OUT	GAS+TG+CW	-100086	139.52	0.000	0.0	0.0	0	OK
1109	S	OUT	GAS+TG+CW	-302035	169.53	0.000	0.0	0.0	0	OK
1110	S	OUT	GAS+TG+CW	-302152	160.91	0.000	0.0	0.0	0	OK
1111	S	OUT	GAS+TG+CW	-303646	147.99	0.000	0.0	0.0	0	OK
1112	S	OUT	GAS+TG+CW	-306947	130.49	0.000	0.0	0.0	0	OK
1003-A	S	IN	GAS+TG+CW	-6020	164.49	2.172	-118900.2	0.0	-105822	OK
1003-A	S	IN	GAS+TG+CW	-6020	164.49	2.172	-118900.2	0.0	-105822	OK
1003-A	S	IN	GAS+TG+CW	-6020	164.49	2.172	-118900.2	0.0	-105822	OK
1009-A	S	OUT	GAS+TG+CW	-19604	192.10	2.214	-181162.4	11833.1	125933	OK
1009-A	S	OUT	GAS+TG+CW	-19604	192.10	2.214	-181162.4	11833.1	125933	OK
1009-A	S	OUT	GAS+TG+CW	-19604	192.10	2.214	-181162.4	11833.1	125933	OK
1010-A	S	OUT	GAS+TG+CW	-16593	196.13	0.022	-1829.9	160.2	1299	OK
1010-A	S	OUT	GAS+TG+CW	-16593	196.13	0.022	-1829.9	160.2	1299	OK
1010-A	S	OUT	GAS+TG+CW	-16593	196.13	0.022	-1829.9	160.2	1299	OK
1201-A	S	IN	GAS+TG+CW	-278742	73.33	4.158	-1252981.4	3543.6	-90311	OK
1201-A	S	IN	GAS+TG+CW	-278742	73.33	4.158	-1252981.4	3543.6	-90311	OK
1201-A	S	IN	GAS+TG+CW	-278742	73.33	4.158	-1252981.4	3543.6	-90311	OK
1204	S	OUT	GAS+TG+CW	-277139	77.42	0.558	-168025.7	694.7	12785	OK
1206	S	OUT	GAS+TG+CW	-277139	77.42	11.709	-3528112.6	14587.0	268459	OK

1209	S	OUT	GAS+TG+CW	-277945	75.40	0.208	-62806.1	216.5	4654	OK
1303-A	S	IN	GAS+TG+CW	-285558	53.18	13.431	-4046874.6	63.6	-211525	OK
1303-B	S	IN	GAS+TG+CW	-285558	53.18	13.431	-4046874.6	63.6	-211525	OK
1306	S	OUT	GAS+TG+CW	-284235	57.51	26.862	-8093749.1	1174.0	457526	OK
835	S	OUT	GAS+TG+CW	-284620	56.27	0.825	-248690.8	23.2	13753	OK
802	S	IN	GAS+TG+CW	-284234	57.51	0.825	-248690.8	36.9	-14058	OK
Other users	P	OUT	GAS+TG+CW					23164.0	0	OK
Gen Loss	P	OUT	GAS+TG+CW					566.0	0	OK
Gen Loss	P	OUT	GAS+TG+CW					566.0	0	OK
Gen Loss	P	OUT	GAS+TG+CW					566.0	0	OK
1003-A	S	IN	1000-GT	-6020	164.49	2.172	-118900.2	0.0	-105822	OK
1003-A	S	IN	1000-GT	-6020	164.49	2.172	-118900.2	0.0	-105822	OK
1003-A	S	IN	1000-GT	-6020	164.49	2.172	-118900.2	0.0	-105822	OK
1002-A	S	IN	1000-GT	-97821	156.57	0.053	-64088.3	56489.9	-2444	OK
1002-A	S	IN	1000-GT	-97821	156.57	0.053	-64088.3	56489.9	-2444	OK
1002-A	S	IN	1000-GT	-97821	156.57	0.053	-64088.3	56489.9	-2444	OK
1009-A	S	OUT	1000-GT	-19604	192.10	2.214	-181162.4	11833.1	125933	OK
1009-A	S	OUT	1000-GT	-19604	192.10	2.214	-181162.4	11833.1	125933	OK
1009-A	S	OUT	1000-GT	-19604	192.10	2.214	-181162.4	11833.1	125933	OK
1010-A	S	OUT	1000-GT	-16593	196.13	0.022	-1829.9	160.2	1299	OK
1010-A	S	OUT	1000-GT	-16593	196.13	0.022	-1829.9	160.2	1299	OK
1010-A	S	OUT	1000-GT	-16593	196.13	0.022	-1829.9	160.2	1299	OK
C1001A	P	IN	1000-GT					32634.0	0	OK
C1001A	P	IN	1000-GT					32634.0	0	OK
C1001A	P	IN	1000-GT					32634.0	0	OK
T1001A	P	OUT	1000-GT					51501.8	0	OK
T1001A	P	OUT	1000-GT					51501.8	0	OK
T1001A	P	OUT	1000-GT					51501.8	0	OK
1201-A	S	IN	1000-GT	-278742	73.33	4.158	-1252981.4	3543.6	-90311	OK

1201-A	S	IN	1000-GT	-278742	73.33	4.158	-1252981.4	3543.6	-90311	OK
1201-A	S	IN	1000-GT	-278742	73.33	4.158	-1252981.4	3543.6	-90311	OK
1202-A	S	OUT	1000-GT	-277139	77.42	4.158	-1252981.4	5180.5	95341	OK
1202-A	S	OUT	1000-GT	-277139	77.42	4.158	-1252981.4	5180.5	95341	OK
1202-A	S	OUT	1000-GT	-277139	77.42	4.158	-1252981.4	5180.5	95341	OK
1303-A	S	IN	800-CW System	-285558	53.18	13.431	-4046874.6	63.6	-211525	OK
1303-B	S	IN	800-CW System	-285558	53.18	13.431	-4046874.6	63.6	-211525	OK
830	S	IN	800-CW System	-283160	60.86	24.248	-7306298.2	3123.6	-437015	OK
1306	S	OUT	800-CW System	-284235	57.51	26.862	-8093749.1	1174.0	457526	OK
832	S	OUT	800-CW System	-284615	56.26	24.248	-7306298.2	832.2	404021	OK
P-802A	P	IN	800-CW System					56.0	0	OK
P-802B	P	IN	800-CW System					56.0	0	OK
P-801	P	IN	800-CW System					126.5	0	OK

Table B3.1.4. Streams exergy flow- Multiple paralleled compressors – 100% FPSO gas load – RER-1

Stream	Stream Type S/P	Direction In/Out	System	H (kJ/kgmol)	S (kJ/kgmol.K)	Flow (kgmol/s)	$\sum N_k.\mu_k^0$ (kW)	$H-T_0S+P_0V-\sum Nk.\mu_k^0$ (kW)	S_K kW	Check Ex >0
102	S	IN	Overall Gas Plant	-123689	163.76	2.173	-2281951.7	1907850.8	-105369	OK
201	S	IN	Overall Gas Plant	-156362	183.40	0.030	-51158.7	44918.0	-1609	OK
208	S	IN	Overall Gas Plant	-176963	176.71	0.098	-173097.0	150557.8	-5144	OK
803	S	IN	Overall Gas Plant	-284622	56.26	5.394	-1625184.2	149.3	-89868	OK
805	S	IN	Overall Gas Plant	-284622	56.26	0.028	-8563.0	0.8	-474	OK
807	S	IN	Overall Gas Plant	-284622	56.26	0.109	-32694.6	3.0	-1808	OK
809	S	IN	Overall Gas Plant	-284622	56.26	0.304	-91748.2	8.4	-5073	OK
811	S	IN	Overall Gas Plant	-284622	56.26	0.386	-116320.6	10.7	-6432	OK
813	S	IN	Overall Gas Plant	-284622	56.26	4.690	-1413300.6	129.8	-78152	OK
815	S	IN	Overall Gas Plant	-284622	56.26	5.318	-1602345.2	147.2	-88605	OK
817	S	IN	Overall Gas Plant	-284622	56.26	1.048	-315688.3	29.0	-17457	OK
819	S	IN	Overall Gas Plant	-284622	56.26	1.340	-403707.8	37.1	-22324	OK
821	S	IN	Overall Gas Plant	-284622	56.26	1.715	-516649.3	47.5	-28569	OK
823	S	IN	Overall Gas Plant	-284622	56.26	2.131	-642009.6	59.0	-35501	OK
825	S	IN	Overall Gas Plant	-284622	56.26	1.270	-382547.8	35.1	-21154	OK
827	S	IN	Overall Gas Plant	-284622	56.26	1.995	-601016.6	55.2	-33235	OK
804	S	OUT	Overall Gas Plant	-283068	61.15	5.394	-1625184.2	715.7	97684	OK
806	S	OUT	Overall Gas Plant	-284235	57.51	0.028	-8563.0	1.2	484	OK
808	S	OUT	Overall Gas Plant	-283067	61.15	0.109	-32694.6	14.5	1965	OK
810	S	OUT	Overall Gas Plant	-283846	58.74	0.304	-91748.2	20.9	5297	OK
812	S	OUT	Overall Gas Plant	-283068	61.15	0.386	-116320.6	51.2	6992	OK
814	S	OUT	Overall Gas Plant	-283068	61.15	4.690	-1413300.6	622.4	84949	OK
816	S	OUT	Overall Gas Plant	-283068	61.15	5.318	-1602345.2	705.6	96312	OK
818	S	OUT	Overall Gas Plant	-283068	61.15	1.048	-315688.3	139.0	18975	OK
820	S	OUT	Overall Gas Plant	-283068	61.15	1.340	-403707.8	177.8	24266	OK
822	S	OUT	Overall Gas Plant	-283068	61.15	1.715	-516649.3	227.5	31054	OK

824	S	OUT	Overall Gas Plant	-283068	61.15	2.131	-642009.6	282.7	38589	OK
826	S	OUT	Overall Gas Plant	-283068	61.15	1.270	-382547.8	168.5	22994	OK
828	S	OUT	Overall Gas Plant	-283846	58.74	1.995	-601016.6	137.2	34702	OK
510	S	OUT	Overall Gas Plant	-99660	134.20	1.652	-1923425.2	1693169.5	65645	OK
402	S	OUT	Overall Gas Plant	-96059	156.34	0.146	-170595.3	149740.2	6783	OK
705	S	OUT	Overall Gas Plant	-245893	118.14	0.474	-332755.7	199640.8	16581	OK
1101	S	OUT	Overall Gas Plant	-285880	52.60	0.000	-64.0	0.0	3	OK
1102	S	OUT	Overall Gas Plant	-284254	57.53	0.000	-27.6	0.0	2	OK
1103	S	OUT	Overall Gas Plant	-180564	87.06	0.025	-78132.1	73044.5	636	OK
1104	S	OUT	Overall Gas Plant	-286952	49.90	0.003	-789.2	0.6	39	OK
1105	S	OUT	Overall Gas Plant	-286498	49.59	0.001	-235.2	0.1	11	OK
1106	S	OUT	Overall Gas Plant	-123654	77.86	0.000	0.0	0.0	0	OK
1107	S	OUT	Overall Gas Plant	-127302	118.83	0.000	0.0	0.0	0	OK
1108	S	OUT	Overall Gas Plant	-97534	146.03	0.000	0.0	0.0	0	OK
1109	S	OUT	Overall Gas Plant	-239668	172.88	0.000	0.0	0.0	0	OK
1110	S	OUT	Overall Gas Plant	-239507	165.12	0.000	0.0	0.0	0	OK
1111	S	OUT	Overall Gas Plant	-240046	155.27	0.000	0.0	0.0	0	OK
1112	S	OUT	Overall Gas Plant	-241741	142.64	0.000	0.0	0.0	0	OK
C-101-A_P	P	IN	Overall Gas Plant					4058.8	0	OK
C-101-B_P	P	IN	Overall Gas Plant					4058.8	0	OK
C-201-A_P	P	IN	Overall Gas Plant					42.9	0	OK
C-201-B_P	P	IN	Overall Gas Plant					42.9	0	OK
C-201-C_P	P	IN	Overall Gas Plant					42.9	0	OK
C-202-A_P	P	IN	Overall Gas Plant					180.0	0	OK
C-202-B_P	P	IN	Overall Gas Plant					180.0	0	OK
C-202-C_P	P	IN	Overall Gas Plant					180.0	0	OK
C-501-A_P	P	IN	Overall Gas Plant					1618.7	0	OK
C-501-B_P	P	IN	Overall Gas Plant					1618.7	0	OK
C-501-C_P	P	IN	Overall Gas Plant					1618.7	0	OK
C-502-A_P	P	IN	Overall Gas Plant					1583.6	0	OK
C-502-B_P	P	IN	Overall Gas Plant					1583.6	0	OK

C-502-C_P	P	IN	Overall Gas Plant					1583.6	0	OK
C-601_P	P	IN	Overall Gas Plant					1707.3	0	OK
C-602_P	P	IN	Overall Gas Plant					1824.1	0	OK
C-603_P	P	IN	Overall Gas Plant					1864.4	0	OK
C-604_P	P	IN	Overall Gas Plant					1762.3	0	OK
C-701-A_P	P	IN	Overall Gas Plant					1551.8	0	OK
C-701-B_P	P	IN	Overall Gas Plant					0.0	0	OK
C-901-A_P	P	IN	Overall Gas Plant					229.4	0	OK
C-901-B_P	P	IN	Overall Gas Plant					229.4	0	OK
1208	S	IN	Overall Gas Plant	-277139	77.42	0.767	-231176.8	955.8	-17591	OK
1209	S	OUT	Overall Gas Plant	-277945	75.40	0.767	-231176.8	796.8	17131	OK
102	S	IN	GAS+TG+CW	-123689	163.76	2.173	-2281951.7	1907850.8	-105369	OK
201	S	IN	GAS+TG+CW	-156362	183.40	0.030	-51158.7	44918.0	-1609	OK
208	S	IN	GAS+TG+CW	-176963	176.71	0.098	-173097.0	150557.8	-5144	OK
510	S	OUT	GAS+TG+CW	-99660	134.20	1.652	-1923425.2	1693169.5	65645	OK
705	S	OUT	GAS+TG+CW	-245893	118.14	0.474	-332755.7	199640.8	16581	OK
1101	S	OUT	GAS+TG+CW	-285880	52.60	0.000	-64.0	0.0	3	OK
1102	S	OUT	GAS+TG+CW	-284254	57.53	0.000	-27.6	0.0	2	OK
1103	S	OUT	GAS+TG+CW	-180564	87.06	0.025	-78132.1	73044.5	636	OK
1104	S	OUT	GAS+TG+CW	-286952	49.90	0.003	-789.2	0.6	39	OK
1105	S	OUT	GAS+TG+CW	-286498	49.59	0.001	-235.2	0.1	11	OK
1106	S	OUT	GAS+TG+CW	-123654	77.86	0.000	0.0	0.0	0	OK
1107	S	OUT	GAS+TG+CW	-127302	118.83	0.000	0.0	0.0	0	OK
1108	S	OUT	GAS+TG+CW	-97534	146.03	0.000	0.0	0.0	0	OK
1109	S	OUT	GAS+TG+CW	-239668	172.88	0.000	0.0	0.0	0	OK
1110	S	OUT	GAS+TG+CW	-239507	165.12	0.000	0.0	0.0	0	OK
1111	S	OUT	GAS+TG+CW	-240046	155.27	0.000	0.0	0.0	0	OK
1112	S	OUT	GAS+TG+CW	-241741	142.64	0.000	0.0	0.0	0	OK
1003-A	S	IN	GAS+TG+CW	-6020	164.49	2.791	-152750.7	0.0	-135949	OK
1003-A	S	IN	GAS+TG+CW	-6020	164.49	2.791	-152750.7	0.0	-135949	OK
1009-A	S	OUT	GAS+TG+CW	-19787	193.16	2.848	-235672.9	16424.5	162902	OK

1009-A	S	OUT	GAS+TG+CW	-19787	193.16	2.848	-235672.9	16424.5	162902	OK
1010-A	S	OUT	GAS+TG+CW	-17445	196.24	0.029	-2380.5	207.0	1672	OK
1010-A	S	OUT	GAS+TG+CW	-17445	196.24	0.029	-2380.5	207.0	1672	OK
1201-A	S	IN	GAS+TG+CW	-278742	73.33	4.158	-1252981.4	3543.6	-90311	OK
1201-A	S	IN	GAS+TG+CW	-278742	73.33	4.158	-1252981.4	3543.6	-90311	OK
1204	S	OUT	GAS+TG+CW	-277139	77.42	6.193	-1866070.3	7715.3	141992	OK
1206	S	OUT	GAS+TG+CW	-277139	77.42	1.356	-408715.7	1689.8	31100	OK
1209	S	OUT	GAS+TG+CW	-277945	75.40	0.767	-231176.8	796.8	17131	OK
1303-A	S	IN	GAS+TG+CW	-285558	53.18	15.030	-4528857.0	70.8	-236717	OK
1303-B	S	IN	GAS+TG+CW	-285558	53.18	15.030	-4528857.0	70.8	-236717	OK
1306	S	OUT	GAS+TG+CW	-284236	57.51	30.061	-9057714.1	1313.3	512008	OK
835	S	OUT	GAS+TG+CW	-284620	56.27	3.522	-1061333.6	98.6	58694	OK
802	S	IN	GAS+TG+CW	-284234	57.51	3.522	-1061333.6	157.6	-59995	OK
Other users	P	OUT	GAS+TG+CW					23164.0	0	OK
Gen Loss	P	OUT	GAS+TG+CW					790.3	0	OK
Gen Loss	P	OUT	GAS+TG+CW					790.3	0	OK
1003-A	S	IN	1000-GT	-6020	164.49	2.791	-152750.7	0.0	-135949	OK
1003-A	S	IN	1000-GT	-6020	164.49	2.791	-152750.7	0.0	-135949	OK
1002-A	S	IN	1000-GT	-96059	158.13	0.073	-85297.6	74831.2	-3430	OK
1002-A	S	IN	1000-GT	-96059	158.13	0.073	-85297.6	74831.2	-3430	OK
1009-A	S	OUT	1000-GT	-19787	193.16	2.848	-235672.9	16424.5	162902	OK
1009-A	S	OUT	1000-GT	-19787	193.16	2.848	-235672.9	16424.5	162902	OK
1010-A	S	OUT	1000-GT	-17445	196.24	0.029	-2380.5	207.0	1672	OK
1010-A	S	OUT	1000-GT	-17445	196.24	0.029	-2380.5	207.0	1672	OK
C1001A	P	IN	1000-GT					41337.8	0	OK
C1001A	P	IN	1000-GT					41337.8	0	OK
T1001A	P	OUT	1000-GT					67682.1	0	OK
T1001A	P	OUT	1000-GT					67682.1	0	OK
1201-A	S	IN	1000-GT	-278742	73.33	4.158	-1252981.4	3543.6	-90311	OK

1201-A	S	IN	1000-GT	-278742	73.33	4.158	-1252981.4	3543.6	-90311	OK
1202-A	S	OUT	1000-GT	-277139	77.42	4.158	-1252981.4	5180.5	95341	OK
1202-A	S	OUT	1000-GT	-277139	77.42	4.158	-1252981.4	5180.5	95341	OK
1303-A	S	IN	800-CW System	-285558	53.18	15.030	-4528857.0	70.8	-236717	OK
1303-B	S	IN	800-CW System	-285558	53.18	15.030	-4528857.0	70.8	-236717	OK
830	S	IN	800-CW System	-283266	60.53	29.249	-8813109.3	3477.9	-524333	OK
1306	S	OUT	800-CW System	-284236	57.51	30.061	-9057714.1	1313.3	512008	OK
832	S	OUT	800-CW System	-284615	56.26	29.249	-8813109.3	1003.9	487346	OK
P-802A	P	IN	800-CW System					63.1	0	OK
P-802B	P	IN	800-CW System					63.1	0	OK
P-801	P	IN	800-CW System					157.6	0	OK

Table B3.1.5. Streams exergy flow- Multiple paralleled compressors – 50% FPSO gas load – RER-1

Stream	*Stream Type S/P*	*Direction In/Out*		*H (kJ/kgmol)*	*S (kJ/kgmol.K)*	*Flow (kgmol/s)*	*∑ $N_k.\mu_k^0$ (kW)*	*$H-T_0S+P_0V-\sum Nk.\mu_k^0$ (kW)*	*S_K kW*	*Check Ex >0*
102	S	IN	Overall Gas Plant	-146519	164.81	1.298	-1321446.9	1067969.5	-63339	OK
201	S	IN	Overall Gas Plant	-178368	183.66	0.016	-26695.9	22925.0	-881	OK
208	S	IN	Overall Gas Plant	-204760	176.13	0.046	-74560.7	62658.7	-2416	OK
803	S	IN	Overall Gas Plant	-284622	56.26	3.683	-1109831.4	101.9	-61371	OK
805	S	IN	Overall Gas Plant	-284622	56.26	0.040	-12180.4	1.1	-674	OK
807	S	IN	Overall Gas Plant	-284622	56.26	0.060	-18115.0	1.7	-1002	OK
809	S	IN	Overall Gas Plant	-284622	56.26	0.132	-39764.9	3.7	-2199	OK
811	S	IN	Overall Gas Plant	-284622	56.26	0.149	-44804.8	4.1	-2478	OK
813	S	IN	Overall Gas Plant	-284622	56.26	2.219	-668756.7	61.4	-36980	OK
815	S	IN	Overall Gas Plant	-284622	56.26	2.585	-778940.0	71.6	-43073	OK
817	S	IN	Overall Gas Plant	-284622	56.26	0.882	-265819.6	24.4	-14699	OK
819	S	IN	Overall Gas Plant	-284622	56.26	1.180	-355461.3	32.7	-19656	OK
821	S	IN	Overall Gas Plant	-284622	56.26	1.547	-466125.2	42.8	-25775	OK
823	S	IN	Overall Gas Plant	-284622	56.26	1.934	-582608.8	53.5	-32217	OK
825	S	IN	Overall Gas Plant	-284622	56.26	1.057	-318397.9	29.2	-17606	OK
827	S	IN	Overall Gas Plant	-284622	56.26	1.349	-406417.2	37.3	-22474	OK
804	S	OUT	Overall Gas Plant	-283068	61.15	3.683	-1109831.4	488.7	66708	OK
806	S	OUT	Overall Gas Plant	-284235	57.51	0.040	-12180.4	1.8	689	OK
808	S	OUT	Overall Gas Plant	-283067	61.15	0.060	-18115.0	8.0	1089	OK
810	S	OUT	Overall Gas Plant	-283846	58.74	0.132	-39764.9	9.1	2296	OK
812	S	OUT	Overall Gas Plant	-283068	61.15	0.149	-44804.8	19.7	2693	OK
814	S	OUT	Overall Gas Plant	-283068	61.15	2.219	-668756.7	294.5	40197	OK
816	S	OUT	Overall Gas Plant	-283068	61.15	2.585	-778940.0	343.0	46819	OK
818	S	OUT	Overall Gas Plant	-283068	61.15	0.882	-265819.6	117.1	15978	OK
820	S	OUT	Overall Gas Plant	-283068	61.15	1.180	-355461.3	156.5	21366	OK
822	S	OUT	Overall Gas Plant	-283068	61.15	1.547	-466125.2	205.3	28017	OK

824	S	OUT	Overall Gas Plant	-283068	61.15	1.934	-582608.8	256.6	35019	OK
826	S	OUT	Overall Gas Plant	-283068	61.15	1.057	-318397.9	140.2	19138	OK
828	S	OUT	Overall Gas Plant	-283846	58.74	1.349	-406417.2	92.7	23466	OK
510	S	OUT	Overall Gas Plant	-100221	134.02	0.805	-951393.1	838826.0	31933	OK
402	S	OUT	Overall Gas Plant	-96648	155.92	0.122	-144185.2	126770.2	5630	OK
705	S	OUT	Overall Gas Plant	-273135	115.64	0.414	-273771.2	146500.7	14179	OK
1101	S	OUT	Overall Gas Plant	-285273	54.86	0.000	0.0	0.0	0	OK
1102	S	OUT	Overall Gas Plant	-284261	57.54	0.000	-54.2	0.0	3	OK
1103	S	OUT	Overall Gas Plant	-181522	85.12	0.016	-52360.4	48960.9	415	OK
1104	S	OUT	Overall Gas Plant	-287081	50.33	0.003	-768.6	0.6	38	OK
1105	S	OUT	Overall Gas Plant	-286420	49.86	0.001	-158.0	0.1	8	OK
1106	S	OUT	Overall Gas Plant	-123639	77.92	0.000	0.0	0.0	0	OK
1107	S	OUT	Overall Gas Plant	-129428	116.12	0.000	0.0	0.0	0	OK
1108	S	OUT	Overall Gas Plant	-98082	145.88	0.000	0.0	0.0	0	OK
1109	S	OUT	Overall Gas Plant	-266336	171.41	0.000	0.0	0.0	0	OK
1110	S	OUT	Overall Gas Plant	-266086	163.95	0.000	0.0	0.0	0	OK
1111	S	OUT	Overall Gas Plant	-266675	154.00	0.000	0.0	0.0	0	OK
1112	S	OUT	Overall Gas Plant	-268594	140.81	0.000	0.0	0.0	0	OK
C-101-A_P	P	IN	Overall Gas Plant					2482.2	0	OK
C-101-B_P	P	IN	Overall Gas Plant					2482.2	0	OK
C-201-A_P	P	IN	Overall Gas Plant					34.9	0	OK
C-201-B_P	P	IN	Overall Gas Plant					34.9	0	OK
C-201-C_P	P	IN	Overall Gas Plant					0.0	0	OK
C-202-A_P	P	IN	Overall Gas Plant					139.7	0	OK
C-202-B_P	P	IN	Overall Gas Plant					139.7	0	OK
C-202-C_P	P	IN	Overall Gas Plant					0.0	0	OK
C-501-A_P	P	IN	Overall Gas Plant					1156.2	0	OK
C-501-B_P	P	IN	Overall Gas Plant					1156.2	0	OK
C-501-C_P	P	IN	Overall Gas Plant					0.0	0	OK
C-502-A_P	P	IN	Overall Gas Plant					1140.3	0	OK
C-502-B_P	P	IN	Overall Gas Plant					1140.3	0	OK

C-502-C_P	P	IN	Overall Gas Plant					0.0	0	OK
C-601_P	P	IN	Overall Gas Plant					1476.1	0	OK
C-602_P	P	IN	Overall Gas Plant					1587.8	0	OK
C-603_P	P	IN	Overall Gas Plant					1612.1	0	OK
C-604_P	P	IN	Overall Gas Plant					1484.2	0	OK
C-701-A_P	P	IN	Overall Gas Plant					1280.5	0	OK
C-701-B_P	P	IN	Overall Gas Plant					0.0	0	OK
C-901-A_P	P	IN	Overall Gas Plant					155.1	0	OK
C-901-B_P	P	IN	Overall Gas Plant					155.1	0	OK
1208	S	IN	Overall Gas Plant	-277139	77.42	0.457	-137710.3	569.4	-10479	OK
1209	S	OUT	Overall Gas Plant	-277945	75.40	0.457	-137710.3	474.6	10205	OK
102	S	IN	GAS+TG+CW	-146519	164.81	1.298	-1321446.9	1067969.5	-63339	OK
201	S	IN	GAS+TG+CW	-178368	183.66	0.016	-26695.9	22925.0	-881	OK
208	S	IN	GAS+TG+CW	-204760	176.13	0.046	-74560.7	62658.7	-2416	OK
510	S	OUT	GAS+TG+CW	-100221	134.02	0.805	-951393.1	838826.0	31933	OK
705	S	OUT	GAS+TG+CW	-273135	115.64	0.414	-273771.2	146500.7	14179	OK
1101	S	OUT	GAS+TG+CW	-285273	54.86	0.000	0.0	0.0	0	OK
1102	S	OUT	GAS+TG+CW	-284261	57.54	0.000	-54.2	0.0	3	OK
1103	S	OUT	GAS+TG+CW	-181522	85.12	0.016	-52360.4	48960.9	415	OK
1104	S	OUT	GAS+TG+CW	-287081	50.33	0.003	-768.6	0.6	38	OK
1105	S	OUT	GAS+TG+CW	-286420	49.86	0.001	-158.0	0.1	8	OK
1106	S	OUT	GAS+TG+CW	-123639	77.92	0.000	0.0	0.0	0	OK
1107	S	OUT	GAS+TG+CW	-129428	116.12	0.000	0.0	0.0	0	OK
1108	S	OUT	GAS+TG+CW	-98082	145.88	0.000	0.0	0.0	0	OK
1109	S	OUT	GAS+TG+CW	-266336	171.41	0.000	0.0	0.0	0	OK
1110	S	OUT	GAS+TG+CW	-266086	163.95	0.000	0.0	0.0	0	OK
1111	S	OUT	GAS+TG+CW	-266675	154.00	0.000	0.0	0.0	0	OK
1112	S	OUT	GAS+TG+CW	-268594	140.81	0.000	0.0	0.0	0	OK
1003-A	S	IN	GAS+TG+CW	-6020	164.49	2.436	-133352.4	0.0	-118685	OK
1003-A	S	IN	GAS+TG+CW	-6020	164.49	2.436	-133352.4	0.0	-118685	OK
1009-A	S	OUT	GAS+TG+CW	-19329	192.58	2.483	-203394.8	13755.4	141638	OK

1009-A	S	OUT	GAS+TG+CW	-19329	192.58	2.483	-203394.8	13755.4	141638	OK
1010-A	S	OUT	GAS+TG+CW	-16644	196.15	0.025	-2054.5	179.8	1457	OK
1010-A	S	OUT	GAS+TG+CW	-16644	196.15	0.025	-2054.5	179.8	1457	OK
1201-A	S	IN	GAS+TG+CW	-278742	73.33	4.158	-1252981.4	3543.6	-90311	OK
1201-A	S	IN	GAS+TG+CW	-278742	73.33	4.158	-1252981.4	3543.6	-90311	OK
1204	S	OUT	GAS+TG+CW	-277139	77.42	2.623	-790324.3	3267.6	60137	OK
1206	S	OUT	GAS+TG+CW	-277139	77.42	5.237	-1577928.3	6523.9	120067	OK
1209	S	OUT	GAS+TG+CW	-277945	75.40	0.457	-137710.3	474.6	10205	OK
1303-A	S	IN	GAS+TG+CW	-285557	53.18	10.021	-3019416.3	48.0	-157824	OK
1303-B	S	IN	GAS+TG+CW	-285557	53.18	10.021	-3019416.3	48.0	-157824	OK
1306	S	OUT	GAS+TG+CW	-284236	57.51	20.042	-6038832.6	875.7	341360	OK
835	S	OUT	GAS+TG+CW	-284620	56.27	3.650	-1099717.2	103.1	60816	OK
802	S	IN	GAS+TG+CW	-284234	57.51	3.650	-1099717.2	163.3	-62164	OK
Other users	P	OUT	GAS+TG+CW					23164.0	0	OK
Gen Loss	P	OUT	GAS+TG+CW					635.8	0	OK
Gen Loss	P	OUT	GAS+TG+CW					635.8	0	OK
1003-A	S	IN	1000-GT	-6020	164.49	2.436	-133352.4	0.0	-118685	OK
1003-A	S	IN	1000-GT	-6020	164.49	2.436	-133352.4	0.0	-118685	OK
1002-A	S	IN	1000-GT	-96648	157.69	0.061	-72092.6	63353.1	-2847	OK
1002-A	S	IN	1000-GT	-96648	157.69	0.061	-72092.6	63353.1	-2847	OK
1009-A	S	OUT	1000-GT	-19329	192.58	2.483	-203394.8	13755.4	141638	OK
1009-A	S	OUT	1000-GT	-19329	192.58	2.483	-203394.8	13755.4	141638	OK
1010-A	S	OUT	1000-GT	-16644	196.15	0.025	-2054.5	179.8	1457	OK
1010-A	S	OUT	1000-GT	-16644	196.15	0.025	-2054.5	179.8	1457	OK
C1001A	P	IN	1000-GT					36600.7	0	OK
C1001A	P	IN	1000-GT					36600.7	0	OK
T1001A	P	OUT	1000-GT					57792.9	0	OK
T1001A	P	OUT	1000-GT					57792.9	0	OK
1201-A	S	IN	1000-GT	-278742	73.33	4.158	-1252981.4	3543.6	-90311	OK

1201-A	S	IN	1000-GT	-278742	73.33	4.158	-1252981.4	3543.6	-90311	OK
1202-A	S	OUT	1000-GT	-277139	77.42	4.158	-1252981.4	5180.5	95341	OK
1202-A	S	OUT	1000-GT	-277139	77.42	4.158	-1252981.4	5180.5	95341	OK
1303-A	S	IN	800-CW System	-285557	53.18	10.021	-3019416.3	48.0	-157824	OK
1303-B	S	IN	800-CW System	-285557	53.18	10.021	-3019416.3	48.0	-157824	OK
830	S	IN	800-CW System	-283330	60.33	20.467	-6166940.4	2321.9	-365703	OK
1306	S	OUT	800-CW System	-284236	57.51	20.042	-6038832.6	875.7	341360	OK
832	S	OUT	800-CW System	-284615	56.26	20.467	-6166940.4	702.4	341017	OK
P-802A	P	IN	800-CW System					41.2	0	OK
P-802B	P	IN	800-CW System					41.2	0	OK
P-801	P	IN	800-CW System					104.2	0	OK

Table B3.1.6. Streams exergy flow- Multiple paralleled compressors – 25% FPSO gas load – RER-1

Stream	*Stream Type S/P*	*Direction In/Out*		*H (kJ/kgmol)*	*S (kJ/kgmol.K)*	*Flow (kgmol/s)*	$\sum N_k.\mu_k^0$ *(kW)*	$H\text{-}T_0S + P_0V - \sum Nk.\mu_k^0$ *(kW)*	S_K *kW*	*Check Ex >0*
102	S	IN	Overall Gas Plant	-193477	164.61	0.581	-536568.9	395934.5	-28303	OK
201	S	IN	Overall Gas Plant	-225649	181.98	0.006	-7996.2	6352.3	-317	OK
208	S	IN	Overall Gas Plant	-254182	174.37	0.019	-25648.8	19752.7	-996	OK
803	S	IN	Overall Gas Plant	-284622	56.26	1.851	-557702.2	51.2	-30839	OK
805	S	IN	Overall Gas Plant	-284622	56.26	0.006	-1714.2	0.2	-95	OK
807	S	IN	Overall Gas Plant	-284622	56.26	0.021	-6443.1	0.6	-356	OK
809	S	IN	Overall Gas Plant	-284622	56.26	0.046	-13802.5	1.3	-763	OK
811	S	IN	Overall Gas Plant	-284622	56.26	0.056	-16854.6	1.5	-932	OK
813	S	IN	Overall Gas Plant	-284622	56.26	0.000	0.0	0.0	0	OK
815	S	IN	Overall Gas Plant	-284622	56.26	0.000	0.0	0.0	0	OK
817	S	IN	Overall Gas Plant	-284622	56.26	0.564	-170056.2	15.6	-9404	OK
819	S	IN	Overall Gas Plant	-284622	56.26	0.834	-251322.7	23.1	-13897	OK
821	S	IN	Overall Gas Plant	-284622	56.26	1.620	-488056.4	44.8	-26988	OK
823	S	IN	Overall Gas Plant	-284622	56.26	2.208	-665227.8	61.1	-36785	OK
825	S	IN	Overall Gas Plant	-284622	56.26	1.264	-380897.8	35.0	-21063	OK
827	S	IN	Overall Gas Plant	-284622	56.26	0.584	-175892.0	16.2	-9726	OK
804	S	OUT	Overall Gas Plant	-283068	61.15	1.851	-557702.2	245.6	33522	OK
806	S	OUT	Overall Gas Plant	-284235	57.51	0.006	-1714.2	0.2	97	OK
808	S	OUT	Overall Gas Plant	-283067	61.15	0.021	-6443.1	2.9	387	OK
810	S	OUT	Overall Gas Plant	-283846	58.74	0.046	-13802.5	3.1	797	OK
812	S	OUT	Overall Gas Plant	-283068	61.16	0.056	-16854.6	7.4	1013	OK
814	S	OUT	Overall Gas Plant	0	0.00	0.000	0.0	0.0	0	OK
816	S	OUT	Overall Gas Plant	0	0.00	0.000	0.0	0.0	0	OK
818	S	OUT	Overall Gas Plant	-283068	61.15	0.564	-170056.2	74.9	10222	OK
820	S	OUT	Overall Gas Plant	-283068	61.15	0.834	-251322.7	110.7	15106	OK
822	S	OUT	Overall Gas Plant	-283068	61.15	1.620	-488056.4	214.9	29335	OK

824	S	OUT	Overall Gas Plant	-283068	61.15	2.208	-665227.8	292.9	39985	OK
826	S	OUT	Overall Gas Plant	-283068	61.15	1.264	-380897.8	167.7	22894	OK
828	S	OUT	Overall Gas Plant	-283846	58.74	0.584	-175892.0	40.1	10156	OK
402	S	OUT	Overall Gas Plant	-97760	154.88	0.097	-117905.5	103955.1	4455	OK
405	S	OUT	Overall Gas Plant	-97760	154.88	0.000	0.0	0.0	0	OK
705	S	OUT	Overall Gas Plant	-221506	121.21	0.500	-431717.8	302892.1	17966	OK
1101	S	OUT	Overall Gas Plant	-284838	56.72	0.000	0.0	0.0	0	OK
1102	S	OUT	Overall Gas Plant	-284275	57.55	0.000	-6.0	0.0	0	OK
1103	S	OUT	Overall Gas Plant	-192973	82.99	0.006	-19978.1	18644.5	151	OK
1104	S	OUT	Overall Gas Plant	-287563	50.60	0.002	-522.5	0.6	26	OK
1105	S	OUT	Overall Gas Plant	-286432	49.82	0.000	-80.1	0.0	4	OK
1106	S	OUT	Overall Gas Plant	-123645	77.89	0.000	0.0	0.0	0	OK
1107	S	OUT	Overall Gas Plant	-134540	111.38	0.000	0.0	0.0	0	OK
1108	S	OUT	Overall Gas Plant	0	0.00	0.000	0.0	0.0	0	OK
1109	S	OUT	Overall Gas Plant	-302216	168.76	0.000	0.0	0.0	0	OK
1110	S	OUT	Overall Gas Plant	-301763	162.00	0.000	0.0	0.0	0	OK
1111	S	OUT	Overall Gas Plant	-219786	118.38	0.000	0.0	0.0	0	OK
1112	S	OUT	Overall Gas Plant	-217511	145.10	0.000	0.0	0.0	0	OK
C-101-A_P	P	IN	Overall Gas Plant					2269.6	0	OK
C-101-B_P	P	IN	Overall Gas Plant					0.0	0	OK
C-201-A_P	P	IN	Overall Gas Plant					26.0	0	OK
C-201-B_P	P	IN	Overall Gas Plant					0.0	0	OK
C-201-C_P	P	IN	Overall Gas Plant					0.0	0	OK
C-202-A_P	P	IN	Overall Gas Plant					117.8	0	OK
C-202-B_P	P	IN	Overall Gas Plant					0.0	0	OK
C-202-C_P	P	IN	Overall Gas Plant					0.0	0	OK
C-501-A_P	P	IN	Overall Gas Plant					0.0	0	OK
C-501-B_P	P	IN	Overall Gas Plant					0.0	0	OK
C-501-C_P	P	IN	Overall Gas Plant					0.0	0	OK
C-502-A_P	P	IN	Overall Gas Plant					0.0	0	OK
C-502-B_P	P	IN	Overall Gas Plant					0.0	0	OK

C-502-C_P	P	IN	Overall Gas Plant					0.0	0	OK
C-601_P	P	IN	Overall Gas Plant					1008.9	0	OK
C-602_P	P	IN	Overall Gas Plant					1103.6	0	OK
C-603_P	P	IN	Overall Gas Plant					1804.1	0	OK
C-604_P	P	IN	Overall Gas Plant					1755.3	0	OK
C-701-A_P	P	IN	Overall Gas Plant					1634.9	0	OK
C-701-B_P	P	IN	Overall Gas Plant					0.0	0	OK
C-901-A_P	P	IN	Overall Gas Plant					129.9	0	OK
C-901-B_P	P	IN	Overall Gas Plant					0.0	0	OK
1208	S	IN	Overall Gas Plant	-277139	77.42	0.208	-62651.6	259.0	-4767	OK
1209	S	OUT	Overall Gas Plant	-277945	75.40	0.208	-62651.6	215.9	4643	OK
102	S	IN	GAS+TG+CW	-193477	164.61	0.581	-536568.9	395934.5	-28303	OK
201	S	IN	GAS+TG+CW	-225649	181.98	0.006	-7996.2	6352.3	-317	OK
208	S	IN	GAS+TG+CW	-254182	174.37	0.019	-25648.8	19752.7	-996	OK
405	S	OUT	GAS+TG+CW	-97760	154.88	0.000	0.0	0.0	0	OK
705	S	OUT	GAS+TG+CW	-221506	121.21	0.500	-431717.8	302892.1	17966	OK
1101	S	OUT	GAS+TG+CW	-284838	56.72	0.000	0.0	0.0	0	OK
1102	S	OUT	GAS+TG+CW	-284275	57.55	0.000	-6.0	0.0	0	OK
1103	S	OUT	GAS+TG+CW	-192973	82.99	0.006	-19978.1	18644.5	151	OK
1104	S	OUT	GAS+TG+CW	-287563	50.60	0.002	-522.5	0.6	26	OK
1105	S	OUT	GAS+TG+CW	-286432	49.82	0.000	-80.1	0.0	4	OK
1106	S	OUT	GAS+TG+CW	-123645	77.89	0.000	0.0	0.0	0	OK
1107	S	OUT	GAS+TG+CW	-134540	111.38	0.000	0.0	0.0	0	OK
1108	S	OUT	GAS+TG+CW	0	0.00	0.000	0.0	0.0	0	OK
1109	S	OUT	GAS+TG+CW	-302216	168.76	0.000	0.0	0.0	0	OK
1110	S	OUT	GAS+TG+CW	-301763	162.00	0.000	0.0	0.0	0	OK
1111	S	OUT	GAS+TG+CW	-219786	118.38	0.000	0.0	0.0	0	OK
1112	S	OUT	GAS+TG+CW	-217511	145.10	0.000	0.0	0.0	0	OK
1003-A	S	IN	GAS+TG+CW	-6020	164.49	2.014	-110206.6	0.0	-98085	OK
1003-A	S	IN	GAS+TG+CW	-6020	164.49	2.014	-110206.6	0.0	-98085	OK
1009-A	S	OUT	GAS+TG+CW	-19653	191.74	2.051	-167471.3	10673.9	116482	OK

1009-A	S	OUT	GAS+TG+CW	-19653	191.74	2.051	-167471.3	10673.9	116482	OK
1010-A	S	OUT	GAS+TG+CW	-16403	196.11	0.021	-1691.6	148.3	1203	OK
1010-A	S	OUT	GAS+TG+CW	-16403	196.11	0.021	-1691.6	148.3	1203	OK
1201-A	S	IN	GAS+TG+CW	-278742	73.33	4.158	-1252981.4	3543.6	-90311	OK
1201-A	S	IN	GAS+TG+CW	-278742	73.33	4.158	-1252981.4	3543.6	-90311	OK
1204	S	OUT	GAS+TG+CW	-277139	77.42	0.558	-168025.7	694.7	12785	OK
1206	S	OUT	GAS+TG+CW	-277139	77.42	7.551	-2275285.6	9407.2	173129	OK
1209	S	OUT	GAS+TG+CW	-277945	75.40	0.208	-62651.6	215.9	4643	OK
1303-A	S	IN	GAS+TG+CW	-285556	53.18	5.284	-1592279.1	25.6	-83232	OK
1303-B	S	IN	GAS+TG+CW	-285556	53.18	5.284	-1592279.1	25.6	-83232	OK
1306	S	OUT	GAS+TG+CW	-284235	57.51	10.569	-3184558.2	462.0	180018	OK
835	S	OUT	GAS+TG+CW	-284621	56.26	0.825	-248690.8	23.5	13753	OK
802	S	IN	GAS+TG+CW	-284234	57.51	0.825	-248690.8	36.9	-14058	OK
Other users	P	OUT	GAS+TG+CW					23164.0	0	OK
Gen Loss	P	OUT	GAS+TG+CW					513.6	0	OK
Gen Loss	P	OUT	GAS+TG+CW					513.6	0	OK
1003-A	S	IN	1000-GT	-6020	164.49	2.014	-110206.6	0.0	-98085	OK
1003-A	S	IN	1000-GT	-6020	164.49	2.014	-110206.6	0.0	-98085	OK
1002-A	S	IN	1000-GT	-97760	156.61	0.049	-58952.7	51952.7	-2252	OK
1002-A	S	IN	1000-GT	-97760	156.61	0.049	-58952.7	51952.7	-2252	OK
1009-A	S	OUT	1000-GT	-19653	191.74	2.051	-167471.3	10673.9	116482	OK
1009-A	S	OUT	1000-GT	-19653	191.74	2.051	-167471.3	10673.9	116482	OK
1010-A	S	OUT	1000-GT	-16403	196.11	0.021	-1691.6	148.3	1203	OK
1010-A	S	OUT	1000-GT	-16403	196.11	0.021	-1691.6	148.3	1203	OK
C1001A	P	IN	1000-GT					30610.2	0	OK
C1001A	P	IN	1000-GT					30610.2	0	OK
T1001A	P	OUT	1000-GT					47729.1	0	OK
T1001A	P	OUT	1000-GT					47729.1	0	OK
1201-A	S	IN	1000-GT	-278742	73.33	4.158	-1252981.4	3543.6	-90311	OK

1201-A	S	IN	1000-GT	-278742	73.33	4.158	-1252981.4	3543.6	-90311	OK
1202-A	S	OUT	1000-GT	-277139	77.42	4.158	-1252981.4	5180.5	95341	OK
1202-A	S	OUT	1000-GT	-277139	77.42	4.158	-1252981.4	5180.5	95341	OK
1303-A	S	IN	800-CW System	-285556	53.18	5.284	-1592279.1	25.6	-83232	OK
1303-B	S	IN	800-CW System	-285556	53.18	5.284	-1592279.1	25.6	-83232	OK
830	S	IN	800-CW System	-283211	60.70	9.879	-2976660.3	1228.4	-177585	OK
1306	S	OUT	800-CW System	-284235	57.51	10.569	-3184558.2	462.0	180018	OK
832	S	OUT	800-CW System	-284616	56.26	9.879	-2976660.3	339.0	164601	OK
P-802A	P	IN	800-CW System					21.4	0	OK
P-802B	P	IN	800-CW System					21.4	0	OK
P-801	P	IN	800-CW System					48.2	0	OK

- *RER-2*

Table B3.1.7. Streams exergy flow- Single-shaft compressors – 100% FPSO gas load – RER-2

Stream	Stream Type S/P	Direction In/Out	System	H (kJ/kgmol)	S (kJ/kgmol.K)	Flow (kgmol/s)	$\sum N_k.\mu_k^0$ Flow (kW)	$H-T_0S+P_0V-\sum Nk.\mu_k^0$ Flow (kW)	S_K (kW)	Check Ex >0
102	S	IN	Overall Gas Plant	-123689	163.76	2.173	-446929.1	72828.2	-105369	OK
201	S	IN	Overall Gas Plant	-156362	183.40	0.030	-7474.2	1233.6	-1609	OK
208	S	IN	Overall Gas Plant	-176963	176.71	0.098	-26693.3	4154.1	-5144	OK
803	S	IN	Overall Gas Plant	-284622	56.26	5.463	-1646213.1	151.2	-91031	OK
805	S	IN	Overall Gas Plant	-284622	56.26	0.028	-8563.0	0.8	-474	OK
807	S	IN	Overall Gas Plant	-284622	56.26	0.115	-34726.0	3.2	-1920	OK
809	S	IN	Overall Gas Plant	-284622	56.26	0.304	-91748.2	8.4	-5073	OK
811	S	IN	Overall Gas Plant	-284622	56.26	0.430	-129531.9	11.9	-7163	OK
813	S	IN	Overall Gas Plant	-284622	56.26	4.522	-1362576.3	125.2	-75347	OK
815	S	IN	Overall Gas Plant	-284622	56.26	5.168	-1557150.0	143.0	-86106	OK
817	S	IN	Overall Gas Plant	-284622	56.26	1.315	-396246.1	36.4	-21911	OK
819	S	IN	Overall Gas Plant	-284622	56.26	1.608	-484492.7	44.5	-26791	OK
821	S	IN	Overall Gas Plant	-284622	56.26	1.955	-588977.4	54.1	-32569	OK
823	S	IN	Overall Gas Plant	-284622	56.26	2.304	-694244.5	63.8	-38390	OK
825	S	IN	Overall Gas Plant	-284622	56.26	4.611	-1389279.6	127.6	-76823	OK
827	S	IN	Overall Gas Plant	-284622	56.26	2.031	-612079.3	56.2	-33846	OK
804	S	OUT	Overall Gas Plant	-283068	61.15	5.463	-1646213.1	724.9	98948	OK
806	S	OUT	Overall Gas Plant	-284235	57.51	0.028	-8563.0	1.2	484	OK
808	S	OUT	Overall Gas Plant	-283067	61.15	0.115	-34726.0	15.4	2087	OK
810	S	OUT	Overall Gas Plant	-283846	58.74	0.304	-91748.2	20.9	5297	OK
812	S	OUT	Overall Gas Plant	-283068	61.15	0.430	-129531.9	57.0	7786	OK
814	S	OUT	Overall Gas Plant	-283068	61.15	4.522	-1362576.3	600.0	81900	OK
816	S	OUT	Overall Gas Plant	-283068	61.15	5.168	-1557150.0	685.7	93595	OK
818	S	OUT	Overall Gas Plant	-283068	61.15	1.315	-396246.1	174.5	23817	OK

820	S	OUT	Overall Gas Plant	-283068	61.15	1.608	-484492.7	213.4	29121	OK
822	S	OUT	Overall Gas Plant	-283068	61.15	1.955	-588977.4	259.4	35401	OK
824	S	OUT	Overall Gas Plant	-283068	61.15	2.304	-694244.5	305.7	41729	OK
826	S	OUT	Overall Gas Plant	-283068	61.15	4.611	-1389279.6	611.8	83505	OK
828	S	OUT	Overall Gas Plant	-283846	58.74	2.031	-612079.3	139.7	35340	OK
510	S	OUT	Overall Gas Plant	-99659	134.20	1.624	-293318.9	66904.8	64552	OK
402	S	OUT	Overall Gas Plant	-96058	156.34	0.174	-31436.0	6656.1	8059	OK
705	S	OUT	Overall Gas Plant	-245894	118.13	0.474	-148975.3	15853.1	16581	OK
1101	S	OUT	Overall Gas Plant	-285888	52.58	0.000	-67.6	0.0	3	OK
1102	S	OUT	Overall Gas Plant	-284367	57.17	0.000	-50.2	0.0	3	OK
1103	S	OUT	Overall Gas Plant	-180135	87.06	0.025	-6259.1	1163.5	638	OK
1104	S	OUT	Overall Gas Plant	-286955	49.90	0.003	-783.2	0.6	38	OK
1105	S	OUT	Overall Gas Plant	-286501	49.58	0.001	-234.8	0.1	11	OK
1106	S	OUT	Overall Gas Plant	-122967	80.40	0.000	0.0	0.0	0	OK
1107	S	OUT	Overall Gas Plant	-127699	118.00	0.000	0.0	0.0	0	OK
1108	S	OUT	Overall Gas Plant	-97645	145.67	0.000	0.0	0.0	0	OK
1109	S	OUT	Overall Gas Plant	-239637	172.98	0.000	0.0	0.0	0	OK
1110	S	OUT	Overall Gas Plant	-239613	164.78	0.000	0.0	0.0	0	OK
1111	S	OUT	Overall Gas Plant	-240373	154.22	0.000	0.0	0.0	0	OK
1112	S	OUT	Overall Gas Plant	-242403	140.59	0.000	0.0	0.0	0	OK
C-101_P	P	IN	Overall Gas Plant					8222.8	0	OK
C-201_P	P	IN	Overall Gas Plant					139.0	0	OK
C-202_P	P	IN	Overall Gas Plant					604.8	0	OK
C-501_P	P	IN	Overall Gas Plant					4635.3	0	OK
C-502_P	P	IN	Overall Gas Plant					4576.7	0	OK
C-601_P	P	IN	Overall Gas Plant					2122.9	0	OK
C-602_P	P	IN	Overall Gas Plant					2241.1	0	OK
C-603_P	P	IN	Overall Gas Plant					2237.8	0	OK
C-604_P	P	IN	Overall Gas Plant					2031.7	0	OK
C-701_P	P	IN	Overall Gas Plant					6744.0	0	OK
C-901_P	P	IN	Overall Gas Plant					493.8	0	OK

1208	S	IN	Overall Gas Plant	-277139	77.42	0.767	-231168.6	955.8	-17590	OK
1209	S	OUT	Overall Gas Plant	-277945	75.40	0.767	-231168.6	796.7	17131	OK
1303-A	S	IN	800-CW System	-285558	53.18	17.466	-5262603.5	81.4	-275068	OK
1303-B	S	IN	800-CW System	-285558	53.18	17.466	-5262603.5	81.4	-275068	OK
830	S	IN	800-CW System	-283242	60.61	33.378	-10057161.8	4037.5	-599089	OK
1306	S	OUT	800-CW System	-284236	57.51	34.931	-10525207.1	1525.4	594950	OK
832	S	OUT	800-CW System	-284615	56.26	33.378	-10057161.8	1145.6	556141	OK
P-802A	P	IN	800-CW System					74.3	0	OK
P-802B	P	IN	800-CW System					74.3	0	OK
P-801	P	IN	800-CW System					185.7	0	OK
102	S	IN	100-Main Comp.	-123689	163.76	2.173	-446929.1	72828.2	-105369	OK
803	S	IN	100-Main Comp.	-284622	56.26	5.463	-1646213.1	151.2	-91031	OK
107	S	OUT	100-Main Comp.	-126529	155.67	2.315	-483882.1	84325.0	106702	OK
804	S	OUT	100-Main Comp.	-283068	61.15	5.463	-1646213.1	724.9	98948	OK
1101	S	OUT	100-Main Comp.	-285888	52.58	0.000	-67.6	0.0	3	OK
214	S	IN	100-Main Comp.	-168313	160.53	0.142	-37020.6	6345.6	-6756	OK
C-101_P	P	IN	100-Main Comp.					8222.8	0	OK
404	S	IN	500-Export Comp.	-96058	156.34	1.624	-293318.9	62105.9	-75199	OK
813	S	IN	500-Export Comp.	-284622	56.26	4.522	-1362576.3	125.2	-75347	OK
815	S	IN	500-Export Comp.	-284622	56.26	5.168	-1557150.0	143.0	-86106	OK
510	S	OUT	500-Export Comp.	-99659	134.20	1.624	-293318.9	66904.8	64552	OK
814	S	OUT	500-Export Comp.	-283068	61.15	4.522	-1362576.3	600.0	81900	OK
816	S	OUT	500-Export Comp.	-283068	61.15	5.168	-1557150.0	685.7	93595	OK
1107	S	OUT	500-Export Comp.	-127699	118.00	0.000	0.0	0.0	0	OK
1108	S	OUT	500-Export Comp.	-97645	145.67	0.000	0.0	0.0	0	OK
C-501_P	P	IN	500-Export Comp.					4635.3	0	OK
C-502_P	P	IN	500-Export Comp.					4576.7	0	OK
403	S	IN	600-CO2 Comp.	-239668	172.88	0.474	-148975.3	11119.9	-24265	OK
817	S	IN	600-CO2 Comp.	-284622	56.26	1.315	-396246.1	36.4	-21911	OK
819	S	IN	600-CO2 Comp.	-284622	56.26	1.608	-484492.7	44.5	-26791	OK
821	S	IN	600-CO2 Comp.	-284622	56.26	1.955	-588977.4	54.1	-32569	OK

823	S	IN	600-CO2 Comp.	-284622	56.26	2.304	-694244.5	63.8	-38390	OK
620	S	OUT	600-CO2 Comp.	-245003	126.37	0.474	-148975.3	15119.2	17737	OK
818	S	OUT	600-CO2 Comp.	-283068	61.15	1.315	-396246.1	174.5	23817	OK
820	S	OUT	600-CO2 Comp.	-283068	61.15	1.608	-484492.7	213.4	29121	OK
822	S	OUT	600-CO2 Comp.	-283068	61.15	1.955	-588977.4	259.4	35401	OK
824	S	OUT	600-CO2 Comp.	-283068	61.15	2.304	-694244.5	305.7	41729	OK
1109	S	OUT	600-CO2 Comp.	-239637	172.98	0.000	0.0	0.0	0	OK
1110	S	OUT	600-CO2 Comp.	-239613	164.78	0.000	0.0	0.0	0	OK
1111	S	OUT	600-CO2 Comp.	-240373	154.22	0.000	0.0	0.0	0	OK
1112	S	OUT	600-CO2 Comp.	-242403	140.59	0.000	0.0	0.0	0	OK
C-601_P	P	IN	600-CO2 Comp.					2122.9	0	OK
C-602_P	P	IN	600-CO2 Comp.					2241.1	0	OK
C-603_P	P	IN	600-CO2 Comp.					2237.8	0	OK
C-604_P	P	IN	600-CO2 Comp.					2031.7	0	OK
620	S	IN	700-EOR Comp.	-245003	126.37	0.474	-148975.3	15119.2	-17737	OK
825	S	IN	700-EOR Comp.	-284622	56.26	4.611	-1389279.6	127.6	-76823	OK
705	S	OUT	700-EOR Comp.	-245894	118.13	0.474	-148975.3	15853.1	16581	OK
826	S	OUT	700-EOR Comp.	-283068	61.15	4.611	-1389279.6	611.8	83505	OK
C-701_P	P	IN	700-EOR Comp.					6744.0	0	OK
307	S	IN	400-MP Unit	-126286	155.39	2.272	-473730.2	82223.5	-104563	OK
401	S	OUT	400-MP Unit	-96058	156.34	1.798	-324754.9	68762.0	83258	OK
403	S	OUT	400-MP Unit	-239668	172.88	0.474	-148975.3	11119.9	24265	OK
1208	S	IN	400-MP Unit	-277139	77.42	0.767	-231168.6	955.8	-17590	OK
1209	S	OUT	400-MP Unit	-277945	75.40	0.767	-231168.6	796.7	17131	OK
901	S	IN	900-C3 Cycle	-106646	141.76	0.101	-21354.6	6396.1	-4225	OK
827	S	IN	900-C3 Cycle	-284622	56.26	2.031	-612079.3	56.2	-33846	OK
907	S	OUT	900-C3 Cycle	-117416	101.30	0.101	-21354.6	6518.3	3019	OK
828	S	OUT	900-C3 Cycle	-283846	58.74	2.031	-612079.3	139.7	35340	OK
C-901_P	P	IN	900-C3 Cycle					493.8	0	OK

201	S	IN	200-VRU	-156362	183.40	0.030	-7474.2	1233.6	-1609	OK
208	S	IN	200-VRU	-176963	176.71	0.098	-26693.3	4154.1	-5144	OK
317	S	IN	200-VRU	-154621	111.94	0.039	-9162.3	1820.2	-1296	OK
805	S	IN	200-VRU	-284622	56.26	0.028	-8563.0	0.8	-474	OK
807	S	IN	200-VRU	-284622	56.26	0.115	-34726.0	3.2	-1920	OK
809	S	IN	200-VRU	-284622	56.26	0.304	-91748.2	8.4	-5073	OK
811	S	IN	200-VRU	-284622	56.26	0.430	-129531.9	11.9	-7163	OK
806	S	OUT	200-VRU	-284235	57.51	0.028	-8563.0	1.2	484	OK
808	S	OUT	200-VRU	-283067	61.15	0.115	-34726.0	15.4	2087	OK
810	S	OUT	200-VRU	-283846	58.74	0.304	-91748.2	20.9	5297	OK
812	S	OUT	200-VRU	-283068	61.15	0.430	-129531.9	57.0	7786	OK
214	S	OUT	200-VRU	-168313	160.53	0.142	-37020.6	6345.6	6756	OK
1102	S	OUT	200-VRU	-284367	57.17	0.000	-50.2	0.0	3	OK
1103	S	OUT	200-VRU	-180135	87.06	0.025	-6259.1	1163.5	638	OK
C-201_P	P	IN	200-VRU					139.0	0	OK
C-202_P	P	IN	200-VRU					604.8	0	OK
303	S	IN	300-HCDP Adj.	-127848	150.50	2.299	-479959.6	83592.0	-102463	OK
305	S	OUT	300-HCDP Adj.	-128021	149.37	2.272	-473730.2	82330.1	100514	OK
312	S	OUT	300-HCDP Adj.	-153765	106.80	0.027	-6229.4	1283.9	844	OK
907	S	IN	300-HCDP Adj.	-117416	101.30	0.101	-21354.6	6518.3	-3019	OK
901	S	OUT	300-HCDP Adj.	-106646	141.76	0.101	-21354.6	6396.1	4225	OK
801	S	IN	Oil Plant	-284622	56.26	3.522	-1061333.6	97.5	-58689	OK
802	S	OUT	Oil Plant	-284234	57.51	3.522	-1061333.6	157.6	59995	OK

Table B3.1.8. Streams exergy flow - Single-shaft compressors – 50% FPSO gas load – RER approach II

Stream	Stream Type S/P	Direction In/Out	System	H (kJ/kgmol)	S (kJ/kgmol.K)	Flow (kgmol/s)	$\sum N_k.\mu_k^0$ Flow (kW)	$H-T_0S+P_0V-\sum N_k.\mu_k^0$ Flow (kW)	Check Ex >0
102	S	IN	Overall Gas Plant	-146519	164.81	1.298	-295989.8	42512.4	OK
201	S	IN	Overall Gas Plant	-178368	183.66	0.016	-4408.1	637.2	OK
208	S	IN	Overall Gas Plant	-204760	176.13	0.046	-13722.7	1820.7	OK
803	S	IN	Overall Gas Plant	-284622	56.26	5.843	-1760425.3	161.7	OK
805	S	IN	Overall Gas Plant	-284622	56.26	0.040	-12180.4	1.1	OK
807	S	IN	Overall Gas Plant	-284622	56.26	0.103	-31057.8	2.9	OK
809	S	IN	Overall Gas Plant	-284622	56.26	0.132	-39764.9	3.7	OK
811	S	IN	Overall Gas Plant	-284622	56.26	0.340	-102381.6	9.4	OK
813	S	IN	Overall Gas Plant	-284622	56.26	3.392	-1022120.6	93.9	OK
815	S	IN	Overall Gas Plant	-284622	56.26	3.648	-1099152.0	101.0	OK
817	S	IN	Overall Gas Plant	-284622	56.26	1.290	-388600.7	35.7	OK
819	S	IN	Overall Gas Plant	-284622	56.26	1.586	-477876.2	43.9	OK
821	S	IN	Overall Gas Plant	-284622	56.26	1.899	-572142.2	52.6	OK
823	S	IN	Overall Gas Plant	-284622	56.26	2.167	-652824.6	60.0	OK
825	S	IN	Overall Gas Plant	-284622	56.26	4.376	-1318543.4	121.1	OK
827	S	IN	Overall Gas Plant	-284622	56.26	1.703	-513218.8	47.1	OK
804	S	OUT	Overall Gas Plant	-283068	61.15	5.843	-1760425.3	775.2	OK
806	S	OUT	Overall Gas Plant	-284235	57.51	0.040	-12180.4	1.8	OK
808	S	OUT	Overall Gas Plant	-283067	61.15	0.103	-31057.8	13.8	OK
810	S	OUT	Overall Gas Plant	-283846	58.74	0.132	-39764.9	9.1	OK
812	S	OUT	Overall Gas Plant	-283068	61.15	0.340	-102381.6	45.1	OK
814	S	OUT	Overall Gas Plant	-283068	61.15	3.392	-1022120.6	450.1	OK
816	S	OUT	Overall Gas Plant	-283068	61.15	3.648	-1099152.0	484.0	OK
818	S	OUT	Overall Gas Plant	-283068	61.15	1.290	-388600.7	171.1	OK
820	S	OUT	Overall Gas Plant	-283068	61.15	1.586	-477876.2	210.4	OK
822	S	OUT	Overall Gas Plant	-283068	61.15	1.899	-572142.2	252.0	OK
824	S	OUT	Overall Gas Plant	-283068	61.15	2.167	-652824.6	287.5	OK

826	S	OUT	Overall Gas Plant	-283068	61.15	4.376	-1318543.4	580.6	OK
828	S	OUT	Overall Gas Plant	-283846	58.74	1.703	-513218.8	117.1	OK
510	S	OUT	Overall Gas Plant	-100232	134.01	0.760	-137929.7	31574.5	OK
402	S	OUT	Overall Gas Plant	-96657	155.92	0.167	-30253.4	6440.0	OK
705	S	OUT	Overall Gas Plant	-273140	115.63	0.414	-140865.2	13583.2	OK
1101	S	OUT	Overall Gas Plant	-285676	53.53	0.001	-175.4	0.0	OK
1102	S	OUT	Overall Gas Plant	-284732	56.03	0.000	-99.7	0.0	OK
1103	S	OUT	Overall Gas Plant	-180790	86.07	0.016	-4041.0	760.8	OK
1104	S	OUT	Overall Gas Plant	-287076	50.34	0.002	-599.4	0.5	OK
1105	S	OUT	Overall Gas Plant	-286416	49.88	0.001	-158.6	0.1	OK
1106	S	OUT	Overall Gas Plant	-118741	94.93	0.000	0.0	0.0	OK
1107	S	OUT	Overall Gas Plant	-132940	108.54	0.000	0.0	0.0	OK
1108	S	OUT	Overall Gas Plant	-99269	141.93	0.000	0.0	0.0	OK
1109	S	OUT	Overall Gas Plant	-266265	171.66	0.000	0.0	0.0	OK
1110	S	OUT	Overall Gas Plant	-266266	163.39	0.000	0.0	0.0	OK
1111	S	OUT	Overall Gas Plant	-267244	152.16	0.000	0.0	0.0	OK
1112	S	OUT	Overall Gas Plant	-269677	137.26	0.000	0.0	0.0	OK
C-101_P	P	IN	Overall Gas Plant					8313.4	OK
C-201_P	P	IN	Overall Gas Plant					136.5	OK
C-202_P	P	IN	Overall Gas Plant					603.1	OK
C-501_P	P	IN	Overall Gas Plant					4196.2	OK
C-502_P	P	IN	Overall Gas Plant					4027.6	OK
C-601_P	P	IN	Overall Gas Plant					2109.2	OK
C-602_P	P	IN	Overall Gas Plant					2219.4	OK
C-603_P	P	IN	Overall Gas Plant					2159.1	OK
C-604_P	P	IN	Overall Gas Plant					1846.1	OK
C-701_P	P	IN	Overall Gas Plant					6438.8	OK
C-901_P	P	IN	Overall Gas Plant					574.5	OK
1208	S	IN	Overall Gas Plant	-277139	77.42	0.457	-137799.6	569.7	OK
1209	S	OUT	Overall Gas Plant	-277945	75.40	0.457	-137799.6	474.9	OK
1303-A	S	IN	800-CW System	-285558	53.18	15.652	-4716189.7	73.5	OK

1303-B	S	IN	800-CW System	-285558	53.18	15.652	-4716189.7	73.5	OK
830	S	IN	800-CW System	-283253	60.57	30.168	-9090005.8	3621.1	OK
1306	S	OUT	800-CW System	-284236	57.51	31.304	-9432379.3	1367.2	OK
832	S	OUT	800-CW System	-284615	56.26	30.168	-9090005.8	1035.4	OK
P-802A	P	IN	800-CW System					66.0	OK
P-802B	P	IN	800-CW System					66.0	OK
P-801	P	IN	800-CW System					163.7	OK
102	S	IN	100-Main Comp.	-146519	164.81	1.298	-295989.8	42512.4	OK
803	S	IN	100-Main Comp.	-284622	56.26	5.843	-1760425.3	161.7	OK
107	S	OUT	100-Main Comp.	-149531	155.29	1.373	-317311.2	48780.4	OK
804	S	OUT	100-Main Comp.	-283068	61.15	5.843	-1760425.3	775.2	OK
1101	S	OUT	100-Main Comp.	-285676	53.53	0.001	-175.4	0.0	OK
214	S	IN	100-Main Comp.	-191775	162.13	0.076	-21496.0	3204.2	OK
C-101_P	P	IN	100-Main Comp.					8313.4	OK
404	S	IN	500-Export Comp.	-96657	155.92	0.760	-137929.7	29361.0	OK
813	S	IN	500-Export Comp.	-284622	56.26	3.392	-1022120.6	93.9	OK
815	S	IN	500-Export Comp.	-284622	56.26	3.648	-1099152.0	101.0	OK
510	S	OUT	500-Export Comp.	-100232	134.01	0.760	-137929.7	31574.5	OK
814	S	OUT	500-Export Comp.	-283068	61.15	3.392	-1022120.6	450.1	OK
816	S	OUT	500-Export Comp.	-283068	61.15	3.648	-1099152.0	484.0	OK
1107	S	OUT	500-Export Comp.	-132940	108.54	0.000	0.0	0.0	OK
1108	S	OUT	500-Export Comp.	-99269	141.93	0.000	0.0	0.0	OK
C-501_P	P	IN	500-Export Comp.					4196.2	OK
C-502_P	P	IN	500-Export Comp.					4027.6	OK
403	S	IN	600-CO2 Comp.	-266339	171.41	0.414	-140865.2	9558.5	OK
817	S	IN	600-CO2 Comp.	-284622	56.26	1.290	-388600.7	35.7	OK
819	S	IN	600-CO2 Comp.	-284622	56.26	1.586	-477876.2	43.9	OK
821	S	IN	600-CO2 Comp.	-284622	56.26	1.899	-572142.2	52.6	OK
823	S	IN	600-CO2 Comp.	-284622	56.26	2.167	-652824.6	60.0	OK
620	S	OUT	600-CO2 Comp.	-272265	123.61	0.414	-140865.2	12966.2	OK
818	S	OUT	600-CO2 Comp.	-283068	61.15	1.290	-388600.7	171.1	OK

820	S	OUT	600-CO2 Comp.	-283068	61.15	1.586	-477876.2	210.4	OK
822	S	OUT	600-CO2 Comp.	-283068	61.15	1.899	-572142.2	252.0	OK
824	S	OUT	600-CO2 Comp.	-283068	61.15	2.167	-652824.6	287.5	OK
1109	S	OUT	600-CO2 Comp.	-266265	171.66	0.000	0.0	0.0	OK
1110	S	OUT	600-CO2 Comp.	-266266	163.39	0.000	0.0	0.0	OK
1111	S	OUT	600-CO2 Comp.	-267244	152.16	0.000	0.0	0.0	OK
1112	S	OUT	600-CO2 Comp.	-269677	137.26	0.000	0.0	0.0	OK
C-601_P	P	IN	600-CO2 Comp.					2109.2	OK
C-602_P	P	IN	600-CO2 Comp.					2219.4	OK
C-603_P	P	IN	600-CO2 Comp.					2159.1	OK
C-604_P	P	IN	600-CO2 Comp.					1846.1	OK
620	S	IN	700-EOR Comp.	-272265	123.61	0.414	-140865.2	12966.2	OK
825	S	IN	700-EOR Comp.	-284622	56.26	4.376	-1318543.4	121.1	OK
705	S	OUT	700-EOR Comp.	-273140	115.63	0.414	-140865.2	13583.2	OK
826	S	OUT	700-EOR Comp.	-283068	61.15	4.376	-1318543.4	580.6	OK
C-701_P	P	IN	700-EOR Comp.					6438.8	OK
307	S	IN	400-MP Unit	-149330	155.00	1.341	-309048.3	47254.1	OK
401	S	OUT	400-MP Unit	-96657	155.92	0.927	-168183.1	35801.0	OK
403	S	OUT	400-MP Unit	-266339	171.41	0.414	-140865.2	9558.5	OK
1208	S	IN	400-MP Unit	-277139	77.42	0.457	-137799.6	569.7	OK
1209	S	OUT	400-MP Unit	-277945	75.40	0.457	-137799.6	474.9	OK
901	S	IN	900-C3 Cycle	-106648	141.75	0.069	-14744.1	4416.2	OK
827	S	IN	900-C3 Cycle	-284622	56.26	1.703	-513218.8	47.1	OK
907	S	OUT	900-C3 Cycle	-117416	101.30	0.069	-14744.1	4500.5	OK
828	S	OUT	900-C3 Cycle	-283846	58.74	1.703	-513218.8	117.1	OK
C-901_P	P	IN	900-C3 Cycle					574.5	OK
201	S	IN	200-VRU	-178368	183.66	0.016	-4408.1	637.2	OK
208	S	IN	200-VRU	-204760	176.13	0.046	-13722.7	1820.7	OK
317	S	IN	200-VRU	-171930	112.91	0.030	-7506.0	1347.1	OK

805	S	IN	200-VRU	-284622	56.26	0.040	-12180.4	1.1	OK
807	S	IN	200-VRU	-284622	56.26	0.103	-31057.8	2.9	OK
809	S	IN	200-VRU	-284622	56.26	0.132	-39764.9	3.7	OK
811	S	IN	200-VRU	-284622	56.26	0.340	-102381.6	9.4	OK
806	S	OUT	200-VRU	-284235	57.51	0.040	-12180.4	1.8	OK
808	S	OUT	200-VRU	-283067	61.15	0.103	-31057.8	13.8	OK
810	S	OUT	200-VRU	-283846	58.74	0.132	-39764.9	9.1	OK
812	S	OUT	200-VRU	-283068	61.15	0.340	-102381.6	45.1	OK
214	S	OUT	200-VRU	-191775	162.13	0.076	-21496.0	3204.2	OK
1102	S	OUT	200-VRU	-284732	56.03	0.000	-99.7	0.0	OK
1103	S	OUT	200-VRU	-180790	86.07	0.016	-4041.0	760.8	OK
C-201_P	P	IN	200-VRU					136.5	OK
C-202_P	P	IN	200-VRU					603.1	OK
303	S	IN	300-HCDP Adj.	-150800	150.26	1.359	-313432.5	48117.3	OK
305	S	OUT	300-HCDP Adj.	-151092	148.89	1.341	-309048.3	47317.6	OK
312	S	OUT	300-HCDP Adj.	-171059	107.28	0.018	-4384.1	818.0	OK
907	S	IN	300-HCDP Adj.	-117416	101.30	0.069	-14744.1	4500.5	OK
901	S	OUT	300-HCDP Adj.	-106648	141.75	0.069	-14744.1	4416.2	OK
801	S	OUT	Oil Plant	-284622	56.26	3.650	-1099717.2	101.0	OK
802	S	IN	Oil Plant	-284234	57.51	3.650	-1099717.2	163.3	OK

Table B3.1.9. Streams exergy flow - Single-shaft compressors – 25% FPSO gas load – RER-2

Stream	Stream Type S/P	Direction In/Out	System	H (kJ/kgmol)	S (kJ/kgmol.K)	Flow (kgmol/s)	$\sum N_k.\mu_k^0$ Flow (kW)	$H-T_0S+P_0V-\sum N_k.\mu_k^0$ Flow (kW)	Check Ex >0
102	S	IN	Overall Gas Plant	-193477	164.61	0.581	-158649.3	18014.9	OK
201	S	IN	Overall Gas Plant	-225649	181.98	0.006	-1844.7	200.8	OK
208	S	IN	Overall Gas Plant	-254181	174.38	0.019	-6562.0	665.8	OK
803	S	IN	Overall Gas Plant	-284622	56.26	5.658	-1704929.6	156.6	OK
805	S	IN	Overall Gas Plant	-284622	56.26	0.006	-1714.2	0.2	OK
807	S	IN	Overall Gas Plant	-284622	56.26	0.094	-28201.7	2.6	OK
809	S	IN	Overall Gas Plant	-284622	56.26	0.046	-13809.6	1.3	OK
811	S	IN	Overall Gas Plant	-284622	56.26	0.338	-101853.6	9.4	OK
813	S	IN	Overall Gas Plant	-284622	56.26	2.702	-814069.2	74.8	OK
815	S	IN	Overall Gas Plant	-284622	56.26	2.584	-778458.4	71.5	OK
817	S	IN	Overall Gas Plant	-284622	56.26	1.261	-380016.5	34.9	OK
819	S	IN	Overall Gas Plant	-284622	56.26	1.523	-458840.6	42.1	OK
821	S	IN	Overall Gas Plant	-284622	56.26	1.702	-512874.3	47.1	OK
823	S	IN	Overall Gas Plant	-284622	56.26	1.749	-526925.7	48.4	OK
825	S	IN	Overall Gas Plant	-284622	56.26	4.031	-1214669.5	111.6	OK
827	S	IN	Overall Gas Plant	-284622	56.26	1.730	-521244.5	47.9	OK
804	S	OUT	Overall Gas Plant	-283068	61.15	5.658	-1704929.6	750.8	OK
806	S	OUT	Overall Gas Plant	-284235	57.51	0.006	-1714.2	0.2	OK
808	S	OUT	Overall Gas Plant	-283067	61.15	0.094	-28201.7	12.5	OK
810	S	OUT	Overall Gas Plant	-283846	58.74	0.046	-13809.6	3.2	OK
812	S	OUT	Overall Gas Plant	-283068	61.15	0.338	-101853.6	44.9	OK
814	S	OUT	Overall Gas Plant	-283068	61.15	2.702	-814069.2	358.5	OK
816	S	OUT	Overall Gas Plant	-283068	61.15	2.584	-778458.4	342.8	OK
818	S	OUT	Overall Gas Plant	-283068	61.15	1.261	-380016.5	167.3	OK
820	S	OUT	Overall Gas Plant	-283068	61.15	1.523	-458840.6	202.1	OK
822	S	OUT	Overall Gas Plant	-283068	61.15	1.702	-512874.3	225.9	OK
824	S	OUT	Overall Gas Plant	-283068	61.15	1.749	-526925.7	232.0	OK

826	S	OUT	Overall Gas Plant	-283068	61.15	4.031	-1214669.5	534.9	OK
828	S	OUT	Overall Gas Plant	-283846	58.74	1.730	-521244.5	119.0	OK
510	S	OUT	Overall Gas Plant	-100257	134.26	0.145	-26339.0	6042.8	OK
402	S	OUT	Overall Gas Plant	-97821	154.85	0.158	-28921.2	6206.7	OK
705	S	OUT	Overall Gas Plant	-309848	111.68	0.289	-108476.8	9260.3	OK
1101	S	OUT	Overall Gas Plant	-286104	52.78	0.001	-326.1	0.1	OK
1102	S	OUT	Overall Gas Plant	-284945	55.42	0.000	-28.3	0.0	OK
1103	S	OUT	Overall Gas Plant	-192339	87.03	0.005	-1434.0	249.0	OK
1104	S	OUT	Overall Gas Plant	-287549	50.63	0.001	-207.0	0.2	OK
1105	S	OUT	Overall Gas Plant	-286423	49.85	0.000	-80.9	0.0	OK
1106	S	OUT	Overall Gas Plant	-83662	201.20	0.000	0.0	0.0	OK
1107	S	OUT	Overall Gas Plant	-130193	106.31	0.006	-1246.0	303.1	OK
1108	S	OUT	Overall Gas Plant	-100086	139.52	0.000	0.0	0.0	OK
1109	S	OUT	Overall Gas Plant	-302035	169.53	0.000	0.0	0.0	OK
1110	S	OUT	Overall Gas Plant	-302152	160.91	0.000	0.0	0.0	OK
1111	S	OUT	Overall Gas Plant	-303646	147.99	0.000	0.0	0.0	OK
1112	S	OUT	Overall Gas Plant	-306947	130.49	0.000	0.0	0.0	OK
C-101_P	P	IN	Overall Gas Plant					8161.0	OK
C-201_P	P	IN	Overall Gas Plant					138.2	OK
C-202_P	P	IN	Overall Gas Plant					612.2	OK
C-501_P	P	IN	Overall Gas Plant					3970.1	OK
C-502_P	P	IN	Overall Gas Plant					3702.3	OK
C-601_P	P	IN	Overall Gas Plant					2091.4	OK
C-602_P	P	IN	Overall Gas Plant					2174.0	OK
C-603_P	P	IN	Overall Gas Plant					1979.2	OK
C-604_P	P	IN	Overall Gas Plant					1484.6	OK
C-701_P	P	IN	Overall Gas Plant					6032.8	OK
C-901_P	P	IN	Overall Gas Plant					1005.6	OK
1208	S	IN	Overall Gas Plant	-277139	77.42	0.208	-62806.1	259.7	OK
1209	S	OUT	Overall Gas Plant	-277945	75.40	0.208	-62806.1	216.5	OK
1303-A	S	IN	800-CW System	-285558	53.18	13.431	-4046874.6	63.6	OK

1303-B	S	IN	800-CW System	-285558	53.18	13.431	-4046874.6	63.6	OK
830	S	IN	800-CW System	-283160	60.86	24.248	-7306298.2	3123.6	OK
1306	S	OUT	800-CW System	-284235	57.51	26.862	-8093749.1	1174.0	OK
832	S	OUT	800-CW System	-284615	56.26	24.248	-7306298.2	832.2	OK
P-802A	P	IN	800-CW System					56.0	OK
P-802B	P	IN	800-CW System					56.0	OK
P-801	P	IN	800-CW System					126.5	OK
102	S	IN	100-Main Comp.	-193477	164.61	0.581	-158649.3	18014.9	OK
803	S	IN	100-Main Comp.	-284622	56.26	5.658	-1704929.6	156.6	OK
107	S	OUT	100-Main Comp.	-196887	153.66	0.614	-169510.5	20672.1	OK
804	S	OUT	100-Main Comp.	-283068	61.15	5.658	-1704929.6	750.8	OK
1101	S	OUT	100-Main Comp.	-286104	52.78	0.001	-326.1	0.1	OK
214	S	IN	100-Main Comp.	-238694	160.88	0.035	-11187.4	1302.1	OK
C-101_P	P	IN	100-Main Comp.					8161.0	OK
404	S	IN	500-Export Comp.	-97821	154.85	0.151	-27585.0	5919.9	OK
813	S	IN	500-Export Comp.	-284622	56.26	2.702	-814069.2	74.8	OK
815	S	IN	500-Export Comp.	-284622	56.26	2.584	-778458.4	71.5	OK
510	S	OUT	500-Export Comp.	-100257	134.26	0.145	-26339.0	6042.8	OK
814	S	OUT	500-Export Comp.	-283068	61.15	2.702	-814069.2	358.5	OK
816	S	OUT	500-Export Comp.	-283068	61.15	2.584	-778458.4	342.8	OK
1107	S	OUT	500-Export Comp.	-130193	106.31	0.006	-1246.0	303.1	OK
1108	S	OUT	500-Export Comp.	-100086	139.52	0.000	0.0	0.0	OK
C-501_P	P	IN	500-Export Comp.					3970.1	OK
C-502_P	P	IN	500-Export Comp.					3702.3	OK
403	S	IN	600-CO2 Comp.	-302265	168.76	0.289	-108477.0	6563.7	OK
817	S	IN	600-CO2 Comp.	-284622	56.26	1.261	-380016.5	34.9	OK
819	S	IN	600-CO2 Comp.	-284622	56.26	1.523	-458840.6	42.1	OK
821	S	IN	600-CO2 Comp.	-284622	56.26	1.702	-512874.3	47.1	OK
823	S	IN	600-CO2 Comp.	-284622	56.26	1.749	-526925.7	48.4	OK
620	S	OUT	600-CO2 Comp.	-309043	119.18	0.289	-108477.0	8851.2	OK
818	S	OUT	600-CO2 Comp.	-283068	61.15	1.261	-380016.5	167.3	OK

820	S	OUT	600-CO2 Comp.	-283068	61.15	1.523	-458840.6	202.1	OK
822	S	OUT	600-CO2 Comp.	-283068	61.15	1.702	-512874.3	225.9	OK
824	S	OUT	600-CO2 Comp.	-283068	61.15	1.749	-526925.7	232.0	OK
1109	S	OUT	600-CO2 Comp.	-302035	169.53	0.000	0.0	0.0	OK
1110	S	OUT	600-CO2 Comp.	-302152	160.91	0.000	0.0	0.0	OK
1111	S	OUT	600-CO2 Comp.	-303646	147.99	0.000	0.0	0.0	OK
1112	S	OUT	600-CO2 Comp.	-306947	130.49	0.000	0.0	0.0	OK
C-601_P	P	IN	600-CO2 Comp.					2091.4	OK
C-602_P	P	IN	600-CO2 Comp.					2174.0	OK
C-603_P	P	IN	600-CO2 Comp.					1979.2	OK
C-604_P	P	IN	600-CO2 Comp.					1484.6	OK
620	S	IN	700-EOR Comp.	-309043	119.18	0.289	-108477.0	8851.2	OK
825	S	IN	700-EOR Comp.	-284622	56.26	4.031	-1214669.5	111.6	OK
705	S	OUT	700-EOR Comp.	-309848	111.68	0.289	-108476.8	9260.3	OK
826	S	OUT	700-EOR Comp.	-283068	61.15	4.031	-1214669.5	534.9	OK
C-701_P	P	IN	700-EOR Comp.					6032.8	OK
307	S	IN	400-MP Unit	-196983	153.38	0.598	-164983.2	19974.9	OK
401	S	OUT	400-MP Unit	-97821	154.85	0.309	-56506.1	12126.6	OK
403	S	OUT	400-MP Unit	-302265	168.76	0.289	-108477.0	6563.7	OK
1208	S	IN	400-MP Unit	-277139	77.42	0.208	-62806.1	259.7	OK
1209	S	OUT	400-MP Unit	-277945	75.40	0.208	-62806.1	216.5	OK
901	S	IN	900-C3 Cycle	-106645	141.76	0.031	-6656.2	1993.7	OK
827	S	IN	900-C3 Cycle	-284622	56.26	1.730	-521244.5	47.9	OK
907	S	OUT	900-C3 Cycle	-117416	101.30	0.031	-6656.2	2031.8	OK
828	S	OUT	900-C3 Cycle	-283846	58.74	1.730	-521244.5	119.0	OK
C-901_P	P	IN	900-C3 Cycle					1005.6	OK
201	S	IN	200-VRU	-225649	181.98	0.006	-1844.7	200.8	OK
208	S	IN	200-VRU	-254181	174.38	0.019	-6562.0	665.8	OK
317	S	IN	200-VRU	-209972	113.61	0.015	-4243.0	615.7	OK

805	S	IN	200-VRU	-284622	56.26	0.006	-1714.2	0.2	OK
807	S	IN	200-VRU	-284622	56.26	0.094	-28201.7	2.6	OK
809	S	IN	200-VRU	-284622	56.26	0.046	-13809.6	1.3	OK
811	S	IN	200-VRU	-284622	56.26	0.338	-101853.6	9.4	OK
806	S	OUT	200-VRU	-284235	57.51	0.006	-1714.2	0.2	OK
808	S	OUT	200-VRU	-283067	61.15	0.094	-28201.7	12.5	OK
810	S	OUT	200-VRU	-283846	58.74	0.046	-13809.6	3.2	OK
812	S	OUT	200-VRU	-283068	61.15	0.338	-101853.6	44.9	OK
214	S	OUT	200-VRU	-238694	160.88	0.035	-11187.4	1302.1	OK
1102	S	OUT	200-VRU	-284945	55.42	0.000	-28.3	0.0	OK
1103	S	OUT	200-VRU	-192339	87.03	0.005	-1434.0	249.0	OK
C-201_P	P	IN	200-VRU					138.2	OK
C-202_P	P	IN	200-VRU					612.2	OK
303	S	IN	300-HCDP Adj.	-198411	148.49	0.606	-167190.5	20325.2	OK
305	S	OUT	300-HCDP Adj.	-198808	147.05	0.598	-164983.2	20004.0	OK
312	S	OUT	300-HCDP Adj.	-211405	107.91	0.008	-2207.3	330.1	OK
907	S	IN	300-HCDP Adj.	-117416	101.30	0.031	-6656.2	2031.8	OK
901	S	OUT	300-HCDP Adj.	-106645	141.76	0.031	-6656.2	1993.7	OK
801	S	IN	Oil Plant	-284622	56.26	0.825	-248690.8	22.8	OK
802	S	OUT	Oil Plant	-284234	57.51	0.825	-248690.8	36.9	OK

Table B3.1.10. Streams exergy flow - Multiple paralleled compressors – 100% FPSO gas load – RER-2

Stream	*Stream Type S/P*	*Direction In/Out*	*System*	*H (kJ/kgmol)*	*S (kJ/kgmol.K)*	*Flow (kgmol/s)*	*$\sum N_k.\mu_k^0$ (kW)*	*$H-T_0S+P_0V-\sum Nk.\mu_k^0$ (kW)*	*S_K (kW)*	*Check Ex >0*
102	S	IN	Overall Gas Plant	-123689	163.76	2.173	-446929.1	72828.2	-105369	OK
201	S	IN	Overall Gas Plant	-156362	183.40	0.030	-7474.2	1233.6	-1609	OK
208	S	IN	Overall Gas Plant	-176963	176.71	0.098	-26693.3	4154.1	-5144	OK
803	S	IN	Overall Gas Plant	-284622	56.26	5.394	-1625184.2	149.3	-89868	OK
805	S	IN	Overall Gas Plant	-284622	56.26	0.028	-8563.0	0.8	-474	OK
807	S	IN	Overall Gas Plant	-284622	56.26	0.109	-32694.6	3.0	-1808	OK
809	S	IN	Overall Gas Plant	-284622	56.26	0.304	-91748.2	8.4	-5073	OK
811	S	IN	Overall Gas Plant	-284622	56.26	0.386	-116320.6	10.7	-6432	OK
813	S	IN	Overall Gas Plant	-284622	56.26	4.690	-1413300.6	129.8	-78152	OK
815	S	IN	Overall Gas Plant	-284622	56.26	5.318	-1602345.2	147.2	-88605	OK
817	S	IN	Overall Gas Plant	-284622	56.26	1.048	-315688.3	29.0	-17457	OK
819	S	IN	Overall Gas Plant	-284622	56.26	1.340	-403707.8	37.1	-22324	OK
821	S	IN	Overall Gas Plant	-284622	56.26	1.715	-516649.3	47.5	-28569	OK
823	S	IN	Overall Gas Plant	-284622	56.26	2.131	-642009.6	59.0	-35501	OK
825	S	IN	Overall Gas Plant	-284622	56.26	1.270	-382547.8	35.1	-21154	OK
827	S	IN	Overall Gas Plant	-284622	56.26	1.995	-601016.6	55.2	-33235	OK
804	S	OUT	Overall Gas Plant	-283068	61.15	5.394	-1625184.2	715.7	97684	OK
806	S	OUT	Overall Gas Plant	-284235	57.51	0.028	-8563.0	1.2	484	OK
808	S	OUT	Overall Gas Plant	-283067	61.15	0.109	-32694.6	14.5	1965	OK
810	S	OUT	Overall Gas Plant	-283846	58.74	0.304	-91748.2	20.9	5297	OK
812	S	OUT	Overall Gas Plant	-283068	61.15	0.386	-116320.6	51.2	6992	OK
814	S	OUT	Overall Gas Plant	-283068	61.15	4.690	-1413300.6	622.4	84949	OK
816	S	OUT	Overall Gas Plant	-283068	61.15	5.318	-1602345.2	705.6	96312	OK
818	S	OUT	Overall Gas Plant	-283068	61.15	1.048	-315688.3	139.0	18975	OK
820	S	OUT	Overall Gas Plant	-283068	61.15	1.340	-403707.8	177.8	24266	OK
822	S	OUT	Overall Gas Plant	-283068	61.15	1.715	-516649.3	227.5	31054	OK

824	S	OUT	Overall Gas Plant	-283068	61.15	2.131	-642009.6	282.7	38589	OK
826	S	OUT	Overall Gas Plant	-283068	61.15	1.270	-382547.8	168.5	22994	OK
828	S	OUT	Overall Gas Plant	-283846	58.74	1.995	-601016.6	137.2	34702	OK
510	S	OUT	Overall Gas Plant	-99660	134.20	1.652	-298296.2	68040.5	65645	OK
402	S	OUT	Overall Gas Plant	-96059	156.34	0.146	-26456.9	5601.9	6783	OK
705	S	OUT	Overall Gas Plant	-245893	118.14	0.474	-148965.9	15851.1	16581	OK
1101	S	OUT	Overall Gas Plant	-285880	52.60	0.000	-64.0	0.0	3	OK
1102	S	OUT	Overall Gas Plant	-284254	57.53	0.000	-27.6	0.0	2	OK
1103	S	OUT	Overall Gas Plant	-180564	87.06	0.025	-6242.4	1154.8	636	OK
1104	S	OUT	Overall Gas Plant	-286952	49.90	0.003	-789.2	0.6	39	OK
1105	S	OUT	Overall Gas Plant	-286498	49.59	0.001	-235.2	0.1	11	OK
1106	S	OUT	Overall Gas Plant	-123654	77.86	0.000	0.0	0.0	0	OK
1107	S	OUT	Overall Gas Plant	-127302	118.83	0.000	0.0	0.0	0	OK
1108	S	OUT	Overall Gas Plant	-97534	146.03	0.000	0.0	0.0	0	OK
1109	S	OUT	Overall Gas Plant	-239668	172.88	0.000	0.0	0.0	0	OK
1110	S	OUT	Overall Gas Plant	-239507	165.12	0.000	0.0	0.0	0	OK
1111	S	OUT	Overall Gas Plant	-240046	155.27	0.000	0.0	0.0	0	OK
1112	S	OUT	Overall Gas Plant	-241741	142.64	0.000	0.0	0.0	0	OK
C-101-A_P	P	IN	Overall Gas Plant					4058.8	0	OK
C-101-B_P	P	IN	Overall Gas Plant					4058.8	0	OK
C-201-A_P	P	IN	Overall Gas Plant					42.9	0	OK
C-201-B_P	P	IN	Overall Gas Plant					42.9	0	OK
C-201-C_P	P	IN	Overall Gas Plant					42.9	0	OK
C-202-A_P	P	IN	Overall Gas Plant					180.0	0	OK
C-202-B_P	P	IN	Overall Gas Plant					180.0	0	OK
C-202-C_P	P	IN	Overall Gas Plant					180.0	0	OK
C-501-A_P	P	IN	Overall Gas Plant					1618.7	0	OK
C-501-B_P	P	IN	Overall Gas Plant					1618.7	0	OK
C-501-C_P	P	IN	Overall Gas Plant					1618.7	0	OK
C-502-A_P	P	IN	Overall Gas Plant					1583.6	0	OK
C-502-B_P	P	IN	Overall Gas Plant					1583.6	0	OK

C-502-C_P	P	IN	Overall Gas Plant					1583.6	0	OK
C-601_P	P	IN	Overall Gas Plant					1707.3	0	OK
C-602_P	P	IN	Overall Gas Plant					1824.1	0	OK
C-603_P	P	IN	Overall Gas Plant					1864.4	0	OK
C-604_P	P	IN	Overall Gas Plant					1762.3	0	OK
C-701-A_P	P	IN	Overall Gas Plant					1551.8	0	OK
C-701-B_P	P	IN	Overall Gas Plant					0.0	0	OK
C-901-A_P	P	IN	Overall Gas Plant					229.4	0	OK
C-901-B_P	P	IN	Overall Gas Plant					229.4	0	OK
1208	S	IN	Overall Gas Plant	-277139	77.42	0.767	-231176.8	955.8	-17591	OK
1209	S	OUT	Overall Gas Plant	-277945	75.40	0.767	-231176.8	796.8	17131	OK
1303-A	S	IN	800-CW System	-285558	53.18	15.030	-4528857.0	70.8	-236717	OK
1303-B	S	IN	800-CW System	-285558	53.18	15.030	-4528857.0	70.8	-236717	OK
830	S	IN	800-CW System	-283266	60.53	29.249	-8813109.3	3477.9	-524333	OK
1306	S	OUT	800-CW System	-284236	57.51	30.061	-9057714.1	1313.3	512008	OK
832	S	OUT	800-CW System	-284615	56.26	29.249	-8813109.3	1003.9	487346	OK
P-802A	P	IN	800-CW System					63.1	0	OK
P-802B	P	IN	800-CW System					63.1	0	OK
P-801	P	IN	800-CW System					157.6	0	OK
102	S	IN	100-Main Comp.	-123689	163.76	2.173	-446929.1	72828.2	-105369	OK
803	S	IN	100-Main Comp.	-284622	56.26	5.394	-1625184.2	149.3	-89868	OK
107	S	OUT	100-Main Comp.	-126532	155.67	2.315	-483975.5	84343.9	106720	OK
804	S	OUT	100-Main Comp.	-283068	61.15	5.394	-1625184.2	715.7	97684	OK
1101	S	OUT	100-Main Comp.	-285880	52.60	0.000	-64.0	0.0	3	OK
214	S	IN	100-Main Comp.	-168264	160.43	0.142	-37110.4	6364.6	-6770	OK
C-101-A_P	P	IN	100-Main Comp.					4058.8	0	OK
C-101-B_P	P	IN	100-Main Comp.					4058.8	0	OK
404	S	IN	500-Export Comp.	-96059	156.34	1.652	-298296.2	63159.8	-76474	OK
813	S	IN	500-Export Comp.	-284622	56.26	4.690	-1413300.6	129.8	-78152	OK
815	S	IN	500-Export Comp.	-284622	56.26	5.318	-1602345.2	147.2	-88605	OK
510	S	OUT	500-Export Comp.	-99660	134.20	1.652	-298296.2	68040.5	65645	OK

814	S	OUT	500-Export Comp.	-283068	61.15	4.690	-1413300.6	622.4	84949	OK
816	S	OUT	500-Export Comp.	-283068	61.15	5.318	-1602345.2	705.6	96312	OK
1107	S	OUT	500-Export Comp.	-127302	118.83	0.000	0.0	0.0	0	OK
1108	S	OUT	500-Export Comp.	-97534	146.03	0.000	0.0	0.0	0	OK
C-501-A_P	P	IN	500-Export Comp.					1618.7	0	OK
C-501-B_P	P	IN	500-Export Comp.					1618.7	0	OK
C-501-C_P	P	IN	500-Export Comp.					1618.7	0	OK
C-502-A_P	P	IN	500-Export Comp.					1583.6	0	OK
C-502-B_P	P	IN	500-Export Comp.					1583.6	0	OK
C-502-C_P	P	IN	500-Export Comp.					1583.6	0	OK
403	S	IN	600-CO2 Comp.	-239667	172.88	0.474	-148965.9	11119.3	-24264	OK
817	S	IN	600-CO2 Comp.	-284622	56.26	1.048	-315688.3	29.0	-17457	OK
819	S	IN	600-CO2 Comp.	-284622	56.26	1.340	-403707.8	37.1	-22324	OK
821	S	IN	600-CO2 Comp.	-284622	56.26	1.715	-516649.3	47.5	-28569	OK
823	S	IN	600-CO2 Comp.	-284622	56.26	2.131	-642009.6	59.0	-35501	OK
620	S	OUT	600-CO2 Comp.	-245004	126.36	0.474	-148965.9	15118.5	17735	OK
818	S	OUT	600-CO2 Comp.	-283068	61.15	1.048	-315688.3	139.0	18975	OK
820	S	OUT	600-CO2 Comp.	-283068	61.15	1.340	-403707.8	177.8	24266	OK
822	S	OUT	600-CO2 Comp.	-283068	61.15	1.715	-516649.3	227.5	31054	OK
824	S	OUT	600-CO2 Comp.	-283068	61.15	2.131	-642009.6	282.7	38589	OK
1109	S	OUT	600-CO2 Comp.	-239668	172.88	0.000	0.0	0.0	0	OK
1110	S	OUT	600-CO2 Comp.	-239507	165.12	0.000	0.0	0.0	0	OK
1111	S	OUT	600-CO2 Comp.	-240046	155.27	0.000	0.0	0.0	0	OK
1112	S	OUT	600-CO2 Comp.	-241741	142.64	0.000	0.0	0.0	0	OK
C-601_P	P	IN	600-CO2 Comp.					1707.3	0	OK
C-602_P	P	IN	600-CO2 Comp.					1824.1	0	OK
C-603_P	P	IN	600-CO2 Comp.					1864.4	0	OK
C-604_P	P	IN	600-CO2 Comp.					1762.3	0	OK
620	S	IN	700-EOR Comp.	-245004	126.36	0.474	-148965.9	15118.5	-17735	OK

825	S	IN	700-EOR Comp.	-284622	56.26	1.270	-382547.8	35.1	-21154	OK
705	S	OUT	700-EOR Comp.	-245893	118.14	0.474	-148965.9	15851.1	16581	OK
826	S	OUT	700-EOR Comp.	-283068	61.15	1.270	-382547.8	168.5	22994	OK
C-701-A_P	P	IN	700-EOR Comp.					1551.8	0	OK
C-701-B_P	P	IN	700-EOR Comp.					0.0	0	OK
307	S	IN	400-MP Unit	-126285	155.39	2.272	-473719.1	82222.3	-104561	OK
401	S	OUT	400-MP Unit	-96059	156.34	1.798	-324753.2	68761.6	83257	OK
403	S	OUT	400-MP Unit	-239667	172.88	0.474	-148965.9	11119.3	24264	OK
1208	S	IN	400-MP Unit	-277139	77.42	0.767	-231176.8	955.8	-17591	OK
1209	S	OUT	400-MP Unit	-277945	75.40	0.767	-231176.8	796.8	17131	OK
901	S	IN	900-C3 Cycle	-106651	141.74	0.101	-21491.4	6437.2	-4252	OK
827	S	IN	900-C3 Cycle	-284622	56.26	1.995	-601016.6	55.2	-33235	OK
907	S	OUT	900-C3 Cycle	-117416	101.30	0.101	-21491.4	6560.1	3039	OK
828	S	OUT	900-C3 Cycle	-283846	58.74	1.995	-601016.6	137.2	34702	OK
C-901-A_P	P	IN	900-C3 Cycle					229.4	0	OK
C-901-B_P	P	IN	900-C3 Cycle					229.4	0	OK
201	S	IN	200-VRU	-156362	183.40	0.030	-7474.2	1233.6	-1609	OK
208	S	IN	200-VRU	-176963	176.71	0.098	-26693.3	4154.1	-5144	OK
317	S	IN	200-VRU	-154625	111.92	0.039	-9212.9	1830.2	-1303	OK
805	S	IN	200-VRU	-284622	56.26	0.028	-8563.0	0.8	-474	OK
807	S	IN	200-VRU	-284622	56.26	0.109	-32694.6	3.0	-1808	OK
809	S	IN	200-VRU	-284622	56.26	0.304	-91748.2	8.4	-5073	OK
811	S	IN	200-VRU	-284622	56.26	0.386	-116320.6	10.7	-6432	OK
806	S	OUT	200-VRU	-284235	57.51	0.028	-8563.0	1.2	484	OK
808	S	OUT	200-VRU	-283067	61.15	0.109	-32694.6	14.5	1965	OK
810	S	OUT	200-VRU	-283846	58.74	0.304	-91748.2	20.9	5297	OK
812	S	OUT	200-VRU	-283068	61.15	0.386	-116320.6	51.2	6992	OK
214	S	OUT	200-VRU	-168264	160.43	0.142	-37110.4	6364.6	6770	OK
1102	S	OUT	200-VRU	-284254	57.53	0.000	-27.6	0.0	2	OK
1103	S	OUT	200-VRU	-180564	87.06	0.025	-6242.4	1154.8	636	OK

C-201-A_P	P	IN	200-VRU					42.9	0	OK
C-201-B_P	P	IN	200-VRU					42.9	0	OK
C-201-C_P	P	IN	200-VRU					42.9	0	OK
C-202-A_P	P	IN	200-VRU					180.0	0	OK
C-202-B_P	P	IN	200-VRU					180.0	0	OK
C-202-C_P	P	IN	200-VRU					180.0	0	OK
303	S	IN	300-HCDP Adj.	-127848	150.51	2.299	-480004.8	83602.2	-102475	OK
305	S	OUT	300-HCDP Adj.	-128021	149.37	2.272	-473719.1	82328.9	100511	OK
312	S	OUT	300-HCDP Adj.	-153751	106.79	0.027	-6285.7	1295.6	851	OK
907	S	IN	300-HCDP Adj.	-117416	101.30	0.101	-21491.4	6560.1	-3039	OK
901	S	OUT	300-HCDP Adj.	-106651	141.74	0.101	-21491.4	6437.2	4252	OK
801	S	OUT	Oil Plant	-284622	56.26	3.522	-1061333.6	97.5	58689	OK
802	S	IN	Oil Plant	-284234	57.51	3.522	-1061333.6	157.6	-59995	OK

Table B3.1.11. Streams exergy flow - Multiple paralleled compressors – 50% FPSO gas load – RER-2

Stream	*Stream Type S/P*	*Direction In/Out*	*System*	*H (kJ/kgmol)*	*S (kJ/kgmol.K)*	*Flow (kgmol/s)*	*$\sum N_k.\mu_k^0$ Flow (kW)*	*$H-T_0S+P_0V-\sum Nk.\mu_k^0$ Flow (kW)*	*S_K (kW)*	*Check Ex >0*
102	S	IN	Overall Gas Plant	-146519	164.81	1.298	-295989.8	42512.4	-63339	OK
201	S	IN	Overall Gas Plant	-178368	183.66	0.016	-4408.1	637.2	-881	OK
208	S	IN	Overall Gas Plant	-204760	176.13	0.046	-13722.7	1820.7	-2416	OK
803	S	IN	Overall Gas Plant	-284622	56.26	3.683	-1109831.4	101.9	-61371	OK
805	S	IN	Overall Gas Plant	-284622	56.26	0.040	-12180.4	1.1	-674	OK
807	S	IN	Overall Gas Plant	-284622	56.26	0.060	-18115.0	1.7	-1002	OK
809	S	IN	Overall Gas Plant	-284622	56.26	0.132	-39764.9	3.7	-2199	OK
811	S	IN	Overall Gas Plant	-284622	56.26	0.149	-44804.8	4.1	-2478	OK
813	S	IN	Overall Gas Plant	-284622	56.26	2.219	-668756.7	61.4	-36980	OK
815	S	IN	Overall Gas Plant	-284622	56.26	2.585	-778940.0	71.6	-43073	OK
817	S	IN	Overall Gas Plant	-284622	56.26	0.882	-265819.6	24.4	-14699	OK
819	S	IN	Overall Gas Plant	-284622	56.26	1.180	-355461.3	32.7	-19656	OK
821	S	IN	Overall Gas Plant	-284622	56.26	1.547	-466125.2	42.8	-25775	OK
823	S	IN	Overall Gas Plant	-284622	56.26	1.934	-582608.8	53.5	-32217	OK
825	S	IN	Overall Gas Plant	-284622	56.26	1.057	-318397.9	29.2	-17606	OK
827	S	IN	Overall Gas Plant	-284622	56.26	1.349	-406417.2	37.3	-22474	OK
804	S	OUT	Overall Gas Plant	-283068	61.15	3.683	-1109831.4	488.7	66708	OK
806	S	OUT	Overall Gas Plant	-284235	57.51	0.040	-12180.4	1.8	689	OK
808	S	OUT	Overall Gas Plant	-283067	61.15	0.060	-18115.0	8.0	1089	OK
810	S	OUT	Overall Gas Plant	-283846	58.74	0.132	-39764.9	9.1	2296	OK
812	S	OUT	Overall Gas Plant	-283068	61.15	0.149	-44804.8	19.7	2693	OK
814	S	OUT	Overall Gas Plant	-283068	61.15	2.219	-668756.7	294.5	40197	OK
816	S	OUT	Overall Gas Plant	-283068	61.15	2.585	-778940.0	343.0	46819	OK
818	S	OUT	Overall Gas Plant	-283068	61.15	0.882	-265819.6	117.1	15978	OK
820	S	OUT	Overall Gas Plant	-283068	61.15	1.180	-355461.3	156.5	21366	OK
822	S	OUT	Overall Gas Plant	-283068	61.15	1.547	-466125.2	205.3	28017	OK

824	S	OUT	Overall Gas Plant	-283068	61.15	1.934	-582608.8	256.6	35019	OK
826	S	OUT	Overall Gas Plant	-283068	61.15	1.057	-318397.9	140.2	19138	OK
828	S	OUT	Overall Gas Plant	-283846	58.74	1.349	-406417.2	92.7	23466	OK
510	S	OUT	Overall Gas Plant	-100221	134.02	0.805	-145982.4	33415.3	31933	OK
402	S	OUT	Overall Gas Plant	-96648	155.92	0.122	-22123.9	4708.9	5630	OK
705	S	OUT	Overall Gas Plant	-273135	115.64	0.414	-140851.6	13581.2	14179	OK
1101	S	OUT	Overall Gas Plant	-285273	54.86	0.000	0.0	0.0	0	OK
1102	S	OUT	Overall Gas Plant	-284261	57.54	0.000	-54.2	0.0	3	OK
1103	S	OUT	Overall Gas Plant	-181522	85.12	0.016	-4181.3	781.7	415	OK
1104	S	OUT	Overall Gas Plant	-287081	50.33	0.003	-768.6	0.6	38	OK
1105	S	OUT	Overall Gas Plant	-286420	49.86	0.001	-158.0	0.1	8	OK
1106	S	OUT	Overall Gas Plant	-123639	77.92	0.000	0.0	0.0	0	OK
1107	S	OUT	Overall Gas Plant	-129428	116.12	0.000	0.0	0.0	0	OK
1108	S	OUT	Overall Gas Plant	-98082	145.88	0.000	0.0	0.0	0	OK
1109	S	OUT	Overall Gas Plant	-266336	171.41	0.000	0.0	0.0	0	OK
1110	S	OUT	Overall Gas Plant	-266086	163.95	0.000	0.0	0.0	0	OK
1111	S	OUT	Overall Gas Plant	-266675	154.00	0.000	0.0	0.0	0	OK
1112	S	OUT	Overall Gas Plant	-268594	140.81	0.000	0.0	0.0	0	OK
C-101-A_P	P	IN	Overall Gas Plant					2482.2	0	OK
C-101-B_P	P	IN	Overall Gas Plant					2482.2	0	OK
C-201-A_P	P	IN	Overall Gas Plant					34.9	0	OK
C-201-B_P	P	IN	Overall Gas Plant					34.9	0	OK
C-201-C_P	P	IN	Overall Gas Plant					0.0	0	OK
C-202-A_P	P	IN	Overall Gas Plant					139.7	0	OK
C-202-B_P	P	IN	Overall Gas Plant					139.7	0	OK
C-202-C_P	P	IN	Overall Gas Plant					0.0	0	OK
C-501-A_P	P	IN	Overall Gas Plant					1156.2	0	OK
C-501-B_P	P	IN	Overall Gas Plant					1156.2	0	OK
C-501-C_P	P	IN	Overall Gas Plant					0.0	0	OK
C-502-A_P	P	IN	Overall Gas Plant					1140.3	0	OK
C-502-B_P	P	IN	Overall Gas Plant					1140.3	0	OK

C-502-C_P	P	IN	Overall Gas Plant					0.0	0	OK
C-601_P	P	IN	Overall Gas Plant					1476.1	0	OK
C-602_P	P	IN	Overall Gas Plant					1587.8	0	OK
C-603_P	P	IN	Overall Gas Plant					1612.1	0	OK
C-604_P	P	IN	Overall Gas Plant					1484.2	0	OK
C-701-A_P	P	IN	Overall Gas Plant					1280.5	0	OK
C-701-B_P	P	IN	Overall Gas Plant					0.0	0	OK
C-901-A_P	P	IN	Overall Gas Plant					155.1	0	OK
C-901-B_P	P	IN	Overall Gas Plant					155.1	0	OK
1208	S	IN	Overall Gas Plant	-277139	77.42	0.457	-137710.3	569.4	-10479	OK
1209	S	OUT	Overall Gas Plant	-277945	75.40	0.457	-137710.3	474.6	10205	OK
1303-A	S	IN	800-CW System	-285557	53.18	10.021	-3019416.3	48.0	-157824	OK
1303-B	S	IN	800-CW System	-285557	53.18	10.021	-3019416.3	48.0	-157824	OK
830	S	IN	800-CW System	-283330	60.33	20.467	-6166940.4	2321.9	-365703	OK
1306	S	OUT	800-CW System	-284236	57.51	20.042	-6038832.6	875.7	341360	OK
832	S	OUT	800-CW System	-284615	56.26	20.467	-6166940.4	702.4	341017	OK
P-802A	P	IN	800-CW System					41.2	0	OK
P-802B	P	IN	800-CW System					41.2	0	OK
P-801	P	IN	800-CW System					104.2	0	OK
102	S	IN	100-Main Comp.	-146519	164.81	1.298	-295989.8	42512.4	-63339	OK
803	S	IN	100-Main Comp.	-284622	56.26	3.683	-1109831.4	101.9	-61371	OK
107	S	OUT	100-Main Comp.	-149576	155.28	1.372	-316995.0	48685.0	63092	OK
804	S	OUT	100-Main Comp.	-283068	61.15	3.683	-1109831.4	488.7	66708	OK
1101	S	OUT	100-Main Comp.	-285273	54.86	0.000	0.0	0.0	0	OK
214	S	IN	100-Main Comp.	-192756	162.62	0.074	-21005.3	3108.8	-3578	OK
C-101-A_P	P	IN	100-Main Comp.					2482.2	0	OK
C-101-B_P	P	IN	100-Main Comp.					2482.2	0	OK
404	S	IN	500-Export Comp.	-96648	155.92	0.805	-145982.4	31071.1	-37152	OK
813	S	IN	500-Export Comp.	-284622	56.26	2.219	-668756.7	61.4	-36980	OK
815	S	IN	500-Export Comp.	-284622	56.26	2.585	-778940.0	71.6	-43073	OK
510	S	OUT	500-Export Comp.	-100221	134.02	0.805	-145982.4	33415.3	31933	OK

814	S	OUT	500-Export Comp.	-283068	61.15	2.219	-668756.7	294.5	40197	OK
816	S	OUT	500-Export Comp.	-283068	61.15	2.585	-778940.0	343.0	46819	OK
1107	S	OUT	500-Export Comp.	-129428	116.12	0.000	0.0	0.0	0	OK
1108	S	OUT	500-Export Comp.	-98082	145.88	0.000	0.0	0.0	0	OK
C-501-A_P	P	IN	500-Export Comp.					1156.2	0	OK
C-501-B_P	P	IN	500-Export Comp.					1156.2	0	OK
C-501-C_P	P	IN	500-Export Comp.					0.0	0	OK
C-502-A_P	P	IN	500-Export Comp.					1140.3	0	OK
C-502-B_P	P	IN	500-Export Comp.					1140.3	0	OK
C-502-C_P	P	IN	500-Export Comp.					0.0	0	OK
403	S	IN	600-CO2 Comp.	-266335	171.41	0.414	-140851.6	9557.7	-21018	OK
817	S	IN	600-CO2 Comp.	-284622	56.26	0.882	-265819.6	24.4	-14699	OK
819	S	IN	600-CO2 Comp.	-284622	56.26	1.180	-355461.3	32.7	-19656	OK
821	S	IN	600-CO2 Comp.	-284622	56.26	1.547	-466125.2	42.8	-25775	OK
823	S	IN	600-CO2 Comp.	-284622	56.26	1.934	-582608.8	53.5	-32217	OK
620	S	OUT	600-CO2 Comp.	-272261	123.61	0.414	-140851.6	12965.4	15157	OK
818	S	OUT	600-CO2 Comp.	-283068	61.15	0.882	-265819.6	117.1	15978	OK
820	S	OUT	600-CO2 Comp.	-283068	61.15	1.180	-355461.3	156.5	21366	OK
822	S	OUT	600-CO2 Comp.	-283068	61.15	1.547	-466125.2	205.3	28017	OK
824	S	OUT	600-CO2 Comp.	-283068	61.15	1.934	-582608.8	256.6	35019	OK
1109	S	OUT	600-CO2 Comp.	-266336	171.41	0.000	0.0	0.0	0	OK
1110	S	OUT	600-CO2 Comp.	-266086	163.95	0.000	0.0	0.0	0	OK
1111	S	OUT	600-CO2 Comp.	-266675	154.00	0.000	0.0	0.0	0	OK
1112	S	OUT	600-CO2 Comp.	-268594	140.81	0.000	0.0	0.0	0	OK
C-601_P	P	IN	600-CO2 Comp.					1476.1	0	OK
C-602_P	P	IN	600-CO2 Comp.					1587.8	0	OK
C-603_P	P	IN	600-CO2 Comp.					1612.1	0	OK
C-604_P	P	IN	600-CO2 Comp.					1484.2	0	OK
620	S	IN	700-EOR Comp.	-272261	123.61	0.414	-140851.6	12965.4	-15157	OK

825	S	IN	700-EOR Comp.	-284622	56.26	1.057	-318397.9	29.2	-17606	OK
705	S	OUT	700-EOR Comp.	-273135	115.64	0.414	-140851.6	13581.2	14179	OK
826	S	OUT	700-EOR Comp.	-283068	61.15	1.057	-318397.9	140.2	19138	OK
C-701-A_P	P	IN	700-EOR Comp.					1280.5	0	OK
C-701-B_P	P	IN	700-EOR Comp.					0.0	0	OK
307	S	IN	400-MP Unit	-149333	155.01	1.341	-308957.9	47232.4	-61537	OK
401	S	OUT	400-MP Unit	-96648	155.92	0.926	-168106.3	35780.0	42782	OK
403	S	OUT	400-MP Unit	-266335	171.41	0.414	-140851.6	9557.7	21018	OK
1208	S	IN	400-MP Unit	-277139	77.42	0.457	-137710.3	569.4	-10479	OK
1209	S	OUT	400-MP Unit	-277945	75.40	0.457	-137710.3	474.6	10205	OK
901	S	IN	900-C3 Cycle	-106641	141.78	0.068	-14519.8	4348.9	-2873	OK
827	S	IN	900-C3 Cycle	-284622	56.26	1.349	-406417.2	37.3	-22474	OK
907	S	OUT	900-C3 Cycle	-117416	101.30	0.068	-14519.8	4432.0	2053	OK
828	S	OUT	900-C3 Cycle	-283846	58.74	1.349	-406417.2	92.7	23466	OK
C-901-A_P	P	IN	900-C3 Cycle					155.1	0	OK
C-901-B_P	P	IN	900-C3 Cycle					155.1	0	OK
201	S	IN	200-VRU	-178368	183.66	0.016	-4408.1	637.2	-881	OK
208	S	IN	200-VRU	-204760	176.13	0.046	-13722.7	1820.7	-2416	OK
317	S	IN	200-VRU	-172156	112.94	0.028	-7109.9	1274.2	-949	OK
805	S	IN	200-VRU	-284622	56.26	0.040	-12180.4	1.1	-674	OK
807	S	IN	200-VRU	-284622	56.26	0.060	-18115.0	1.7	-1002	OK
809	S	IN	200-VRU	-284622	56.26	0.132	-39764.9	3.7	-2199	OK
811	S	IN	200-VRU	-284622	56.26	0.149	-44804.8	4.1	-2478	OK
806	S	OUT	200-VRU	-284235	57.51	0.040	-12180.4	1.8	689	OK
808	S	OUT	200-VRU	-283067	61.15	0.060	-18115.0	8.0	1089	OK
810	S	OUT	200-VRU	-283846	58.74	0.132	-39764.9	9.1	2296	OK
812	S	OUT	200-VRU	-283068	61.15	0.149	-44804.8	19.7	2693	OK
214	S	OUT	200-VRU	-192756	162.62	0.074	-21005.3	3108.8	3578	OK
1102	S	OUT	200-VRU	-284261	57.54	0.000	-54.2	0.0	3	OK
1103	S	OUT	200-VRU	-181522	85.12	0.016	-4181.3	781.7	415	OK

C-201-A_P	P	IN	200-VRU					34.9	0	OK
C-201-B_P	P	IN	200-VRU					34.9	0	OK
C-201-C_P	P	IN	200-VRU					0.0	0	OK
C-202-A_P	P	IN	200-VRU					139.7	0	OK
C-202-B_P	P	IN	200-VRU					139.7	0	OK
C-202-C_P	P	IN	200-VRU					0.0	0	OK
303	S	IN	300-HCDP Adj.	-150801	150.26	1.357	-313165.1	48062.3	-60404	OK
305	S	OUT	300-HCDP Adj.	-151094	148.90	1.341	-308957.9	47295.9	59113	OK
312	S	OUT	300-HCDP Adj.	-171194	107.31	0.017	-4207.2	784.2	536	OK
907	S	IN	300-HCDP Adj.	-117416	101.30	0.068	-14519.8	4432.0	-2053	OK
901	S	OUT	300-HCDP Adj.	-106641	141.78	0.068	-14519.8	4348.9	2873	OK
801	S	OUT	Oil Plant	-284622	56.26	3.650	-1099717.2	101.0	60811	OK
802	S	IN	Oil Plant	-284234	57.51	3.650	-1099717.2	163.3	-62164	OK

Table B3.1.12. Streams exergy flow- Multiple paralleled compressors – 25% FPSO gas load – RER-2

Stream	*Stream Type S/P*	*Direction In/Out*	*System*	*H (kJ/kgmol)*	*S (kJ/kgmol.K)*	*Flow (kgmol/s)*	*$\sum N_k.\mu_k^0$ Flow (kW)*	*$H-T_0S+P_0V-\sum Nk.\mu_k^0$ Flow (kW)*	*S_K (kW)*	*Check Ex >0*
102	S	IN	Overall Gas Plant	-193477	164.61	0.581	-158649.3	18014.9	-28303	OK
201	S	IN	Overall Gas Plant	-225649	181.98	0.006	-1844.7	200.8	-317	OK
208	S	IN	Overall Gas Plant	-254182	174.37	0.019	-6562.0	665.8	-996	OK
803	S	IN	Overall Gas Plant	-284622	56.26	1.851	-557702.2	51.2	-30839	OK
805	S	IN	Overall Gas Plant	-284622	56.26	0.006	-1714.2	0.2	-95	OK
807	S	IN	Overall Gas Plant	-284622	56.26	0.021	-6443.1	0.6	-356	OK
809	S	IN	Overall Gas Plant	-284622	56.26	0.046	-13802.5	1.3	-763	OK
811	S	IN	Overall Gas Plant	-284622	56.26	0.056	-16854.6	1.5	-932	OK
813	S	IN	Overall Gas Plant	-284622	56.26	0.000	0.0	0.0	0	OK
815	S	IN	Overall Gas Plant	-284622	56.26	0.000	0.0	0.0	0	OK
817	S	IN	Overall Gas Plant	-284622	56.26	0.564	-170056.2	15.6	-9404	OK
819	S	IN	Overall Gas Plant	-284622	56.26	0.834	-251322.7	23.1	-13897	OK
821	S	IN	Overall Gas Plant	-284622	56.26	1.620	-488056.4	44.8	-26988	OK
823	S	IN	Overall Gas Plant	-284622	56.26	2.208	-665227.8	61.1	-36785	OK
825	S	IN	Overall Gas Plant	-284622	56.26	1.264	-380897.8	35.0	-21063	OK
827	S	IN	Overall Gas Plant	-284622	56.26	0.584	-175892.0	16.2	-9726	OK
804	S	OUT	Overall Gas Plant	-283068	61.15	1.851	-557702.2	245.6	33522	OK
806	S	OUT	Overall Gas Plant	-284235	57.51	0.006	-1714.2	0.2	97	OK
808	S	OUT	Overall Gas Plant	-283067	61.15	0.021	-6443.1	2.9	387	OK
810	S	OUT	Overall Gas Plant	-283846	58.74	0.046	-13802.5	3.1	797	OK
812	S	OUT	Overall Gas Plant	-283068	61.16	0.056	-16854.6	7.4	1013	OK
814	S	OUT	Overall Gas Plant	0	0.00	0.000	0.0	0.0	0	OK
816	S	OUT	Overall Gas Plant	0	0.00	0.000	0.0	0.0	0	OK
818	S	OUT	Overall Gas Plant	-283068	61.15	0.564	-170056.2	74.9	10222	OK
820	S	OUT	Overall Gas Plant	-283068	61.15	0.834	-251322.7	110.7	15106	OK
822	S	OUT	Overall Gas Plant	-283068	61.15	1.620	-488056.4	214.9	29335	OK

824	S	OUT	Overall Gas Plant	-283068	61.15	2.208	-665227.8	292.9	39985	OK
826	S	OUT	Overall Gas Plant	-283068	61.15	1.264	-380897.8	167.7	22894	OK
828	S	OUT	Overall Gas Plant	-283846	58.74	0.584	-175892.0	40.1	10156	OK
510	S	OUT	Overall Gas Plant	0	0.00	0.000	0.0	0.0	0	OK
402	S	OUT	Overall Gas Plant	-97760	154.88	0.097	-17760.7	3810.3	4455	OK
705	S	OUT	Overall Gas Plant	-221506	121.21	0.500	-147073.0	18247.3	17966	OK
1101	S	OUT	Overall Gas Plant	-284838	56.72	0.000	0.0	0.0	0	OK
1102	S	OUT	Overall Gas Plant	-284275	57.55	0.000	-6.0	0.0	0	OK
1103	S	OUT	Overall Gas Plant	-192973	82.99	0.006	-1614.3	280.7	151	OK
1104	S	OUT	Overall Gas Plant	-287563	50.60	0.002	-522.5	0.6	26	OK
1105	S	OUT	Overall Gas Plant	-286432	49.82	0.000	-80.1	0.0	4	OK
1106	S	OUT	Overall Gas Plant	-123645	77.89	0.000	0.0	0.0	0	OK
1107	S	OUT	Overall Gas Plant	-134540	111.38	0.000	0.0	0.0	0	OK
1108	S	OUT	Overall Gas Plant	0	0.00	0.000	0.0	0.0	0	OK
1109	S	OUT	Overall Gas Plant	-302216	168.76	0.000	0.0	0.0	0	OK
1110	S	OUT	Overall Gas Plant	-301763	162.00	0.000	0.0	0.0	0	OK
1111	S	OUT	Overall Gas Plant	-219786	118.38	0.000	0.0	0.0	0	OK
1112	S	OUT	Overall Gas Plant	-217511	145.10	0.000	0.0	0.0	0	OK
C-101-A_P	P	IN	Overall Gas Plant					2269.6	0	OK
C-101-B_P	P	IN	Overall Gas Plant					0.0	0	OK
C-201-A_P	P	IN	Overall Gas Plant					26.0	0	OK
C-201-B_P	P	IN	Overall Gas Plant					0.0	0	OK
C-201-C_P	P	IN	Overall Gas Plant					0.0	0	OK
C-202-A_P	P	IN	Overall Gas Plant					117.8	0	OK
C-202-B_P	P	IN	Overall Gas Plant					0.0	0	OK
C-202-C_P	P	IN	Overall Gas Plant					0.0	0	OK
C-501-A_P	P	IN	Overall Gas Plant					0.0	0	OK
C-501-B_P	P	IN	Overall Gas Plant					0.0	0	OK
C-501-C_P	P	IN	Overall Gas Plant					0.0	0	OK
C-502-A_P	P	IN	Overall Gas Plant					0.0	0	OK
C-502-B_P	P	IN	Overall Gas Plant					0.0	0	OK

C-502-C_P	P	IN	Overall Gas Plant					0.0	0	OK
C-601_P	P	IN	Overall Gas Plant					1008.9	0	OK
C-602_P	P	IN	Overall Gas Plant					1103.6	0	OK
C-603_P	P	IN	Overall Gas Plant					1804.1	0	OK
C-604_P	P	IN	Overall Gas Plant					1755.3	0	OK
C-701-A_P	P	IN	Overall Gas Plant					1634.9	0	OK
C-701-B_P	P	IN	Overall Gas Plant					0.0	0	OK
C-901-A_P	P	IN	Overall Gas Plant					129.9	0	OK
C-901-B_P	P	IN	Overall Gas Plant					0.0	0	OK
1208	S	IN	Overall Gas Plant	-277139	77.42	0.208	-62651.6	259.0	-4767	OK
1209	S	OUT	Overall Gas Plant	-277945	75.40	0.208	-62651.6	215.9	4643	OK
1303-A	S	IN	800-CW System	-285556	53.18	5.284	-1592279.1	25.6	-83232	OK
1303-B	S	IN	800-CW System	-285556	53.18	5.284	-1592279.1	25.6	-83232	OK
830	S	IN	800-CW System	-283211	60.70	9.879	-2976660.3	1228.4	-177585	OK
1306	S	OUT	800-CW System	-284235	57.51	10.569	-3184558.2	462.0	180018	OK
832	S	OUT	800-CW System	-284616	56.26	9.879	-2976660.3	339.0	164601	OK
P-802A	P	IN	800-CW System					21.4	0	OK
P-802B	P	IN	800-CW System					21.4	0	OK
P-801	P	IN	800-CW System					48.2	0	OK
102	S	IN	100-Main Comp.	-193477	164.61	0.581	-158649.3	18014.9	-28303	OK
803	S	IN	100-Main Comp.	-284622	56.26	1.851	-557702.2	51.2	-30839	OK
107	S	OUT	100-Main Comp.	-197062	153.61	0.612	-168944.7	20529.7	27835	OK
804	S	OUT	100-Main Comp.	-283068	61.15	1.851	-557702.2	245.6	33522	OK
1101	S	OUT	100-Main Comp.	-284838	56.72	0.000	0.0	0.0	0	OK
214	S	IN	100-Main Comp.	-244174	161.29	0.031	-10295.5	1159.3	-1495	OK
C-101-A_P	P	IN	100-Main Comp.					2269.6	0	OK
C-101-B_P	P	IN	100-Main Comp.					0.0	0	OK
405	S	IN	500-Export Comp.	-97760	154.88	0.000	0.0	0.0	0	OK
813	S	IN	500-Export Comp.	-284622	56.26	0.000	0.0	0.0	0	OK
815	S	IN	500-Export Comp.	-284622	56.26	0.000	0.0	0.0	0	OK
510	S	OUT	500-Export Comp.	0	0.00	0.000	0.0	0.0	0	OK

814	S	OUT	500-Export Comp.	0	0.00	0.000	0.0	0.0	0	OK
816	S	OUT	500-Export Comp.	0	0.00	0.000	0.0	0.0	0	OK
1107	S	OUT	500-Export Comp.	-134540	111.38	0.000	0.0	0.0	0	OK
1108	S	OUT	500-Export Comp.	0	0.00	0.000	0.0	0.0	0	OK
C-501-A_P	P	IN	500-Export Comp.					0.0	0	OK
C-501-B_P	P	IN	500-Export Comp.					0.0	0	OK
C-501-C_P	P	IN	500-Export Comp.					0.0	0	OK
C-502-A_P	P	IN	500-Export Comp.					0.0	0	OK
C-502-B_P	P	IN	500-Export Comp.					0.0	0	OK
C-502-C_P	P	IN	500-Export Comp.					0.0	0	OK
403	S	IN	600-CO2 Comp.	-302215	168.76	0.289	-108459.9	6563.7	-14460	OK
406	S	IN	600-CO2 Comp.	-97760	154.88	0.211	-38613.1	8283.8	-9686	OK
817	S	IN	600-CO2 Comp.	-284622	56.26	0.564	-170056.2	15.6	-9404	OK
819	S	IN	600-CO2 Comp.	-284622	56.26	0.834	-251322.7	23.1	-13897	OK
821	S	IN	600-CO2 Comp.	-284622	56.26	1.620	-488056.4	44.8	-26988	OK
823	S	IN	600-CO2 Comp.	-284622	56.26	2.208	-665227.8	61.1	-36785	OK
620	S	OUT	600-CO2 Comp.	-220847	128.84	0.500	-147073.0	17446.0	19097	OK
818	S	OUT	600-CO2 Comp.	-283068	61.15	0.564	-170056.2	74.9	10222	OK
820	S	OUT	600-CO2 Comp.	-283068	61.15	0.834	-251322.7	110.7	15106	OK
822	S	OUT	600-CO2 Comp.	-283068	61.15	1.620	-488056.4	214.9	29335	OK
824	S	OUT	600-CO2 Comp.	-283068	61.15	2.208	-665227.8	292.9	39985	OK
1109	S	OUT	600-CO2 Comp.	-302216	168.76	0.000	0.0	0.0	0	OK
1110	S	OUT	600-CO2 Comp.	-301763	162.00	0.000	0.0	0.0	0	OK
1111	S	OUT	600-CO2 Comp.	-219786	118.38	0.000	0.0	0.0	0	OK
1112	S	OUT	600-CO2 Comp.	-217511	145.10	0.000	0.0	0.0	0	OK
C-601_P	P	IN	600-CO2 Comp.					1008.9	0	OK
C-602_P	P	IN	600-CO2 Comp.					1103.6	0	OK
C-603_P	P	IN	600-CO2 Comp.					1804.1	0	OK
C-604_P	P	IN	600-CO2 Comp.					1755.3	0	OK

620	S	IN	700-EOR Comp.	-220847	128.84	0.500	-147073.0	17446.0	-19097	OK
825	S	IN	700-EOR Comp.	-284622	56.26	1.264	-380897.8	35.0	-21063	OK
705	S	OUT	700-EOR Comp.	-221506	121.21	0.500	-147073.0	18247.3	17966	OK
826	S	OUT	700-EOR Comp.	-283068	61.15	1.264	-380897.8	167.7	22894	OK
C-701-A_P	P	IN	700-EOR Comp.					1634.9	0	OK
C-701-B_P	P	IN	700-EOR Comp.					0.0	0	OK
307	S	IN	400-MP Unit	-197022	153.39	0.598	-164833.6	19943.1	-27147	OK
401	S	OUT	400-MP Unit	-97760	154.88	0.308	-56373.7	12094.0	14141	OK
403	S	OUT	400-MP Unit	-302215	168.76	0.289	-108459.9	6563.7	14460	OK
1208	S	IN	400-MP Unit	-277139	77.42	0.208	-62651.6	259.0	-4767	OK
1209	S	OUT	400-MP Unit	-277945	75.40	0.208	-62651.6	215.9	4643	OK
901	S	IN	900-C3 Cycle	-106645	141.77	0.030	-6372.9	1908.8	-1261	OK
827	S	IN	900-C3 Cycle	-284622	56.26	0.584	-175892.0	16.2	-9726	OK
907	S	OUT	900-C3 Cycle	-117416	101.30	0.030	-6372.9	1945.3	901	OK
828	S	OUT	900-C3 Cycle	-283846	58.74	0.584	-175892.0	40.1	10156	OK
C-901-A_P	P	IN	900-C3 Cycle					129.9	0	OK
C-901-B_P	P	IN	900-C3 Cycle					0.0	0	OK
201	S	IN	200-VRU	-225649	181.98	0.006	-1844.7	200.8	-317	OK
208	S	IN	200-VRU	-254182	174.37	0.019	-6562.0	665.8	-996	OK
317	S	IN	200-VRU	-210693	113.69	0.012	-3509.1	507.2	-414	OK
805	S	IN	200-VRU	-284622	56.26	0.006	-1714.2	0.2	-95	OK
807	S	IN	200-VRU	-284622	56.26	0.021	-6443.1	0.6	-356	OK
809	S	IN	200-VRU	-284622	56.26	0.046	-13802.5	1.3	-763	OK
811	S	IN	200-VRU	-284622	56.26	0.056	-16854.6	1.5	-932	OK
806	S	OUT	200-VRU	-284235	57.51	0.006	-1714.2	0.2	97	OK
808	S	OUT	200-VRU	-283067	61.15	0.021	-6443.1	2.9	387	OK
810	S	OUT	200-VRU	-283846	58.74	0.046	-13802.5	3.1	797	OK
812	S	OUT	200-VRU	-283068	61.16	0.056	-16854.6	7.4	1013	OK
214	S	OUT	200-VRU	-244174	161.29	0.031	-10295.5	1159.3	1495	OK
1102	S	OUT	200-VRU	-284275	57.55	0.000	-6.0	0.0	0	OK

1103	S	OUT	200-VRU	-192973	82.99	0.006	-1614.3	280.7	151	OK
C-201-A_P	P	IN	200-VRU					26.0	0	OK
C-201-B_P	P	IN	200-VRU					0.0	0	OK
C-201-C_P	P	IN	200-VRU					0.0	0	OK
C-202-A_P	P	IN	200-VRU					117.8	0	OK
C-202-B_P	P	IN	200-VRU					0.0	0	OK
C-202-C_P	P	IN	200-VRU					0.0	0	OK
303	S	IN	300-HCDP Adj.	-198452	148.50	0.604	-166741.9	20248.6	-26574	OK
305	S	OUT	300-HCDP Adj.	-198844	147.08	0.598	-164833.6	19972.1	26030	OK
312	S	OUT	300-HCDP Adj.	-211834	107.98	0.007	-1908.3	284.6	213	OK
907	S	IN	300-HCDP Adj.	-117416	101.30	0.030	-6372.9	1945.3	-901	OK
901	S	OUT	300-HCDP Adj.	-106645	141.77	0.030	-6372.9	1908.8	1261	OK
801	S	OUT	Oil Plant	-284622	56.26	0.825	-248690.8	22.8	13752	OK
802	S	IN	Oil Plant	-284234	57.51	0.825	-248690.8	36.9	-14058	OK

B3.2. Exergy balances

Table B3.2.1. Exergy balance for single-shaft compressors (base case) – RER-1

System	Ex_{in} (kW)	Ex_{out} (kW)	$Ex_{destroyed}$ (kW)	$S_{generated}$ (kW)	Error	$Ex_{destroyed}$	Ex_{waste} (kW)	$Ex_{waste+destroyed}$	η_{ex}
Case				**SSLC - 100% Gas Load - RER I**					
1000-GT	291411	216366	75044	75057	-0.016%	25.8%	38374	38.9%	61.1%
800-CW System	4535	2671	1864	1865	-0.080%	41.1%	1525	74.7%	25.3%
Overall Gas Plant	2139159	2120495	18664	18873	-1.118%	0.9%		0.9%	99.1%
GAS+TG+CW	2114278	2018301	95977	95968	0.009%	4.5%	39899	6.4%	93.6%
Case				**SSLC - 50% Gas Load - RER I**					
1000-GT	284161	210810	73350	73362	-0.016%	25.8%	37102	38.9%	61.1%
800-CW System	4064	2403	1661	1661	-0.011%	40.9%	1367	74.5%	25.5%
Overall Gas Plant	1187481	1164827	22654	22669	-0.064%	1.9%		1.9%	98.1%
GAS+TG+CW	1164494	1066452	98042	97857	0.189%	8.4%	38469	11.7%	88.3%
Case				**SSLC - 25% Gas Load - RER I**					
1000-GT	278003	206026	71976	71988	-0.016%	25.9%	35980	38.8%	61.2%
800-CW System	3489	2006	1483	1481	0.115%	42.5%	1174	76.2%	23.8%
Overall Gas Plant	454299	428449	25849	25869	-0.076%	5.7%		5.7%	94.3%
GAS+TG+CW	432834	333226	99609	99437	0.172%	23.0%	37154	31.6%	68.4%

Table B3.2.2 Exergy balance for Multiple paralleled compressors – RER-1

System	Ex_{in} (kW)	Ex_{out} (kW)	$Ex_{destroyed}$ (kW)	$S_{generated}$ (kW)	Error	$Ex_{destroyed}$	Ex_{waste} (kW)	$Ex_{waste+destroyed}$	η_{ex}
Case	**MSCP - 100% Gas Load - RER I**								
1000-GT	239425	178988	60437	60447	-0.017%	25.2%	32065	38.6%	61.4%
800-CW System	3903	2317	1586	1586	0.000%	40.6%	1265	73.0%	27.0%
Overall Gas Plant	2132556	2119657	12899	12729	1.320%	0.6%		0.6%	99.4%
GAS+TG+CW	2110713	2035477	75236	74917	0.424%	3.6%	33330	5.1%	94.9%
Case	**MSCP - 50% Gas Load - RER I**								
1000-GT	206995	153817	53178	53186	-0.016%	25.7%	27148	38.8%	61.2%
800-CW System	2604	1578	1026	1026	0.000%	39.4%	849	72.0%	28.0%
Overall Gas Plant	1172246	1163666	8579	8567	0.145%	0.7%			100.0%
GAS+TG+CW	1160900	1097839	63061	62911	0.237%	5.4%	27997	7.8%	92.2%
Case	**MSCP - 25% Gas Load - RER I**								
1000-GT	172213	127463	44749	44757	-0.016%	26.0%	21393	38.4%	61.6%
800-CW System	1371	801	570	570	0.000%	41.6%	452	74.5%	25.5%
Overall Gas Plant	432399	426869	5530	5526	0.077%	1.3%		1.3%	98.7%
GAS+TG+CW	429215	378176	51039	50916	0.241%	11.9%	21845	17.0%	83.0%

Table B3.2.3. Exergy balance for single-shaft compressors (base case) – RER-2

System	Ex_{in} (kW)	Ex_{out} (kW)	$Ex_{destroyed}$ (kW)	$S_{generated}$ (kW)	Error	$Ex_{destroyed}$	η_{ex}
Case			**SSLC - 100% Gas Load - RER II**				
100-Main Comp.	87548	85050	2498	2498	0.01%	2.9%	97.1%
200-VRU	7976	7604	372	372	0.00%	4.7%	95.3%
300-HCDP Adj.	90110	90010	100	100	0.00%	0.1%	99.9%
900-C3 Cycle	6946	6658	288	288	0.04%	4.1%	95.9%
400-MP Unit	83179	80679	2501	2501	0.00%	3.0%	97.0%
500-Export Comp.	71586	68191	3395	3396	0.00%	4.7%	95.3%
600-CO2 Comp.	19952	16072	3880	3880	0.01%	19.4%	80.6%
700-EOR Comp.	21991	16465	5526	5526	0.00%	25.1%	74.9%
800-CW System	4535	2671	1864	1865	-0.08%	41.1%	58.9%
Overall Gas Plant	114048	95185	18863	18873	-0.05%	16.5%	83.5%
Case			**SSLC - 50% Gas Load - RER II**				
100-Main Comp.	54192	49556	4636	4637	-0.02%	8.6%	91.4%
200-VRU	4562	4035	527	527	0.00%	11.6%	88.4%
300-HCDP Adj.	52618	52552	66	66	-0.05%	0.1%	99.9%
900-C3 Cycle	5038	4618	420	420	-0.01%	8.3%	91.7%
400-MP Unit	47824	45834	1989	1989	0.00%	4.2%	95.8%
500-Export Comp.	37780	32509	5271	5271	-0.01%	14.0%	86.0%
600-CO2 Comp.	18084	13887	4197	4197	0.00%	23.2%	76.8%
700-EOR Comp.	19526	14164	5362	5362	0.00%	27.5%	72.5%
800-CW System	4064	2403	1661	1661	-0.01%	40.9%	59.1%
Overall Gas Plant	78898	56232	22666	22669	-0.01%	28.7%	71.3%
Case			**SSLC - 25% Gas Load - RER II**				
100-Main Comp.	27635	21423	6211	6212	0.00%	22.5%	77.5%
200-VRU	2246	1612	634	634	0.00%	28.2%	71.8%
300-HCDP Adj.	22357	22328	29	29	-0.03%	0.1%	99.9%
900-C3 Cycle	3047	2151	896	896	0.00%	29.4%	70.6%
400-MP Unit	20235	18907	1328	1328	0.00%	6.6%	93.4%
500-Export Comp.	13739	7047	6691	6691	0.00%	48.7%	51.3%
600-CO2 Comp.	14465	9678	4787	4787	0.00%	33.1%	66.9%
700-EOR Comp.	14996	9795	5200	5200	0.01%	34.7%	65.3%
800-CW System	3489	2006	1483	1481	0.11%	42.5%	57.5%
Overall Gas Plant	51141	25273	25868	25869	0.00%	50.6%	49.4%

Table B3.2.4. Exergy balance for Multiple paralleled compressors – RER-2

System	Ex_{in} (kW)	Ex_{out} (kW)	$Ex_{destroyed}$ (kW)	$S_{generated}$ (kW)	Error	$Ex_{destroyed}$	η_{ex}
Case	**MSCP - 100% Gas Load - RER II**						
100-Main Comp.	87460	85060	2400	2400	0.00%	2.7%	97.3%
200-VRU	7909	7607	302	302	0.00%	3.8%	96.2%
300-HCDP Adj.	90162	90062	101	101	0.00%	0.1%	99.9%
900-C3 Cycle	6951	6697	254	254	0.00%	3.7%	96.3%
400-MP Unit	83178	80678	2500	2500	0.00%	3.0%	97.0%
500-Export Comp.	73044	69368	3675	3675	0.00%	5.0%	95.0%
600-CO2 Comp.	18450	15946	2504	2504	0.00%	13.6%	86.4%
700-EOR Comp.	16706	16020	686	686	0.00%	4.1%	95.9%
800-CW System	3903	2317	1586	1586	0.00%	40.6%	59.4%
Overall Gas Plant	107445	94710	12735	12729	0.05%	11.9%	88.1%
Case	**MSCP - 50% Gas Load - RER II**						
100-Main Comp.	50688	49174	1514	1514	0.00%	3.0%	97.0%
200-VRU	4092	3929	163	163	0.00%	4.0%	96.0%
300-HCDP Adj.	52494	52429	65	65	0.00%	0.1%	99.9%
900-C3 Cycle	4696	4525	172	172	0.00%	3.7%	96.3%
400-MP Unit	47802	45812	1989	1989	0.00%	4.2%	95.8%
500-Export Comp.	35797	34053	1744	1744	0.00%	4.9%	95.1%
600-CO2 Comp.	15871	13701	2170	2170	0.00%	13.7%	86.3%
700-EOR Comp.	14275	13721	554	554	0.00%	3.9%	96.1%
800-CW System	2604	1578	1026	1026	0.00%	39.4%	60.6%
Overall Gas Plant	63663	55096	8567	8567	0.00%	13.5%	86.5%
Case	**MSCP - 25% Gas Load - RER II**						
100-Main Comp.	21495	20775	720	720	0.00%	3.3%	96.7%
200-VRU	1521	1454	68	68	0.00%	4.4%	95.6%
300-HCDP Adj.	22194	22165	28	28	0.00%	0.1%	99.9%
900-C3 Cycle	2055	1985	69	69	0.00%	3.4%	96.6%
400-MP Unit	20202	18874	1329	1329	0.00%	6.6%	93.4%
500-Export Comp.	-	-	-	-	-	-	-
600-CO2 Comp.	20664	18139	2525	2525	0.00%	12.2%	87.8%
700-EOR Comp.	19116	18415	701	701	0.00%	3.7%	96.3%
800-CW System	1371	801	570	570	0.00%	41.6%	58.4%
Overall Gas Plant	29241	23715	5526	5526	0.00%	18.9%	81.1%

References of Appendix B

Cruz, M. de A.; Araújo, O. de Q. F.; De Medeiros, J. L. Deep seawater intake for primary cooling in tropical offshore processing of natural gas with high carbon dioxide content: Energy, emissions and economic assessments. **Journal of Natural Gas Science and Engineering**, v. 56, n. June, p. 193–211, 2018.

SUPPLEMENTARY MATERIALS C

CRUZ, M. DE A. et al. Impact of solid waste treatment from spray dryer absorber on the levelized cost of energy of a coal-fired power plant. **Journal of Cleaner Production**, v. 164, 2017a.

Supplement C1. FBR solid product and air flows determination

Supplement C2. Aspen process economic analysis

Supplement C3. Sensitivity analysis (LCOE versus treated residue revenue price)

References of Supplementary Materials C

Supplement C1. FBR solid product and air flows determination

Table C1.1. FBR Solid Product Stream.

Component	MW (kg/mol)	Flow (mol/h)	Flow (kg/h)	% Weight
$CaSO_3.½H_2O$	1.29E-01	-	-	0.00%
$CaSO_4.2H_2O$	1.72E-01	-	-	0.00%
$Ca(OH)_2$	7.40E-02	-	-	0.00%
$CaSO_3$	1.20E-01	6186	742	3.66%
$CaSO_4$	1.36E-01	55671	7571	37.34%
CaO	5.60E-02	23307	1305	6.44%
H_2O*	1.80E-02	-	-	0.00%
Inert	-	-	10660	52.57%
Total			20279	100.00%

Table C1.2. FBR Air Inlet and Outlet Streams.

FBR Air Inlet Stream				
	MW (kg/mol)	**Flow (mol/h)**	**Flow (kg/h)**	**% Molar**
O_2	0.032	32475	1039	21.00%
N_2	0.028	122167	3421	79.00%
Air	0.029	154642	4460	100.00%
FBR Air Outlet Stream				
O_2	0.032	4639	148	2.27%
N_2	0.028	122167	3421	59.85%
H_2O	0.018	77325	1392	37.88%
Air	0.024	204131	4961	100.00%

Supplement C2. Aspen process economic analysis

Table C2.1. Aspen Process Economic Analysis Equipment Inputs.

Reactor (FBR)	
Vessel Diameter (mm)	101.6
Vessel Height (m)	5.08
Design Gauge Pressure (kPa)	100
Design Temperature (°C)	800
Operating Temperature (°C)	550
Design Temperature (°C)	750
Solids Volume (% of vessel's volume)	30
Compressor	
Actual Gas Flow Rate (m^3/h)	3717.5
Design Gauge Pressure (kPa)	148.67
Design Temperature Inlet (°C)	20
Air Heater	
Material	SS304
Duty (MW)	0.5572
Gas Flow Rate (Sm3/h)	3466
Process Type	GAS
Design Gauge Pressure (kPa)	250
Design Temperature (°C)	550
Economizer	
Heat Transfer Area (m^2)	17.1
Number of Shells	1
TEMA symbol	BEU
Tube Material	SS304
Tube Design Gauge Pressure (kPa)	200
Tube Operating Temperature (°C)	350
Tube Outside Diameter (mm)	19.05
Shell Material	SS304
Shell Design Gauge Pressure (kPa)	100
Shell Operating Temperature (°C)	550
Shell Diameter (mm)	406
Air Filter	
Gas Flow Rate (Sm3/h)	4575
Air Temperature (°C)	400
Cyclones	
Gas Flow Rate (Sm3/h)	4575

Table C2.2. Aspen Process Economic Analysis Financial Set Parameters.

Time Period		
Period Description		Year
Operating Hours per Period	Hours/period	7451
Number of Weeks per Period	Weeks/period	52
Number of Periods for Analysis	Period	30
Capital Costs Parameters		
Working Capital Percentage	%/period	5
Operating Costs Parameters		
Operating Supplies (lump-sum)	Cost/period	25
Laboratory Charges (lump-sum)	Cost/period	0
User Entered Operating Charge (%)	%/period	25
Operating Charges (% of Operating Labor Costs)	%/period	0
Plant Overhead (% of O&M Costs)	%/period	50
G and A Expenses (% of Subtotal Operating Costs)	%/period	8
Operating Labor and Maintenance Costs		
Operating Labour		
Operators per Shift		2
Unit Cost	Cost/Operator/H	20
Supervision		
Supervisors per Shift		1
Unit Cost	Cost/Supervisor/H	35
Utilities Costs		
Electricity Unit Cost	Cost/kWh	0.095
General Investment Parameters		
Project Type		Grass Roots
Tax Rate	%/period	40
Interest Rate (or discount rate)	%/period	8
Economic Life of Project	Period	30
Salvage Value (Fraction of Initial Capital Cost)	%	20
Depreciation Method		Straight Line
Escalation		
Project Capital Escalation	%/period	5
Products Escalation	%/period	5
Raw Material Escalation	%/period	3.5
Operating and Maintenance Labor Escalation	%/period	3
Utilities Escalation	%/period	3

Table C2.3. Semi-Dry FGD Treatment Unit CAPEX.

Component Name	Total Direct Cost (USD)*	Equipment Cost (USD)*	Equipment Weight (kg)	Installed Weight (kg)
Compressor	400,100.00	250,800.00	6,500.00	13,671.00
Reactor (FBR)	223,400.00	49,500.00	1,700.00	9,748.00
Heater	324,700.00	194,400.00	13,500.00	19,636.00
Economizer	120,800.00	19,900.00	760	6,149.00
Air Filter	29,500.00	13,800.00	1,900.00	3,294.00
Cyclones	25,300.00	14,200.00	260	735
Total	1,123,800.00	542,600.00	24,620	53,233

*1st quarter 2014 price basis.

Supplement C3. Sensitivity analysis.

Table C3.1. Sensitivity Analysis Fixed Parameters

Fixed Parameters	Value
Sales (ton/h)	20.3
Operating Hours (h/yr)	7,451
Sales (ton/yr)	151,255
Project Lifetime (yr)	30
Interest Rate (%/yr)	8
Total Utilities Cost ($/yr)	112,257.85
Annualised Capital Cost ($/yr)	604,384.20
O&M Fixed Cost ($/yr)	573,261.31
AE (MWh/yr)	2,535,000
Base Plant LCOE ($/MWh)	94.97
FGD waste disposal cost ($/MWh)	0.53

Table C3.2. Sensitivity Analysis of LCOE versus Treated Semi-dry FGD Revenue Price

Residue Price ($/ton)	Anual Revenue ($/yr)	Sales Profit ($/yr)	TAC * ($/yr)	ΔLCOE ($/MWh)	FINAL LCOE ($/MWh)	ΔLCOE (%)
0	0.00	-112257.85	-1289903.36	0.02	94.95	0.0%
10	1512553.00	1400295.15	222649.64	0.62	94.35	0.7%
20	3025106.00	2912848.15	1735202.64	1.21	93.76	1.3%
30	4537659.00	4425401.15	3247755.64	1.81	93.16	1.9%
40	6050212.00	5937954.15	4760308.64	2.41	92.56	2.5%
47	7108999.10	6996741.25	5819095.74	2.83	92.14	3.0%
50	7562765.00	7450507.15	6272861.64	3.00	91.97	3.2%
60	9075318.00	8963060.15	7785414.64	3.60	91.37	3.8%
70	10587871.00	10475613.15	9297967.64	4.20	90.77	4.4%
80	12100424.00	11988166.15	10810520.64	4.79	90.18	5.0%
90	13612977.00	13500719.15	12323073.64	5.39	89.58	5.7%
100	15125530.00	15013272.15	13835626.64	5.99	88.98	6.3%

* TAC = Total Annualized Cost of semi-dry FGD solid waste treatment unit = sales profit - annualized capital cost - O&M fixed cost.

APPENDIX I – PILOT-PLANT DETAILED DESIGN

I.1. Process Simulation

Preliminary process simulation was developed in Aspen HYSYS v8.8 (Aspentech, 2020), according to the process design. A blend of MEA/1-propanol/Water was considered as the PCAS. The Acid Gas fluid package was chosen to perform the simulation. This thermodynamic package does not predict phase split when the solvent absorbs CO_2. A stream splitter module was used to force the phase-split, based on the volume ratios determined experimentally at the PCASP. The information generated in the simulation was used as a design basis for sizing and specification of the main equipment, instruments, valves and pipes. Figure I.1 shows the simulation flowsheet and Table I.1 summarizes the main simulation inputs, constrains, targets and other assumptions.

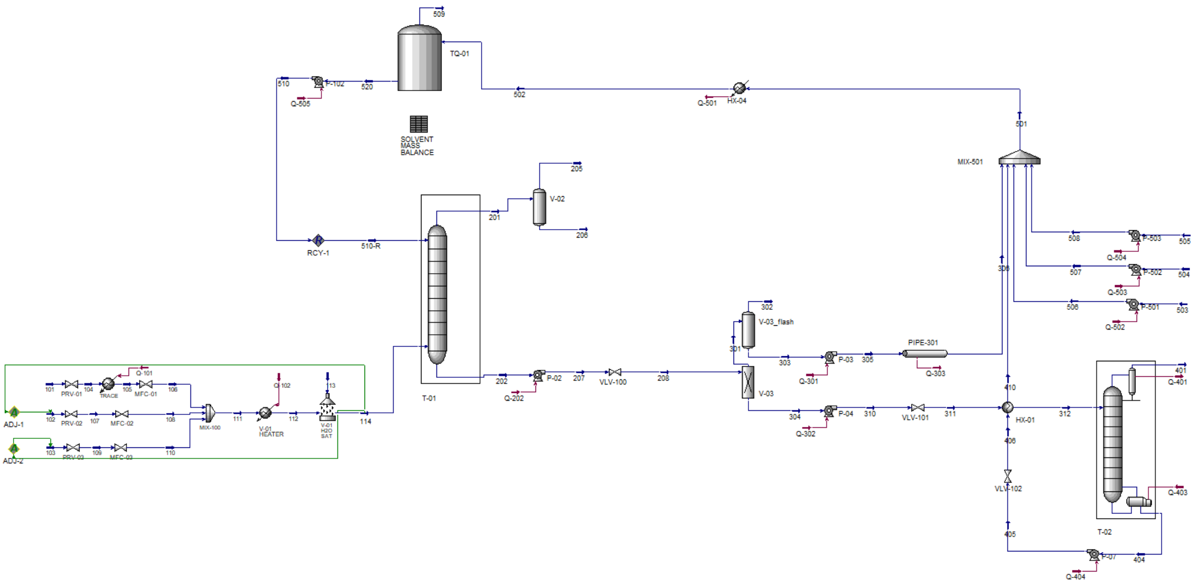

Figure I.1. PCAPP Simulation Flowsheet

Table I.1. PCAPP Simulation assumptions

Parameter	Value
Flue-Gas CO_2 flow rate	2.5 – 5.0 kg/h
Flue-Gas CO_2 concentration	4% - 15% (mol/mol)
Lean solvent composition	30% MEA, 40% 1-propanol (w/w)
Solvent flow rate	50 – 200 kg/h
Absorption column pressure	101-200 kPa
Absorption column internals	MELLAPAK 500Y metal, 135mm diameter, 4400mm section height
Minimum CO_2 capture efficiency	90%
Integration heat exchanger minimum approach	10ºC
Regeneration pressure	150 – 300 kPa
Reboiler maximum temperature	130ºC
Condenser temperature	40ºC
Regeneration column internals	MELLAPAK 500Y metal, 108mm diameter, 4400mm section height

I.2. Equipment Design and Specification

- **Towers**

To design the columns, it was considered a hypothetical wet flue-gas from a natural gas combined cycle (NGCC) power plant. The flue-gas CO_2 molar concentration was considered 4% at 200 kPa and 40ºC. The flue-gas inlet flow rate is manipulated to reach a CO_2 flow rate of 5kg/h. The solvent flow rate was considered 100 kg/h (30%MEA, 40% 1-propanol).

The diameters of the absorption and desorption towers were defined in 5” (141mm internal diameter) and 4” (114mm internal diameter), respectively. Both columns have 2 sections of packed beds with 2.2m of height each. The column's height is limited in around 8 meters by the ceiling of the shed. The hydraulics of the towers were checked using the software KG-Tower (Koch-Glitsch, 2020). This software requires the properties summarized in Table I.2 to calculate the pressure drop through the packed beds, % of flooding, and other operational parameters. All inputs were imported from the process simulations.

Table I.2. KG-Tower Inputs

	Inputs
Liquid (*for each theoretical stage or the plate with maximum internal flow rate*)	Nominal, Minimum and Maximum Flow Rates (kg/h); Density (kg/m³); Viscosity (cP); Surface Tension (dyne/cm)
Vapor (*for each theoretical stage or the plate with maximum internal flow rate*)	Nominal, Minimum and Maximum Flow Rates (kg/h); Density (kg/m³); Viscosity (cP)
Tower	System Factor; Packing Type; Height (m), Diameter (m)

The KG-Tower reports generated for the T-01 and T-02 are depicted in Figs. I.2 and I.3.

KOCH-GLITSCH®
KG-TOWER® Software v 5.4
Registered To: Matheus Cruz, UFRJ

Customer's copy.
Strictly confidential. Property of Koch-Glitsch.
PACKED TOWER RATING DATA

Project Name UPAS2F — Date : 02-Mar-2020 — Page : 1
Tower Name T-01 Absorption Tower — File : T01-10_REVD.kgt
Case Name 100kg/h 30MEA40PROP 5kg/h CO2 — By : Matheus — Revision : 0

ZONE		Top	Top	Top
DESCRIPTION		Max Liq	Max Liq	Max Liq
BED NUMBER		3	MIN	MAX
% OF LOADING	(%V/%L)	100	50/ 75	105/ 200
LOADINGS				
Vapor Rate	kg/hr	88	44	92
Vapor Density	kg/m3	1.829	1.829	1.829
Vapor Volume	m3/s	0.01	0.01	0.01
Vapor Viscosity	cP	0.0187	0.0187	0.0187
Liquid Rate	kg/hr	103	77	206
Liquid Density	kg/m3	948.17	948.17	948.17
Liquid Volume	m3/hr	0.11	0.08	0.22
Surface Tension	mN/m	26.26	26.26	26.26
Liquid Viscosity	cP	1.789	1.789	1.789
System Factor		0.70	0.70	0.70
Packing Type		FLEXIPAC® 500Y structured packing METAL	FLEXIPAC® 500Y structured packing METAL	FLEXIPAC® 500Y structured packing METAL
Tower Diameter	mm	135	135	135
Tower Area	m2	0.01	0.01	0.01
Packing Height	mm	4400	4400	4400
Fs	m/s*(kg/m3)^0.5	1.26	0.63	1.32
Cv	m/s	0.04	0.02	0.04
Liquid Loading	m3/hr/m2	7.58	5.68	15.15
Calculated Capacity Constant L/V	%	92	49	109
Pressure Drop	mbar/m	1.69	<0.5	N/A

Total Packing Pressure Drop mm Hg 5.57 (Min. 1.42 Max. N/A)
Note: The total packing pressure drop is the sum of the calculated pressure drop for each loading.

WARNINGS: 1, 2,3,

Figure I.2. KG-Tower Report for the T-01 Hydraulic Analysis

KOCH-GLITSCH®

KG-TOWER® Software v 5.4

Registered To: Matheus Cruz, UFRJ

Customer's copy.

Strictly confidential. Property of Koch-Glitsch.

PACKED TOWER RATING DATA

Project Name	UPAS2F	**Date :** 02-Mar-2020	**Page :** 1
Tower Name	T-02 Stripper	**File :** T02-5_REV0.kgt	
Case Name	100kg/h 30MEA40PROP 5kg/h CO2	**By :** Matheus	**Revision :** 0

ZONE		Bottom	Bottom	Bottom
DESCRIPTION		Max L&G Rates	Max L&G Rates	Max L&G Rates
BED NUMBER		20	MIN	MAX
% OF LOADING	(%V/%L)	100	50/ 75	105/ 200
LOADINGS				
Vapor Rate	kg/hr	11	5	11
Vapor Density	kg/m3	2.854	2.854	2.854
Vapor Volume	m3/s	0.00	0.00	0.00
Vapor Viscosity	cP	0.0140	0.0140	0.0140
Liquid Rate	kg/hr	81	61	162
Liquid Density	kg/m3	959.75	959.75	959.75
Liquid Volume	m3/hr	0.08	0.06	0.17
Surface Tension	mN/m	23.65	23.65	23.65
Liquid Viscosity	cP	0.711	0.711	0.711
System Factor		0.70	0.70	0.70
Packing Type		FLEXIPAC® 500Y structured packing METAL	FLEXIPAC® 500Y structured packing METAL	FLEXIPAC® 500Y structured packing METAL
Tower Diameter	mm	102	102	102
Tower Area	m2	0.01	0.01	0.01
Packing Height	mm	4400	4400	4400
Fs	m/s*(kg/m3)^0.5	0.22	0.11	0.23
Cv	m/s	0.01	0.00	0.01
Liquid Loading	m3/hr/m2	10.26	7.69	20.51
Calculated Capacity Constant L/V	%	26	15	35
Pressure Drop	mbar/m	<0.5	<0.5	<0.5

Total Packing Pressure Drop mm Hg 0.19 (Min. 0.05 Max. 0.23)

Note: The total packing pressure drop is the sum of the calculated pressure drop for each loading.

Figure I.3. KG-Tower Report for the T-02 Hydraulic Analysis

The % of flooding is above 90% for the T-01 at 100% CO_2 capacity (5kg/h). This result is above 80%, the maximum recommended by the manufacturers of tower internals. Thus, if the flooding occurs the plant should operate with a lower CO_2 inlet flow rate. The hydraulic analysis of T-02 unveiled that it will operate far from the flooding point because of the small internal vapor flow rates.

Figs. I.4 and I.5 present the internals and nozzles of the towers T-01 and T-02, respectively. The description of each nozzle is presented in Table I.3.

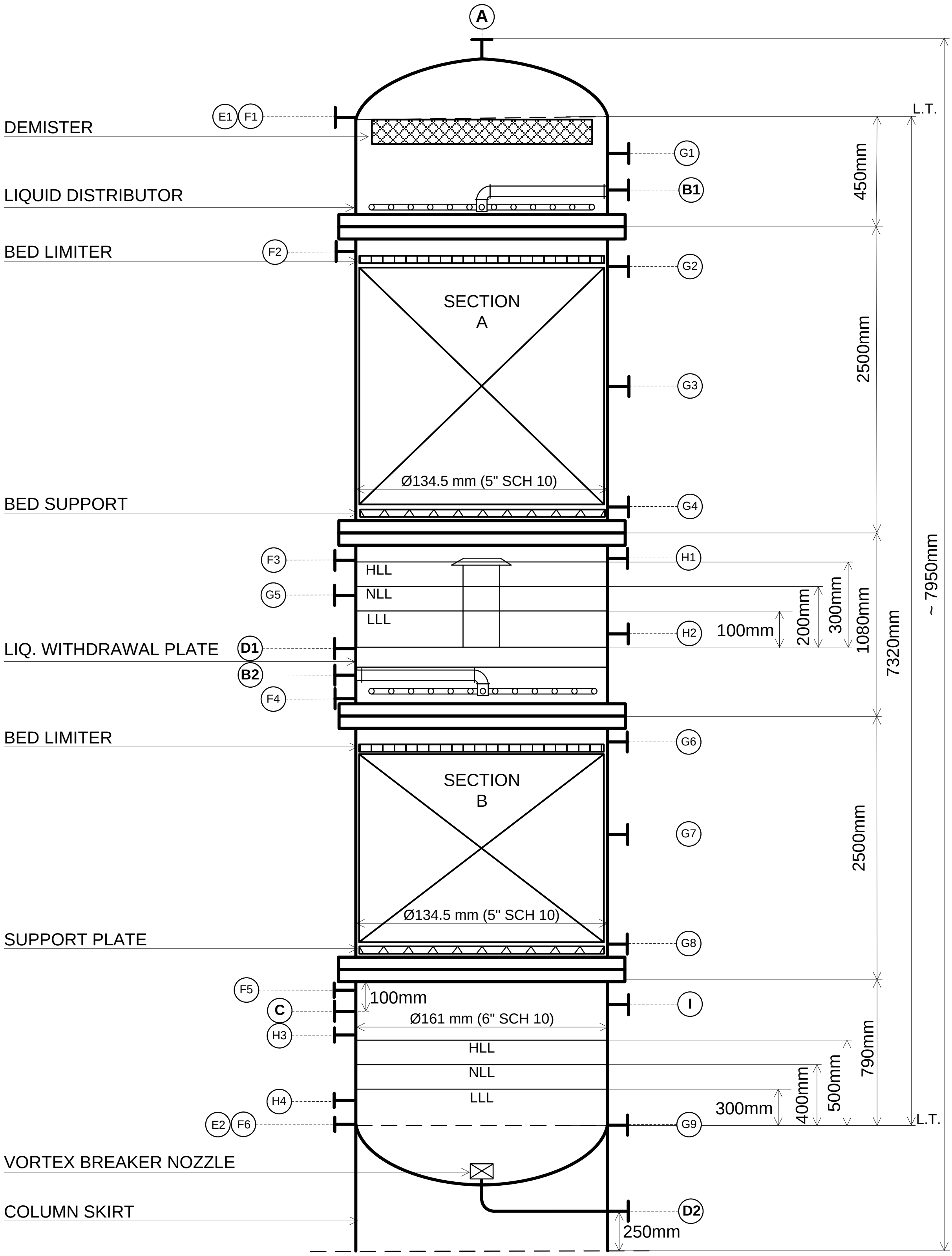

Figure I.4. Absorber (T-01) Internals and Nozzles

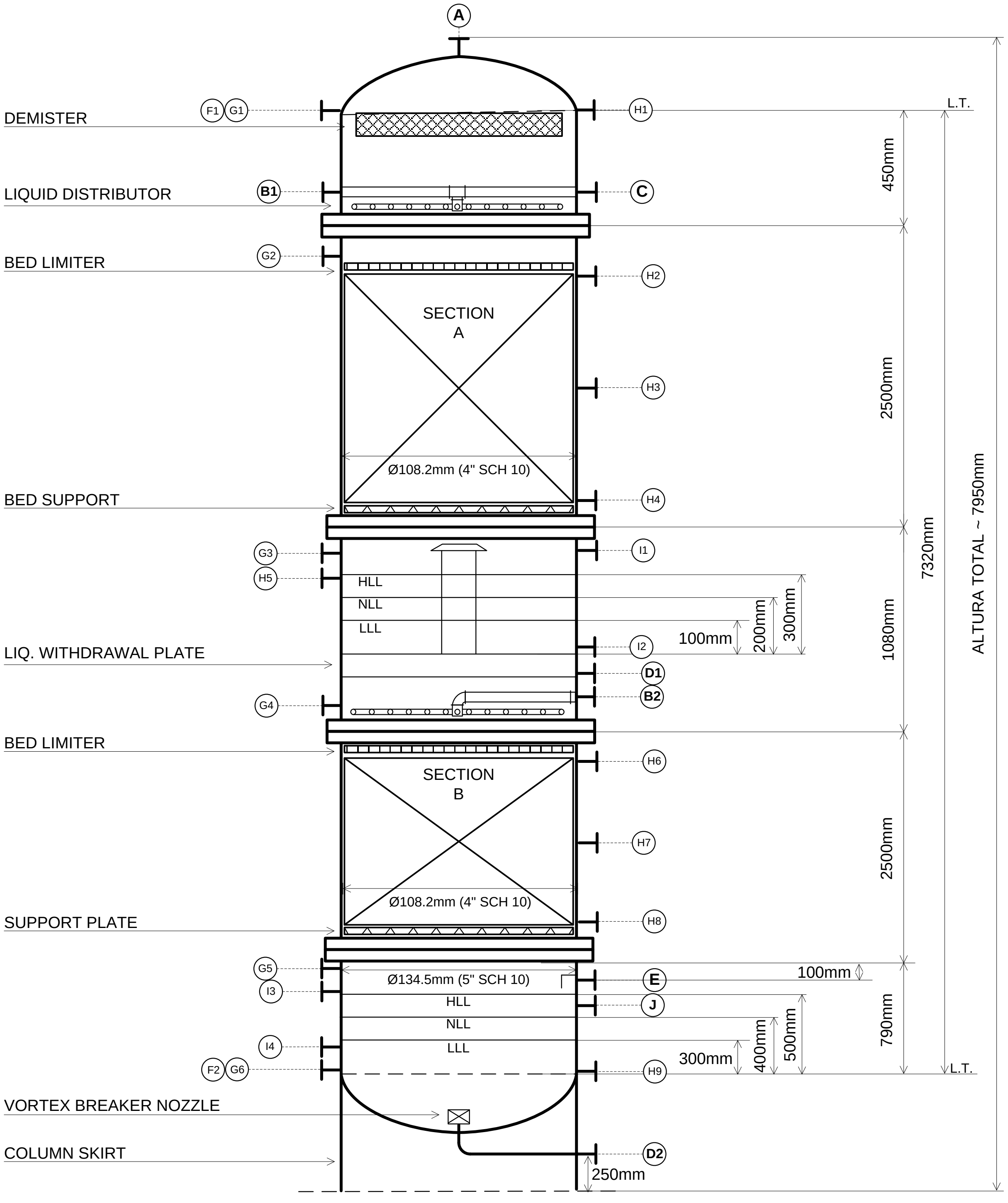

Figure I.5. Stripper (T-02) Internals and Nozzles

Table I.3. Nozzles list of the absorption and desorption columns

	ABSORBER (T-01)			STRIPPER (T-02)		
NOZZLE	QUANT.	DIAM. (in)	DESCRIPTION	QUANT.	DIAM. (in)	DESCRIPTION
A	1	1	Top gas outlet	1	1	Top gas outlet
B	2	1/2	Liquid inlet	2	1	Liquid inlet
C	1	1	Gas inlet	1	1/2	Liquid inlet (reflux)
D	2	1	Liquid outlet	2	1	Liquid outlet
E	2	1/4	Pressure gauge	1	1	Gas inlet
F	6	1/4	Pressure sensor	2	1/4	Pressure gauge
G	9	1/4	Temperature sensor	6	1/4	Pressure sensor
H	4	1/2	Level sensor	9	1/4	Temperature sensor
I	1	1/2	Liquid inlet	4	1/2	Level sensor
J	-	-	-	1	1	Liquid inlet

Fig. I.6 shows pictures of the columns and their internals.

Figure I.6. PCAPP Columns and their internals

- **Heat Exchangers**

Table I.4 summarize the heat exchangers design.

Table I.4. PCAPP Heat Exchangers

TAG	TEMA Type	Duty (kW)	DN Shell (mm)	Tubes Length (mm)	Tubes Design T (°C)	Shell Design T (°C)	Tubes Design P (kPa)	Shell Design P (kPa)	Heat Exchange Area (m²)
HX-01	BEW	4,5	67	2500	155	155	400	500	1
HX-02	BEW	0,6	67	900	70	125	400	500	0,2
HX-03	BKU	7,0	161	600	215	155	400	500	0,8
HX-04	BEW	5,0	95	1400	105	105	400	500	0,7

Fig. I.7 shows pictures of the heat exchangers.

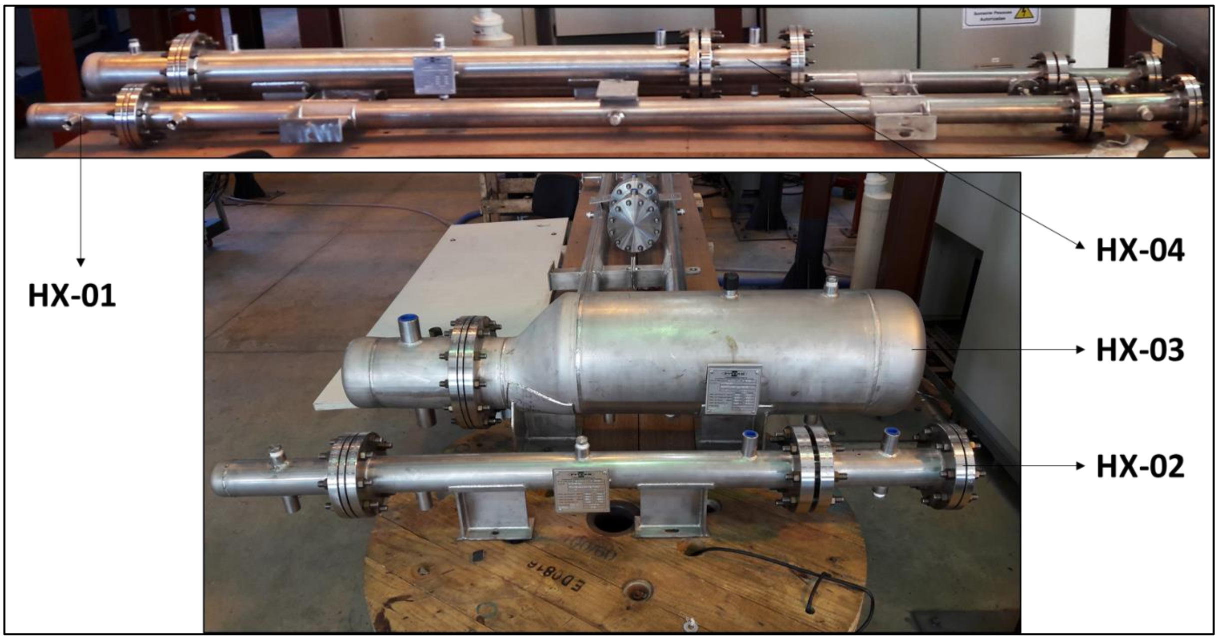

Figure I.7. PCAPP Heat Exchangers

- **Pressure Vessels**

Table I.5 summarize the pressure vessels design.

Table I.5. PCAPP Pressure Vessels

TAG	Volume (l)	Design P (kPag)	Design T (°C)	DN (in)	Height (m)	Service
V-01	15,0	500	70	4	1,70	Flue-Gas heating and saturation with H_2O
V-02	10,0	500	80	6	0,53	Knock-Out
V-03	15,0	500	90	8	0,90	Liquid-liquid phase separation
V-04	1,50	500	140	4	0,58	Reflux condensate separation

The vessel V-03 is illustrated in Fig. I.8 and its nozzles list is shown in Table I.6.

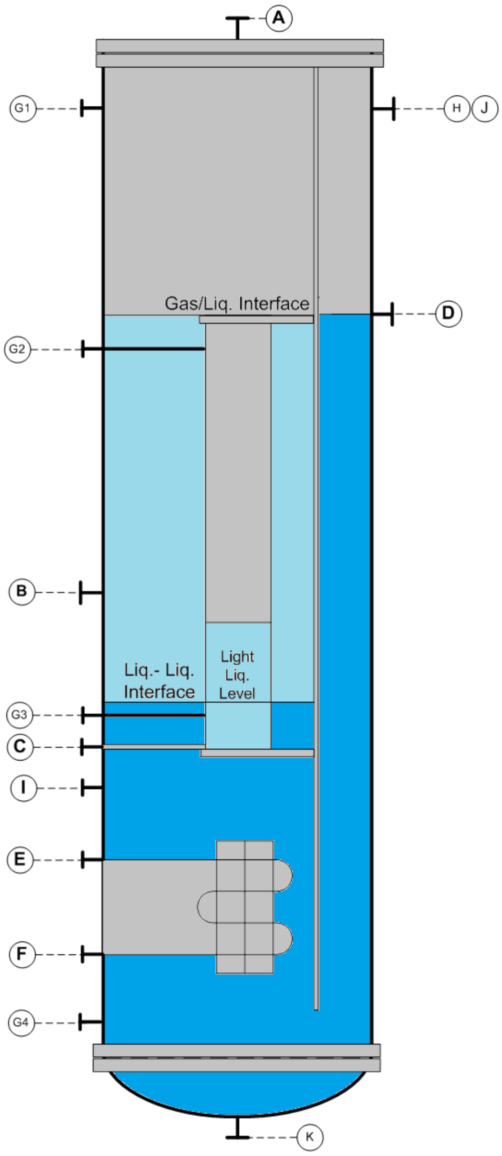

Figure I.8. V-03 Internals and Nozzles

Table I.6. Nozzles list of the V-03

NOZZLE	QUANT.	DIAM. (in)	DESCRIPTION
A	1	1/2	Top gas outlet
B	1	1/2	Liquid inlet
C	1	1/2	Light liquid outlet
D	1	1/2	Heavy liquid outlet
E	1	1/2	Thermal fluid inlet
F	1	1/2	Thermal fluid outlet
G	4	1/2	Level sensor
H	1	1/4	Pressure gauge
I	1	1/4	Temperature sensor
J	1	1/4	Pressure sensor
K	1	1	Drain

Fig. I.9 shows pictures of the four vessels of the PCAPP.

V-01	V-02	V-03	V-04
			

Figure I.9. PCAPP Pressure Vessels

- **Pumps**

The pump selection was challenging due to the very low flow rates, high temperatures and chemical aggressivity of the fluids. The Micropump external gear pumps (Micropump, 2020) GA and GB series were considered suitable for the service. Table I.7 summarize the specification of the pumps.

However, the PCAPP is intended to deal with multiple PCAS and CO_2 flow rates and partial pressures. As a result, a great flow rate flexibility is necessary. To meet this demand VSD and gearboxes were adopted. Table I.8 shows the range of flow rates and revolutions per minute (rpm) necessary to achieve the range of flow rates shown in Table I.7.

Table I.7. PCAPP Pumps

TAG	Volumetric Flow Rates Min (l/h)	Volumetric Flow Rates Nominal (l/h)	Volumetric Flow Rates Max (l/h)	P_{inlet} (barg)	P_{outlet} (barg)	$T_{operation}$ (°C)	T_{design} (°C)	Max viscosity (cP)	Design density (kg/m³)
P-01	36	90	210	0.5	3.0	45	80	250	1200
P-02	36	90	210	0.5	1.5	40	80	250	1200
P-03	15	30	120	0.1	3.0	40	90	250	1200
P-04	24	66	180	0.1	3.0	40	90	250	1200
P-05A	9.0	24.0	36.0	1.0	3.0	40	90	1.1	1000
P-05B	1.0	3.6	6.0	1.0	3.0	40	90	1.1	1000
P-06	36	75	210	2.0	3.0	130	150	20	1000
P-07	36	75	210	2.0	3.0	130	150	20	1000
P-08	36	105	210	0,0	3.0	40	50	250	1200
P-12	36	75	210	2.0	3.0	130	150	20	1000

Table I.8. PCAPP pumps: drives, variable speed drives, gearboxes and rpm range

TAG	Pump Model	Drive	VSD	Gearbox Ratio	RPM RANGE RPM max = 3440 @ 60Hz Min	Nom	Max	Min*	Nom*	Max
P-01	GB	WEG - 220/380V 3PH 60Hz 0,75CV, IEC 71-B14	WEG CFW 500	2:1	570	1425	3325	33%	83%	97%
P-02	GB	WEG - 220/380V 3PH 60Hz 0,75CV, IEC 71-B14	WEG CFW 500	2:1	570	1425	3325	33%	83%	97%
P-03	GB	WEG - 220/380V 3PH 60Hz 0,75CV, IEC 71-B14	WEG CFW 500	4:1	238	475	1900	28%	55%	55%
P-04	GB	WEG - 220/380V 3PH 60Hz 0,75CV, IEC 71-B14	WEG CFW 500	3:1	380	1045	2850	33%	91%	83%
P-05A	GB	WEG - 220/380V 3PH 60Hz 0,75CV, IEC 71-B14	WEG CFW 500	2:1	599	1596	2394	35%	93%	70%
P-05B	GA	WEG - 220/380V 3PH 60Hz 0,75CV, IEC 71-B14	WEG CFW 500	4:1	204	733	1221	24%	85%	71%
P-06	GB	WEG - 220/380V 3PH 60Hz 0,75CV, IEC 71-B14	WEG CFW 500	2:1	570	1188	3325	33%	69%	97%
P-07	GB	WEG - 220/380V 3PH 60Hz 0,75CV, IEC 71-B14	WEG CFW 500	2:1	570	1188	3325	33%	69%	97%
P-08	GB	WEG - 220/380V 3PH 60Hz 0,75CV, IEC 71-B14	WEG CFW 500	2:1	570	1663	3325	33%	97%	97%
P-12	GB	WEG - 220/380V 3PH 60Hz 0,75CV, IEC 71-B14	WEG CFW 500	2:1	570	1188	3325	33%	69%	97%

*considering gearbox

- **Instruments, Control and Automation**

Table I.9 lists all the instruments specified to the PCAPP

Table I.9. PCAPP List of Instruments

Type	Qnt.	Sign
Pressure Sensor/Transmitter (PT)	15	4 – 20 mA
Temperature Sensor/Transmitter (TT)	35	4 – 20 mA
Differential Pressure Sensor/Transmitter (PDT)	4	4 – 20 mA
Flow Meter/Transmitter (FT)	12	4 – 20 mA
Level Sensor/Transmitter (PT)	7	4 – 20 mA
Analyzers (AT)	8	4 – 20 mA

Table I.10 lists all the control loops of the PCAPP.

Table I.10. PCAPP List of Control Loops

Type	Qnt.	Control Element
Pressure Control	3	Valve (PCV)
	2	Valve (TCV)
Temperature Control	1	Solid State Relay (SSR)
	2	Process Thermostat
Mass Flow Control	3	Mass Flow Controller (MFC)
Level Control	9	VSD of pumps
Tank Mixer rpm	1	VSD

Table I.11 lists the control panel components and Fig. I.10 shows a picture of the panel.

Table I.11. PCAPP List of components of Programmable Logic Control Panel

Description	Qnt.
Programmable Logic Control Wago model PFC200	1
CPU - 24 Vdc, Modbus TCP/IP, PFC200, Slot Micro SD	1
Analog Card 8 inputs, 4..20mA	11
Digital Card 16 inputs, 24Vdc, 3ms	2
Digital Card 16 outputs, 24Vdc	2
Analog Card 4 outputs, 4..20mA	4
Analog Card 4 outputs, 0..20mA	2
Module	1
Power source: In:100..240Vac / Out:24Vdc, 10A	1
Relay, 24Vdc	64
Jumper (for relay) 10 ways	10

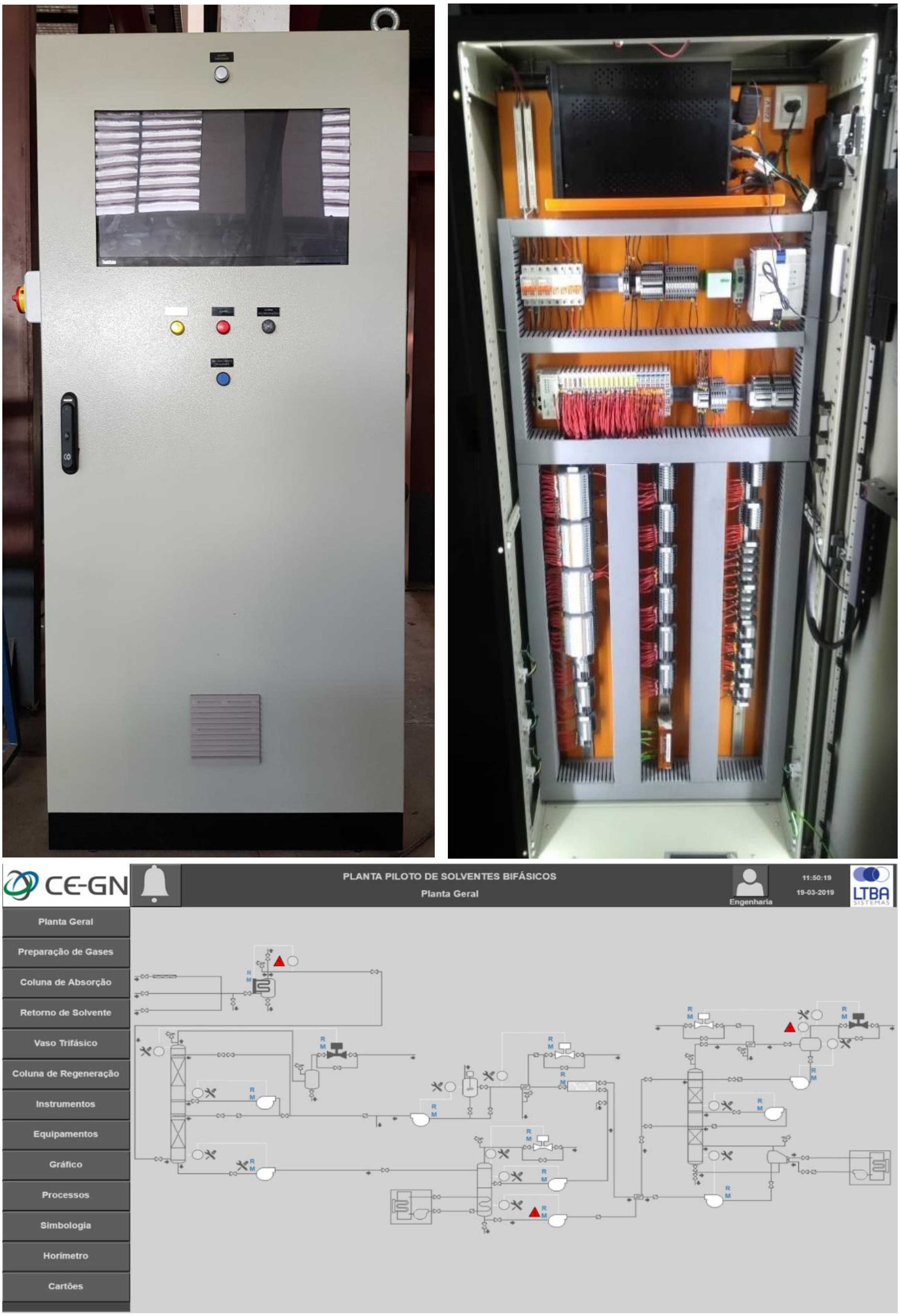

Figure I.10. PCAPP Control Panel

ERRATUM

CRUZ, M. D. A. et al. Environmental Performance of a Solid Waste Monetization Process Applied to a Coal-Fired Power Plant with Semi-Dry Flue Gas Desulfurization. **Journal of Sustainable Development of Energy, Water and Environment Systems**, v. 7, n. 3, p. 506–520, 2018.

1 – The reference [31] (CONAMA 03/1990), cited in the page 510, line 13 of the original article (reproduced in the Chapter 6 of this thesis) is a national regulation for air quality in Brazil. However, the limit of 400 mg/Nm^3 for SO_2 emissions from coal-fired Power Plants is stablished by the BNDES, through the following reference:

BNDES, 2020. Environmental criteria to support the power generation segment. [WWW Document]. URL http://www.https://www.bndes.gov.br/SiteBNDES/bndes/bndes_en/Institucional/Social_and_Environmental_Responsibility/socioenvironmental_policy/environmental_criteria_power_generation.html (accessed 5.15.20).

2 – In the last line of Tables 6, 7, and 8 (Tables 6.6, 6.7, and 6.8 of this thesis): where it reads "SO_4", it should read "$CaSO_4$".